Interaction between the V0 subunit of V-ATPase and the exchange factor ARNO and its functional involvement in regulated exocytosis

Qili Wang

UNIVERSITÉ DE STRASBOURG

École Doctorale des Sciences de la Vie et de la Santé

INCI – CNRS UPR 3212

THÈSE

Présentée Pour l'obtention du grade de :

Docteur de l'Université de Strasbourg
Discipline : Sciences du Vivant
Spécialité : Aspects moléculaires et cellulaires de la biologie

Par

Qili WANG

Interaction entre la sous unité V0 de la V-ATPase et le facteur d'échange ARNO et son implication fonctionnelle dans l'exocytose régulée

Soutenue mecredi le 18 septembre 2019, devant le jury composé de :

Dr. SIMONNEAUX Valérie	**Présidente du jury**
Dr. EL FAR Oussama	**Rapporteur externe**
Pr. OLIVIER Jean-Luc	**Rapporteur externe**
Dr. VITALE Nicolas	**Directeur de thèse**

Remerciements

Je souhaiterais tout d'abord remercier les membres de mon jury de thèse, **Dr. SIMONNEAUX Valérie, Dr. EL FAR Oussama et Pr. OLIVIER Jean-Luc**, qui m'ont fait le grand honneur d'avoir accepté de lire, commenter et juger mon travail de thèse.

Je voudrais également remercier mon directeur de thèse **Dr. VITALE Nicolas**. Tu m'as encadré pendant 4 ans et tu m'as suivi pas a pas dans mon apprentissage de la recherche avec tes qualités scientifiques et humaines. Je veux bien profiter de cette occasion pour t'exprimer mes sincères remerciements pour ta confiance et les libértés que tu m'as données dans la recherche. Merci pour tout.

Mes remerciements vont également à tous les membres de l'équipe pour leur aide :

Dr. Marie France BADER, pour m'avoir accueillie à l'INCI alors qu'elle en était la directrice.

Dr. Stéphane GASMAN, co-responsable de l'équipe, pour tes remarques constructives et sa bonne humeur.

Dr. Stéphane ORY, pour les discussions scientifiques et les conseils notamment en imagerie.

Dr. Sylvette CHASSEROT-GOLAZ, pour la formation à la microscopie confocale.

Tam THAHOULY, un grand merci pour les manips de biologie moléculaire et pour les cultures de chromaffines bovines.

Claudine BOISSIER, pour ta serviabilité, et la gestion des stocks et commandes.

Anne-Marie HAEBERLE, pour ton aide en microscopie électronique par transmission durant mon stage de master et le début de ma thèse.

Dr. Petra TOTH, pour les discussions scientifiques ou non-scientifiques.

Sebahat OZKAN, plus récemment arrivée dans l'équipe, merci pour tes conseils de clonage.

Valérie CALCO, pour ton aide à la culture des cellules PC12.

De même, un grand merci à **Emeline Tanguy, Marion RAME, Marion GABEL** et **Marion MILLET** pour tous les moments de discussion et les aides durant les 4 ans dans notre laboratoire. Merci aussi à Marion Millet, Laura et Margherita, je vous souhaite bonne chance pour la suite de votre thèse.

Je souhaiterais remercier tous ma famille. Merci à mes parents pour votre soutiens sans réserve depuis toujours. Merci à ma sœur pour toute son aide.

Enfin, un grand merci pour ma femme **Yidan**. Sans ta patience et ton soutien tout au long de ma thèse, je n'aurais certainement pas réussi à la mener à bien. J'en profite pour t'exprimer mon grand amour et ma grande fierté.

Abbreviations

AD	Alzheimer Disease
ADHD	Attention deficit/ hyperactivity disorder
AL	Autolysosomes
AP	Autophagosome
APP	Amyloid precursor protein
ARF6	ADP-ribosylation factor 6
ARNO	Cytohesin 2
ATP	Adenosine Triphosphate
ARCL	Autosomal recessive cutis laxa
α-SNAP	NSF cofactor
BoNT	Botulinum neurotoxin
CMA	Chaperone-mediated autophagy
c-AMP	Cyclic adenosine monophosphate
dRTA	Distal renal tubular acidosis
EE	Early endosomes
ER	Endoplasmic reticulum
F-ATPase	ATP-synthase
FLIM	Fluorescence-lifetime imaging microscopy
FRAP	Fluorescence recovery after photobleaching
FRET	Förster resonance energy transfer
GEF	Guanine Nucleotide Exchange Factor
GTP	Guanosine-5'-triphosphate
ISG	Immature secretory granules
LE	Late endosomes
MMs	Matrix metalloproteinase isoforms
MRXSH	X-linked Mental Retardation Hedera type
MSG	Mature secretory granules
Munc-18	Mammalian uncoordinated-18
MVB	Multi-vesicular bodies
NHE3	Na^+-H^+ exchanger isoform 3
NSF	N-ethylmaleimide sensitive factor
NTs	Neurotransmitters
PA	Phosphatidic acid
PAS	Preautophagosomal structure
PI-3 kinase	Phosphatidylinositol 3-kinase
PI(3)P	Phosphatidylinositol-3-phosphate
PI(4)P	Phophatidylinositol-4-phosphate
PI(3,5)P2	Phosphatidylinositol-3,5-bisphosphate
PI(4,5)P2	Phosphatidylinositol-4,5-bisphosphate
PLD	Phospholipase D
PS1	Presenilin-1
PS2	Presenilin-2

PUFA	Polyunsaturated fatty acids
Rab	One of five families of small GTPases
Ras	cAMP-dependent protein kinase
RAVE	Regulator of acidification of vacuoles and endosomes
RRP	Readily releasable pool
SM protein	Sec1/Munc18 protein
SNARE	Soluble N-éthylmaleimide-sensitive-factor Attachment protein Receptor
SNAP-25	Q-SNARE protein synaptosome associated protein 25
t-SNARE	Target SNARE
TeNT	Tetanus neurotoxin
TGF-β	Transforming growth factor beta
TGM	Triple glycosylation mutant
TGN	Trans-Golgi network
TIRF	Dynamic live imaging
TMD	Transmembrane domain
TRACE/ADAM 17	Tumor necrosis factor-alpha converting enzyme
TCSPC	Time-correlated single-photon counting
V-ATPase	Vacuolar ATPases
v-SNARE	Vesicular SNARE
V0	Transmembrane domain of V-ATPase
V1	Peripheral domain of V-ATPase
VACHT	Vesicular acetylcholine transporter
VAMP	Vesicle-associated membrane proteins
VGCC	Voltage-gated calcium channel
VGLUT	Inhibitor of the glutamate vesicular transporter
XMEA	X-linked myopathy with excessive autophagy
XPDS	X-linked Parkinson Disease with Spasticity

List of figures

Table of Contents

Introduction

Chapter 1: The V-ATPase

Chapter 2: Regulated Exocytosis

Results

Introduction

Chapter 1: The V-ATPase

1.1 A short historical point on V-ATPase

The fact that some compartments of the eukaryotic cell are acidic is known since the 60's. The chemo-osmotic theory established that this accumulation of protons on one side of a biological membrane is a source of free energy [*Mitchell, 1961*]. This energy can be used for example by the F-ATPase of the inner membrane of mitochondria to produce ATP or by co-transporters, for the accumulation of solutes against their concentration gradient. However, the molecular aspects of proton transport against their concentration gradient were little known at that time.

It is through pharmacological approaches that different ATPases capable of transporting protons through a lipid membrane against their concentration gradient have been identified. F-ATPase, also known as ATP-synthase or V-complex of the electron transfer chain of mitochondria, is capable of hydrolyzing ATP. However, its main role is to use proton transport through the inner membrane of mitochondria to produce ATP. A second subgroup of H^+-ATPase was revealed by its sensitivity to the phosphatase inhibitor vanadate. These proton pumps were called pH-ATPases and a member of this family is, for example, the H^+/K^+ -ATPase of secretory cells of the stomach.

Finally, a class of vacuolar ATPases has been identified through their sensitivity to Bafilomycin-A [*Bowman et al., 1988*]. They are expressed in all eukaryotic cells and are essential for survival. V-ATPases are present in the membrane of many cellular compartments allowing proton accumulation in their lumen, forming an electrochemical gradient of protons between interior and exterior of acidic organelles.

1.2 Structure and function

The Vacuolar-type H^+-ATPase or V-ATPase is a multi-protein complex that forms a highly conserved evolutionarily enzyme in eukaryotic organisms [*Nelson et al., 2000*]. V-ATPases have remarkably diverse functions as they acidify many intracellular organelles. Indeed, the V-ATPase forms a proton pump that crosses membranes and translocate proton into intracellular organelles after the hydrolysis of ATP.

V-ATPases are found at the membranes of many organelles, such as lysosomes, endosomes and secretory vesicles in different tissues, where they play a variety but important roles for their functions. For example, an H^+/Ca^{2+} antiporter system drives calcium uptake into the vacuole in yeast by the proton gradient across the yeast vacuolar membrane that is generated by V-ATPases [*Ohya et al., 1991*]. In synaptic transmission in neuronal cells, V-ATPase acidifies synaptic vesicles in order to the filling of neurotransmitters [*Wienisch and Klingauf, 2006*]. V-ATPases are also found in the plasma membranes of various cells such as osteoclasts, intercalated cells of the kidney, neutrophils, macrophages, sperm, and certain tumor cells [*Izumi et al., 2003*]. V-ATPases are involved in processes of pH homeostasis, coupled transport, and tumor metastasis. The translocation of protons onto the bone surface produced by V-ATPases in the osteoclast plasma membrane is needed for bone resorption. In the intercalated cells of the kidney, protons are pumped into the urine by V-ATPase, in order to allow bicarbonate reabsorption into the blood. The acidification produced by V-ATPase in the acrosomal membrane of sperm activates proteases that is required for drilling through the plasma membrane of the egg (Figure 1).

As multi-protein complexes, the V-ATPases are constituted by two major domains; a transmembrane domain called V0, directly responsible for the translocation of protons and another domain V1 that hydrolyses ATP, providing the energy needed for proton translocation across membranes (Figure 2). Each of these two domains is actually constituted by the assembly of several different sub-units (Figure 2, Table 1).

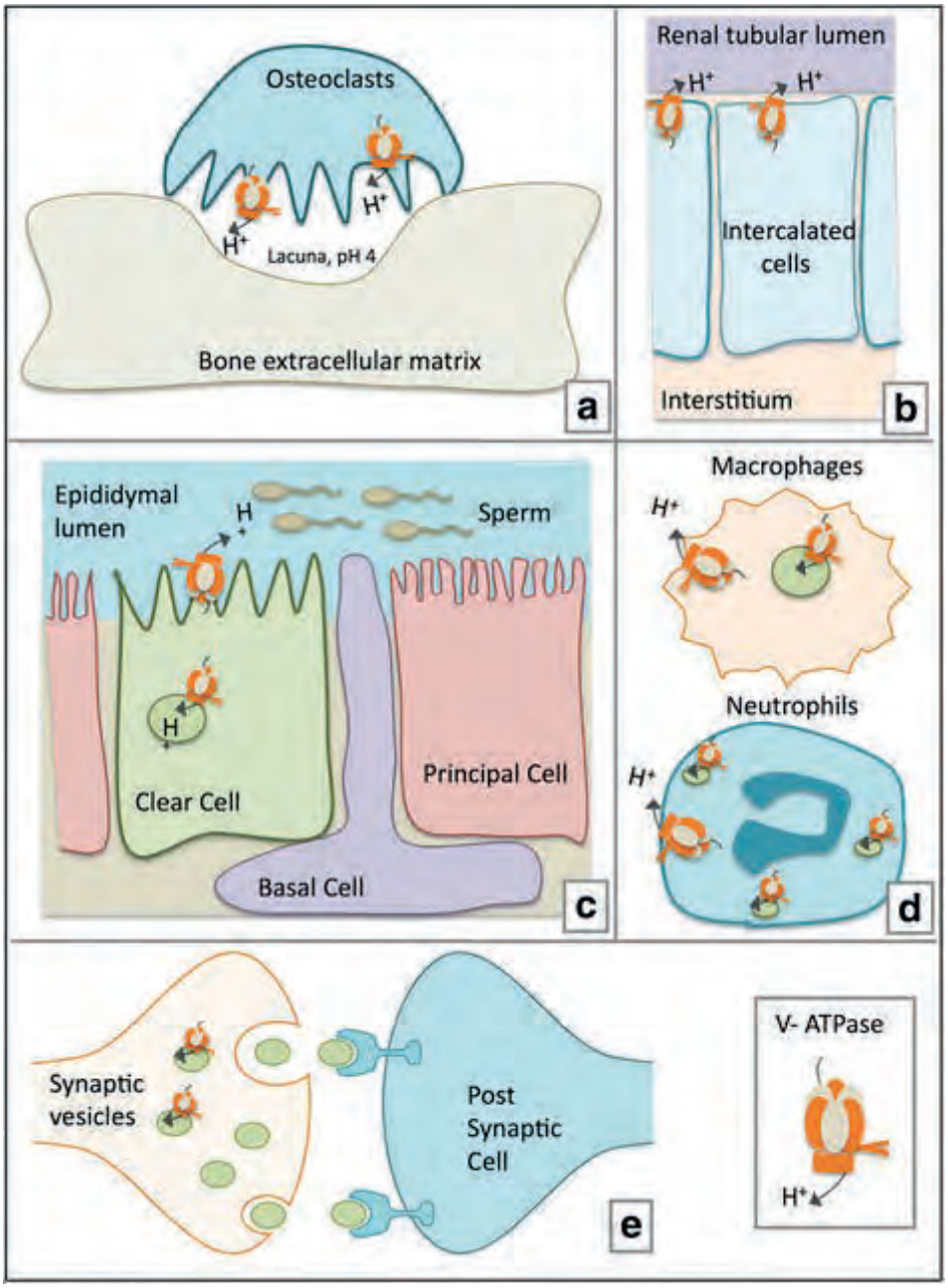

Figure 1: Physiological role of V-ATPase (from *Pamarthy et al., 2018*) a) Bone resorption: V-ATPase located on the plasma membrane of osteoclasts mediates extracellular acidification for bone demineralization during bone resorption. b) Renal function: In the kidney, intercalated cells maintain systemic acidosis and achieve urinary acidification by proton pumping activity of V-ATPases expressed on apical membrane. c) Sperm maturation: In the epididymis, V-ATPase expressing in the clear cells acidify the lumen, a process that is crucial for the proper maturation and motility of spermatozoa. d) Innate immune responses: V-ATPases mediated vesicular acidification has an important role in trafficking and exocytosis of neutrophil granules. V-ATPase is constitutively expressed on the plasma membrane of monocytes and activated lymphocytes and contributes to pH related inflammatory responses. e) Neurotransmission: V-ATPase provides the crucial proton gradient force necessary for the acidification of synaptic vesicles and subsequent accumulation of neurotransmitters. V-ATPase also provides the crucial electrochemical potential necessary for accumulation of neurotransmitters during the replenishment of recycling secretory synaptic vesicles after fusion.

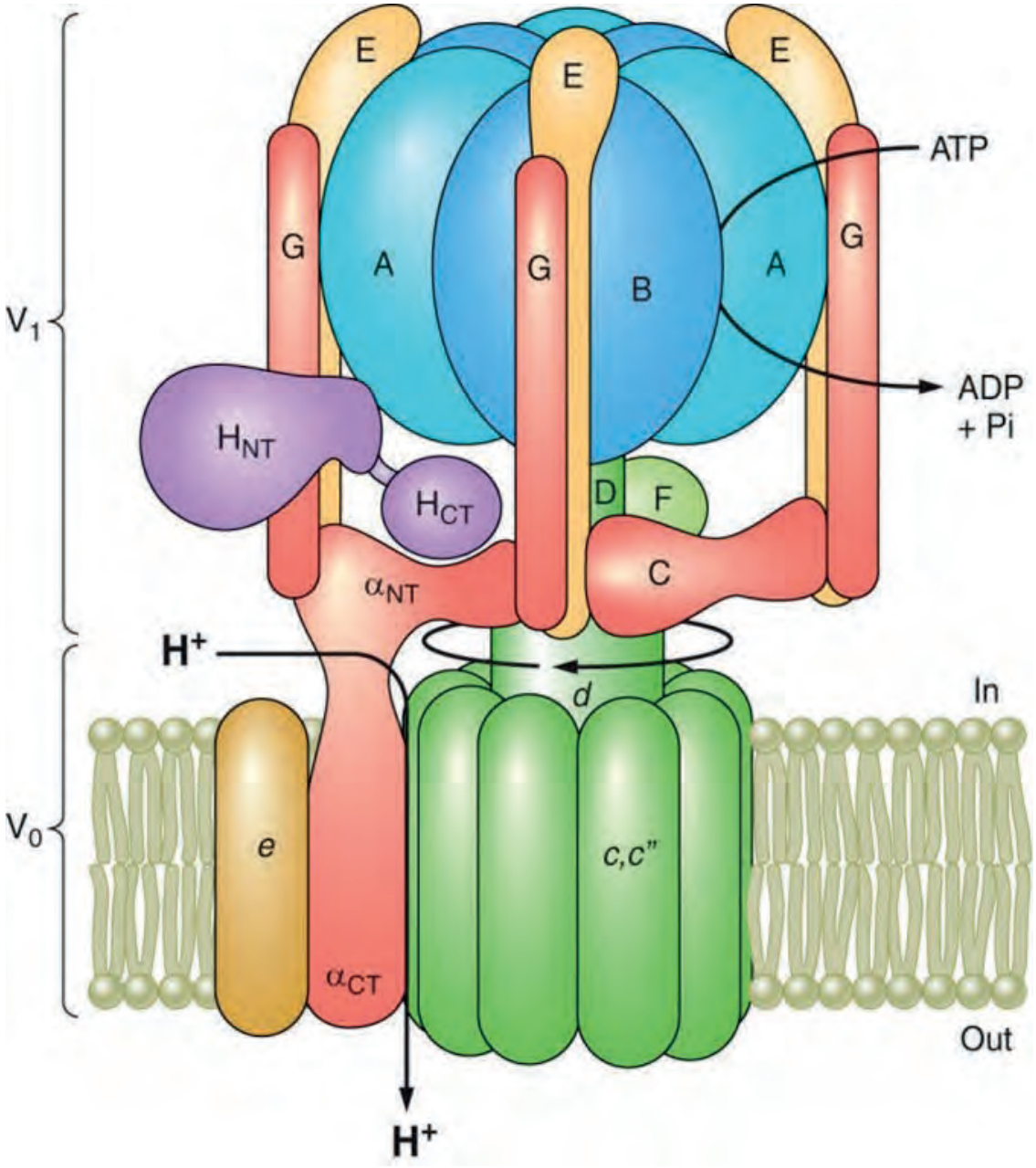

Figure 2: Structure and function of the V-ATPase complex (from *Stransky et al. 2016*). The V-ATPase is composed of a peripheral V1 domain that hydrolyzes ATP and an integral V0 domain that translocates protons. ATP hydrolysis occurs at nucleotide binding sites located at the interface of the A and B subunits and drives rotation of a central rotary complex composed of subunits D and F of V1 and subunit d and the ring of proteolipid subunits (c and c") of V0 relative to the remainder of the complex. Rotation of the proteolipid ring relative to subunit a drives unidirectional proton transport from the cytoplasm to the lumen (see text for details). The A3B3 catalytic head is held fixed relative to subunit a by peripheral stalks composed of three EG heterodimers that connect to subunits C and H and the NH2-terminal cytoplasmic domain of subunit a.

Table 1: Characteristics of V-ATPase subunits (adapted from *Masashi et al. 2011*)

Subunit	**Mammalian Isoforms**		**Subunit function**
V1 domain	**Tissue / cell type**	**Alternative splicing**	
A			ATP hydrolytic site, regulation via non-homologous domain,
B	B1 (renal, epididymis, olfactory epithelium); B2 (ubiquitous)		Non-catalytic ATP site, binds actin and aldolase,
C	C1 (ubiquitous); C2 (lung, renal, epididymis)	C2a (lung) C2b (renal)	Regulatory, stator subunit, binds actin
D			Rotary subunit
E	E1 (testis, olfactory epithelium); E2 (ubiquitous)		Stator subunit, binds RAVE and aldolase
F			Rotary subunit
G	G1 (ubiquitous); G2 (neural); G3 (renal, epididymis)		Stator subunit, binds RAVE
H		SFD-α, SFD-β	Regulatory, stator subunit, binds NEF
V0 domain	**Tissue / cell type**	**Alternative splicing**	
a	a1 (neural); a2 (endothelial, neurons); a3 (osteoclasts, pancreatic β-cells, premature melanosomes); a4 (renal, epididymis)	a1-I (brain, neurons), a1-II (ubiquitous), a1-III (ubiquitous), a1-IV (neurons), a3-I (ubiquitous), a3-II (ubiquitous), a3-III (heart, lung), a4-I (kidney, heart, lung, skeletal muscle, testis), a4-II (kidney, lung, liver, testis)	H^+ transport, targeting, binds aldolase, stator subunit
d	d1 (ubiquitous) d2 (renal, epididymis, osteoclast, dendritic cells)		Coupling, rotary subunit
e			Unknown
c			H^+ transport, rotary subunit
c′	No mammalian gene		H^+ transport, binds Vma21 assembly factor, rotary subunit
c″			H^+ transport, rotary subunit
Ac45	Ac45 Ac45LP (*Xenopus*)		unknown

1.2.1 V0 domain

1.2.1.1 The a subunit

In yeast, all the V-ATPase subunits are encoded by single genes but the a subunit is encoded by two genes (VPH1 and STV1) [*Manolson et al., 1994*]. In mammalian cells the a subunit has four isoforms (a1, a2, a3, and a4) and in humans, the four isoforms display 47-61% identity at the amino acid level [*Wagner et al., 2004*].

The a1 and a2 isoforms are mostly found in cells originating from the neuronal crest and displaying neurosecretory activity with a1 isoform found in both presynaptic membranes and synaptic vesicles [*Morel et al., 2003*]. V-ATPase complexes containing a1 acidify synaptic vesicles, but the early discovery of the presence of a1 in both synaptic vesicle and synaptic plasma membrane, has long suggested that V0 may also play a more direct role in membrane fusion during neurotransmitter release [*Hiesinger et al., 2005*]. Accordingly, the a1 subunit is also implicated in fusion between phagosomes and lysosomes during phagocytosis in the brain [*Peri and Nüsslein-Volhard, 2008*], suggesting that a1 may play a role in the endocytic pathway.

The a2 isoform also expresses in apical endosomes of proximal tubule cells of the kidney to provide a low pH necessary, in order to release endocytosed peptides from the receptors megalin and cubulin that are involved in their absorptive uptake from the renal fluid [*Hurtado-Lorenzo et al., 2006*].

The a3 isoform is heavily expressed in osteoclasts where it is involved in bone resorption [*Toyomura et al., 2003*]. It has also been found on insulin-containing secretory vesicles in pancreatic islet cells in order to contributes the acidic environment which is required for proteolytic processing of insulin. Interestingly, a3 gene knock-out in mice, does not impair insulin process but alters insulin secretion [*Sun-Wada et al., 2006*]. Another study suggests that the a2 isoform can replace a3 for

acidification of insulin-containing compartments but that a2 is unable to replace the role of a3 for insulin secretion [*Sun-Wada et al., 2007*].

The a4 isoform is expressed almost exclusively in renal cells [*Wagner et al., 2004*]. Dysfunction of a4 induces defective urinary acid secretion associated with renal tubular acidosis [*Smith et al., 2000*]. Interestingly, a4 is also fund in epididymal clear cells, required for acidification of the epididymal lumen [*Pietrement et al., 2006*]. There exist two types of the mouse a4 subunit, a4-I and a4-II, which show distinct tissue and developmental expression patterns. The a4-I expresses strongly in kidney and is detected in skeletal muscle, heart, lung and testis. The a4-II is detected in liver, lung and testis. During development, a4-I expression begins with the early embryonic stage, and a4-II is expressed from day 17 [*Kawasaki-Nishi et al., 2007*]. The a3 and a4 isoforms were also shown to be involved in tumor cells development. MB231, a highly invasive human breast tumor cell line, expresses much more of both a3 and a4 isoforms than MCF7, a poorly invasive cell line, and the knock-down of a3 and a4 gene can inhibit the invasiveness of MB231 cells [*Hinton et al., 2009*].

1.2.1.2 The c, c' and c" subunits

The c subunit of the Vo sub-domain forms the main transmembrane subunit of the V-ATPase. Three isoforms (c, c′ and c′′) form what is called the proteolipid domain of the V-ATPase that is part of the proton-conducting pore, each containing a buried glutamic acid residue that is essential for proton transport, and together they form a hexametric ring spanning the membrane [*Inoue and Forgac, 2005; Jones et al., 2003*]. The c-subunit has also been shown as a critical component of the mitochondrial permeability transition pore [*Bonora et al., 2013*].

1.2.1.3 The d subunit

There are two isoforms of d (d1 and d2) that are both non-integral necessary membrane component of V0 domain [*Toei et al., 2010*]. In human and mouse, d1 is expressed ubiquitously whereas d2 is expressed in osteoclasts in addition to kidney and epididymis [*Smith et al., 2002; Sun-Wada et al., 2003; Smith et al., 2005*]. Due to defects of multinucleated osteoclasts, d2 knockout mice may develop osteopetrosis [*Lee et al., 2006*], suggesting that the d2 could play a specific role in osteoclast fusion. Both d1 and d2 have been demonstrated to directly associate with subunits D and F of the central stalk, suggesting that the d subunit could be part of the central rotor [*Smith et al., 2008*].

1.2.1.4 The e subunit

The e subunit is a membrane sector-associated protein of V –ATPase. Although it was identified in the 1990s [*Ludwig et al., 1998*], almost nothing is known about its function up to now.

1.2.2 The V1 sub domain

The V1 domain is made from eight different subunits (A-H) and its most appreciated function is the hydrolyzation of ATP [*Forgac, 2007; Kane,2006*]. The sites of ATP hydrolysis are located at the interface of A and B subunits [*Liu et al., 1996; Liu et al., 1997*]. The V1 and V0 domains associate by multiple stalks: a central stalk that is made by subunits D, F and d and three peripheral stalks constituted by subunits C, E, G and H [*Zhang et al., 2008*] (Figure 1).

1.2.2.1 The A and B subunits

In each V-ATPase, three copies of A and B form the site for ATP hydrolysis. Two isoform of subunit B have been identified. B1 isoform is expressed in renal cells, epididymal cells and hair cells of the inner ear [*Karet et al., 1999*]. Mutations of B1 have been shown to lead to renal tubular acidosis deafness. In contrast, B2 is expressed in all cells and predominantly localize at intracellular compartments, suggesting that B1 and B2 may have different functions [*Paunescu et al., 2004*]. However, some studies revealed that B2 can at least compensate some functional consequences in B1 knock out mice [*Da Silva et al., 2007; Brown et al., 2009*]. In the mouse olfactory epithelium, B1 localizes to the apical membrane and subapical region of olfactory cells while B2 is cytoplasmic. Once B1 is knocked-out, B2 expression is upregulated but B2 cannot be found in the apical membrane [*Paunescu et al., 2008*].

1.2.2.2 The C subunit

As a part of V1 domain, subunit C localizes at the interface between V0 and V1 domain and plays an essential role in the assembly of V-ATPase as a flexible stator that connects V0 and V1 domain together [*Dorey et al., 2004*]. The structure of V1C reveals two slightly twined, long α-helices that provide flexibility and enable movement of the 'head' in relation to the 'foot' domain. Indeed, the structure that was solved from the sitting-drop crystals shows a remarkable movement of the 'head' domain in relation to the 'foot' domain (Figure 3 A, B). Whereas minor structural changes were detected in the 'foot' domain, most of the structural changes took place in the middle of the 'neck' and in the 'head' domains. The free movement of about 12° to both sides may provide the flexibility required for the smooth operation of the ATP-dependent proton transport by V-ATPase [*Drory et al., 2004*]. Also, subunit C was shown to have the property of actin binding in mammalian and insect V-ATPases, respectively [*Holliday et al, 2000; Vitavska et al, 2003*].

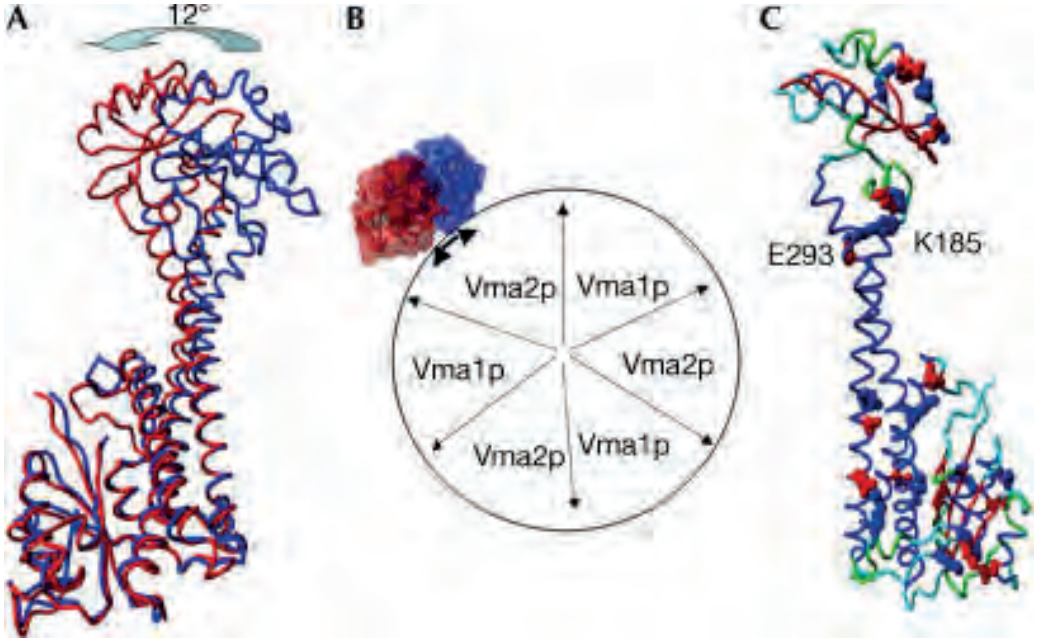

Figure 3: Elasticity of Vma5p (from *Dory et al., 2004*). A) Superposition of the two conformations of Vma5p. The movement of the 'head' is indicated. A 1.75 AÅstructure is in red and a 2.9 AÅstructure in blue. B) Top view of possible interaction between the catalytic sector (modeled as F-ATPase) with subunit C in the two conformations. C) Salt bridges in the high-resolution structure of Vma5p. The protein is colored according to the secondary structures. Blue, α-helix; red, βsheet; green, turns; cyan, loops. Negatively charged amino acids are in red, and positively charged in blue. The only salt bridge that connects the two long α-helices is indicated.

1.2.2.3 The D and F subunits

The subunits D and F form the central rotor axle of V1 domain [*Kitagawa et al., 2008*]. The central stalk formed by D and F subunits bridges and stabilizes V1/ V0 interaction and thus the formation of the holocomplex of V-ATPase. This stalks also couples the energy released from A3B3 to proton translocation in V0 [*Tomashek et al., 1997a*]. Additionally the F subunit interacts with both the V0 sector and other subunits of the V1 sector and is thus crucial in coupling ATP hydrolysis with rotation [*Tomashek et al., 1997b*].

1.2.2.4 The E and G subunits

As for A and B subunits, three copies of E and G subunits are needed for the assembly of a functional V1 domain of V-ATPase. These subunits are important for the assemblage of V-ATPase and its activity as the rotary motor V1 is stabilized by three peripheral stalks constituted by three E-G heterodimers that connect the N-terminal domain of a subunit of the V0 sub-domain (V0a) to the A3B3 hexamer via subunits H and C [*Zhao et al., 2015*].

1.2.2.5 The H subunit

The H subunit plays an important role in the regulation of V-ATPase since it is located at the interface of V1 and V0. H subunit is needed for the ATPase activity in holo-V-ATPase and also for stabilizing the Mg-ADP-inhibited state in membrane-detached V1. The deletion of the N-terminal region of H subunit abolishes ATPase activity while proton-pumping activity requires the C-terminal part of H subunits [*Ho et al., 1993; Maxfield and McGraw, 2004*].

1.3 V-ATPase and organelle function

V-ATPase is present in many intracellular organelles such as lysosome, endosome, autophagosome, Golgi and secretory vesicles, where it plays one or several roles for the normal function of these organelles.

Lysosomes constitute the main catabolic compartments of eukaryotic cells and play a key role in the degradation of the extracellular matrix (ECM) [*Saftig and Klumperman, 2009*]. V-ATPase is required for the function of lysosomes as it is responsible for the acidification of lysosome [*Saftig and Klumperman, 2009*]. But is also

important to note that V-ATPase contributes to lysosomal trafficking. Indeed, the lysosomal maturation could be inhibited at an early endosomal stage in presence of V-ATPase inhibitors (Figure 4) [*Mindell, 2012; Hurtado-Lorenzo et al., 2006*].

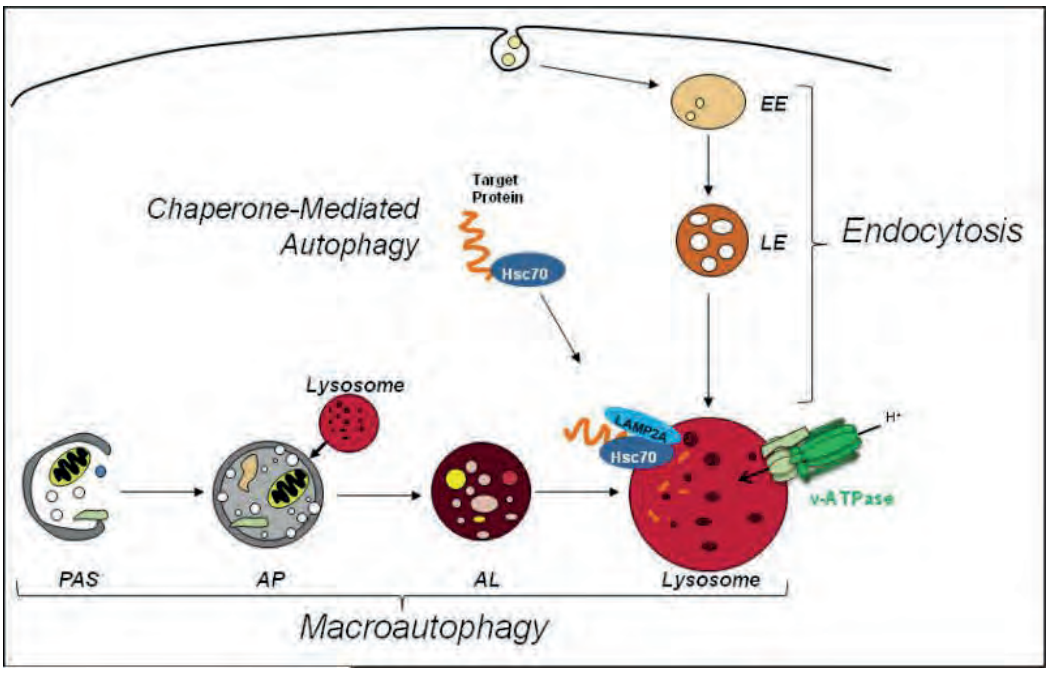

Figure 4: The Lysosomal System (from *Colacurcio and Nixon, 2016*). The lysosomal system refers to the autophagic pathway and the endocytic pathway, and mediates the transport and proteolytic degradation of cellular waste. In the endocytic pathway, early endosomes (EE) mature into late endosomes (LE) prior to full acidification (Lysosome). In the autophagic (macroautophagy) pathway, a preautophagosomal structure (PAS) is formed, enveloping an area of cytoplasm or a selected substrate, before developing into a double-membrane autophagosome (AP). Lysosomes fuse with autophagosomes, generating single-membrane autolysosomes (AL), and ultimately lysosomes. Upon fusion with autophagosomes, lysosomes introduce proteolytic enzymes to carry out the degradation of substrates as the compartment becomes more acidic. The acidification of these compartments is mediated by the V-ATPase. Chaperone-mediated autophagy (CMA) is another type of autophagy, during which a chaperone protein complex (Hsc70 complex) recognizes a cytoplasmic target protein via a KFERQ motif, and shuttles the target protein to the lysosomal lumen for digestion via interaction with the LAMP2 protein complex, which serves as the lysosomal CMA receptor [*Nixon, 2013; Colacurcio and Nixon, 2016*].

V-ATPase activity is also required for neurotransmitter fill-in of synaptic vesicles in neurons and secretory granules in neuroendocrine cells. As a proton pump, V-ATPase translocates proton from cytoplasm across vesicle membrane to acidify the vesicles. Subsequently different neurotransmitters are loaded into the vesicles by different transporters that use this electrochemical gradient (proton gradient) [Sandoval et al., 2006]. In consequence, V-ATPase activity was shown to be primordial for transmitter loading in secretory and synaptic vesicles. Of note this activity is operating both after vesicles biogenesis from the Golgi apparatus but also after the recycling of the constituents of synaptic and secretory vesicles by compensatory endocytosis following fusion with the plasma membrane.

1.4 Regulation of V-ATPase activity

Cells can temporally regulate pH in different cell compartments, such as the endocytic pathway and the secretary vesicle production. The luminal pH decreases from early endosomes through late endosomes to lysosomes [*Forgac, 2007*], which is essential for the regulation in the endocytic process [*Maxfield and McGraw, 2004*]. Similarly, the trans-Golgi network is less acidic than late endosomes, the pH of other Golgi compartments is higher than in late endosome [*Kim et al., 1996*]. In addition, the translocation of proton across the plasma membrane without changing pH is also sometimes needed by cells. In conclusion, since different proton transports produced by V-ATPase are necessary for various cell functions, the regulation mechanism of V-ATPase activity must be diverse.

1.4.1 Regulation of V-ATPase by reversible disulfide formation

The first identified mechanism for regulating V-ATPase activity is the reversible disulfide bond between conserved cysteine residues at the catalytic site of the V-ATPase

[*Feng and Forgac,1992; Feng and Forgac,1994*]. The V-ATPase activity is reversibly inhibited by a disulfide bond formed between a highly conserved cysteine of the catalytic A subunit and a second highly conserved cysteine residue located in the C-terminal domain of the same subunit.

1.4.2 Regulation of V-ATPase by modification of density

V-ATPase activity is also controlled by pump density. Particularly this is important for V-ATPase-dependent proton transport occurring across the plasma membrane of epithelial cells. Both in renal alpha intercalated cells and epididymal clear cells, the proton translocation across the apical membrane is controlled by reversible fusion with the apical membrane of intracellular vesicles with a high density of V-ATPases [*Pietrement et al., 2006*].

1.4.3 Regulation of V-ATPase by reversible disulfide formation

Another important mechanism of controlling V-ATPase activity is the reversible dissociation of the complex between V1 and V0 domains (Figure 4), which was first defined in yeast and insect cells [*Kane, 2006; Beyenbach and Wieczorek, 2006*] and is also present in mammalian cells. V-ATPase dissociation in yeast responds to glucose depletion from the media and its assembly in renal cells is thus directly responsive to glucose levels [*Sautin et al, 2005*]. The acidification of lysosome is necessary for normal antigen processing and an increase of assembly of V-ATPase has been detected when dendritic cells are active to process antigen [*Trombetta et al., 2003*], and it is likely that reversible dissociation will be shown to control V-ATPase activity in others cell process (Figure 5).

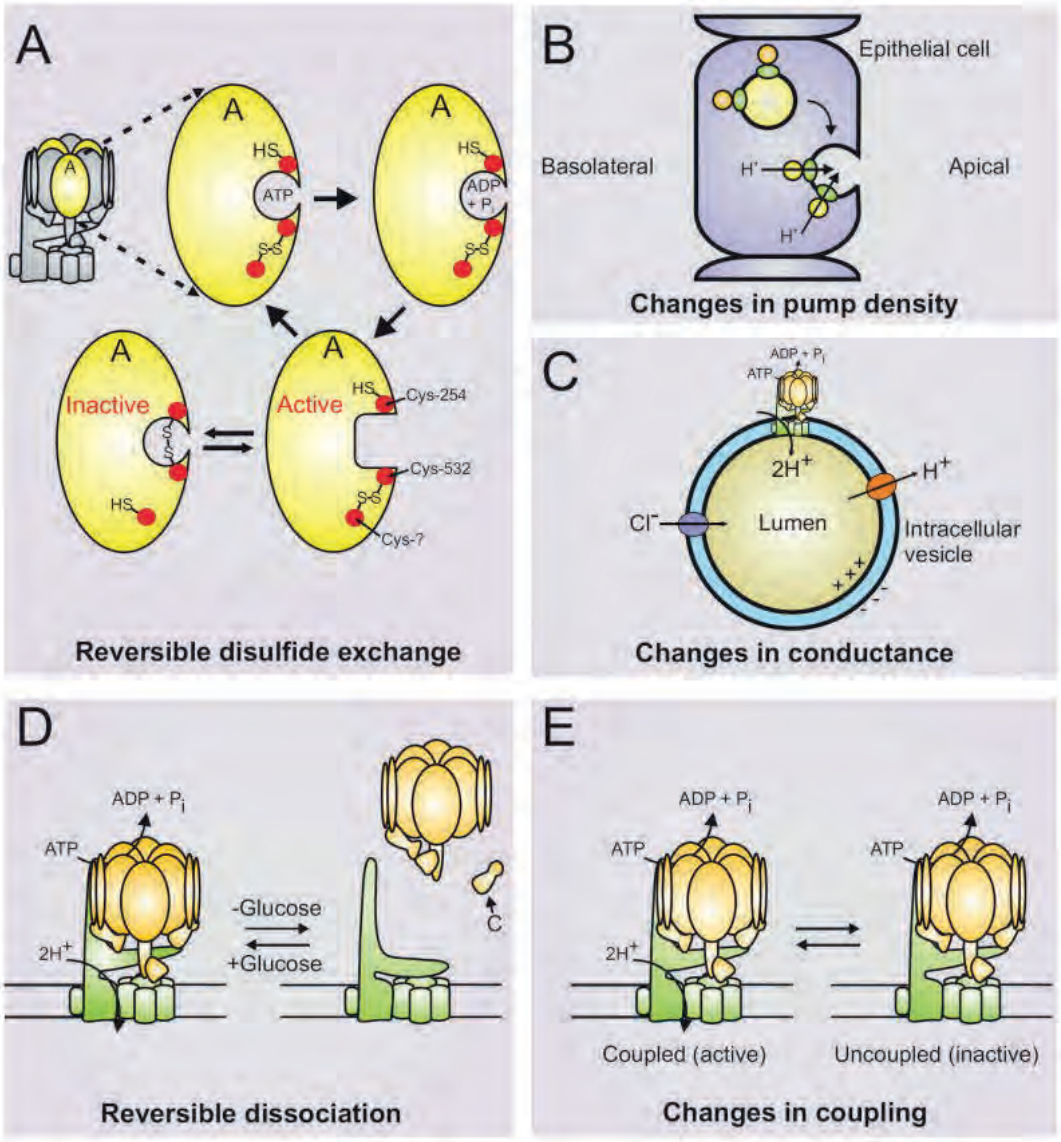

Figure 5: Regulation of the V-ATPase (*Daniel et al. 2008*). V-ATPases are regulated by a number of different mechanisms including: A, reversible disulfide bond formation between conserved cysteine residues that prevent the catalytic site from cycling between the open and closed conformations required by the binding change mechanism; B, changes in pump density through fusion of vesicles containing a high number of V-ATPase; C, changes in either Cl^- or H^+ conductance through distinct channels; D, reversible dissociation into inactive V1 and V0 domains; and E, changes in coupling efficiency.

In yeast the dissociation is fast, reversible and does not need new protein synthesis [*Kane, 1995; Parra and Kane, 1998; Qi and Forgac, 2007*]. The ATP hydrolysis and passive proton translocation are inhibited following the dissociation of V1 and V0

domain, to prevent deleterious effects of releasing an uncoupled ATP hydrolytic domain into the cytosol or an uncontrollable passive proton translocation. ATP hydrolysis at V1 can be inhibited by a conformational change [*Diab et al., 2009*], subunit H [*Parra et al., 2000*], or by bridging of peripheral and central stalks [Jefferies and Forgac, 2008]. Dissociation and association use different mechanism to be controlled. Thus dissociation needs an intact microtubular network [*Xu and Forgac, 2001*], whereas association needs the protein RAVE (regulator of acidification of vacuoles and endosomes) [*Seol et al., 2001*], which is a complex of three proteins (Rav1p, Rav2p and Skp1) that was shown to bind to subunits V1C, V1E and V1G [*Smardon et al., 2002; Smardon and Kane, 2007*]. In both glucose-regulated process and normal biosynthetic pathway, the dissociated V1 domain could be stabilized by RAVE [*Smardon et al., 2002*].

In yeast, the glucose-dependent association of V1 and V0 domain is activated by the Ras/cAMP/protein kinase A pathway [*Bond and Forgac, 2008*]. The Ras GAPs Ira1p and Ira2p are inhibited by raising glucose levels, leading to an increase of GTP-bound Ras and Ras levels, which activates adenylate cyclase resulting in a raising cellular cAMP level. Hence the catalytic subunits of kinase A are activated by dissociation of its regulatory subunits caused by high cAMP level. In insect cells, kinase A has been demonstrated to promote assembly of the V-ATPase and then to phosphorylate subunit V1C, which is otherwise not phosphorylated in V-ATPase [*Voss et al., 2007*]. In renal epithelial cells, glucose-dependent association has been shown to be regulated by phosphatidylinositol 3-kinase (PI-3 kinase) [*Sautin et al., 2005*], and may also be regulated by other signaling pathways.

There is a “non-homologous” region at the catalytic V1A subunit, which is important for the reversible association/dissociation of V-ATPase and this region is highly conserved in different species [*Wilkens et al., 1999*]. Mutations in this region have been shown to potentially prevent the glucose-dependent dissociation of V-ATPase without affecting catalytic activity [*Shao et al., 2003*]. Moreover, a binding of the non-homologous region (using a separate epitope-tagged construct) to V0 has been

detected in a glucose-dependent manner in case of absence of other subunits of V1 domain [*Shao and Forgac, 2004*]. This means that interaction between the non-homologous region of V1A and V0 domain, probably the N-terminal domain of subunit V0a, may regulate the association/dissociation of V-ATPase.

Reversible dissociation of the V-ATPase is also sensitive to the cellular environment. V-ATPases containing Stv1p, which is localized to the Golgi apparatus and does not dissociate, can dissociate if this type of V-ATPase is re-located to the vacuole by directed overexpression [*Kawasaki-Nishi et al., 2001*]. Although the environmental factor(s) responsible for this phenomenon has not been identified, it has been shown that luminal pH affects dissociation of V-ATPase [*Shao and Forgac, 2004*].

1.4.4 Other regulatory mechanisms of V-ATPase activity.

Change in chlorine or proton conductance of specific channels may also lead to the regulation of the pumping activity of V-ATPase by indirectly affecting charge gradient in organelles. Finally, the coupling efficiency of the V-ATPase switch from active to inactive form can also modulated leading modulation of pumping activity.

1.5 Genetic diseases related to the V-ATPase

Since V-ATPase is involved in many basic cellular functions, defaults of V-ATPase could in theory result in many diseases. Accordingly, genetic disease such as osteopetrosis, distal renal tubular acidosis, X-linked myopathy with excessive autophagy (XMEA) and Cutis laxa autosomal recessive type II have been attributed to mutations in genes encoding V-ATPase subunits or regulators (Figure 6).

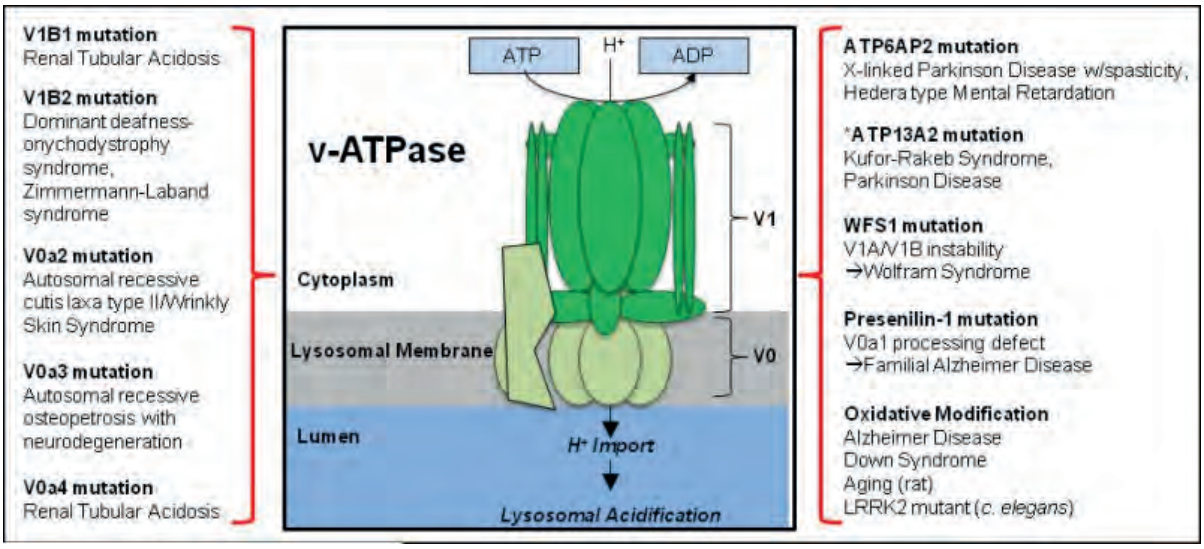

Figure 6: V-ATPase defects and associated neurodegenerative diseases (from *Colacurcio et al. 2016*). Shown in the left column are disease-associated mutations in the genes encoding for individual V-ATPase subunits (bold). Shown in the right column are changes in V-ATPase-related proteins (bold) and corresponding neurodegenerative diseases. *ATP13A2, while not directly linked to V-ATPase function, is shown due to its suspected role in lysosomal acidification and its implication in both Kufor-Rakeb Syndrome and Parkinson Disease.

1.5.1 Osteopetrosis

Osteopetrosis is an extremely rare inherited disorder whereby the bones harden, becoming denser. Osteopetrosis can cause bones to dissolve and break [*Lam et al., 2007*]. Default in one of at least ten genes can lead to various types of osteopetrosis. For example, mutations in the CLCN7 gene cause about 10-15% of cases of autosomal recessive osteopetrosis, most cases of autosomal dominant osteopetrosis and all known cases of intermediate autosomal osteopetrosis. More importantly, mutations in the TCIRG1 gene (V0a3) cause about 50% of cases of autosomal recessive osteopetrosis [*Stark and Savarirayan, 2009; Sobacchi et al., 2001*].

The V0a3 isoform is highly expressed in osteoclasts and the V-ATPase containing

V0a3 locate at plasma membrane of these cells, where it is involved in bone resorbtion. Osteoclasts use V-ATPase to acidify extracellular compartment between the bone surface and the ruffled border membrane [*Kornak et al., 2000; Baron et al., 1985*]. The low pH is required for both optimal function of proteases that degrade the organic bone matrix and dissolving inorganic bone material [*Blair, 1998*]. In pre-osteoclast cells, V0a3 is localized to lysosomes and is likely re-directed to the plasma membrane when these cells differentiate into mature osteoclasts [*Sobacchi et al., 2001; Baron et al., 1985*].

1.5.2 Autosomal recessive cutis laxa (ARCL) type II

ARCL is a genetic disease with three phenotypes [*Morava et al., 2009*]. ARCL type I is a fatal form occurring at an early age that leads to cardiopulmonary complications. ARCL type II is a spectrum of connective tissue disorders characterized by the association of wrinkled, redundant and sagging inelastic skin with growth and developmental delay, and skeletal anomalies. ARCL Type III, also known as De Barsy syndrome, has a progeroid appearance with corneal clouding and athetoid movements. Patients with ARCL type II can be divided in two major groups – children with ARCL type II associated without the presence of metabolic disorder and with a combined N- and O-linked glycosylation defect. So far, mutations on both alleles of V0a2 gene have been detected in all ARCL II cases with combined glycosylation defect [*Kornak et al., 2008; Rajab et al., 2008*].

1.5.3 Distal renal tubular acidosis (dRTA)

Distal RTA is the classical form of RTA and characterized by a failure of acid secretion by the alpha intercalated cells of the cortical collecting duct of the distal nephron, resulting in an inability to acidify urine to a pH bellow 5.3 [*Batlle and Haque, 2012*]. About 90%

secretion of protons over the apical membrane produce by Na^+-H^+ exchanger isoform 3 (NHE3) that exchanges sodium for protons over the apical membrane and the remaining 10% of protons secretion is carried out by V-ATPase present in the distal tubule. Mutations of V1B and V0a4 are usually responsible for patients with autosomal recessive dRTA [*Batlle and Haque, 2012*]. Indeed 12 different mutations of V1B1 and 24 different mutations of V0a4 have been shown to lead to dRTA [*Karet et al., 1999; Stover et al., 2002*]. In some case dRTA caused by V0a4 mutations could also be associated with deafness produced by anomal acidification at the endolymph of the inner ear [*Stehberger et al., 2003*].

1.5.4 X-linked myopathy with excessive autophagy (XMEA)

XMEA is a rare childhood onset disease characterized by slow progressive vacuolation and atrophy of skeletal muscle. It is a myopathy with onset of slowly progressive proximal weakness and elevated serum creatine kinase in the first decade of age. Mutations in the vacuolar ATPase assembly integral membrane protein (VMA21) gene, have be shown to increase lysosomal pH, thereby reducing degradative ability of lysosomes by reducing lysosomal hydrolase activity and ultimately inhibiting autophagy. The VMA21 protein actually regulates the assembly of V0 domain of V-ATPase required to acidify the lysosome. To summarize increased lysosomal pH and poor degradation of cellular debris resulting from VMA21 mutation may secondarily stimulate autophagy and lead to accumulation of autophagolysosomes with sarcolemmal features [*Dowling et al., 2015*].

1.6 Autophagy and V-ATPase: Aging and neurodegenerative disease

Autophagy and endocytosis deliver useless cellular materials to lysosomes for

degradation, which is needed for various pathways of nutrient homeostasis and intracellular metabolism. The low range of intraluminal pH produced by V-ATPase is important for these pathways. V-ATPase activity and lysosomal pH dysregulation are involved in cellular aging, longevity and adult-onset neurodegenerative diseases, including Parkinson Disease and Alzheimer Disease. More and more genetic defects of V-ATPase subunits or proteins related with V-ATPase have been found in familial neurodegenerative diseases [*Colacurcio and Nixon, 2016*].

Mutations in the brain-specific subunit V1B of V-ATPase are found in two very rare genetic disorders, dominant deafness-onychodystrophy syndrome and Zimmermann-Laband syndrome [*Kortum et al., 2015*]. Mutations of accessory proteins required for v-ATPase function also induce severe congenital disorders associated with neurodegeneration. X-linked Parkinson Disease with Spasticity (XPDS) is an extremely rare progressive Parkinsonism with a disease onset varying between age of 14 and 58 years old [*Poorkaj et al., 2010*]. It was shown that a point mutation in the ATP6AP2 gene induces altered splicing of ATP6AP2 in XPDS [*Korvatska et al., 2013*]. ATP6AP2 is a V-ATPase-interacting protein essential for V-ATPase assembly, specifically for the assembly of the V0 domain [*Korvatska et al., 2013; Malkus et al., 2004*]. Ablation of ATP6AP2 in cells reduces expression of several V0 subunits, impairs V-ATPase function, de-acidifies intracellular compartments and increases the amount of autophagic vacuoles [*Kinouchi et al., 2011; Kinouchi et al., 2013*]. This mutation is also involved in another neurological condition, the X-linked Mental Retardation Hedera type (MRXSH), a congenital form of mental retardation with epilepsy and sometimes ataxia [*Hedera et al., 2002*].

V-ATPase involvement was long time ago shown in the early onset neurodegenerative disease: the childhood disorder Wolfram syndrome [*Venzano et al., 1980*], an autosomal-recessive neurodegenerative disease related with broad sensory, autonomic nervous system deficits and childhood-onset diabetes mellitus, which is often fatal [*Rigoli and Di Bella, 2012*]. It also induces brain stem atrophy, optic atrophy,

seizures and peripheral neuropathy [*Genis et al., 1997; Urano, 2016*]. Wolfram Syndrome is caused by mutations in WFS1 gene, which encodes a nine-pass transmembrane protein of the endoplasmic reticulum (ER) membrane [*Inoue et al., 1998; Strom et al., 1998*]. Although WFS1 is not involved directly in lysosomal acidification, it is needed to stabilize the V1A subunit. This process occurs via interaction between the cytosolic N-terminus of WFS1 and cytosolic V1A subunits, which prevents the degradation of V1A subunits through an unknown proteasome-independent mechanism [*Gharanei et al., 2013*].

Alzheimer Disease (AD) is the most prevalent neurodegenerative disease in old age but in about 5% of all cases, an "early onset" form of familial AD induced by mutations of Presenilin-1 (PS1), Presenilin-2 (PS2), or amyloid precursor protein (APP) genes have been described. In the most common form of early-onset AD, mutations of Presenilin-1 prevent proteolysis and lysosomal acidification. PS1 holoprotein is a specific ligand of V0a1, required for proper N-glycosylation, stability, and targeting to lysosomes [*Lee et al., 2010; Wolfe et al., 2013*]. Cells from AD patients with PS1 mutations exhibit defective V0a1 maturation and increased lysosomal pH. Cells lacking PS1 or both PS1 and PS2 show even greater elevations of lysosomal pH and AD-like autophagic vacuole pathology. Lysosomes isolated from PS1-KO cells have just about 30% of V0a1 subunit compared with wild type cells [*Wolfe et al., 2013*].

1.7 V-ATPase and regulation of signaling pathways

The signaling pathways to be associated with V-ATPase namely Notch, Wnt and TGF-β, have similar expression patterns and cellular functions during both development and disease. However, there are other steps of the signaling pathways known to be pH dependent, which warrant future investigation. Maturation of Notch and TGF-β by glycosylation in Trans Golgi Network (TGN) activates their signaling pathways. Further *a*1 and *a*2 subunits of V-ATPase are important for the protein glycosylation that

is a key role of the TGM (triple glycosylation mutant) [*Marshansky and Futai, 2008*]. We and others have shown that surface expression of V-ATPase modulates MMPs thereby leading the proliferation of cancer cells [*Fan et al., 2015; Kulshrestha et al., 2015*]. However, V-ATPase dependent activity of TRACE/ADAM 17 has not been explored and might hold important clues for V-ATPase and signaling crosstalk mechanism. Furthermore, enzymes like γ-secretase that activate signaling pathway mediators are efficient at acidic pH [*Pasternak et al., 2003*]. Similarly, the involvement of V-ATPase in activation of acid proteases during lysosomal degradation to regulate signal turnover cannot be ignored [*Kissing et al., 2017*] (Figure 7). V-ATPase could have profound effects on cell fate by influencing signaling molecules that depend on pH. The research on V-ATPase regulation of signaling pathways is a field waiting to be explored that will have a tremendous impact in physiology and pathology.

1.8 V-ATPase and cancer

Induction of apoptosis by V-ATPase inhibition has been reported in many tumor types [*Stransky et al., 2016*]. As V-ATPases play essential roles in fundamental cellular processes (Figure 7), it is not surprising that inhibition of V-ATPase activity is fatal to cells. However, cancer cells are particularly reliant on the V-ATPase for survival but more sensitive to V-ATPase inhibition than normal cells [*Damaghi et al., 2013*].

V-ATPase was found on the plasma membrane of invasive breast cancer cells and participates in control of cytoplasmic pH [*Sennoune et al., 2004*]. The V-ATPase has since been found located on the plasma membranes in many different invasive cancer cells, including melanoma, breast, Ewing sarcoma, lung, liver, esophageal, prostate, ovarian, and pancreatic cancers [*Damaghi et al., 2013*]. Moreover, particular V-ATPase subunits have been found to be overexpressed in both human cancer cell lines and human tumor samples. For instance, V1C is overexpressed in oral squamous cell carcinoma samples [*García-García et al., 2012*], and V0c is overexpressed in human

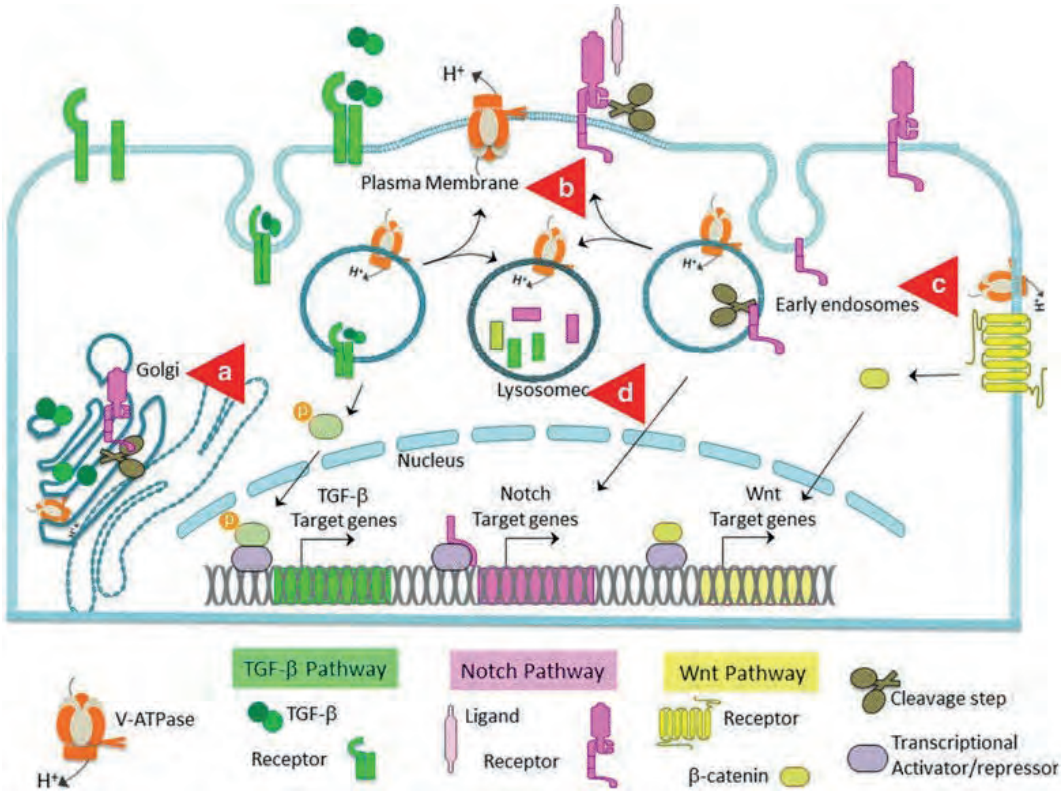

Figure 7: V-ATPase and cellular signaling (*Pamarthy et al., 2018*). V-ATPase (orange) acidifies intracellular vesicles thereby regulating Notch signaling and other pathways like Wnt and TGF-β, which depend on endolysosomal system for sustenance. In Notch Signaling, the Notch receptor (dark pink) is cleaved in Golgi and translocated to the plasma membrane where further cleavage of the receptor occurs in response to Notch ligand (light pink) binding. Cleaved Notch intracellular domain is translocated to nucleus activating Notch target genes. TGF-β (dark green) protein is glycosylated in the Golgi to form mature TGF-β and secreted into the extracellular space. TGF-β bound to its receptor (TGF-βR) (bright green) results in endocytosis and phosphorylation of Smad2 (olive green), which in turn activates TGF-β target genes. During canonical Wnt signaling, the binding of ligands to the Wnt receptor complex (bright yellow) inhibits the phosphorylation of β-catenin (dark yellow) by GSK-3β and directs the translocation of β-catenin into the nucleus where it activates the transcription of target genes Cyclin D1 and oncogene c-Myc. V-ATPase-mediated acidification can affect signaling in the following ways: **a)** Maturation of signaling molecules Notch receptor and TGF-β by furin glycosylation in the golgi vesicles. **b)** Cleavage and activation of pathway mediators by acid-dependent enzyme like matrix metallo proteinases (MMPs) and γ-secretase. **c)** Maintenance of basal signaling by recycling endocytosis of both ligand and receptor. **d)** Degradation of signaling molecules in lysosomes.

hepatocellular carcinoma samples [*Xu et al., 2012*] and pancreatic cancer samples [*Ohta et al., 1998*]. V1E and V1A are also increased in pancreatic cancer and gastric cancer. Overexpression of V-ATPase subunits has also been detected in lung, breast, and esophageal cancer tissues [*Hendrix et al., 2013; Huang et al., 2012; Lu et al., 2013*]. The V0a exist in four isoforms in mammalian cells allowing localization to specific membranes in cell and each of these V0a isoforms are overexpressed in many different cancer cells.

The presence of the V-ATPase on the plasma membrane of invasive cancer cells and the overexpression of V-ATPase subunits in human cancer samples has suggested a possible role for the V-ATPase in cancer cell migration and invasion. Several studies have demonstrated that both in vitro invasion and migration of human breast cancer cells is dependent on V-ATPase activity. Treatment of highly invasive MB231 and MCF10CA1a human breast cancer cells with the specific V-ATPase inhibitors concanamycin A and bafilomycin results in a significant decrease in *in vitro* invasion as measured by transwell assays [*Sennoune et al., 2004*]. Similar results have been obtained with other cancer cell types.

Chapter 2: Regulated Exocytosis

2.1 Exocytosis

Exocytosis is an evolved process by which cells bring molecules such as channels and receptors to the plasma membrane or release molecules such as neurotransmitters, hormones and proteins to the extracellular space in order to communicate with other cells even at distance in the organism. Exocytosis and its counterpart, endocytosis, are used by all cells since most chemical substances important are large polar molecules that cannot pass through the cell membrane by passive means. In exocytosis, molecules stored in secretory vesicles are carried to plasma membrane, and their contents are secreted into the extracellular environment after merging of plasma and vesicular membranes. For instance, neurons release neurotransmitters stored in synaptic vesicles into the synaptic cleft after a rise of Ca^{2+} in the cytoplasm and therefore called regulated exocytosis.

2.1.1 Constitutive exocytosis

Constitutive exocytosis is a mechanism by which cells are able to locate molecules into plasma membrane such as ion channels, cell receptors, lipids, and other components. It is required by all type of cells and also serves the release of extracellular matrix after the fusion of the transport vesicle.

2.1.2 Regulated exocytosis

In specialized secretory cells, there is a second secretory pathway in which soluble proteins and other substances are initially stored in secretory vesicles for later release.

This release mechanism is tightly controlled and is generally triggered by a rise in intracellular calcium levels after cell stimulation and is thereby called “regulated exocytosis”. It is found mainly in cells specialized for devoted to rapid secretion of informative molecules on demand—such as hormones, neurotransmitters, or digestive enzymes. I will in the following sections give more details about the molecular aspects of this complex process.

In the nervous system, neurons are highly specialized cells capable in response to a stimulus of generating a nerve impulse that will propagate up to its connecting units with other neurons called synapses. Neurons are composed of dendrites, a cell body and an axon. A synapse includes the presynaptic compartment (endings of the axon), the synaptic cleft, and the postsynaptic compartment (either a dendrite or a neuron cell body). Along the axons propagates an electrical message in the form of action potentials (APs). These APs reach the presynaptic compartment where they cause the opening of voltage-dependent calcium channels on the presynaptic membrane. As calcium is more concentrated outside the cell it enters the presynapse according the gradient of concentration. The more action potentials reaching the presynaptic compartment, the higher the calcium concentration in the presynaptic compartment will be. This increase in calcium concentration will affect several calcium sensitive proteins (including synaptotagmins, calmodulin, and NCS-1) allowing the release of neurotransmitters into the synaptic cleft by exocytosis of synaptic vesicles filled with neurotransmitters.

2.2 The life cycle of a secretory vesicle: from Golgi to plasma membrane

The secretory pathway is a fundamental cellular process that requires synthesis, modification, sorting and release of secretory proteins/molecules to the extracellular milieu or delivery of different components to the cell surface. These proteins are synthesized on endoplasmic reticulum (ER)-bound ribosomes and translocated into the

ER lumen where they are folded, assembled and glycosylated [*Braakman and Bulleid, 2011*]. Cargo proteins are transported from ER exit sites to the entry side of the Golgi complex by the tubulo-vesicular components of the ER-Golgi complex intermediate compartment and successively pass through the different Golgi stacks, where proteins undergo further processing and maturation [*Wilson et al., 2010*]. At the most distal region of the Golgi complex, the trans-Golgi network (TGN), proteins are sorted into different vesicular carriers for trafficking and delivery to their final destinations, such as endo-lysosomal system and plasma membrane, by constitutive or regulated exocytic pathway. In the constitutive pathway, newly synthesized proteins are packaged into constitutive secretory vesicles that are transported directly to the cell surface and secreted without any extracellular or intracellular stimuli [*Burgessand Kelly, 1987*]. In contrast, the regulated pathway is a hallmark of specialized secretory cells such as neurons, exocrine and endocrine cells, and requires the concentration and condensation of the secretory products into secretory granules. These granules are transported in the cytoplasm towards the cell periphery to await exocytosis stimulated by cell surface signal [*Burgessand Kelly, 1987*] (Figure 8a).

2.3 The different steps of exocytosis

Like for most, if not all, complex cellular processes, biologists have divided the successive sequences that lead to exocytosis in several specific steps (Figure 9).

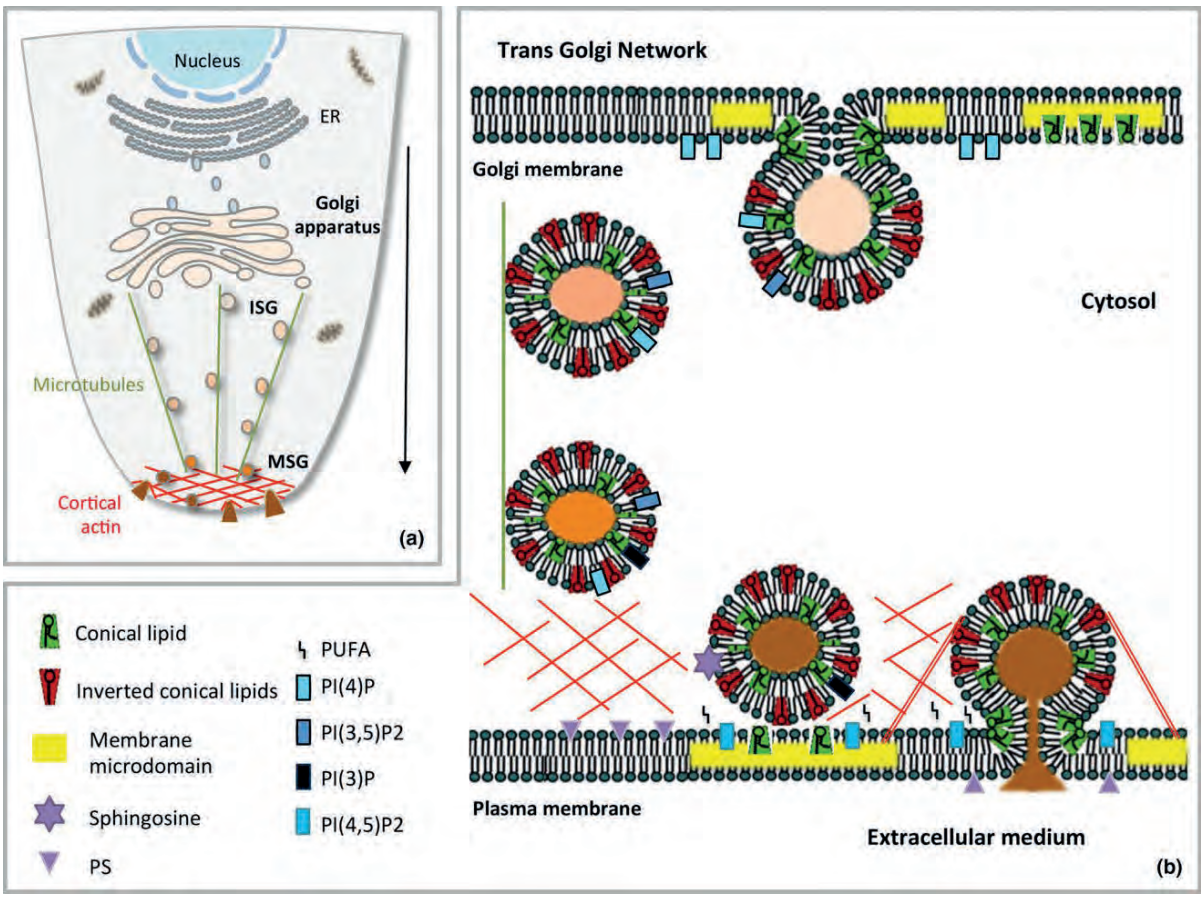

Figure 8: Model of life cycle of secretory granule from biogenesis to fusion (*Tanguy et al, 2016*)..(a) The regulated secretory pathway from the Golgi apparatus to the plasma membrane. Immature secretory granules (ISG) are transported along microtubules from the trans-Golgi network (TGN) up to the cortical actin. During their active transport they are converted into mature secretory granules (MSG). (b) Lipids involved in the journey of secretory granules. Specific minor lipids directly control directionality and functionality of the regulated secretory pathway. Conical lipids include cholesterol, diacylglycerol, phospha- tidic acid, and phosphatidylethanolamine. Inverted conical lipids include lysophospholipids and PI(4,5)P_2. Omega-6 and omega-3 forms of polyunsaturated fatty acids (PUFA) are released in the cytosol by phospholipases. Membrane microdomains enriched in cholesterol, gangliosides, and sphingolipids are highlighted at the budding membrane of the TGN and at the exocytotic sites of the plasma membrane.

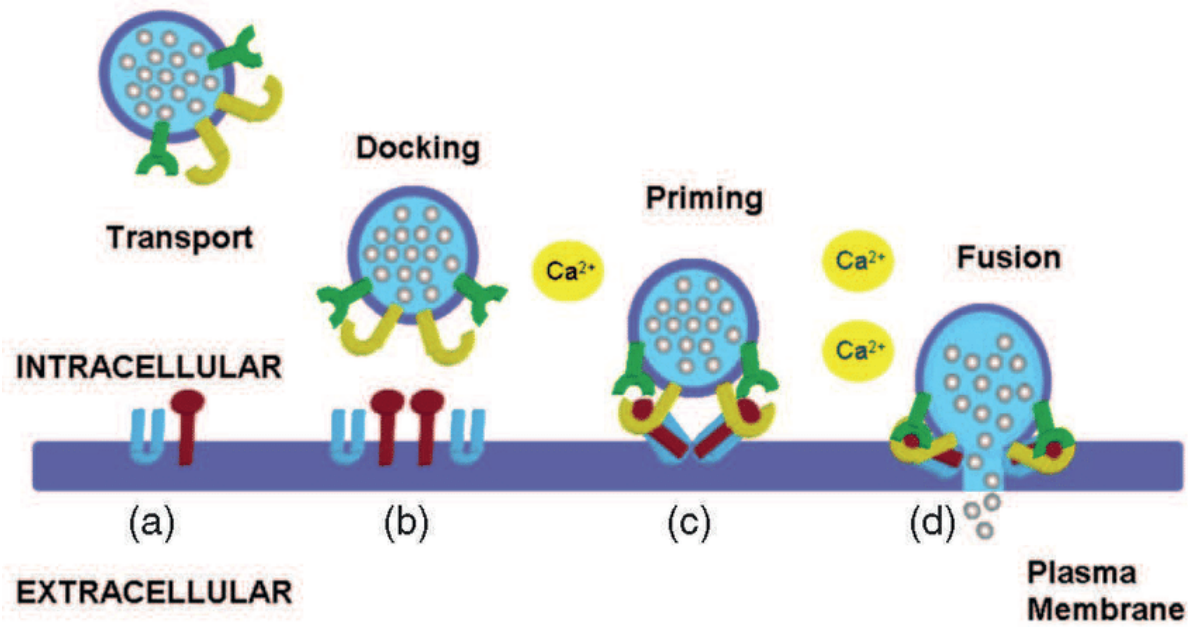

Figure 9: The different stages of exocytosis in secretory cells (Díaz et al., 2010). Regulated exocytosis requires the SNARE machinery (colored lines) and for the ultimate and penultimate steps calcium ions. (a) Formation of vesicles, (b) vesicle "docking," (c) the transformation of vesicles into fusion-competent vesicles ("priming"), and (d) fusion.

2.3.1 Production of secretory vesicles

Neuronal synaptic vesicles are organelles of the presynaptic compartment filled with neurotransmitters, whereas secretory granules of neuroendocrine cells in addition to neurotransmitters also contain large proteins such as members of the granin family and neuropeptides. Both synaptic vesicles and secretory granules are produced at the TGN levels, but they are also actively recycled and reused after exocytosis and after maturation steps.

Since most neurotransmitters are synthesized in the cytoplasm, their accumulation in the vesicle lumen is achieved by a transporter located in the vesicle membrane [*Edwards, 2007*]. Each carrier is specific to one neurotransmitter. For instance, the transporter of glutamate is VGLUT whereas that of acetylcholine is VACHT. These carriers exchange the proton output of the lumen of the vesicle against the

neurotransmitters input. It is therefore necessary that the vesicular lumen is acidic to allow their loading in neurotransmitters. As determined by quantitative mass spectrometry this acidification of the synaptic vesicular luminal medium is achieved by one or two molecules of V-ATPase per vesicle inserted into membrane [*Takamori et al., 2006*]. It must be noted however that this analysis was performed on purified rat brain synaptic vesicles that by essence are not homogenous and thus those numbers may vary significantly for synaptic vesicles with different origin or for larger secretory granules.

2.3.2 The docking of the vesicle

Neurotransmitter-loaded synaptic vesicles are specifically directed to a domain of the presynaptic membrane called the active zone [*Neher and Sakaba., 2008*]. Therefore, there is mutual recognition of the vesicle membranes and the active zone promoting the exocytosis of the vesicles in this zone. This recognition involves members of the exocyst complex as well as Rab proteins and coincides with the step of attaching the vesicle to the target membrane, also known as tethering [*Stenmark 2009*]. Rab proteins are small GTPases. There are more than 60 identified Rab genes in humans. As a result, among the proteins involved in intracellular trafficking, they are the most diverse [*Stenmark 2009*]. Rab proteins are reversibly associated with lipid membranes by hydrophobic geranylgeranyl groups. The distribution of each Rab is specific, giving each compartment a surface identity [*Stenmark 2009*]. For example, synaptic vesicle membranes are associated with Rab3 proteins.

After this tethering step, the initial assembly of the SNARE complex allows for docking if synaptic vesicles or secretory granules to the exocytotic sites (Figure 9). It is indeed believed that the SNARE complex is partially zipped during the docking stage.

2.3.3 Getting ready for secretion

Once the vesicle is attached to the target membrane, it is stapled by a closer association of SNAREs complexes. It should be noted that the borderline between docking and stowage is unclear and that these steps are likely to be very close in time [*Karatekin et al., 2008*]. It is also of notice that the concept of docking may not represent the exact same steps of exocytosis when studied by electronic microscopy, dynamic live imaging (TIRF), or by electrophysiological means such as capacitance recording.

2.3.4 Release of contents of vesicle

The next step corresponds to the priming of vesicles for release. It is known for a long time that this steps is ATP-dependent and involves the phosphoinositide $PI(4,5)P_2$. It is likely that this step also involves rearrangements in the structure and organization of the SNARE complexes allowing vesicles to get closer to the plasma membrane. Further zippering of the SNARE complex is thought to provide the needed energy to overcome the repulsion between the two membranes allowing for the formation of a hemifusion intermediate where the cytosolic leaflets of the two membranes have fused. The next step represents the complete merging of the proximal membranes and the formation of a fusion pore. At this stage vesicles can release their contents by at least two different modes of release. The first is classical mode of exocytosis where the secretory vesicle fully inserts into the plasma membrane allows for the complete release of vesicle content. The second mode of exocytosis consists in a transient opening of a pore between vesicular and plasma membranes allowing a direct connection of the vesicular lumen and the extracellular medium and partial release of vesicle content (*He and Wu, 2007*). This later mode is also known as the "kiss and run". Regardless of the type of membrane fusion, there is a formation of membrane fusion pore that requires the formation of the complex SNAREs.

2.4 Factors involved in membrane fusion

2.4.1 Lipids

Membrane fusion consists above all of the merging of two membrane bilayers. It is thus rather logical to speculate that lipids also play an important role. First neglected this aspect has been more intensely studied over the last two decades [*Ammar et al., 2013*]. These studies have led to models where specific lipid organize exocytotic sites whereas other lipids present fusogenic capacities. Following is a review I contributed too, that recapitulates the different roles that were established for lipids in exocytosis [*Tanguy et al., 2016*].

Some lipids, such as cholesterol, PI(4,5)P_2, and sphingolipids are clustered to microdomains in plasma membrane. Biochemical and high-resolution imaging observations have shown that these microdomains serve to concentrate and regulate SNARE proteins activity, in order to active exocytotic sites [*Salaun et al., 2005*]. Furthermore, it has been demonstrated that PI(4,5)P_2-enriched microdomains co-localize with SNARE clusters that is docked on secretory granules, from analysis of immunogold labeled plasma membrane sheets obtained from chromaffin cells [*Umbrecht-Jenck et al., 2010*]. Recent work from our group has further shown that annexin A2 generates lipid domains sites by connecting cortical actin and docked secretory granules to active fusion sites [*Gabel et al., 2015*]. These findings suggest that exocytotic sites may be defined by specific lipids, such as cholesterol and PI(4,5)P_2, and orchestrated by the cytoskeleton that altogether contribute to sequestering and/or stabilizing components of the exocytotic machinery (Figure 8b)

This chapter is further detailed in a review I contributed to and that was published in the Journal of Neurochemistry.

Journal of Neurochemistry

JOURNAL OF NEUROCHEMISTRY | 2016 | 137 | 904–912 doi: 10.1111/jnc.13577

REVIEW

Lipids implicated in the journey of a secretory granule: from biogenesis to fusion

Emeline Tanguy,*[,1] Ophélie Carmon,†[,1] Qili Wang,* Lydie Jeandel,† Sylvette Chasserot-Golaz,* Maité Montero-Hadjadje† and Nicolas Vitale*

*Institut des Neurosciences Cellulaires et Intégratives (INCI), UPR-3212 Centre National de la Recherche Scientifique & Université de Strasbourg, Strasbourg, France

†INSERM U982, Laboratoire de Différenciation et Communication Neuronale et Neuroendocrine, Institut de Recherche et d'Innovation Biomédicale, Université de Rouen, Mont-Saint-Aignan, France

Abstract

The regulated secretory pathway begins with the formation of secretory granules by budding from the Golgi apparatus and ends by their fusion with the plasma membrane leading to the release of their content into the extracellular space, generally following a rise in cytosolic calcium. Generation of these membrane-bound transport carriers can be classified into three steps: (i) cargo sorting that segregates the cargo from resident proteins of the Golgi apparatus, (ii) membrane budding that encloses the cargo and depends on the creation of appropriate membrane curvature, and (iii) membrane fission events allowing the nascent carrier to separate from the donor membrane. These secretory vesicles then mature as they are actively transported along microtubules toward the cortical actin network at the cell periphery. The final stage known as regulated exocytosis involves the docking and the priming of the mature granules, necessary for merging of vesicular and plasma membranes, and the subsequent partial or total release of the secretory vesicle content. Here, we review the latest evidence detailing the functional roles played by lipids during secretory granule biogenesis, recruitment, and exocytosis steps.

Keywords: exocytosis, lipid, membrane, microdomain, secretion, secretory granule budding.

J. Neurochem. (2016) **137**, 904–912.

This article is part of a mini review series on Chromaffin cells (ISCCB Meeting, 2015).

The secretory pathway is an essential cellular activity that requires synthesis, modification, sorting, and release of secretory proteins/molecules outside cells, as well as transport of cell surface components. These proteins are first created on endoplasmic reticulum (ER)-bound ribosomes and translocated into the ER lumen, where they are folded, assembled, and N-glycosylated (Braakman and Bulleid 2011). Cargo proteins (either membrane associated or soluble) are conveyed from the ER exit sites to the entry side of the Golgi apparatus and then successively pass through the different Golgi stacks, where the proteins undergo maturation and processing (Wilson *et al.* 2011). At the trans-Golgi network (TGN), proteins are sorted into specific vesicular carriers for transport and distribution to their ultimate destinations, including the endolysosomal system and the plasma membrane, by the constitutive or regulated exocytosis pathway (Gerdes 2008). On one side, all cell types recycle membranes, proteins, and extracellular matrix components through constitutive secretory vesicles that are transported directly to the cell surface where they

Received December 24, 2015; revised manuscript received January 20, 2016; accepted February 3, 2016.

Address correspondence and reprint requests to Nicolas Vitale, Institut des Neurosciences Cellulaires et Intégratives (INCI), UPR-3212 Centre National de la Recherche Scientifique & Université de Strasbourg, 5 rue Blaise Pascal, 67084 Strasbourg, France. E-mail: vitalen@unistra.fr

Maité Montero-Hadjadje, INSERM U982, Laboratoire de Différenciation et Communication Neuronale et Neuroendocrine, Institut de Recherche et d'Innovation Biomédicale, Université de Rouen, 76821 Mont-Saint-Aignan, France. E-mail: maite.montero@univ-rouen.fr

[1]These authors contributed equally to this work.

Abbreviations used: AA, arachidonic acid; AP, adaptor protein; AQP, aquaporin; BAR, Bin/amphiphysin/Rvs; CAPS, calcium-activator protein for secretion; CERT, ceramide transport protein; DAG, diacylglycerol; ER, endoplasmic reticulum; ISG, immature secretory granules; LPA, lysophosphatidic acid; LPC, lyso-phosphatidylcholine; MSG, mature secretory granules; PA, phosphatidic acid; PE, phosphatidylethanolamine; PI(3)P, phosphatidylinositol-3-phosphate; PI(3,5)P2, phosphatidylinositol 3,5-bisphosphate; PI(4)P, phophatidylinositol 4-phosphate; PI(4,5)P2, phosphatidylinositol 4,5-bisphosphate; PI3K, phosphatidylinositol 3-kinase; PKD, protein kinase D; PLD, phospholipase D; PS, phosphatidylserine; PUFA, polyunsaturated fatty acid; SNARE, soluble *N*-ethylmaleimide-sensitive factor attachment protein receptor; TGN, trans-Golgi network; VAMP, vesicle-associated membrane protein; V-ATPase, vacuolar H-ATPase.

REVIEW

fuse with the plasma membrane in the absence of any kind of stimuli. On the other side, the regulated pathway is a trademark of specialized secretory cells, such as neurons, endocrine, and exocrine cells, and requires the accumulation of the secretory material into dedicated organelles, the secretory granules (Vázquez-Martínez *et al.* 2012). The latter are transported through the cytoplasm toward the cell periphery, where they are exocytosed after stimulation of the cell (Burgess and Kelly 1987).

In addition to the function of important protein players in the journey of a secretory granules, lipids also contribute to key steps. Cell membranes are indeed composed of a broad spectrum of lipids with specific properties that can directly influence membrane topology, dynamics, and tasks. In addition, the lipid composition and transbilayer arrangement vary strikingly between organelles and there is compelling evidence that the collective properties of bulk lipids profoundly define organelle identity and function (Holthuis and Menon 2014). Of particular interest are changes in the physical properties of the membrane that are directly under the control of lipids, and mark the transition from early to late organelles in the secretory pathway. These include bilayer thickness, lipid packing density, and surface charge. Here, we highlight the latest evidence supporting the notion that in addition to the collective action of bulk lipids, specific minor lipids directly control directionality and functionality of the secretory pathway.

Lipids and biogenesis of secretory granules

Lipids involved in formation of budding sites at the TGN membrane

The biogenesis of secretory granules destined for the regulated secretory pathway begins like other transport vesicles by active budding at the TGN membrane. This process needs several concomitant events: the sorting of cargo and membrane components, the membrane curvature, and the recruitment of cytosolic proteins. A role for lipids in the formation of post-Golgi carriers has long been proposed, including their interactions with enzymes and other membrane-associated proteins. The development of cellular lipidomic approaches (especially mass spectrometry) has revealed (i) that the Golgi membrane of the mammalian cell contains the same lipids as those found in the plasma membrane, but in different proportions and (ii) that the two leaflets of the Golgi membrane bilayers display specific lipid compositions, sphingolipids being enriched in the lumenal leaflet, whereas phosphatidylserine (PS) and phosphatidylethanolamine are concentrated in the cytosolic leaflet (van Meer and de Kroon 2011). Beside these lipids, the recruitment of enzymes at the cytosolic face of the TGN membrane contributes to its remodeling through the generation of lipid metabolites, such as diacylglycerol (DAG), phosphatidic acid (PA), and phosphoinositides (Ha *et al.* 2012). These lipids play a central role in the formation of secretory granules. For instance, the accumulation of PA in the TGN membrane is a key factor for the budding of secretory granules (Siddhanta and Shields 1998). At low pH and high calcium concentrations, PA adopts a conical shape that favors changes in membrane topology (Kooijman *et al.* 2003). DAG also exhibits a conical shape and its accumulation in the TGN membrane has been found to facilitate membrane curvature leading to the budding of secretory granules (Asp *et al.* 2009).

The Golgi membrane also exhibits a dynamic lipid asymmetry, with the ability of cholesterol, DAG, and other glycerophospholipids to translocate spontaneously or in P4-ATPase-stimulated manner (Tang *et al.* 1996). Flippases generally maintain lipid asymmetry, but their lipid transfer activity between the two leaflets can also potentially lead to membrane curvatures that drive the budding of post-Golgi vesicles (Leventis and Grinstein 2010).

Cells are able to maintain differences in lipid composition between their organelles despite the lateral diffusion of lipids in cellular membranes. The physical differences between glycerolipids and sphingolipids make them segregate in the presence of cholesterol (Marsh 2009). In the Golgi membrane, for example, domains with different lipid compositions are targeted with unique transmembrane proteins into separate secretory vesicles. This segregation of lipids and proteins forms the sorting mechanism which cells use to maintain the specific composition of their membranes (van Meer *et al.* 2008). Originally, lipid self-organization was considered to be the major driving force behind lateral membrane organization. The formation of such functional lipid micro- or nano-domains in the bilayer remains difficult to visualize because of the lack of effective lipid probes to study molecule dynamics in living cells. Although this self-organization plays an essential role, it is plausible that membrane proteins influence lipid organization, and conversely that protein function and clustering are under the control of lipids. Notwithstanding the so-called 'lipid rafts' in Golgi membrane have been predicted to regulate the function and clustering of proteins involved in the budding of secretory granules (Surma *et al.* 2012).

Lipids involved in protein recruitment at the budding sites

The enrichment of secretory granule membrane in sphingolipids and cholesterol suggests their participation in the formation of functional microdomains involved in the budding of these organelles from the Golgi membrane (Wang and Silvius 2000). Lipid microdomains are implicated in the sorting of proteins destined for the regulated secretory pathway (Tooze *et al.* 2001), as they possess the ability to attract peripheral proteins such as carboxypeptidase E (Dhanvantari and Loh 2000), prohormone convertase PC2 (Blázquez *et al.* 2000), and secretogranin III (Hosaka *et al.*

2004). These proteins act as chaperones by tethering soluble or aggregated proteins to the secretory granule membrane (Dikeakos and Reudelhuber 2007). In secretory cells, lipid microdomains also attract aquaporins (AQP), which are transmembrane proteins that remove water, thereby allowing the condensation of aggregated granule proteins in the TGN (Arnaoutova *et al.* 2008). In the low pH and high calcium conditions found in the Golgi compartment, members of a family of soluble proteins called chromogranins induce aggregation of proteins destined to the regulated secretory pathway (Montero-Hadjadje *et al.* 2008). TGN acidification is achieved by proton pumps of the vacuolar H-ATPase (V-ATPase) family (Schapiro and Grinstein 2000). Interestingly, Li *et al.* (2014) have demonstrated that the signaling lipid phosphatidylinositol 3,5-bisphosphate (PI(3,5)P2) is a significant regulator of V-ATPase assembly and activity. Furthermore, phosphoinositides on the cytosolic surface recruit organelle-specific effector proteins of vesicle trafficking and signal transduction (Di Paolo and De Camilli 2006). For example, the serine/threonine protein kinase D (PKD) is recruited by binding to DAG and the GTPase ARF1, and this promotes the production of phophatidylinositol 4-phosphate (PI(4)P) by activating the lipid kinase PI(4)-kinase IIIß. At the TGN, PI(4)P can recruit lipid transfer proteins, such as oxysterol-binding protein 1 and ceramide transport protein that control sphingolipid and sterol levels, respectively. Ceramide transport protein-mediated transport of ceramide to the TGN has been proposed to increase the local production of DAG, which is converted into PA and lysophosphatidic acid; all these lipids being necessary for fission of secretory vesicles. PKD also regulates the recruitment of Arfaptin-1 (a Bin/amphiphysin/Rvs domain protein) to PI(4)P at the TGN membrane (Cruz-Garcia *et al.* 2013). In this study, Arfaptin-1 also appears important for the sorting of chromogranin A, a member of the chromogranin family, to the regulated secretory pathway in human BON carcinoid tumor cells. These results suggest that DAG-dependent PKD recruitment is crucial for the biogenesis of secretory granules. Indeed, PKD-mediated Arfaptin-1 phosphorylation is necessary to ensure the fission of secretory granules at the TGN of pancreatic β cells (Gehart *et al.* 2012). Such a role is compatible with previous reports showing that other cellular components, such as chromogranin-induced prohormone aggregates are important for driving TGN vesicle budding after their association with membrane rafts (Gondré-Lewis *et al.* 2012).

The journey of secretory granules begins

Hormone precursors, along with other proteins of the regulated secretory pathway in neuroendocrine cells, are sorted and packaged into immature secretory granules that bud off from the TGN. These organelles are rapidly conveyed to the cell periphery through their interaction with microtubules via kinesin motors (Park *et al.* 2009). The maturation process comprises an acidification-dependent processing of cargo, condensation of the secretory granule content, and removal of lipids and proteins not destined for mature secretory granules. The acidification process occurs along the regulated secretory route resulting in a decrease in pH from the TGN (6.5–6.2), to immature secretory granules (6.3–5.7), and finally to mature secretory granules (5.5–5.0). In chromaffin cells, an increase in the proton pump density and a diminution in proton permeability of the granule membrane allow a pH drop (Apps *et al.* 1989). Moreover, the selective V-ATPase inhibitor bafilomycin A1 demonstrated the role of acidification on trafficking of specific granule proteins through the regulated secretory pathway in PC12 cells (Taupenot *et al.* 2005), a process potentially under the control of phosphoinositide levels.

During maturation in endocrine and exocrine cells, granules decrease in size as their content undergoes condensation, along with the concomitant efflux of Na^+, K^+, Cl^-, and water from the granules. Water removal is ensured by the lipid microdomain-associated AQP. AQP1 is found in secretory granules of pituitary and chromaffin cells, as well as in synaptic vesicles and pancreatic zymogen granules, whereas AQP5 is found in parotid gland secretory vesicles (Ishikawa *et al.* 2005; Arnaoutova *et al.* 2008). They facilitate condensation of granular content during maturation. Upon their arrival at the cell periphery, secretory granules are trapped in the dense cortical actin network. Myosin Va together with Rab3D regulate distinct steps of the granule maturation, with an essential role of myosin Va in membrane remodeling (Kögel and Gerdes 2010) and a crucial function of Rab3D in the cargo processing (Kögel *et al.* 2013). Interestingly in yeast, oxysterol-binding protein Osh4p-recruited PI(4)P and Rab proteins are in association with a myosin V type (Myo2p) in the membrane of secretory compartments and are implicated in vesicle maturation (Santiago-Tirado *et al.* 2011).

Membrane remodeling also induces a decrease of the size of secretory granules. The presence of a clathrin coat on patches of secretory granule membrane causes shrinkage of material, mediated by the clathrin adaptator protein (AP)-1 (Dittie *et al.* 1996). As a result, membrane proteins like vesicle-associated membrane protein 4 (VAMP4), furin, and mannose 6-phosphate receptors, which have a canonical AP-1-binding site in their cytosolic domain, are present in immature secretory granules, but not anymore in mature secretory granules (Klumperman *et al.* 1998; Teuchert *et al.* 1999; Hinners *et al.* 2003). AP-1 accumulates at the cytosolic face of TGN membrane likely through PI(4)P interaction (Wang *et al.* 2003). Their transport along microtubules toward the cortical actin, a step that has not been linked to lipid yet, and the concomitant granular modifications result in the maturation and storage of secretory granules, competent for exocytosis.

Lipids and exocytosis of secretory granules

And the journey of secretory granules ends

The final stage of the secretory pathway is regulated exocytosis, a well-defined multistep process triggered by an exocytotic stimulus (Pang and Südhof 2010). The molecular machinery underlying regulated exocytosis involves assembly of a tripartite soluble *N*-ethylmaleimide-sensitive factor attachment protein receptor (SNARE) complex between plasma and granular proteins as well as accessory proteins (Jahn and Fasshauer 2012). Extensive work over the last two decades has also shed light on the importance of lipids in the exocytosis process. In the following sections, the major contributions of membrane lipids for each step of secretory granule exocytosis will be described.

Lipids involved in formation of exocytotic sites and the docking step

Mature granules, once tethered, are recruited to exocytotic sites and this represents the initial contact between secretory granules and plasma membrane. Some lipids, such as cholesterol, phosphatidylinositol 4,5-bisphosphate (PI(4,5)P2), and sphingolipids are clustered in ordered microdomains in plasma membrane, also called membrane rafts. Biochemical and high-resolution imaging observations indicate that these detergent-resistant microdomains serve to concentrate and regulate SNARE proteins, arguing for the constitution of active exocytotic sites (Salaün *et al.* 2005). Spatial definition of exocytotic sites is cholesterol dependent, as depletion of cholesterol from the plasma membrane negatively affects cluster integrity and results in reduced secretory activity by neuroendocrine cells (Lang *et al.* 2001). Furthermore, we have demonstrated that PI(4,5)P2-enriched microdomains co-localize with SNARE clusters and docked secretory granules from analysis of immunogold labeled plasma membrane sheets (Umbrecht-Jenck *et al.* 2010).

PI(4,5)P2 plays a critical role in translocating secretory vesicles to the plasma membrane (Wen *et al.* 2011), but also binds and regulates a large subset of proteins involved in the docking step, and therefore plays an essential role in granule recruitment at exocytotic sites (recently reviewed by Martin 2015). For instance, by modulating actin polymerization, PI(4,5)P2 controls actin-based delivery of secretory vesicles to exocytotic sites (Trifaró *et al.* 2008). Moreover, PI(4,5)P2 clusters organized by syntaxin-1A could act as a platform for granule docking in membrane rafts (Honigmann *et al.* 2013). Studies in chromaffin cells have demonstrated that generation of microdomains is positively regulated by recruitment of annexin A2, a calcium- and PI(4,5)P2-binding protein present at docking sites near SNARE complexes (Chasserot-Golaz *et al.* 2005; Umbrecht-Jenck *et al.* 2010). Using 3D electron tomography, we have recently shown that annexin A2 generates lipid domains sites by connecting cortical actin and docked secretory granules to active fusion sites (Gabel *et al.* 2015). The actin-bundling activity of annexin A2 promotes the formation of ganglioside GM1-enriched microdomains, increases the number of morphologically docked granules at the plasma membrane, and controls the number and the kinetic of individual exocytotic events.

Altogether, these findings raise the possibility that exocytotic sites are defined by specific lipids, such as cholesterol and PI(4,5)P2, that contribute to sequestering or stabilizing components of the exocytotic machinery. There are also indications that other lipids contribute to the establishment of exocytotic sites. For instance, PS resides mostly in the cytosolic leaflet of plasma membrane in unstimulated conditions. However, during exocytosis of secretory granules in numerous secretory cell types, notably neuroendocrine cells, PS translocates to the outer leaflet (Vitale *et al.* 2001). An ultrastructural analysis has recently demonstrated that PS is externalized in the vicinity of the docking sites of secretory granules, although the functional relevance of this PS externalization for fusion is still under debate (Ory *et al.* 2013). Another lipid implicated in regulated exocytosis is PA. Silencing of the PA-producing enzyme phospholipase D1 (PLD1) and the ectopic expression of a catalytically dead PLD1 form in chromaffin cells affected the number of exocytotic events, as revealed by capacitance recordings and carbon fiber amperometry (Zeniou-Meyer *et al.* 2007). In line with these observations, PA has recently been proposed to regulate docking in sea urchin eggs (Rogasevskaia and Coorssen 2015). Finally, analysis of plasma membrane SNARE microdomains in chromaffin cells by total internal reflection fluorescent microscopy suggests that exogenous addition of the polyunsaturated fatty acid arachidonic acid (AA) enhances docking of granules (García-Martínez *et al.* 2013). Thus, investigations using novel high-resolution imaging techniques combined with acute modifications of individual lipid composition in a given membrane will probably further elucidate the contribution of lipids to the organization of the exocytotic platform.

Lipids regulating molecular mechanisms of priming steps

Priming steps depend on molecular events, essentially involving SNARE complex assembly, and are necessary to render vesicles fusion competent (Klenchin and Martin 2000). There is also growing evidence that lipids are implicated in priming, as indicated by lipid reorganization provoked by inositol kinases and lipases during this step. Phosphoinositides such as PI(4,5)P2 seem to be key regulators of secretion, not only by regulating the docking step but also by controlling the size and refilling rate of the readily releasable pool of granules. Electrophysiological studies modulating PI(4,5)P2 levels and using over-expressed PI(4,5)P2 fluorescent probes revealed that a high level of PI(4,5)P2 in chromaffin cells positively modulates secretion by increasing the size of the primed vesicle pool,

whereas the constants of the fusion rate were not affected (Milosevic *et al.* 2005). In agreement with this concept, we recently found that the HIV protein Tat sequesters plasmalemmal PI(4,5)P2 in neuroendocrine cells and subsequently reduces the number of exocytotic events, without significantly affecting the kinetics of fusion (Tryoen-Toth *et al.* 2013). Moreover, *in vitro* experiments using liposomes have previously reported that PI(4,5)P2 can recruit priming factors such as calcium-activator protein for secretion (CAPS), which facilitates SNARE-dependent fusion (James *et al.* 2008). However, it seems that a well-regulated balance between plasmalemmal PI(4,5)P2 synthesis and breakdown is mandatory for exocytosis. Indeed, DAG production through hydrolysis of PI(4,5)P2 by phospholipase C is crucial for exocytosis in mast cells (Hammond *et al.* 2006). As for PI(4,5)P2, DAG formation is essential for priming, leading to activation of protein kinase C and Munc-13, which then modulate the function of syntaxin-1A (Sheu *et al.* 2003; Bauer *et al.* 2007).

On the granule membrane, phosphoinositides have also been implicated in priming. For instance, experiments on permeabilized chromaffin cells have shown that synthesis of phosphatidylinositol-3-phosphate (PI(3)P) on secretory granules positively regulates secretion. Formation of PI3P is mediated by an isoform of phosphatidylinositol 3-kinase (PI3K), PI3K-C2α, particularly enriched on chromaffin granule membranes, suggesting that PI3K-C2α production of PI(3)P has a specific role in the ATP-dependent priming phase of exocytosis (Meunier *et al.* 2005). Genetic and pharmalogical inhibition of PI3K-C2α activity resulted in a complete inhibition of secretion, suggesting that PI(3)P synthesis is necessary for exocytosis to occur (Meunier *et al.* 2005). This notion has been validated by experiments showing that stimulation of exocytosis up-regulated PI(3)P levels on granules, whereas enzymatic conversion of PI3P in PI(3,5)P2 negatively affected exocytosis (Osborne *et al.* 2008; Wen *et al.* 2008). A similar effect on insulin secretion has been reported in pancreatic β cells with impaired PI3K-C2α activity (Dominguez *et al.* 2011). Taken together, PI(3)P production by PI3K-C2α on chromaffin granule membrane can be proposed to act as an essential priming signal for secretory granules, although the effectors directly involved remain to be characterized. Altogether these observations suggest that phosphoinositide metabolism is finely regulated to control the number of fusion-competent granules.

Other lipids have recently emerged as additional modulators of the priming step. AA, a polyunsaturated fatty acid of the omega-6 family has been described to potentiate exocytosis from chromaffin cells (Vitale *et al.* 1994, 2010; Latham *et al.* 2007). *In vitro* assays on protein interactions have revealed that AA can directly interact with SNAREs, like syntaxin-1a or syntaxin-3, and potentiate their assembly with SNAP-25 (Darios and Davletov 2006). Interestingly, this effect of AA on SNARE complex formation *in vitro* can be reproduced by other omega-3 and omega-6 fatty acids, suggesting that polyunsaturated lipids may physiologically regulate SNARE complex assembly by targeting syntaxin isoforms (Darios and Davletov 2006). Along this line, work with snake phospholipase acting as neurotoxin substantiates the notion that free fatty acids and lysophopholipids promote neurosecretion (Rigoni *et al.* 2005). Furthermore, production of sphingosine, *via* hydrolysis of vesicular membrane sphingolipids, also facilitated SNARE complex assembly by activating the vesicular SNARE synaptobrevin (Darios *et al.* 2009). Finally, *in vitro* fusion assays have demonstrated that PA binds syntaxin-1 and promotes SNARE complex assembly (Lam *et al.* 2008; Mima and Wickner 2009).

'Fusogenic lipids' for membrane merging and release of content

Many observations are in agreement that lipids have also a crucial role in the fusion reaction. Thus, the most widely accepted lipidic model for membrane fusion is the stalk pore model, defined by the merging of cis-contacting monolayers, leading to a negatively curved lipid structure called a stalk (Chernomordik and Kozlov 2008). During exocytosis, the outer leaflet of the granule and the inner leaflet of the plasma membrane seemingly form the stalk. As a result of differences in the geometry of lipids, lipid composition of membranes presumably influences the structure of the stalk and subsequently efficacy of exocytosis. Theoretically, cone-shaped lipids such as cholesterol, DAG, or PA, which have intrinsic negative curvatures when found in the inner (cis) leaflets of contacting bilayers could promote fusion. On the contrary, inverted cone-shaped lipids (PS, gangliosides, or lysophospholipids) are supposed to be present in the outer (trans) leaflets. This concept has been partially validated using reconstituted fusion assays and directly by adding lipids to cell cultures. These results indicate that PA, DAG, and cholesterol, may promote fusion by changing the spontaneous curvature of membranes (Ammar *et al.* 2013).

PA is present in the inner leaflet of the plasma membrane, but presumably in very small quantities in resting conditions. Based on the pivotal role of this lipid in exocytosis (Bader and Vitale 2009), the visualization of local formation of PA has been a recurring issue. Use of PA-specific probes coupled to ultrastructural analysis allowed us to visualize PA accumulation at the plasma membrane in stimulated chromaffin cells, near morphological docking sites (Zeniou-Meyer *et al.* 2007). Moreover, silencing of PLD1 has suggested that PA production is necessary to facilitate membrane fusion after early steps of exocytosis, probably by modifying membrane topology in the proximity of docking sites. In favor of this model, extracellular lyso-phosphatidylcholine (LPC) application partially rescued secretion from PLD1-depleted cells (Zeniou-Meyer *et al.* 2007). PLD1 activity at the plasma membrane, and subsequently PA

synthesis during exocytosis, is itself regulated by PI(4,5)P2 (Du *et al.* 2003). As PA is also an essential co-factor of PI5K, which produces PI(4,5)P2, a positive feedback loop for the synthesis of these two lipids may be activated during exocytosis (Cockcroft 2009).

In conclusion, the local accumulation of different fusogenic lipids, such as PA, PI(4,5)P2, DAG, and cholesterol at or near granule docking sites may have a synergistic effect on membrane curvature and thereby promote fusion. However, the precise localization of these lipids during the course of the fusion pore formation, expansion, and closure remains elusive and requires significant advances in imaging techniques and lipid sensors. Finally, a novel mass spectrometry method has recently revealed that saturated free fatty acids are actively generated in stimulated neurosecretory cells and neurons (Narayana *et al.* 2015), but at present it is not known if these fatty acids have a direct role in exocytosis or if they are degradation products of fusogenic lipids.

Ending the journey or a new beginning?

Membrane fusion during exocytosis can occur through three different modes in secretory cells, depending on the physiological demand: kiss and run, cavicapture, or full-collapse fusion. After full-collapse fusion of the granules upon stimulation, the secretory granule membrane components can be entirely recycled by a clathrin-mediated compensatory endocytotic process (Ceridono *et al.* 2011). Molecular mechanisms underlying the preservation of granule mem-

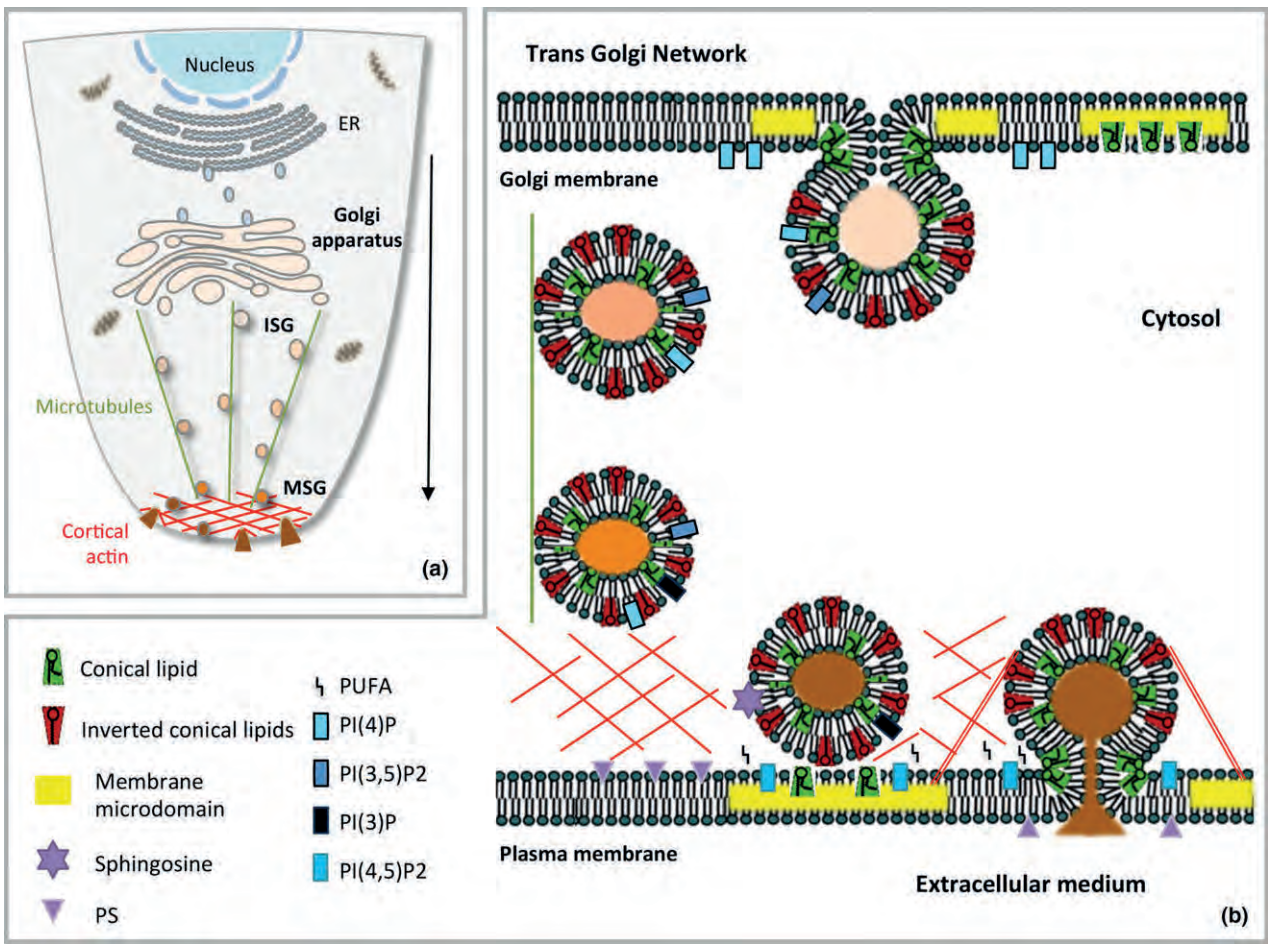

Fig. 1 Model highlighting the importance of lipids from secretory granule biogenesis to fusion**.** (a) The regulated secretory pathway from the Golgi apparatus to the plasma membrane. Immature secretory granules (ISG) are transported along microtubules from the trans-Golgi network (TGN) up to the cortical actin. During their active transport they are converted into mature secretory granules (MSG). (b) Lipids involved in the journey of secretory granules. Specific minor lipids directly control directionality and functionality of the regulated secretory pathway. Conical lipids include cholesterol, diacylglycerol, phosphatidic acid, and phosphatidylethanolamine. Inverted conical lipids include lysophospholipids and PI(4,5)P2. Omega-6 and omega-3 forms of polyunsaturated fatty acids (PUFA) are released in the cytosol by phospholipases. Membrane microdomains enriched in cholesterol, gangliosides, and sphingolipids are highlighted at the budding membrane of the TGN and at the exocytotic sites of the plasma membrane.

brane identity after fusion with plasma membrane remains unclear, but it has been proposed that specific lipid microdomains might contribute to prevent diffusion of granular components. Hence, exo-endocytosis coupling leads then to recycling of post-exocytotic internalized granule membrane back to the Golgi apparatus, starting a new life for the secretory granule (Houy *et al.* 2013). Recently lipids generated upon exocytosis have been proposed to contribute to the exo-endocytosis coupling (Yuan *et al.* 2015).

Conclusion

Lipids undoubtedly appear to contribute to almost every step along the regulated secretory pathway from the biogenesis of secretory granules to the exocytosis process (Fig. 1). However, despite the important advances in our understanding, many important answers remain far beyond our reach. The contribution of individual molecular lipid species is not known. Addressing this issue will require following the dynamics of individual lipid species at the nanometric scale, an aspect that may be achieved through the development of mass spectrometric imaging. Clearly this remains one of the most challenging issues in modern cell biology, given the large number of lipid molecules to analyze. Probing the physiological relevance of these lipids in different secretory processes is another challenging aspect for the near future. Indeed there is no doubt that an alteration of the fine cellular lipid balance, either as a consequence of an alteration of lipid metabolism or a bad diet, could contribute to dysfunction of the secretory pathway. On the other hand, determining the influence of lipid shape to membrane topology during the different steps of membrane remodeling across the secretory pathway will probably require better *in vitro* modeling of the different steps involved.

Acknowledgements and conflict of interest disclosure

We thank Dr N. Grant for critical reading of the manuscript. This work was supported by the Ministère de l'Enseignement Supérieur et de la Recherche, a grant from La Ligue contre le Cancer to NV, and by a grant from the Région Haute-Normandie to MM-H. The authors declare no conflict of interest.

References

Ammar M. R., Kassas N., Chasserot-Golaz S., Bader M.-F. and Vitale N. (2013) Lipids in regulated exocytosis: what are they doing? *Front. Endocrinol.* **4**, 125.

Apps D. K., Percy J. M. and Perez-Castineira J. R. (1989) Topography of a vacuolar-type H+-translocating ATPase: chromaffin-granule membrane ATPase I. *Biochem. J.* **263**, 81–88.

Arnaoutova I., Cawley N. X., Patel N., Kim T., Rathod T. and Loh Y. P. (2008) Aquaporin 1 is important for maintaining secretory granule biogenesis in endocrine cells. *Mol. Endocrinol.* **22**, 1924–1934.

Asp L., Kartberg F., Fernandez-Rodriguez J. *et al.* (2009) Early stages of Golgi vesicle and tubule formation require diacylglycerol. *Mol. Biol. Cell* **20**, 780–790.

Bader M.-F. and Vitale N. (2009) Phospholipase D in calcium-regulated exocytosis: lessons from chromaffin cells. *Biochim. Biophys. Acta* **1791**, 936–941.

Bauer C. S., Woolley R. J., Teschemacher A. G. and Seward E. P. (2007) Potentiation of exocytosis by phospholipase C-coupled G-Protein-Coupled Receptors requires the priming protein Munc13-1. *J. Neurosci.* **27**, 212–219.

Blázquez M., Thiele C., Huttner W. B., Docherty K. and Shennan K. I. (2000) Involvement of the membrane lipid bilayer in sorting prohormone convertase 2 into the regulated secretory pathway. *Biochem. J.* **349**, 843–852.

Braakman I. and Bulleid N. J. (2011) Protein folding and modification in the mammalian endoplasmic reticulum. *Annu. Rev. Biochem.* **80**, 71–99.

Burgess T. L. and Kelly R. B. (1987) Constitutive and regulated secretion of proteins. *Annu. Rev. Cell Biol.* **3**, 243–293.

Ceridono M., Ory S., Momboisse F. *et al.* (2011) Selective recapture of secretory granule components after full collapse exocytosis in neuroendocrine chromaffin cells. *Traffic* **12**, 72–88.

Chasserot-Golaz S., Vitale N., Umbrecht-Jenck E., Knight D., Gerke V. and Bader M.-F. (2005) Annexin 2 promotes the formation of lipid microdomains required for calcium-regulated exocytosis of dense-core vesicles. *Mol. Biol. Cell* **16**, 1108–1119.

Chernomordik L. V. and Kozlov M. M. (2008) Mechanics of membrane fusion. *Nat. Struct. Mol. Biol.* **15**, 675–683.

Cockcroft S. (2009) Phosphatidic acid regulation of phosphatidylinositol 4-phosphate 5-kinases. *Biochim. Biophys. Acta* **1791**, 905–912.

Cruz-Garcia D., Ortega-Bellido M., Scarpa M., Villeneuve J., Jovic M., Porzner M., Balla T., Seufferlein T. and Malhotra V. (2013) Recruitment of arfaptins to the trans-Golgi network by PI(4)P and their involvement in cargo export. *EMBO J.* **32**, 1717–1729.

Darios F. and Davletov B. (2006) Omega-3 and omega-6 fatty acids stimulate cell membrane expansion by acting on syntaxin 3. *Nature* **440**, 813–817.

Darios F., Wasser C., Shakirzyanova A. *et al.* (2009) Sphingosine facilitates SNARE complex assembly and activates synaptic vesicle exocytosis. *Neuron* **62**, 683–694.

Dhanvantari S. and Loh Y. P. (2000) Lipid raft association of carboxypeptidase E is necessary for its function as a regulated secretory pathway sorting receptor. *J. Biol. Chem.* **275**, 29887–29893.

Di Paolo G. and De Camilli P. (2006) Phosphoinositides in cell regulation and membrane dynamics. *Nature* **443**, 651–657.

Dikeakos J. D. and Reudelhuber T. L. (2007) Sending proteins to dense core secretory granules: still a lot to sort out. *J. Cell Biol.* **177**, 191–196.

Dittie A. S., Hajibagheri N. and Tooze S. A. (1996) The AP-1 adaptor complex binds to immature secretory granules from PC12 cells, and is regulated by ADP-ribosylation factor. *J. Cell Biol.* **132**, 523–536.

Dominguez V., Raimondi C., Somanath S. *et al.* (2011) Class II Phosphoinositide 3-Kinase regulates exocytosis of insulin granules in pancreatic cells. *J. Biol. Chem.* **286**, 4216–4225.

Du G., Altshuller Y. M., Vitale N., Huang P., Chasserot-Golaz S., Morris A. J., Bader M.-F. and Frohman M. A. (2003) Regulation of phospholipase D1 subcellular cycling through coordination of multiple membrane association motifs. *J. Cell Biol.* **162**, 305–315.

Gabel M., Delavoie F., Demais V., Royer C., Bailly Y., Vitale N., Bader M.-F. and Chasserot-Golaz S. (2015) Annexin A2-dependent actin bundling promotes secretory granule docking to the plasma membrane and exocytosis. *J. Cell Biol.* **210**, 785–800.

García-Martínez V., Villanueva J., Torregrosa-Hetland C. J., Bittman R., Higdon A., Darley-Usmar V. M., Davletov B. and Gutiérrez L. M. (2013) Lipid metabolites enhance secretion acting on SNARE microdomains and altering the extent and kinetics of single release events in bovine adrenal chromaffin cells. *PLoS ONE* **8**, e75845.

Gehart H., Goginashvili A., Beck R., Morvan J., Erbs E., Formentini I., De Matteis M. A., Schwab Y., Wieland F. T. and Ricci R. (2012) The BAR domain protein arfaptin-1 controls secretory granule biogenesis at the trans-Golgi network. *Dev. Cell* **23**, 756–768.

Gerdes H.-H. (2008) Membrane traffic in the secretory pathway. *Cell. Mol. Life Sci.* **65**, 2777–2780.

Gondré-Lewis M. C., Park J. J. and Loh Y. P. (2012) Cellular mechanisms for the biogenesis and transport of synaptic and dense-core vesicles. *Int. Rev. Cell Mol. Biol.* **299**, 27–115.

Ha K. D., Clarke B. A. and Brown W. J. (2012) Regulation of the Golgi complex by phospholipid remodeling enzymes. *Biochim. Biophys. Acta* **1821**, 1078–1088.

Hammond G. R. V., Dove S. K., Nicol A., Pinxteren J. A., Zicha D. and Schiavo G. (2006) Elimination of plasma membrane phosphatidylinositol (4,5)-bisphosphate is required for exocytosis from mast cells. *J. Cell Sci.* **119**, 2084–2094.

Hinners I., Wendler F., Fei H., Thomas L., Thomas G. and Tooze S. A. (2003) AP-1 recruitment to VAMP4 is modulated by phosphorylation-dependent binding of PACS-1. *EMBO Rep.* **4**, 1182–1189.

Holthuis J. C. M. and Menon A. K. (2014) Lipid landscapes and pipelines in membrane homeostasis. *Nature* **510**, 48–57.

Honigmann A., van den Bogaart G., Iraheta E. *et al.* (2013) Phosphatidylinositol 4,5-bisphosphate clusters act as molecular beacons for vesicle recruitment. *Nat. Struct. Mol. Biol.* **20**, 679–686.

Hosaka M., Suda M., Sakai Y., Izumi T., Watanabe T. and Takeuchi T. (2004) Secretogranin III binds to cholesterol in the secretory granule membrane as an adapter for chromogranin A. *J. Biol. Chem.* **279**, 3627–3634.

Houy S., Croisé P., Gubar O., Chasserot-Golaz S., Tryoen-Tóth P., Bailly Y., Ory S., Bader M.-F. and Gasman S. (2013) Exocytosis and endocytosis in neuroendocrine cells: inseparable membranes!. *Front. Endocrinol.* **4**, 135.

Ishikawa Y., Yuan Z., Inoue N., Skowronski M. T., Nakae Y., Shono M., Cho G., Yasui M., Agre P. and Nielsen S. (2005) Identification of AQP5 in lipid rafts and its translocation to apical membranes by activation of M3 mAChRs in interlobular ducts of rat parotid gland. *Am. J. Physiol. Cell Physiol.* **289**, 1303–1311.

Jahn R. and Fasshauer D. (2012) Molecular machines governing exocytosis of synaptic vesicles. *Nature* **490**, 201–207.

James D. J., Khodthong C., Kowalchyk J. A. and Martin T. F. J. (2008) Phosphatidylinositol 4,5-bisphosphate regulates SNARE-dependent membrane fusion. *J. Cell Biol.* **182**, 355–366.

Klenchin V. A. and Martin T. F. (2000) Priming in exocytosis: attaining fusion-competence after vesicle docking. *Biochimie* **82**, 399–407.

Klumperman J., Kuliawat R., Griffith J. M., Geuze H. J. and Arvan P. (1998) Mannose 6-phosphate receptors are sorted from immature secretory granules via adaptor protein AP-1, clathrin, and syntaxin 6-positive vesicles. *J. Cell Biol.* **141**, 359–371.

Kögel T. and Gerdes H. H. (2010) Roles of myosin Va and Rab3D in membrane remodeling of immature secretory granules. *Cell. Mol. Neurobiol.* **30**, 1303–1308.

Kögel T., Rudolf R., Hodneland E., Copier J., Regazzi R., Tooze S. A. and Gerdes H. H. (2013) Rab3D is critical for secretory granule maturation in PC12 cells. *PLoS ONE* **8**, e57321.

Kooijman E. E., Chupin V., de Kruijff B. and Burger K. N. J. (2003) Modulation of membrane curvature by phosphatidic acid and lysophosphatidic acid. *Traffic* **4**, 162–174.

Lam A. D., Tryoen-Toth P., Tsai B., Vitale N. and Stuenkel E. L. (2008) SNARE-catalyzed fusion events are regulated by syntaxin1A–lipid interactions. *Mol. Biol. Cell* **19**, 485–497.

Lang T., Bruns D., Wenzel D., Riedel D., Holroyd P., Thiele C. and Jahn R. (2001) SNAREs are concentrated in cholesterol-dependent clusters that define docking and fusion sites for exocytosis. *EMBO J.* **20**, 2202–2213.

Latham C. F., Osborne S. L., Cryle M. J. and Meunier F. A. (2007) Arachidonic acid potentiates exocytosis and allows neuronal SNARE complex to interact with Munc18a. *J. Neurochem.* **100**, 1543–1554.

Leventis P. A. and Grinstein S. (2010) The distribution and function of phosphatidylserine in cellular membranes. *Annu. Rev. Biophys.* **39**, 407–427.

Li S. C., Diakov T. T., Xu T., Tarsio M., Zhu W., Couoh-Cardel S. and Weisman L. S., Kane P. M. (2014) The signaling lipid PI(3,5)P_2 stabilizes V_1-V(o) sector interactions and activates the V-ATPase. *Mol. Biol. Cell* **25**, 1251–1262.

Marsh D. (2009) Cholesterol-induced fluid membrane domains: a compendium of lipid-raft ternary phase diagrams. *Biochim. Biophys. Acta* **1788**, 2114–2123.

Martin T. F. J. (2015) PI(4,5)P2-binding effector proteins for vesicle exocytosis. *Biochim. Biophys. Acta* **1851**, 785–793.

van Meer G. and de Kroon A. I. P. M. (2011) Lipid map of the mammalian cell. *J. Cell Sci.* **124**, 5–8.

van Meer G., Voelker D. and Feigenson G. (2008) Membrane lipids - where they are and how they behave. *Nat. Rev. Mol.* **9**, 112–124.

Meunier F. A., Osborne S. L., Hammond G. R., Cooke F. T., Parker P. J., Domin J. and Schiavo G. (2005) Phosphatidylinositol 3-kinase C2α is essential for ATP-dependent priming of neurosecretory granule exocytosis. *Mol. Biol. Cell* **16**, 4841–4851.

Milosevic I., Sørensen J. B., Lang T., Krauss M., Nagy G., Haucke V., Jahn R. and Neher E. (2005) Plasmalemmal phosphatidylinositol-4,5-bisphosphate level regulates the releasable vesicle pool size in chromaffin cells. *J. Neurosci.* **25**, 2557–2565.

Mima J. and Wickner W. (2009) Complex lipid requirements for SNARE- and SNARE chaperone-dependent membrane fusion. *J. Biol. Chem.* **284**, 27114–27122.

Montero-Hadjadje M., Vaingankar S., Elias S., Tostivint H., Mahata S. K. and Anouar Y. (2008) Chromogranins A and B and secretogranin II: evolutionary and functional aspects. *Acta Physiol.* **192**, 309–324.

Narayana V. K., Tomatis V. M., Wang T., Kvaskoff D. and Meunier F. A. (2015) Profiling of free fatty acids using stable isotope tagging uncovers a role for saturated fatty acids in neuroexocytosis. *Chem. Biol.* **22**, 1552–1561.

Ory S., Ceridono M., Momboisse F. *et al.* (2013) Phospholipid scramblase-1-induced lipid reorganization regulates compensatory endocytosis in neuroendocrine cells. *J. Neurosci.* **33**, 3545–3556.

Osborne S. L., Wen P. J., Boucheron C., Nguyen H. N., Hayakawa M., Kaizawa H., Parker P. J., Vitale N. and Meunier F. A. (2008) PIKfyve negatively regulates exocytosis in neurosecretory cells. *J. Biol. Chem.* **283**, 2804–2813.

Pang Z. P. and Südhof T. C. (2010) Cell biology of Ca^{2+}-triggered exocytosis. *Curr. Opin. Cell Biol.* **22**, 496–505.

Park J. J., Koshimizu H. and Loh Y. P. (2009) Biogenesis and transport of secretory granules to release site in neuroendocrine cells. *J. Mol. Neurosci.* **37**, 151–159.

Rigoni M., Caccin P., Gschmeissner S., Koster G., Postle A. D., Rossetto O., Schiavo G. and Montecucco C. (2005) Equivalent effects of snake PLA2 neurotoxins and lysophospholipid-fatty acid mixtures. *Science* **310**, 1678–1680.

Rogasevskaia T. P. and Coorssen J. R. (2015) The role of phospholipase D in regulated exocytosis. *J. Biol. Chem.* **290**, 28683–28696.

Salaün C., Gould G. W. and Chamberlain L. H. (2005) Lipid raft association of SNARE proteins regulates exocytosis in PC12 cells. *J. Biol. Chem.* **280**, 19449–19453.

Santiago-Tirado F. H., Legesse-Miller A., Schott D. and Bretscher A. (2011) PI4P and Rab inputs collaborate in myosin-V-dependent transport of secretory compartments in yeast. *Dev. Cell* **20**, 47–59.

Schapiro F. B. and Grinstein S. (2000) Determinants of the pH of the Golgi complex. *J. Biol. Chem.* **275**, 21025–21032.

Sheu L., Pasyk E. A., Ji J., Huang X., Gao X., Varoqueaux F., Brose N. and Gaisano H. Y. (2003) Regulation of insulin exocytosis by Munc13-1. *J. Biol. Chem.* **278**, 27556–27563.

Siddhanta A. and Shields D. (1998) Secretory vesicle budding from the trans-Golgi network is mediated by phosphatidic acid levels. *J. Biol. Chem.* **273**, 17995–17998.

Surma M. A., Klose C. and Simons K. (2012) Lipid-dependent protein sorting at the trans Golgi network. *Biochim. Biophys. Acta* **1821**, 1059–1067.

Tang X., Halleck M. S., Schlegel R. A. and Williamson P. (1996) A subfamily of P-type ATPases with aminophospholipid transporting activity. *Science* **272**, 1495–1497.

Taupenot L., Harper K. L. and O'Connor D. T. (2005) Role of H+-ATPase-mediated acidification in sorting and release of the regulated secretory protein chromogranin A: evidence for a vesiculogenic function. *J. Biol. Chem.* **280**, 3885–3897.

Teuchert M., Schäfer W., Berghöfer S., Hoflack B., Klenk H. D. and Garten W. (1999) Sorting of furin at the trans-Golgi network. Interaction of the cytoplasmic tail sorting signals with AP-1 Golgi-specific assembly proteins. *J. Biol. Chem.* **274**, 8199–8207.

Tooze S. A., Martens G. J. M. and Huttner W. B. (2001) Secretory granule biogenesis: rafting to the SNARE. *Trends Cell Biol.* **11**, 116–122.

Trifaró J.-M., Gasman S. and Gutiérrez L. M. (2008) Cytoskeletal control of vesicle transport and exocytosis in chromaffin cells: cytoskeleton and the secretory vesicle cycle. *Acta Physiol.* **192**, 165–172.

Tryoen-Toth P., Chasserot-Golaz S., Tu A., Gherib P., Bader M.-F., Beaumelle B. and Vitale N. (2013) HIV-1 Tat protein inhibits neurosecretion by binding to phosphatidylinositol 4,5-bisphosphate. *J. Cell Sci.* **126**, 454–463.

Umbrecht-Jenck E., Demais V., Calco V., Bailly Y., Bader M.-F. and Chasserot-Golaz S. (2010) S100A10-mediated translocation of annexin-A2 to SNARE proteins in adrenergic chromaffin cells undergoing exocytosis. *Traffic* **11**, 958–971.

Vázquez-Martínez R., Díaz-Ruiz A., Almabouada F., Rabanal-Ruiz Y., Gracia-Navarro F. and Malagón M. M. (2012) Revisiting the regulated secretory pathway: from frogs to human. *Gen. Comp. Endocrinol.* **175**, 1–9.

Vitale N., Thiersé D., Aunis D. and Bader M.-F. (1994) Exocytosis in chromaffin cells: evidence for a MgATP-independent step that requires a pertussis toxin-sensitive GTP-binding protein. *Biochem. J.* **300**, 217–227.

Vitale N., Caumont A.-S., Chasserot-Golaz S., Du G., Wu S., Sciorra V. A., Morris A. J., Frohman M. A. and Bader M.-F. (2001) Phospholipase D1: a key factor for the exocytotic machinery in neuroendocrine cells. *EMBO J.* **20**, 2424–2434.

Vitale N., Thiersé D. and Bader M.-F. (2010) Melittin promotes exocytosis in neuroendocrine cells through the activation of phospholipase A_2. *Regul. Pept.* **165**, 111–116.

Wang T. and Silvius J. R. (2000) Different sphingolipids show differential partitioning into sphingolipid/cholesterol-rich domains in lipid bilayers. *Biophys. J .* **79**, 1478–1489.

Wang Y. J., Wang J., Sun H. Q., Martinez M., Sun Y. X., Macia E., Kirchhausen T., Albanesi J. P., Roth M. G. and Yin H. L. (2003) Phosphatidylinositol 4 phosphate regulates targeting of clathrin adaptor AP-1 complexes to the Golgi. *Cell* **114**, 299–310.

Wen P. J., Osborne S. L., Morrow I. C., Parton R. G., Domin J. and Meunier F. A. (2008) Ca2+-regulated pool of phosphatidylinositol-3-phosphate produced by phosphatidylinositol 3-kinase C2α on neurosecretory vesicles. *Mol. Biol. Cell* **19**, 5593–5603.

Wen P. J., Osborne S. L., Zanin M. *et al.* (2011) Phosphatidylinositol (4,5)bisphosphate coordinates actin-mediated mobilization and translocation of secretory vesicles to the plasma membrane of chromaffin cells. *Nat. Commun.* **2**, 491.

Wilson C., Venditti R., Rega L. R., Colanzi A., D'Angelo G. and De Matteis M. A. (2011) The Golgi apparatus: an organelle with multiple complex functions. *Biochem. J.* **433**, 1–9.

Yuan T., Liu L., Zhang Y. *et al.* (2015) Diacylglycerol guides the hopping of clathrin-coated pits along microtubules for exo-endocytosis coupling. *Dev. Cell* **35**, 120–130.

Zeniou-Meyer M., Zabari N., Ashery U. *et al.* (2007) Phospholipase D1 production of phosphatidic acid at the plasma membrane promotes exocytosis of large dense-core granules at a late stage. *J. Biol. Chem.* **282**, 21746–21757.

2.4.2 SNARE proteins

SNAREs are small, abundant, sometimes tail-anchored proteins which are often post-translationally inserted into membranes by a C-terminal transmembrane domain. There are at least 24 different SNAREs in yeasts and more than 60 in mammalian cells [*Burri and Lithgow, 2004*]. The SNAREs that mediate docking of synaptic vesicles with the presynaptic membrane in neurons are best studied. As mentioned previously one important role of SNARE proteins is to mediate synaptic and secretory vesicle fusion.

Two categories of SNAREs have been defined: vesicle or v-SNAREs, which are incorporated into the membranes of vesicles during budding, and target or t-SNAREs, which are associated with nerve terminal membranes and form stable subcomplexes that help v-SNARE to complete the SNARE complex [*Malsam and Söllner, 2011*]. Accounting by structural features, SNAREs were later divided into R-SNAREs and Q-SNAREs. Usually, R-SNAREs act as v-SNAREs and Q-SNAREs act as t-SNAREs. R-SNAREs are proteins that contribute an arginine (R) residue in the formation of the zero ionic layer in the assembled core SNARE complex. Q-SNAREs are proteins that contribute a glutamine (Q) residue in the formation of the zero ionic layer in the assembled core SNARE complex (see below and figure 11). Q-SNAREs include syntaxin and SNAP-25, whereas VAMP-2 is a member of the R-SNARE family. For some SNAREs, such as SNAP-25, a transmembrane domain is not present and lipid modifications such as palmitoylation are responsible for membrane anchoring [*Hong and Lev, 2014*].

2.4.2.1 Structure and interaction of SNAREs

Although SNAREs vary in structure and size, they all share a segment in the cytosolic domain that contains heptad repeats, which is able to form coiled-coil structures. v-SNAREs and t-SNAREs can assemble reversibly into a four-helix bundles called trans-SNARE complexes. In synaptic vesicles these complexes are formed by three

SNAREs: two t-SNAREs (syntaxin 1 and SNAP-25) and synaptobrevin (also referred to as vesicle-associated membrane protein or VAMP-2), a v-SNAREs.

In neuronal exocytosis, syntaxin and synaptobrevin are moored in membranes by their C-terminal domains, whereas SNAP-25 is tethered to the plasma membrane via several cysteine-linked palmitoyl chains. The core trans-SNARE complex is a four-α-helix bundle, where syntaxin 1 and synaptobrevin contribute one by each, and SNAP-25 contributes two [*Sutton et al., 1998*] (figure 10). The interacting amino acid residues that zip the SNARE complex can be grouped into layers. Each layer has 4 amino acid residues - one residue per each of the 4 α-helices. In the center of the complex is the zero ionic layer that compose one arginine and three glutamine residues, and it is flanked by leucine zippering. At the center of the complex, most closely layers as '-1', '+1' and '+2', follow ideal leucine-zipper geometry and amino acid composition [*Fasshauer et al., 1998*]. The zero ionic layer is composed of Q226 from syntaxin-1A, R56 from VAMP-2, Q174 from Sn2 and Q53 from Sn1, and is completely buried within the leucine-zipper layers. The positively charged guanidino group of the arginine residue interacts with the carboxyl groups of each of the three glutamine residues (figure 11).

2.4.3 SNAREs and membrane fusion

During membrane fusion, v-SNARE and t-SNARE proteins on separate membranes combine to form a trans-SNARE complex. After fusion the membranes merge and SNARE proteins are then referred to as a cis-SNARE complex, which is then bound and disassembled by an adaptor protein, alpha-SNAP. Then, the SNARE complex unfolds in an ATP-dependent reaction, which is catalyzed by the hexametric AAA-ATPase NSF, in order to release them for recycling.

SNAREs are proposed to be the key components of the fusion machinery and can

work independently. This was demonstrated by engineering flipped SNAREs, disposing the SNARE domains facing the extracellular space. When these engineered cells expressing flipped t-SNAREs contact cells with flipped v-SNAREs, trans-SNARE complexes form and cell-cell fusion ensues [*Hu et al., 2003*].

2.4.3.1 Assembly of the SNARE complex

To provide the force that is required for vesicle fusion, SNARE proteins must assemble into trans-SNARE complexes. The rate-limiting step in the assembly of complexes is the association of the syntaxin SNARE domain, since its ability of interacting with other SNARE proteins is generally blocked by a closed state [*Burkhardt et al., 2008*]. When syntaxin 1 transits towards an open state, the four SNARE domains begin associating together at their N-terminal. The SNARE domains proceed in forming a coiled-coil motif in the direction of the C-termini of their respective domains.

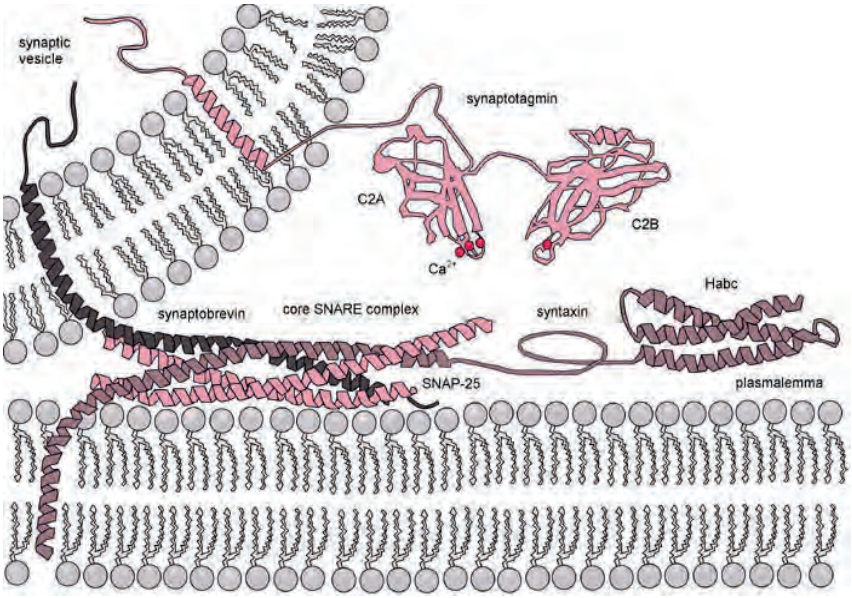

Figure 10: The SNARE complex. The core SNARE complex is formed by four α-helices contributed by synaptobrevin, syntaxin and SNAP-25, synaptotagmin serves as a calcium sensor and regulates intimately the SNARE zipping [By Danko Mimchev Georgiev].

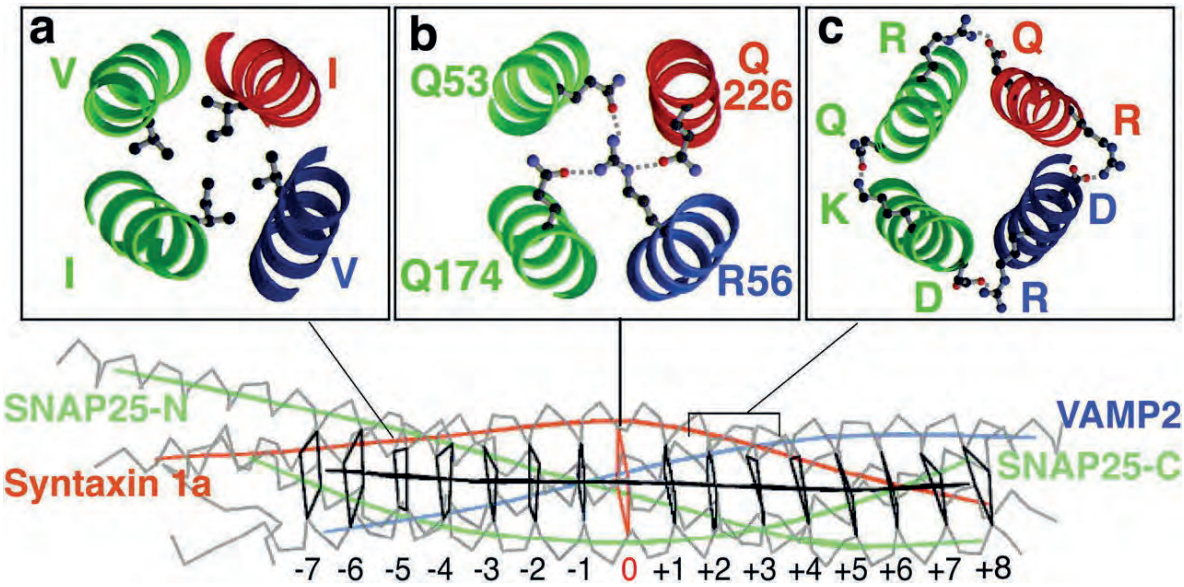

Figure 11: Structure of the neuronal SNARE complex [Fasshauer et al., 1998]. Structure of the four-helical bundle of the cis-SNARE (postfusion) core complex, with the syntaxin 1a coil in red, VAMP-2 in blue, and the two SNAP-25 coils in green. The central black polygons denote the 15 hydrophobic layers of the complex, with the central red ionic layer referred to as the zero layer. a) A cross section of a typical (the −5) hydrophobic layer, with ball and stick structures representing the indicated amino acids. b) The ionic layer with its three glutamines, Q226 from syntaxin, Q53 from SNAP-25 N-terminal coil, and Q174 from SNAP-25 C-terminal coil, and the arginine R56 of VAMP. The dotted lines indicate the three hydrogen bonds formed between these residues in the wild-type complex. c) Examples of electrostatic surface interactions (dotted lines) between the SNARE coils.

The SM protein (Sec1/Munc18 protein) is thought to act on the assembly of the SNARE complex, although its mechanism of action remains controversial. However it is well admitted that Munc18 acts as a chaperone protein for syntaxin 1 allowing its transport from the TGN to the plasma membrane. It is also well known that the clasp of Munc18 locks syntaxin in a closed conformation by binding to its alpha-helix SNARE domain, which inhibits the entry of synaptic fusion proteins into the SNARE complex [Burkhardt et al., 2008]. One hypothesis suggests that during the assembly of the SNARE complex, the Munc18 clasp releases the closed syntaxin remains associated with the N-terminal peptide of syntaxin and is then relegated to the newly formed four-helix SNARE complex [*Südhof and Rothman, 2009*]. It was more recently shown by single

molecule tracking by super-resolution that Munc18 regulates the formation of nanoclusters of syntaxin [*Kasula et al., 2016*].

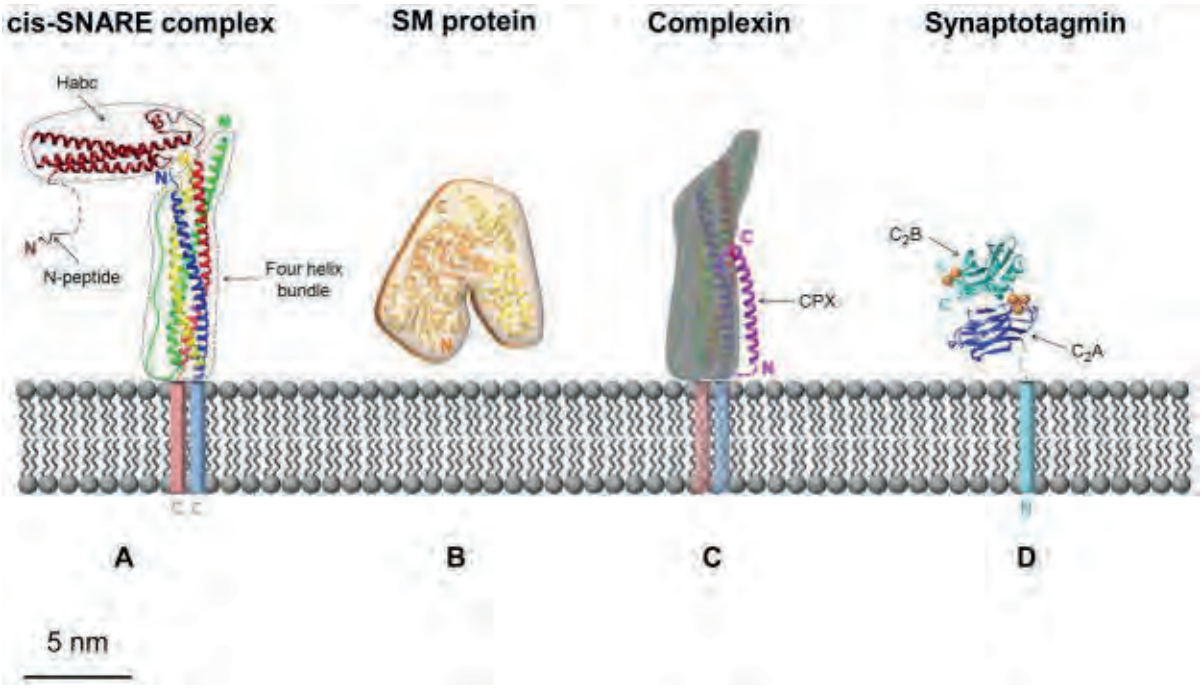

Figure 11: Structure of SNARE and SM proteins and some proteins that grapple with them (from *Südhof and Rothman, 2009)*.A) SNARE complex (also called cis-SNARE complex) of VAMP/synaptobrevin-2 (blue helix), Syntaxin-1A (red helix), and SNAP-25 (green and yellow helices for the N- and C-terminal domains, respectively). The Habc domain of Syntaxin-1A (brown helices) is positioned arbitrarily. B) An SM protein, highlighting its arch-like structure (Munc18). C) Complexin, bound to the SNARE complex (Complexin-1, shown in magenta), has a helical region that binds at the interface of v- and t-SNARE in an anti-parallel orientation. D) Synaptotagmin, the calcium sensor for synchronous synaptic transmission (Synaptotagmin-1), with its membrane-proximal (C2A) and membrane-distal (C2B) C2 domains labeled and the position of critical bound calcium ions (orange) shown. All proteins are at the same scale and the bilayer thickness is approximately on the same scale.

This possible dissociation mechanism and subsequent recombination with the SNARE domain may be calcium-dependent [*Jahn and Fasshauer, 2012*]. This supports the notion that Munc18 plays a key regulatory role in vesicle fusion. Under normal conditions the SNARE complex is blocked by Munc18, but when exocytosis is triggered,

Munc18 assists the SNARE-complex assembly, thereby acting as a fusion catalyst [*Südhof and Rothman, 2009*] (Figure 11). Recent work shows that two mutations in the vesicle-anchored v-SNARE selectively impair the ability of Munc18-1 to promote trans-SNARE zippering, whereas other known Munc18-1/SNARE-binding modes are unaffected. And these v-SNARE mutations strongly inhibit spontaneously as well as evoked neurotransmitter release, providing genetic evidence for the trans-SNARE-regulating function of Munc18-1 in synaptic exocytosis [*Shen et al., 2015*].

2.4.3.2 Membrane fusion

Membrane fusion is an energy-demanding event that requires translocation of proteins in the membrane, formation of highly curved membrane structure, before disruption of the lipid bilayer. The process of combining two membranes requires an input of energy to overcome the repulsive electrostatic forces between the membranes. The mechanism by which the movement of membrane-associated proteins away from the membrane contact zone is adjusted before fusion is unknown, but a local increase in membrane curvature is believed to contribute to the process. SNARE produces energy through protein-lipid and protein-protein interactions as a driving force for membrane fusion.

One model assumes that the force required to bind the two membranes together during fusion comes from the conformational change of the trans SNARE complex to form a cis SNARE complex. The assumption that currently describes this process is known as the SNARE "zipper." [*Chen and Scheller, 2001*]

When the trans SNARE complex is formed, the SNARE protein is still found on the opposite membrane. As the SNARE domains continue to coil during the spontaneous process, they form a tighter, more stable four-helix bundle. During this "zippering" of the SNARE complex, it is believed that a portion of the released energy from the bond is stored as molecular bending stress in each SNARE motif. It is assumed that this

mechanical stress is stored in the semi-rigid connection between the transmembrane domain (known as the stalk) and the SNARE helical beam [*Kiessling and Tamm, 2003; Wang et al., 2001*]. When the composite moves to the film fusion site on the periphery, the energy-favorable bending is minimized. As a result, the relief of stress overcomes the repulsive force between the vesicle and the cell membrane and presses the two membranes together [*Risselada et al., 2011*]. Following the "zippering" hypothesis, when the SNARE complex is formed, the tightening of the helical bundle exerts a torsional force on the transmembrane domain of synaptic vesicle proteins and synaptic fusion proteins [*Fang and Lindau, 2014*]. This causes the transmembrane domain to tilt within a separate membrane because the protein is more tightly entangled.

The unstable configuration of the transmembrane domain ultimately leads to the fusion of the two membranes, and the SNARE proteins cluster together in the same membrane, which is called the "cis"-SNARE complex. Due to lipid rearrangement, the fusion pores open and allow the chemical components of the vesicles to leak into the external environment (Figure 12).

Molecular simulations indicate that the proximity of the membrane enables the lipid to unfold, with a population of lipids inserting their hydrophobic tail into the adjacent membrane - effectively maintaining a "foot" in each membrane. The resolution of the unfolded lipid state proceeds spontaneously to form a stem structure. In this molecular view, the unfolded intermediate state of the lipid is the rate determining barrier rather than the formation of the stem, which now becomes the free energy minimum (Figure 13). The energy barrier to establish an expanded lipid conformation is proportional to the membrane spacing. Thus, the SNARE complex and its pressing of the two membranes together provide the free energy required to overcome the barrier [*Risselada and Grubmüller, 2012*]. The energy input required for SNARE-mediated fusion comes from the complex disassembly of SNARE. The suspected source of energy is an ATPase associated with membrane fusion, N-ethylmaleimide sensitive factor (NSF). The NSF homo hexamer, together with the NSF cofactor α-SNAP, binds and dissociates the SNARE complex by coupling this process to ATP hydrolysis [*Söllner et al., 1993*]. This process allows for the uptake of synaptic vesicle proteins for further use in vesicles,

while other SNARE proteins are still associated with cell membranes.

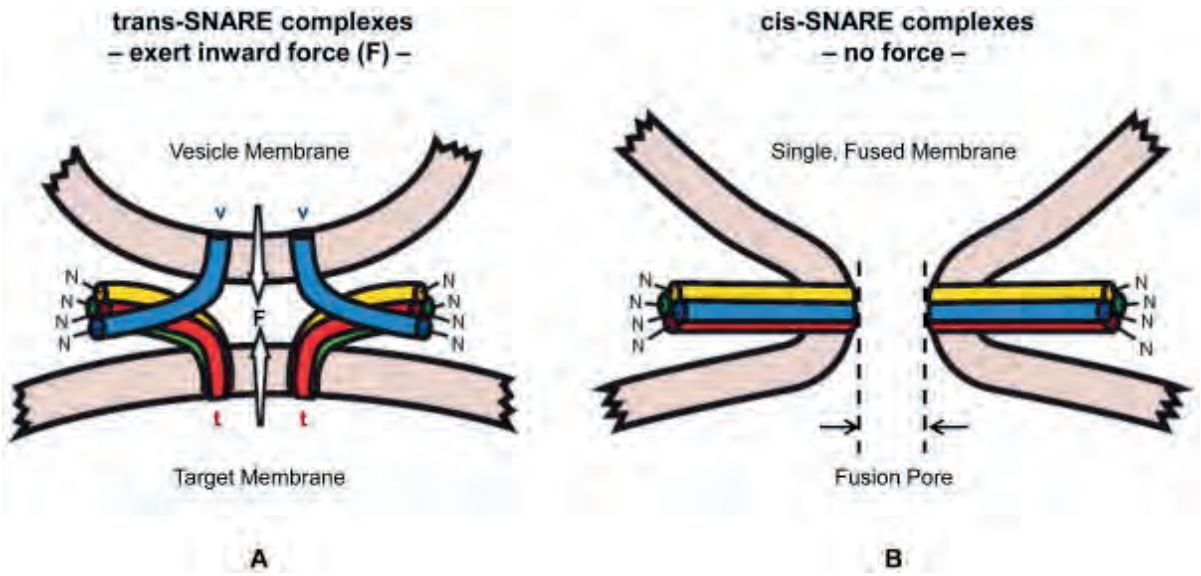

Figure 12: SNARE zippering model (Südhof and Rothman, 2009). A) The zippering model for SNARE-catalyzed membrane fusion. Three helices anchored in one membrane (the t-SNARE) assemble with the fourth helix anchored in the other membrane (v-SNARE) to form trans-SNARE complexes, or SNARE pins. Assembly proceeds progressively from the membrane-distal N-termini towards the membrane-proximal C-termini of the SNAREs. This generates an inward force vector (F) that pulls the bilayers together, forcing them to fuse. Complete zippering is sterically prevented until fusion occurs, so that fusion and the completion of zippering are thermodynamically coupled. B) Therefore, when fusion has occurred, the force vanishes and the SNAREs are in the low energy cis-SNARE complex

The dissociated SNARE protein has a higher energy state than the more stable cis SNARE complex. It is believed that the energy that drives the fusion comes from a transition to a lower energy cis-SNARE complex. The ATP hydrolysis coupled dissociation of the SNARE complex is an energy investment that can be compared to a "warp gun" so that once the vesicle fusion is triggered, the process spontaneously occurs at an optimal rate. A similar process occurs in the muscle where the myosin head must first hydrolyze ATP to accommodate the necessary conformation with actin interaction and subsequent power stroke.

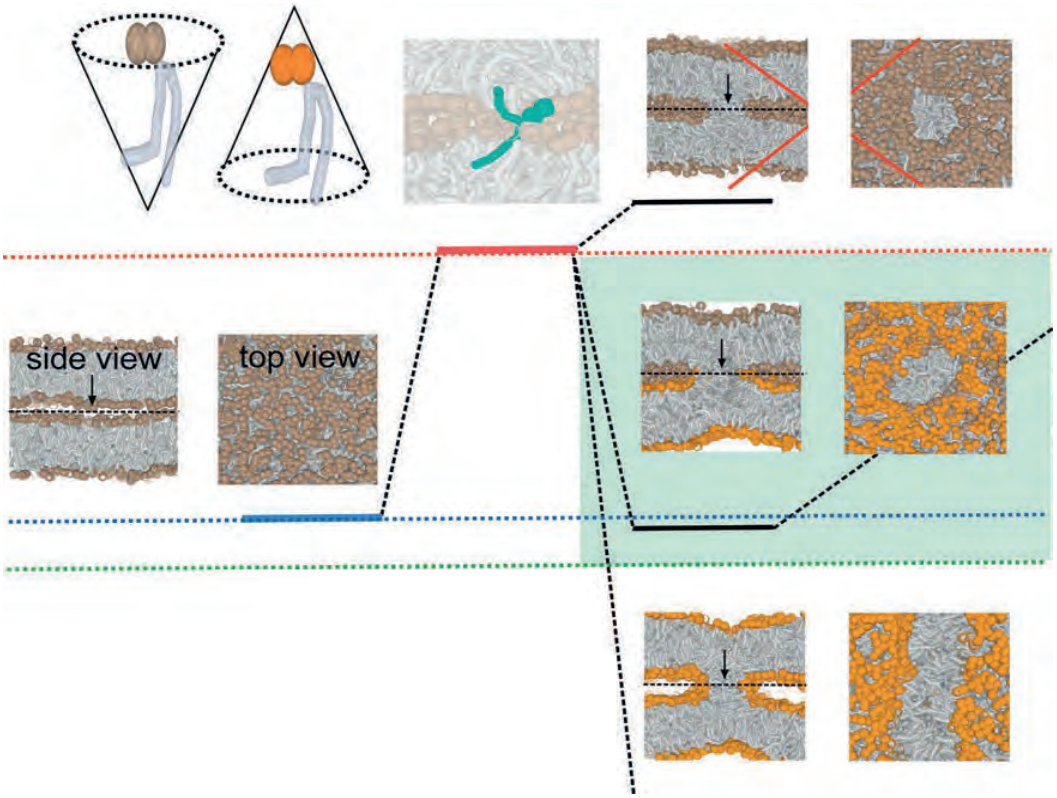

Figure 13: Energetics of stalk formation [*Risselada and Grubmüller, 2012*].

(a) Unfused bilayers. (b) At a constant inter-membrane distance, the free energy of the splayed lipid (DG) is not expected to depend on the head-group type (spontaneous curvature). (b), (c) and (e) The free energy of the stalk itself, however, depends on both the spontaneous curvature (plotted cone) and separation distance and these will determine whether a formed stalk is metastable or not [31_]. (c) At such an inter-membrane distance, the stalk formed between two DOPC membranes is an unstable transient intermediate. (d) The stalk is metastable when its free energy is lower than both the dissociation barrier and expansion barrier. (e) In the HII-phase the formed hourglass-shaped (rhombohedral) stalk structure is unstable (no expansion barrier) and the stalk will continuously elongate to maximize its energetically favorable negatively curved perimeter. The barrier of stalk formation is determined by the free energy of the stalk intermediate (DG). However, this barrier excludes the additional energy that is required to bring the two membranes within such proximity (inter-membrane repulsion). This inter-membrane repulsion includes the known relation between spontaneous curvature and fusogenicity. Hence, an intrinsic negative curvature reflects the inability of the lipid head-group to sufficiently shield its hydrophobic moiety when arranged in a planar conformation. As a result the membrane surface becomes more hydrophobic which lowers the energetic cost of leaflet approach.

2.5 After Membrane fusion

Membrane fusion during exocytosis can occur through three different modes in secretory cells, depending on the physiological demand: kiss and run, cavicapture, or full-collapse fusion [*Tanguy et al., 2016*]. After full-collapse fusion of the synaptic vesicles or secretory granules upon stimulation, the vesicular membrane components can be entirely recycled by a clathrin-mediated compensatory endocytotic process for secretory granules [*Ceridono et al. 2011*] and by ultrafast, bulk or clathrin-mediated endocytosis for synaptic vesicles [*Maritzen and Haucke, 2018*]. It is of note that these processes allow cells to maintain membrane size homeostasis despite intensive membrane addition by exocytosis. Molecular mechanisms underlying the preservation of granule membrane identity after fusion with plasma membrane remains unclear, but it has been proposed that specific lipid microdomains might contribute to prevent diffusion of membrane components for secretory granules. Hence, exo-endocytosis coupling leads then to recycling of post-exocytotic internalized granule membrane back to the Golgi apparatus or to a recycling pool of vesicles, starting a new life for the secretory vesicle [*Houy et al. 2013*]. Recently lipids generated upon exocytosis have also been proposed to contribute to the exo-endocytosis coupling [*Yuan et al. 2015*].

2.6 Regulation of the SNARE complex

A) Regulation via SNAP-25 palmitoylation

The Q-SNARE protein synaptosome associated protein 25 (SNAP-25) consists of two alpha-helical domains joined by a randomly coiled linker. The most striking aspect of the random coil junction region is its four cysteine residues [*Bock et al., 2010*]. The α-helical domain binds to synaptic fusion proteins and synaptic vesicle proteins (also known as vesicle-associated membrane proteins or VAMP) to form a 4-α-helical

coiled-coil SNARE complex that is essential for effective exocytosis.

Although both syntaxin and synpatobrevin contain transmembranes domain that allows for docking to the target membrane and vesicle membrane, the function of SNAP-25 is dependent on palmytoylation of these cysteine residues found in the random coiled region. Acylation of SNAP-25 allows its docking to the target membrane. Some studies have shown that the association of SNARE interactions with synapses precludes the need for such docking mechanisms. However, synaptic knockdown studies failed to show a decrease in membrane-bound SNAP-25, suggesting the existence of alternative docking means [*Greaves et al., 2010b*]. Thus, covalent attachment of a fatty acid chain to SNAP-25 by attachment of a thioester to one or more cysteine residues provides for the regulation of docking and eventual SNARE-mediated exocytosis. This process is mediated by a specialized family of enzymes called DHHC palmitoyl transferases [*Greaves et al., 2010a*]. The cysteine-rich SNAP-25 domain also appears to be weakly associated with the plasma membrane, possibly localizing it near the enzyme for subsequent palmitoylation. The reversal of this process is carried out by another enzyme called palmitoyl thioesterase.

The availability of SNAP-25 in the SNARE complex is also theoretically likely to be spatially regulated by the localization of lipid domains in the target membrane. The palmitoylated cysteine residue can be localized to the desired target membrane region by a favorable lipid environment (possibly rich in cholesterol) complementary to the fatty acid chain to which the cysteine residue of SNAP-25 is bound [*Greaves et al., 2010b*].

When the action potential reaches the end of the axon, the depolarization event stimulates the opening of the voltage-gated calcium channel (VGCC), allowing calcium to flow rapidly to lower its electrochemical gradient. Calcium major stimulation action of exocytosis occurs through binding to synaptotagmin-1. However, surprisingly SNAP-25 has been shown to negatively regulate VGCC function in glutamatergic

neuronal cells. SNAP-25 causes a decrease in current density through VGCC, and thus a decrease in the amount of calcium bound to synaptotagmin, resulting in a decrease in neuronal glutamatergic vomiting. In contrast, low expression of SNAP-25 increases VGCC current density and increases exocytosis [*Condliffe et al., 2010*].

Further studies suggest that there may be a link between SNAP-25 expression levels and various brain diseases. In the attention deficit/ hyperactivity disorder (ADHD), the polymorphism of the human SNAP-25 locus is associated with the disease [*Corradini et al., 2009*], which is further demonstrated by a heterogeneous SNAP-25 knockout study of the coloboma mutant mice model. This led to the phenotypic characteristics of ADHD [*Hess et al., 1992*]. Studies have also shown a correlation between SNAP-25 expression level and the onset of schizophrenia [*Thompson et al. 1998; Gabriel et al., 1997*].

B) Syntaxin and Habc domains

The synaptic fusion protein consists of a transmembrane domain (TMD), an alpha-helical SNARE domain, a short linker region, and a Habc domain consisting of three alpha-helix regions. The SNARE domain in syntaxin serves as a target site for docking of SNAP-25 and synaptic vesicle proteins to form a SNARE complex and a four-helix bundle necessary for subsequent fusion. However, the Habc domain acts as an autoinhibitory domain in syntaxin. It has been shown to fold and associate with the SNARE domain of the syntaxin to induce a "closed" state, thereby forming a physical barrier to the formation of the SNARE motif. In contrast, the Habc domain can again dissociate from the SNARE domain, allowing syntaxin to bind freely to SNAP-25 and synaptic vesicle proteins [*MacDonald et al., 2010*].

C) Syntaxin interaction with lipids

The juxtamembrane domain adjacent to the TMD of syntaxin 1 was shown to bind to anionic lipids such as phosphoinositides and phosphatidic acid [*Lam et al., 2008*].

Mutations in this domain reduced the number of exocytotic events in bovine chromaffin cells, but also affected the fusion pore stability arguing that the interaction of syntaxin 1 with specific lipids is important for proper membrane fusion [*Lam et al., 2008*].

D) Syntaxin 1B and an easily released vesicle pool

There is a huge diversity of syntaxin subtypes, and there are 15 variants in the human genome [*Teng et al., 2001*]. It has been suggested that syntaxin1B plays a role in regulating the number of synaptic vesicles prepared by exocytosis in the axon terminal. This is called readily releasable pool (RRP). A knockout study in 2014 showed that the lack of syntaxin1B led to a significant decline in RRP size [*Mishima et al., 2014*]. Many neurotoxins directly affect the SNARE complex. These toxins, such as botulinum and tetanus toxins, act by targeting the SNARE component. These toxins prevent proper vesicle recirculation, leading to poor muscle control, paralysis, paralysis, and even death (figure 14).

2.7 Exocytosis and V-ATPase

V-ATPase is a protein essential for cell survival by its proton pump activity. Accordingly studying an additional role of V-ATPase independent of proton transport has been difficult by approaches involving robust depletion of V-ATPase such as knockdown or knockout. Moreover, since V-ATPase is involved in neurotransmitter loading of synaptic vesicles, it is very difficult to study an independent role of this protein in exocytosis. Indeed, disrupting V-ATPase by conventional approaches, including the use of drugs inhibiting V-ATPase, will inevitably disrupt the loading of vesicles into neurotransmitters. Despite these difficulties, several teams have demonstrated in various organisms the role of V-ATPase, and more specifically of its V0 domain, in exocytosis independently of its role of proton transport.

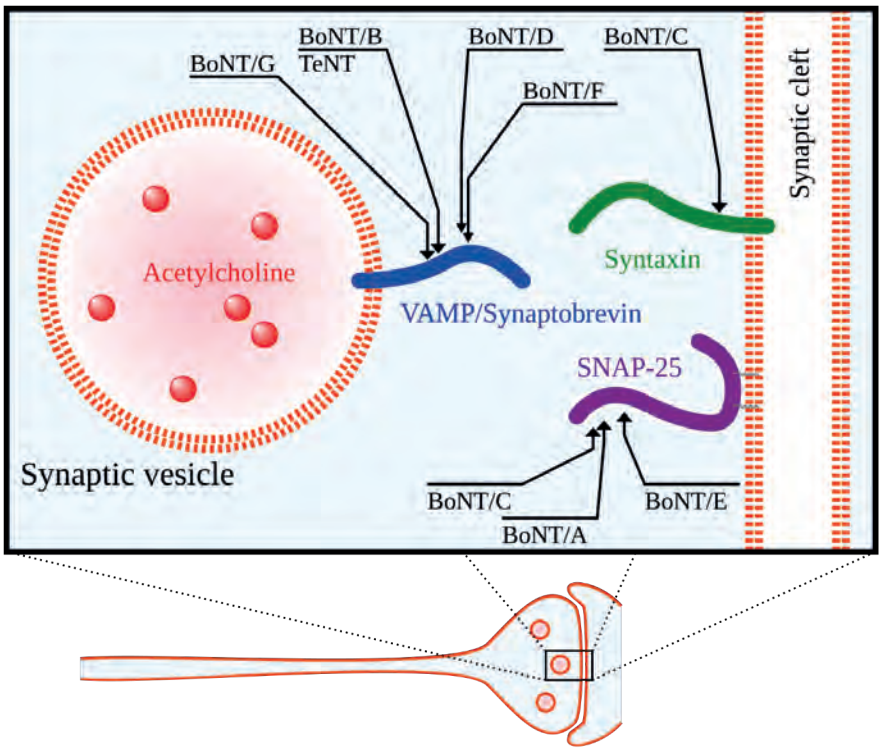

Figure14: Target SNARE proteins of botulinum neurotoxin (BoNT) and tetanus neurotoxin (TeNT) in the axon terminal [*Barr et al., 2005*].

2.7.1 V-ATPase and fusion of yeast vacuoles

The presence of the V0 domain of V-ATPase in the yeast vacuole membrane is required for their fusion [*Peters et al., 2001, Bayer et al., 2003*]. This role of V0 appears independent of proton transport by V-ATPase since it is conserved under conditions where domain VI is absent [*Peters et al., 2001*]. These authors also observed that trans-dimers of V0 domains are formed during the fusion reaction after the formation of SNARE complexes. Finally, by double immunoprecipitation experiments, the authors have shown that the V0 trans-dimer interacts with the Q-SNARE proteins. These experiments, therefore, lead to a yeast vacuole fusion model in which the binding of the vacuoles by the SNAREs complexes allows the formation of a protein fusion pore formed by a trans-dimer of V0 domains. However, the fusion of yeast vacuoles remains

possible if V-ATPase V0 domains are present in at least one of the two vacuoles [*Takeda et al., 2008; El Far and Seagar, 2011*]. The presence of a V0 domain is necessary for the fusion of yeast vacuoles but the trans-dimer of V0 is not an obligatory step of the fusion.

2.7.2 Role of V0 in exocytosis

Many researches showed that v-ATPase had a role in exocytosis independent of its role as a proton pump. For instance, drosophila-carrying mutations of the gene encoding the a1 subunit lose their sight [*Hiesinger et al., 2005*]. Interestingly, it has been shown by electrophysiology that the amplitude of the spontaneous postsynaptic potentials is not modified in the mutants of this gene while their frequency is decreased. An interpretation of these observations is that the secretory vesicles are well filled with neurotransmitters, but that their release seems to be hampered. The absence of the a-subunit must therefore probably be compensated by another isoform of the a subunit to allow the acidification, and thus the loading of NTs into the vesicles. Moreover, the amplitude of the post-synaptic potentials evoked is very small in the mutants, reflecting a decrease in the number of vesicles released. These mutations thus seem to prevent the a1 subunit from playing a role in the exocytosis of the secretory vesicles.

In 2006, the role of the V0 domain of V-ATPase in exocytosis was also shown in Caenorhabditis elegans [*Liegeois et al., 2006*]. The authors followed the release of morphogenic factors leading to the formation of a structure called Alae on the surface of the worm. The secretion of these factors is made from multi-vesicular bodies (MVB), which are acidic organelles. It had been found that some mutations of the subunit α-5 isoform affect proton transport and the role of V0 domain in exocytosis of MVB. The phenotypes associated with these two perturbations are: 1) transport of protons alteration: The excretory canal, the equivalent of the urine collecting tube in mammals, has an increased surface compensating for the least good transport of protons by the v-ATPases containing vha-5 2) exocytosis alteration: a defect of formation of Alae. Some

mutations of vha-5 have no effect on the excretory canal but prevent the formation of Alae. These mutations, therefore, disrupt the role of V0 in the exocytosis of MVBs. Interestingly, in these mutants, the absence of other malformations of the epidermis shows that the role of vha-5 in proton transport can be compensated by another isoform of the a: vha-7 subunit (not expressed in the excretory duct). On the other hand, the role of the V0 domain in exocytosis seems to be specific to V0 containing the isoform vha-5 of the subunit a. Indeed, vha-7 expressed in this fabric doesn't allow its compensation.

In a search for mutants defective in insulin secretion in response to glucose administration, a decrease of insulin level in the blood had been measured in mice not expressing the a3 subunit of V-ATPase [*Sun-Wada et al., 2006; Xiong et al., 2017*]. However, secretory vesicles were well loaded with mature insulin in these mutants. Maturation of insulin occurs only in an acid compartment. It was shown that these mutants expressed the isoform a2, which compensated for the absence of a3 and allowed the acidification of these vesicles, but could not compensate for exocytosis. This suggests that the a3 subunit is involved in the release of insulin regardless of its role in proton transport.

It has been also proposed that the V-ATPase membrane domain is a sensor of granular pH that controls the exocytotic machinery [*Poëa-Guyon et al., 2013*]. A rapid decrease in neurotransmitter release after acute photoinactivation of the V0 a1-I subunit in neuronal pairs was shown. Inactivation of the V0 a1-I subunit in chromaffin cells resulted in a decreased frequency and prolonged kinetics of amperometric spikes induced by depolarization and dissipation of the granular pH gradient was associated with an inhibition of exocytosis and correlated with the V1–V0 association status in secretory granules. Thus it had been proposed that V0 serves as a sensor of intragranular pH that controls exocytosis and synaptic transmission via the reversible dissociation of V1 at acidic pH. Hence, the V-ATPase membrane domain would allow the

exocytotic machinery to discriminate fully loaded and acidified vesicles from vesicles undergoing neurotransmitter reloading.

2.7.3 Interaction between V-ATPase and SNAREs

It has been proposed early on that V0 could be a component of the fusion pore [*Morel et al., 2001; Peters et al., 2001*] and could favor lipid mixing and the formation of a lipidic fusion pore [*El Far and Seagar, 2011; Strasser et al., 2011*], but recent work shows that V-ATPase membrane V0 sector has no direct role in synaptic vesicle fusion [Bodzęta et al., 2017]. Indeed, V0 has been shown to interact with SNARE proteins in various models and may thus contribute to exocytosis by regulating the SNARE machinery rather than forming a pore by itself [*Peters et al., 2001; Morel et al., 2003; Di Giovanni et al., 2010*].

Some studies have shown that V-ATPase and more particularly its V0 domain interacts with SNARE proteins, so that interactions between VAMP2 and the V0 domain have been demonstrated in rat synaptosomes, as well as in PC12 cells [*Galli et al., 1996; Morel et al., 2003*]. This interaction occurs between VAMP2 and a subunit of V0 domain having lost its domain VI [*Galli et al., 1996; Morel et al., 2003; Xiong et al., 2017*]. Recently, this interaction has been characterized as a direct interaction between the subunit c of the V0 domain and the VAMP2 at the proximal domain, between the transmembrane domain and the SNARE motif [*Di Giovanni et al. 2010*].

Other studies have demonstrated interactions between the V0 domain of V-ATPase and Q-SNAREs. In the yeast vacuole fusion model, an interaction between the V0 domain and yeast syntaxin was reported [*Peters et al., 2001*]. Thereafter, direct interactions between the a1 subunit of the V0 domain of Drosophila and syntaxin-1/SNAP25 have been demonstrated [*Hiesinger et al., 2005*]. The interaction

between syntaxin-1 and V0 seems to involve the proximal domain of syntaxin-1, as the interaction between VAMP2 and subunit c [*Li et al., 2005*].

Moreover, the V-ATPase, which in the nerve terminal is essentially known for its localization to synaptic vesicles, has been demonstrated to be also present in the presynaptic membrane [*Morel et al., 2003*]. The interactions between the V0 domain and Q-SNAREs can therefore potentially occur in *cis* (all proteins in the presynaptic membrane), or in *trans* (V0 in the vesicle and Q-SNAREs in the presynaptic membrane). Finally, the interaction between SNAREs complexes and the V0 domain of V-ATPase was observed by immunoprecipitation using an antibody specifically recognizing assembled SNARE complexes [*Morel et al., 2003*].

Altogether these results have thus shown that V-ATPase, in addition to its critical role in secretory vesicle acidification, also directly contributes to exocytosis as a constituent of the fusion machinery.

Chapter 3: Objectives

3.1 V-ATPase and the regulation of exocytosis: Modulation of fusogenic lipid synthesis

It was shown in several secretory cell model systems, including neuroendocrine cells, that the enzyme phospholipase D1 (PLD1) produces phosphatidic acid (PA) that favors one or several steps of the late stages of exocytosis (*Tanguy et al., 2017*). The PA produced in this specific location may favor the membrane curvatures necessary for the fusion and/or modulate the functions of the SNARE complex (*Vitale et al., 2001; Zeniou-Meyer et al., 2007*). It has also been shown that the activity of PLD1 during exocytosis is regulated by GTPase ARF6 and its GEF ARNO, both playing a positive role in regulated exocytosis (*Caumont et al., 2000; Vitale et al., 2002; Béglé et al., 2009*).

Interestingly, ARNO interacts with the a2 subunit of the V-ATPase and Arf6 interacts with the subunit c of V-ATPase on endosome from epithelial cells (*Hurtado-Lorenzo et al., 2006*). It was further shown that V0 recruits ARNO and Arf6 to endosomes in an acidification-dependent manner (*Hurtado-Lorenzo et al., 2006)*

Since V-ATPase is present on secretory granules where Arf6 was also identified (*Caumont et al., 2000*), I wanted to probe the possibility that V0 could, in addition to its ability to regulate SNARE function, also control membrane fusion via the regulation of ARNO-Arf6-PLD1 triade.

3.2 Is V-ATPase a sensor for fusion competence?

The V-ATPase activity generates a large electrochemical proton gradient in synaptic

vesicles of neurons and in secretary granules of neuroendocrine chromaffin cells for an inter-vesicle pH between 5.2–5.5 [*Michaelson and Angel, 1980; Füldner and Stadler, 1982*]. This electrochemical proton gradient energizes the filling of neurotransmitters in synaptic vesicles and secretory granules. A low intragranular pH is also required for catecholamine binding to chromogranins within the secretory granules [*Camacho et al., 2006*].

Independently of its well-established role in proton translocation, V0 has also been implicated in neurotransmitter release [*Hiesinger et al., 2005*], in intracellular membrane fusion [*Peters et al., 2001; Peri and Nüsslein-Volhard, 2008; Williamson et al., 2010; Strasser et al., 2011*], and in exocytosis [*Liégeois et al., 2006*], suggesting that V0 could be directly involved in the fusion between two membrane compartments. The work of our team has shown that the trans-membrane domain of V-ATPase could be an intra vesicular pH sensor during exocytosis [*Poëa-Guyon et al., 2013*]. Although the dissociation of V1 and V0 domain could be a pH-depend process [*Hurtado-Lorenzo et al., 2006*], the mechanism associated with pH sensing to regulate exocytosis is not clear.

Thus, in the second party of my thesis I wanted to probe the notion that V0/V1 association/dissociation could represent a sensor for vesicle replenishment in neurotransmitter. Indeed it is possible that the vesicle that will be used for release only represent the proportion of fully loaded vesicles in neurotransmitter. To probe this model I probed a) the relationship between intra vesicular pH and the dissociation of V1 and V0 domain, b) the dynamic of interaction between V0 domain and ARNO, and the relation between this interaction and intra vesicular pH.

Chapter 4: Results

4.1 Results of part I

Recent pioneer studies have shown that lipid compartmentalization is important at the exocytotic sites and validated the contribution of fusogenic lipids such as phosphatidic acid (PA) for membrane fusion. The V-ATPase is involved both in vesicle loading in neurotransmitters and vesicle fusion. Indeed the V1 and V0 subdomains were shown to dissociate during stimulation allowing subunits of the vesicular V0 to interact with different proteins of the secretory machinery. We show here that V0a1 interacts with the exchange factor ARNO and promotes Arf6 activation during exocytosis in neuroendocrine cells. Interfering with the V0a1-ARNO interaction prevented phospholipase D (PLD) activation, phosphatididic acid synthesis during exocytosis, and altered the kinetic parameters of individual fusion events. These results are shown here as a manuscript in preparation for publication.

V-ATPase modulates exocytosis in neuroendocrine cells through the activation of an ARNO-Arf6-PLD pathway and the synthesis of phosphatidic acid.

Qili WANG[1], Tamou THAHOULY[1], Ludovic RICHERT[2], Yves MELLY[2], Sylvette CHASSEROT-GOLAZ[1], Stéphane ORY[1], Stéphane GASMAN[1], Marie-France BADER[1], and Nicolas VITALE[1]*

[1] Institut des Neurosciences Cellulaires et Intégratives, CNRS UPR 3212 and Université de Strasbourg, 5 rue Blaise Pascal, Strasbourg 67000, France

[2]Laboratoire de Bioimagerie et Pathologies, CNRS UMR 7213 and Université de Strasbourg, Faculté de Pharmacie, 74 route du Rhin, Illkirch 67401, France

[*] Corresponding authors: vitalen@inci-cnrs.unistra.fr

Key words: Arf6, ARNO, exocytosis, phosphatidic acid, phospholipase D, V-ATPase

Abstract

Despite increasing evidence that lipids play key cellular functions and are involved in an increasing number of human diseases, little information is available on there exact function. This is especially the case in neurosecretion that relies on the fusion of specific membrane organelle with the plasma membrane for which relatively little attention has been paid to the necessary role of lipids. However recent pioneer studies have established the importance of lipid compartmentalization at the exocytotic sites and validated the contribution of fusogenic lipids such as phosphatidic acid (PA) for membrane fusion. Nevertheless the mechanisms allowing the regulation of the fine dynamics of these key lipids during neurosecretion remains poorly understood. The V-ATPase is involved both in vesicle loading in neurotransmitters and vesicle fusion seems to represent an ideal candidate to regulate the fusogenic status of secretory vesicles according to their replenishment state. Indeed the V1 and V0 subdomains were shown to dissociate during stimulation allowing subunits of the vesicular V0 to interact with different proteins of the secretory machinery. We show here that V0a1 interacts with the exchange factor ARNO and promotes Arf6 activation during exocytosis in neuroendocrine cells. Interfering with the V0a1-ARNO interaction prevented phospholipase D (PLD) activation, phosphatididic acid synthesis during exocytosis, and altered the kinetic parameters of individual fusion events. Altogether these data suggest that V1 dissociation from V0

could represent the signal that triggers the activation of the ARNO-Arf6-PLD1 pathway and promotes PA synthesis needed for efficient exocytosis in neuroendocrine cells.

Introduction

Neurotransmitters, neuropeptides and hormones are released by neurons and neuroendocrine cells by calcium-regulated exocytosis of synaptic vesicle (SV) and large dense core vesicle (LDCV), respectively. This process can be divided into multiple steps including vesicle biogenesis, maturation and transport, followed by vesicle docking at the exocytotic site and priming, when vesicles fully acquire the ability to fuse and release their contents in response to Ca^{2+} influx (1). Ca^{2+} entry through voltage-gated channels is detected by Ca^{2+} sensor proteins, which ultimately trigger the membrane fusion machinery (2). A transient fusion pore connecting the vesicle lumen to the extracellular space opens allowing diffusion of neurotransmitters and hormones outside cells. Based on the “kiss and run” model, this pore can either close or expand to allow partial or full vesicle collapse into the plasma membrane (3). Ultimately partially or fully empty secretory vesicles are retrieved by endocytosis and recycled for a novel round of secretion after replenishment with neurotransmitters.

The implication of SNARE proteins in vesicular transport is ubiquitous in eukaryotes. The classical SNARE complex responsible for neurosecretion involves the v-SNARE synaptobrevin (VAMP2), anchored in the vesicle membrane, and the t-SNAREs syntaxin 1 and SNAP-25, which are predominantly inserted in the plasma membrane (4). It is generally accepted that SNAREs, assisted by the Ca^{2+}-sensor synaptotagmin, can directly promote lipid bilayer fusion. The nature of the fusion pore is also a matter of debate and it seems likely that distinct modes of transmitter release reflect differences in the molecular organization of the membrane fusion machinery. Thus SNARE assembly might provide force to mix lipids mechanically or alternatively pin membranes together and provide scaffolding for proteins that act downstream to form a channel-like pore or catalyze rearrangements of lipid pore intermediates (5, 6).

V-ATPases are large multimeric enzymes organized in two domains, V1 and V0. The cytosolic V1 domain contains eight different subunits (A-H) with subunits A responsible for ATP hydrolysis, thereby providing the energy for the V0 membrane domain to translocate protons. V0 contains a, c”, d and e subunits associated to five subunits c (7). V-ATPase is expressed in all eukaryotic cells, with the primary function of proton pumping. V-ATPase activity can be

controlled by different means, including subcellular targeting of different isoforms, expression level and stability of the different subunits, coupling efficiency of ATP-hydrolysis to proton transport, and reversible association of V0 and V1 subdomains (8). V-ATPase is virtually found in all intracellular membrane compartments, including synaptic vesicles and secretory granules where it generates vesicular proton gradients and membrane potential. Acidification of these organelles is required for many cellular processes (e.g. maturation or degradation of proteins, receptor-mediated endocytosis, proton-coupled transport of small molecules) (7). These gradient and potential are also needed for neurotransporter uptake by selective transporters in synaptic vesicles and secretory granules (9).

Independent of its role in proton translocation, V0 has been more recently implicated in intra-cellular membrane fusion (10-13), neurotransmitter release (14-15) and exocytosis (16-17), suggesting that V0 is directly involved in the fusion between two membrane compartments. Exocytotic release of transmitter molecules packaged in synaptic vesicles or secretory granules is a highly regulated process that allows vesicles to fuse with the plasma membrane and it was originally proposed that V0 could be a component of the fusion pore (10, 18), or that it could favor lipid mixing and the formation of a lipidic fusion pore (13, 19). Indeed V0 has been shown to interact with SNARE proteins (10, 14, 20-22). In addition V0 could also behave as a pH sensor (23, 24) that could participate in the priming steps that render secretory vesicles competent for exocytosis (21). The drawbacks of these earlier studies relying on genetic long-term invalidation of specific subunits are that these approaches do not allow excluding the possibility that the observed membrane fusion deficits indirectly result from alterations in the pH gradient. The use chromophore-assisted light inactivation (CALI) technique inserting a small tetracystein motif and allowing specific inactivation of V0 or V1 subunits upon light illumination more recently validated to notion that photo-inactivation of the V0c or V0a subunits leads to a rapid impairment of synaptic transmission in neurons and of catecholamine release in chromaffin cells (17, 25).

Although the original idea that V0 could form the fusion pore between synaptic or secretory vesicles and the plasma membrane has been recently ruled out (26, 27), the exact mode of action by which V-ATPase regulates exocytosis remains elusive. Interestingly, a direct interaction between V0c and VAMP2 has been observed in mammalian neurons, establishing a first link with SNARE-dependent exocytosis. A second interesting lead comes from a fascinating study revealing an interaction between V-ATPase

and the pair Arf6/ARNO in endosomes (23). Arf6 is a mall GTPase mainly involved in vesicular trafficking and control of signaling lipid synthesis, whereas ARNO is a guanine exchange factor (GEF) for Arf proteins including Arf6. As Arf6 and ARNO were shown to be essential regulators of exocytosis through the activation of phospholipase D1 (PLD1) and the synthesis of phosphatidic acid near exocytotic sites (28-37), we decided to explore the possibility that the V-ATPase could modulate this pathway. We report here that V0a1 interacts with ARNO in neuroendocrine cells. Overexpression of a GFP-tagged N-terminal V0 peptide, thereby inhibiting the interaction between V0 and ARNO, prevented both Arf6 and PLD activation, and also strongly reduced exocytosis recorded from cells by carbon fiber amperometry, in a manner very similar to what was found after PLD1 knockout, supporting the notion of interplay between V0 and the ARNO/Arf6/PLD pathway in regulated exocytosis.

Results

ARNO and V0a interact during exocytosis in neuroendocrine cells. Both co-immunoprecipitation and pull-down experiments revealed an interaction of ARNO with the V0a2 subunit of the V-ATPase along the endolysosomal pathway in epithelial cells (38). We used a FRET approach based on lifetime measurements by fluorescence lifetime imaging microscopy (FLIM) to investigate the interaction between ARNO and V0a1, the a subunit of V0 that is associated with secretory granules in chromaffin cells (Figure 1). In FLIM-FRET, the nanosecond-scale decay pattern of emission, known as fluorescence lifetime, is measured. Exciting the donor with an ultra-short pulse of light and then measuring the photon distribution at the nanosecond scale provides information on fluorescence lifetime values. Quenching of donor emission by FRET interaction results in a decrease in the lifetime of the acceptor. Compared to the classical intensity-based FRET approaches, FLIM-FRET has many advantages as i) lifetime decay is not as sensitive to fluorescence intensity and does not require calibration, ii) no interference of possible spectral cross-talk between acceptor and donor, iii) it is internally calibrated and thus independent of donor and acceptor concentrations, iv) it enables the identification of fractions of molecules involved in FRET. However the major drawback of the technique is that since many photons need to be measured to achieve a high signal-to-noise ratio, acquisition times for conventional laser scanning FLIM are in the order of minutes.

FLIM measurements of V0a1-nowGFP revealed a significant reduction in the lifetime of nowGFP after 2 minutes of

stimulation of exocytosis. Interestingly we noted a strong increase of FLIM signal between 1800 and 1950 ps (Figure 1, blue box) at the expense of the signal observed between 2100 and 2250 ps (Figure 1, red box). These observations suggest that a subpopulation of V0a1-nowGFP is probably getting in close proximity to ARNO-shadowG after cell stimulation. It is of note that our FRET-FLIM measurements take around 60s, which does not allow to precisely follow individual V0a1 signal on individual secretory granules, of which most display significant motion during this time interval. Quantification analysis indicated that individual cells did not respond with similar kinetics, but that on average the most important drop in half-life appeared after 2 minutes of stimulation and that the signal was close to the control non-stimulated condition, 5 minutes after stimulation (Figure 1).

Preventing V0a-ARNO interaction abolishes Arf6 activation during exocytosis in neuroendocrine cells. We previously reported that Arf6, a key regulator of PLD1 for exocytosis (32), is activated by the GEF ARNO (36). Overexpression of the amino-terminal domain of V0a1 was previously shown *in vitro* to prevent the GDP/GTP exchange activity of ARNO on Arf6 (23). Combining this approach by expressing this short competing peptide fused to GFP together with the expression of MT2-YFP, a reporter for GTP-loaded active Arf6 in cells (36, 39), we found that Arf6 activation observed when exocytosis is triggered in PC12 cells by a depolarizing potassium solution was severely impaired by GFP-V0a1 N-terminus expression. Indeed in control untransfected cells or cells expressing GFP, MT2-YFP was recruited to the plasma membrane upon cell stimulation as revealed by an increase of colocalization with the plasma membrane marker SNAP-25 (Figure 2). This plasma membrane recruitment of MT2 in stimulated cells is largely abolished in cells expressing GFP-V0a1 (Figure 2). These data suggest that V0a-ARNO interaction may be essential for proper activation of Arf6 during exocytosis. In other words V0a1 could be a regulator of the GEF activity of ARNO towards Arf6 during exocytosis.

Preventing V0a-ARNO interaction abolishes PLD activation during exocytosis in neuroendocrine cells. An increase in PLD activity during exocytosis was reported in different cellular models including neuroendocrine chromaffin and PC12 cells and appears to predominantly depend on PLD1 activation (29, 40). Several regulators of PLD1 during exocytosis have been identified including the kinase Rsk2 (41) and several small GTPases, including RalA, Rac1, and Arf6 (36, 42-44). Accordingly

PLD activity measured from cell extracts nearly doubled after exocytosis stimulation in control mock-transfected cells or in cells expressing GFP alone (Figure 3). Strikingly overexpression of V0a1-YFP strongly prevented this activity-dependent increase in PLD activity (Figure 3), suggesting that V0a-ARNO interaction may be essential for optimal stimulation of PLD during exocytosis. These data also reveal that the Arf6 activation pathway represents a major contributor of PLD activity required for exocytosis.

Preventing V0a-ARNO interaction abolishes PA synthesis at the exocytotic sites during exocytosis in neuroendocrine cells. Increased levels of phosphatidic acid (PA), the product of PLD activity, were reported in various secreting cells. The PA-binding domain of the yeast protein Spo20p fused to GFP (Spo20p-PABD-GFP), acting as a PA sensor (45, 46) revealed particularly useful to visualize this increase of PA at the plasma membrane. Further morphometric electronic microscopy analysis revealed that this PA sensor was found to be enriched in portion of the plasma membrane were secretory granule appears morphologically docked, suggesting that PA is synthesized near exocytotic sites (47). Accordingly we found in control untransfected cells or in cells expressing GFP, that Spo20p-PABD-YFP was recruited to the plasma membrane upon cell stimulation as revealed by an increase of colocalization with the plasma membrane marker SNAP-25 (Figure 4). This plasma membrane recruitment of Spo20p-PABD-YFP in stimulated cells is largely abolished in cells expressing GFP-V0a1 (Figure 4). These data suggest that V0a-ARNO interaction is also critical for the synthesis of PA at the plasma membrane during exocytosis.

Preventing V0a-ARNO interaction affects exocytosis in neuroendocrine cells. Carbon fiber amperometry represents an elegant and powerful approach to evaluate kinetic parameters of exocytosis from single cells secreting catecholamines, as it allows measuring various parameters of individual secretion events (see Figure 5A). A typical amperomtric profile shown in Figure 5B displays successive spikes each corresponding to the detection of single secretory granule fusion events. Interestingly expression of GFP-V0a1, compared to untransfected cells or cells expressing GFP alone, reduced the number of spikes per cells but also various spike parameter, including spike half-width and amplitude, but without significant effect on the charge (Figure 5), indicating that i) the total number of event is reduced, ii) the kinetic of individual fusion event is modified, and iii) the total amount of catecholamine released by event is not modified. More precisely an increase in the

time to pick (rise time) observed upon GFP-V0a1 expression most likely represents a slow-down in the speed of the fusion pore expansion. Spikes are often preceded by small increases in current amplitude called prespike foot that are believed to represent the detection of small amounts of catecholamine leaking through the initial fusion pore (48). Expression of GFP-V0a1 significantly increased the amplitude and duration of prespike foot indicating V0a-ARNO interaction affects the pore size and stability (Figure 6). Interestingly very similar change in these spikes and prespike parameters were observed when chromaffin cells were treated with PLD inhibitor FIPI (Figures 5, 6), highlighting the link between V0 and PLD activation during exocytosis.

Discussion

In neurosecretory cells the production of specific lipids at and near exocytotic sites appears to be an important regulatory element of the fusogenic status of secretory vesicles (49). Although the pathway involving the production of PA through PLD activation by Arf6 was shown to be an important trigger for exocytosis in different cell types (26-35), the exact signal that engages this pathway has remained elusive. The Arf6 GEF ARNO was reported to activate Arf6 in different membrane trafficking processes (50-52), but again the activation mechanism of ARNO was never clearly identified. The identification that different subunits of the V-ATPase, a known participant in exocytosis (10-22), interact with ARNO/Arf6 on early endosomes to regulate the endocytic degradative pathway in epithelial cells (23), prompted us to probe the possible involvement of the V-ATPase in the regulation of the ARNO-Arf6-PLD pathway in neuroendocrine cells.

The c subunit of V0 was shown to specifically interact with Arf6 in epithelial cells, but the functional consequences of this interaction were not investigated and the domains involved in either protein were not identified (23). The same study further established by co-immunoprecipitation and pull-down experiments that the a2 subunit of V0 directly interacts with ARNO on early endosomes (23). In this case, the amino-terminal domain of V0a2 is involved in the interaction with ARNO and the expression of the V0a2-Nt peptide fused to GFP was reported to act as competitor (23). Finally this interaction was reported to promote the GEF activity of ARNO and therefore led to Arf6 activation (23). Using a FLIM-FRET based approach we found here that V0a1 expressed on chromaffin granules interacts with ARNO within 2 minutes after cell stimulation, suggesting that V0a1 could be an activator of the ARNO-Arf6-PLD pathway during exocytosis. It is of note that this timing is compatible with a previous

study reporting by FRET that the highest Arf6 activation was detected nearly 2 minutes after exocytosis stimulation in PC12 cells (36).

We found that overexpression of V0a2-Nt-GFP in PC12 cells inhibited the activation of Arf6 as detected by a reduced recruitment of the active Arf6 sensor MT2, decreased the stimulation of PLD activity, and prevented the PA synthesis at the plasma membrane as visualized by a lower recruitment of the PA probe Spo20p-PABD. One possible interpretation of these observations is that V0a1 interaction with the plasma membrane associated ARNO occurs after granule tethering/docking at the exocytotic site. The association of Arf6 with V0c that we also detected by co-immunoprecipitation in PC12 cells (data not shown) may also contribute to close contact between V-ATPase, ARNO, and Arf6 and the subsequent activation of Arf6 leading to PLD activation and PA synthesis to favor granule docking and ultimately fusion.

Hampering with V0a1-ARNO interaction dramatically reduced the number of events and affected the kinetics of single exocytosis events in chromaffin cells as reported by carbon fiber amperometry recordings, highlighting the importance of this interaction for granule docking and fusion. Overall the profile of the remaining single spike was smaller and broader, in agreement with a delay in the expansion of the fusion pore when V0a1-Nt-GFP is expressed. In line with this model the duration of prespike foot was found to be increased indicating a-greater fusion pore stability. Of importance similar observations were also found in cells treated with the PLD inhibitor FIPI, suggesting that a major outcome of V0a1-Nt-GFP expression is reminiscent of an alteration of PA synthesis. It is however also of note that V0a1-Nt-GFP expression uniquely affected prespike foot amplitude, raising the possibility that other targets of the V-ATPase might also be affected. Among those the SNARE protein VAMP2 that interacts directly with V0c is a prominent candidate (22).

We previously reported using co-immunoprecipitation experiments that the V0/V1 assembly is dependent on intragranular pH (17). In line with our findings, fluorescence recovery after photobleaching (FRAP) of GFP-tagged V-ATPase subunits indicated also that V0/V1 assembly is correlated with intragranular pH, with most acidic synaptic vesicles displaying low amounts of V1 (53). Furthermore an optogenetic approach revealed that incompletely filled synaptic vesicles fuse with lower release probability (54). We can thus propose that the V0/V1 association-dissociation represents a mechanism allowing for preferential fusion of fully acidified and filled vesicles devoid of V1. This mechanism may thus provide a control

step to avoid exocytosis of empty or incompletely filled vesicles. Clearly the V-ATPase also plays an important role in synaptic vesicle recycling and refilling (53). Since most constituents of secretory granules from neuroendocrine cells are also recycled by compensatory endocytosis (55), the possible involvement of the pathway described here for secretory vesicle recycling remains to be explored.

Material and methods

Antibody and chemicals – Anti-SNAP-25 was purchased from BioLegend (Cat #: 836303) and Hoechst 33342 from ThermoFisher

Plasmids – Oligonucleotides corresponding to the 19 residues of the N-terminal part of V0a1 were annealed and cloned into pEGFP-N3 through BglII and BamHI restriction sites as described (23). NowGFP (Addgene plasmid #74749) was cloned into pV0a1 IV-EGFP in KpnI and MunI restriction sites, whereas ARNO was cloned into CMV-shadowG (Addgene plasmid #104620) in BglII and HindIII restriction sites, essentially as described previously (56).

Chrommafin cell culture and catecholamine release - Freshly dissected primary bovine chromaffin cells were cultured in DMEM in the presence of 10 % fetal calf serum, 10 µM cytosine arabinoside, 10 µM fluorodeoxyuridine and antibiotics as described previously (57). Plasmid expressing GFP-V0a1-Nt was introduced into chromaffin cells (5 x 10^6 cells) by Amaxa Nucleofactor systems (Lonza) according to manufacturer's instructions and as described previously (58). 48h/72h after transfection, catecholamine secretion was evoked by applying K^+ (100 mM) in Locke's solution without ascorbic acid for 10 s to single cells by mean of a glass micropipette positioned at a distance of 30-50 µm from the cell. Electrochemical measurements of catecholamine secretion were performed using 5 μm diameter carbon-fiber electrodes (ALA Scientific) held at a potential of +650 mV compared with the reference electrode (Ag/AgCl) and approached closely to the transfected cells essentially as described previously (59). Amperometric recordings were performed with an AMU130 (Radiometer Analytical) amplifier, sampled at 5 kHz, and digitally low-pass filtered at 1 kHz. Analysis of amperometric recordings was done as described previously (60), allowing automatic spike detection and extraction of spike parameters. The number of amperometric spikes was counted as the total number of spikes with an amplitude > 5 pA.

PC12 cell culture and transfection - PC12 cells were grown in Dulbecco's modified

Eagle's medium supplemented with glucose (4500 mg/liter) and containing 30 mM $NaHCO_3$, 5% fetal bovine serum, 10% horse serum, and 100 units/ml penicillin/streptomycin and 100 µg/ml Kanamycin as described previously (36). For immunofluorescence experiments, expression vectors were introduced into PC12 cells using lipofectamin 2000 on adherent cells according to the manufacturer's instructions. Under these conditions, the transfection efficiency ranged from 60 to 75% and co-transfection rate was greater than 90%.

FRET-FLIM imaging – Chromaffin cells expressing V0a1-nowGFP and ARNO-shadowG (ShadowG is a mutation of GFP that be used as a dark acceptor in FRET experience) incubated in Locke's solution in Ibidi plates were imaged using a homemade two-photon excitation microscopy. Cells were then stimulated by addition of concentrated nicotine solution to reach 20µM final concentration. All RAW data were treated by SPCImage (version7.4).

Immunolabeling and confocal microscopy PC12 cells expressing YFP-MT2 or YFP-PABD constructs together of not with GFP or V0a1-Nt-GFP were fixed with 4% paraformaldehyde in serum free medium for 10 min at room temperature. Cells were then permeabilized in PBS containing 4% paraformaldehyde and 0.1% Triton-X100, for 10 min at room temperature. SNAP-25 (1:500 dilution) antibodies were used as markers for the plasma membrane and revealed with a goat-anti-mouse IgG-Alexa 647 (1:1000 dilution, Molecular Probes, Thermo Scientific). Cell nuclei were also labeled with Hoechst. The cellular distributions of the Arf6-GTP and PA probes and markers were examined with a Leica SP5 II confocal microscope equipped with an oil immersion 63x objective (Plan Apochromat n.a.=1.4). Digital images were acquired in the equatorial and basal planes and quantification performed as described previously (36, 47).

Statistical analysis - Number of experiments and repeats are indicated in figure legends. Normality of the data distribution was verified with ANOVA test and statistical analysis was performed with t-tests relative to the indicated control.

Acknowledgements

We thank Nicolas Morel for sharing valuable V-ATPase constructs. This work was supported by a grant from "Fondation pour la Recherche Médicale" to NV.

Abbreviations

ATPase, adenosine triphosphatase; FLIM, fluorescence lifetime imaging microscopy; FRAP, fluorescence recovery after photobleaching; FRET, fluorescence resonance energy transfer; GEF, guanine nucleotide exchange factor; GFP, green fluorescent protein; PA, phosphatidic acid; PABD, PA-binding domain; PBS, phosphate buffered saline, PLD, phospholipase D; V-ATPase, vacuolar-ATPase

The authors declare that they have no conflicts of interest with the contents of this article.

Contributions

Q.W., T.T., L.R. and N.V. performed experiments. Q.W., L.R., Y.M., S.C-G., S.O., S.G., M-F. B. designed and analyzed the experiments. N.V. wrote the manuscript. All authors revised the manuscript.

Figure legends

Figure 1: Increased V0a1-ARNO interaction after chromaffin cell stimulation. A) Chromaffin cells expressing V0a1-nowGFP and ARNO-shadowG were stimulated for different time with 10 µM of nicotine and the half-life of nowGFP was measured by FLIM. Bar = 10 µm. B) Profile of the lifetime signal of cells images in A at the different time of stimulation. Blue and Red boxes at the t=2 min indicate and increase and a decrease in lifetime, respectively after cell stimulation. C) Quantification of lifetime signal obtained from n = 10 analysis performed from cells obtained from 2 independent cell preparation. Data are presented as box plot were plain bars represent median and scattered bars represent means.

Figure 2: Interfering with V0a1-ARNO interaction reduces Arf6 activation after PC12 cells stimulation. Distribution of MT2-YFP probe in mock-transfected PC12 cells or in cells co-expressing GFP or V0a1-GFP in resting (R) condition or after a-10 minutes stimulation with 59 mM K^+ solution (S). After fixation cells were immunostained for SNAP25 and labeled with Hoechst. Bar = 10 µm. Colocalization levels of MT2-YFP and SNAP25 were measured and presented as mean ± SEM (n = 50 cells for each condition from two independent experiments).

Figure 3: Interfering with V0a1-ARNO interaction reduces PLD activation after PC12 cells stimulation. Mock-transfected cells or cells expressing GFP or V0a1-GFP were kept in Locke's solution (Resting) or stimulated with 59 mM K^+ solution for 10 minutes (Stimulated). Cells were lysed on ice and lysats were used to measure PLD activity. Data are mean values from triplicate values ± SD obtained from independent experiments (n = 3), each obtained from quadruplicates in individual experiments.

Figure 4: Interfering with V0a1-ARNO interaction reduces PA synthesis at the plasma membrane after PC12 cells stimulation. Distribution of Spo20p-PABD-YFP probe in in cells co-expressing GFP or V0a1-GFP in resting (R) condition or after a-10 minutes stimulation with 59 mM K^+ solution (S). After fixation cells were immunostained for SNAP25 and labeled with Hoechst. Arrows indicate a cell co-expressing Spo20p-PABD-GFP and V0a1-GFP in the stimulated condition. A cell only expressing Spo20p-PABD-GFP is also present on the picture. Bars = 10 µm. Colocalization levels of Spo20p-PABD-YFP and SNAP25 were measured and presented as mean ± SEM (n = 75 cells for each condition from three independent experiments).

Figure 5: Interfering with V0a1-ARNO interaction affects individual spike kinetic parameters from chromaffin cells. A) Schema showing the different parameter of amperometric spikes that were analysed. B-E) Chromaffin cells in culture expressing GFP (control) or V0a1-Nt-GFP or untransfected cells treated with 750 nM of FIPI were stimulated with a local application of 100 µM of nicotine for 10 s and catecholamine secretion was monitored using carbon fiber amperometry. B) The histogram illustrates the number of amperometric spikes recorded per cell. Parameters of individual spike include spike charge (C), half width (D), and spike amplitude (E). Data are expressed as means ± S.D. (n > 75 cells for each condition from three independent cell cultures). D) Average spike profile for cell expressing GFP (Control) or V0a1-Nt-GFP (V0a1) or treated with FIPI (FIPI).

Figure 6: Interfering with V0a1-ARNO interaction affects prespike kinetic parameters from chromaffin cells. Parameters of individual prespike from cells recorded in figure 5 include prespike duration (A), and prespike amplitude (B), and charge (C). Data are expressed as means ± S.D. (n > 75 cells for each condition from three independent cell cultures). D) Average prespike profile for cell expressing GFP (Control) or V0a1-Nt-GFP (V0a1) or treated with FIPI (FIPI).

Reference:

1. Tanguy E, Carmon O, Wang Q, Jeandel L, Chasserot-Golaz S, Montero-Hadjadje M, Vitale N.（2016）Lipids implicated in the journey of a secretory granule: from biogenesis to fusion. J Neurochem. 137(6):904-912.
2. Rizo J.（2018）Mechanism of neurotransmitter release coming into focus. Protein Sci. 27(8):1364-1391.
3. Yu X, Taylor AMW, Nagai J, Golshani P, Evans CJ, Coppola G, Khakh BS. (2018) Reducing Astrocyte Calcium Signaling In Vivo Alters Striatal Microcircuits and Causes Repetitive Behavior. Neuron. 19;99(6):1170-1187.e9.
4. Sutton RB, Fasshauer D, Jahn R, Brunger AT. (1998) Crystal structure of a SNARE complex involved in synaptic exocytosis at 2.4 A resolution. Nature. 24;395(6700):347-53.
5. Jahn R, Südhof TC. (1999) Membrane fusion and exocytosis. Annu Rev Biochem. 68:863-911.
6. Lauwers E, Goodchild R, Verstreken P. (2016) Membrane Lipids in Presynaptic Function and Disease. Neuron. 90(1):11-25.
7. Forgac M. (2007) Vacuolar ATPases: rotary proton pumps in physiology and pathophysiology. Nat Rev Mol Cell Biol. 8(11):917-29.
8. Maxson ME, Grinstein S. (2014) The vacuolar-type H -ATPase at a glance - more than a proton pump. J Cell Sci. 127(Pt 23):4987-93.
9. Moriyama Y, Maeda M, Futai M. (1992) The role of V-ATPase in neuronal and endocrine systems. J Exp Biol. 172:171-8.
10. Peters C, Bayer MJ, Bühler S, Andersen JS, Mann M, Mayer A. (2001) Trans-complex formation by proteolipid channels in the terminal phase of membrane fusion. Nature. 409(6820):581-8.
11. Peri F, Nüsslein-Volhard C. (2008) Live imaging of neuronal degradation by microglia reveals a role for v0-ATPase a1 in phagosomal fusion in vivo. Cell. 133(5):916-27.
12. Williamson WR, Wang D, Haberman AS, Hiesinger PR. (2010) A dual function of V0-ATPase a1 provides an endolysosomal degradation mechanism in Drosophila melanogaster photoreceptors. J Cell Biol. 189(5):885-99.
13. Strasser B, Iwaszkiewicz J, Michielin O, Mayer A. (2010) The V-ATPase proteolipid cylinder promotes the lipid-mixing stage of SNARE-dependent fusion of yeast

vacuoles. EMBO J. 30(20):4126-41.

14. Hiesinger PR, Fayyazuddin A, Mehta SQ, Rosenmund T, Schulze KL, Zhai RG, Verstreken P, Cao Y, Zhou Y, Kunz J, Bellen HJ. (2005) The v-ATPase V0 subunit a1 is required for a late step in synaptic vesicle exocytosis in Drosophila. Cell. 121(4):607-620.
15. Bodzęta A, Kahms M, Klingauf J. (2017) The Presynaptic v-ATPase Reversibly Disassembles and Thereby Modulates Exocytosis but Is Not Part of the Fusion Machinery. Cell Rep. 20(6):1348-1359.
16. Liégeois S., Benedetto A., Garnier J.M., Schwab Y., Labouesse M. (2006) The V0-ATPase mediates apical secretion of exosomes containing Hedgehog-related proteins in Caenorhabditis elegans. J. Cell Biol. 173:949–961.
17. Poëa-Guyon S, Ammar MR, Erard M, Amar M, Moreau AW, Fossier P, Gleize V, Vitale N, Morel N. (2013) The V-ATPase membrane domain is a sensor of granular pH that controls the exocytotic machinery. J Cell Biol. 203(2):283-98.
18. Morel N, Dunant Y, Israël M. (2001) Neurotransmitter release through the V0 sector of V-ATPase. J Neurochem. 79(3) :485-8.
19. El Far O, Seagar M. (2011) A role for V-ATPase subunits in synaptic vesicle fusion? J Neurochem. 117(4):603-12.
20. Galli T, McPherson PS, De Camilli P. (1996) The V0 sector of the V-ATPase, synaptobrevin, and synaptophysin are associated on synaptic vesicles in a Triton X-100-resistant, freeze-thawing sensitive, complex. J Biol Chem. 271(4):2193-8.
21. Morel N, Dedieu JC, Philippe JM. (2003) Specific sorting of the a1 isoform of the V-H+ATPase a subunit to nerve terminals where it associates with both synaptic vesicles and the presynaptic plasma membrane. J Cell Sci. 116(Pt 23):4751-62.
22. Di Giovanni J., Boudkkazi S., Mochida S., Bialowas A., Samari N., Lévêque C., Youssouf F., Brechet A., Iborra C., Maulet Y., et al. (2010) V-ATPase membrane sector associates with synaptobrevin to modulate neurotransmitter release. Neuron. 67:268–279
23. Hurtado-Lorenzo A, Skinner M, El Annan J, Futai M, Sun-Wada GH, Bourgoin S, Casanova J, Wildeman A, Bechoua S, Ausiello DA, Brown D, Marshansky V. (2006) V-ATPase interacts with ARNO and Arf6 in early endosomes and regulates the protein degradative pathway. Nat Cell Biol. 8(2):124-136.
24. Hosokawa H, Dip PV, Merkulova M, Bakulina A, Zhuang Z, Khatri A, Jian X, Keating SM, Bueler SA, Rubinstein JL, Randazzo PA, Ausiello DA, Grüber G,

Marshansky V. (2013) The N termini of a-subunit isoforms are involved in signaling between vacuolar H+-ATPase (V-ATPase) and cytohesin-2. J Biol Chem. 288(8):5896-913.

25. Rama S, Boumedine-Guignon N, Sangiardi M, Youssouf F, Maulet Y, Lévêque C, Belghazi M, Seagar M, Debanne D, El Far O. (2019) Chromophore-Assisted Light Inactivation of the V-ATPase V0c Subunit Inhibits Neurotransmitter Release Downstream of Synaptic Vesicle Acidification. Mol Neurobiol. 56(5):3591-3602.
26. Morel N, Poëa-Guyon S, Ammar MR, Vitale N. (2014) V-ATPase is a pH sensor controlling vesicular membrane fusion. Med Sci (Paris). 30(6-7):631-3.
27. Morel N, Poëa-Guyon S. (2015) The membrane domain of vacuolar H(+)ATPase: a crucial player in neurotransmitter exocytotic release. Cell Mol Life Sci. 72(13):2561-73.
28. Galas MC, Helms JB, Vitale N, Thiersé D, Aunis D, Bader MF. (1997) Regulated exocytosis in chromaffin cells. A potential role for a secretory granule-associated ARF6 protein. J Biol Chem. 272(5):2788-93.
29. Caumont AS, Galas MC, Vitale N, Aunis D, Bader MF. (1998) Regulated exocytosis in chromaffin cells. Translocation of ARF6 stimulates a plasma membrane-associated phospholipase D. J Biol Chem. 273(3):1373-9.
30. Yang CZ, Mueckler M. (1999) ADP-ribosylation factor 6 (ARF6) defines two insulin-regulated secretory pathways in adipocytes. J Biol Chem. 274(36):25297-300.
31. Caumont AS, Vitale N, Gensse M, Galas MC, Casanova JE, Bader MF. (2000) Identification of a plasma membrane-associated guanine nucleotide exchange factor for ARF6 in chromaffin cells. Possible role in the regulated exocytotic pathway. J Biol Chem 275(21):15637-44.
32. Vitale N, Chasserot-Golaz S, Bailly Y, Morinaga N, Frohman MA, Bader MF. (2002) Calcium-regulated exocytosis of dense-core vesicles requires the activation of ADP-ribosylation factor (ARF)6 by ARF nucleotide binding site opener at the plasma membrane. J Cell Biol. 159(1):79-89.
33. Vitale N, Chasserot-Golaz S, Bader MF. (2002) Regulated secretion in chromaffin cells: an essential role for ARF6-regulated phospholipase D in the late stages of exocytosis. Ann N Y Acad Sci. 971:193-200.
34. Matsukawa J, Nakayama K, Nagao T, Ichijo H, Urushidani T. (2003) Role of ADP-ribosylation factor 6 (ARF6) in gastric acid secretion. J Biol Chem. 278(38):36470-5.
35. Liu L, Liao H, Castle A, Zhang J, Casanova J, Szabo G, Castle D. (2005) SCAMP2

interacts with Arf6 and phospholipase D1 and links their function to exocytotic fusion pore formation in PC12 cells. Mol Biol Cell. 16(10):4463-72.

36. Béglé A, Tryoen-Tóth P, de Barry J, Bader MF, Vitale N. (2009) ARF6 regulates the synthesis of fusogenic lipids for calcium-regulated exocytosis in neuroendocrine cells. J Biol Chem. 284(8):4836-45.
37. Pelletán LE, Suhaiman L, Vaquer CC, Bustos MA, De Blas GA, Vitale N, Mayorga LS, Belmonte SA. (2015) ADP ribosylation factor 6 (ARF6) promotes acrosomal exocytosis by modulating lipid turnover and Rab3A activation. J Biol Chem. 290(15):9823-41.
38. Recchi C, Chavrier P. (2006) V-ATPase: a potential pH sensor. Nat Cell Biol. 8(2):107-9.
39. Tanguy E, Tran Nguyen AP, Kassas N, Bader MF, Grant NJ, Vitale N. (2019) Regulation of Phospholipase D by Arf6 during FcγR-Mediated Phagocytosis. J Immunol. 202(10):2971-2981.
40. Vitale N, Caumont AS, Chasserot-Golaz S, Du G, Wu S, Sciorra VA, Morris AJ, Frohman MA, Bader MF. (2001) Phospholipase D1: a key factor for the exocytotic machinery in neuroendocrine cells. EMBO J. 20(10):2424-34.
41. Zeniou-Meyer M, Liu Y, Béglé A, Olanich ME, Hanauer A, Becherer U, Rettig J, Bader MF, Vitale N. (2008) The Coffin-Lowry syndrome-associated protein RSK2 is implicated in calcium-regulated exocytosis through the regulation of PLD1. Proc Natl Acad Sci U S A. 105(24):8434-9.
42. Vitale N, Mawet J, Camonis J, Regazzi R, Bader MF, Chasserot-Golaz S. (2005) The Small GTPase RalA controls exocytosis of large dense core secretory granules by interacting with ARF6-dependent phospholipase D1. J Biol Chem. 280(33):29921-8.
43. Momboisse F, Lonchamp E, Calco V, Ceridono M, Vitale N, Bader MF, Gasman S. (2009) betaPIX-activated Rac1 stimulates the activation of phospholipase D, which is associated with exocytosis in neuroendocrine cells. J Cell Sci. 122(Pt 6):798-806.
44. Bader MF, Vitale N. (2009) Phospholipase D in calcium-regulated exocytosis: lessons from chromaffin cells. Biochim Biophys Acta. 1791(9):936-41.
45. Kassas N, Tryoen-Tóth P, Corrotte M, Thahouly T, Bader MF, Grant NJ, Vitale N. (2012) Genetically encoded probes for phosphatidic acid. Methods Cell Biol. 108:445-59.
46. Kassas N, Tanguy E, Thahouly T, Fouillen L, Heintz D, Chasserot-Golaz S, Bader MF, Grant NJ, Vitale N. (2017) Comparative Characterization of Phosphatidic Acid

Sensors and Their Localization during Frustrated Phagocytosis. J Biol Chem. 292(10):4266-4279.

47. Zeniou-Meyer M, Zabari N, Ashery U, Chasserot-Golaz S, Haeberlé AM, Demais V, Bailly Y, Gottfried I, Nakanishi H, Neiman AM, Du G, Frohman MA, Bader MF, Vitale N. (2007) Phospholipase D1 production of phosphatidic acid at the plasma membrane promotes exocytosis of large dense-core granules at a late stage. J Biol Chem. 282(30):21746-57.
48. Tryoen-Tóth P, Chasserot-Golaz S, Tu A, Gherib P, Bader MF, Beaumelle B, Vitale N. (2013) HIV-1 Tat protein inhibits neurosecretion by binding to phosphatidylinositol 4,5-bisphosphate. J Cell Sci. 126(Pt 2):454-63.
49. Gasman S, Vitale N. (2017) Lipid remodelling in neuroendocrine secretion. Biol Cell. 109(11):381-390.
50. Hernández-Deviez DJ, Roth MG, Casanova JE, Wilson JM. (2004) ARNO and ARF6 regulate axonal elongation and branching through downstream activation of phosphatidylinositol 4-phosphate 5-kinase alpha. Mol Biol Cell. 15(1):111-20.
51. Eva R, Crisp S, Marland JR, Norman JC, Kanamarlapudi V, ffrench-Constant C, Fawcett JW. (2012) ARF6 directs axon transport and traffic of integrins and regulates axon growth in adult DRG neurons. J Neurosci. 32(30):10352-64.
52. Zhu W, Shi DS, Winter JM, Rich BE, Tong Z, Sorensen LK, Zhao H, Huang Y, Tai Z, Mleynek TM, Yoo JH, Dunn C, Ling J, Bergquist JA, Richards JR, Jiang A, Lesniewski LA, Hartnett ME, Ward DM, Mueller AL, Ostanin K, Thomas KR, Odelberg SJ, Li DY. (2017) Small GTPase ARF6 controls VEGFR2 trafficking and signaling in diabetic retinopathy. J Clin Invest. 127(12):4569-4582.
53. Bodzęta A, Kahms M, Klingauf J. (2017) The Presynaptic v-ATPase Reversibly Disassembles and Thereby Modulates Exocytosis but Is Not Part of the Fusion Machinery. Cell Rep. 20(6):1348-1359.
54. Herman MA, Trimbuch T, Rosenmund C. (2018) Differential pH Dynamics in Synaptic Vesicles from Intact Glutamatergic and GABAergic Synapses. Front Synaptic Neurosci. 10:44.
55. Ceridono M, Ory S, Momboisse F, Chasserot-Golaz S, Houy S, Calco V, Haeberlé AM, Demais V, Bailly Y, Bader MF, Gasman S. (2011) Selective recapture of secretory granule components after full collapse exocytosis in neuroendocrine chromaffin cells. Traffic. 12(1):72-88.
56. Vitale N, Moss J, Vaughan M. (1996) ARD1, a 64-kDa bifunctional protein containing

an 18-kDa GTP-binding ADP-ribosylation factor domain and a 46-kDa GTPase-activating domain. Proc Natl Acad Sci U S A. 93(5):1941-4.

57. Vitale N, Mukai H, Rouot B, Thiersé D, Aunis D, Bader MF. (1993) Exocytosis in chromaffin cells. Possible involvement of the heterotrimeric GTP-binding protein G(o). J Biol Chem. 268(20):14715-23.
58. Chasserot-Golaz S, Vitale N, Umbrecht-Jenck E, Knight D, Gerke V, Bader MF. (2005) Annexin 2 promotes the formation of lipid microdomains required for calcium-regulated exocytosis of dense-core vesicles. Mol Biol Cell. 16(3):1108-19.
59. Gabel M, Delavoie F, Demais V, Royer C, Bailly Y, Vitale N, Bader MF, (2015) Chasserot-Golaz S. Annexin A2-dependent actin bundling promotes secretory granule docking to the plasma membrane and exocytosis. J Cell Biol. 210(5):785-800.
60. Houy S, Estay-Ahumada C, Croisé P, Calco V, Haeberlé AM, Bailly Y, Billuart P, Vitale N, Bader MF, Ory S, Gasman S. (2015) Oligophrenin-1 Connects Exocytotic Fusion to Compensatory Endocytosis in Neuroendocrine Cells. J Neurosci. 35(31):11045-55.

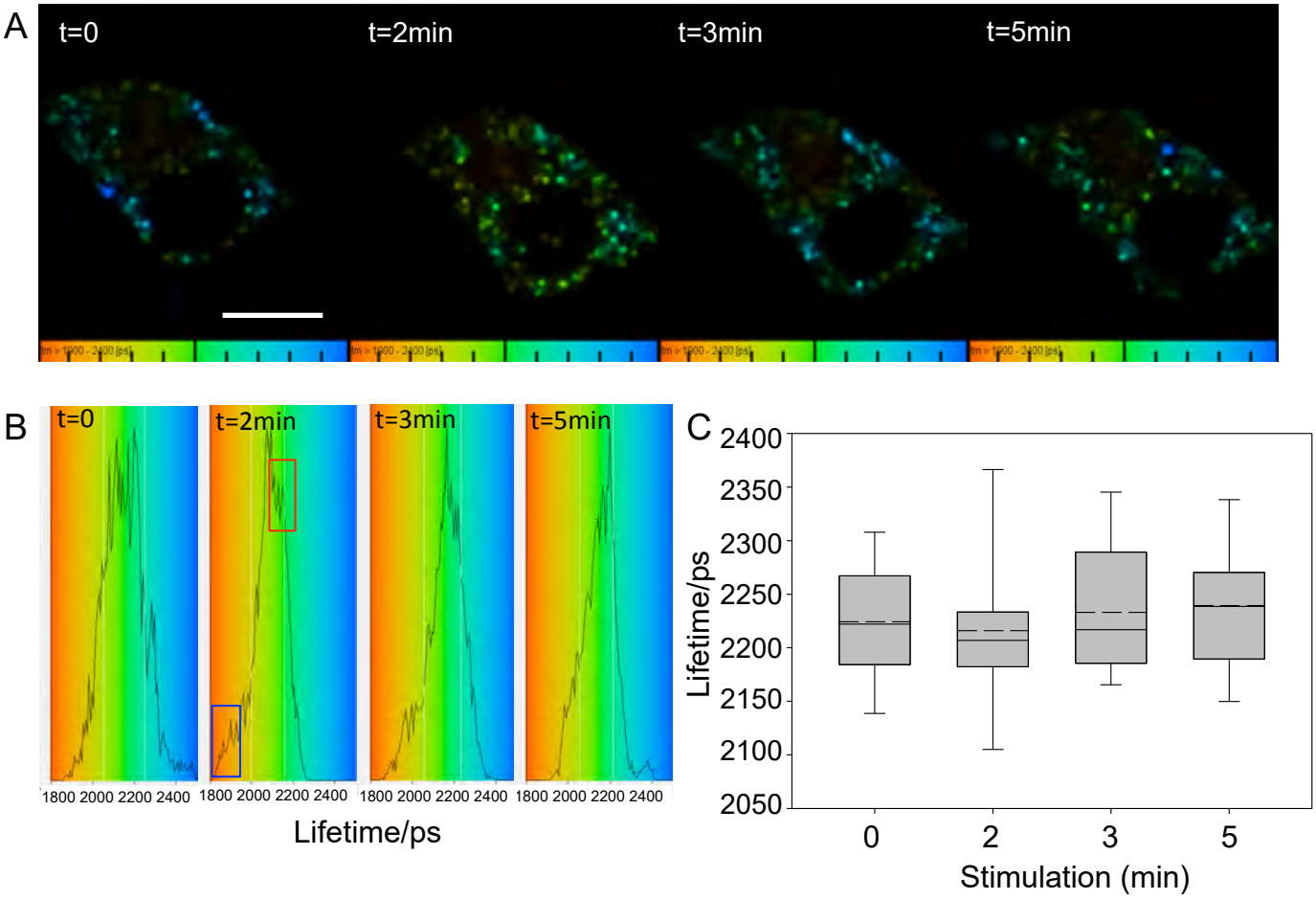
A
t=0
t=2min
t=3min
t=5min
B
t=0
t=2min
t=3min
t=5min
1800 2000 2200 2400
1800 2000 2200 2400
1800 2000 2200 2400
1800 2000 2200 2400
Lifetime/ps
C
2400
2350
2300
2250
2200
2150
2100
2050
Lifetime/ps
0
2
3
5
Stimulation (min)

Figure 1

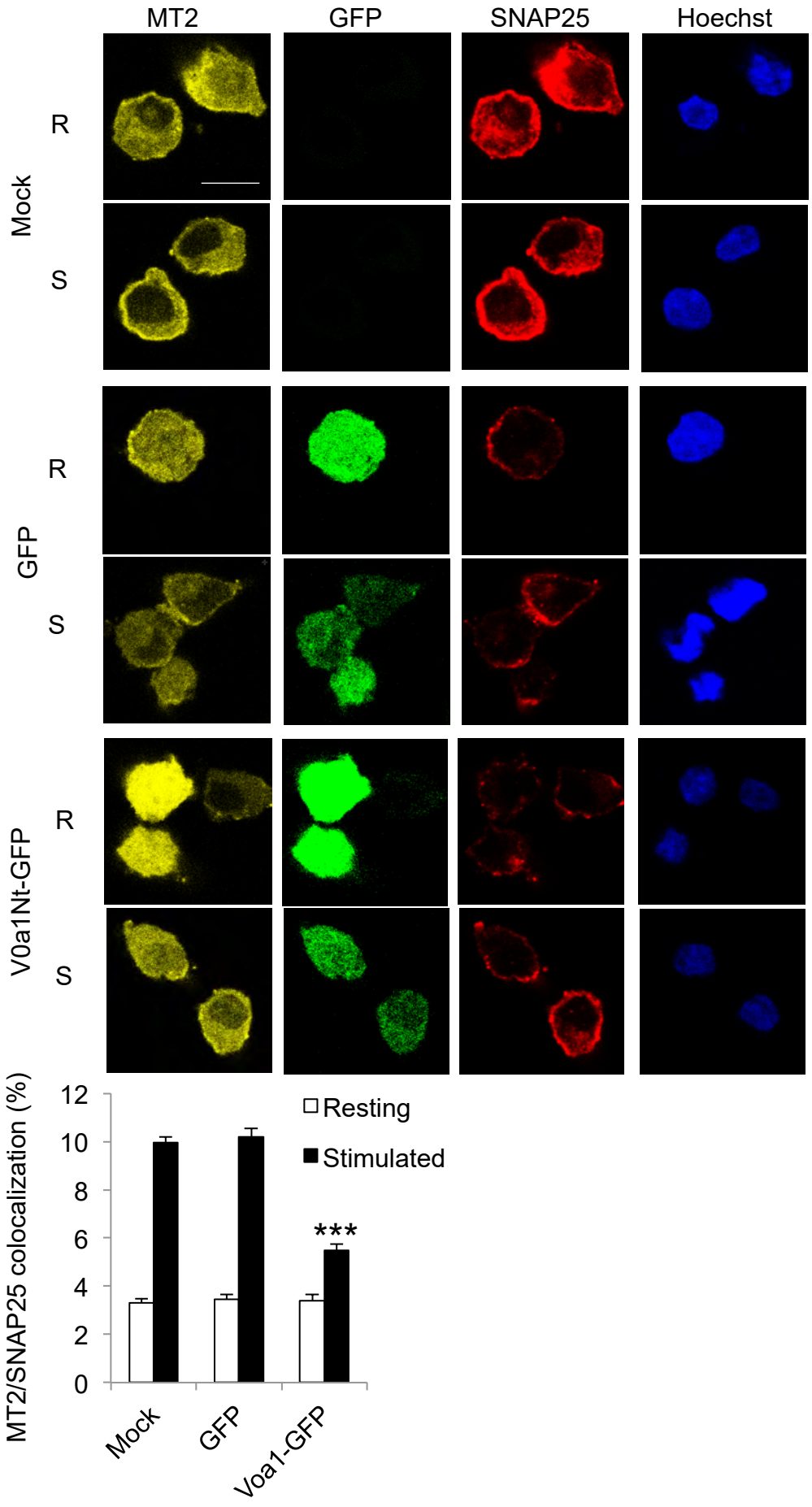
MT2
GFP
SNAP25
Hoechst
Mock
R
S
GFP
R
S
V0a1Nt-GFP
R
S
MT2/SNAP25 colocalization (%)
12
10
8
6
4
2
0
Resting
Stimulated
***
Mock
GFP
Voa1-GFP

Figure 2

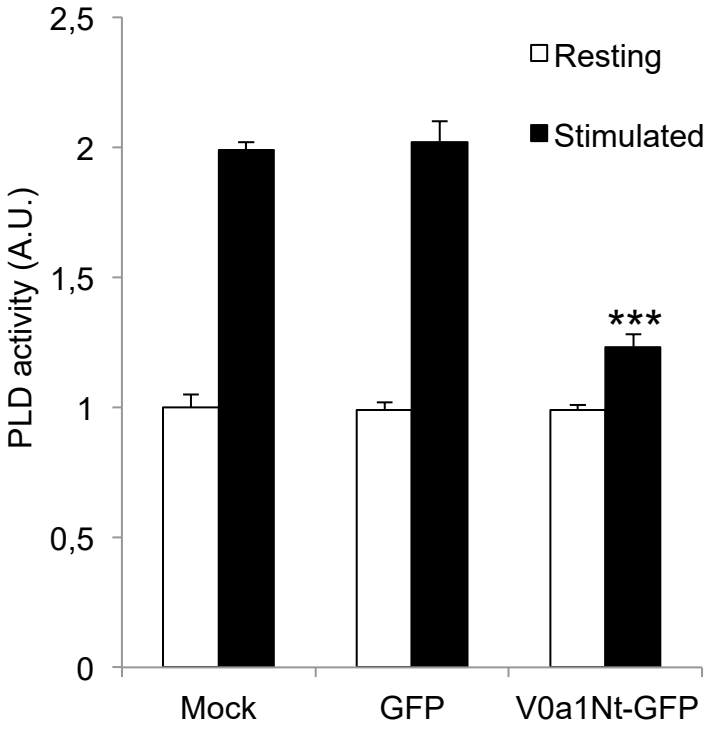
2,5
2
1,5
1
0,5
0
PLD activity (A.U.)
Resting
Stimulated
***
Mock
GFP
V0a1Nt-GFP

Figure 3

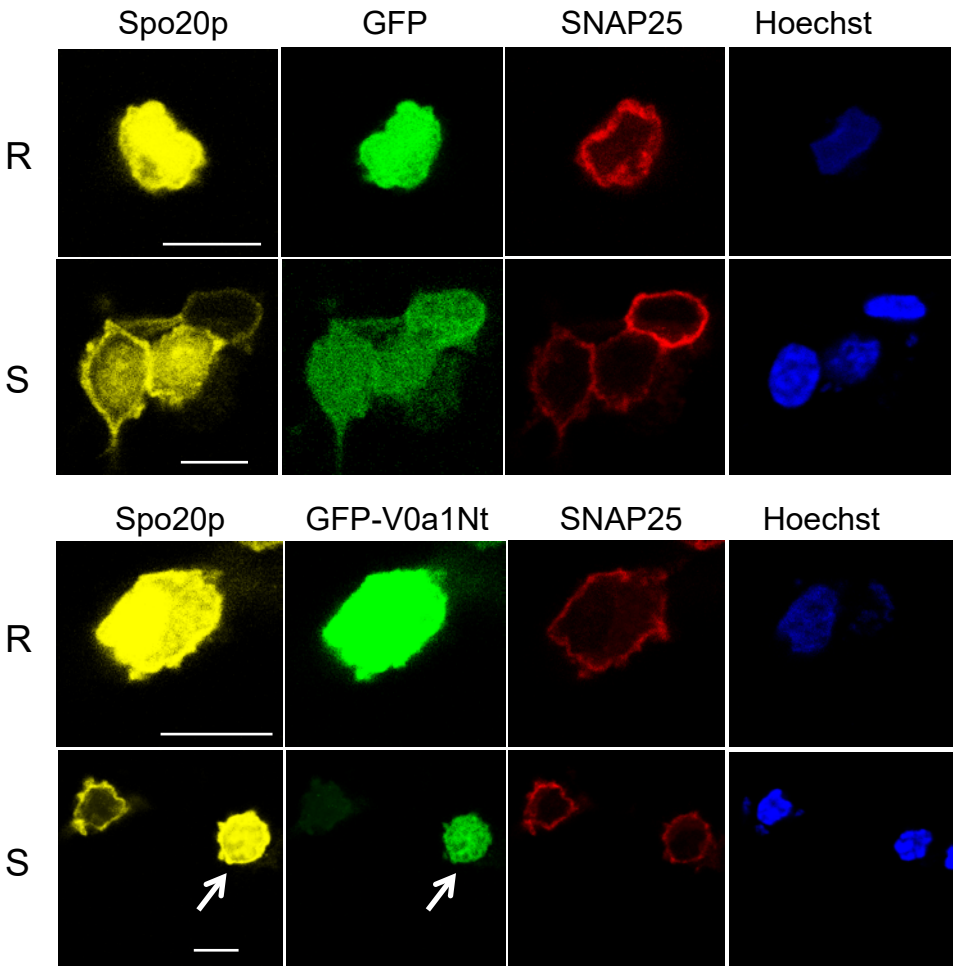
Spo20p
GFP
SNAP25
Hoechst
R
S
Spo20p
GFP-V0a1Nt
SNAP25
Hoechst
R
S

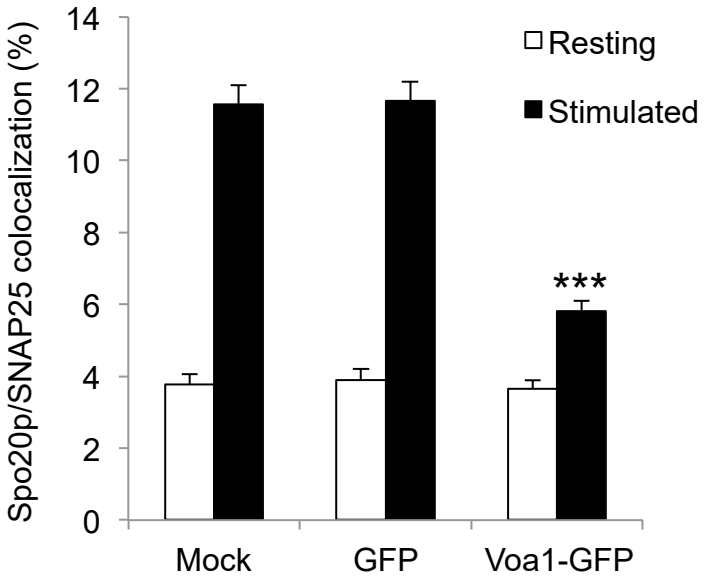
Spo20p/SNAP25 colocalization (%)
14
12
10
8
6
4
2
0
Resting
Stimulated
***
Mock
GFP
Voa1-GFP

Figure 4

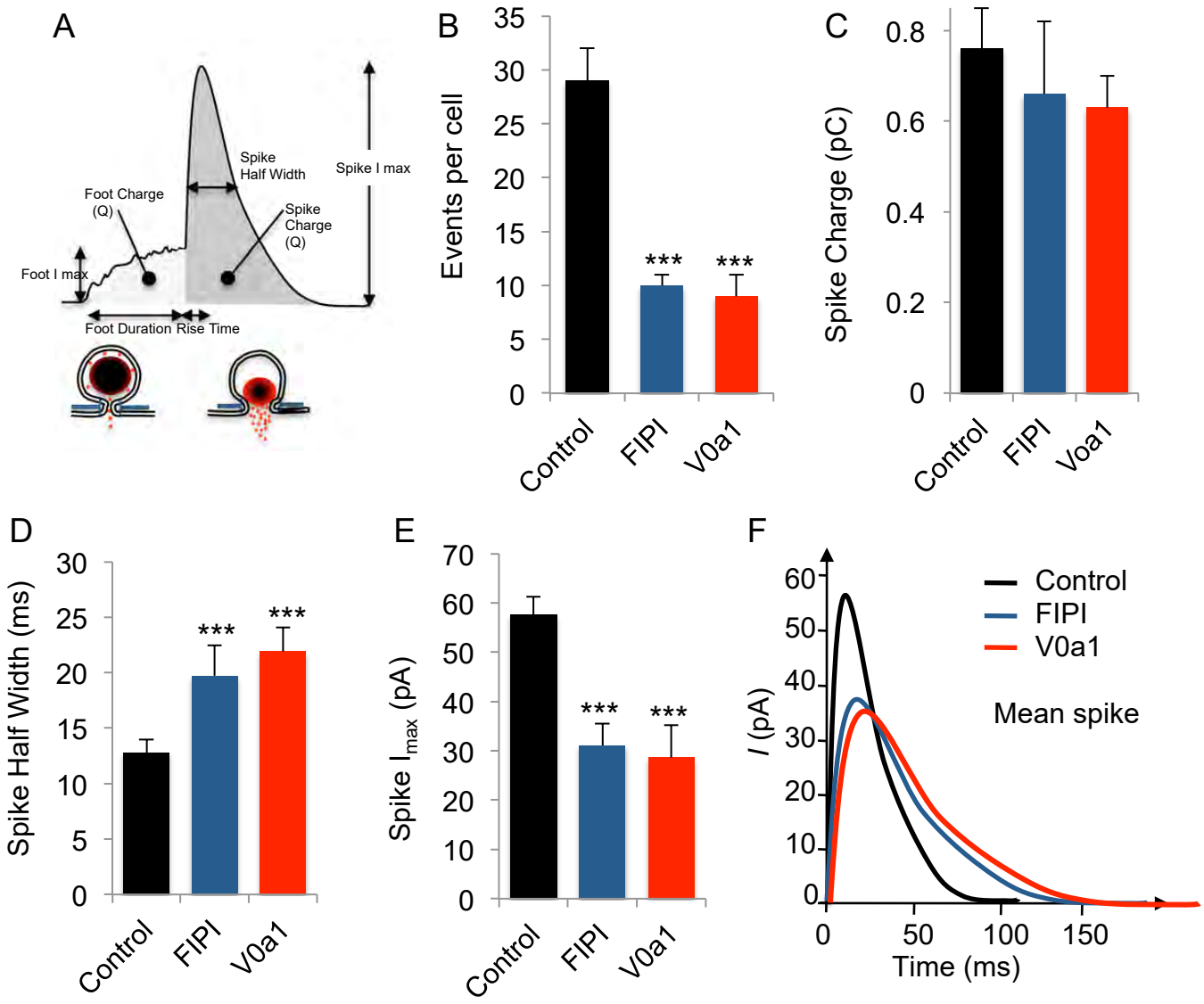
A
Spike
Half Width
Spike I max
Foot Charge
(Q)
Spike
Charge
(Q)
Foot I max
Foot Duration Rise Time
B
Events per cell
35
30
25
20
15
10
5
0
***
***
Control
FIPI
V0a1
C
Spike Charge (pC)
0.8
0.6
0.4
0.2
0
Control
FIPI
Voa1
D
Spike Half Width (ms)
30
25
20
15
10
5
0
***
***
Control
FIPI
V0a1
E
Spike I$_{max}$ (pA)
70
60
50
40
30
20
10
0
***
***
Control
FIPI
V0a1
F
I (pA)
60
50
40
30
20
10
0
Control
FIPI
V0a1
Mean spike
0
50
100
150
Time (ms)

Figure 5

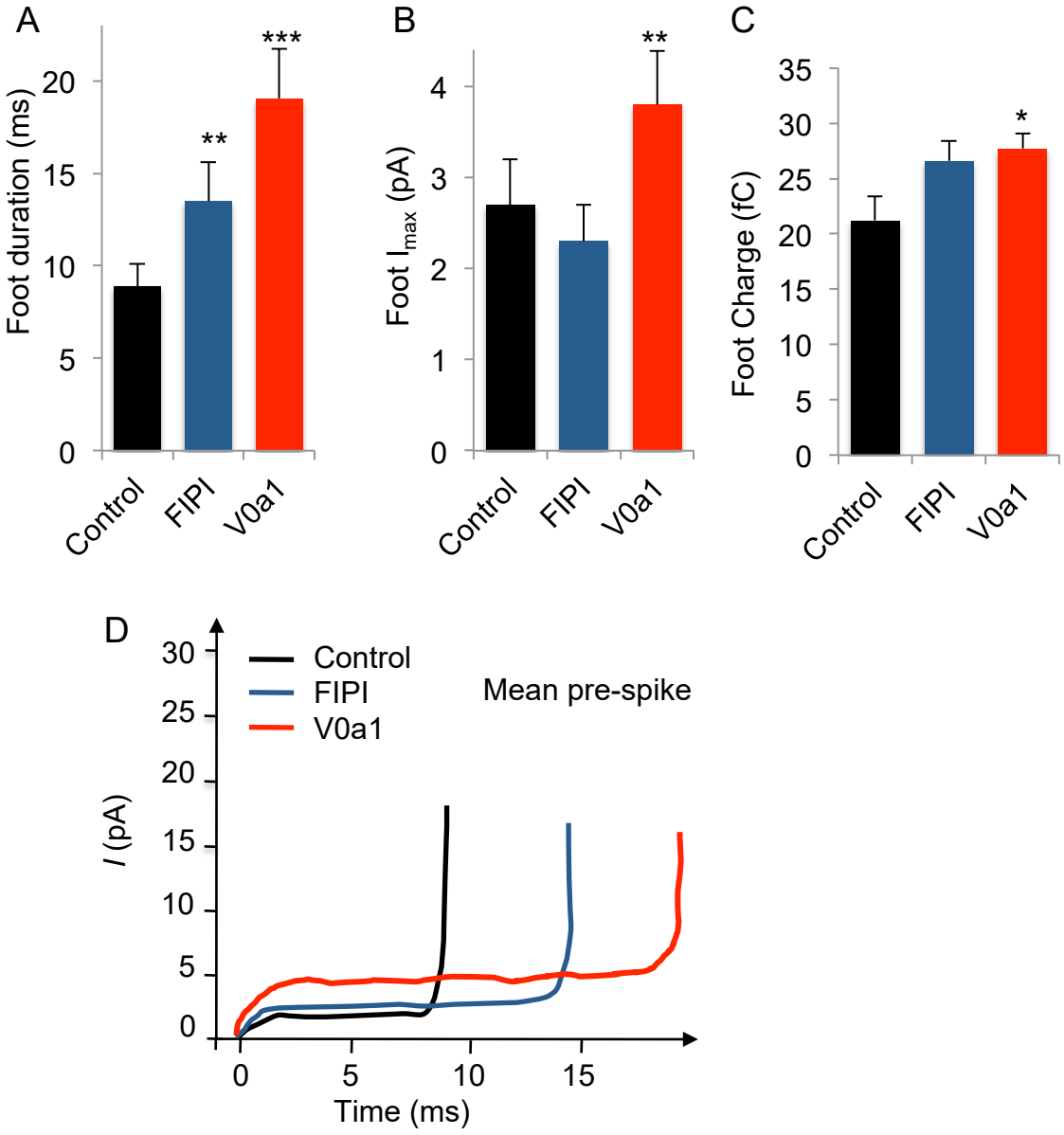
A
Foot duration (ms)
20
15
10
5
0
**
***
Control
FIPI
V0a1
B
Foot I max (pA)
4
3
2
1
0
**
Control
FIPI
V0a1
C
Foot Charge (fC)
35
30
25
20
15
10
5
0
*
Control
FIPI
V0a1
D
I (pA)
30
25
20
15
10
5
0
Control
FIPI
V0a1
Mean pre-spike
0
5
10
15
Time (ms)

Figure 6

4.2 Results of part II

In the second part of this work, I wanted to answer if V-ATPase is sensing intravesicular pH to check for granule content in neurotransmitter to provide fusion competence to fully loaded granules. So FLIM was used as a major technique to measure intra vesicular pH and simultaneously evaluate the interaction between pairs such as V0a1-ARNO or V1-V0 domains. In this work, all FLIM experiences are performed with a two photons laser microscopy by time-correlated single-photon counting (TCSPC) method for measurement.

4.2.1 Lifetime and pH

Fluorescence-lifetime imaging microscopy or FLIM is an imaging technique for producing an image based on the differences in the exponential decay rate of the fluorescence from a fluorescent sample. When a fluorophore is excited by a photon it will drop to the ground state with a certain probability based on the decay rates through a number of different (radiative and/or nonradiative) decay pathways. Since the fluorescence lifetime of a fluorophore depends on both radiative (i.e. fluorescence) and non-radiative (i.e. quenching, FRET) processes, energy transfer from the donor molecule to the acceptor molecule will decrease the lifetime of the donor. Furthermore the lifetime of fluorescent protein such as GFP is also sensible to pH, which makes it possible to measure intra vesicular pH and interaction between two proteins at the same time.

Originally I had chosen a red fluorescent protein pHuji as a pH sensor to establisher the relationship between lifetime and pH. However after many experiences that were difficult to evaluate, we found that chromaffin granules display a significant red autofluorescence. At this level of autofluorescence it is impossible to isolate the pHuji signal.

CgA-EGFP was then used as the intravesicular pH sensor. The calibration curve of the EGFP fluorescence lifetimes at different pH is shown in figure 15.

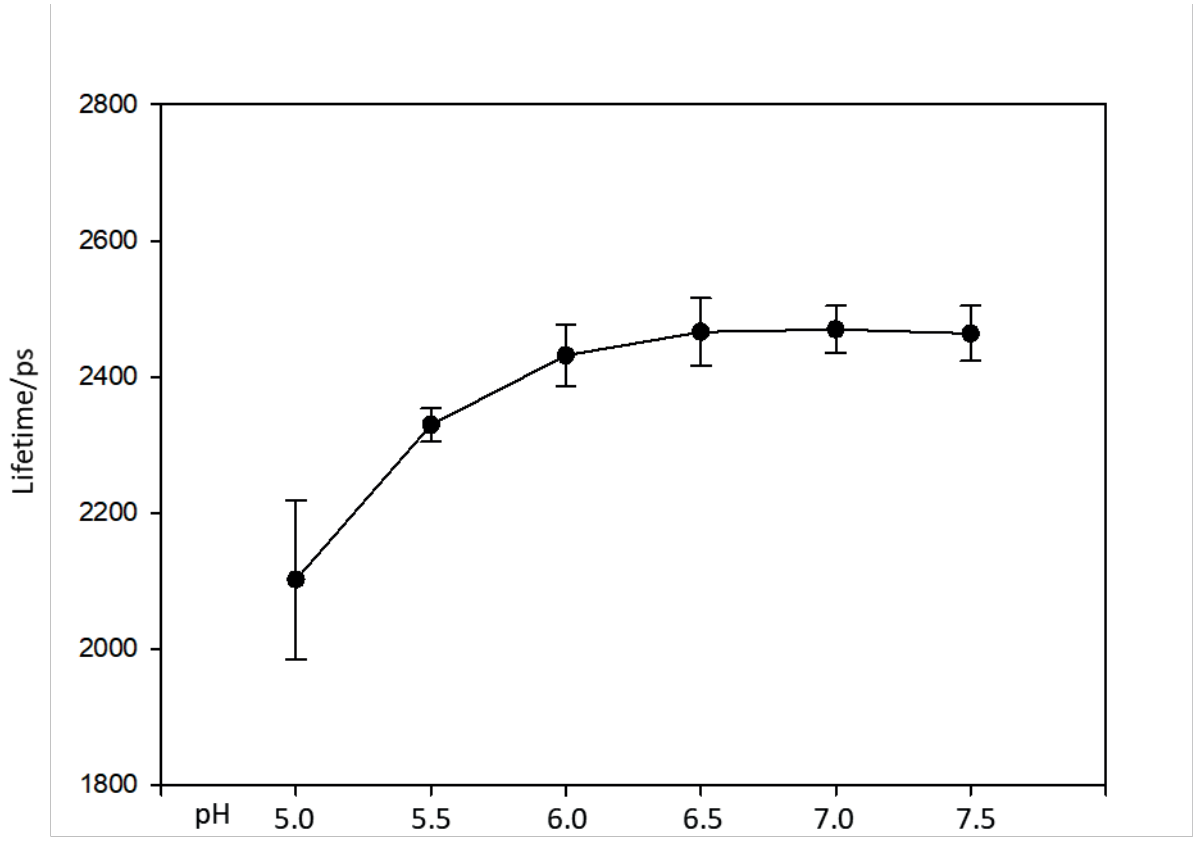

Figure 15: Calibration curve of the EGFP fluorescence lifetimes in different pH. Chromaffin cells were transfected with pCgA-EGFP and permeabilized with 10 µM nigericin in buffers having the desired pH between 5.0 and 7.5.

4.2.2 Intra vesicular pH and the dissociation of V1 and V0 domain.

Since we changed the intra vesicular pH sensor to CgA-EGFP, the FRET pair ECFP-EYFP could not be used. Thus I had generated another FRET pair based on the couple NowGFP-ShadowG. The ShadowG is a mutation of GFP that is be used as a dark acceptor in FRET experience. Although EGFP and NowGFP are both green, their lifetime

is totally different. Two GFP with different lifetime and a dark FRET acceptor of GFP, make it possible to measure pH and interaction between two proteins at the same time.
In order to prevent the uncertainty of co-transfection by three plasmids, which is relatively high in chromaffin cells, I have generated a tricistronic plasmid including all three genes needed, CgA-EGFP, V0a1 IV-NowGFP and ARNO-ShadowG. Each gene has its own CMV promoter for expression in mammalian cells. These experiments are still in progress and will hopefully be done soon.

4.2.3 Intra vesicular pH and the interaction between V0 domain and ARNO

Also, to prevent the uncertainty of co-transfection, I have generated a plasmid including CgA-EGFP, V0a1 IV-NowGFP and V1C1-ShadowG. This allows us to evaluate the dynamic of V0a-ARNO interaction and the relationship between V0a-ARNO interaction and intra vesicular pH.
These experiments are still in progress and will hopefully be done soon.

Chapter 5: Discussion and perspective

In neurosecretory cells the production of specific lipids at and near exocytotic sites appears to be an important regulatory element of the secretion of secretory vesicles [*Gasman and Vitale, 2017*]. Among these lipids, PA appears to play a prominent role, as it seems to control several steps of the secretory pathway from the secretory vesicle biogenesis, to its transport, docking and fusion at the plasma membrane (see Tanguy et al., and Carmon et al., in the annex section, two manuscript currently under evaluation). The major pathway regulating PA synthesis in neuroendocrine cells seems to involve PLD1 activity [*Vitale et al., 2001, Zeniou-Meyer et al., 2007*]. Stimulation of PLD1 activity involves kinases such as RSK2 [*Zeniou-Meyer et al., 2008*], but also small GTPases, including RalA [*Vitale et al., 2005*], Rac1 [*Momboisse et al., 2009*], and Arf6 [*Vitale et al., 2002; Béglé et al., 2009*]. Calcium, the main trigger of exocytosis was shown to promote RSK2 activity and PLD1 phosphorylation through the activation of the ERK pathway, but to date there is no information regarding the way calcium levels regulates the activity of RalA, Rac1, or Arf6.

Some studies have shown that the Arf GEF ARNO activates Arf6 in different membrane trafficking processes [*Hernández-Deviez et al., 2004; Eva et al., 2012; Zhu et al., 2017*]. Similarly ARNO was shown to promote Arf6 activation and PLD activity during exocytosis in neuroendocrine cells (*Caumont et al., 2000*), but the activation mechanism of ARNO is remaining unclearly until now. Since different subunits of the V-ATPase, known to be key participant in exocytosis, could also interact with ARNO/Arf6 on early endosomes to regulate the endocytic degradative pathway in epithelial cells [*Hurtado-Lorenzo et al., 2006*], we speculated that some subunits of the V-ATPase could in part regulate exocytosis via the ARNO-Arf6-PLD pathway in neuroendocrine cells.

Arf6 was shown to interact with c subunit of V0 in epithelial cells, but the functional implications of this interaction are not known [*Hurtado-Lorenzo et al., 2006*]. The same study further established that the amino-terminal domain of V0a2 is involved

in the interaction with ARNO and that the expression of the V0a2-Nt peptide fused to GFP could act as competitor to prevent the V0a-ARNO interaction [*Hurtado-Lorenzo et al., 2006*]. During my PhD work I found that V0a1 expressed on chromaffin granules interacts with ARNO within 2 minutes after cell stimulation by using a FLIM-FRET based approach, suggesting that V0a1 could be an activator of the ARNO-Arf6-PLD pathway during exocytosis. This timing is compatible with a previous study reporting by FRET that the highest Arf6 activation was detected around 2 minutes after exocytosis stimulation in PC12 cells [*Béglé et al.,2009*].

The overexpression of V0a1-Nt-GFP in PC12 cells inhibits the activation of Arf6 as detected by a reduced recruitment of the active Arf6 sensor MT2. It also decreases the stimulation of PLD activity and prevents PA synthesis at the plasma membrane as visualized by a lower recruitment of the PA probe Spo20p-PABD. These observations suggest that the interaction between plasma membrane associated ARNO and the granule associated V0a could occurs after granule tethering/docking at the exocytotic site. We also detected that Arf6 associated with V0c subunit by co-immunoprecipitation in PC12 cells (data not shown). This interaction may also contribute to close contact between V-ATPase, ARNO, and Arf6 and the activation of Arf6 resulting in PLD activation and PA synthesis to favor granule docking and ultimately membrane fusion.

The inhibition of V0a1-ARNO interaction reduced the number of events and affected the kinetics of single exocytosis events in chromaffin cells, showing the importance of this interaction for granule docking and fusion. A similar result was observed in cells treated with the PLD inhibitor FIPI suggesting that a major outcome of V0a1-Nt-GFP expression is reminiscent of an alteration of PA synthesis by the activation of PLD1 via ARNO-Arf6-PLD1 pathway.

We previously reported that the V0/V1 assembly is dependent on intragranular pH [*Poëa-Guyon et al., 2013*]. Also fluorescence recovery after photobleaching (FRAP) of

GFP-tagged V-ATPase subunits indicated that V0/V1 assembly is correlated with intragranular pH, with most acidic synaptic vesicles displaying low amounts of V1 [*Bodzęta et al., 2017*]. Furthermore an optogenetic approach revealed that incompletely filled synaptic vesicles fuse with lower release probability [*Herman et al., 2018*]. We can thus propose that the subdomain V0 of V-ATPase is an intragranular pH sensor that controls the V0/V1 association-dissociation, thus allowing the liberation of N-terminal of subunit V0a in order to interact with ARNO to product PA nearby exocytosis sites since PA synthesis at plasma membrane is regulated by Arf6 and its activator ARNO (Figure 16). This mechanism may thus provide a control step to avoid exocytosis of empty or incompletely filled vesicles since the fill-in of a secretory vesicle needs a certain gradient of protons, which makes the filled granule to show an acid pH around 5.5. Since most constituents of secretory granules from neuroendocrine cells are also recycled by compensatory endocytosis [*Ceridono et al., 2011*] and the V-ATPase also plays an important role in synaptic vesicle recycling and refilling [*Bodzęta et al., 2017*], the possible involvement of the pathway described here for secretory vesicle recycling remains to be explored.

The V-ATPase has since been found located on the plasma membranes in many different invasive cancer cells, including melanoma, breast, Ewing sarcoma, lung, liver, esophageal, prostate, ovarian, and pancreatic cancers [*Damaghi et al., 2013*]. Moreover, particular V-ATPase subunits have been found to be overexpressed in both human cancer cell lines and human tumor samples such as V1C [*García-García et al., 2012*], V0c [*Xu et al., 2012; Ohta et al., 1998*]. Overexpression of V-ATPase subunits has also been detected in lung, breast, and esophageal cancer tissues [*Hendrix et al., 2013; Huang et al., 2012; Lu et al., 2013*]. The V0a exist in four isoforms in mammalian cells allowing localization to specific membranes in cell and each of these V0a isoforms are overexpressed in many different cancer cells. This shows us the possibility that the interaction between subunits of V0 sector of V-ATPase and ARNO could be also a key regulator for the survival of certain cancer cells, which is interestingly to be explored. Indeed many cancer cells, show elevated PLD activity and PA synthesis that favor

survival and cell proliferation through the activation of multiple signaling pathway, among which the mTor pathway is the most prominent one.

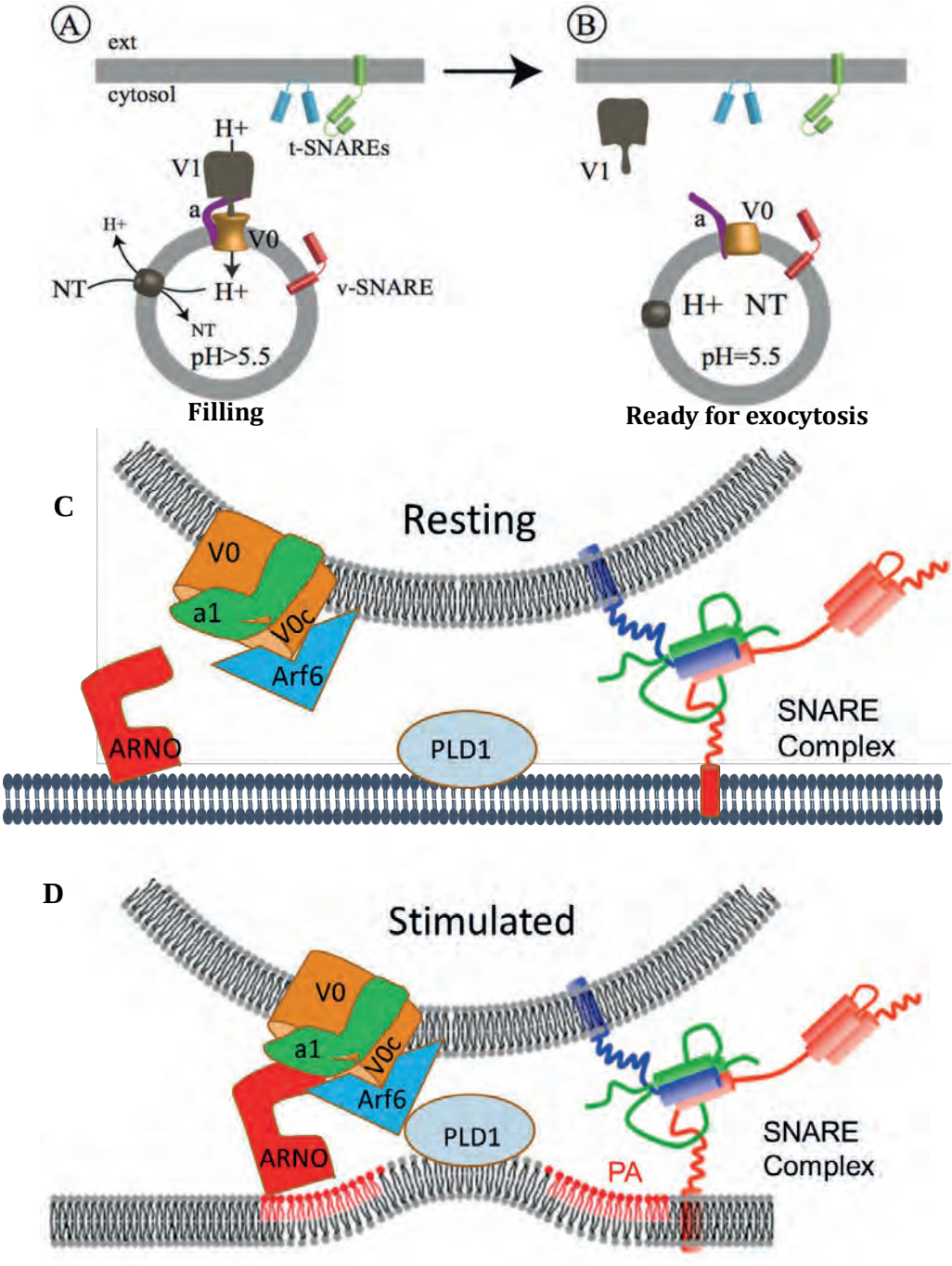

Figure 16: How V-ATPase regulate exocytosis: A) V-ATPase is functional with V0 associated with V1 allowing the filling of secretory granule that requires granule acidification. B) Once the granule is filled with neurotransmitter V1 and V0 domains dissociate allowing an interaction between the N terminal part of V0a and ARNO. C) Before stimulation the filled secretory vesicle can be tethered to the plasma membrane. D) The stimulation of exocytosis allows filled vesicle to further dock with plasma membrane and the subsequent interaction between ARNO and V0a triggering PA synthesis at exocytotic site by activating Arf6 to stimulate the activity of PLD1. Note that in this model we don't know when Arf6 and V0c interact.

Chapter 6: Materials and Methods

6.1 Molecular biology

The following plasmids were used to direct the expression of recombinant proteins. All inserted coding sequences and the junctions with the vectors were verified by sequencing. All plasmids in this work were generated in our laboratory and were amplified according to a standard protocol, including transformation and bacterial culture, followed by purification of the recombinant plasmids by the Qiagen endotoxin-free kit. All plasmids that I had generated in this work are shown below:

pV0a1 IV-EGFP	pV0a1 IV-ECFP	pV0a1 IV-EYFP	pV0a1 IV Nt-EGFP	pV0a1 II Nt-EGFP
pV0a1 II-EGFP	pV0a1 II-ECFP	pV0a1 II-EYFP	pV0a2-EGFP	pV0a2-ECFP
pV0a2-EYFP	pV0c-EGFP	pV1C1-EGFP	pV1C1-ECFP	pV1C1-EYFP
pV1C2-EGFP	pV1C2-ECFP	pV1C2-EYFP	pECFP-ARNO(WT)	pECFP-ARNO(M)
pArf6-EYFP		pARNO-ShadowG		pV0a1 IV-NowGFP
pARNO-ShadowG-V0a1IV-NowGFP-CgA-EGFP			pV1C1-ShadowG-V0a1IV-NowGFP-CgA-EGFP	
pARNO-ShadowG-V0a1IV-NowGFP			pCgA-pHuji	

6.2 Cell culture and transfection

6.2.1 Primary culture of bovine chromaffin cells (BCC)

The cells were seeded on fibronectin-coated glass slides at 250,000 cells/coverslip and used within three days of culture for immunofluorescence experiments. To induce exocytosis, intact chromaffin cells were washed twice with Locke's solution (140 mM NaCl, 4.7 mM KCl, 2.5 mM $CaCl_2$, 1.2 mM KH_2PO_4, 1.2 mM $MgSO_4$, 11 mM glucose, 0.56 mM ascorbic acid, 0.01 mM EDTA and 15 mM Hepes, pH 7.5), and then stimulated with Locke's solution containing 20 μM nicotine or a depolarising Locke solution containing K^+ 59mM.

6.2.2 PC12 cell line (rat pheochromocytoma)

The PC12 line is an adherent cell line obtained in rats from pheochromocytoma, a tumor of the adrenal gland. We use these cells in parallel with the primary culture of chromaffin cells because they have the advantage of being able to be transfected more efficiently.

PC12 cells are cultured in 10 cm diameter dishes in DMEM medium containing 4.5 g/L of glucose and 30 mM of NaHCO3 (Sigma, D5796), supplemented with 5% fetal calf serum (FBS) and 10% horse serum (HS) to obtain complete medium. During the weekly passage, the confluent cells are dissociated from the support by incubation for a few minutes with trypsin at room temperature (Gibco). After adding complete medium in order to inactivate the trypsin, the cell suspension is centrifuged for 5 minutes at 800 rpm and the pellet is resuspended in complete medium. The cells are inoculated at a dilution of 1/40 in complete medium and are then placed at 37°C in a humid atmosphere containing 5% of CO_2. Renewal of the medium is carried out 4 days after the passage. To carry out the experiments, PC12 cells are seeded in 8-well microplates (IBIDI) at a level of 70,000 cells / well for immunofluorescence or 50,000 cells/well for transfection. The supports are previously coated with poly-L-lysine at 10 µg / ml (PLL, Sigma).

6.2.3 Transfection of cells by lipofection

Lipofection or transfection by lipidic agent consists in including nucleic acids in micellar structures, liposomes, which by virtue of their structural properties analogous to those of cell membranes can then fuse with them and release their contents into the cell.

Transfection of PC12 cells is performed the day after seeding when the cells have reached 70-90% confluency. One hour before transfection, the medium is replaced by serum-depleted Opti-MEM medium (Gibco). For each transfection, the

DNA is complexed with Lipofectamine 2000 (Invitrogen). DNA and Lipofectamine are first diluted separately in Opti-MEM at a rate of 4 µg plasmid/250µl and 10 µl of Lipofectamine/250µl. The two solutions are then mixed and incubated for 5 to 10 minutes at room temperature. The nucleic acid-lipofectamine complex is added to the cells. The cells are then incubated at 37°C in a humid atmosphere containing 5% CO_2, and the Opti-MEM medium is replaced 4-6 hours after transfection. The cells are used 24 to 48 hours after the transfection. The transfection efficiency varied between 30 and 70%.

6.2.4 Transfection of cells by nucleofection

Isolated bovine chromaffin cells were transfected by electroporation using Basic Nucleofector™ Kit for Primary Mammalian Neurons (Lonza, Catalog #: VPI-1003). The device used for electroporation is Nucleofector™ 2b (Lonza, Catalog #: AAB-1001)

6.3 Confocal microscopy acquisitions

Acquisitions are performed using a confocal laser-scanning microscope (Leica TCS SP5 II) with the LAS-AF (Leica Application Suite Advanced Fluorescence) program. The virtual sections are made at the median plane of the cell with an objective x63, numerical aperture 1.4. In order to compare several conditions, all images were acquired with the same settings. Fluorescent markings are visualized using different lasers capable of exciting fluorophores.

6.4 Amperometry

Bovine chromaffin cells were washed with Locke's solution and processed for catecholamine release measurements by amperometry. Carbon-fiber electrode of 5 µm diameter (ALA Scientific) was held at a potential of +650 mV compared with the reference electrode (Ag/AgCl) and approached closely to GFP expressing cells. Catecholamine's secretion was induced by 10 seconds pressure ejection of 100 µM nicotine in Locke's solution or 100 mM K^+ solution from a micropipette positioned at 20 µm from the cell and recorded for 60 seconds. Amperometric recordings were performed with an AMU130 (Radiometer Analytical) amplifier, sampled at 5 kHz, and digitally low-passed filtered at 1 kHz. Analysis of amperometric recordings was done with a macro (obtained from Dr. R. Borges laboratory; http://webpages.ull.es/users/rborges/) written for Igor software (Wavemetrics), allowing automatic spike detection and extraction of spike parameters. The number of amperometric spikes was counted as the total number of spikes with an amplitude >5 pA within 60 seconds. The spike parameters analysis was restricted to spikes with amplitudes of 5 pA. Quantal size (Q) of individual spike is measured by calculating the spike area above the baseline. For foot-signal, the analysis was restricted to spikes with foot amplitudes of 1.5 pA.

6.5 FLIM of intragranular pH sensor

For pH calibration, cells transfected with CgA-EGFP (vector pEGFP-N2) were incubated in buffers containing 15 mM MES, 15 mM Hepes, 140 mM KCl, and 10 µM nigericin at pH ranging from 5 to 7.5. Time-resolved, laser-scanning, time-correlated two photon counting microscopy was performed on a homemade setup based on a microscope (TE2000; Nikon) equipped with a 60×, 1.2 NA water immersion objective. The FLIM setup allows real-time monitoring of EGFP lifetime variations and provides highly reproducible results (Poëa-Guyon et al., 2013).

6.6 FLIM-FRET

In a FRET experiment the potential binding partners are labeled with spectrally distinct fluorophores in such a way that the emission spectrum of the donor molecule overlaps the excitation spectrum of the acceptor molecule. If both interaction partners are in close contact at a distance of only a few nanometers, the excited donor can transfer its energy to the acceptor. In turn, the acceptor emits a fluorescence photon and the fluorescence lifetime of the donor molecule decreases.

In this study the FRET pair is V0a1 IV-NowGFP-ARNO-ShadowG and V0a1 IV-NowGFP-V1C1-ShadowG, the ShadowG is a mutation of GFP that be used as a dark acceptor in FRET experience. The bovine chromaffin cells or PC12 cells were transfected with plasmids expressing FRET pair and observed after 48 hours. To determine the FRET, the lifetime of V0a1 IV-NowGFP was measured in resting or stimulated condition. All RAW data were treated by SPCImage (version7.4).

References:

Ammar M. R., Kassas N., Chasserot-Golaz S., Bader M.-F. and Vitale N. (2013) Lipids in regulated exocytosis: what are they doing? Front. Endocrinol. 4, 125.

Baron, R., Neff, L., Louvard, D. and Courtoy, P.J. (1985) Cell-mediated extracellular acidification and bone resorption: evidence for a low pH in resorbing lacunae and localization of a 100-kD lysosomal membrane protein at the osteoclast ruffled border. J. Cell Biol., 101, 2210–2222.

Barr JR, Moura H, Boyer AE, Woolfitt AR, Kalb SR, Pavlopoulos A, McWilliams LG, Schmidt JG, Martinez RA, Ashley DL. Botulinum neurotoxin detection and differentiation by mass spectrometry. Emerg Infect Dis. 2005 Oct;11(10):1578-83.

Batlle D, Haque SK. Genetic causes and mechanisms of distal renal tubular acidosis. Nephrol Dial Transplant. 2012 Oct;27(10):3691-704.

Bayer MJ, Reese C, Buhler S, Peters C, Mayer A. Vacuole membrane fusion: V0 functions after trans-SNARE pairing and is coupled to the Ca2+-releasing channel. J Cell Biol. 2003 Jul 21;162(2):211-22.

Béglé A, Tryoen-Tóth P, de Barry J, Bader MF, Vitale N. ARF6 regulates the synthesis of fusogenic lipids for calcium-regulated exocytosis in neuroendocrine cells. J Biol Chem. 2009 Feb 20;284(8):4836-45.

Beyenbach KW, Wieczorek H. The V-type H+ ATPase: molecular structure and function, physiological roles and regulation. J Exp Biol. 2006 Feb;209(Pt 4):577-89.

Blair, H.C. (1998) How the osteoclast degrades bone. Bioessays , 20, 837–846

Bock LV, Hutchings B, Grubmüller H, Woodbury DJ. Chemomechanical regulation of SNARE proteins studied with molecular dynamics simulations. Biophys J. 2010 Aug 9;99(4):1221-30.

Bodzęta A, Kahms M, Klingauf J. The Presynaptic v-ATPase Reversibly Disassembles and Thereby Modulates Exocytosis but Is Not Part of the Fusion Machinery. Cell Rep. 2017 Aug 8;20(6):1348-1359.

Bond S, Forgac M. The Ras/cAMP/protein kinase A pathway regulates glucose-dependent assembly of the vacuolar (H+)-ATPase in yeast. J Biol Chem. 2008; 283:36513–36521.

Bonora M, Bononi A, De Marchi E, Giorgi C, Lebiedzinska M, Marchi S, Patergnani S, Rimessi A, Suski JM, Wojtala A, Wieckowski MR, Kroemer G, Galluzzi L, Pinton P (Feb 15, 2013). "Role of the c subunit of the FO ATP synthase in mitochondrial permeability transition". Cell cycle (Georgetown, Tex.). 12 (4): 674–83.

Bowman EJ, Siebers A, Altendorf K. Bafilomycins: a class of inhibitors of membrane ATPases from microorganisms, animal cells, and plant cells. Proc Natl Acad Sci U S A. 1988 Nov;85(21):7972-6.

Braakman I, Bulleid NJ. Protein folding and modification in the mammalian endoplasmic reticulum. Annu Rev Biochem. 2011;80:71-99.

Brown D, Paunescu TG, Breton S, Marshansky V. Regulation of the V-ATPase in kidney epithelial cells: dual role in acid-base homeostasis and vesicle trafficking. J Exp Biol. 2009 Jun;212(Pt 11):1762-72.

Burgess TL, Kelly RB, Constitutive and regulated secretion of proteins, Annu. Rev. Cell Biol. 3 (1987) 243–293.

Burkhardt P, Hattendorf DA, Weis WI, Fasshauer D. Munc18a controls SNARE assembly through its interaction with the syntaxin N-peptide. EMBO J. 2008 Apr 9;27(7):923-33.

Burri L, Lithgow T. A complete set of SNAREs in yeast. Traffic. 2004 Jan;5(1):45-52.

Camacho M., Machado J.D., Montesinos M.S., Criado M., Borges R. 2006. Intragranular pH rapidly modulates exocytosis in adrenal chromaffin cells. J. Neurochem. 96:324–334

Caumont AS, Galas MC, Vitale N, Aunis D and Bader MF (1998) Regulated exocytosis in chromaffin cells. Translocation of ARF6 stimulates a plasma membrane-associated phospholipase D. J Biol Chem, 273, 1373–1379.

Ceridono M., Ory S., Momboisse F. et al. (2011) Selective recapture of secretory granule components after full collapse exocytosis in neuroendocrine chromaffin cells. Traffic 12, 72–88.

Chen YA, Scheller RH. SNARE-mediated membrane fusion. Nat Rev Mol Cell Biol.2001 Feb;2(2):98-106.

Colacurcio DJ, Nixon RA. Disorders of lysosomal acidification-The emerging role of v-ATPase in aging and neurodegenerative disease. Ageing Res Rev. 2016 Dec; 32:75-88.

Condliffe SB, Corradini I, Pozzi D, Verderio C, Matteoli M. Endogenous SNAP-25 regulates native voltage-gated calcium channels in glutamatergic neurons. J Biol Chem. 2010 Aug 6;285(32):24968-76.

Corradini I, Verderio C, Sala M, Wilson MC, Matteoli M. SNAP-25 in neuropsychiatric disorders. Ann N Y Acad Sci. 2009 Jan; 1152:93-9

Da Silva N, Shum WW, El-Annan J, Păunescu TG, McKee M, Smith PJ, Brown D, Breton S. Relocalization of the V-ATPase B2 subunit to the apical membrane of epididymal clear cells of mice deficient in the B1 subunit. Am J Physiol Cell Physiol. 2007 Jul;293(1):C199-210.

Damaghi M, Wojtkowiak JW, Gillies RJ. pH sensing and regulation in cancer. Front Physiol 4: 370, 2013.

Di Giovanni J., Boudkkazi S., Mochida S., Bialowas A., Samari N., Lévêque C., Youssouf F., Brechet A., Iborra C., Maulet Y., et al. 2010. V-ATPase membrane sector associates with synaptobrevin to modulate neurotransmitter release. Neuron. 67:268–279

Diab H, Ohira M, Liu M, Cobb E, Kane PM. Subunit interactions and requirements for inhibition of the yeast V1-ATPase. J Biol Chem. 2009; 284:13316–13325.

Díaz E, Ayala G, Díaz ME, Gong LW, Toomre D. Automatic detection of large dense-core vesicles in secretory cells and statistical analysis of their intracellular distribution. IEEE/ACM Trans Comput Biol Bioinform. 2010 Jan-Mar;7(1):2-11.

Dowling JJ, Moore SA, Kalimo H, Minassian BA. X-linked myopathy with excessive autophagy: a failure of self-eating. Acta Neuropathol. 2015 Mar;129(3):383-90.

Drory O, Frolow F, Nelson N. Crystal structure of yeast V-ATPase subunit C reveals its stator function. EMBO Rep. 2004 Dec;5(12):1148-52.

Edwards RH. The neurotransmitter cycle and quantal size. Neuron. 2007 Sep 20;55(6):835-58.

El Far O, Seagar M. A role for V-ATPase subunits in synaptic vesicle fusion? J Neurochem. 2011 May;117(4):603-12.

Eva R, Crisp S, Marland JR, Norman JC, Kanamarlapudi V, ffrench-Constant C, Fawcett JW. (2012) ARF6 directs axon transport and traffic of integrins and regulates axon growth in adult DRG neurons. J Neurosci. 32(30):10352-64.

Fan SH, Wang YY, Lu J, Zheng YL, Wu DM, Zhang ZF, Shan Q, Hu B, Li MQ, Cheng W. CERS2 suppresses tumor cell invasion and is associated with decreased V-ATPase and MMP-2/MMP-9 activities in breast cancer. J Cell Biochem. 2015;116(4):502–513.

Fang Q, Lindau M. How could SNARE proteins open a fusion pore? Physiology (Bethesda). 2014 Jul;29(4):278-85

Fasshauer D, Sutton RB, Brunger AT, Jahn R. Conserved structural features of the synaptic fusion complex: SNARE proteins reclassified as Q- and R-SNAREs. Proc Natl Acad Sci USA.1998 Dec22;95(26):15781-6

Feng Y, Forgac M. A novel mechanism for regulation of vacuolar acidification. J Biol Chem. 1992 Oct 5;267(28):19769-72.

Feng Y, Forgac M. Inhibition of vacuolar H (+)-ATPase by disulfide bond formation between cysteine 254 and cysteine 532 in subunit A. J Biol Chem. 1994 May 6;269(18):13224-30.

Forgac M. Vacuolar ATPases: rotary proton pumps in physiology and pathophysiology. Nat Rev Mol Cell Biol. 2007 Nov;8(11):917-29.

Füldner H.H., Stadler H. 1982. 31P-NMR analysis of synaptic vesicles. Status of ATP and internal pH. Eur. J. Biochem. 121:519–524

Gabel M., Delavoie F., Demais V., Royer C., Bailly Y., Vitale N., Bader M.-F. and Chasserot-Golaz S. (2015) Annexin A2-dependent actin bundling promotes secretory granule docking to the plasma membrane and exocytosis. J. Cell Biol. 210, 785–800.

Gabriel SM, Haroutunian V, Powchik P, Honer WG, Davidson M, Davies P, Davis KL. Increased concentrations of presynaptic proteins in the cingulate cortex of subjects with schizophrenia. Arch Gen Psychiatry. 1997 Jun;54(6):559-66.

Galli T, McPherson PS, De Camilli P. The V0 sector of the V-ATPase, synaptobrevin, and synaptophysin are associated on synaptic vesicles in a Triton X-100-resistant, freeze-thawing sensitive, complex. J Biol Chem. 1996 Jan 26;271(4):2193-8.

García-García A, Pérez-Sayáns García M, Rodríguez MJ, Antúnez-López J, Barros-Angueira F, Somoza-Martín M, Gándara-Rey JM, Aguirre-Urízar JM. Immunohistochemical localization of C1 subunit of V-ATPase (ATPase C1) in oral squamous cell cancer and normal oral mucosa. Biotech Histochem 87: 133–139, 2012.

Gasman S, Vitale N. (2017) Lipid remodelling in neuroendocrine secretion. Biol Cell. 109(11):381-390.

Genis D, Davalos A, Molins A, Ferrer I. Wolfram syndrome: a neuropathological study. Acta Neuropathol. 1997; 93:426–429.

Gharanei S, Zatyka M, Astuti D, Fenton J, Sik A, Nagy Z, Barrett TG. Vacuolar-type H+-ATPase V1A subunit is a molecular partner of Wolfram syndrome 1 (WFS1) protein, which regulates its expression and stability. Hum Mol Genet. 2013; 22:203–217.

Greaves J, Gorleku OA, Salaun C, Chamberlain LH. Palmitoylation of the SNAP25 protein family: specificity and regulation by DHHC palmitoyl transferases. J Biol Chem. 2010 Aug 6;285(32):24629-38.

Greaves J, Prescott GR, Gorleku OA, Chamberlain LH. Regulation of SNAP-25 trafficking and function by palmitoylation. Biochem Soc Trans. 2010 Feb;38(Pt1):163-6.

Hammond SM et al. (1997) Characterization of two alternately spliced forms of phospholipase D1. Activation of the purified enzymes by phosphatidylinositol 4,5-bisphosphate, ADP-ribosylation factor and Rho family monomeric GTP-binding proteins and protein kinase C-α. J Biol Chem, 272, 3860–3868.

He L, Wu LG. The debate on the kiss-and-run fusion at synapses. Trends Neurosci. 2007 Sep;30(9):447-55.

Hedera P, Alvarado D, Beydoun A, Fink JK. Novel mental retardation-epilepsy syndrome linked to Xp21.1-p11.4. Ann Neurol. 2002; 51:45–50.

Hendrix A, Sormunen R, Westbroek W, Lambein K, Denys H, Sys G, Braems G, Van den Broecke R, Cocquyt V, Gespach C, Bracke M, De Wever O. Vacuolar H+ ATPase expression and activity is required for Rab27B-dependent invasive growth and metastasis of breast cancer. Int J Cancer 133: 843–854, 2013.

Herman MA, Trimbuch T, Rosenmund C. (2018) Differential pH Dynamics in Synaptic Vesicles from Intact Glutamatergic and GABAergic Synapses. Front Synaptic Neurosci. 10:44.

Hernández-Deviez DJ, Roth MG, Casanova JE, Wilson JM. (2004) ARNO and ARF6 regulate axonal elongation and branching through downstream activation of phosphatidylinositol 4-phosphate 5-kinase alpha. Mol Biol Cell. 15(1):111-20.

Hess EJ, Jinnah HA, Kozak CA, Wilson MC. Spontaneous locomotor hyperactivity in a mouse mutant with a deletion including the Snap gene on chromosome 2. J Neurosci. 1992 Jul;12(7):2865-74.

Hiesinger PR, Fayyazuddin A, Mehta SQ, Rosenmund T, Schulze KL, Zhai RG, Verstreken P, Cao Y, Zhou Y, Kunz J, Bellen HJ. The v-ATPase V0 subunit a1 is required for a late step in synaptic vesicle exocytosis in Drosophila. Cell. 2005 May 20;121(4):607-620.

Hinton A, Sennoune SR, Bond S, Fang M, Reuveni M, Sahagian GG, Jay D, Martinez-Zaguilan R, Forgac M. Function of a subunit isoforms of the V-ATPase in pH homeostasis and in vitro invasion of MDA-MB231 human breast cancer cells. J Biol Chem. 2009 Jun 12;284(24):16400-8.

Ho MN, Hirata R, Umemoto N, Ohya Y, Takatsuki A, Stevens TH, Anraku Y. VMA13 encodes a 54-kDa vacuolar H(+)-ATPase subunit required for activity but not assembly of the enzyme complex in Saccharomyces cerevisiae. J Biol Chem. 1993 Aug 25;268(24):18286-92.

Holliday LS, Lu M, Lee BS, Nelson RD, Solivan S, Zhang L, Gluck SL (2000) The amino-terminal domain of the B subunit of vacuolar H+-ATPase contains a filamentous actin binding site. J Biol Chem 275: 32331–32337.

Hong W, Lev S. Tethering the assembly of SNARE complexes. Trends Cell Biol.2014 Jan;24(1):35-43.

Houy S., Crois,e P., Gubar O., Chasserot-Golaz S., Tryoen-T,oth P., Bailly Y., Ory S., Bader M.-F. and Gasman S. (2013) Exocytosis and endocytosis in neuroendocrine cells: inseparable membranes!. Front. Endocrinol. 4, 135.

Hu C, Ahmed M, Melia TJ, Söllner TH, Mayer T, Rothman JE. Fusion of cells by flipped SNAREs. Science. 2003 Jun 13;300(5626):1745-9.

Huang L, Lu Q, Han Y, Li Z, Zhang Z, Li X. ABCG2/V-ATPase was associated with the drug resistance and tumor metastasis of esophageal squamous cancer cells. Diagn Pathol 7: 180, 2012.

Hurtado-Lorenzo A, Skinner M, El Annan J, Futai M, Sun-Wada GH, Bourgoin S, Casanova J, Wildeman A, Bechoua S, Ausiello DA, Brown D, Marshansky V. V-ATPase interacts with ARNO and Arf6 in early endosomes and regulates the protein degradative pathway. Nat Cell Biol. 2006 Feb;8(2):124-136.

Inoue H, Tanizawa Y, Wasson J, Behn P, Kalidas K, Bernal-Mizrachi E, Mueckler M, Marshall H, Donis-Keller H, Crock P, et al. A gene encoding a transmembrane protein is mutated in patients with diabetes mellitus and optic atrophy (Wolfram syndrome). Nat Genet. 1998; 20:143–148.

Inoue T, Forgac M (2005). "Cysteine-mediated cross-linking indicates that subunit C of the V-ATPase is in close proximity to subunits E and G of the V1 domain and subunit a of the V0 domain". J. Biol. Chem. 280 (30): 27896–27903.

Izumi H, Torigoe T, Ishiguchi H, Uramoto H, Yoshida Y, Tanabe M, Ise T, Murakami T, Yoshida T, Nomoto M, Kohno K (December 2003). "Cellular pH regulators: potentially promising molecular targets for cancer chemotherapy". Cancer Treatment Reviews. 29 (6): 541–9.

Jahn R, Fasshauer D. Molecular machines governing exocytosis of synaptic vesicles. Nature. 2012 Oct 11;490(7419):201-7.

Jefferies KC, Forgac M. Subunit H of the vacuolar (H+) ATPase inhibits ATP hydrolysis by the free V1 domain by interaction with the rotary subunit F. J Biol Chem. 2008;283:4512–4519.

Jones R, Findlay JB, Harrison M, Durose L, Song CF, Barratt E, Trinick J (2003). "Structure and function of the vacuolar H+-ATPase: moving from low-resolution models to high-resolution structures". J. Bioenerg. Biomembr. 35 (4): 337–345.

Kane PM. Disassembly and reassembly of the yeast vacuolar H (+)-ATPase in vivo. J Biol Chem. 1995; 270:17025–17032.

Kane PM. The where, when, and how of organelle acidification by the yeast vacuolar H+-ATPase. Microbiol Mol Biol Rev. 2006 Mar;70(1):177-91.

Karatekin E, Tran VS, Huet S, Fanget I, Cribier S, Henry JP. A 20-nm step toward the cell membrane preceding exocytosis may correspond to docking of tethered granules. Biophys J. 2008 Apr 1;94(7):2891-905.

Karet FE, Finberg KE, Nelson RD, Nayir A, Mocan H, Sanjad SA, Rodriguez-Soriano J,

Santos F, Cremers CW, Di Pietro A, Hoffbrand BI, Winiarski J, Bakkaloglu A, Ozen S, Dusunsel R, Goodyer P, Hulton SA, Wu DK, Skvorak AB, Morton CC, Cunningham MJ, Jha V, Lifton RP. Mutations in the gene encoding B1 subunit of H+-ATPase cause renal tubular acidosis with sensorineural deafness. Nat Genet. 1999 Jan;21(1):84-90.

Kasula R, Chai YJ, Bademosi AT, Harper CB, Gormal RS, Morrow IC, Hosy E, Collins BM, Choquet D, Papadopulos A, Meunier FA. The Munc18-1 domain 3a hinge-loop controls syntaxin-1A nanodomain assembly and engagement with the SNARE complex during secretory vesicle priming. J Cell Biol. 2016 Sep 26;214(7):847-58.

Kawasaki-Nishi S, Bowers K, Nishi T, Forgac M, Stevens TH. The amino-terminal domain of the vacuolar proton-translocating ATPase a subunit controls targeting and in vivo dissociation, and the carboxyl-terminal domain affects coupling of proton transport and ATP hydrolysis. J Biol Chem. 2001; 276:47411–47420.

Kawasaki-Nishi S, Yamaguchi A, Forgac M, Nishi T. Tissue specific expression of the splice variants of the mouse vacuolar proton-translocating ATPase a4 subunit. Biochem Biophys Res Commun. 2007 Dec 28 ;364(4):1032-6.

Kiessling V, Tamm LK. Measuring distances in supported bilayers by fluorescence interference-contrast microscopy: polymer supports and SNARE proteins. Biophys J. 2003 Jan;84(1):408-18.

Kim JH, Lingwood CA, Williams DB, Furuya W, Manolson MF, Grinstein S. Dynamic measurement of the pH of the Golgi complex in living cells using retrograde transport of the verotoxin receptor. J Cell Biol. 1996 Sep;134(6):1387-99.

Kinouchi K, Ichihara A, Itoh H. Functional characterization of (pro)renin receptor in association with V-ATPase. Front Biosci (Landmark Ed) 2011; 16:3216–3223.

Kinouchi K, Ichihara A, Sano M, Sun-Wada GH, Wada Y, Ochi H, Fukuda T, Bokuda K, Kurosawa H, Yoshida N, et al. The role of individual domains and the significance of shedding of ATP6AP2/(pro)renin receptor in vacuolar H(+)-ATPase biogenesis. PLoS One. 2013;8:e78603.

Kissing S, Saftig P, Haas A. Vacuolar ATPase in phago(lyso)some biology. Int J Med Microbiol. 2017.

Kitagawa N, Mazon H, Heck AJ, Wilkens S. Stoichiometry of the peripheral stalk subunits E and G of yeast V1-ATPase determined by mass spectrometry. J Biol Chem. 2008 Feb 8;283(6):3329-37.

Kornak U, Reynders E, Dimopoulou A, van Reeuwijk J, Fischer B, Rajab A, et al. Impaired glycosylation and cutis laxa caused by mutations in the vesicular H+-ATPase subunit ATP6V0A2. Nat Genet. 2008; 40:32–4.

Kornak U, Schulz A, Friedrich W, Uhlhaas S, Kremens B, Voit T, Hasan C, Bode U, Jentsch TJ, Kubisch C. Mutations in the a3 subunit of the vacuolar H (+)-ATPase cause infantile malignant osteopetrosis. Hum Mol Genet. 2000 Aug 12 ;9(13) :2059-63.

Kortum F, Caputo V, Bauer CK, Stella L, Ciolfi A, Alawi M, Bocchinfuso G, Flex E, Paolacci S, Dentici ML, et al. Mutations in KCNH1 and ATP6V1B2 cause Zimmermann-Laband syndrome. Nat Genet. 2015; 47:661–667.

Korvatska O, Strand NS, Berndt JD, Strovas T, Chen DH, Leverenz JB, Kiianitsa K, Mata IF, Karakoc E, Greenup JL, et al. Altered splicing of ATP6AP2 causes X-linked

parkinsonism with spasticity (XPDS). Hum Mol Genet. 2013; 22:3259–3268.
Kulshrestha A, Katara GK, Ibrahim S, Pamarthy S, Jaiswal MK, Sachs AG, Beaman KD. Vacuolar ATPase 'a2' isoform exhibits distinct cell surface accumulation and modulates matrix metalloproteinase activity in ovarian cancer. Oncotarget. 2015;6(6):3797–3810.
Lam DK, Sándor GK, Holmes HI, Carmichael RP, Clokie CM. Marble bone disease: a review of osteopetrosis and its oral health implications for dentists. J Can Dent Assoc. 2007 Nov;73(9):839-43
Lee J-HH, Yu WH, Kumar A, Lee S, Mohan PS, Peterhoff CM, Wolfe DM, Martinez-Vicente M, Massey AC, Sovak G, et al. Lysosomal proteolysis and autophagy require presenilin 1 and are disrupted by Alzheimer-related PS1 mutations. Cell. 2010; 141:1146–1158
Lee SH, Rho J, Jeong D, Sul JY, Kim T, Kim N, Kang JS, Miyamoto T, Suda T, Lee SK, Pignolo RJ, Koczon-Jaremko B, Lorenzo J, Choi Y. v-ATPase V0 subunit d2-deficient mice exhibit impaired osteoclast fusion and increased bone formation. Nat Med. 2006 Dec;12(12):1403-9.
Li G, Yang Q, Alexander EA, Schwartz JH. Syntaxin 1A has a specific binding site in the H3 domain that is critical for targeting of H+-ATPase to apical membrane of renal epithelial cells. Am J Physiol Cell Physiol. 2005 Sep;289(3):C665-72.
Liégeois S., Benedetto A., Garnier J.M., Schwab Y., Labouesse M. 2006. The V0-ATPase mediates apical secretion of exosomes containing Hedgehog-related proteins in *Caenorhabditis elegans*. J. Cell Biol. 173:949–961.
Liu Q, Kane PM, Newman PR, Forgac M. Site-directed mutagenesis of the yeast V-ATPase B subunit (Vma2p). J Biol Chem. 1996 Jan 26;271(4):2018-22.
Liu Q, Leng XH, Newman PR, Vasilyeva E, Kane PM, Forgac M. Site-directed mutagenesis of the yeast V-ATPase A subunit. J Biol Chem. 1997 May 2;272(18):117506.
Lu Q, Lu S, Huang L, Wang T, Wan Y, Zhou CX, Zhang C, Zhang Z, Li X. The expression of V-ATPase is associated with drug resistance and pathology of non-small-cell lung cancer. Diagn Pathol 8: 145, 2013.
Ludwig J, Kerscher S, Brandt U, Pfeiffer K, Getlawi F, Apps DK, Schägger H.Identification and characterization of a novel 9.2-kDa membrane sector-associated protein of vacuolar proton-ATPase from chromaffin granules. J Biol Chem. 1998 May 1;273(18):10939-47.
MacDonald C, Munson M, Bryant NJ. Autoinhibition of SNARE complex assembly by a conformational switch represents a conserved feature of syntaxins. Biochem Soc Trans. 2010 Feb;38(Pt 1):209-12.
Malkus P, Graham LA, Stevens TH, Schekman R. Role of Vma21p in assembly and transport of the yeast vacuolar ATPase. Mol Biol Cell. 2004; 15:5075–5091.
Malsam J, Söllner TH. Organization of SNAREs within the Golgi stack. Cold Spring Harb Perspect Biol. 2011 Oct 1;3(10): a005249.
Manolson MF, Wu B, Proteau D, Taillon BE, Roberts BT, Hoyt MA, Jones EW. STV1 gene encodes functional homologue of 95-kDa yeast vacuolar H (+)-ATPase subunit Vph1p. J Biol Chem. 1994 May 13;269(19):14064-74.

Maritzen T, Haucke V. Coupling of exocytosis and endocytosis at the presynaptic active zone. Neurosci Res. 2018 Feb;127:45-52.

Marshansky V, Futai M. The V-type H+-ATPase in vesicular trafficking: targeting, regulation and function. Curr Opin Cell Biol. 2008;20(4):415–426.

Maxfield FR, McGraw TE. Endocytic recycling. Nat Rev Mol Cell Biol. 2004 Feb;5(2):121-32.

Michaelson DM, Angel I. Determination of delta pH in cholinergic synaptic vesicles: its effect on storage and release of acetylcholine. Life Sci. 1980 Jul 7;27(1):39-44.

Mindell JA. Lysosomal acidification mechanisms. Annual review of physiology. 2012; 74:69–86.

Mishima T, Fujiwara T, Sanada M, Kofuji T, Kanai-Azuma M, Akagawa K. Syntaxin 1B, but not syntaxin 1A, is necessary for the regulation of synaptic vesicle exocytosis and of the readily releasable pool at central synapses. PLoS One. 2014 Feb 28;9(2): e90004.

MITCHELL P. Coupling of phosphorylation to electron and hydrogen transfer by a chemi-osmotic type of mechanism. Nature. 1961 Jul 8; 191:144-8.

Momboisse F, Lonchamp E, Calco V, Ceridono M, Vitale N, Bader MF, Gasman S. (2009) betaPIX-activated Rac1 stimulates the activation of phospholipase D, which is associated with exocytosis in neuroendocrine cells. J Cell Sci. 122(Pt 6):798-806.

Morava E, Guillard M, Lefeber DJ, Wevers RA. Autosomal recessive cutis laxa syndrome revisited. Eur J Hum Genet. 2009; 17:1099–110.

Morel N, Dedieu JC, Philippe JM. Specific sorting of the a1 isoform of the V-H+ATPase a subunit to nerve terminals where it associates with both synaptic vesicles and the presynaptic plasma membrane. J Cell Sci. 2003 Dec 1;116(Pt 23):4751-62.

Morel N, Dunant Y, Israël M. Neurotransmitter release through the V0 sector of V-ATPase. J Neurochem. 2001 Nov ;79(3) :485-8.

Neher E, Sakaba T. Multiple roles of calcium ions in the regulation of neurotransmitter release. Neuron. 2008 Sep 25;59(6):861-72.

Nelson N, Perzov N, Cohen A, Hagai K, Padler V, Nelson H (January 2000). "The cellular biology of proton-motive force generation by V-ATPases". The Journal of Experimental Biology. 203 (Pt 1): 89–95.

Nixon RA. The role of autophagy in neurodegenerative disease. Nat Med. 2013 Aug;19(8):983-97.

Ohta T, Arakawa H, Futagami F, Fushida S, Kitagawa H, Kayahara M, Nagakawa T, Miwa K, Kurashima K, Numata M, Kitamura Y, Terada T, Ohkuma S. Bafilomycin A1 induces apoptosis in the human pancreatic cancer cell line Capan-1. J Pathol 185: 324–330, 1998.

Ohya Y, Umemoto N, Tanida I, Ohta A, Iida H, Anraku Y (July 1991). "Calcium-sensitive cls mutants of Saccharomyces cerevisiae showing a Pet- phenotype are ascribable to defects of vacuolar membrane H(+)-ATPase activity". The Journal of Biological Chemistry. 266 (21): 13971–7.

Pamarthy S, Kulshrestha A, Katara GK, Beaman KD. The curious case of vacuolar ATPase: regulation of signaling pathways. Mol Cancer. 2018 Feb15;17(1):41.

Parra KJ, Kane PM. Reversible association between the V1 and V0 domains of yeast

vacuolar H+-ATPase is an unconventional glucose-induced effect. Mol Cell Biol. 1998; 18:7064–7074.

Parra KJ, Keenan KL, Kane PM. The H subunit (Vma13p) of the yeast V-ATPase inhibits the ATPase activity of cytosolic V1 complexes. J Biol Chem. 2000; 275:21761–21767.

Pasternak SH, Bagshaw RD, Guiral M, Zhang S, Ackerley CA, Pak BJ, Callahan JW, Mahuran DJ. Presenilin-1, nicastrin, amyloid precursor protein, and gamma-secretase activity are co-localized in the lysosomal membrane. J Biol Chem. 2003;278(29):26687–26694.

Paunescu TG, Da Silva N, Marshansky V, McKee M, Breton S, Brown D. Expression of the 56-kDa B2 subunit isoform of the vacuolar H(+)-ATPase in proton-secreting cells of the kidney and epididymis. Am J Physiol Cell Physiol. 2004 Jul;287(1):C149-62.

Paunescu TG, Jones AC, Tyszkowski R, Brown D. V-ATPase expression in the mouse olfactory epithelium. Am J Physiol Cell Physiol. 2008 Oct;295(4):C923-30.

Peri F, Nüsslein-Volhard C. Live imaging of neuronal degradation by microglia reveals a role for v0-ATPase a1 in phagosomal fusion in vivo. Cell. 2008 May 30;133(5):916-27.

Peters C, Bayer MJ, Bühler S, Andersen JS, Mann M, Mayer A. Trans-complex formation by proteolipid channels in the terminal phase of membrane fusion. Nature. 2001 Feb 1;409(6820):581-8

Pietrement C, Sun-Wada GH, Silva ND, McKee M, Marshansky V, Brown D, Futai M, Breton S. Distinct expression patterns of different subunit isoforms of the V-ATPase in the rat epididymis. Biol Reprod. 2006 Jan;74(1):185-94.

Poorkaj P, Raskind WH, Leverenz JB, Matsushita M, Zabetian CP, Samii A, Kim S, Gazi N, Nutt JG, Wolff J, et al. A novel X-linked four-repeat tauopathy with Parkinsonism and spasticity. Mov Disord. 2010; 25:1409–1417.

Poëa-Guyon S, Ammar MR, Erard M, Amar M, Moreau AW, Fossier P, Gleize V, Vitale N, Morel N. The V-ATPase membrane domain is a sensor of granular pH that controls the exocytotic machinery. J Cell Biol. 2013 Oct 28;203(2):283-98.

Qi J, Forgac M. Cellular environment is important in controlling V-ATPase dissociation and its dependence on activity. J Biol Chem. 2007; 282:24743–24751.

Rajab A, Kornak U, Budde BS, Hoffmann K, Jaeken J, Nürnberg P, et al. Geroderma osteodysplasticum hereditaria and wrinkly skin syndrome in 22 patients from Oman. Am J Med Genet A. 2008; 146:965–76.

Rigoli L, Di Bella C. Wolfram syndrome 1 and Wolfram syndrome 2. Curr Opin Pediatr. 2012; 24:512–517.

Risselada HJ, Kutzner C, Grubmüller H. Caught in the act: visualization of SNARE-mediated fusion events in molecular detail. Chembiochem. 2011 May 2;12(7):1049-55.

Risselada HJ, Grubmüller H. How SNARE molecules mediate membrane fusion:recent insights from molecular simulations. Curr Opin Struct Biol. 2012 Apr;22(2):187-96.

Rubinstein JL, Walker JE, Henderson R (2003) Structure of the mitochondrial ATP synthase by electron cryomicroscopy. EMBO J 22: 6182–6192

Saftig P, Klumperman J. Lysosome biogenesis and lysosomal membrane proteins: trafficking meets function. Nature reviews Molecular cell biology. 2009; 10:623–635.

Salaun C., Gould G. W. and Chamberlain L. H. (2005) Lipid raft association of SNARE proteins regulates exocytosis in PC12 cells. J. Biol. Chem. 280, 19449–19453

Sandoval GM, Duerr JS, Hodgkin J, Rand JB, Ruvkun G. A genetic interaction between the vesicular acetylcholine transporter VAChT/UNC-17 and synaptobrevin/SNB-1 in C. elegans. Nat Neurosci. 2006 May;9(5):599-601.

Sautin YY, Lu M, Gaugler A, Zhang L, Gluck SL. Phosphatidylinositol 3-kinase-mediated effects of glucose on vacuolar H+-ATPase assembly, translocation, and acidification of intracellular compartments in renal epithelial cells. Mol Cell Biol. 2005 Jan;25(2):575-89.

Sennoune SR, Bakunts K, Martínez GM, Chua-Tuan JL, Kebir Y, Attaya MN, Martínez-Zaguilán R. Vacuolar H+-ATPase in human breast cancer cells with distinct metastatic potential: distribution and functional activity. Am J Physiol Cell Physiol 286: C1443–C1452, 2004.

Seol JH, Shevchenko A, Deshaies RJ. Skp1 forms multiple protein complexes, including RAVE, a regulator of V-ATPase assembly. Nat Cell Biol. 2001; 3:384–391.

Shao E, Forgac M. Involvement of the nonhomologous region of subunit A of the yeast V-ATPase in coupling and in vivo dissociation. J Biol Chem. 2004; 279:48663–48670.

Shao E, Nishi T, Kawasaki-Nishi S, Forgac M. Mutational analysis of the non-homologous region of subunit A of the yeast V-ATPase. J Biol Chem. 2003; 278:12985–12991.

Shen C, Rathore SS, Yu H, Gulbranson DR, Hua R, Zhang C, Schoppa NE, Shen J. The trans-SNARE-regulating function of Munc18-1 is essential to synaptic exocytosis. Nat Commun. 2015 Nov 17;6:8852.

Smardon AM, Kane PM. RAVE is essential for the efficient assembly of the C subunit with the vacuolar H (+)-ATPase. J Biol Chem. 2007; 282:26185–26194.

Smardon AM, Tarsio M, Kane PM. The RAVE complex is essential for stable assembly of the yeast V-ATPase. J Biol Chem. 2002; 277:13831–13839.

Smith AN, Borthwick KJ, Karet FE. Molecular cloning and characterization of novel tissue-specific isoforms of the human vacuolar H (+)-ATPase C, G and d subunits, and their evaluation in autosomal recessive distal renal tubular acidosis. Gene. 2002 Sep 4;297(1-2):169-77.

Smith AN, Francis RW, Sorrell SL, Karet FE. The d subunit plays a central role in human vacuolar H(+)-ATPases. J Bioenerg Biomembr. 2008 Aug;40(4):371-80.

Smith AN, Jouret F, Bord S, Borthwick KJ, Al-Lamki RS, Wagner CA, Ireland DC, Cormier-Daire V, Frattini A, Villa A, Kornak U, Devuyst O, Karet FE. Vacuolar H+-ATPase d2 subunit: molecular characterization, developmental regulation, and localization to specialized proton pumps in kidney and bone. J Am Soc Nephrol. 2005 May;16(5):1245-56.

Smith AN, Skaug J, Choate KA, Nayir A, Bakkaloglu A, Ozen S, Hulton SA, Sanjad SA, Al-Sabban EA, Lifton RP, Scherer SW, Karet FE. Mutations in ATP6N1B, encoding a

new kidney vacuolar proton pump 116-kD subunit, cause recessive distal renal tubular acidosis with preserved hearing. Nat Genet. 2000 Sep;26(1):71-5.

Sobacchi C, Frattini A, Orchard P, Porras O, Tezcan I, Andolina M, Babul-Hirji R, Baric I, Canham N, Chitayat D, Dupuis-Girod S, Ellis I, Etzioni A, Fasth A, Fisher A, Gerritsen B, Gulino V, Horwitz E, Klamroth V, Lanino E, Mirolo M, Musio A, Matthijs G, Nonomaya S, Notarangelo LD, Ochs HD, Superti Furga A, Valiaho J, van Hove JL, Vihinen M, Vujic D, Vezzoni P, Villa A. The mutational spectrum of human malignant autosomal recessive osteopetrosis. Hum Mol Genet. 2001 Aug 15 ;10(17) :1767-1773.

Söllner T, Bennett MK, Whiteheart SW, Scheller RH, Rothman JE. A protein assembly-disassembly pathway in vitro that may correspond to sequential steps of synaptic vesicle docking, activation, and fusion. Cell. 1993 Nov 5;75(3):409-18.

Stransky L, Cotter K, Forgac M. The Function of V-ATPases in Cancer. Physiol Rev. 2016 Jul;96(3):1071-91.

Stark Z, Savarirayan R. Osteopetrosis. Orphanet J Rare Dis. 2009 Feb 20 ; 4 :5.

Stehberger PA, Schulz N, Finberg KE, Karet FE, Giebisch G, Lifton RP, Geibel JP, Wagner CA. Localization and regulation of the ATP6V0A4 (a4) vacuolar H+-ATPase subunit defective in an inherited form of distal renal tubular acidosis. J Am Soc Nephrol. 2003 Dec;14(12):3027-38.

Stenmark H. Rab GTPases as coordinators of vesicle traffic. Nat Rev Mol Cell Biol. 2009 Aug;10(8):513-25.

Stover EH, Borthwick KJ, Bavalia C, Eady N, Fritz DM, Rungroj N, Giersch AB, Morton CC, Axon PR, Akil I, Al-Sabban EA, Baguley DM, Bianca S, Bakkaloglu A, Bircan Z, Chauveau D, Clermont MJ, Guala A, Hulton SA, Kroes H, Li Volti G, Mir S, Mocan H, Nayir A, Ozen S, Rodriguez Soriano J, Sanjad SA, Tasic V, Taylor CM, Topaloglu R, Smith AN, Karet FE. Novel ATP6V1B1 and ATP6V0A4 mutations in autosomal recessive distal renal tubular acidosis with new evidence for hearing loss. J Med Genet. 2002 Nov;39(11):796-803.

Strasser B, Iwaszkiewicz J, Michielin O, Mayer A. The V-ATPase proteolipid cylinder promotes the lipid-mixing stage of SNARE-dependent fusion of yeast vacuoles. EMBO J. 2011 Sep 20;30(20):4126-41.

Strom TM, Hortnagel K, Hofmann S, Gekeler F, Scharfe C, Rabl W, Gerbitz KD, Meitinger T. Diabetes insipidus, diabetes mellitus, optic atrophy and deafness (DIDMOAD) caused by mutations in a novel gene (wolframin) coding for a predicted transmembrane protein. Hum Mol Genet. 1998; 7:2021–2028.

Südhof TC, Rothman JE. Membrane fusion: grappling with SNARE and SM proteins. Science. 2009 Jan 23;323(5913):474-7.

Sun-Wada GH, Tabata H, Kawamura N, Futai M, Wada Y. Differential expression of a subunit isoforms of the vacuolar-type proton pump ATPase in mouse endocrine tissues. Cell Tissue Res. 2007 Aug;329(2):239-48.

Sun-Wada GH, Toyomura T, Murata Y, Yamamoto A, Futai M, Wada Y. The a3 isoform of V-ATPase regulates insulin secretion from pancreatic beta-cells. J Cell Sci. 2006 Nov 1;119(Pt 21):4531-40.

Sun-Wada GH, Yoshimizu T, Imai-Senga Y, Wada Y, Futai M. Diversity of mouse proton-translocating ATPase: presence of multiple isoforms of the C, d and G subunits. Gene. 2003 Jan 2;302(1-2):147-53.

Sutton RB, Fasshauer D, Jahn R, Brunger AT. Crystal structure of a SNARE complex involved in synaptic exocytosis at 2.4 A resolution. Nature. 1998 Sep 24;395(6700):347-53.

Takamori S, Holt M, Stenius K, Lemke EA, Grønborg M, Riedel D, Urlaub H, Schenck S, Brügger B, Ringler P, Müller SA, Rammner B, Gräter F, Hub JS, De Groot BL, Mieskes G, Moriyama Y, Klingauf J, Grubmüller H, Heuser J, Wieland F, Jahn R. Molecular anatomy of a trafficking organelle. Cell. 2006 Nov 17; 127 (4): 831-46.

Takeda K, Cabrera M, Rohde J, Bausch D, Jensen ON, Ungermann C. The vacuolar V1/V0-ATPase is involved in the release of the HOPS subunit Vps41 from vacuoles, vacuole fragmentation and fusion. FEBS Lett. 2008 Apr 30;582 (10):1558-63.

Tanguy E, Carmon O, Wang Q, Jeandel L, Chasserot-Golaz S, Montero-Hadjadje M, Vitale N.（2016）Lipids implicated in the journey of a secretory granule: from biogenesis to fusion. J Neurochem. 137(6):904-912.

Teng FY, Wang Y, Tang BL. The syntaxins. GenomeBiol .2001;2(11): REVIEWS3012. Epub 2001 Oct 24.

Thompson PM, Sower AC, Perrone-Bizzozero NI. Altered levels of the synaptosomal associated protein SNAP-25 in schizophrenia. Biol Psychiatry. 1998 Feb 15;43(4):239-43.

Toei M, Saum R, Forgac M. Regulation and isoform function of the V-ATPases. Biochemistry. 2010;49(23):4715–4723.

Tomashek JJ, Garrison BS, Klionsky DJ. Reconstitution in vitro of the V1 complex from the yeast vacuolar proton-translocating ATPase. Assembly recapitulates mechanism. J Biol Chem. 1997; 272:16618–23.

Tomashek JJ, Graham LA, Hutchins MU, Stevens TH, Klionsky DJ. V1-situated stalk subunits of the yeast vacuolar proton-translocating ATPase. J Biol Chem. 1997; 272:26787–93.

Toyomura T, Murata Y, Yamamoto A, Oka T, Sun-Wada GH, Wada Y, Futai M. From lysosomes to the plasma membrane: localization of vacuolar-type H+ -ATPase with the a3 isoform during osteoclast differentiation. J Biol Chem. 2003 Jun 13;278(24):22023-30. Epub 2003 Apr 2.

Trombetta ES, Ebersold M, Garrett W, Pypaert M, Mellman I. Activation of lysosomal function during dendritic cell maturation. Science. 2003 Feb 28;299(5611):1400-3.

Umbrecht-Jenck E., Demais V., Calco V., Bailly Y., Bader M.-F. and Chasserot-Golaz S. (2010) S100A10-mediated translocation of annexin-A2 to SNARE proteins in adrenergic chromaffin cells undergoing exocytosis. Traffic 11, 958–971.

Urano F. Wolfram Syndrome: Diagnosis, Management, and Treatment. Curr Diab Rep. 2016; 16:6

Venzano V, Conforti G, Marchesi A, Minetti C, Iester A. [The association of juvenile diabetes mellitus, primary optic atrophy and deafness (the Wolfram and Ikkos syndrome). Apropos of a personal case]. Minerva Pediatr. 1980; 32:685–692.

Vitale N, Chasserot-Golaz S, Bader MF. Regulated secretion in chromaffin cells: an essential role for ARF6-regulated phospholipase D in the late stages of exocytosis. Ann N Y Acad Sci. 2002 Oct; 971:193-200.

Vitale N, Chasserot-Golaz S, Bailly Y, Morinaga N, Frohman MA, Bader MF. Calcium-regulated exocytosis of dense-core vesicles requires the activation of ADP-ribosylation factor (ARF)6 by ARF nucleotide binding site opener at the plasma membrane. J Cell Biol. 2002 Oct 14;159(1):79-89.

Vitale N, Caumont AS, Chasserot-Golaz S, Du G, Wu S, Sciorra VA, Morris AJ, Frohman MA, Bader MF. Phospholipase D1: a key factor for the exocytotic machinery in neuroendocrine cells. EMBO J. 2001 May 15;20(10):2424-34.

Vitale N, Mawet J, Camonis J, Regazzi R, Bader MF, Chasserot-Golaz S. The Small GTPase RalA controls exocytosis of large dense core secretory granules by interacting with ARF6-dependent phospholipase D1. J Biol Chem. 2005 Aug 19;280(33):29921-8.

Vitale N., Thierse D., Aunis D. and Bader M.-F. (1994) Exocytosis in chromaffin cells: evidence for a MgATP-independent step that requires a pertussis toxin-sensitive GTP-binding protein. Biochem. J. 300, 217–227.

Voss M, Vitavska O, Walz B, Wieczorek H, Baumann O. Stimulus-induced phosphorylation of vacuolar H (+)-ATPase by protein kinase A. J Biol Chem. 2007;282:33735–33742.

Wagner CA, Finberg KE, Breton S, Marshansky V, Brown D, Geibel JP. Renal vacuolar H+-ATPase. Physiol Rev. 2004 Oct;84(4):1263-314.

Wang Y, Dulubova I, Rizo J, Südhof TC. Functional analysis of conserved structural elements in yeast syntaxin Vam3p. J Biol Chem. 2001 Jul 27;276(30):28598-605.

Wienisch M, Klingauf J (August 2006). "Vesicular proteins exocytosed and subsequently retrieved by compensatory endocytosis are nonidentical". Nature Neuroscience. 9 (8): 1019–27.

Wilkens S, Vasilyeva E, Forgac M. Structure of the vacuolar ATPase by electron microscopy. J Biol Chem. 1999; 274:31804–31810.

Williamson W.R., Wang D., Haberman A.S., Hiesinger P.R. 2010. A dual function of V0-ATPase a1 provides an endolysosomal degradation mechanism in Drosophila melanogaster photoreceptors. J. Cell Biol. 189:885–899

Wilson C, Venditti R, Rega LR, Colanzi A, D'Angelo G, De Matteis MA, The Golgi apparatus: an organelle with multiple complex functions, Biochem. J. 433 (2010) 1–9.

Wolfe DM, Lee JH, Kumar A, Lee S, Orenstein SJ, Nixon RA. Autophagy failure in Alzheimer's disease and the role of defective lysosomal acidification. Eur J Neurosci. 2013; 37:1949–1961.

Xiong QY, Yu C, Zhang Y, Ling L, Wang L, Gao JL. Key proteins involved in insulin vesicle exocytosis and secretion. Biomed Rep. 2017 Feb;6(2):134-139.

Xu J, Xie R, Liu X, Wen G, Jin H, Yu Z, Jiang Y, Zhao Z, Yang Y, Ji B, Dong H, Tuo B. Expression and functional role of vacuolar H+-ATPase in human hepatocellular carcinoma. Carcinogenesis 33: 2432–2440, 2012.

Xu T, Forgac M. Microtubules are involved in glucose-dependent dissociation of the yeast vacuolar [H+]-ATPase in vivo. J Biol Chem. 2001; 276:24855–24861.

Yuan T., Liu L., Zhang Y. et al. (2015) Diacylglycerol guides the hopping of clathrin-coated pits along microtubules for exo- endocytosis coupling. Dev. Cell 35, 120–130.

Zeniou-Meyer M, Liu Y, Béglé A, Olanich ME, Hanauer A, Becherer U, Rettig J, Bader MF, Vitale N. The Coffin-Lowry syndrome-associated protein RSK2 is implicated in calcium-regulated exocytosis through the regulation of PLD1. Proc Natl Acad Sci U S A. 2008 Jun 17;105(24):8434-9.

Zeniou-Meyer M, Zabari N, Ashery U, Chasserot-Golaz S, Haeberlé AM, Demais V, Bailly Y, Gottfried I, Nakanishi H, Neiman AM, Du G, Frohman MA, Bader MF, Vitale N. Phospholipase D1 production of phosphatidic acid at the plasma membrane promotes exocytosis of large dense-core granules at a late stage. J Biol Chem. 2007 Jul 27;282(30):21746-57.

Zhang Z, Zheng Y, Mazon H, Milgrom E, Kitagawa N, Kish-Trier E, Heck AJ, Kane PM, Wilkens S. Structure of the yeast vacuolar ATPase. J Biol Chem. 2008 Dec 19;283(51):35983-95.

Zhao J, Benlekbir S, Rubinstein JL. Electron cryomicroscopy observation of rotational states in a eukaryotic V-ATPase. Nature. 2015 May 14;521(7551):241-5.

Zhu W, Shi DS, Winter JM, Rich BE, Tong Z, Sorensen LK, Zhao H, Huang Y, Tai Z, Mleynek TM, Yoo JH, Dunn C, Ling J, Bergquist JA, Richards JR, Jiang A, Lesniewski LA, Hartnett ME, Ward DM, Mueller AL, Ostanin K, Thomas KR, Odelberg SJ, Li DY. (2017) Small GTPase ARF6 controls VEGFR2 trafficking and signaling in diabetic retinopathy. J Clin Invest. 127(12):4569-4582.

Annex

I. Liste des publications :

V-ATPase is an intravesical pH sensor and a regulator of the regulated secretion in neuroendocrine cells though the production of fusogenic lipids.
Wang Q., Chasserot-Golaz S., Ory S., Gasman S., Bader M-F. and Vitale N. (en préparation pour *Embo J*)

ChromograninA -phosphatidicacidinteraction contributesto secretorygranule biogenesis
Carmon O., Laguerre F., Riachy L., Wang Q., Haeberlé A-M.,Delestre-Delacour C., Tanguy E., Thahouly T., Fouillen L., Rezazgui O., Haefelé A., Renard P-Y., Alexandre S. , Anouar Y., Vitale N. & Montero-Hadjadje M. (en préparation pour *Embo J*)

Mono and polyunsaturated phosphatidic acid regulate distinct steps of regulated exocytosis in neuroendocrine cells
Tanguy E., Costé de Bagneaux P., Kassas N., Ammar M-R., Wang Q., Heaberlé A-M., Raherindratsara J., Fouillen L., Renard P-Y., Montero M., Chasserot-Golaz S., Ory S., Gasman S., Bader M-F. and Vitale N. (en préparation pour *PNAS*)

***Prion Proteins and Neuronal Death in the Cerebellum*.**
Ragagnin A., Wang Q., Guillemain A., Dole S., Wilding A-S., Demais V., Royer C., Haeberlé A-M., Vitale N., Gasman S., Grant NJ. and Bailly Y**.** Prions**-**Some Physiological and Pathophysiological Aspects DOI: 10.5772/intechopen.74080**,** ISBN: 978-1-78985-018-5, *30 Jan 2019*

(Revue) **Phosphatidic Acid: From Pleiotropic Functions to Neuronal Pathology.**
Tanguy E., Wang Q., Moine H., and Vitale N. *Frontiers in Cellular Neuroscience. 2019 Jan;13:2*

(Revue) **Role of Phospholipase D-Derived Phosphatidic Acid in Regulated Exocytosis and Neurological Disease.**
Tanguy E., Wang Q., and Vitale N. *Handbook of Experimental Pharmacology. 2018 Dec. [Epub ahead of print]*

Different species of phosphatidic acid are produced during neuronal growth and neurosecretion.
Tanguy E., Wang Q., Coste de Bagneaux P., Fouillen L., Thahouly T., Ammar M.-R., and Vitale N.
Oilseeds and fats, Crops and Lipids, publié en ligne le 30 Mars 2018

(Revue) **Lipids implicated in the journey of a secretory granule: from biogenesis to fusion**.
Tanguy E., Carmon O., Wang Q., Jeandel L., Chasserot-Golaz S., Montero-Hadjadje M., and Vitale N. *Journal of Neurochemistry, 2016 Jun; 137(6):904-12*

II. Liste des communications orales :

Multiple regulatory functions of phospholipase D-derived phosphatidic acid in neuroendocrine secretion.
Tanguy E., Coste de Bagneaux P., Wang Q., Ammar M-R, Chasserot-Golaz S., Bailly Y., Haeberle

A- M, Bader M-F, and Vitale N. *21è congrès annuel du Club Exocytose-Endocytose (Mai 2018 - Sant Feliu de Guixols, Espagne)*

(Blitz) **Role of phospholipase D-derived phosphatidic acid in calcium-regulated exocytosis.** Tanguy E., Coste de Bagneaux P., Wang Q., Ammar M-R, Chasserot-Golaz S., Bailly Y., Haeberle A- M, Bader M-F, and Vitale N. *Federative Day for Neuroscience in Strasbourg (Avril 2018 - Strasbourg)*

III. Liste des communications affichées :

V-ATPase regulates an ARNO-Arf6-PLD pathway and regulated exocytosis in neuroendocrine cells
Wang Q. and Vitale N. *21è congrès annuel du Club Exocytose-Endocytose (Mai 2018 - Sant Feliu de Guixols, Espagne)*

Regulation of secretory granules exocytosis by phospholipase D-derived phosphatidic acid
Tanguy E., Coste de Bagneaux P., Wang Q., Ammar M-R, Chasserot-Golaz S., Bailly Y., Haeberle A- M, Bader M-F, and Vitale N. *42ème colloque de la Société de Neuroendocrinologie (Septembre 2017- Dijon)*

Implication of phosphatidic acid in regulated exocytosis during neurosecretion. Tanguy E., Coste de Bagneaux P., Wang Q., Ammar M-R, Chasserot-Golaz S., Bailly Y., Haeberle A- M, Bader M-F, and Vitale N. *Congrès Européen des Doubles Cursus Médecine/Pharmacie-Sciences (Juin 2016 - Strasbourg*

Chromogranin A - phosphatidic acid interaction contributes to secretory granule biogenesis

Ophélie Carmon[1†], Fanny Laguerre[1†], Lina Riachy[1†], Qili Wang[3], Charlène Delestre-Delacour[1,2], Emeline Tanguy[3], , Lydie Jeandel[1], Dorthe Cartier[1], Tamou Thahouly[3], Anne-Marie Haeberlé[3], Laetitia Fouillen[4], Olivier Rezazgui[5], Alexandre Haefelé[5], Yannick Goumon[3], Pierre-Yves Renard[5], Stéphane Alexandre[6], Nicolas Vitale[3§], Youssef Anouar[1§] & Maité Montero-Hadjadje[1§£]

[1] Normandie Univ, UNIROUEN, INSERM, U1239, Laboratoire de Différenciation et Communication Neuronale et Neuroendocrine, Institut de Recherche et d'Innovation Biomédicale de Normandie, 76000, Rouen, France
[2] Normandie Univ, UNIROUEN, Laboratoire GLYCOMEV, Fédération de recherche Normandie-Végétal - FED 4277, GDR CNRS 3711 COSM'ACTIFS, 76000, Rouen, France
[3] Centre National de la Recherche Scientifique, Université de Strasbourg, Institut des Neurosciences Cellulaires et Intégratives, F-67000 Strasbourg, France
[4] Laboratoire de Biogénèse Membranaire, UMR-5200 CNRS, Plateforme Métabolome, Université de Bordeaux, 33883 Villenave D'Ornon, France
[5] Normandie Univ, UNIROUEN, COBRA, UMR 6014 & FR 3038, INSA Rouen, CNRS, 76000 Rouen, France
[6] Normandie Univ, UNIROUEN, CNRS, UMR 6270, Polymères, Biopolymères, Surfaces Laboratory, 76000, Rouen, France

[†] These authors equally contributed to this work.

[§] These authors equally contributed to this work.

[£] Corresponding author; Tel: +33 235146643; e-mail: maite.montero@univ-rouen.fr

Running title: CgA/PA interaction and granulogenesis

Key words: chromogranin A / phosphatidic acid / membrane dynamics / organelle biogenesis / hormone sorting

ABSTRACT

Previous studies demonstrated that chromogranin A (CgA) mediates the biogenesis of secretory granules at the level of the *trans*-Golgi network but the mechanisms involved remains obscure. Here, we investigate the possibility that CgA acts synergistically with specific membrane lipids to trigger the formation of secretory granules. We observe that Golgi PA is involved in the biogenesis of CgA-containing granules in secretory cells. Moreover, CgA preferentially interacts with immobilized PA and a bioinformatic analysis of CgA sequence predicted a PA-binding domain (PABD). We identify PA (36:1) and PA (40:6) as predominant species in Golgi and granule membranes of secretory cells by LC-MS/MS. We show that, through its predicted PABD, CgA is able to bind PA-enriched liposomes, to promote membrane deformation and remodeling, and to regulate secretory granule biogenesis. Furthermore, we demonstrate that depletion of CgA PABD or PLD1 activity significantly alters secretory granule biogenesis in secretory cells. These results suggest that CgA controls secretory granule biogenesis by directly interacting with PLD1-generated PA to induce membrane remodeling and curvature necessary for secretory granule budding.

INTRODUCTION

Secretory granules are vesicular and membrane-surrounded organelles which materialize the regulated secretory pathway in secretory cells, allowing hormone release in endocrine and neuroendocrine cells, but also in most neurons. Secretory granules are formed by budding from the *trans*-Golgi network (TGN) membrane. It is well established that molecular remodeling at this level is an important process for secretory granule budding (Tanguy *et al*, 2016), but the identity of the molecular actors, the sequence of their intervention and their mechanisms of action are not elucidated to date. In addition to different important proteins, the TGN membrane is composed of a broad spectrum of lipids with specific properties that profoundly define its identity and function (Holthuis & Menon 2014). Membrane proteins are known to influence lipid organization, and conversely protein function and clustering are under the control of lipids, leading to the formation of TGN membrane microdomains that have been predicted to regulate the function and clustering of proteins involved in the budding of secretory granules (Surma *et al*, 2012). As an example, the regulated production and organization of sphingomyelin, which assembles with cholesterol to generate microdomains in the membranes, has been demonstrated to be crucial for the biogenesis of transport carriers at the Golgi membranes (Duran *et al*, 2012). Besides the TGN membrane components, luminal and cytosolic molecular components also influence membrane organization. Among the luminal components, chromogranin A (CgA) is a soluble glycoprotein known as a key actor of the regulated secretory pathway involved in hormone aggregation and the biogenesis of secretory granules (Kim *et al*, 2001; Carmon *et al*, 2017). The *Chga* gene knockout led to decreased secretory granule number and associated metabolic complications such as hypertension and obesity in mice (Mahapatra *et al*, 2005; Bandyopadhyay & Mahata 2017), thus arguing for an important role of this glycoprotein in hormone storage and release. In previous studies, we have shown that CgA can induce the formation of secretory granule-like

structures in a model of non-endocrine cells, confirming its important role in granulogenesis (Montero-Hadjadje *et al*, 2009; Elias *et al*, 2012). However, whether and how CgA acts at the level of the TGN membrane to trigger the formation of secretory granules is still unknown. The first indication for a role of CgA at the TGN level is related to the acidic nature of the protein that confers to this protein the ability to aggregate with neuropeptides and hormones in the TGN lumen (Chanat & Huttner 1991). Besides these soluble aggregates, a fraction of CgA was found to be tightly associated with the membrane of secretory granules (Kang & Yoo 1997), suggesting that CgA/hormone aggregates might interact with the TGN membrane.

In vitro and *in vivo* studies revealed that depletion of cholesterol alters secretory granule biogenesis (Dhanvantari & Loh 2000; Gondre-Lewis *et al*, 2006). Moreover, cholesterol has been shown to interact notably with another granin family member secretogranin III (SgIII) (Hosaka *et al*, 2005), which has been shown to interact with CgA, and then targets CgA aggregates to the regulated secretory pathway (Hosaka *et al*, 2002, 2004). However, the CgA domain of interaction with SgIII ($CgA_{41–109}$) is not fully conserved through evolution and SgIII is not expressed in all cell types displaying secretory granules, indicating that various mechanisms of hormone sorting mediated by CgA remain to be elucidated. In a previous study, we showed that CgA controls the biogenesis of secretory granules and CgA sorting to the Golgi apparatus through its conserved N and/or C-terminal regions (Montero-Hadjadje *et al*, 2009). Interestingly, these regions exhibit a conserved α-helical organization (Elias *et al*, 2010) and a recent study revealed that CgA regulates fusion pore expansion (Abbineni *et al*, 2019), suggesting a potential interaction of CgA with membranes. Supporting this hypothesis, CgA-derived peptides with such α-helical conformation have been demonstrated to interact with membrane lipids. For instance, the conserved N-terminal peptide vasostatin I ($hCgA_{1-76}$) interacts with phosphatidylserine in phospholipid monolayers (Blois *et al*, 2006) and cell surface (Dondossola *et al*, 2010),

whereas catestatin ($hCgA_{352-372}$) binds to phosphatidylcholine micelles (Sugawara *et al*, 2010). As it is now well established that membrane lipid properties define organelle identity and function, we hypothesized that an interaction between CgA and certain lipid(s) of the TGN membrane could promote secretory granule biogenesis. In this study, we observed that overexpression of a cytosolic probe for Golgi phosphatidic acid (PA) impairs the formation of CgA-containing granules in secretory cells. Moreover, we found that CgA specifically interacts with few PA species enriched in purified Golgi and secretory granule membranes *in vitro*, through a predicted PA-binding domain (PABD). Using giant unilamellar vesicles (GUV) enriched with Golgi and secretory granule PA species, we observed that CgA interaction induces GUV membrane remodeling and deformation in a dose-dependent manner. Interestingly, deletion of the predicted PABD in the CgA sequence significantly reduced secretory granule biogenesis in CgA-expressing cells. Finally, genetic and pharmacological evidence reveal that phospholipase D1 (PLD1) is a major source of PA production for secretory granule formation in endocrine cells.

Results

Golgi PA is involved in the biogenesis of CgA-containing secretory granules

To probe the importance of PA in the formation of CgA-induced secretory granules in secretory cells, we overexpressed the PABD of cytosolic phosphodiesterase PDE4A1, that was previously shown to specifically interact with PA at the TGN in COS1 cells (Huston *et al*, 2006) and RAW264.7 macrophages (Kassas *et al*, 2017). We found that PDE4A1(PABD)-GFP (PDE4A1 WT) not only exhibited an expected Golgi-confined localization, but also significantly reduced secretory granule biogenesis (Fig. 1A). Moreover, mutations that abolished *in vitro* binding of PDE4A1(PABD)-GFP to PA (PDE4A1 Mut) prevented the recruitment of this PA sensor to the Golgi apparatus and did not impact the number of CgA-

induced granules (Fig. 1A), reinforcing the crucial role of Golgi PA in the biogenesis of secretory granules.

Chromogranin A interacts preferentially with PA through a putative PA-binding domain

Due to the presence of two helicoidal motives in its N- and C-terminal conserved regions (Elias *et al*, 2010), we analyzed the capacity of CgA to interact with membrane lipids. A lipid overlay assay was performed by incubating recombinant CgA with a nitrocellulose sheet where different membrane lipids were adsorbed. Using an antibody raised against CgA (Montero-Hadjadje *et al*, 2002), this overlay assay revealed that CgA interacts with PA and phosphoinositides (PIP, PIP_2 and PIP_3) (Fig. 1B). Quantification of the CgA-lipid interaction signals revealed that CgA preferentially interacts with PA (Fig. 1B). To further characterize the PABD of CgA, we compared the CgA helicoidal motifs with that of proteins with known PABD, notably the Golgi PA sensor PDE4A1. This analysis revealed a potential PABD within residues 352-381 of CgA, a sequence of positively charged and hydrophobic amino acids (Fig. 1C). Indeed, a bioinformatics analysis using Heliquest software (Gautier *et al*, 2008) further refined this PABD to residues 364 and 381 (Fig. 1C) that shares the characteristics of typical PABDs (Tanguy *et al*, 2018). It is predicted that this PABD adopts an amphipathic α-helical conformation with five positively charged residues (arginines) sequestered in one side of the helix, which could interact with negatively charged PA, and three surface exposed hydrophobic residues (tryptophane, phenylalanine, leucine) on the other side of the helix which could insert CgA within membranes and interact with the fatty acid chains of PA (Fig. 1D). Interestingly, a model of CgA PABD confirmed that this domain displays an alpha helix when its structure was examined using MacPyMol software (shown as a ribbon, Fig. 1E). Using a semi-quantitative *in vitro* assay with NBD-labeled liposomes (Kassas *et al*, 2017), we investigated the PA binding capacity of three different GST fusion

proteins containing the C-terminal helicoidal motif of CgA or parts of it: $CgA_{352-381}$, $CgA_{352-372}$ and $CgA_{373-381}$. Thus, we found that GST-$CgA_{352-381}$ linked to GSH-Sepharose very efficiently bound PA-containing liposomes, while the binding of $CgA_{352-372}$ was greatly reduced and that of $CgA_{373-381}$ was negligible (Fig. 1F). These data not only indicate that the whole sequence corresponding to PABD is important for PA binding but also that CgA proteolysis generating catestatin (Fig. 1C) amends this functionality.

Specific PA species are predominant and common to Golgi and secretory granule membranes from CgA-expressing cells

We analyzed and compared the PA composition of Golgi and secretory granule membrane fractions purified from COS7-CgA and PC12 cells (Elias *et al*, 2012), and their purity was evaluated by western blotting (Fig. S1). Detailed lipidomics analysis of these fractions revealed that over the 44 distinct species potentially detected, few specific PA species are predominantly detected in secretory granule and Golgi membranes of COS7-CgA cells, *i.e.* PA (36:1), PA (38:2), PA (38:6) and PA (40:6) (Fig. 2A). Furthermore, we compared the Golgi membrane of COS7-WT and COS7-CgA cells to examine the potential impact of CgA expression on the PA content. We found that the Golgi membrane of COS7-WT and COS7-CgA cells exhibit the same predominant PA species, *i.e.* PA (36:1), PA (38:2) and PA (40:6), but we also noticed a significant increase in PA (36:1) and PA (36:2) enrichment in Golgi membranes after CgA expression, mainly at the expense of PA (40:6) (Fig. 2B). The presence of the same major PA species, *i.e.* PA (36:1), PA (38:2) and PA (40:6), was also found in secretory granule membranes isolated from neuroendocrine PC12 cells, but with a major contribution of PA (40:6) in PC12 cells (Fig. 2C).

Chromogranin A interacts with Golgi/secretory granule PA species included in liposomes and induces membrane deformation of PA-enriched GUVs

We used a liposome flotation assay to test the interaction between CgA from COS7-CgA cell extracts and the predominant PA species identified in Golgi and secretory granule membranes (Fig. 3A). Following the flotation assay, the different fractions were analyzed by western blotting using a CgA specific antibody (Montero-Hadjadje *et al*, 2002). This analysis revealed a specific interaction between CgA and liposomes enriched with PA species identified previously by lipidomics analysis, *i.e.* PA (36:1) and PA (40:6), with an apparent preference for the first one and less with PIP_2-enriched liposomes (Fig. 3B). In contrast, no interaction was found with liposomes enriched with PC, PS, in accordance with the results obtained using lipid strips, or with PA (36:0) (Fig. 3B) (Fig. 1B). These results demonstrate that endogenous CgA interacts specifically with predominant PA species identified in Golgi and secretory granule membranes from CgA-expressing cells.

To examine membrane dynamics following CgA and PA interaction, we developed a model of GUVs enriched in PA (36:1) or PA (40:6), whose formation is assisted by a polyvinyl alcohol gel. To analyze their morphology using confocal microscopy, we generated PA-enriched GUVs containing a fluorescent lipid, PE-NBD. We observed that the formed GUVs exhibit a diameter ranging between 5 and 50 μm. After image acquisitions during 1 min, we observed that the fluorescence is homogeneously distributed around GUVs (Fig. 3C). Addition of 2 μM CgA to PA-enriched GUVs often provoked a marked fluorescence concentration in a confined membrane domain of several GUVs just before a budding event and the formation of a resulting small vesicle (Fig. 3D). The quantification of membrane deformations revealed that the number of budding events depends on CgA concentration (Fig. 3E). After addition of 2 μM CgA-Alexa488 on non-fluorescent PA-enriched GUVs, CgA was

first rapidly and homogenously distributed in GUV membranes. Within a minute, budding events were detected from CgA-enriched membrane domains (Fig. 3F).

Thermodynamic characteristics of CgA/PA interaction indicate that PA favors CgA incorporation in the SUV membrane

To investigate the CgA/PA interaction in more details, we conducted an isothermal titration calorimetry (ITC) analysis, which quantifies the binding equilibrium directly by measuring the heat change resulting from the association of a ligand with its binding partner (Pierce *et al*, 1999; Miao *et al*, 2019). ITC thermograms showed that injection of a water suspension of small unilamellar vesicles (SUV) composed of DOPC or DOPC/PA (36:1) induced an exothermic process resulting from the dilution process heat of SUV in water (Fig. 4A,B, upper panels). When we injected DOPC or DOPC/PA (36:1) SUV suspension into CgA solution, the ITC results showed sequential exothermic and endothermic processes (Fig 4A,B, lower panels). Enthalpy curves (Fig. 4C) were obtained from the integrated energy values obtained from A and B traces in lower panels, using A and B traces in upper panels as blank, respectively. These curves were fitted using two simple one-site binding model to yield thermodynamic parameters (Table 1). Comparing the enthalpy curves obtained after DOPC and DOPC/PA (36:1) injection in CgA solution, we observed an increase due to an exothermic process related to the binding of CgA with DOPC that could result from hydrogen bonding and/or electrostatic force (Blois *et al*, 2006). We also noticed that the maximum of enthalpy is reached after 14 injections of DOPC SUV while it is reached after only 6 injections of DOPC/PA (36:1) SUV (Fig. 4C). In addition, for the exothermic process, the calculated enthalpy ratio $\Delta H^{exo}_{DOPC/POPA}/\Delta H^{exo}_{DOPC}$ is close to 7, the enthalpy ratio $\Delta H^{endo}_{DOPC/POPA}/\Delta H^{endo}_{DOPC}$ is equal to 12, and the stoichiometry (n) for both processes is lower with DOPC/PA (36:1) SUVs (Table 1). Moreover, the endothermic phase leads to the

enthalpy decrease (Fig. 4C) and the stoichiometric ratio, which is the ratio between the total number of lipids and the number of lipids on the outer surface of the SUV, is close to 1.8, suggesting a reorganization of the protein/lipid complex in the SUV membrane. Together, these results clearly show that PA favors the incorporation of CgA in the SUV membrane.

Chromogranin A induces the remodeling of supported membrane bilayers enriched with Golgi/secretory granule PA species

Using atomic force microscopy, we studied the impact of CgA on supported bilayers composed of DOPC or DOPC/PA (36:1). Addition of 0.6 and 1.2 µM CgA during 15 min and 75 min on a DOPC membranes revealed small alterations of their topographical profile corresponding to protrusions with a maximal height of 4 nm (Fig. 5A). After addition of CgA on DOPC/PA (36:1) membrane, analysis of images obtained showed a profile change of the membrane with a height above 4-16 nm (Fig. 5B). These results suggest that CgA interacts with PA-enriched lipid bilayers in a concentration and time-dependent manner and that this interaction modifies membrane topology. Of note, the grain size analysis of 11-15 images obtained with 1.2 µM CgA during 75 min revealed that the total number of CgA-induced domains increased by a factor of 3 after PA (36:1) addition in DOPC bilayers (41±23 domains per 100 μm^2 DOPC bilayer (Fig. 6A) versus 120±41 domains per 100 μm^2 DOPC/PA (36:1) bilayer (Fig. 6B)). Moreover, domains with an area greater than 20 μm^2 were clearly more abundant in presence of PA (36:1) in the supported bilayer, and their height increased with their area to reach a mean of 21±3 nm (Fig. 6B).

Chromogranin A PABD is required for secretory granule biogenesis

COS7 cells stably expressing CgA display CgA-containing secretory granule-like structures (Delestre-Delacour *et al*, 2017; Elias *et al*, 2012; Montero-Hadjadje *et al*, 2009**)**. To analyze

the role of the predicted CgA PABD on secretory granule formation, we deleted the PABD-encoding region in CgA-GFP. After verifying this deletion did not affect CgA-GFP integrity (Fig. S2), we expressed CgAΔPABD-GFP in COS7 cells and we observed its accumulation within the Golgi associated with a significant decrease of the number of induced granules (Fig. 7). These results support the idea that the interaction of CgA with PA through the PADB is important for granule biogenesis and CgA export from the Golgi.

Inhibition of PLD-mediated PA synthesis alters the biogenesis of secretory granules

To identify the source of Golgi PA involved in the biogenesis of CgA-containing secretory granules, we altered PLD-mediated PA synthesis since PLD appears to be the most important provider of PA in the Golgi (Freyberg *et al*, 2001, 2003). First, secretory cells were treated with the pan-PLD inhibitor FIPI and we found a reduction in the number of CgA-induced granules in CgA-expressing COS7 cells (Fig. 8A) and in PC12 cells (Fig. 8B) without any apparent effect on the granin levels in COS7-CgA and PC12 cells (Fig. S3A and S3B). Interestingly, in mice lacking *Pld1* gene, we observed by electron microscopy a significant reduction in the number of secretory granules (Fig. 8C,D) associated to an apparent granule deformation in chromaffin cells (Fig. 8C,E), consistent with the defects in granule biogenesis and morphology seen in chromaffin cells from CgA knockout mice (Pasqua *et al*, 2016). In conclusion, pharmacological and genetic invalidation of PLD activity and expression, respectively, supported the notion that PLD1 is an important provider of PA required for CgA-induced secretory granule biogenesis.

DISCUSSION

Although considerable efforts have been deployed to identify the molecular mechanism at the origin of secretory granule formation, many aspects of this fundamental process remain to be

elucidated. The biogenesis of secretory granules depends on TGN membrane dynamics that rely on interactions of luminal and cytosolic proteins with molecular components of the TGN membrane, such as microtubule-associated motor proteins and actin-based motors which are key factors in membrane deformation leading to the budding of post-Golgi carriers (Yamada *et al*, 2014; Carmon *et al*, 2017). Among luminal proteins, members of the granin protein family have been long considered as major actors of secretory granule biogenesis but direct mechanistic evidence in favor of this hypothesis is still lacking (Gondré-Lewis *et al*, 2012). The TGN soluble granin, SgIII, has been shown to interact with membrane cholesterol to control secretory granule biogenesis (Hosaka *et al*, 2005), but SgIII is not ubiquitously expressed in neuroendocrine cells. Another member of the granin family, CgB, has been very recently shown to penetrate into phospholipid membranes and to form anionic channels (Yadav *et al*, 2018).

Here, we first revealed the ability of the coiled-coil soluble glycoprotein CgA to bind acidic phospholipids, in particular PA, using a lipid-overlay. *In silico* identification of $CgA_{364-381}$ sequence as a PABD led us to confirm CgA/PA interaction using PA-enriched liposomes, as this sequence specifically binds PA. Interestingly, CgA PABD binds PA at level similar to that observed for PDE4A1, a *bona fide* PA sensor in Golgi membranes characterized previously (Kassas *et al*, 2017). In contrast, $CgA_{352-372}$ and $CgA_{373-381}$ shorter fragments, corresponding to the expected cleavage of CgA occurring during secretory granule maturation to generate catestatin, exhibited only a weak interaction with PA. We can therefore speculate that CgA/PA interaction might be regulated during secretory granule maturation and CgA processing. The CgA PABD sequence may allow hydrophobic residue insertion into lipid bilayers and direct ionic interaction between basic residues and several PA molecules. Thus, CgA may participate to TGN remodeling by interacting with TGN predominant PA species that could induce the formation of PA-enriched microdomains. Accumulation of the conical-

shaped PA enables membrane bending (Kooijman *et al*, 2003), and this phenomenon could generate TGN membrane curvature preceding secretory granule budding.

Since PA was suspected to play a role in secretory granule biogenesis (Siddhanta & Shields 1998), we overexpressed a cytosolic Golgi PA probe, PDE4A1, and we observed a decrease of CgA-containing secretory granules in PC12 cells, suggesting the occurrence of a link between TGN membrane PA and luminal CgA to generate secretory granules. Then, we analyzed and compared the PA composition in Golgi and secretory granule membranes from CgA-expressing COS7 cells by mass spectrometry, and found a close correlation in the PA species composition in these two membranes isolated from CgA-expressing COS7 cells. Among these PA species, we observed a predominance of several common PA species in secretory granule and Golgi membranes, including mono- and poly-unsatured forms, *i.e.* PA (36:1) and PA (40:6). Interestingly, these PA species were also identified in the membrane of secretory granules from neuroendocrine PC12 cells, but in significantly different ratios. The apparent differences in the ratio of PA (36:1) or PA (40:6) between COS7-CgA and PC12 cells may actually result from different PA metabolic enzymes present at the TGN in these two cell types. It is of note that PC12 cells also express other granins such as CgB and SgII that may contribute to secretory granule biogenesis through alternative mechanisms. Together, these results suggest that synthesis of specific PA species occurs at the Golgi membrane of CgA-expressing cells to induce the biogenesis of secretory granules and that one or some of these species have a key role in this process. Using liposome models enriched with distinct phospholipids, we observed that CgA preferentially interacts with PA (36:1) and PA (40:6), and that CgA provokes membrane deformation of PA (36:1)- or PA (40:6)-enriched artificial membranes in a dose-dependent manner. The analysis of the thermodynamic characteristics of CgA/PA (36:1) interaction by isothermal titration calorimetry consolidated the observation that CgA strongly interacts with PA (36:1)-enriched membranes and favors

membrane deformation. Atomic force microscopy on supported membrane bilayers revealed that PA (36:1) enrichment increased the number, the height and the surface of CgA-induced domains resulting from either CgA aggregation, membrane deformation, microdomain formation, or any combination of these. These data support a central role of PA in the formation of CgA-induced domains as observed by confocal microscopy and ITC. Altogether, these results support the idea that CgA/PA (36:1) or PA (40:6) interaction plays a key role in the membrane remodeling process necessary for secretory granule budding.

In line with this model, we showed that expression of CgA deleted from the PABD led to a significant decrease of CgA granule number with a retention of the truncated CgA in the Golgi area in COS7 cells. Therefore, these data support the notion that CgA PABD region is involved in granule biogenesis and that CgA/PA interaction is critical for the initiation of the neurosecretory process in neuroendocrine cells. Interestingly, this CgA PABD region includes the C-terminal sequence of catestatin ($CgA_{352-372}$) where several single nucleotide polymorphisms have been detected in humans that are associated with cardiovascular and metabolic disorders (Sahu *et al*, 2012; Kiranmayi *et al*, 2016).

An important source of Golgi PA is the conversion of PC by the enzymatic activity of PLD. Pharmacological inhibition of PLD in COS7-CgA and PC12 cells, and *Pld1* knockout in mice chromaffin cells both reduced secretory granule biogenesis. Interestingly, this reduction in secretory granule number was also accompanied by an alteration in the shape of these organelles, very similarly to what was found in CgA-knockout chromaffin cells (Pasqua *et al*, 2016), showing that PLD1 depletion partially phenocopies CgA deficiency regarding the impact on secretory granule biogenesis. These observations strongly suggest that CgA and PLD1-generated PA are two cooperating molecular actors involved in the formation of secretory granules in neuroendocrine cells.

Altogether, our data suggest that CgA binds to specific species of PA at the TGN to generate membrane remodeling and curvature in order to initiate secretory granule budding, concomitantly or prior to the recruitment of cytosolic proteins such as arfaptins (Cruz-Garcia *et al*, 2013), the acto-myosin 1b complex (Delestre-Delacour *et al*, 2017) or the membrane-associated myristoylated protein HID1 (Hummer *et al*, 2017). Future studies are now needed to evaluate the role of CgA/PA interaction during secretory granule biogenesis in living neuroendocrine cells.

Materials and Methods

Cell culture

African green monkey kidney fibroblast-derived COS7 cells (American Type Culture Collection ; CRL 1651) stably expressing CgA developed previously (Elias *et al*, 2012) were maintained in Dulbecco's Modified Eagle's Medium (DMEM, Gibco, Thermo Fisher Scientific) supplemented with 5% heat-inactivated fetal bovine serum (Sigma - Aldrich), 100 U ml^{-1} penicillin, 100 µg ml^{-1} streptomycin (Gibco, Thermo Fisher Scientific) and 300 µg ml^{-1} geneticin (G-418 sulfate, Life Technologies, Inc, UK) to maintain gene resistance selection, at 37°C in 5% CO_2. Rat pheochromocytoma PC12 cells (American Type Culture Collection; CRL 1721) were routinely grown in Dulbecco's Modified Eagle's Medium (DMEM, Gibco, Thermo Fisher Scientific) supplemented with 5% sterile-filtered fetal bovine serum (Sigma-Aldrich), 10% sterile-filtered HyClone Donor Equine serum (GE Healthcare, Life Sciences), 100 U ml^{-1} penicillin, 100 µg ml^{-1} streptomycin (Gibco, Thermo Fisher Scientific) and 1% L-glutamine (Gibco, Thermo Fisher Scientific), at 37°C in 5% CO_2. For IF experiments, COS7-WT cells were transfected with 0.8 µg of DNA encoding GFP-tagged human CgA (CgA-GFP), GFP-tagged human ΔPABD CgA (CgAΔPABD-GFP) or GFP-tagged rat PDE4A1-

PABD (PDE4A1-GFP), and 2 µl Lipofectamine 2000 (Invitrogen) per well (24-well plate) according to the manufacturer's protocol. Four or five hours after the beginning of transfection, the culture medium was replaced by supplemented DMEM, and cells were additionally cultured for 24–48 h. For WB experiments, COS7-WT cells were transfected with 4 µg of DNA encoding GFP-tagged human CgA (CgA-GFP) or GFP-tagged human ΔPABD CgA (CgAΔPABD-GFP), and 8 µl Lipofectamine 2000 (Invitrogen) per well (6-well plate) according to the manufacturer's protocol. Four or five hours after the beginning of transfection, the culture medium was replaced by supplemented DMEM, and cells were additionally cultured for 48 h.

Plasmid constructs

Full-length CgA-GFP (pCgA-EGFP-N2) kindly provided by M. Courel (UPMC, Paris, France) was used to amplify the sequence of CgA encoding region by PCR cloning into a pGEM-T vector (Promega, Charbonnieres, France) using the sense primer (5'-CTCGAGGCCACCATGCGCTCCGCCGCTGTCTCGGCTTCTT-3'), including an Xho1 restriction site (underlined bases), and the antisense primer (5'-CCGCGGGCGCCCCGCCGTAGTGCCTGCA-3'), including a SacII restriction site. Site-directed mutagenesis was conducted by using the QuikChange® II XL Site-Directed Mutagenesis Kit (Agilent technologies, Les Ulis, France) and specific primers (sense: 5'-CTCTCCTTCCGGGCCCGGGCCTACGAGGACAGCCTTGAGGCGGGCCTG-3';
antisense: (5'-CAGGCCCGCCTCAAGGCTGTCCTCGTAGGCCCGGGCCCGGAAGGAG
AG-3') designed to remove the CgA PABD sequence. The amplified mutated CgA (with deleted $CgA_{364\text{-}381}$ region was named CgAΔPABD) was digested with the appropriate enzymes (Xho1 and SacII) and subcloned into the eukaryotic expression vector pEGFP-N2. All the constructs were verified by restriction enzyme digestion and their nucleotide sequence

was verified by DNA sequencing. PDE4A1 WT - GFP and PDE4A1 Mut - GFP constructs were described previously (Kassas *et al*, 2017).

Animals

Pld1 knockout mice were described previously (Ammar *et al*, 2013; Ammar *et al*, 2015). They were housed and raised at Chronobiotron UMS 3415. All experiments were carried out in accordance with the European Communities Council Directive of 24th November 1986 (86/609/EEC) and resulting French regulations. Accordingly, the CREMEAS local ethical committee approved all experimental protocols. Every effort was made to minimize the number of animals used and their suffering.

Proteins and antibodies

Recombinant CgA (human chromogranin A 19-457aa, His tag, *E. coli*, ATGP0323, Atgen global) was used for lipid strip and GUVs experiments. For CgA-Alexa488 coupling, all reactants and solvents were purchased from TCI-Chemicals and Alfa Aesar. CgA labeling was performed according to a modified version of protocol cited in Chevalier *et al* (2013). First, 82 µl (1 eq.) of Alexa488 solution (2 mg ml^{-1} in anhydrous DMF) were introduced into a 1 ml round-bottom flask. TSTU (70 µg, 1.2 eq.) and DIEA (0.04 ml, 1.2 eq.) were added, reaction medium was placed under argon, with magnetic stirring and at RT during 1 h, to obtain the NHS activated ester. A solution of 250 µg of CgA in PBS buffer (pH 7.2, 0.5 mg ml^{-1}, 1 eq.) was then slowly added dropwise in reaction medium, for a ratio Alexa488/CgA 10/1. Reaction was placed under argon, magnetic stirring and at RT overnight. Purification was performed using 10 kDa centrifugation filters (Spin-X® UF 500, CORNING) previously conditioned with PBS to remove glycerol and others biocidal compounds. Labeled protein was collected in PBS buffer following 3 centrifugations of 10 min at 7,500 rpm. Grafting rate

was evaluated by Western-blot and UV-Vis spectroscopy (λabs = 494 nm), with a maximum labeling rate of 5.6 Alexa488 molecules per protein.

Primary antibodies used were goat polyclonal anti-CgA (Santa-Cruz Biotechnology inc.; sc-23556) (1:200), rabbit polyclonal anti-CgA (WE-14; Montero-Hadjadje *et al*, 2002) (1:1,000), rabbit polyclonal anti-CgA (RV31.4; Montero-Hadjadje *et al*, 2009) (1 :1,000), rabbit polyclonal anti-SgII (EM66; Anouar *et al*, 1998) (1:1,000), goat polyclonal anti-CgB (Santa-Cruz Biotechnology inc.; sc-1489) (1:1,000), mouse monoclonal anti-GM130 (BDBiosciences) (1:1,000), mouse monoclonal anti-CALR (Sigma-Aldrich, clone 1G11-1A9) (1:1,000), mouse monoclonal ant-GLUD1 (Sigma-Aldrich; clone 3C2) (1:500), rabbit monoclonal anti-ZO-3 (Cell signaling; D57G7) (1:1,000), mouse monoclonal anti-PCNA (Santa-Cruz Biotechnology; sc-25280) (1:500), mouse monoclonal anti-α-tubulin (Sigma-Aldrich; T5168) (1:5,000). For IF, secondary antibodies used were Alexa 488-conjugated donkey anti-rabbit IgG; Alexa 594-conjugated donkey anti-mouse IgG (Invitrogen) (1:500). For Western blotting, anti-rabbit, anti-mouse and anti-goat secondary antibodies conjugated to horseradish peroxydase (Thermo Fisher Scientific) (1:5,000) were used.

Protein-lipid binding assay

Membrane lipid strips (P-6002, Echelon Biosciences) were saturated in PBS-T buffer (0,1% v/v Tween 20 in PBS) supplemented with 3% fatty acid-free BSA for 1 h at room temperature, and then incubated with 500 ng ml^{-1} recombinant human purified CgA diluted in this buffer for an additional hour at room temperature. After several washes with PBS-T, the membranes were incubated with anti-WE-14 antibody (1:1,000) 1 h at RT in the saturation buffer. After washing with PBS-T, membranes were incubated with a secondary antibody coupled to horseradish peroxydase (Thermo Fisher Scientific) and visualized by enhanced

chemiluminescence. Densitometric analysis was performed to determine the relative affinity of CgA binding to various phospholipids.

Subcellular fractionation

Cells were collected in PBS and sedimented by centrifugation at 400 *g* for 5 min at 4°C. The cell pellet was disrupted by 5 pulls/pushes through a 21- and then a 25-gauge needle attached to a syringe, in ice-cold buffer (0.32 M sucrose, 20 mM Tris-HCl, pH 8; 1 ml g^{-1} of cells). The resulting lysate was centrifuged at 800 *g* for 30 min at 4°C.

Golgi membrane purification

Pellets containing Golgi membranes were suspended in 1.4 M sucrose. The homogenate was deposited on a succession of 2 ml 1.6, 1.8, 2.0 and 2.2 M sucrose cushions and then covered with 2 ml 1.2 and 1 M sucrose cushions and 10 ml 0.32 M sucrose cushion, all sucrose cushions containing 10 mM Tris-HCl at pH 7.4. The extracts were then centrifuged at 10,000 *g* for 18 h at 4°C. The different fractions were collected in hemolysis tubes and kept at -20°C. An aliquot of each fraction was used for the localization of Golgi apparatus by Western blot using specific plasma membrane, Golgi, nucleus, mitochondria and endoplasmic reticulum antibodies.

Secretory granule purification

Post-nuclear supernatants were centrifuged at 20,000 *g* for 20 min at 4°C. Pellets containing dense core granules were centrifuged on a multi-step gradient of 1 to 2.2 M sucrose (1, 1.2, 1.4, 1.6, 1.8, 2 and 2.2 M sucrose; 5 ml steps), at 100,000 *g* for 12 h at 4°C. All gradient steps were collected from the top of the tube in 5 ml fractions, and analyzed by western blotting to check the granule-containing fractions and to verify their purity. The recovered granule fractions were used for liquid chromatography coupled to tandem mass spectrometry analysis.

Lipidomic analysis

Total lipids from cell samples were extracted by the method of Bligh and Dyer (1959). Lipid extracts were resuspended in 50µl of eluent A. LC-MS/MS (MRM mode) analyses were performed with a MS model QTRAP® 6500 (Sciex) coupled to an LC system (1290 Infinity II, Agilent). Analyses were achieved in the negative (PA); nitrogen was used for the curtain gas (set to 15), gas 1 (set to 20) and gas 2 (set to 0). Needle voltage was at − 4, 500 without needle heating; the declustering potential was adjusted set at − 180 V. The collision gas was also nitrogen; collision energy is set to − 50eV. Reversed phase separations were carried out at 50 °C on a Luna C8 150×1 mm column, with 100 Å pore size, 5 µm particles (Phenomenex). Eluent A was isopropanol/CH_3OH/H_2O+0.2 % formic acid+0.028 % NH_3 and eluent B was isopropanol+0.2 % formic acid+0.028 % NH_3. The gradient elution program was as follows: 0-5 min, 30-50 % B; 5 - 30 min, 50-80 % B; 31–41 min, 95 % B; 42–52 min, 30 % B. The flow rate was set at 40 µl min^{-1}; 3 µl sample volumes were injected. Quantitative PA analyses were made based on MS/MS multiple reaction monitoring (MRM) as described (Shui *et al*, 2010). Briefly, MRM transitions for individual PAs were determined using PA standards (Avanti Polar Lipids, Alabaster, AL). The predominant daughter fragment ions were then used for quantitative MRM analysis. MRM transitions and specific retention times were used to selectively monitor PA using MultiQuant software (v3.0, Sciex).

Liposome and giant unilamellar vesicle formation

Liposome flotation and binding assays

Lipids solubilized in chloroform were purchased from Avanti Polar Lipids (Alabaster, AL) and were used without further purification. Liposome mixtures were prepared in mass ratios

composed of 90% DOPC (1,2-dioleoyl-*sn*-glycero-3-phosphocholine), 5% PE-NBD (1,2-dioleoyl-*sn*-glycero-3-phosphoethanolamine-N-(7-nitro-2-1,3-benzoxadiazol-4-yl)), and 5% PS (1,2-dioleoyl-sn-glycero-3-phospho-L-serine), $PI(4,5)P_2$ (1,2-dioleoyl-sn-glycero-3-phospho-(1'-myo-inositol-4',5'-bisphosphate)), egg PA mix or PA species (36:1 (1-stearoyl-2-oleoyl-*sn*-glycero-3-phosphate), 36:2 (1-stearoyl-2-linoleoyl-sn-glycero-3-phosphate), 40:6 (1-stearoyl-2-docosahexaenoyl-*sn*-glycero-3-phosphate) or 36:0 (1,2-distearoyl-sn-glycero-3-phosphate). Lipids were dried in a stream of nitrogen and kept under vacuum for at least 2 h. Dried lipids were then suspended in liposome-binding buffer (LBB: 20 mM HEPES, pH 7.4, 150 mM NaCl, 1 mM $MgCl_2$) by three freeze and thaw cycles and were extruded using a Mini-Extruder (Avanti Polar Lipids, Alabaster, Alabala, USA) through polycarbonate track-etched membrane filters to produce liposomes of 200 nm in diameter. The liposomes were then diluted (1:10) and incubated with 30 µg of COS7-CgA extract during 20 min. Then samples were centrifuged at 200,000 *g* (1 h at 4°C) on a multi-step gradient sucrose. To determine the association of CgA with liposomes, the fractions were collected after centrifugation, and the presence of CgA was revealed using western blot analysis of the different fractions.

To quantify liposome binding to GST-CgA-PABD linked to GSH-Sepharose beads, GST and GST-PABD constructs (330 pmol) bound to GSH beads were washed once with 1 ml of LBB medium before incubation for 20 min in the dark at room temperature and under agitation with liposomes containing a 10-fold molar excess of PA relative to the quantity of GST proteins in a final volume of 200 µl of LBB. Beads were washed three times with 1 ml of ice-cold LBB and collected by centrifugation at 3,000 rpm for 5 min. Liposome binding to the PABD was estimated by measuring the fluorescence at 535 nm with a Mithras fluorimeter (Berthold). Triplicate measurements were performed for each condition. Fluorescence

measured with GST linked to GSH-Sepharose beads alone was between 3 and 4 A.U. and was subtracted from sample measurements.

Giant unilamellar vesicle preparation

Giant unilamelar vesicles (GUVs) were prepared by polyvinyl acetate (PVA, MW 145000, purchased from VWR International, Fontenay-sous-Bois, France) – assisted swelling. Briefly, Teflon plate was cleaned twice with 99% ethanol. A 5% (w/w) solution of PVA was prepared by stirring PVA in water while heating at 90 °C. PVA-coated substrates were prepared by spreading 100–300 µl of PVA solution on a clean Teflon plate, and dried for 30 min at 80°C. 10–20 µl of lipid mixture (96% of DOPC, 4% of PA (36:1) or (40:6) and 1% of PE-NBD) dissolved in chloroform (1 mg ml^{-1}) was spread on the dried PVA film and placed under vacuum over-night at room temperature to evaporate the solvent. A chamber around the drops of lipids was formed with Vitrex and filled with 100 mM sucrose and 150 mM NaCl solution during 3 h at room temperature, allowing the formation of GUVs with a suitable size. Next, the buffer containing GUVs is recovered using a rib with a wide tip to not destroy the GUVs, and deposited in LabTek wells (LabTek I non-separable, on glass coverslip, 4 culture chambers, Nunc), which were previously coated with a 1 mg ml^{-1} BSA solution. To allow the sedimentation of GUVs, we added the same volume (100 µl) of a solution containing 90 mM glucose and 15 mM NaCl in LabTek wells. The sedimentation of the GUVs takes place for about 1 h at room temperature.

To test the effect of CgA on the GUV membranes, we added CgA or CgA-Alexa488 in GUV-containing Labtek wells at a final concentration of 2, 4 or 6 µM just before the beginning of confocal microscopy acquisitions.

Small unilamellar vesicle preparation

The lipid vesicles were prepared using the standard extrusion method as described previously for liposome formation. Liposome mixtures were prepared in mass ratios composed of 90% DOPC, 10% POPA (PA 36:1) were dissolved in a test tube with chloroform. Lipids were dried under argon gaz. The lipid film thus obtained was hydrated with 500 µl of water and the solution was subjected to vortex mixing for 1 h at room temperature. The multilamellar vesicles were extruded 27 times using the Mini-Extruder equipped with a polycarbonate membrane filter of 100 nm pore diameter to obtain SUVs.

Atomic force microscopy measurements

Membrane preparation

Giant Unilamellar Vesicles (GUVs) were prepared by using 100% DOPC or a mix of 90% DOPC and 10% POPA. The vesicles were prepared in a 200 mM sucrose solution. GUV solution was diluted 100 times in 250 mM glucose solution to promote their sedimentation and to avoid multilayers. Final lipid concentration was 10 μM. The vesicle solution was injected in the AFM liquid cell and put in contact with freshly cleaved mica. After 2 minutes, the vesicle solution is replaced with 250 mM glucose solution in order to maintain the supported lipid bilayers hydrated at all times during imaging. To study protein/lipid interactions, the glucose solution was replaced with a CgA solution (0.6 or 1.2 μM), and the sample was imaged again.

Microscopy imaging

AFM measurements were performed on a multimode atomic force microscope (Nanoscope IIIA, Veeco, USA). Supported lipid bilayers images were taken in tapping mode in the fluid cell. A soft cantilever with a typical spring constant of 0.06 N/m and equipped with a silicon nitride tip was used. The tip velocity was set between 5-10 μm/s by varying the scan rate according to the scan size. The cantilever oscillation was tuned to a frequency between 20 and 30 kHz, and the amplitude was set between 0.8 V and 2 V. All the experiments were carried out at a temperature of 21°C.

High-sensitivity isothermal titration calorimetry (ITC)

Isothermal titration calorimetry was performed on an Affinity instrument (TA Instrument, New Castle, DE) equipped with a 185 μl reaction chamber. Solutions were degassed under

low pressure before use to avoid the formation of air bubbles while titrating. The CgA solution (5 µM) was placed in the calorimeter chamber and SUV suspension (10 mM) was injected in aliquots of 2.5 µl. The period between two successive injections was typically 200 sec to allow the system to reach equilibrium. The solution was stirred continuously at 125 rpm and the experiments were carried out at a temperature of 10°C. The resulting heat changes after SUV injection were recorded as a function of time. The heat of reaction was obtained by integrating the area under each peak of heat flow tracings, using the heat of SUV dilution in water as blank sample. The data were acquired by using the Nanoanalyze software (v.3.10.0, TA Instrument).

Immunofluorescence labelling

COS7-CgA cells were cultured in 24-well plates (Costar® 24 Well Clear TC-Treated Multiple Well Plates, Corning), onto glass coverslips and fixed with 4% paraformaldehyde (Sigma – Aldrich) in PBS at room temperature for 15 min. Cells were permeabilized and blocked for 30 min with 0.3% Triton X-100 (Thermo Fisher Scientific), in PBS containing 5% normal donkey serum (Sigma – Aldrich) (1:50) and 1% BSA (Bovine Serum Albumin, Sigma – Aldrich)). Cells were then incubated for 2 h at room temperature with primary antibodies, and, after washing with PBS, for 1 h with secondary antibodies. Nuclei were stained with DAPI (4',6-diamidino-2-phénylindole, Molecular probes #D3571, 1 µg ml^{-1}). To verify the specificity of the immunoreactions, the primary or secondary antibodies were substituted with PBS.

Protein electrophoresis and Western blotting

Cells were harvested by scraping, homogenized, and proteins were separated by SDS-PAGE followed by Western blotting. Membranes were incubated in a blocking buffer containing 5% non-fat dry milk in phosphate-buffered saline containing 0.5% Tween 20 (Sigma - Aldrich) (PBS-T) for 1 h at room temperature, and overnight with primary antibodies at 4°C. Then, membranes were washed for 45 min with PBS-T. Blots were subsequently incubated for 1 h with appropriate HRP (Horse Radish Peroxidase)-conjugated secondary antibody (Thermo Fisher Scientific) in blocking buffer. Membranes were washed for 45 min with PBS-T. Immunoreactive proteins were detected by chemiluminescence (BioRad Biotechnology). Quantification was performed using Image Lab software (5.0 build 18, 2013 version, Bio-Rad Laboratories). The mean intensity of each individual band of interest was calculated after background value subtraction.

Image acquisition

For GUVs experiments, real-time videomicroscopy was carried out with an inverse confocal microscope TCS-SP5 AOBS (*Acousto-Optical Beam Splitter*), equipped with pulsed white light laser (WLL) and with a 63X oil immersion objective (Leica Microsystems). PE–NBD was excited at 463 nm and observed in a 510-550 nm window. Images were acquired at a speed of one frame per 2 s during 1 min.

For immunocytochemistry experiments, confocal microscopy was carried out with a TCS-SP8 upright confocal laser-scanning microscope equipped with 63X oil immersion objective (NA=1.4; Leica, Microsystems). Alexa 488 and GFP were excited at 488 nm and observed in a 505–540 nm window. Alexa 594 was excited at 594 nm and observed in a 600–630nm window. For dual color acquisition, images were sequentially acquired in line scan mode (average line = 2). Overlays were performed with post acquisition Leica Confocal Software functions to obtain the presented snapshots.

Transmission electron microscopy of WT and Pld1$^{-/-}$ chromaffin cells in situ

WT and *Pld1*$^{-/-}$ mice were anesthetized with a mixture of ketamine (100 mg kg^{-1}) and xylazine (5 mg kg^{-1}) and transcardiacally perfused with 0.1 M phosphate buffer, pH 7.3, containing 2% paraformaldehyde and 2.5% glutaraldehyde. The 2-mm-thick slices were cut from the adrenal glands and postfixed in 1% glutaraldehyde in phosphate buffer overnight at 4°C. The slices were then immersed for 1h in OsO4 0.5% in phosphate buffer. 1 mm^3 blocks were cut in the adrenal medulla, dehydrated, and processed classically for embedding in Araldite and ultramicrotomy. Ultrathin sections were counterstained with uranyl acetate and examined with a Hitachi 7500 transmission electron microscope.

Statistical analysis

Data were analyzed with the Prism program (GraphPad 6.04 Software). For the quantification of the number of CgA granules, statistical significance was determined by Mann-Whitney U test. Values are expressed as means ± s.e.m., and the level of significance is designated in the figure legend as follows: * P<0.05, ** P<0.001, *** P<0.0001. For the quantification of CgA signal in lipid strip experiments, statistical significance was determined by an Anova one-way analysis of variance test with Bonferroni's comparison test. Values are expressed as means ± s.e.m., and the level of significance is designated in the figure legend as follows: *** P<0.0001. For the quantification of membrane deformation after CgA addition on GUVs, statistical significance was determined by Mann-Whithney U test. Values are expressed as means ± s.e.m., and the level of significance is designated in the figure legend as follows: *** P<0.0001.

Post-acquisition analysis

The following procedure was used to measure the number of CgA granules. The confocal section generated by the Leica TCS-SP8 confocal microscope was analyzed with Imaris and converted into an Imaris file. A broad region of interest (ROI) was defined around a cell. Then with the tool 'spots detection' on Imaris, the number of spots with a 500 nm diameter was quantified. Spots statistics are automatically computed for each spot object. It provides a procedure to automatically detect point-like structures, an editor to manually correct detection errors, a viewer to visualize the point-like structures as spheres, and statistics output.

To analyze secretory granule density in wild type and *Pld1* knock-out chromaffin cells, secretory granules were counted in 50 chromaffin cells from WT and *Pld1* KO mice with a visible nucleus randomly selected in ultrathin sections from several blocks (1 section/block) from each mouse (n=3 mice per genotype). Dense core diameter was measured from 950 randomly selected granules for each genotype using the line segment tool of Image J. To minimize the bias measurements, samples were blinded.

Acknowledgements

We thank the Normandy Platform of Cell Imaging (PRIMACEN), particularly Damien Schapman and Ludovic Galas. We thank Jérôme Leprince for fruitful discussion for PABD modelization. This work was supported by institutional funding from INSERM, University of Rouen-Normandie, Région Normandie and the European Regional Development Fund (ERDF) (DO-IT2015 program), and grants from the Medical Research Foundation (FRM) (project number DEI20151234424) to MM-H, P-YR and NV. OC and CD-D were supported by fellowships from the Ministère de la Recherche et de l'Enseignement Supérieur. FL is co-supported by European Union and Région Normandie. Europe gets involved in Normandie with ERDF. Lipidomic analyses were performed on the Bordeaux Metabolome Facility-MetaboHUB (ANR-11-INBS-0010).

Author contributions

OC and FL: designed and performed most of the experiments, analyzed the data and contributed to writing the paper. LR: designed and performed AFM and ITC experiments, analyzed the data. CD-D: performed and analyzed lipid overlay assays. LJ: managed cell line culture and secretion experiments. DC: contributed to CgA-GFP and CgAΔPABD-GFP cloning. TT and ET: performed the experiments related to liposome flotation and binding assays. AMH and QW: performed electron microscopy experiments. LF: performed the lipidome analysis using LC-MS/MS. OR, AH and P-YR: produced CgA coupled to Alexa Fluor 488 dye. SA: designed AFM and ITC setup, and analyzed AFM and ITC data. NV: designed liposome flotation and binding assays, analyzed data from electron microscopy experiments and performed PA-binding domain prediction, and contributed to writing of the paper. YA: contributed to experiment design, data analysis and interpretation, and writing of the paper. MM-H: coordinated the study, designed, analyzed and interpreted data, and wrote the paper.

References

Abbineni PS, Bittner MA, Axelrod D, Holz RW (2019) Chromogranin A, the major lumenal protein in chromaffin granules, controls fusion pore expansion. *J Gen Physiol* 151:118-130

Ammar MR, Humeau Y, Hanauer A, Nieswandt B, Bader MF, Vitale N (2013) The Coffin-Lowry syndrome-associated protein RSK2 regulates neurite outgrowth through phosphorylation of phospholipase D1 (PLD1) and synthesis of phosphatidic acid. *J Neurosci* 33:19470-19479

Ammar MR, Thahouly T, Hanauer A, Stegner D, Nieswandt B, Vitale N (2015) PLD1 participates in BDNF-induced signalling in cortical neurons. *Sci Rep* 5:14778

Anouar Y, Desmoucelles C, Yon L, Leprince J, Breault L, Gallo-Payet N, Vaudry H (1998) Identification of a novel secretogranin II-derived peptide (SgII(187-252)) in adult and fetal human adrenal glands using antibodies raised against the human recombinant peptide. *J Clin Endocrinol Metab* 83:2944-2951

Bandyopadhyay GK, Mahata SK (2017) Chromogranin A Regulation of Obesity and Peripheral Insulin Sensitivity. *Front Endocrinol* 8:20

Bligh EG, Dyer WJ (1959) A rapid method of total lipid extraction and purification. *Can J Biochem Physiol* 37: 911-917

Blois A, Holmsen H, Martino G, Corti A, Metz-Boutigue MH, Helle KB (2006) Interactions of chromogranin A-derived vasostatins and monolayers of phosphatidylserine, phosphatidylcholine and phosphatidylethanolamine. *Regul Pept* 134: 30-37

Carmon O, Laguerre F, Jeandel L, Anouar Y, Montero-Hadjadje M (2017) Chromogranins at the crossroads between hormone aggregation and secretory granule biogenesis. Chromogranins: from cell biology to physiology and biomedicine. UNIPA Springer Angelone, Cerra and Tota Eds, pp 39-48

Chanat E, Huttner WB (1991) Milieu-induced, selective aggregation of regulated secretory proteins in the trans-Golgi network. *J Cell Biol* 115: 1505-1519

Chevalier A, Massif C, Renard PY, Romieu A (2013) Bioconjugatable Azo-Based Dark-Quencher Dyes: Synthesis and Application to Protease-Activatable Far-Red Fluorescent Probes. *Chem Eur J* 19: 1686–1699

Cruz-Garcia D, Ortega-Bellido M, Scarpa M, Villeneuve J, Jovic M, Porzner M, Balla T, Seufferlein T, Malhotra V (2013) Recruitment of arfaptins to the trans-Golgi network by PI(4)P and their involvement in cargo export. *EMBO J* 32: 1717-1729

Delestre-Delacour C, Carmon O, Laguerre F, Estay-Ahumada C, Courel M, Elias S, Jeandel L, Rayo MV, Peinado JR, Sengmanivong L, Gasman S, Coudrier E, Anouar Y, Montero-Hadjadje M (2017) Myosin 1b and F-actin are involved in the control of secretory granule biogenesis. *Sci Rep* 7: 5172

Dhanvantari S1, Loh YP (2000) Lipid raft association of carboxypeptidase E is necessary for its function as a regulated secretory pathway sorting receptor. *J Biol Chem* 275: 29887-29893

Dondossola E, Gasparri A, Bachi A, Longhi R, Metz-Boutigue MH, Tota B, Helle KB, Curnis F, Corti A (2010) Role of vasostatin-1 C-terminal region in fibroblast cell adhesion. *Cell Mol Life Sci* 67:2107-2018

Duran JM, Campelo F, van Galen J, Sachsenheimer T, Sot J, Egorov MV, Rentero C, Enrich C, Polishchuk RS, Goni FM, Brugger B, Wieland F, Malhotra V (2012) Sphingomyelin organization is required for vesicle biogenesis at the Golgi complex. *EMBO J* 31: 4535-4546

Elias S, Delestre C, Courel M, Anouar Y, Montero-Hadjadje M (2010) Chromogranin A as a crucial factor in the sorting of peptide hormones to secretory granules. *Cell Mol Neurobiol* 30: 1189-1195

Elias S, Delestre C, Ory S, Marais S, Courel M, Vazquez-Martinez R, Bernard S, Coquet L, Malagon MM, Driouich A, Chan P, Gasman S, Anouar Y, Montero-Hadjadje M (2012) Chromogranin A induces the biogenesis of granules with calcium- and actin-dependent dynamics and exocytosis in constitutively secreting cells. *Endocrinology* 153: 4444-4456

Freyberg Z, Sweeney D, Siddhanta A, Bourgoin S, Frohman M, Shields D (2001) Intracellular localization of phospholipase D1 in mammalian cells. *Mol Biol Cell* 12: 943-955

Freyberg Z, Siddhanta A, Shields D (2003) "Slip, sliding away": phospholipase D and the Golgi apparatus. *Trends Cell Biol* 13: 540-546

Gautier R, Douguet D, Antonny B, Drin G (2008) HELIQUEST: a web server to screen sequences with specific α-helical properties. *Bioinformatics* 24: 2101–2102

Gondré-Lewis MC, Petrache HI, Wassif CA, Harries D, Parsegian A, Porter FD, Loh YP (2006) Abnormal sterols in cholesterol-deficiency diseases cause secretory granule malformation and decreased membrane curvature. *J Cell Sci* 119: 1876-1885

Gondré-Lewis MC, Park JJ, Loh YP (2012) Cellular mechanisms for the biogenesis and transport of synaptic and dense-core vesicles. *Int Rev Cell Mol Biol* 299:27-115

Holthuis JC, Menon AK (2014) Lipid landscapes and pipelines in membrane homeostasis. *Nature* 510: 48-57

Hosaka M, Watanabe T, Sakai Y, Uchiyama Y, Takeuchi T (2002) Identification of a chromogranin A domain that mediates binding to secretogranin III and targeting to secretory granules in pituitary cells and pancreatic beta-cells. *Mol Biol Cell* 13: 3388-3399

Hosaka M, Suda M, Sakai Y, Izumi T, Watanabe T, Takeuchi T (2004) Secretogranin III binds to cholesterol in the secretory granule membrane as an adapter for chromogranin A. *J Biol Chem* 279: 3627-3634

Hosaka M, Watanabe T, Sakai Y, Kato T, Takeuchi T (2005) Interaction between secretogranin III and carboxypeptidase E facilitates prohormone sorting within secretory granules. *J Cell Sci* 118: 4785-4795

Hummer BH, de Leeuw NF, Burns C, Chen L, Joens MS, Hosford B, Fitzpatrick JAJ, Asensio CS (2017) HID-1 controls formation of large dense core vesicles by influencing cargo sorting and trans-Golgi network acidification. *Mol Biol Cell* 28: 3870-3880

Huston E, Gall I, Houslay TM, Houslay MD (2006) Helix-1 of the cAMP-specific phosphodiesterase PDE4A1 regulates its phospholipase-D-dependent redistribution in response to release of Ca2+. *J Cell Sci* 119:3799-3810

Kang YK, Yoo SH (1997) Identification of the secretory vesicle membrane binding region of chromogranin A. *FEBS Lett* 404: 87-90

Kassas N, Tanguy E, Thahouly T, Fouillen L, Heintz D, Chasserot-Golaz S, Bader MF, Grant NJ, Vitale N (2017) Comparative Characterization of phosphatidic acid sensors and their localization during frustrated phagocytosis. *J Biol Chem* 292: 4266-4279

Kim T, Tao-Cheng JH, Eiden LE, Loh YP (2001) Chromogranin A, an "on/off" switch controlling dense-core secretory granule biogenesis. *Cell* 106: 499-509

Kiranmayi M, Chirasani VR, Allu PK, Subramanian L, Martelli EE, Sahu BS, Vishnuprabu D, Kumaragurubaran R, Sharma S, Bodhini D, Dixit M, Munirajan AK, Khullar M, Radha V, Mohan V, Mullasari AS, Naga Prasad SV, Senapati S, Mahapatra NR (2016) Catestatin Gly364Ser Variant Alters Systemic Blood Pressure and the Risk for Hypertension in Human Populations via Endothelial Nitric Oxide Pathway. *Hypertension* 68: 334-347

Kooijman EE, Chupin V, de Kruijff B, Burger KN (2003) Modulation of membrane curvature by phosphatidic acid and lysophosphatidic acid. *Traffic* 4: 162-174

Mahapatra NR, O'Connor DT, Vaingankar SM, Hikim AP, Mahata M, Ray S, Staite E, Wu H, Gu Y, Dalton N, Kennedy BP, Ziegler MG, Ross J, Mahata SK (2005) Hypertension from targeted ablation of chromogranin A can be rescued by the human ortholog. *J Clin Invest* 115:1942-1952

Miao R, Lung SC, Li X, David Li X, Chye ML (2019) Thermodynamic insights into an interaction between acyl-coA-binding protein 2 and lysophospholipase 2 in Arabidopsis. *J Biol Chem* 294: 6214-6226

Montero-Hadjadje M, Vaudry H, Turquier V, Leprince J, Do Rego JL, Yon L, Gallo-Payet N, Plouin PF, Anouar Y (2002) Localization and characterization of evolutionarily conserved chromogranin A-derived peptides in the rat and human pituitary and adrenal glands. *Cell Tissue Res* 310: 223-236

Montero-Hadjadje M, Elias S, Chevalier L, Benard M, Tanguy Y, Turquier V, Galas L, Yon L, Malagon MM, Driouich A, Gasman S, Anouar Y (2009) Chromogranin A promotes peptide hormone sorting to mobile granules in constitutively and regulated secreting cells: role of conserved N- and C-terminal peptides. *J Biol Chem* 284: 12420-12431

Pasqua T, Mahata S, Bandyopadhyay GK, Biswas A, Perkins GA, Sinha-Hikim AP, Goldstein DS, Eiden LE, Mahata SK (2016) Impact of Chromogranin A deficiency on catecholamine storage, catecholamine granule morphology and chromaffin cell energy metabolism in vivo. *Cell Tissue Res* 363: 693-712

Pierce MM, Raman CS, Nall BT (1999) Isothermal titration calorimetry of protein-protein interactions. *Methods* 19: 213-221

Sahu BS, Obbineni JM, Sahu G, Allu PK, Subramanian L, Sonawane PJ, Singh PK, Sasi BK, Senapati S, Maji SK, Bera AK, Gomathi BS, Mullasari AS, Mahapatra NR (2012) Functional genetic variants of the catecholamine-release-inhibitory peptide catestatin in an Indian population: allele-specific effects on metabolic traits. *J Biol Chem* 287: 43840-43852

Shui G, Guan XL, Gopalakrishnan P, Xue Y, Goh JS, Yang H, Wenk MR (2010) Characterization of substrate preference for Slc1p and Cst26p in *Saccharomyces cerevisiae* using lipidomic approaches and an LPAAT activity assay. *PLoS One* 5(8):e11956

Siddhanta A, Shields D (1998) Secretory vesicle budding from the trans-Golgi network is mediated by phosphatidic acid levels. *J Biol Chem* 273:17995-17998

Sugawara M, Resende JM, Moraes CM, Marquette A, Chich JF, Metz-Boutigue MH, Bechinger B (2010) Membrane structure and interactions of human catestatin by multidimensional solution and solid-state NMR spectroscopy. *FASEB J* 24: 1737-1746

Surma MA, Klose C, Simons K (2012) Lipid-dependent protein sorting at the trans-Golgi network. *Biochim Biophys Acta* 1821: 1059-1067

Tanguy E, Carmon O, Wang Q, Jeandel L, Chasserot-Golaz S, Montero-Hadjadje M, Vitale N (2016) Lipids implicated in the journey of a secretory granule: from biogenesis to fusion. *J Neurochem* 137: 904-12

Tanguy E, Kassas N, Vitale N (2018) Protein-Phospholipid Interaction Motifs: A Focus on Phosphatidic Acid. *Biomolecules* 8(2). pii: E20

Vitale N, Caumont AS, Chasserot-Golaz S, Du G, Wu S, Sciorra VA, Morris AJ, Frohman MA, Bader MF (2001) Phospholipase D1: a key factor for the exocytotic machinery in neuroendocrine cells. *EMBO J* 20: 2424-2434

Yadav GP, Zheng H, Yang Q, Douma LG, Bloom LB, Jiang QX (2018) Secretory granule protein chromogranin B (CHGB) forms an anion channel in membranes. *Life Science Alliance* 1(5): 1-18. DOI 10.26508/lsa.201800139

Yamada A, Mamane A, Lee-Tin-Wah J, Di Cicco A, Prévost C, Lévy D, Joanny JF, Coudrier E, Bassereau P (2014) Catch-bond behaviour facilitates membrane tubulation by non-processive myosin 1b. *Nat Commun* 5: 3624

Figure legends

Figure 1. Golgi PA is involved in CgA secretory granule biogenesis and CgA interacts with PA through a putative PABD.

A Involvement of Golgi PA in the formation of CgA-containing secretory granules in PC12 cells. Cells expressing PDE4A1-GFP (PDE4A1 WT) or its PABD-deleted mutant (PDE4A1 Mut) were immunolabelled with anti-CgA antibody. Representative confocal microscopy sections throughout the cells are shown and were used to quantify automatically the granules with a diameter > 200 nm. Values for the number of granules per cell are plotted as the means ± S.D. (n=2; 40 cells per condition). $^{**}P < 0.001$, Mann-Whitney test. The scale bar represents 20 µm.

B Protein–lipid overlay assay in the presence of recombinant CgA (500 ng/ml) using commercial membrane strips where are adsorbed 100 pmol/spot of the following lipids: triglyceride, diacylglycerol (DAG), phosphatidic acid (PA), phosphatidylserine (PS), phosphatidylethanolamine (PE), phosphatidylcholine (PC), phosphatidylglycerol (PG), cardiolipin, phosphatidylinositol (PI), phosphatidylinositol 4-phosphate [PI(4)P], phosphatidylinositol 4,5-bisphosphate [$PI(4,5)P_2$], phosphatidylinositol 3,4,5-trisphosphate [$PI(3,4,5)P_3$], cholesterol, sphingomyelin, or 3-sulfogalactosylceramide (sulfatide). The resulting membrane was immunostained for CgA detected by a WE14 antibody and revealed using a chemiluminescence kit. Plotted are means of CgA binding expressed as percentage normalized to control (blank) $\pm$ s.e.m. ($n = 3$). $^{***}P < 0.0001$, Anova one-way analysis of variance test with Bonferroni's comparison test.

C Human CgA sequence showing a region of 18 amino acids ($hCgA_{364-381}$), encompassing a positive charge cluster and hydrophobic residues that could adopt an α-helical conformation, delimited by arrows, suggesting its function as PA-binding domain (PABD).

D PA binding profile of the putative human CgA-PABD. Amphipathic α-helix projection of the core 18 amino acids of the PABD of CgA obtained with Heliquest software. Arrow indicates hydrophobic moment.

E Model of the putative human CgA-PABD. Ribbon corresponds to the α-helix. Structure was examined using MacPyMOL (v1.74).

F Characterization of the PA binding capacity of human CgA through the putative PABD. Semi-quantitative fluorescent liposome assays with PA-containing fluorescent liposomes (5% PE-NBD, 85% DOPC, 10% PA mix) and GST-CgA-PABD constructs linked to GSH-Sepharose beads. The binding of liposomes with CgA-PABD constructs was monitored by fluorimetry. Results are presented as means ± S.D. (of triplicate measurements pooled from three experiments).

Figure 2. Same predominant PA species are found in Golgi and secretory granule membranes from COS7-WT, COS7-CgA and PC12 cells.

A The levels of distinct PA species were measured in fractions of secretory granule (SG) and Golgi membranes from COS7-CgA cells by duplicate UPLC/MS/MS analysis of two samples (each containing 200 µg of protein) from each fraction. The acyl chain composition of each species is shown on the x axis. The y axis shows the abundance of each species as a percentage of total PA in the sample.

B PA levels were measured in fractions of Golgi membranes from COS7-WT or COS7-CgA cells by duplicate UPLC/MS/MS analysis of two samples (each containing 200 µg of protein) from each fraction. The acyl chain composition of each species is shown on the x axis. The y axis shows the abundance of each species as a percentage of total PA in the sample.

C PA levels were measured in secretory granule-containing fractions from PC12 or COS7-CgA cells by duplicate UPLC/MS/MS analysis of two samples (each containing 200 µg of protein) from each fraction. The acyl chain composition of each species is shown on the x axis. The y axis shows the abundance of each species as a percentage of total PA in the sample.

Figure 3. CgA interacts with PA species identified in Golgi and secretory granule membranes and provokes membrane deformation of PA-enriched GUVs.

A Schematic representation of the liposome flotation assay approach used to study the interaction of CgA from COS7-CgA cell extracts with PA species.

B Detection of CgA in the different fractions (Top (T), Medium (M), Bottom (B)) obtained from liposome assays. COS7-CgA cell extracts were incubated with liposomes containing 5% NBD-PE, 85% of DOPC, and 10% of the indicated phosphatidylcholine (PC), phosphatidylserine (PS), phosphatidylinositol-4,5-bisphosphate (PIP2), a commercial phosphatidic acid mix (PA) or distinct species of PA (PA 36:0, PA 36:1, PA 40:6). Thirty µg of protein from each fraction were run on SDS-PAGE and immunoblotted with the CgA-derived WE14 antibody.

C Formation by PVA-assisted swelling of fluorescent PA-containing GUVs. Stable fluorescent GUVs (96 % DOPC, 10 % PA (36:1) and 1 % PE-NBD) were generated and observed by live confocal microscopy during 1 min. Representative confocal microscopy sections throughout the GUVs are shown. The scale bar represents 30 µm.

D Effect of CgA on fluorescent PA-containing GUVs. Fluorescent GUVs (96 % DOPC, 10 % PA (36:1) or PA (40:6) and 1 % PE-NBD) were incubated with 2 µM CgA. Deformation of GUV membrane was observed by live confocal microscopy during 1 min. Representative confocal microscopy sections throughout the GUVs are shown. The scale bar represents 30 µm.

E Quantification of membrane deformations of PA-containing GUVs. GUVs (90 % DOPC, 10 % PA (36:1)) were incubated with 2, 4 and 6 µM CgA (n=3; 35 movies per condition). ***$P < 0.0001$, Mann-Whitney test. Means ± s.e.m. are plotted.

F Distribution of CgA-Alexa488 on PA-containing GUVs. GUVs (90 % DOPC, 10 % PA (36:1)) were incubated with 2 µM CgA-Alexa488. Staining and budding (arrows) of GUV membrane was observed by live confocal microscopy during 1 min. Representative confocal microscopy sections throughout the GUVs are shown. The scale bar represents 20 µm.

Figure 4. ITC analysis reveals that PA favors membrane incorporation of CgA.

A DOPC SUVs and CgA binding measured by titrating 5 µM CgA in the chamber with 10 mM vesicle suspension in the syringe. Top panel, raw heating power over time obtained with DOPC SUV injection in water; bottom panel, raw heating power over time obtained with DOPC SUV injection in CgA solution.

B DOPC/PA (36:1) SUVs and CgA binding measured by titrating 5 µM CgA in the chamber with 10 mM vesicle suspension in the syringe. Top panel, raw heating power over time obtained with DOPC/PA (36:1) SUV injection in water; bottom panel, raw heating power over time obtained with DOPC/PA (36:1) SUV injection in CgA solution.

C Fit curves of the integrated energy values obtained from A and B traces in bottom panels using A and B traces in upper panels as blank, respectively. Experiments were carried out at 10 °C, and each value is the mean of at least three independent titrations.

Figure 5. CgA induces the remodeling of PA-enriched membrane bilayers.

A Atomic force microscopy topographical images of mica supported bilayer surfaces from DOPC GUVs, incubated without or with 0.6 and 1.2 µM CgA, during 15 min (T1) and 75 min (T2). The scale bar represents 2 µm. The scheme corresponds to a topographical profile through an aggregate (enlarged view) showing a difference of height of 6 nm with the continuous phase.

B Atomic force microscopy topographical images of mica supported bilayer surfaces from DOPC/PA (36:1) (9:1, mol ratio) GUVs, incubated without or with 0.6 and 1.2 µM CgA, during 15 min (T1) and 75 min (T2). Arrow heads indicate aggregates that appeared at T1 and are maintained at T2; arrows indicate aggregates that appeared between T1 and T2. The scale bar represents 2 µm. The scheme corresponds to topographical profiles through aggregates (enlarged views) showing a difference of height of 6 nm (a) and 17 nm (b) with the continuous phase.

Figure 6. Number, surface and height of CgA-induced domains depend on PA enrichment of membrane bilayers.

A Scatter plot showing the number, area and height of domains obtained after incubation of supported bilayer surfaces from DOPC GUVs with 1.2 µM CgA during 75 min. Insert corresponds to enlarged view of the delimited zone emphasizing domains with height below 4 nm and area below 6000 nm^2 (within blue surrounded zone). Analysis of domains was performed on 15 images and domains detected on an image are of the same color.

B Scatter plot showing the number, area and height of domains obtained after incubation of supported bilayer surfaces from DOPC/PA (36:1) (9:1, mol ratio) GUVs with 1.2 µM CgA during 75 min. Insert corresponds to enlarged view of the delimited zone emphasizing domains with height below 4 nm and area below 6000 nm^2 (within blue surrounded zone). Analysis of domains was performed on 11 images and domains detected on an image are of the same color.

Figure 7. CgA PABD and PLD-derived PA are required for secretory granule biogenesis.

COS-7 cells transfected with plasmids encoding full-length CgA-GFP or CgA PABD-truncated form (CgAΔPABD)-GFP were examined for GFP fluorescence and GM130 immunoreactivity using confocal microscopy. Representative confocal microscopy sections throughout the cells are shown and were used to quantify automatically the granules with a diameter > 200 nm. Values for the number of granules/cell are plotted as the means ± s.e.m. (n=3; 65 cells per condition). ***$P < 0.0001$, Mann-Whitney test. The scale bar represents 20 µm.

Figure 8. PLD1 invalidation alters secretory granule biogenesis.

A COS7-CgA cells were treated or not with 75nM FIPI for 6h, fixed and immunolabelled with anti-GM130 and anti-CgA antibodies. Representative confocal microscopy sections throughout the cells are shown. The scale bar represents 17 µm. Values for the number of CgA secretory granules are plotted as the means ± s.e.m. (n=3; 60 cells per condition). ***$P < 0.0001$, Mann-Whitney test.

B PC12 cells were treated or not with 75nM FIPI for 6h, fixed and immunolabelled with anti-GM130 and anti-CgA antibodies. Representative confocal microscopy sections throughout the cells are shown. The scale bar represents 17 µm. Values for the number of CgA secretory granules are plotted as the means ± s.e.m. (n=3; 60 cells per condition). Mann-Whitney test.

C Electron microscopy analysis of chromaffin cells from WT (control) and *Pld1*$^{-/-}$ mice. The scale bars represent 2 µm.

D Quantification of the number of secretory granules (SG) shown in panel (A) (n=6 mice per condition; 50 cells per mouse adrenal medulla). *$P < 0.05$, Mann-Whitney test. Means ± s.e.m. are plotted.

E Quantification of the dense core diameter of secretory granules (SG) shown in panel (A) (n=6 mice per condition; 950 granules). *$P < 0.05$, Mann-Whitney test. Means ± s.e.m. are plotted.

Figure S1. Purification of secretory granule and Golgi membranes by subcellular fractionation using centrifugation on sucrose gradient. Each fraction was collected and analyzed using SDS-PAGE and several antibodies raised against ER (anti-CALR, 70 kDa),

mitochondria (anti-GLUD1, 55 kDa), nucleus (anti-PCNA, 36 kDa), plasma membrane (anti ZO-3, 140 kDa), Golgi (anti-GM130, 130 kDa) and SG (anti-RV29.4, 70 kDa).

Figure S2. Full-length and ΔPABD Chromogranin A expression in COS7 cells.

Upper panel shows a representative Western blot where immunoreactive bands between 130 to 100 kDa correspond to the CgA-GFP fusion protein are detected. Lower panel shows the same Western blot where an immunoreactive band of 55 kDa corresponding to α-tubulin is detected. Tubulin was used as a loading control.

Figure S3. Conditions used for FIPI treatment of secretory cells do not alter granin expression.

A Western blot analysis of CgA content from COS7-CgA cells, treated or not with 75nM of FIPI. Upper panel shows a representative Western blot, where immunoreactive bands of 70 and 55 kDa corresponding to the CgA protein and tubulin respectively are detected. Lower panel shows the quantification of the relative amount of CgA protein. Tubulin was used as a loading control. Means ± s.e.m. from three independent experiments are plotted (Mann-Whitney test).

B Western blot analysis of CgA, CgB and SgII proteins from PC12 cells, treated or not with 75nM of FIPI. Upper panel shows a representative Western blot, where immunoreactive bands of 70, 115, 85 and 55 kDa corresponding to CgA, CgB and SgII proteins and tubulin respectively are detected. Lower panel shows the quantification of the relative amounts

of granin proteins. Tubulin was used as a loading control. Means ± s.e.m. from three independent experiments are plotted (Mann-Whitney test).

Movie S1. Live confocal microscopy observation of DOPC/PA/PE-NBD GUVs during 1 min without CgA highlighting the homogeneous distribution of fluorescence around GUVs.

Movie S2. Live confocal microscopy observation of DOPC/PA/PE-NBD GUVs during 1 min with 2 µM CgA highlighting GUV membrane deformation.

Table 1.

Thermodynamic parameters for CgA binding on DOPC and DOPC/PA SUVs. The values are plotted in Fig. 4.

	DOPC		DOPC:POPA	
	exothermic	endothermic	exothermic	endothermic
Kd (M)	$1.5\ 10^{-4} \pm 0.5\ 10^{-4}$	$2\ 10^{-5} \pm 1\ 10^{-5}$	$1.16\ 10^{-3} \pm 0.03\ 10^{-3}$	$3\ 10^{-4} \pm 0.1\ 10^{-4}$
n	259 ± 30	460 ± 40	199 ± 5	355 ± 5
ΔH (kJ/mol)	-1.82 ± 0.09	0.640 ± 0.06	-12.9 ± 0.3	7.65 ± 0.15
ΔS (J/mol.K)	67.3 ± 3.2	93.4 ± 4.8	10.6 ± 1.3	94.5 ± 0.8

Experiments were carried out at 10 °C, and each value is the mean and standard deviation from the fitted data of three independent experiments. Kd, dissociation constant; n, number of binding sites; ΔH, enthalpy change; ΔS, entropy change.

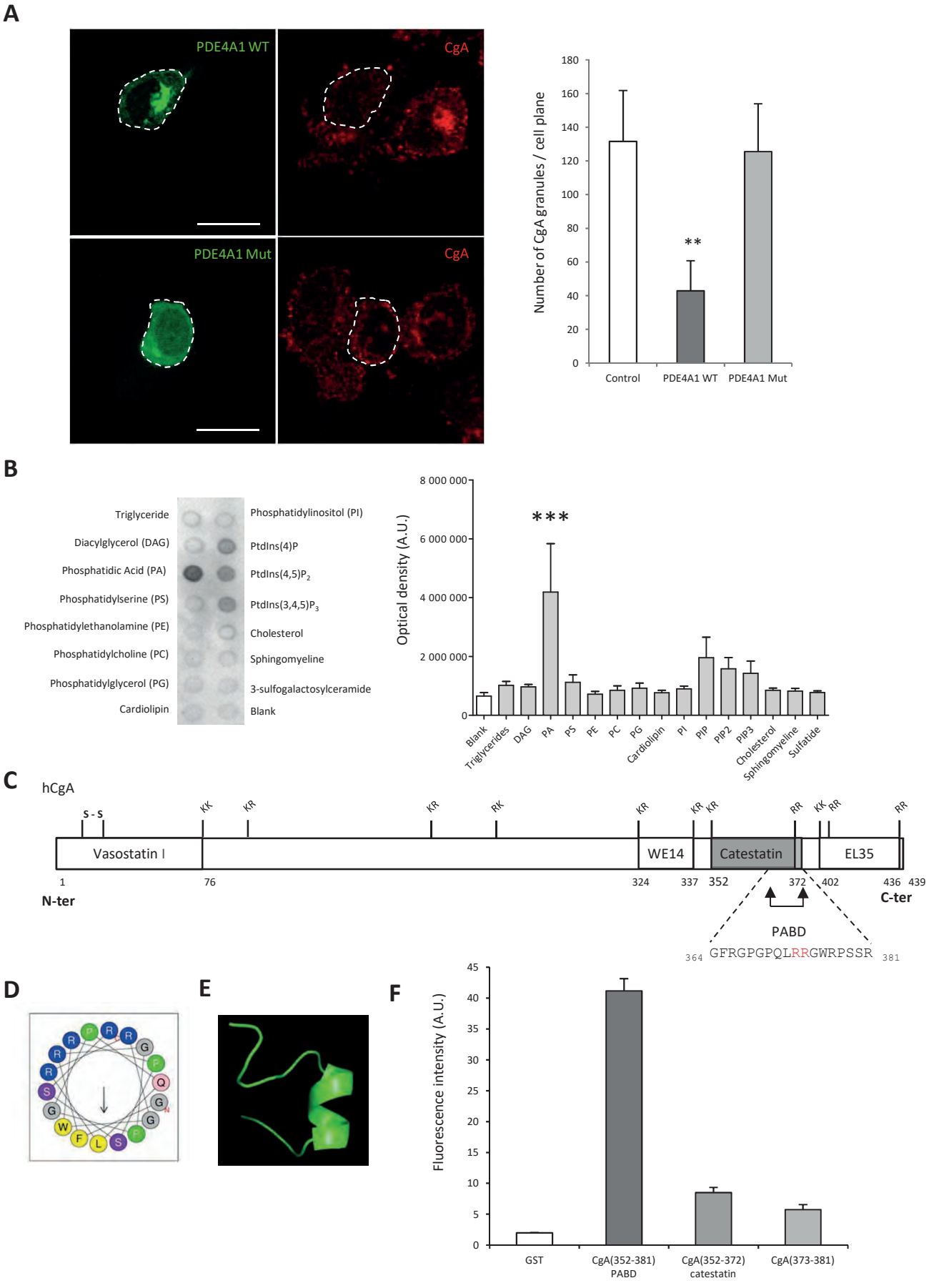
A
PDE4A1 WT
CgA
PDE4A1 Mut
CgA
Number of CgA granules / cell plane
180
160
140
120
100
80
60
40
20
0
**
Control
PDE4A1 WT
PDE4A1 Mut
B
Triglyceride
Diacylglycerol (DAG)
Phosphatidic Acid (PA)
Phosphatidylserine (PS)
Phosphatidylethanolamine (PE)
Phosphatidylcholine (PC)
Phosphatidylglycerol (PG)
Cardiolipin
Phosphatidylinositol (PI)
PtdIns(4)P
PtdIns(4,5)P2
PtdIns(3,4,5)P3
Cholesterol
Sphingomyeline
3-sulfogalactosylceramide
Blank
Optical density (A.U.)
8 000 000
6 000 000
4 000 000
2 000 000
0
***
Blank
Triglycerides
DAG
PA
PS
PE
PC
PG
Cardiolipin
PI
PIP
PIP2
PIP3
Cholesterol
Sphingomyeline
Sulfatide
C
hCgA
S - S
KK
KR
KR
RK
KR
KR
KR
RR
KK
RR
RR
Vasostatin I
WE14
Catestatin
EL35
1
76
324
337
352
372
402
436
439
N-ter
C-ter
PABD
364
GFRGPGPQLRRGWRPSSR
381
D
E
F
Fluorescence intensity (A.U.)
45
40
35
30
25
20
15
10
5
0
GST
CgA(352-381)
PABD
CgA(352-372)
catestatin
CgA(373-381)

Figure 1

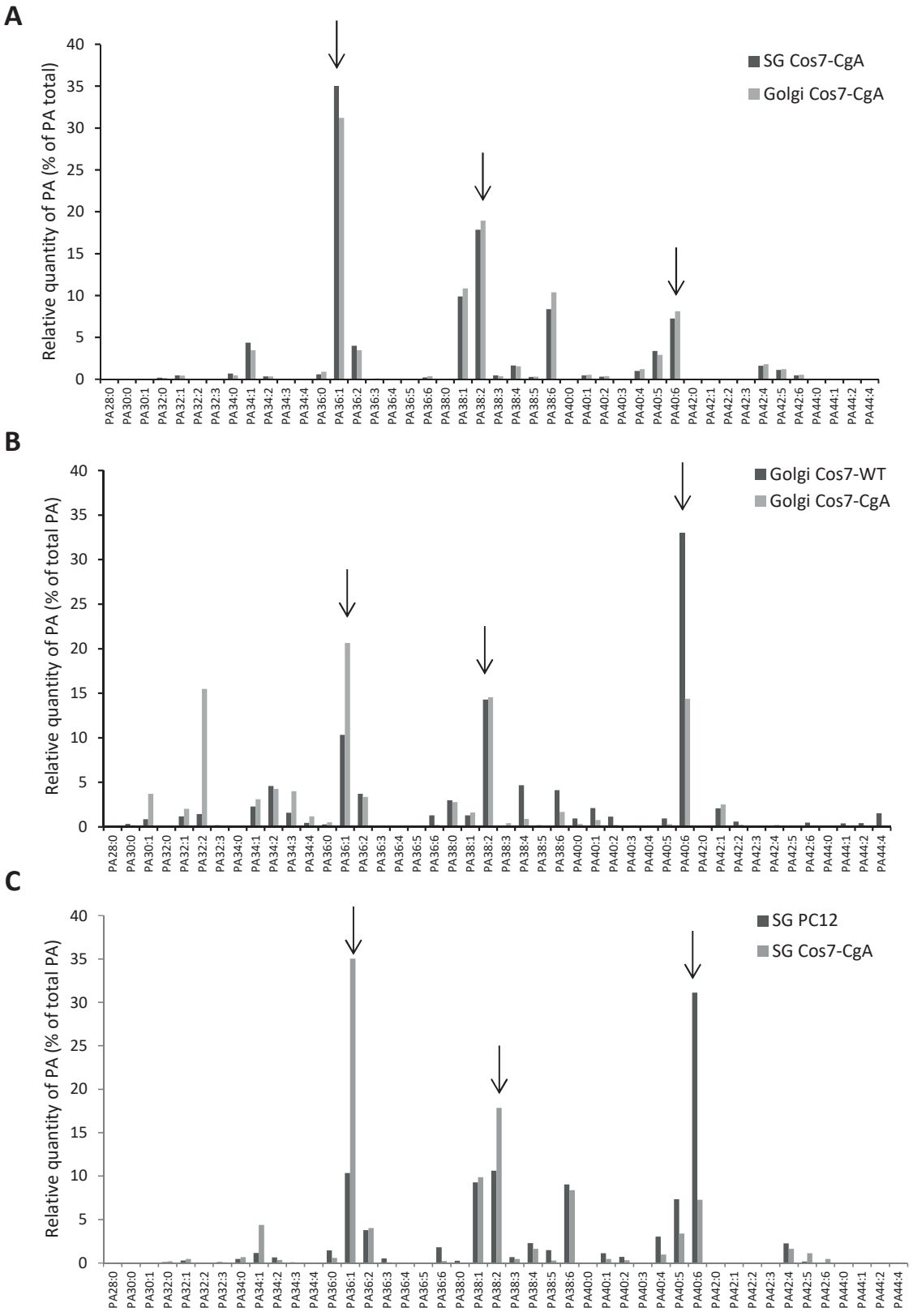
A
Relative quantity of PA (% of PA total)
SG Cos7-CgA
Golgi Cos7-CgA
B
Relative quantity of PA (% of total PA)
Golgi Cos7-WT
Golgi Cos7-CgA
C
Relative quantity of PA (% of total PA)
SG PC12
SG Cos7-CgA
PA28:0 PA30:0 PA30:1 PA32:0 PA32:1 PA32:2 PA32:3 PA34:0 PA34:1 PA34:2 PA34:3 PA34:4 PA36:0 PA36:1 PA36:2 PA36:3 PA36:4 PA36:5 PA36:6 PA38:0 PA38:1 PA38:2 PA38:3 PA38:4 PA38:5 PA38:6 PA40:0 PA40:1 PA40:2 PA40:3 PA40:4 PA40:5 PA40:6 PA42:0 PA42:1 PA42:2 PA42:3 PA42:4 PA42:5 PA42:6 PA44:0 PA44:1 PA44:2 PA44:4

Figure 2

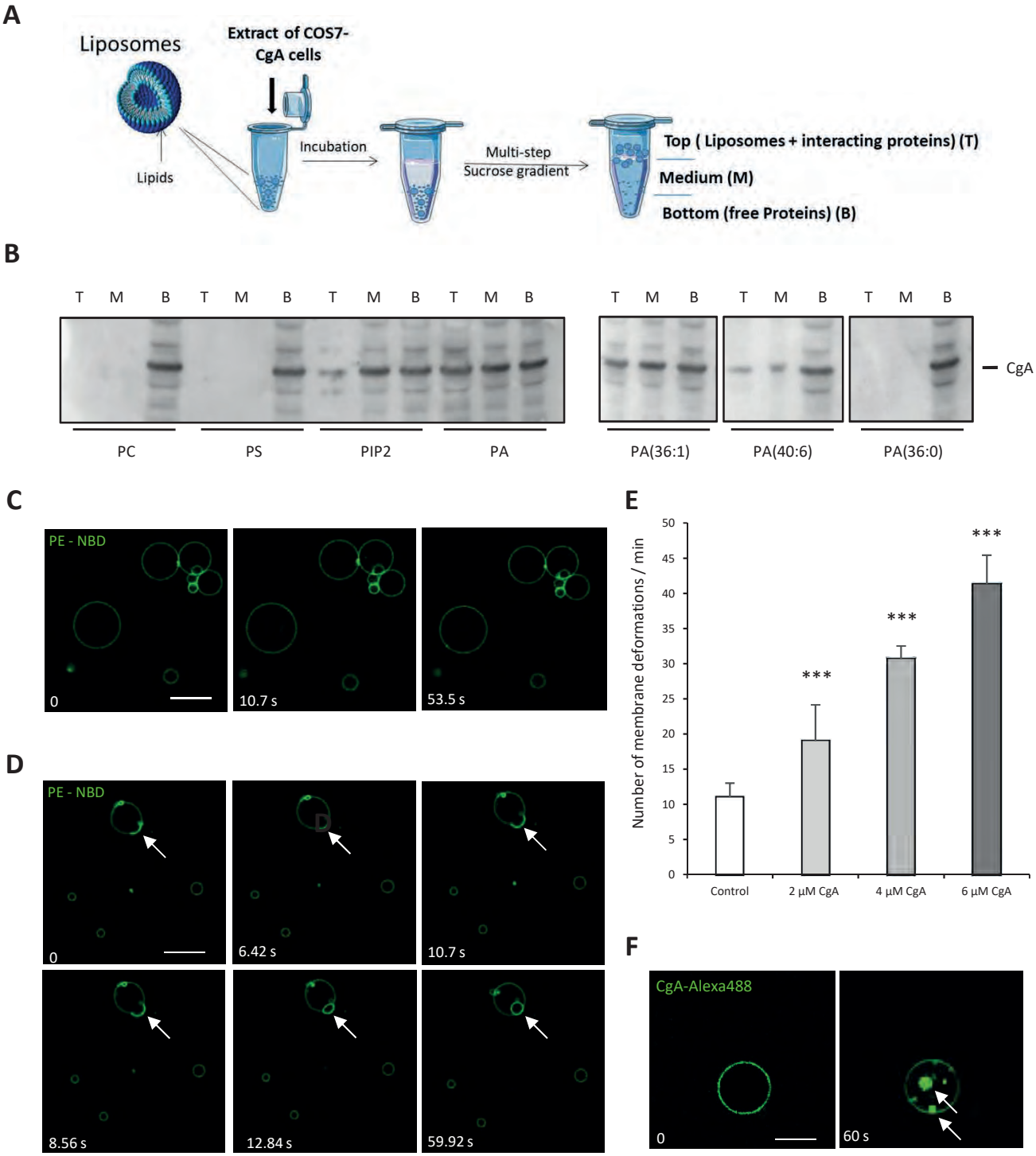
A
Liposomes
Extract of COS7-CgA cells
Lipids
Incubation
Multi-step Sucrose gradient
Top (Liposomes + interacting proteins) (T)
Medium (M)
Bottom (free Proteins) (B)
B
T M B T M B T M B T M B T M B T M B T M B T M B
CgA
PC
PS
PIP2
PA
PA(36:1)
PA(40:6)
PA(36:0)
C
PE - NBD
0
10.7 s
53.5 s
D
PE - NBD
0
6.42 s
10.7 s
8.56 s
12.84 s
59.92 s
E
Number of membrane deformations / min
0
5
10
15
20
25
30
35
40
45
50
***
***
***
Control
2 µM CgA
4 µM CgA
6 µM CgA
F
CgA-Alexa488
0
60 s

Figure 3

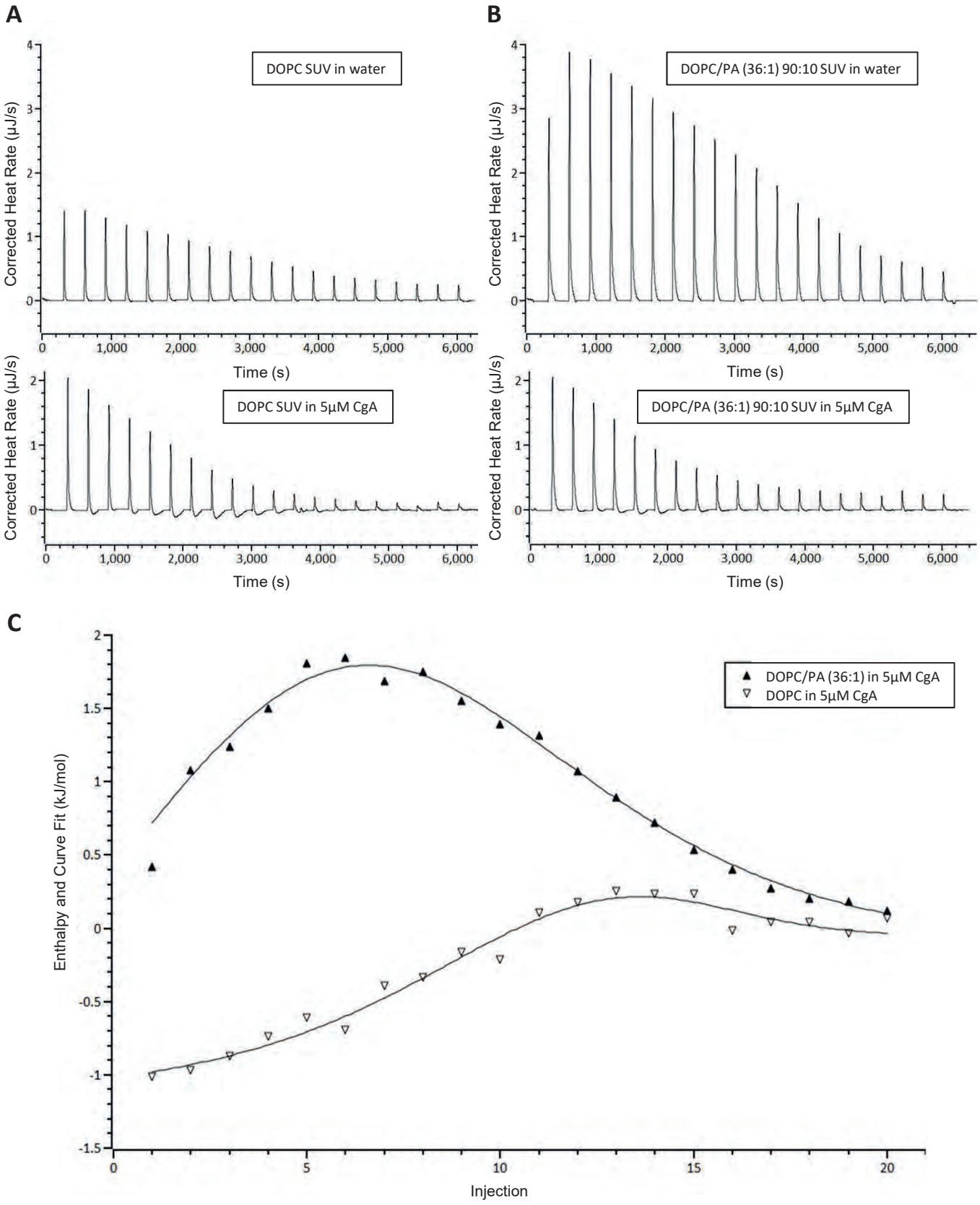
A
DOPC SUV in water
Corrected Heat Rate (µJ/s)
Time (s)
DOPC SUV in 5µM CgA
B
DOPC/PA (36:1) 90:10 SUV in water
DOPC/PA (36:1) 90:10 SUV in 5µM CgA
C
DOPC/PA (36:1) in 5µM CgA
DOPC in 5µM CgA
Enthalpy and Curve Fit (kJ/mol)
Injection

Figure 4

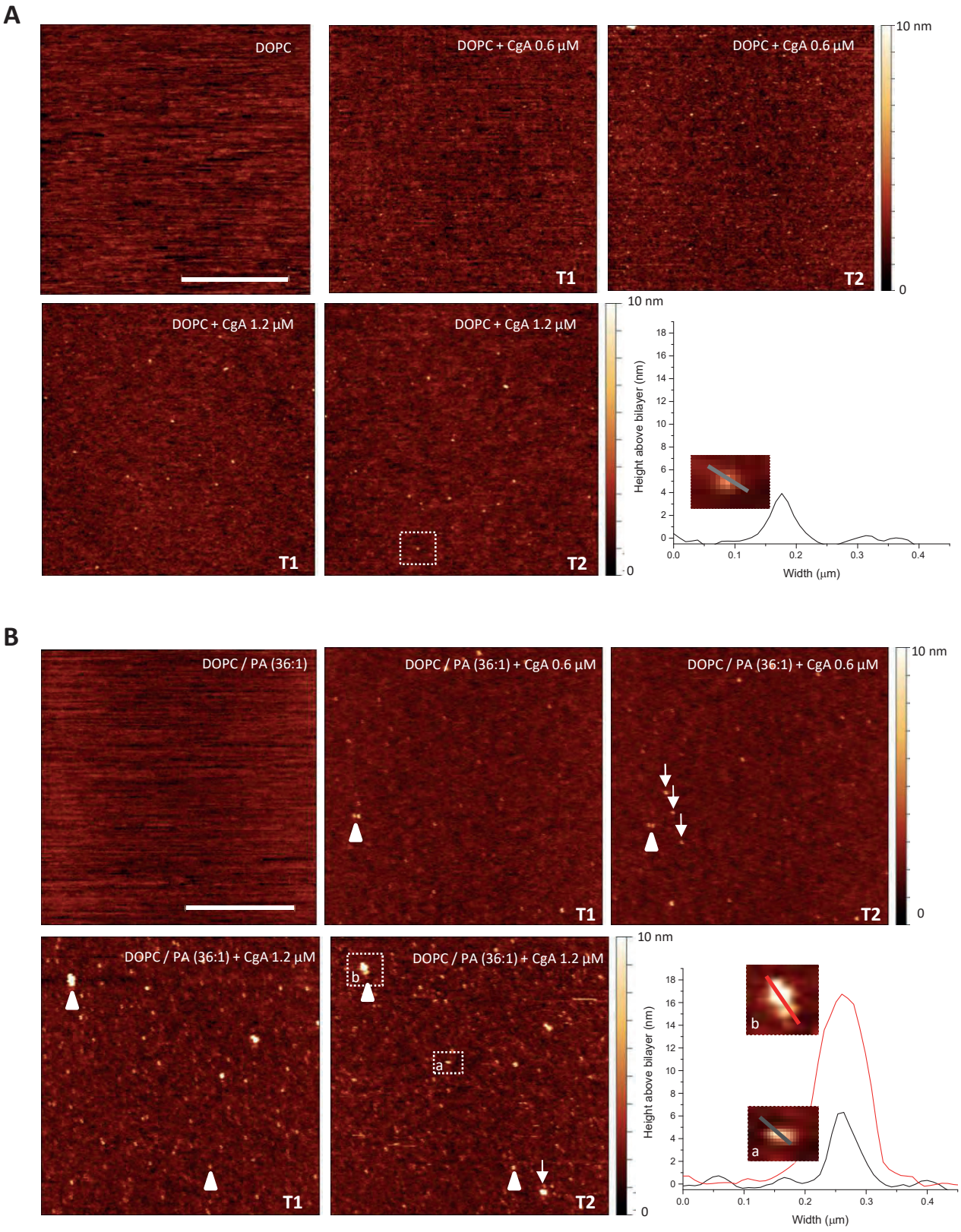
A
DOPC
DOPC + CgA 0.6 µM
T1
DOPC + CgA 0.6 µM
T2
10 nm
0
DOPC + CgA 1.2 µM
T1
DOPC + CgA 1.2 µM
T2
10 nm
0
Height above bilayer (nm)
Width (µm)
B
DOPC / PA (36:1)
DOPC / PA (36:1) + CgA 0.6 µM
T1
DOPC / PA (36:1) + CgA 0.6 µM
T2
10 nm
0
DOPC / PA (36:1) + CgA 1.2 µM
T1
DOPC / PA (36:1) + CgA 1.2 µM
b
a
T2
10 nm
0
Height above bilayer (nm)
Width (µm)

Figure 5

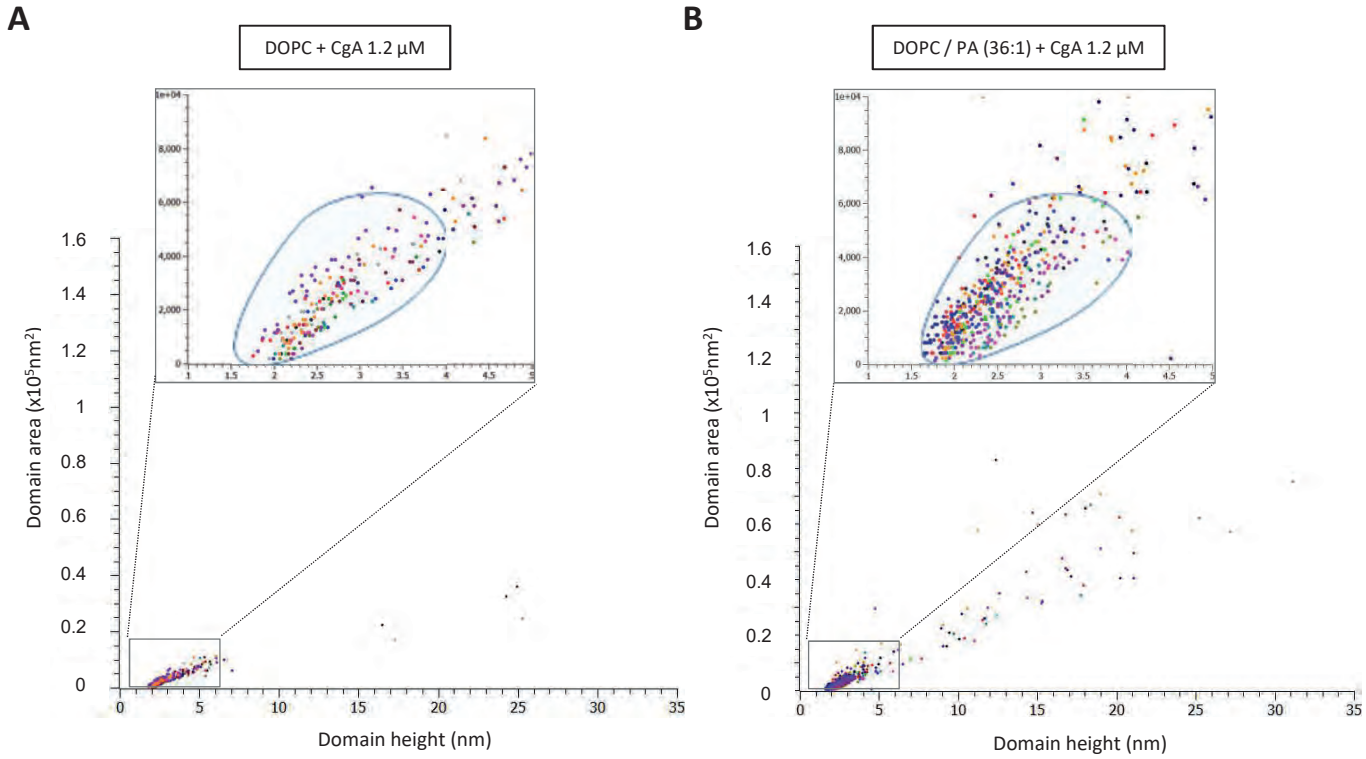
A
DOPC + CgA 1.2 µM
Domain area (x10⁵nm²)
Domain height (nm)
B
DOPC / PA (36:1) + CgA 1.2 µM
Domain area (x10⁵nm²)
Domain height (nm)

Figure 6

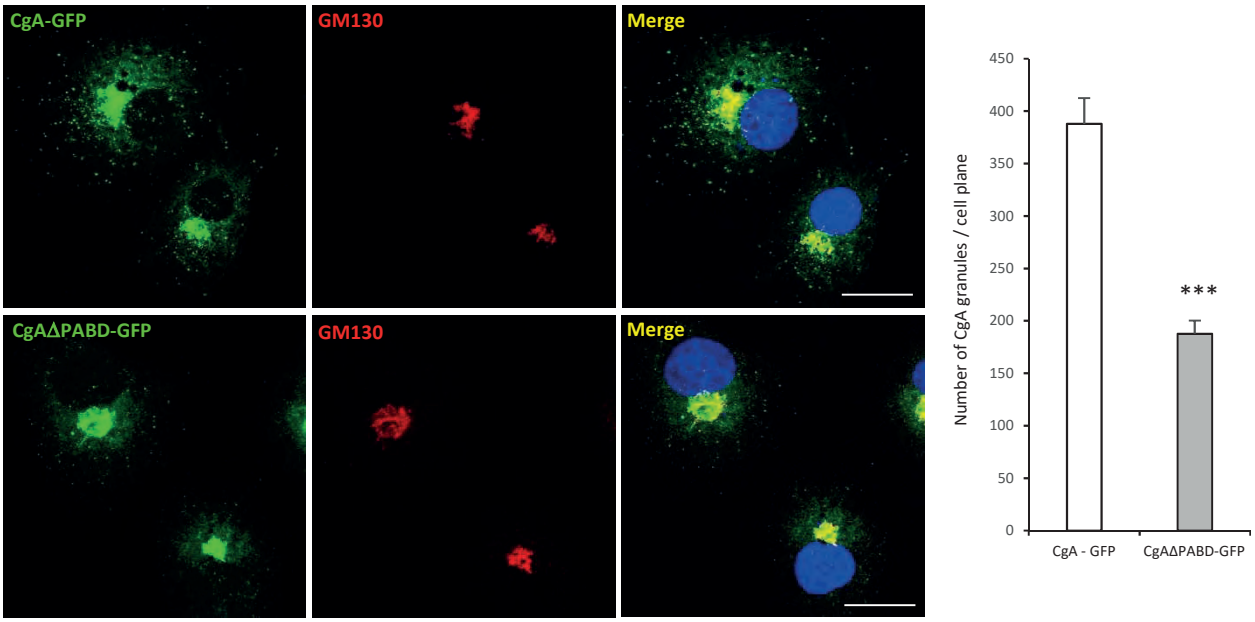
CgA-GFP
GM130
Merge
CgAΔPABD-GFP
GM130
Merge
Number of CgA granules / cell plane
450
400
350
300
250
200
150
100
50
0
***
CgA - GFP
CgAΔPABD-GFP

Figure 7

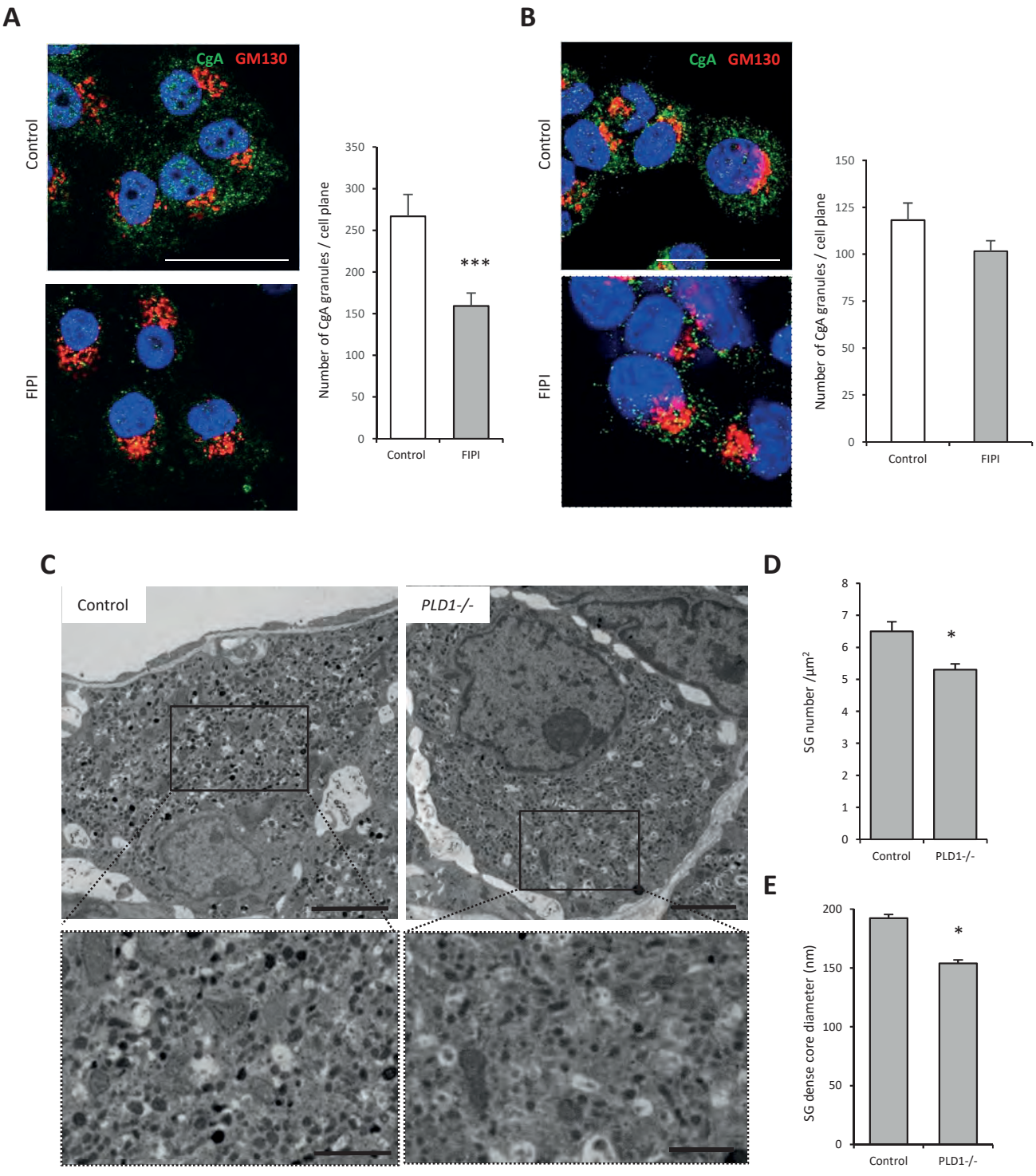
A
CgA GM130
Control
FIPI
Number of CgA granules / cell plane
350
300
250
200
150
100
50
0
***
Control
FIPI
B
CgA GM130
Control
FIPI
Number of CgA granules / cell plane
150
125
100
75
50
25
0
Control
FIPI
C
Control
PLD1-/-
D
SG number /µm²
8
7
6
5
4
3
2
1
0
*
Control
PLD1-/-
E
SG dense core diameter (nm)
200
150
100
50
0
*
Control
PLD1-/-

Figure 8

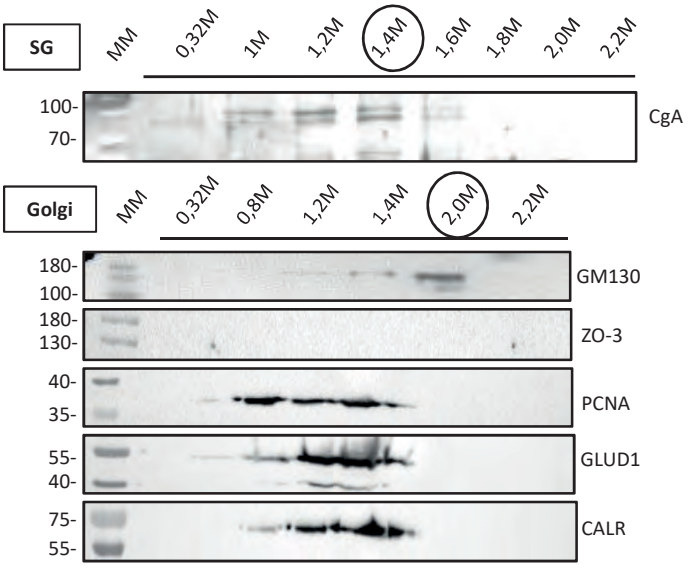
SG
MM
0,32M
1M
1,2M
1,4M
1,6M
1,8M
2,0M
2,2M
100-
70-
CgA
Golgi
MM
0,32M
0,8M
1,2M
1,4M
2,0M
2,2M
180-
100-
GM130
180-
130-
ZO-3
40-
35-
PCNA
55-
40-
GLUD1
75-
55-
CALR

Figure S1

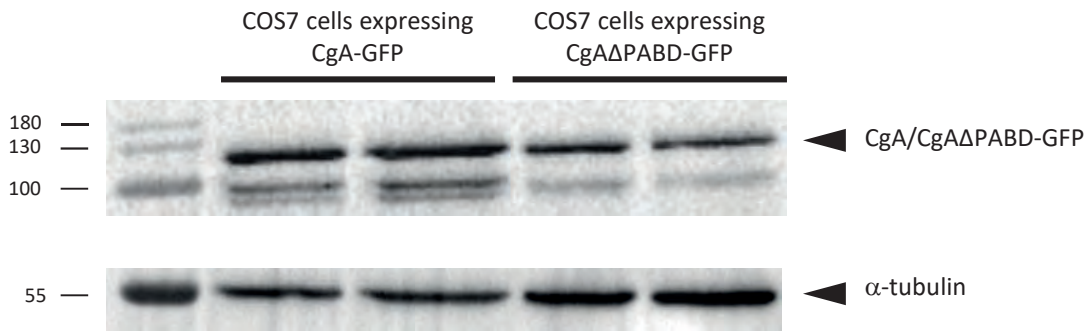
COS7 cells expressing CgA-GFP
COS7 cells expressing CgAΔPABD-GFP
180
130
100
55
CgA/CgAΔPABD-GFP
α-tubulin

Figure S2

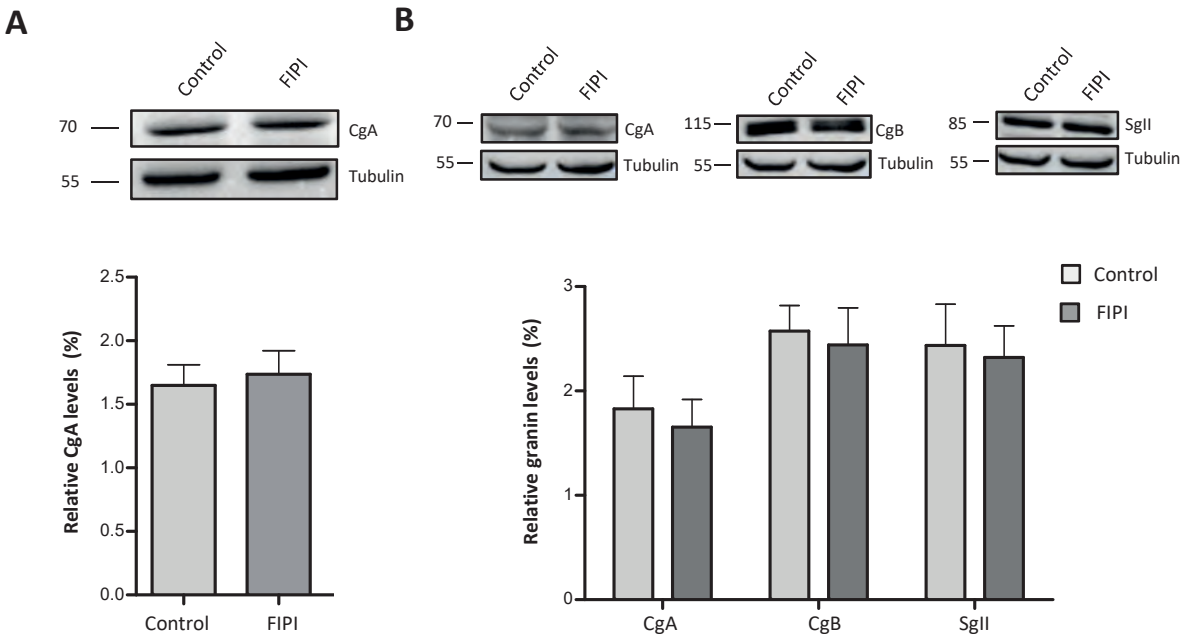
A
Control
FIPI
70
CgA
55
Tubulin
B
Control
FIPI
70
CgA
55
Tubulin
115
CgB
55
Tubulin
85
SgII
55
Tubulin
Relative CgA levels (%)
2.5
2.0
1.5
1.0
0.5
0.0
Control
FIPI
Relative granin levels (%)
3
2
1
0
CgA
CgB
SgII
Control
FIPI

Figure S3

Mono- and polyunsaturated phosphatidic acid regulate distinct steps of regulated exocytosis in neuroendocrine cells

Emeline Tanguy[1], Pierre Costé de Bagneaux[1], Nawal Kassas[1], Mohamed-Raafet Ammar[1], Qili Wang[1], Anne-Marie Haeberlé[1], Juliette Raherindratsara[1], Laetitia Fouillen[2], Pierre-Yves Renard[3], Maité Montero[4], Sylvette Chasserot-Golaz[1], Stéphane Ory[1], Stéphane Gasman[1], Marie-France Bader[1] and Nicolas Vitale[1]

[1]Centre National de la Recherche Scientifique, Université de Strasbourg, Institut des Neurosciences Cellulaires et Intégratives, F-67000 Strasbourg, France

[2]Laboratoire de Biogénèse Membranaire; UMR-5200 Centre National de la Recherche Scientifique, Plateforme Métabolome; Université de Bordeaux; 33883 Villenave D'Ornon, France.

[3]Normandie Univ, UNIROUEN, INSERM, U1239, Laboratoire de Différenciation et Communication Neuronale et Neuroendocrine, Institut de Recherche et d'Innovation Biomédicale de Normandie, 76000, Rouen, France

[4]Normandie Univ, UNIROUEN, COBRA, UMR 6014 & FR 3038, INSA Rouen, Centre National de la Recherche Scientifique, 76000 Rouen, France

Abstract

Specific forms of fatty acids are believed for a long time to have beneficial health effects, although their precise mechanism of action remains elusive. Among them, polyunsaturated fatty acids (PUFA) have been proposed to prevent cognitive decline and accordingly, they have recently been described as essential partners for the core protein machinery involved in neurotransmitter release. PA synthesized by PLD1 has been described to be crucial in regulated exocytosis both in neuroendocrine cells and in neurons. Here, using pharmacological and genetic approaches in neuroendocrine cells, we investigated the role of phosphatidic acid (PA) produced by phospholipase D1 (PLD1) in the docking and fusion of secretory granules. Secretory granule and plasma membranes display a distinct composition in PA as revealed by lipidomic analysis. We identified PA species that significantly increased in the plasma membranes prepared from stimulated cells. Using a specific probe for PA, PA was found to accumulate at granule docking sites in cells stimulated for secretion, suggesting a role for PA in the course of exocytosis. Finally, rescue experiments in cells depleted of PLD1 activity reveal that monounsaturated PA contributes to granule docking while polyunsaturated PA regulates fusion pore stability and expansion. Altogether our work opens a novel comprehension of the cellular functions played by subspecies of the same phospholipid.

Significance

Despite increasing evidence that lipids play key cellular functions and are involved in an increasing number of human diseases, little information is available on their exact mechanism of action. This is especially the case for phosphatidic acid (PA) that has been shown to be involved in many normal and pathological cellular functions. PA lies in the middle of three-enzymatic pathways, which makes it an ideal signaling integrator. We show here that mono- and polyunsaturated forms of PA are involved in different steps of the neurosecretory pathway. Intriguingly the polyunsaturated form of PA appears to control the lifetime of the initial vesicular fusion pore and its expansion before full vesicular fusion, suggesting that this form of PA may contribute to one aspect of the beneficial cognitive function of PUFA by optimizing neurotransmitter release.

Introduction

Phosphatidic acid (PA) is a pleiotropic lipid playing an important structural role as a precursor of glycerophospholipids, but also considered as a key signal integrator in a variety of cellular functions (1-3). Three alternative biosynthetic pathways contribute to the production of signaling forms of PA. The first pathway involves phospholipase D (PLD), which catalyzes the hydrolysis of the distal phosphodiester bond in phosphatidylcholine (PC) to form PA and choline. The second involves diacylglycerol (DAG) kinase (DGK), which phosphorylates DAG, using ATP as a phosphate source, to produce PA. The third implicates acylation of lyso-PA (LPA) to form PA, by LPA-acyltransferases (LPAAT) (4).

PA has been involved in a variety of membrane trafficking events, including endocrine and neuroendocrine exocytosis, synaptic neurotransmission, mast cell degranulation, insulin-stimulated glucose transporter translocation, and phagocytosis (5-10). Yet, little information is still available about its dynamics and role along the secretory pathway. The diversity of the PA biosynthetic routes due to the complexity of the PLD, DGK and LPAAT families, together with the occurrence of many different PA species based on the fatty acyl chain composition opens the possibility for multiple roles in a given cellular function (11). For instance, PA is an important regulator in membrane trafficking, possibly because PA-enriched membranes tend to undergo fusion due to higher curvature, but PA might also serve for recruiting specific proteins or as an intermediate for lipid synthesis. Whether these different roles rely on specific PA subspecies remains unknown and unexplored. Given the awareness of the relevance of PA in a growing number of cellular functions and human diseases (12, 13), understanding the significance of the dynamics and roles of the diverse forms of PA is becoming an important research goal.

In the present manuscript, we use pharmacological and genetic alteration of PLD expression and activity in neuroendocrine chromaffin cells to demonstrate the physiological importance of PA synthesis for stress hormone (catecholamine) secretion (14, 15). At the cellular level, we found that PA governs different steps of the chromaffin granule secretory pathway and we identified specific PA species enriched at the plasma membrane during exocytosis. Rescue experiments in chromaffin cells depleted of PLD activity reveal the specific contribution of monounsaturated PA in the docking of secretory granules and polyunsaturated PA in the lifetime of the fusion pore in the late stages of exocytosis.

Results

Impairing PLD1 expression or activity affects exocytosis in chromaffin cells at distinct stages. We first estimated the role of the two major isoforms of mammalian PLD in catecholamine secretion using *Pld1* or *Pld2* knockout mice chromaffin cells. The physiological significance of PLD for catecholamine secretion was assessed by measuring catecholamine levels in the blood of newborn mice as a dramatic rise in adrenaline and noradrenaline levels after birth have been reported in several mammalian species including humans (16). In wild type mice (control), the blood adrenaline levels were indeed extremely high after birth but rapidly decreased afterwards (Fig. 1*A*). *Pld1* knockout, but not *Pld2*, largely prevented this rise short after birth of adrenaline (Fig. 1*A*) and noradrenaline (SI Appendix, Fig. S1), confirming that PLD1 plays an important modulatory role for catecholamine secretion during stress responses.

To investigate the role of PLD in catecholamine secretion at the cellular level, we used carbon fiber amperometry on cultured mice chromaffin cells to determine the frequency and kinetics of individual exocytotic events (17). Figure 1*B* shows representative amperometric traces recorded from wild type (control), *Pld1*$^{-/-}$, and *Pld2*$^{-/-}$ chromaffin cells stimulated with nicotine. Whereas *Pld2* knockout had no significant effect, *Pld1* knockout decreased the frequency of the amperometric events by nearly 60%, indicating that PLD1 controls the number of secretory granules undergoing exocytosis.

Thereafter, the shape of individual amperometric spikes was analysed. Each amperometric spike is believed to represent a single granule fusion event with the surface area or quantal size being proportional to the amount of catecholamine released per granule, the spike height (amplitude) reflecting the maximal flux of catecholamine, the half-width reflecting the duration of the exocytotic event and the rise time reflecting the kinetics of the fusion pore expansion (Fig. 1*C*). *Pld1* knockout significantly affected some of these spike parameters, whereas *Pld2* knockout had no effect (Fig. 1*C*). While the quantal size of the spikes was not affected (SI Appendix, Fig. S2), the spike half-width and amplitude were modified in cells depleted in PLD1 (Fig. 1*C*). *Pld1*$^{-/-}$ cells also displayed a reduced spike rise-time (SI Appendix, Fig. S2), indicating that the kinetic and duration of the exocytotic event was affected by the absence of PLD1 despite the fact that the total amount of catecholamines released per single granule was not modified.

Amperometric spikes are often preceded by a pre-spike foot (PSF) current believed to reflect the slow catecholamine release through an initial narrow fusion pore before its rapid

expansion, giving rise to the spike. *Pld1*$^{-/-}$ chromaffin cells exhibited significantly longer PSF (Fig. 1*C*), but without significant modification in foot amplitude and charge (SI Appendix, Fig. S2). *Pld1* knockout similarly affected chromaffin cell secretion stimulated by a high potassium depolarizing solution (data not shown), in support for a role for PLD1 activity in the recruitment of secretory granules (number of exocytotic events) and in the late stages of exocytosis (fusion pore stability and/or enlargement for full fusion). To strengthen these findings, we also performed selective silencing of PLD1 using plasmids co-expressing silencing hairpin-RNA together with human growth hormone (GH) as a reporter for the secretory activity of transfected cells (18). Silencing of PLD1 was found to reduce by nearly two-third the secretory activity (GH release) of primary bovine chromaffin cells and rat pheochomocytoma PC12 cells (Fig. 1*D*).

Next, we compared the effect of genetic and pharmacological inhibition of PLD1 in chromaffin cells. Figure 1*E* illustrates the dose-dependent effect of the dual PLD1/PLD2 inhibitor FIPI on chromaffin cell secretion stimulated by nicotine, high-potassium depolarization or direct rise of cytoplasmic calcium by streptolysin-O (SLO)-permeabilization. FIPI induced a similar dose-dependent inhibition of catecholamine secretion triggered by the three secretagogues, indicating that PLD inhibition directly affected the intracellular calcium-dependent exocytotic machinery. PLD1 but not PLD2 is specifically required for efficient catecholamine secretion as illustrated by the use of isoform-specific inhibitors (CAY10593 for PLD1 and CAY10594 for PLD2) (Fig. 1*F*). Note that FIPI and CAY10593, but not CAY10594, modified amperometric spike parameters in a similar manner to that observed in *Pld1*$^{-/-}$ chromaffin cells (SI Appendix, Fig. S3).

In neuroendocrine cells, hormone secretion is also associated with the release of various polypeptides, including chromogranins that constitutes the dense core matrix of the secretory granules (19). It is believed that only free catecholamines diffuse through the narrow initial fusion pore, whereas chromogranins requires fusion pore expansion and full collapse of secretory granules with the plasma membrane to be co-released with catecholamine (20). We examined the effect of the PLD inhibitors on chromogranin A (CgA) release (Fig. 1*G*). Both FIPI and CAY10593 reduced CgA secretion from cells stimulated by high-potassium depolarisation, whereas CAY10594 had no effect. These observations support the idea that PLD1 activity is required for full fusion of secretory granules with the plasma membrane to release both catecholamines and CgA.

Specific PA species are produced at the plasma membrane during chromaffin cell exocytosis. To compare the PA composition of secretory granule and plasmalemmal membranes under resting and stimulated conditions, we used rat PC12 cells to reproducibly obtain sufficient amount of material for comprehensive lipid analysis. PC12 cell secretory granules and plasma membranes were purified by subcellular fractionation on sucrose density gradients. Both granular and plasma membranes contained detectable levels of up to 40 different PA species (SI Appendix, Fig. S4). Secretory granules were particularly enriched in polyunsaturated PA forms (especially PA 40:6 containing the omega-3 docosahexaenoïc (DHA) fatty acid) (SI Appendix, Fig. S4). Surprisingly, the total amount of PA present in the plasma membrane was around 12.5 ± 0.8 nmol/mg of protein, while the amount of PA found in secretory granule membranes was around 36.3 ± 1.1 nmol/mg of protein, and this excess was largely due to the polyunsaturated PAs including PA 40:6. Stimulation with high-potassium decreased the total amount of secretory granules in PC12 cells by ~25%, but the total level of PA per protein as well as the ratio of individual PA species in granule membranes were not significantly modified (data not shown). In contrast, K^+- stimulation increased the level of PA found in the plasma membrane, by more than 6 fold compared to resting cells, to reach 76.5 ± 1.2 nmol/mg of protein. This increase of PA in the plasma membrane upon cell stimulation largely relied on PA containing long chain mono- and diunsaturated fatty acids (PA 36:1, 38:1 and 38:2) although several polyunsaturated PA species including DHA-containing forms were also found in large amounts (Fig. 2*A* and SI Appendix, Fig. S5).

To visualize the precise distribution of PA at the docking site, we prepared native plasma membrane sheets (21) from resting or stimulated cells expressing the PA sensor Spo20p-GFP (18). When expressed in chromaffin cells, Spo20p-GFP is efficiently recruited to the plasma membrane upon nicotine or high-K^+ stimulation, whereas the Spo20p-GFP mutant displaying reduced affinity for PA is not (SI Appendix, Fig. S6), in agreement with our lipidomic observations that secretagogues trigger an increase in plasma membrane PA level. As illustrated in Figure 2*B* by immunogold electron microscopy, native plasma membrane sheets prepared from resting cells displayed only very few gold particles revealing the presence of Spo20p-GFP in most cases found in the close vicinity of docked granules (Fig. 2*B*). Cell stimulation increased the number of docked secretory granules (Fig. 2*B*), but also the amount of gold particles found at the plasma membrane close to docked secretory granules (Fig. 2*B*). Numerical analysis of particle distribution relative to the granule docking site showed that nearly one third of the PA sensor was detected below the secretory granules, while a second

third was concentrated in a 50 nm zone from the edge of the granules and the last third was found equally more distantly distributed (Fig. 2*C*). Note that most of the gold particles that were not found below the granules appeared to be closely associated with filamentous actin structures anchoring secretory granules to the plasma membrane (21) (Fig. *2B,* 2*C*). It is also worth to mention that our analysis most likely minimizes the amount of Spo20p-GFP detected below the secretory granules as gold particles were only seen by transparency in granules that have already at least partially released their content. To assess the specificity of the detection, control experiments were performed with chromaffin cells expressing GFP alone (Fig. 2*B*). Altogether, these findings reveal that various PA species are produced in chromaffin cells undergoing exocytosis both on actin anchors stabilizing docked granules and also below granules potentially close to the fusion pore.

Distinct PA species rescue different steps of regulated exocytosis. Based on pioneer studies from Amatore et al. (2006) (22) showing the effect on secretion of lipid provision, we decided to undertake rescue experiments to identify the function of individual PA species in exocytosis. We first set up experimental conditions to probe that addition of exogenous PA could reach the inner leaflet of the plasma membrane using chromaffin cells expressing Spo20p-GFP. When a mixture of egg-PA or individual forms of PA were added to the medium of cultured chromaffin cells, Spo20p-GFP was rapidly recruited to the plasma membrane whereas a mutated form of the sensor remained in the nucleus (SI Appendix, Fig. S6). Note that the levels of Spo20p-GFP at the plasma membrane after exogenous PA provision was very similar to those observed after nicotine or high-potassium stimulation (SI Appendix, Fig. S6), suggesting that under our experimental conditions, provision of exogenous PA might increase the plasma membrane PA to levels similar to those reached in stimulated cells.

Incubation of chromaffin cells with increasing amounts of a PA mixture did not significantly affect secretion (Fig. 3*A*). However, it largely rescued the inhibition of secretion induced by the PLD1 inhibitor CAY10593 (Fig. 3*A*) and FIPI (Fig. 3*B*). Additionally, mono- (PA 36:1) and di- (PA 36:2) unsaturated forms of PA also rescued the inhibitory effect of FIPI on secretion, whereas polyunsaturated PA 40:6 had little effect (Fig. 3*B*). Note that PA 44:12, a form containing two DHA fatty acid chains and that was not found in our lipidomic analysis, had also no rescue effect on secretion (Fig. 3*B*). The effects of exogenous PA on individual granule exocytosis was further analyzed by amperometry (Fig. 3*C)*. Provision of a mixture of PA in the cell incubation medium rescued the number of exocytotic events (spikes) and the

individual spike parameters in chromaffin cells having PLD1/PLD2 inhibited by FIPI (Fig. 3*C*). Mono- and diunsaturated forms of PA (PA 36:1 and PA 36:2) were able by themselves to rescue the number of exocytotic events, whereas saturated (data not shown) or polyunsaturated forms of PA (PA 40:6, PA 44:12) were ineffective (Fig. 3*C*). However, despite restoring the number of spikes per cell, mono- and diunsaturated forms of PA (PA 36:1 and PA 36:) could not prevent FIPI from increasing spike half width and foot duration, whereas the omega-3 form of PA (PA 40:6) specifically rescued these kinetic parameters (Fig. 3*C*). In other words, the various stages underlying catecholamine secretion i.e. granule docking and subsequent fusion pore formation and/or enlargement seem to implicate distinct PA species.

Monounsaturated PA is involved in secretory granule docking. Figure 4*A* presents the effect of *Pld1* and *Pld2* knockout on the 10 most abundant PA species detected in the adrenal gland from wild type, *Pld1*$^{-/-}$, and *Pld2*$^{-/-}$ mice. In agreement with previous analysis performed on mouse brain (23), *Pld2* knockout did not induce important modifications in the level of the various PA species (Fig. 4*A*). In contrast, *Pld1* knockout had a much more profound effect on many PA species (Fig. 4*A*). Notably the PA containing long mono- and diunsaturated fatty acids (PA 36:1 and PA 36:2), presumably implicated from the amperometry experiments in the number of release events, were reduced by nearly 50% in *Pld1*$^{-/-}$ mice (Fig. 4*A*). We then performed electron microscopy and morphometric analysis on slices from adrenal gland to estimate the number of secretory granules visually considered as docked at the plasma membrane. As illustrated in Figure 4*B*, *Pld1* knockout reduced the number of docked granules by nearly 50%, in good correlation with the reduction in the number of secretory events seen by amperometry in *Pld1*$^{-/-}$ (Fig. 1*B*) or FIPI treated (Fig. 3*C*) chromaffin cells. Finally, we examined native plasma membrane sheets prepared from unstimulated or high-K^+ stimulated chromaffin cells. PLD inhibition by FIPI treatment reduced the number of secretory granules found attached to the inner face of the plasma membrane in high-potassium stimulated cells (Fig. 4 *C*). Incubation of cells with a PA mixture almost completely prevented this inhibitory effect of FIPI on granule docking (Fig. 4*C*). Most interestingly, the monounsaturated PA 36:1 also significantly restored the number of docked granules in stimulated PLD-depleted chromaffin cells whereas the omega-3 form PA 40:6 was without effect. Similar observations were obtained from immunostaining of extracellular dopamine β-hydroxylase (DBH), a granular enzyme which becomes accessible to external antibodies after granule fusion to the plasma membrane. FIPI treatment reduces the number of fusion sites, which can be rescued

by incubation with PA 36:1, confirming that the lack of docked granules is not due to an increase in the fusion process (SI Appendix, Fig. S7*A,C*).

Altogether, our findings support the idea that docking of secretory granules requires mono- (and probably di-) unsatured forms of PA whereas polyunsaturated omega-3 PA 40:6 most likely contributes to the late fusion stages of exocytosis.

Discussion

Important progress in understanding the molecular mechanisms of secretion including hormonal and neurotransmitter release has been made through the discovery of the minimal protein machinery needed for fusion (24), but many regulatory aspects of vesicle release remain elusive (25). For instance there is increasing evidence that lipids play key cellular functions and are involved in many human diseases where secretion is altered but still little information is available on their exact contribution to secretion (26, 27). This is especially the case for phosphatidic acid (PA) that lies in the middle of three-enzymatic pathways, which makes it an ideal signaling integrator (4). Like all phospholipids, PA comes in different flavor based on its fatty acyl chain composition with up to 40 PA species found in mammals, offering to the same lipid family the possibility to support multiple functions. We show here for the first time that PLD1 activity promotes the synthesis of distinct PA species found in the close vicinity of the exocytotic sites and demonstrate that mono- and diunsaturated PA contribute to regulate secretory docking and thereby the number of secretory events, while the omega-3 polyunsaturated PA regulates fusion pore dynamics thereby potentially modulating the type and/or amount of molecules released per vesicle.

The observation that different forms of PA seem to be involved in distinct stages along the secretory pathway suggests that these effects might involve different targets. PA can recruit and/or activate specific proteins to particular membrane locations (8). Among the nearly 50 different proteins that have been shown to date to bind to PA (8), several ones are interesting candidates in regulating exocytosis. For instance, the SNARE protein syntaxin-1 has been shown to bind to several anionic lipids including phophoinositides and PA (28). *In vitro* experiments support the idea that PA directly affects SNARE complex assembly and/or zippering (29), although the function of the different PA forms has not been yet tested. Interestingly, mutations in the polybasic site abolishing the ability of syntaxin 1 to bind PA resulted in a reduction of the number of amperometric spikes and an increase in the PSF duration (28), very similarly to the amperometric response obtained in *Pld1*$^{-/-}$ chromaffin cells

or in cells with inhibited PLD activity. The cytoskeleton that plays a chief role in regulated exocytosis is also a major potential target of PA. Several actin-binding proteins have been shown to bind directly to PA, including small GTPases of the Rho family, which are key conductors of the cytoskeleton dynamics (4, 8). We found that PLD inhibition by FIPI treatment did not affect cortical actin depolymerization required for neuroendocrine secretion (SI Appendix, Fig. S7), but PA might modulate other subtle actin rearrangements that have been observed during exocytosis (21). For instance, annexin-A2, which binds to anionic lipids including PA, was recently shown to promote actin bundling required for efficient granule fusion (30). Of interest, we show here (Fig. 2) that the PA sensor Spo20p-GFP is found closely associated to the large annexin A2-mediated actin bundles that anchor secretory granules to the plasma membrane in stimulated chromaffin cells (21). Finally PA may also act as a lipid second messenger as it is an important regulator of phosphatidylinositol 4,5-bisphosphate (PIP2) synthesis, another crucial lipid in particular for the priming steps of exocytosis (31).

The observation that the omega-3 form of PA specifically regulates the late stages of exocytosis, most likely the fusion pore formation and dynamics, expands our knowledge on the key cellular function of polyunsaturated fatty acids (PUFA) in neurons or neuroendocrine cells. Indeed, it is well admitted that a high PUFA diet has cognitive beneficial effects, but the underlying cellular mechanisms remain elusive (32). A first hint came from the observation that secretory and synaptic vesicles are particularly enriched in PUFA (33). More recently, it was shown by various biophysical and cellular assays that PUFA increase the ability of dynamin and endophilin to deform membranes and support endocytosis, as compared to monounsaturated fatty acids (MUFA) (34). Due to the higher flexibility of their acyl chain, PUFA adapt their conformation to membrane curvature, thereby reducing the energetic cost of various membrane deformations and facilitating fission or fusion events (35). Furthermore the effect of PUFA on membrane packing is actually less disturbing than that of MUFA and phospholipids containing PUFA might soften various molecular stresses in the hydrophobic core of the membrane (36). PA is a cone-shaped lipid that is likely to modulate membrane topology by accumulating at curved membrane areas, resulting in the merging of the inner leaflet of the plasma membrane and the outer leaflet of the vesicular membrane, particularly in the presence of calcium (37). Thus, in the course of exocytosis, synthesis of PA containing a PUFA side chain might well regulate the dynamics of the fusion pore but also the formation of compensatory endocytic vesicles after full collapse of secretory granules in the plasma membrane. Interestingly, we observed on plasma membrane sheets a pool of PA distributed

below the granules after stimulation, that could be involved on fusion or compensatory endocytosis rather than docking step.

One of the more exciting developments in understanding neuronal synaptic function has been the increasing interest in the role of lipids and among them PA appears to play a prominent role (38). We are only at the verge to fully appreciate the functional interconnection in neuronal function between PA, PIP2, and DAG all tightly intertwined in their multiple metabolic pathways (39). For instance, alteration of the tight PA/DAG equilibrium in neurons might be one of the main sources for the neuronal dysfunction in the Fragile-X disease (40), whereas PA synthesis was reported to be altered in the Coffin Lowry Syndrome, an intellectual disability disease (41), as well as in Alzheimer disease (23). The function of individual PA species in these pathologies remain however to be precisely established, but the possibility seen here to restore exocytosis by provision of the adequate PA to cells opens for a better understanding of the role of specific fatty acids in diet to improve human health.

Materials and Methods

Ethics Statement and Mouse Lines. The *Pld1*$^{-/-}$ and *Pld2*$^{-/-}$ mouse lines were described previously (42, 43). They were housed and raised at Chronobiotron UMS 3415. All experiments were carried out in accordance with the European Communities Council Directive of 24th November 1986 (86/609/EEC) and resulting French regulations. Accordingly the CREMEAS local ethical committee approved all experimental protocols. Every effort was made to minimize the number of animals used and their suffering.

Reagents and Plasmids. FIPI, CAY10593, CAY10594 were purchased from Cayman Chemicals. Lipids were obtained from Avanti Polar Lipids. Sequences used for the silencing experiments were described and validated previously (18). Anti-CgA antibodies were described previously (44).

Culture of Chromaffin and PC12 Cells. Bovine and mouse chromaffin cells were isolated as previously described (45, 46). PC12 cells were cultured as described previously (47). See SI Appendix, Supplemental Materials and Methods for details.

Transfection. PC12 cells were transfected at 50-70% confluence with the indicated plasmids using Lipofectamine 2000 according to the manufacturer's protocol (Thermo Scientific) as described previously (47). Bovine chromaffin cells were electroporated (Amaxa Nucleofactor systems, Lonza, Levallois, France) as described previously (17).

Amperometry. Mice or bovine chromaffin cells were washed with Locke's solution and processed for catecholamine release measurements by carbon fiber amperometry after stimulation by 10 seconds pressure ejection of 100 mM K^+ solution or 100 µM nicotine solution from a micropipette positioned at 30 µm from the cell and recorded during 60 seconds as described previously (17, 21). See SI Appendix, Supplemental Materials and Methods for details.

Secretion and catecholamine Elisa assays. Details for catecholamine and GH secretion assays can be found in SI Appendix, Supplemental Materials and Methods. Catecholamine levels from blood samples were measured using the 3-CAT research Elisa kit from LDN (Eurobio, Les Ulis, France) according to the manufacturer's instructions.

Subcellular fractionation and PA lipidomic analysis. 400 x 10^6 PC12 cells grown in 100-mm plates were washed twice with Locke's solution and then incubated for 10 min with Locke's solution (basal release) or stimulated with a 59 mM K^+ solution. Medium was removed and cells immediately scrapped in 1 ml of sucrose 0.32 M (20 mM Tris pH 8.0). Cells were broken before plasma and secretory granule membranes were purified essentially as described previously (47). Adrenal glands were dissected from wild-type, *Pld1*$^{-/-}$ and *Pld2*$^{-/-}$ mouse, weighted, cut into small peace and mixed in 200 µL of sucrose 0.32 M (20 mM Tris pH 8.0). Total lipids were extracted by the method of Bligh & Dyer (48) before lipidomic analysis. Organic phase of lipid extracts were analysed by mass spectrometry essentially as described previously (11, 40). See SI Appendix, Supplemental Materials and Methods for details.

Transmission electron microscopy of chromaffin cells *in situ* and secretory granule docking analysis. Wild-type, *Pld1*$^{-/-}$ and *Pld2*$^{-/-}$ mice were anesthetized with a mixture of ketamine (100 mg/kg) and xylazine (5 mg/kg) and transcardiacally perfused with 0.1 M phosphate buffer, pH 7.3, containing 2% paraformaldehyde and 2.5% glutaraldehyde. The 2-mm-thick slices were cut from the adrenal glands and postfixed in 1% glutaraldehyde in phosphate buffer overnight at 4°C. The slices were then immersed for 1h in OsO4 0.5% in phosphate buffer. 1 mm^3 blocks were cut in the adrenal medulla, dehydrated, and processed classically for embedding in Araldite and ultramicrotomy. Ultrathin sections were counterstained with uranyl acetate and examined with a Hitachi 7500 transmission electron microscope. Secretory granules were counted in 50 chromaffin cells from WT, *Pld1*$^{-/-}$, and *Pld2*$^{-/-}$ mice each with a visible nucleus randomly selected in ultrathin sections from several blocks (1 section/block) from each mouse and were considered to be docked when being less than 50 nm from the plasma membrane.

Plasma membrane sheet preparation, immunolabeling and transmission electron microscopy. Cytoplasmic face-up membrane sheets were prepared and processed as previously described (21). Cells expressing Spo20p-GFP were used <20h after transfection. After blocking in PBS with 1% BSA and 1% acetylated BSA, the immunolabeling was performed and revealed with 15 nm gold particle–conjugated secondary antibodies. Membrane sheets were observed using a Hitachi 7500 transmission electron microscope. The

number of granules and distances were determined manually using Adobe Photoshop. See SI Appendix, Supplemental Materials and Methods for details.

Data Collection and Statistical Analysis. Data were analyzed using SigmaPlot 10 software. In the figure legends, n represents the number of experiments or the number of cells analyzed as specified. Statistical significance has been assessed using *t*-test or the Mann-Withney test when data did not fulfill requirements for parametric tests.

Acknowledgements

We acknowledge the confocal microscopy facilities of Plateforme Imagerie In Vitro, the cytometry facility at INCI, the municipal slaughterhouse of Haguenau (France) for providing the bovine adrenal glands. This work was supported by a grant from the Fondation pour la Recherche Médicale to N.V.

Author contribution statement

Experiments were performed and analysed by E.T., P.C.B., N.K., M.-R.A., Q.W., A.-M.H., J.R., and L.F. Images analysis was performed by E.T., P.C.B and Q.W. with the help of S.C.-G. and S.O. whereas D.H. and L.F. were involved in the lipidomics. P.-Y.R., M.M., S.G., M.-F.B. and N.V. designed experiments and discuss the evolving project. N.V. wrote the manuscript and provided financial grant support. All authors reviewed the manuscript.

Additional Information

The authors declare no competing financial interests.

References

1. Tanguy E, Wang Q, Moine H, Vitale N (2019) Phosphatidic Acid: From Pleiotropic Functions to Neuronal Pathology. *Frontiers in Cellular Neuroscience* 13. doi:10.3389/fncel.2019.00002.

2. Zegarlinska J, Piaścik M, Sikorski AF, Czogalla A (2018) Phosphatidic acid – a simple phospholipid with multiple faces. *Acta Biochimica Polonica* 65(2):163–171.

3. Pokotylo I, Kravets V, Martinec J, Ruelland E (2018) The phosphatidic acid paradox: Too many actions for one molecule class? Lessons from plants. *Progress in Lipid Research* 71:43–53.

4. Ammar M-R, Kassas N, Bader M-F, Vitale N (2014) Phosphatidic acid in neuronal development: A node for membrane and cytoskeleton rearrangements. *Biochimie* 107:51–57.

5. Bader M-F, Vitale N (2009) Phospholipase D in calcium-regulated exocytosis: lessons from chromaffin cells. Biochimica et Biophysica Acta.1791(9):936-41.

6. Ammar MR, Kassas N, Chasserot-Golaz S, Bader M-F, Vitale N (2013) Lipids in Regulated Exocytosis: What are They Doing? *Frontiers in Endocrinology* 4. doi:10.3389/fendo.2013.00125.

7. Barber CN, Huganir RL, Raben DM (2018) Phosphatidic acid-producing enzymes regulating the synaptic vesicle cycle: Role for PLD? *Advances in Biological Regulation* 67:141–147.

8. Tanguy E, Wang Q, Vitale N (2018) Role of Phospholipase D-Derived Phosphatidic Acid in Regulated Exocytosis and Neurological Disease (Springer Berlin Heidelberg, Berlin, Heidelberg). doi:10.1007/164_2018_180.

9. Caumont A-S, Galas M-C, Vitale N, Aunis D, Bader M-F (1998) Regulated exocytosis in chromaffin cells. Translocation of ARF6 stimulates a plasma membrane-associated phospholipase D. *Journal of Biological Chemistry* 273(3):1373-9.

10. Vitale N (2001) Phospholipase D1: a key factor for the exocytotic machinery in neuroendocrine cells. *The EMBO Journal* 20(10):2424–2434.

11. Kassas N, et al. (2017) Comparative Characterization of Phosphatidic Acid Sensors and Their Localization during Frustrated Phagocytosis. *Journal of Biological Chemistry* 292(10):4266–4279.

12. Nelson RK, Frohman MA (2015) Physiological and pathophysiological roles for phospholipase D. *Journal of Lipid Research* 56(12):2229–2237.

13. Di Paolo G, Kim T-W (2011) Linking lipids to Alzheimer's disease: cholesterol and beyond. *Nature Reviews Neuroscience* 12(5):284–296.

14. Niedergang F, Gasman S, Vitale N, Desnos C, Lamaze C (2017) Meeting after meeting: 20 years of discoveries by the members of the Exocytosis-Endocytosis Club: 20 years of discoveries by Exocytosis-Endocytosis Club. *Biology of the Cell* 109(9):339–353.

15. Gasman S, Vitale N (2017) Lipid remodelling in neuroendocrine secretion: Lipid remodelling in neuroendocrine secretion. *Biology of the Cell* 109(11):381–390.

16. Slotkin TA, Seidler FJ (1988) Adrenomedullary catecholamine release in the fetus and newborn: secretory mechanisms and their role in stress and survival. *Journal of developmental physiology* 10(1):1-16.

17. Poëa-Guyon S, et al. (2013) The V-ATPase membrane domain is a sensor of granular pH that controls the exocytotic machinery. *The Journal of Cell Biology* 203(2):283–298.

18. Zeniou-Meyer M, et al. (2007) Phospholipase D1 Production of Phosphatidic Acid at the Plasma Membrane Promotes Exocytosis of Large Dense-core Granules at a Late Stage. *Journal of Biological Chemistry* 282(30):21746–21757.

19. Kim T, Tao-Cheng J-H, Eiden LE, Loh YP (2001) Chromogranin A, an "On/Off" Switch Controlling Dense-Core Secretory Granule Biogenesis. *Cell* 106(4):499–509.

20. Estévez-Herrera J, González-Santana A, Baz-Dávila R, Machado JD, Borges R (2016) The intravesicular cocktail and its role in the regulation of exocytosis. *Journal of Neurochemistry* 137(6):897–903.

21. Gabel M, et al. (2015) Annexin A2–dependent actin bundling promotes secretory granule docking to the plasma membrane and exocytosis. *The Journal of Cell Biology* 210(5):785–800.

22. Amatore C, et al. (2006) Regulation of Exocytosis in Chromaffin Cells by Trans-Insertion of Lysophosphatidylcholine and Arachidonic Acid into the Outer Leaflet of the Cell Membrane. *ChemBioChem* 7(12):1998–2003.

23. Oliveira TG, et al. (2010) Phospholipase D2 Ablation Ameliorates Alzheimer's Disease-Linked Synaptic Dysfunction and Cognitive Deficits. *Journal of Neuroscience* 30(49):16419–16428.

24. Rizo J, Xu J (2015) The Synaptic Vesicle Release Machinery. *Annual Review of Biophysics* 44(1):339–367.

25. Tanguy E, et al. (2016) Lipids implicated in the journey of a secretory granule: from biogenesis to fusion. *Journal of Neurochemistry* 137(6):904–912.

26. Lauwers E, Goodchild R, Verstreken P (2016) Membrane Lipids in Presynaptic Function and Disease. *Neuron* 90(1):11–25.

27. Chasserot-Golaz S, Coorssen JR, Meunier FA, Vitale N (2010) Lipid Dynamics in Exocytosis. *Cellular and Molecular Neurobiology* 30(8):1335–1342.

28. Lam AD, Tryoen-Toth P, Tsai B, Vitale N, Stuenkel EL (2008) SNARE-catalyzed Fusion Events Are Regulated by Syntaxin1A–Lipid Interactions. *Molecular Biology of the Cell* 19(2):485–497.

29. Mima J, Wickner W (2009) Complex Lipid Requirements for SNARE- and SNARE Chaperone-dependent Membrane Fusion. *Journal of Biological Chemistry* 284(40):27114–27122.

30. Gabel M, et al. (2019) Phosphorylation cycling of Annexin A2 Tyr23 is critical for calcium-regulated exocytosis in neuroendocrine cells. *Biochimica et Biophysica Acta (BBA) - Molecular Cell Research* 1866(7):1207–1217.

31. Davletov B, Montecucco C (2010) Lipid function at synapses. *Current Opinion in Neurobiology* 20(5):543–549.

32. Thomas MH, Pelleieux S, Vitale N, Olivier JL (2016) Dietary arachidonic acid as a risk factor for age-associated neurodegenerative diseases: Potential mechanisms. *Biochimie* 130:168–177.

33. Takamori S, et al. (2006) Molecular Anatomy of a Trafficking Organelle. *Cell* 127(4):831–846.

34. Pinot M, et al. (2014) Polyunsaturated phospholipids facilitate membrane deformation and fission by endocytic proteins. *Science* 345(6197):693–697.

35. Manni MM, et al. (2018) Acyl chain asymmetry and polyunsaturation of brain phospholipids facilitate membrane vesiculation without leakage. *eLife* 7. doi:10.7554/eLife.34394.

36. Barelli H, Antonny B (2016) Lipid unsaturation and organelle dynamics. *Current Opinion in Cell Biology* 41:25–32.

37. Jouhet J (2013) Importance of the hexagonal lipid phase in biological membrane organization. *Frontiers in Plant Science* 4. doi:10.3389/fpls.2013.00494.

38. Raben DM, Barber CN (2017) Phosphatidic acid and neurotransmission. *Advances in Biological Regulation* 63:15–21.

39. Di Paolo G, De Camilli P (2006) Phosphoinositides in cell regulation and membrane dynamics. *Nature* 443(7112):651-7.

40. Tabet R, et al. (2016) Fragile X Mental Retardation Protein (FMRP) controls diacylglycerol kinase activity in neurons. *Proceedings of the National Academy of Sciences* 113(26):E3619–E3628.

41. Zeniou-Meyer M, et al. (2008) The Coffin-Lowry syndrome-associated protein RSK2 is implicated in calcium-regulated exocytosis through the regulation of PLD1. *Proceedings of the National Academy of Sciences* 105(24):8434–8439.

42. Ammar MR, et al. (2015) PLD1 participates in BDNF-induced signalling in cortical neurons. *Scientific Reports* 5(1). doi:10.1038/srep14778.

43. Ammar M-R, et al. (2013) The Coffin-Lowry Syndrome-Associated Protein RSK2 Regulates Neurite Outgrowth through Phosphorylation of Phospholipase D1 (PLD1) and Synthesis of Phosphatidic Acid. *Journal of Neuroscience* 33(50):19470–19479.

44. Chasserot-Golaz S (1996) Annexin II in exocytosis: catecholamine secretion requires the translocation of p36 to the subplasmalemmal region in chromaffin cells. *The Journal of Cell Biology* 133(6):1217–1236.

45. Vitale N, Mukai H, Rouot B, Thiersé D, Aunis D, Bader M-F (1993) Exocytosis in chromaffin cells. Possible involvement of the heterotrimeric GTP-binding protein G(o). *Journal of Biological Chemistry* 268(20):14715-23.

46. Houy S, et al. (2015) Oligophrenin-1 Connects Exocytotic Fusion to Compensatory Endocytosis in Neuroendocrine Cells. *Journal of Neuroscience* 35(31):11045–11055.

47. Vitale N, et al. (2002) Calcium-regulated exocytosis of dense-core vesicles requires the activation of ADP-ribosylation factor (ARF)6 by ARF nucleotide binding site opener at the plasma membrane. *The Journal of Cell Biology* 159(1):79–89.

48. Bligh EG, Dyer WJ (1959) A rapid method of total lipid extraction and purification. *Canadian journal of biochemistry and physiology* 37(8):911-7.

Supplemental Method section

Primary Culture of Chromaffin and PC12 Cells. Bovine chromaffin cells were isolated from fresh bovine adrenal glands by retrograde perfusion with collagenase, purified on self-generating Percoll gradients and maintained in culture. To induce exocytosis, intact chromaffin cells were washed twice with Locke's solution (140 mM NaCl, 4.7 mM KCl, 2.5 mM $CaCl_2$, 1.2 mM KH_2PO_4, 1.2 mM $MgSO_4$, 11 mM glucose, 0.56 mM ascorbic acid, 0.01 mM EDTA and 15 mM Hepes, pH 7.5), and then stimulated with Locke's solution containing 20 µM nicotine or depolarising solution, K^+ 59mM. Exocytosis from permeabilized cells was performed as described previously (Vitale et al., 1994). Mouse adrenal glands from 8 to 12-week-old males were dissected and chromaffin cells purified from papain-digested medulla. Cells were seeded on collagen-coated coverslips and maintained at 37°C, 5% CO_2 for 24 to 48 h before experiments. PC12 cells were grown in Dulbecco's modified Eagle's medium supplemented with glucose (4500 mg/liter) and containing 30 mM $NaHCO_3$, 5% fetal bovine serum, 10% horse serum, and 100 units/ml penicillin/streptomycin and 100 µg/ml Kanamycine.

Amperometry. Mice or bovine chromaffin cells were washed with Locke's solution and processed for catecholamine release measurements by amperometry. Carbon-fiber electrode of 5 µm diameter (ALA Scientific) was held at a potential of +650 mV compared with the reference electrode (Ag/AgCl) and approached closely to GFP expressing cells. Catecholamine's secretion was induced by 10 seconds pressure ejection of 100 µM nicotine in Locke's solution or 100 mM K^+ solution from a micropipette positioned at 20 µm from the cell and recorded during 60 seconds. Amperometric recordings were performed with an AMU130 (Radiometer Analytical) amplifier, sampled at 5 kHz, and digitally low-passed filtered at 1 kHz. Analysis of amperometric recordings was done with a macro (obtained from Dr. R. Borges laboratory; http://webpages.ull.es/users/rborges/) written for Igor software (Wavemetrics), allowing automatic spike detection and extraction of spike parameters. The number of amperometric spikes was counted as the total number of spikes with an amplitude >5 pA within 60 seconds. The spike parameters analysis was restricted to spikes with amplitudes of 5 pA. Quantal size (Q) of individual spike is measured by calculating the spike area above the baseline. For foot-signal, the analysis was restricted to spikes with foot amplitudes of 1.5 pA.

Catecholamine, GH, and CgA secretion assays. Chromaffin cells maintained in 96-well plates (Thermo Fisher Scientific, France) were briefly washed twice with Locke and processed as stated in the figure legends. Aliquots of the medium were collected at the end of each experiment and cells were lysed with 1% (v/v) Triton X-100 (Sigma, UK). Both sets of samples were assayed fluorimetrically for catecholamine content. Briefly, 20 µl of sample were transferred to 96-well black-plates (Thermo Fisher Scientific, France), 150 µl of CH_3COONa (1M, pH 6) and 15 µl of $K_3Fe(CN)_6$ (0.25%) were added to each well to oxidize catecholamines to adrenochrome. Next 50 µl of NaOH (5M) containing ascorbic acid (0.3 mg/ml) were added, to convert adrenochrome to adrenolutin. The fluorescence emitted by adrenolutin (λ_{ex}: 430 nm, λ_{em}: 520 nm) is measured with a spectrofluorometer (LB940 Mithras, Berthold). For each experiment a standard curve was determined using known concentration of adrenaline and noradrenaline to demonstrate that the values obtained were in the linear range of detection of the assay. Amounts released were expressed as a percentage of the total amount of catecholamine present in the cells. Plotted data are representative of at least three independent experiments, each carried out in triplicate. PC12 cells (24-well plates, 80% confluent) were transfected with the various siRNA using Lipofectamine 2000 according to the manufacturer's instructions (Invitrogene). 72 h after transfection, cells were washed four times with Locke's solution and then incubated for 10 min in Locke's solution (basal release) or stimulated for 10 min with a depolarizing concentration of K^+. Supernatants were collected and the cells were harvested by scrapping in 10mM phosphate buffered saline (cells were broken by three freeze and thaw cycles). The amounts of GH secreted into the medium or retained within the cells were measured using an ELISA assay (Roche Applied Science). GH secretion is expressed as a percentage of total GH present in the cells before stimulation. Total amount of GH present in cells prior to stimulation was not significantly different in the different condition tested. For CgA secretion assay bovine chromaffin cells were cultured in 24-wells plate for 48-72 hr and then incubated for 60 min with the indicated PLD inhibitors, prior to stimulation in the presence or absence of the PLD inhibitors. 50 µL supernatants were collected and added to 10 µL of 10 x Laemmli buffer. 15 µL aliquots were run on 4-12% Bis-Tris PAGE and CgA detected by Western blot using a rabbit CgA antibody at 1/5000 dilution followed by an anti-rabbit-HRP antibody at 1/50000 dilution and revealed.

Subcellular fractionation. 400 x 10^6 PC12 cells grown in 100-mm plates were washed twice with Locke's solution and then incubated for 10 min with Locke's solution (basal release) or stimulated with an elevated K^+ solution. Medium was removed and cells immediately

scrapped in 1 ml of sucrose 0.32 M (20 mM Tris pH 8.0). Cells were broken and plasma and secretory granule membranes were collected in a Dounce homogenizer and centrifuged at 800 x g for 15 min. The supernatant was further centrifuged at 20 000 x g for 20 min. The resulting supernatant was further centrifuged for 60 min at 100 000 x g to obtain the cytosol (supernatant) and microsomes (pellet enriched in endosomes). The 20 000 x g pellet containing the crude membrane fraction was resuspended in sucrose 0.32 M (20 mM Tris pH 8.0), layered on a cushion sucrose density gradient (sucrose 1-1.6 M, 20 mM Tris pH 8.0) and centrifuged for 90 min at 100 000 x g to separate the plasma membrane from secretory granules. The upper fractions containing SNAP-25 (plasma membrane marker) and the pellet containing dopamine-β-hydroxylase (secretory granule markers) were collected and resuspended before lipid extraction.

PA lipidomic analysis. Total lipids from cell samples were extracted by the method of Bligh & Dyer (35). Extracts were mixed with chloroform:methanol (4:1), vortexed for 10 sec and left under agitation for 1 hr at 4°C. After a 5 min centrifugation at 13,000 rpm, the organic phase (150 µL) was recovered and analyzed by mass spectrometry (UPLC/MS/MS) on an Acquity UPLC system Waters corp. (Milford, USA) coupled to a Quattro Premier XE triple Quadrupole MS system Waters Micromass. The sample (3 µL) was injected into an Acquity UPLC BEH HILIC Amide precolumn (2.1 mm x 5 mm, 1.7 µm particle size), coupled to a Waters Acquity UPLC BEH Amide column (2.1 mm x 100 mm, 1.7 µm particle size) and maintained at 28°C. The column was eluted with a mix of acetonitrile 99.5%, ammonium hydroxide 0.5% (A) and acetonitrile 80%, water 19.5%, ammonium hydroxide 0.5% (B). The flow rate was 0.4 $mL.min^{-1}$ using the following elution protocol: 93% A for 2 min, followed by the gradient, 93% A to 60% A in 1 min, 60% A to 50 % A in 0.5 min, 50% A to 40 % A in 1.5 min. The composition of the mobile phase was then returned to initial conditions as follows: 40% A to 50% A in 2 min, 50% A to 80% A in 2.5 min, 80% A to 93% A in 0.5 min and maintained in 93% A for 2 min. UV spectra were recorded from 200 to 500 nm. The system was run by Mass-Lynx software (version 4.0). The ESI source was used in positive and negative mode with a capillary voltage 3.4 kV; RF lens at 0 V, resolution (LM1, HM1, LM2, HM2) 15, ion energy 1 and 2:0.5. Source and desolvation temperatures were 135 and 400°C. Flows rates of nitrogen for nebulizor and desolvation were 50 and 900 L.h-1. Pressure of the argon collision gas was 3.0 * 10-3 mbar. Full-scan, Selected Ion Recording and Daughter Scan mode were used for qualitative analyses. Quantitative PA analyses were made based on MS/MS Multiple Reaction Monitoring (MRM). Briefly, MRM transitions for

individual PAs were determined using PA standards (Avanti Polar Lipids, Alabaster, AL, USA). The PAs were identified as deprotonated parent ions [M-H^-], cone energy was optimised for each PA and set to 44 V. The predominant daughter fragment ions were then used for quantitative MRM analysis. After optimisation, the collision energy was set to 44V. MRM transitions and specific retention times were used to selectively monitor PA.

Plasma membrane sheet preparation and scanning for electronic microscopy. Carbon-coated Formvar films on nickel electron grids were spilled on unstimulated or nicotine-stimulated chromaffin cells. To prepare membrane sheets, a pressure was applied to the grids for 20 s then grids were lifted so that the fragments of the upper cell surface adhered to the grid. These fragments were fixed in 2% paraformaldehyde for 10 min at 4°C immediately after cell stimulation and sheet preparation, which required less than 30 s. After blocking in PBS with 1% BSA and 1% acetylated BSA, the immune labelling was performed and revealed with 25 nm gold particles-conjugated secondary antibodies. These membrane sheets were fixed in 2.5% glutaraldehyde in PBS, postfixed with 0.5% OsO4, dehydrated in a graded ethanol series, treated with hexamethyldisilazane (Sigma-Aldrich, St. Louis, MO, USA), air-dried and observed using a Hitachi 7500 transmission electron microscope.

Confocal microscopy. For immunocytochemistry, chromaffin cells grown on fibronectin-coated glass coverslips were fixed and labelled. Labelled cells were visualised using a Leica SP5II confocal microscope. The amount of Spo20p-GFP labelling associated with the plasma membrane and nucleus were measured using ROI of equivalent size with ICY software and expressed as the ratio of fluorescence intensity at the plasma membrane and the nucleus.

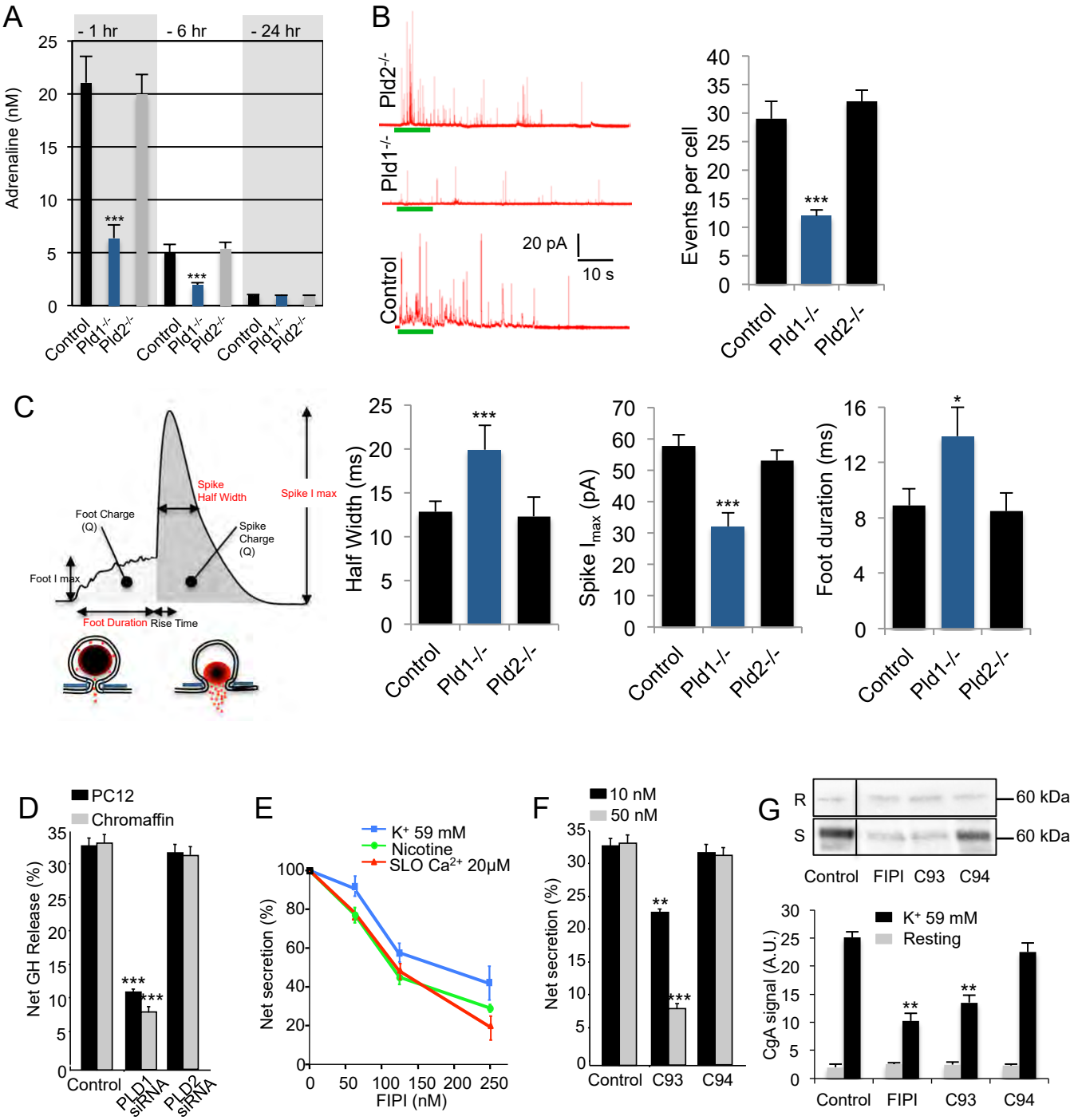

Figure 1: PLD1 activity is required for catecholamine and chromogranin A secretion. A) Adrenaline levels were measured from blood of new-born wild-type (Control), *Pld1*$^{-/-}$ or *Pld2*$^{-/-}$ mice 1 hour (1 hr), 6 hours (6 hr) or 24 hours (24 hr) after birth. Data are expressed as means ± S.D. (n > 9, *** p<0.001). **B-C)** Chromaffin cells in culture were stimulated with a local application of 100 µM of nicotine for 10 s (green bars) and catecholamine secretion was monitored using carbon fiber amperometry. **B)** Typical amperometric recordings obtained from wild-type (Control), *Pld1*$^{-/-}$, or *Pld2*$^{-/-}$ mice chromaffin cells. The histogram illustrates the number of amperometric spikes recorded per cell. **C**) Schema showing the different parameters of the amperometric spike. In red, the three parameters affected in *Pld1*$^{-/-}$ cells namely spike half width, amplitude I max and foot duration. Data are expressed as means ± S.D. (n > 100 cells for each condition from four independent cell cultures).

D) PC12 or chromaffin cells co-expressing GH and the indicated siRNA (control = scrambled PLD1 and PLD2 target sequences) were incubated for 10 min in calcium-free Locke's solution or stimulated for 10 min with 59 mM K^+. The net GH release is obtained by subtracting amounts of basal GH release from GH release after stimulation in each condition. Of note, PLD1 or PLD2 silencing did not significantly modify basal GH release (not shown). **E-G)** Chromaffin cells were treated with the indicated concentration of the PLD inhibitor FIPI, the PLD1 inhibitor CAY10593 (C93) or the PLD2 inhibitor CAY10594 (C94) for 1 hour and stimulated for 10 min with the indicated secretagogues (nicotine 10 µM, 20 µM free Ca^{2+} for streptolysin-O (SLO)-permeabilized cells or K^+ 59 mM) in the presence of PLD inhibitors. Catecholamine release was estimated using the adrenolutine assay and basal release was subtracted to obtain the net catecholamine secretion. CgA release was estimated by Western blot in resting (R) and stimulated condition (S) before quantification. Data are given as the mean values ± S.D. obtained in three experiments performed on different cell cultures (n=3). * p<0.5, ** p<0.01, *** p<0.001.

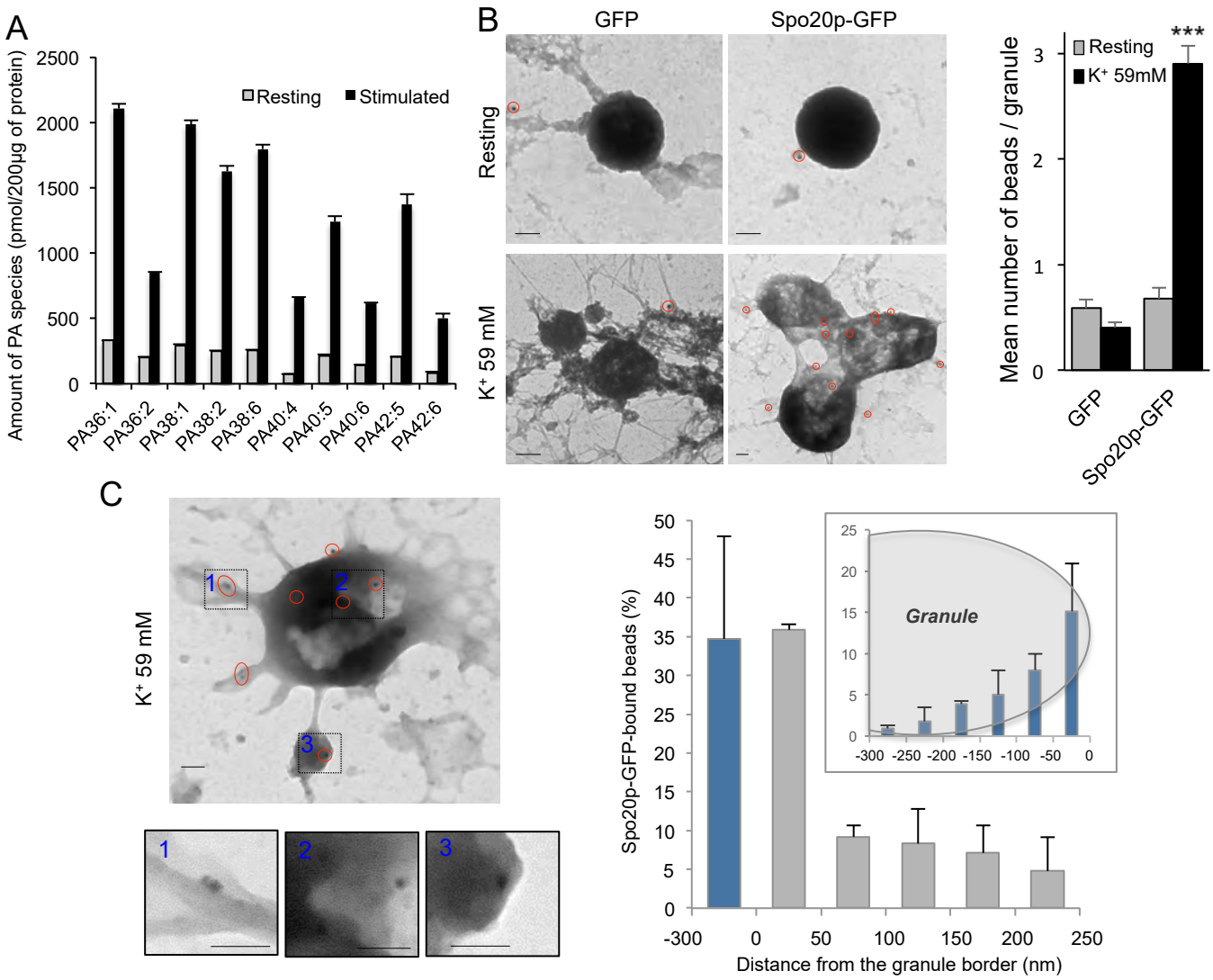

Figure 2: Different PA species are found at granule docking sites during exocytosis. A) Lipidomics identifying the 10 most abundant PA species in the plasma membrane from PC12 cells maintained in resting condition (Resting) or stimulated for 10 min with 59 mM K^+ (Stimulated). Data are means ± S.D. (n=4). **B)** Electron micrograph of anti-GFP immunogold-labeled plasma membrane sheets prepared from chromaffin cells expressing Spo20p-GFP or GFP as a control. Cells were stimulated for 10 min with 59 mM K^+. Bar = 100 nm. Red circles highlight gold particles. **C)** Zooms illustrating the presence of gold particles below secretory granules and close to actin structures. The mean number of gold particles found in the area corresponding to 500 nm from the center of the granule was quantified (error bars indicate ± S.E.M.; n > 65 images from two independent experiments). *** $p<0.001$. Inset shows distribution of particles under the granule.

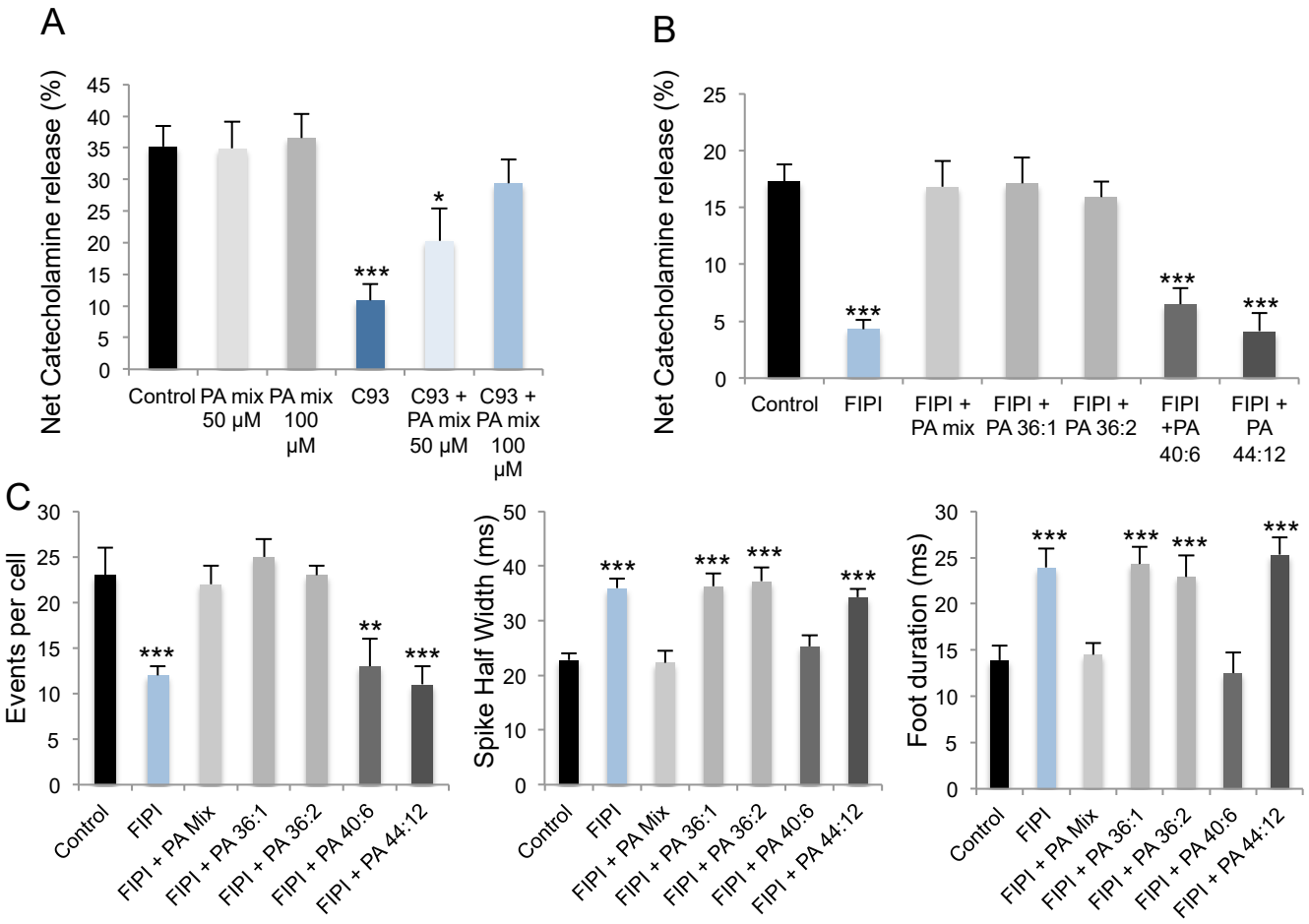

Figure 3: Different PA species rescue distinct stages of exocytosis. A-B) Chromaffin cells were treated with the PLD1 inhibitors CAY10593 50 nM (C93), FIPI 750 nM or vehicle (control) for 1h and incubated with the indicated concentration of a PA mixture or 10 µM of the indicated PA species for 15 min prior to stimulation with 10 µM nicotine. Catecholamine release was estimated using the adrenolutine assay and basal release was subtracted to obtain the net catecholamine secretion. Data are given as the mean values ± S.D. obtained in three experiments performed on different cell cultures (n=3). * p<0.05, *** p<0.001. **C**) Chromaffin cells were treated with FIPI 750 nM or vehicle (control) for 1h and incubated with the indicated PA for 15 min before stimulation with a local application of Locke's solution containing 100 mM K^+ for 10 s. Catecholamine secretion was monitored by carbon fiber amperometry. Data are expressed as means ± S.D. (n > 75 cells for each condition from three independent cell cultures). In cells treated with FIPI, PA mixture rescues the number of exocytotic events and the individual spike parameters (spike half-width and foot duration). Monounsaturated PA rescues only the number of events but not the spike parameters. At the opposite, polyunsaturated PA rescues spike parameters but not the number of events. *** p<0.001.

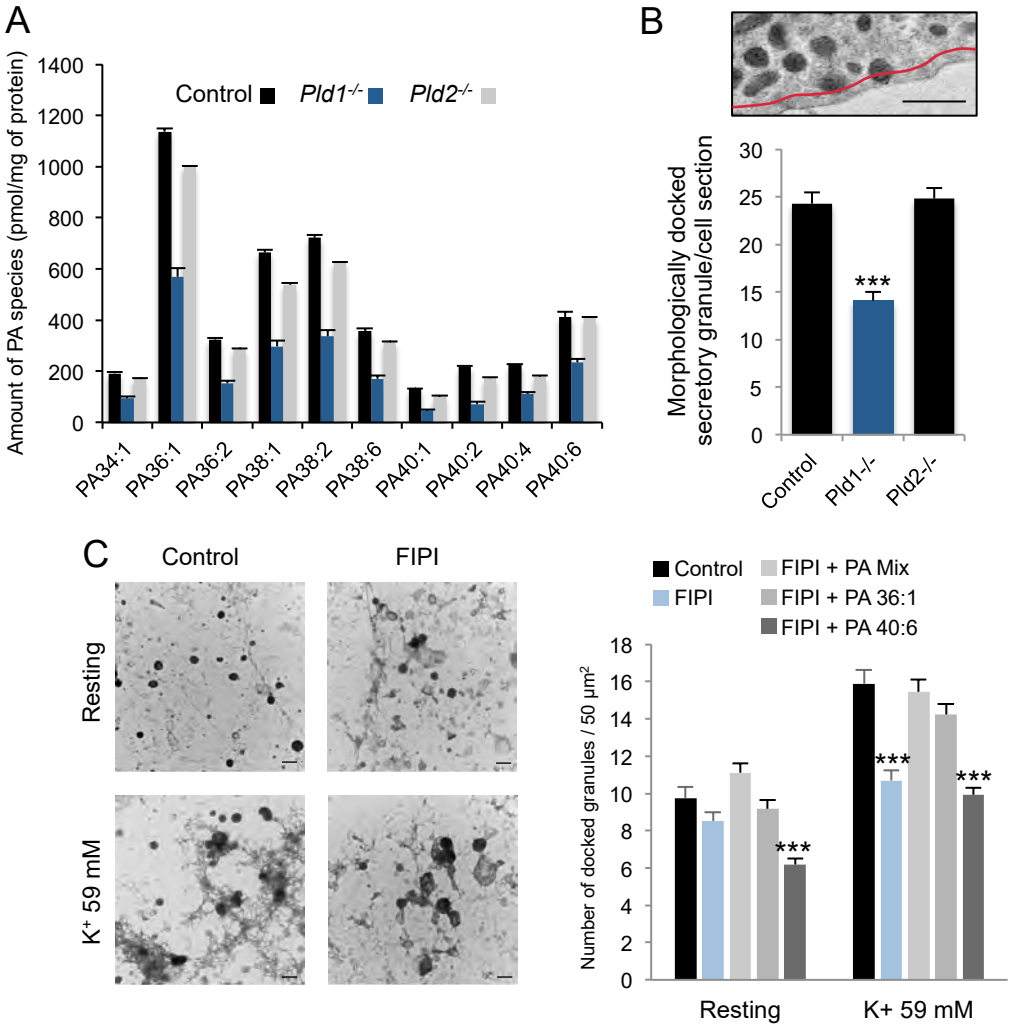

Figure 4: PA modulates secretory granule docking. A) Lipidomic identification of the 10 most abundant PA species in adrenal glands collected from wild-type (WT), *Pld1*$^{-/-}$, or *Pld2*$^{-/-}$ mice. Data are means ± S.D. (n=4). **B)** Representative section of a transmission electron micrograph of an adrenal medulla slice from 3 months old wild-type mice. Number of morphologically docked secretory granules per cell section present in the 50 nm below the plasma membrane (red line) were counted in the adrenal medulla of wild type (Control), *Pld1*$^{-/-}$, *Pld2*$^{-/-}$ mice. n = 6 mice per genotype from which 50 slices were analyzed per mice. *** p<0.001. Bar = 1 µm **C**) Electron micrograph plasma membrane sheets prepared from resting or K^+ 59 mM stimulated (5 min) chromaffin cells. Cells were pre-incubated in the presence or not of FIPI 750 nM with or without the application of the indicated PA for 15 min before stimulation. The number of granules morphologically docked on plasma membrane sheets was quantified manually on random fields. Data are presented as means ± S.E.M. n > 60 images from three different cell cultures for each condition. Bar = 500 nm. *** p<0.001 (Mann-Whitney test)

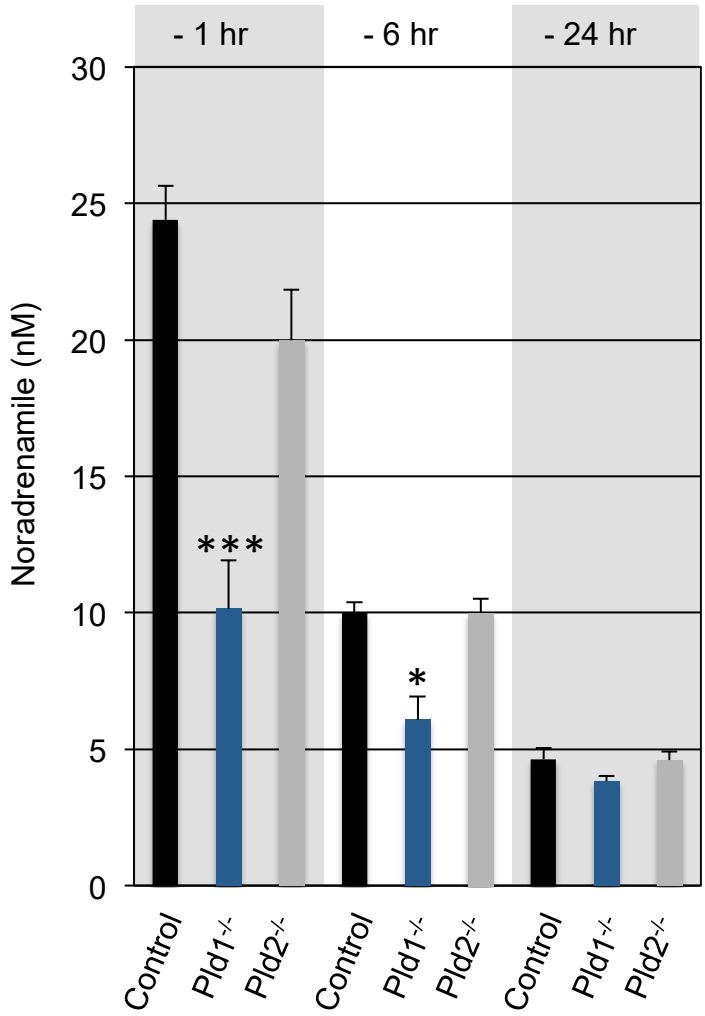

Supplemental Figure1: Noradrenaline levels were measured from blood of new-born wild-type (Control), *Pld1*$^{-/-}$, or *Pld2*$^{-/-}$ mice 1 hour (-1 hr), 6 hours (-6 hr), or 24 hours (-24 hr) after birth. Data are expressed as means ± S.D. (n > 9, *p<0.05, *** p<0.001).

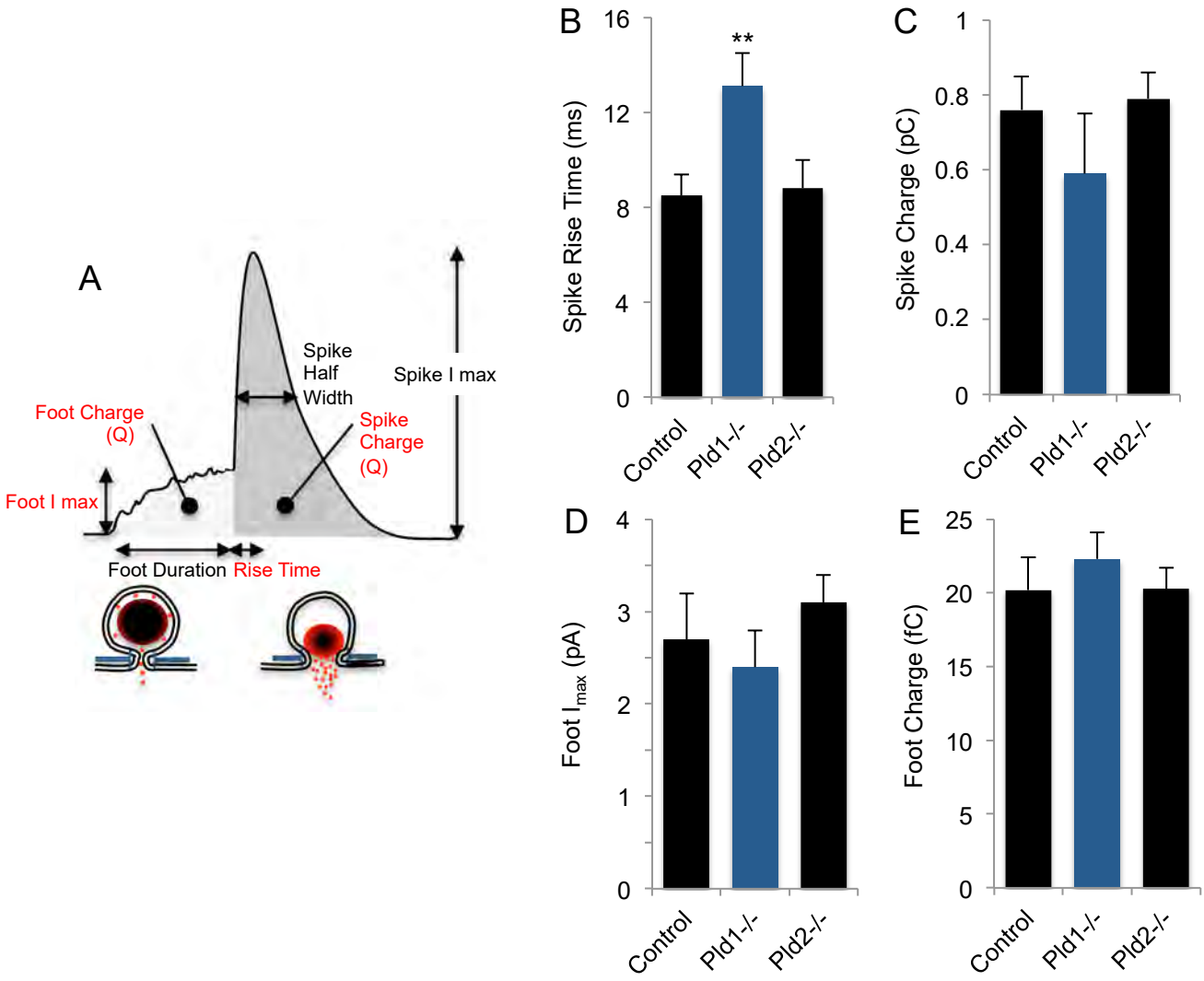

Supplemental Figure 2: Effect of *Pld1* knockout on amperometric spike parameters. **A)** Schema showing the different spike parameters of the amperometric response measured from wild-type (control), *Pld1*$^{-/-}$, and *Pld2*$^{-/-}$ mice chromaffin cells. In red are four parameters measured including spike rise time (**B)** spike charge **(C)**, foot amplitude (**D**), and foot charge **(E)**. Data are expressed as mean ± S.D. (n > 100 cells for each condition from four independent cell cultures). ** p<0.01.

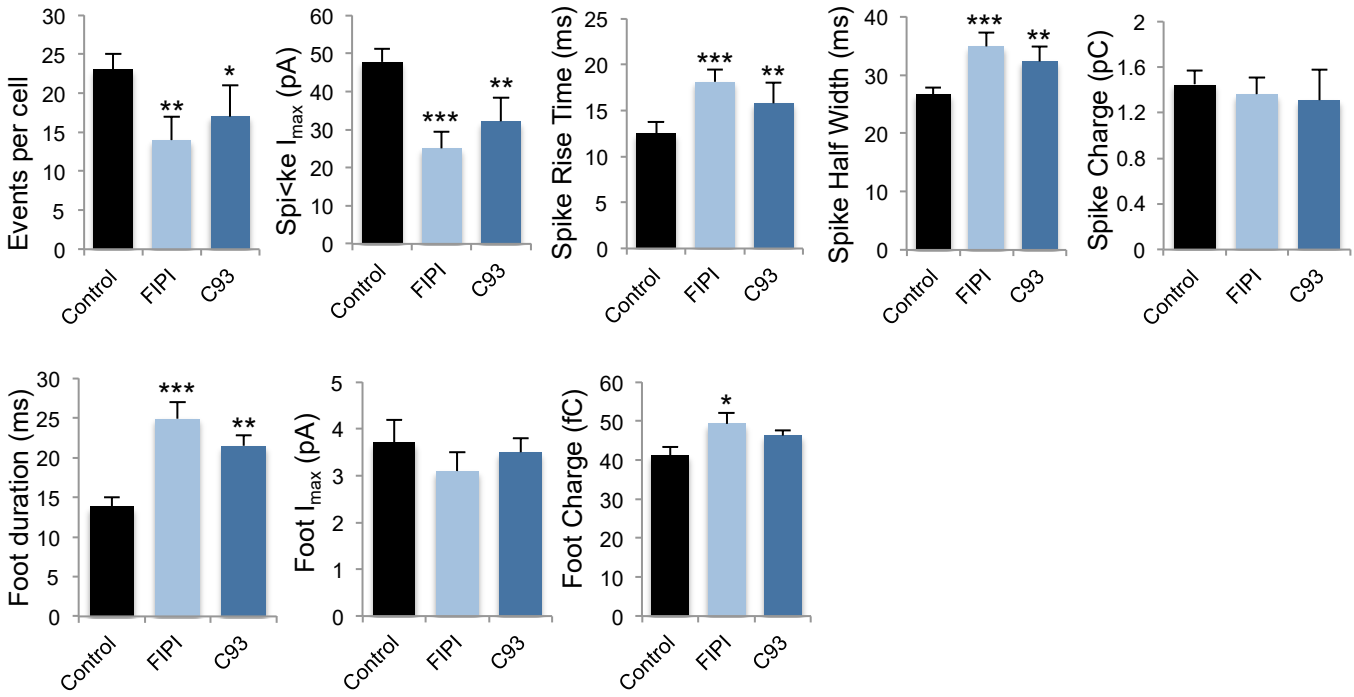

Supplemental Figure 3: Effect of PLD inhibition on amperometric spike parameters from bovine chromaffin cells. Bovine chromaffin cells were incubated 1 hr with or without FIPI 750 nM and CAY93 50 nM and stimulated with a local application of 100 µM of nicotine for 10 s with or without the PLD inhibitors. Catecholamine secretion was monitored using carbon fibre amperometry. The number of events and the indicated spike parameters are expressed as mean ± S.D. (n > 80 cells for each condition from four independent cell cultures). * $p<0.05$, ** $p<0.01$, ***$p<0.001$.

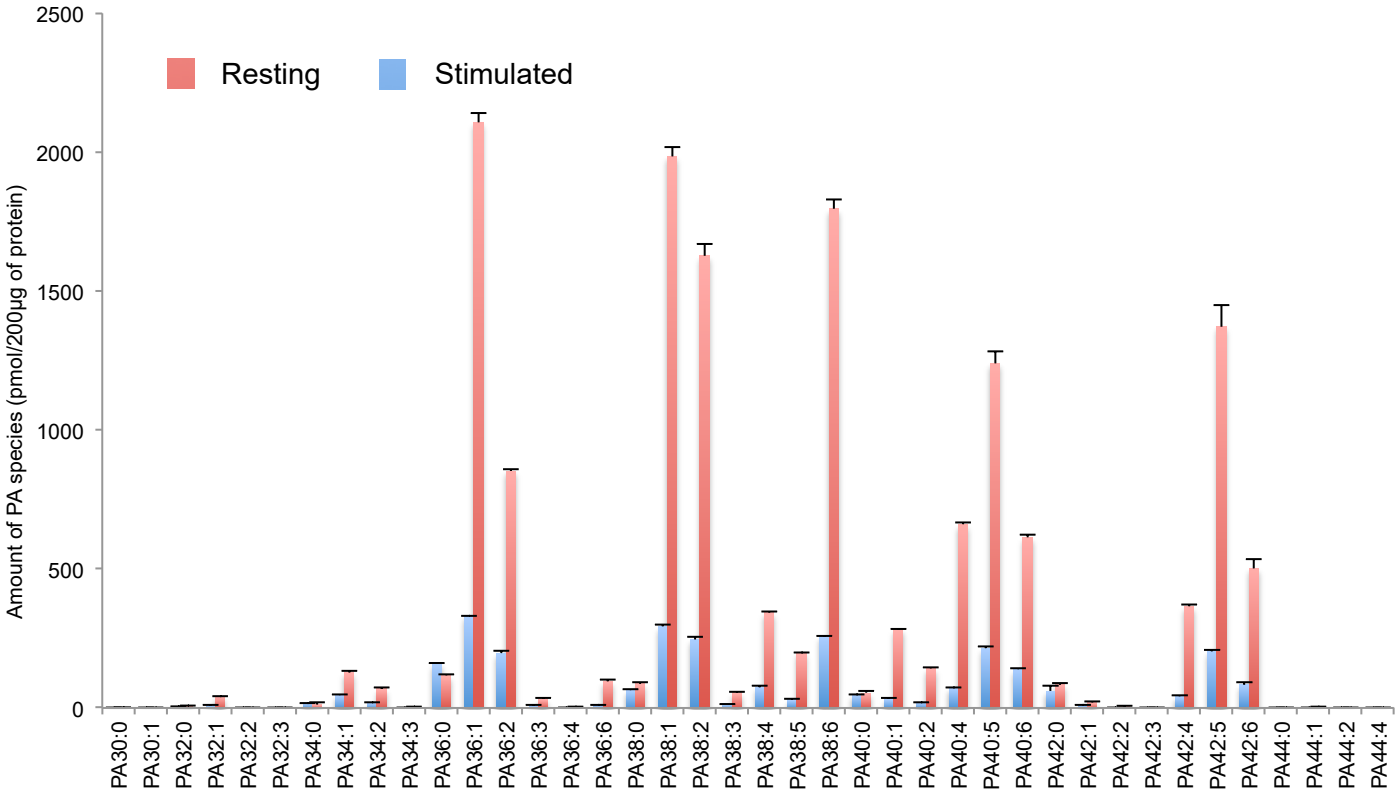

Supplemental Figure 5: Total membranes from 400 x 10^6 resting or 59 mM K^+ stimulated PC12 cells were subjected to ultracentrifugation on sucrose gradient to purify plasma membranes. PA species levels were measured by lipidomics from aliquots containing 200 µg of proteins each. PA amounts are expressed as pmol of PA per 200 µg of proteins. Data are expressed as means ± S.D. (n=4 independent cell cultures).

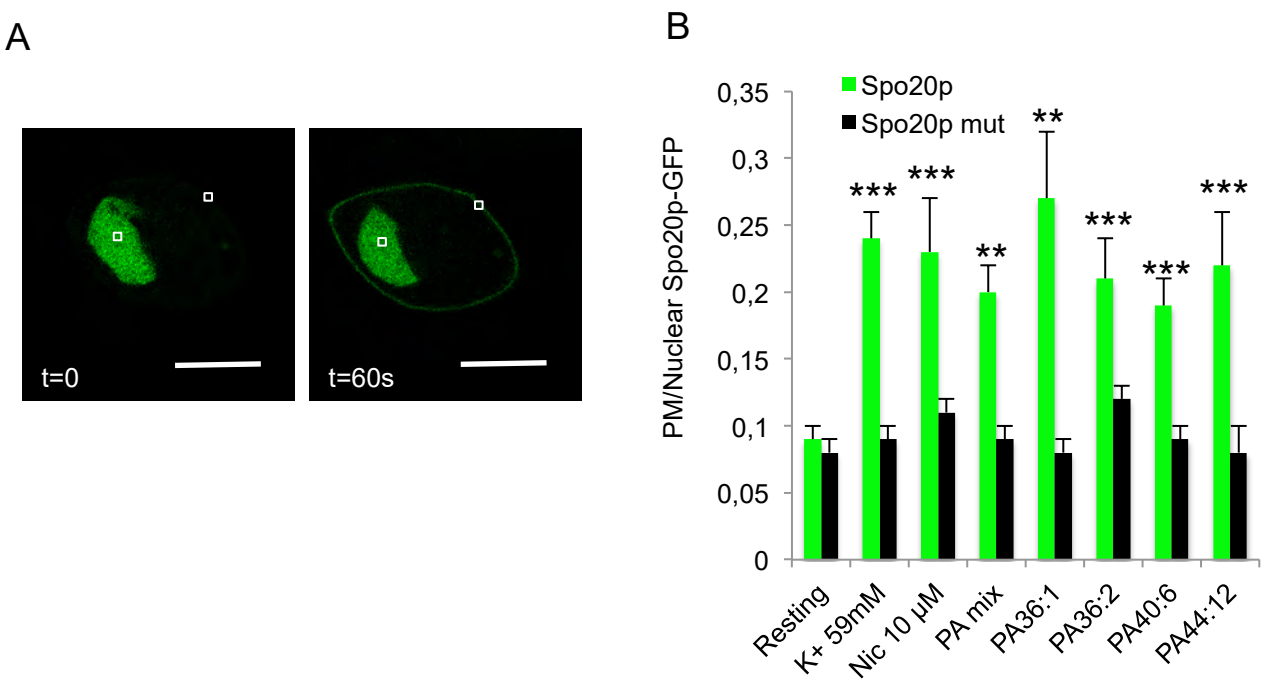

Supplemental Figure 6: **Extracellular PA reaches the inner leaflet of the plasma membrane. A)** Chromaffin cells expressing Spo20p-GFP were incubated with 100 µM of a PA mix and images were taken at the indicated time. **B)** Quantification of the signal ratio of Spo20p-GFP or Spo20p-GFP mutated at the plasma membrane over the nucleus in resting cells, or after stimulation with K^+ 59mM or 10 µM nicotine for 10 minutes, or after a 5 min incubation with the indicated PA. Data are presented as means ± S.D. with n > 30 cells for each condition from two independent cell cultures. ** p<0.01, ***p<0.001.

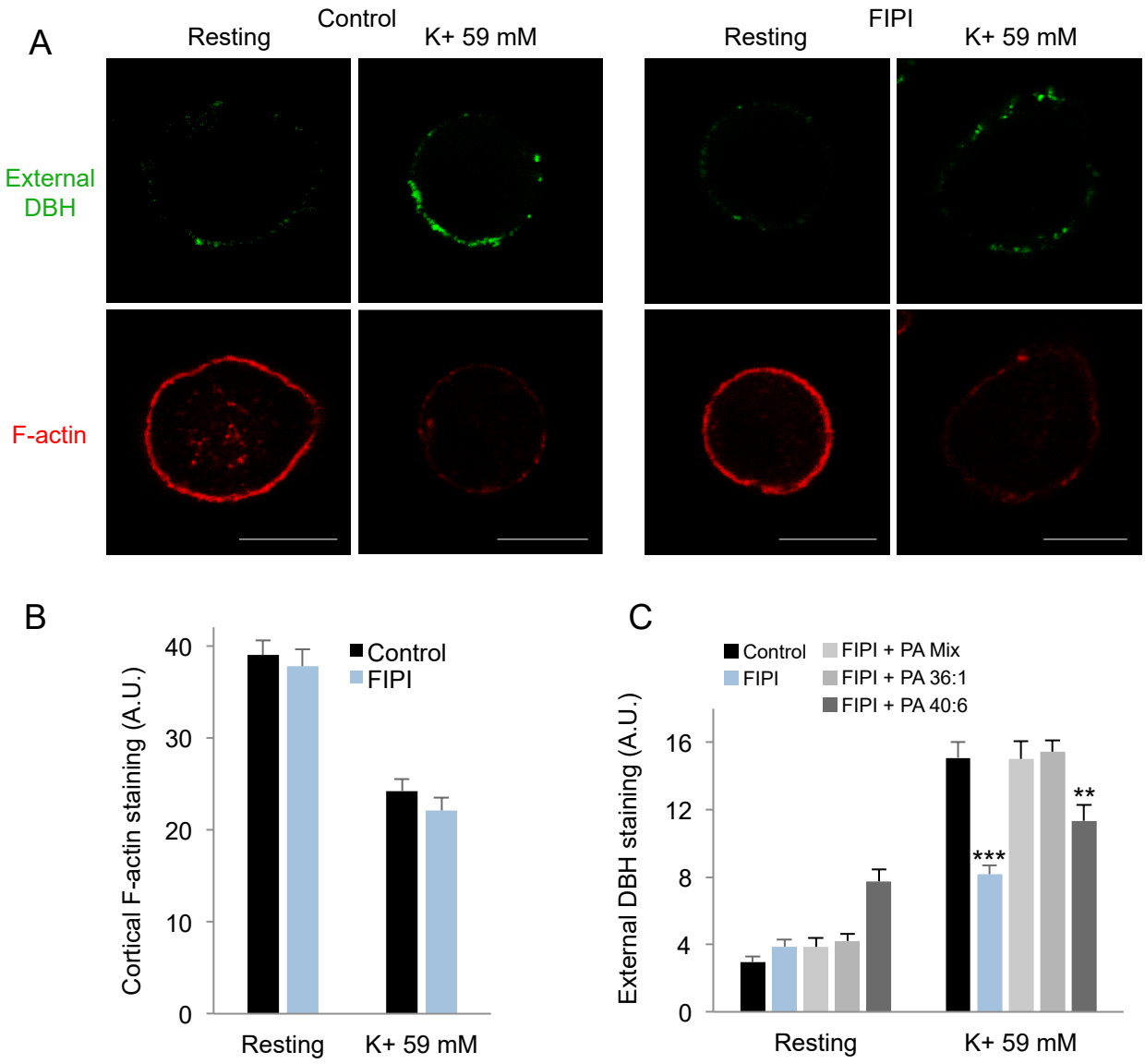

Supplemental Figure 7: **Inhibition of PLD reduces the number of exocytosis sites without preventing cortical actin depolymerization. A)** Chromaffin cells incubated or not with FIPI 750 nM for 1 hr were maintained at rest or stimulated with K^+ 59 mM containing or not FIPI and anti-dopamine β-hydroxylase (DBH) for 5 min. Cortical F-actin was stained by phalloidin-TRITC. **B)** Quantification of cortical F-actin staining. Data are presented as means ± S.E.M. with n > 30 cells for each condition from three independent cell cultures). **C)** Chromaffin cells were treated asin B, but also incubated with the indicated PA for 15 min prior to cell stimulation. Quantification of extracellular staining was performed on n > 30 cells for each condition and given as the mean values ± S.E.M. obtained in three experiments performed on different cell cultures (n=3). ** $p<0.01$, *** $p<0.001$.

Chapter

Prion Proteins and Neuronal Death in the Cerebellum

Audrey Ragagnin, Qili Wang, Aurélie Guillemain, Siaka Dole, Anne-Sophie Wilding, Valérie Demais, Cathy Royer, Anne-Marie Haeberlé, Nicolas Vitale, Stéphane Gasman, Nancy Grant and Yannick Bailly

Abstract

The cellular prion protein, a major player in the neuropathology of prion diseases, is believed to control both death and survival pathways in central neurons. However, the cellular and molecular mechanisms underlying these functions remain to be deciphered. This chapter presents cytopathological studies of the neurotoxic effects of infectious prions and cellular prion protein-deficiency on cerebellar neurons in wild-type and transgenic mice. The immunochemical and electron microscopy data collected in situ and ex vivo in cultured organotypic cerebellar slices indicate that an interplay between apoptotic and autophagic pathways is involved in neuronal death induced either by the infectious prions or by prion protein-deficiency.

Keywords: prion protein, Doppel, apoptosis, autophagy, cerebellum, mouse

1. Introduction

1.1 Prion diseases

Transmissible spongiform encephalopathies (TSEs) or "prion diseases" are fatal neurodegenerative disorders in humans (Creutzfeldt-Jakob disease (CJD), Gerstmann-Straüssler-Scheinker syndrome (GSS), variant CJD (vCJD), fatal familial insomnia (FFI) and kuru) and in animals (bovine spongiform encephalopathy (BSE), transmissible mink encephalopathy (TME), chronic wasting disease of cervids (CWD), camel prion disease (CPD), and scrapie of sheep and goats) [1–4]. Prevailing over a viral etiology, the conformational corruption of host-encoded cellular prion protein (PrP^{c}) by a pathogenic isoform (PrP^{TSE}) is now widely accepted as underlying prion transmission and pathogenesis in TSEs [5–7].

1.2 PrP^{c} functions

Prnp-knockout mice were generated in order to investigate the physiological functions of PrP^{c}. In either mixed C57BL/6 j x129/Sv(ev) (Zurich I, ZrchI, $Prnp^{ZH1/ZH1}$, [8]) or pure 129/Ola (Npu, Edinburgh, Edbg, [9]) or C57BL/6J (Zurich III, ZrchIII, $Prnp^{ZH3/ZH3}$, [10]) genetic backgrounds, the first *Prnp* null

mouse strains produced were viable with no clear abnormality except for their resistance to prion infection [11] and absence of obvious neurodegeneration. Similar absence of neurodegeneration or histopathology resulted from depletion of neuronal PrP^c in adult conditional *Prnp*-knockout NFH-Cre/tg37 mice [12]. Thus, a physiological function of PrP^c that is essential for life seemed to be ruled out unless it is highly redundant or is compensated. Nevertheless, looking at different neuronal and other cell functions in PrP^c-ablated mice has revealed a number of differences that can be attributed to the physiological functions of PrP^c (see [13] for review).

PrP^c has been implicated in neurotransmission, olfaction, proliferation and differentiation of neural precursor cells, neuritic growth, neuronal homeostasis, cell signaling, cell adhesion, myelin maintenance, copper and zinc transport, as well as neuroprotection against toxic insults, such as oxidative stress and excitotoxicity (see [14, 15] for reviews). Increasing evidence links prion protein misfolding and accumulation to neurodegeneration in prion diseases. Accordingly, several nonexclusive mechanisms of prion-mediated neurotoxicity are currently under investigation (see [16] for review). PrP^c has been localized in three major sites: enriched in lipid rafts, anchored in the outer plasma membrane leaflet by its GPI tail [17], and intracellularly in the Golgi apparatus early and late endosomes [18, 19]. Since lipid rafts are pivotal microdomains for signal transduction, PrP^c is likely triggering intracellular signaling pathways [20, 21]. The first evidence that PrP^c might mediate extracellular signals was the caveolin-1-dependent coupling of PrP^c to the tyrosine-protein kinase Fyn [21]. From this pioneering work, accumulating data suggested that PrP^c functions as a "dynamic cell surface platform for the assembly of signaling molecules," partnering with other membrane proteins to transduce cellular signaling [22].

1.3 Synaptic PrP^c

Whereas, PrP^c is highly expressed in both neurons and glial cells of the CNS [19, 23, 24], it is preferentially localized in the pre- and postsynaptic terminals of neurons [19, 24, 25]. Immunocytochemical studies of primate and rodent brains [25, 26] including an EGFP-tagged PrP^c in transgenic mice, showed that PrP^c is enriched along axons and presynaptic terminals [27–29], and undergoes anterograde and retrograde transport [30, 31]. Such a synaptic targeting of PrP^c suggests that it could be involved in preserving synaptic structure and function. Indeed, synaptic dysfunction and loss are early prominent events in prion diseases [32, 33]. However, a functional role of PrP^c at synapses is not consistently supported by functional data and still remains contentious.

Insights into possible mechanisms by which PrP^c modulates synaptic mechanisms and neuronal excitability at a molecular level have been provided by the documented interactions of PrP^c with several ion channels including the voltage-gated calcium channels (VGCCs) [34], the N-methyl-D-aspartate glutamate receptors (NMDARs) [35] and the voltage-gated potassium channels Kv4.2 [36]. PrP^c has been shown to regulate NMDARs due to its affinity for copper that leads to inhibition of glutamate receptors and excitotoxicity [37, 38]. While interaction of PrP^c with these channels may account for some of its functions, a toxic response can also be activated when PrP^c misfolds. A structural change in cell surface PrP^c has been proposed to simultaneously disrupt NMDAR function and plasma membrane permeability, leading to dysregulation of ion homeostasis and neuronal death [39, 40]. PrP^c can also interact with kainate receptor subunits GluR6/7 [41], α-amino-3-hydroxy-5-methyl-4-isoxazolepropionic acid (AMPA) receptors subunits GluA1 and GluA2 [42, 43], and metabotropic glutamate receptors of group 1 mGluR1 and mGluR5 [44, 45]. PrP^c can interact with the β-amyloid peptide (Aβ) and the later [45, 46] is believed to underlie the Aβ

oligomer-induced disruption of LTP in Alzheimer's disease [47]. Thus, PrP^c seems to behave as a cell surface receptor for synaptic oligomers of the Aβ peptide and, of other β-sheet-rich neurotoxic proteins [40].

1.4 PrP^{TSE}-related neurotoxicity in prion diseases

The histopathological signature of TSEs notably relies on the aggregation of PrP^{TSE}, vacuolation of the brain tissue, astrogliosis, and synaptic and neuronal loss. How neurons, the major targets of prions, die, remains a central question in prion diseases. The absence of neurodegenerative phenotypes after depletion of PrP^c suggests that neurotoxicity is not due to a loss of PrP^c function but rather results from a gain of toxicity upon its conversion to PrP^{TSE}, which then acts on the central nervous system (CNS) [48]. Although PrP^c is required for propagation of infectious prions and PrP^{TSE}-mediated toxicity [49], the mechanisms by which prions are lethal for neurons remain mostly unknown. Nevertheless, the endogenous PrP^c conversion has been shown to cause neuronal dysfunction and death, rather than PrP^{TSE} itself which does not seem to be directly neurotoxic. A precise understanding of the factors leading to neurotoxicity in prion infections is crucial to developing targeted therapies and investigating the role of PrP^c in neurons should provide insight.

The conformational conversion of PrP^c begins on the neuronal surface, where PrP^c interacts with exogenous PrP^{TSE}, and then proceeds within endogenous compartments suggesting that neurotoxicity may be triggered by PrP^c misfolding both at the cell surface and inside the cell. In both acquired and genetic prion diseases, intracellular PrP^c misfolding would ultimately alter synaptic proteostasis, either through an indirect unfolded protein response (UPR)-mediated mechanism [50], likely arising either from an impairment of the neuronal ubiquitin-proteasome system (UPS) [51], or a direct interference with secretory trafficking of PrP^c-interacting cargoes [52]. Common features associated with prion infections include Ca^{2+} dysregulation, release of reactive oxygen species, and induction of endoplasmic-reticulum (ER) stress, which has been recently suggested as an important player in pathogenesis [53]. Prion-infected mice show brisk activation of the UPR and specifically of the PERK pathway, resulting in eIF2α phosphorylation and suppression of translational initiation. PERK inhibition protects mice from prion neurotoxicity, confirming an important pathogenic role of ER stress [50]. Since UPR activation and/or increased eIF2α-P levels as well as UPS impairment are commonly seen in prion disorders and in Alzheimer's and Parkinson's diseases, translational control, and UPS stimulation strategies may offer a common therapeutic opportunity to prevent synaptic failure and neuronal loss in protein misfolding diseases [51, 54].

1.5 Loss of PrP^c anti-inflammatory protective function in prion disease

A protective role of PrP^c against a noxious insult mediated by the pro-inflammatory cytokine tumor necrosis factor-α (TNFα) has recently been demonstrated [55]. The α-secretase activity mediated by the TNFα-converting enzyme (TACE) was impaired at the surface of Fukuoka and 22L scrapie prion-infected neurons. Furthermore, the activity of 3-phosphoinositide-dependent kinase-1 (PDK1) which inactivates phosphorylation and caveolin-1-mediated internalization of TACE is increased in scrapie-infected neurons. PDK1 was shown to be controlled by RhoA-associated coiled-coil containing kinases (ROCK) which favored the PrP^{TSE} production. In these neurons, exacerbated ROCK activity overstimulated PDK1 activity which canceled the neuroprotective α-cleavage of PrP^c by TACE α-secretase, physiologically precluding PrP^{TSE} production. Inhibition of ROCK lowered PrP^{TSE} in prion-infected cells as well as in the brain of prion-diseased mice which had

extended lifespans [56]. Indeed, the dysregulation of TACE resulted in PrP^{TSE} accumulation and reduced the shedding of TNFα receptor type 1 (TNFR1) from the neuronal plasma membrane. Inversely, inhibition of PDK1 *in vitro* promoted TACE localization at the plasma membrane, restoring TACE-dependent α-secretase activity and shedding of PrP^{c} and TNFR1, thereby attenuating PrP^{TSE}-induced neurotoxicity. Similarly, inhibition or siRNA-mediated silencing of PDK1 extended survival and reduced motor impairment of scrapie-diseased mice [55]. Mechanistically, PrP^{c} coupling to the NADPH oxidase-TACE α-secretase signaling pathway limits the sensitivity of recipient cells to TNFα by promoting TACE-mediated cleavage of TNFα receptors (TNFRs) and the release of soluble TNFRs. PrP^{c} expression was further shown to be necessary for maintaining TACE α-secretase at the plasma membrane and its TNFR shedding activity. The loss of PrP^{c} provoked TACE internalization, canceling TACE-mediated cleavage of TNFR. This rendered PrP^{c}-depleted cells and *Prnp*-knockout mice highly vulnerable to pro-inflammatory TNFα insult. Thus, abnormal trafficking and activity of TACE in prion diseases likely originates from a loss of PrP^{c} cytoprotective function [57].

Synaptolysis is believed to initiate the neurodegeneration arising after a decrease in depolarization-induced calcium transients that progressively impairs glutamate release [34]. However, although cytoskeletal disruption in dendritic spines plays a major role in neuronal dysfunction, neither changes in postsynaptic densities and presynaptic compartment nor disruption of afferent innervation have been systematically observed, suggesting that even at terminal stages of the disease neuronal loss may not result from deafferentation as previously proposed in the hippocampus and cerebellum of scrapie-infected mice [33, 58, 59]. Thus, neuronal vulnerability to pathological protein misfolding appears to be more strongly dependent than previously thought, on the structure and function of target neurons.

Recent investigations of scrapie pathogenesis in the mouse cerebellum revealed an early upregulation of tumor necrosis factor-α receptor type 1 (TNFR1), a key mediator of neuroinflammation at the membrane of astrocytes enveloping Purkinje cell (PC) excitatory synapses already at the preclinical stage of the disease before PrP^{22L} precipitation, GFAP astrogliosis, and PC death [59]. The contribution of perisynaptic astrocytes to prion pathogenesis through TNFR1 upregulation remains to be clarified and, although the cell types responsible for PrP^{22L} production in the cerebellum are still uncertain, these data suggest a critical role for astrocytes in prion pathogenesis.

2. Mechanisms of neuronal death in prion diseases

Despite the overall advances made in this field during the last decades, the sequence of cellular and molecular events leading to neuronal cell demise in TSEs remains obscure. At present, neuronal cell death can be envisioned as resulting from several parallel, interacting, or sequential pathways involving protein processing and proteasome dysfunction [60], oxidative stress [61], inflammation [55] apoptosis, and autophagy [62]. The repertoire of pathways that lead to neuronal death is however limited [63]. In TSEs, apoptosis is the most popular theory of cell death but is not convincingly documented. In all cases, the probable disruption of both neuronal metabolism and circuits generates a pro-apoptotic signal for neurons. In addition to disruption of cellular proteostasis, UPS dysfunction may lead to neurotoxicity by activating pro-apoptotic pathways. PrP^{TSE} aggresomes can associate with pro-apoptotic factors such as vimentin and caspases [60]. On the other hand, autophagy has been reported in TSEs, but its role in prion disease pathology is not well established [64]. However, the extensive synaptic autophagy observed

in prion diseases [65] has been proposed to contribute to overall synaptic degeneration, a major precocious pathological feature leading to neuronal death in TSEs. This chapter reports recent biochemical and cytopathological studies investigating the involvement of apoptosis and autophagy in neuronal loss induced by infectious prions as well as by PrP^{c}-deficiency in the mouse cerebellum.

Among TSEs, scrapie is a natural ovine prion disease widely studied in mouse models using murine-adapted prion strains (22L, ME7) that, akin to natural prion strains, differ in their rate of disease progression (i.e., duration of the incubation period), as well as the extent and regional pattern of brain histopathology [66, 67]. For example, the characteristic of a prion strain mostly relies on specific biochemical properties related to PrP^{TSE} misfolding. The variable susceptibility of neuronal types to prion infection also emerges as another critical parameter that underlies the complex mechanisms of prion pathogenesis [54, 68, 69] and affects PrP^{TSE} progression along defined anatomical routes [70]. The cellular and molecular mechanisms involved in targeting PrP^{TSE} to specific neuronal populations [33, 71, 72] and neuron-to-neuron spreading of prions in the CNS remain elusive [73].

In several prion diseases, the cerebellum is a preferential prion target for scrapie [74–78], also observed in Creutzfeldt-Jakob disease (CJD) cases [79–87]. Cerebellar circuits are exquisitely patterned and the expression patterns of zebrins in PCs define a topographical map of genetically determined zones controlling sensory-motor behavior [88, 89]. Subsets of PCs expressing zebrins alternate with subsets of zebrin-free PCs, thus forming complementary stripes of biochemically distinct PCs [88]. The most comprehensively studied zonal marker is zebrin II/aldolase C (ZII/AldC) [90]. The expression of ZII/AldC by itself, however, is not sufficient to recapitulate the full complexity of the cerebellar cortex because of the many other PC subtypes [91, 92].

In a recent study [59], the parasagittal compartmentation of the cerebellar cortex restricted 22L scrapie pathogenesis, including PrP^{22L} accumulation, PC neurodegeneration, and gliosis. Indeed, PCs displayed a differential, subtype-specific vulnerability to 22L prions with zebrin-expressing PCs being more resistant to prion toxicity, whereas in stripes where PrP^{22L} accumulated most zebrin-deficient PCs were lost and spongiosis was accentuated (**Figure 1**). Although this banding pattern of PrP^{22L} accumulation is most likely delineated by structural constraints of compartmentation, different biochemical properties of PC subpopulations may well determine their differential resistance to scrapie prions.

2.1 Prion-induced apoptosis

2.1.1 Apoptotic pathways in prion-infected neurons

The mechanism of prion neurotoxicity requires neuronal expression of PrP^{c} and is based on the subversion of its normal function triggered by an interaction with PrP^{TSE} at the cell surface, thereby transducing a toxic signal into the cell. Nevertheless, this has been challenged by the discovery of a monomeric, highly α-helical form of PrP^{c} with strong *in vitro* and *in vivo* neurotoxicity that elicits autophagy and apoptosis with a molecular signature similar to that observed in prion-infected animal brains [93]. This toxic PrP (TPrP) killed PrP-deficient neurons *in vitro* suggesting that a PrP-derived toxic signal can be generated within neurons independently of endogenous membrane-bound PrP^{c}. Indeed, postnatal ablation of PrP^{c} expression in neurons reversed neurodegeneration and affected disease progression in mice even though glial replication was maintained and PrP^{TSE} accumulated [94]. Thus, prion pathogenesis is governed by both cell-autonomous mechanisms responsible for cellular dysfunction and neurodegeneration and noncellular-autonomous mechanisms propagating prion spread [95].

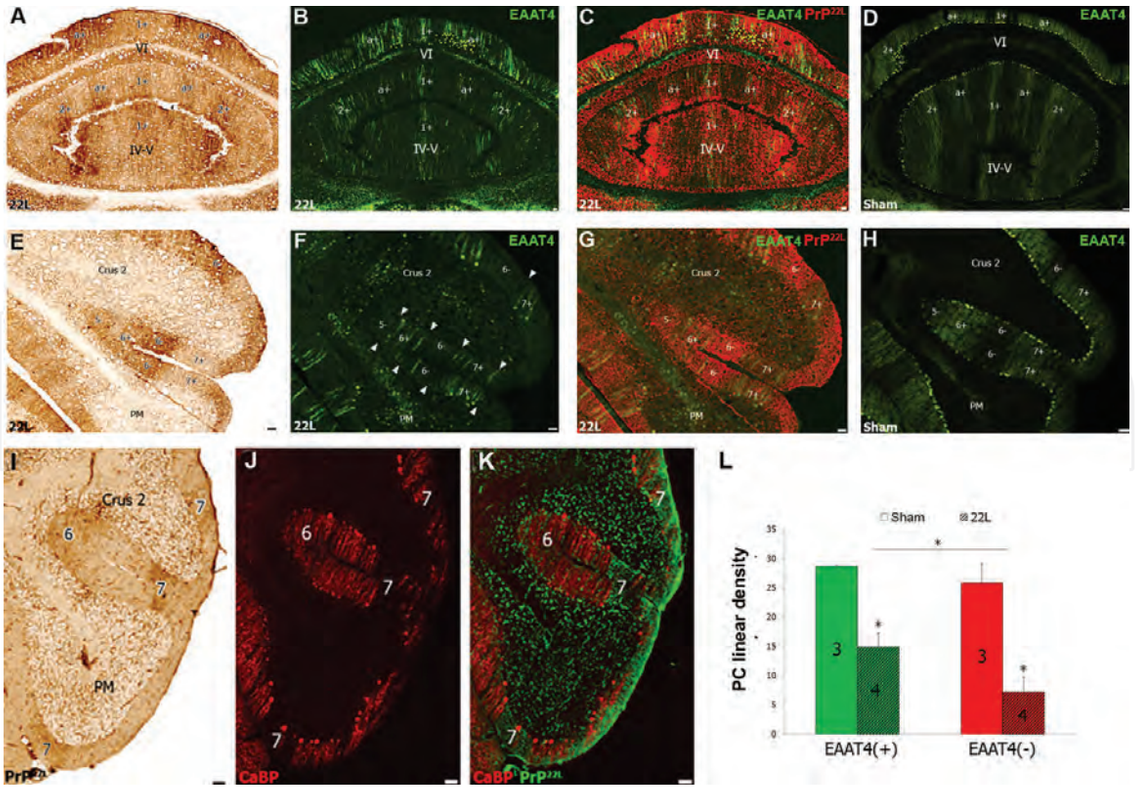

Figure 1.
Banding pattern of PrP^{22L}, EAAT4 zebrin and PC loss in the EAAT4-eGFP mouse cerebellum **A–H**. *The pattern of PrP^{22L} deposits (immunoperoxidase (immunoHRP) in A and E is artificially visualized in red in C and G) correlated with the banding pattern of the zebrin excitatory amino acid transporter 4 (EAAT4-eGFP, green in B, F) in merged PrP^{22L}-EAAT4 images C and G in the cerebellar vermis (A–C) and hemispheres (E–G) infected with 22L ic. (clinical stage 145 dpi). D, H. EAAT4-eGFP PCs in the same regions of the vermis (D) and hemisphere (H) of a noninfected EAAT4-eGFP mouse as shown in the cerebellum of the 22L-infected EAAT4-eGFP mouse (A–G). The zebrin bands are numbered according to the current nomenclature in A–K and indicated by arrowheads in F.* **I–K**. *In the cerebellum infected icb. (preclinical stage), two bands of PrP^{22L} deposits (6 and 7) are visualized by immunoHRP in I and artificially visualized in green in K. These cross crus2 and paramedian lobule (PM) and display a marked loss of CaBP-immunofluorescent PCs (red). Scale bars = 50 μm.* **L**. *Quantitative analysis of EAAT4-expressing and -nonexpressing PCs in the cerebellum of EAAT4-eGFP mice infected i.c. (clinical stage). The EAAT4-nonexpressing PCs are more sensitive to 22L toxicity. *$p < 0.05$. The number of mice analyzed is indicated on the bars in the graph.*

Endoplasmic-reticulum stress has recently been implicated in an apoptotic regulatory pathway activated by changes in Ca^{2+} homeostasis or accumulation of aggregated proteins. In both these situations, Ca^{2+} is released and caspase-12 is activated [96]. ER stress and caspase-12 activation have been identified in prion-infected N2a cells as well as in the brains of prion-diseased mice and CJD patients [97]. The synaptic dysfunction and neuronal death caused by PrP^{TSE} accumulation via dysregulation of the Ca^{2+}-sensitive phosphatase calcineurin (CaN) provides further evidence of the role of ER stress and Ca^{2+} homeostasis in prion-induced neurodegeneration [98]. The increase in Ca^{2+} cytosolic levels following hyperactivation of CaN dysregulates the pro-apoptotic Bcl-2-associated death promoter (Bad), and the transcription factor cAMP response element-binding (CREB). Dephosphorylated Bad interacts with Bax causing mitochondrial stress and apoptosis while dephosphorylated CREB cannot translocate into the nucleus to regulate the transcription of synaptic proteins, resulting in synaptic loss [99].

2.1.2 Mitochondrial apoptosis in prion-infected cerebellar neurons

PrP^{c} has recently been suggested to participate in anti-apoptotic and anti-oxidative processes by interacting with the stress inducible protein 1 (STI-1) to regulate superoxide dismutase (SOD) activation [100]. The PrP^{c} octapeptide repeat

region contains a B-cell-lymphoma 2 (Bcl-2) homology domain 2 (BH2) of the family of apoptosis regulating Bcl-2 proteins involved in the anti-apoptotic function of Bcl-2. A direct interaction between PrPc and the C-terminus of anti-apoptotic Bcl-2 has also been found [101, 102]. In addition, the third helix of PrP^c impaired the BAX conformation changes required for apoptosis activation suggesting that PrP^c may assure the neuroprotective function of Bcl-2 [103]. Along this line, $Prnp^{0/0}$ neurons were more susceptible to apoptotic stimuli such as serum deprivation than their wild-type counterparts, whereas they were rescued by PrP^c or Bcl-2 expression [104, 105]. PrP^c also protected primary neurons against BAX-dependent apoptosis. Furthermore, transgenic expression of *Bax* or *Bax* and *Prnp* indicated that *Prnp* impairs *Bax*-dependent neuronal death [106].

Activation of the mitochondrial apoptotic pathway was observed when primary neurons were exposed to aggregated neurotoxic peptides like PrP106-126 or recombinant mutant PrP [107–109]. Apoptotic neuronal death demonstrated by activation of several caspases and DNA fragmentation is evident in natural prion diseases as well as in experimental models of TSEs [76, 110, 111]. In the cerebellum, apoptotic features have been observed in granule cells in CJD patients [112, 113] as well as in mice experimentally infected with CJD [111] and scrapie strains 301V, 87V, 22A [76], 79A [110], M1000/Fukuoka-1 [114], 127S [115], 22L, 139A, and RML [116, 117]. More recently, activation of caspase-3 was found in PCs of 22L-infected mice [59]. However, cerebral upregulation of the pro-apoptotic factor BAX has been reported in some cases of scrapie-infected rodents [116, 118], whereas no changes in clinical illness and neuropathology could be detected in the brain of Bax-deficient mice infected with 6PB1 mouse-adapted BSE prions [119]. This suggested that BAX-mediated cell death is not involved in the pathological mechanism induced by BSE. Nevertheless, BAX is known to be involved in neuronal death in Tg(PG14) [120] and Ngsk $PrnP^{0/0}$ [121] murine models of PrP-deficiency-linked diseases. In these cases, neuronal death is restricted to cerebellar neurons that are known to undergo BAX and BCL2-dependent apoptosis in other abnormal conditions [122, 123]. This led us to further investigate the involvement of intrinsic mitochondrial apoptotic pathways in a cerebellotropic prion disease such as the 22L scrapie. For this purpose, the pathogenesis of 22L scrapie in the brain of *Bax*-KO ($Bax^{-/-}$) mice [124] and in mice expressing a human Bcl-2 transgene [125] was analyzed. Clinical signs of 22L scrapie (mainly ataxia) were similar to those previously described for C57Bl/6 mice [126]. $Bax^{-/-}$ and HuBcl-2 mice infected by either intraperitoneal (ip.) or intracerebellar (icb.) route displayed ataxia 10–15 days sooner than wild-type mice. Survival times however, were similar in all genotypes (i.e., 223 dpi ip. and 129 dpi icb.). whereas 22L induced more severe cerebellar spongiosis via the icb. route than the ip. route, similar lesion profiles [71] were induced by 22L ip. in the brain of $Bax^{-/-}$ and wild-type mice and lesion profiles were not different in the brain of $Bax^{-/-}$, HuBcl-2 and wild-type mice infected with 22L icb. (**Figure 2**). Anatomopathological analysis of the cerebral and cerebellar cortices of the 22L-diseased $Bax^{-/-}$ and HuBcl-2 mice did not reveal any modified patterns of vacuolation, astrogliosis, and PrP^{22L} deposits irrespective of the inoculation route. Synaptophysin and calcium-binding protein (CaBP) immunohistochemistry also revealed severe synapse and PC loss in all cases (**Figure 3**). Finally, quantitative analysis of the cerebellar granule cells immunolabeled for the nuclear marker NeuN revealed a significant loss of neurons in all genotypes infected by the icb. route (**Figure 4**). Surprisingly, no significant difference could be detected between $Bax^{-/-}$ and wild-type mice infected by the icb. route, whereas HuBcl-2 mice whose granule cells are rescued from developmental cell death [127] lost more granule cells than wild-type and $Bax^{-/-}$ mice (**Figure 4**). These data indicate that neither suppression of *Bax* nor overexpression of Bcl-2 protected cerebellar neurons from 22L scrapie-induced neurotoxicity. Thus, the granule cell

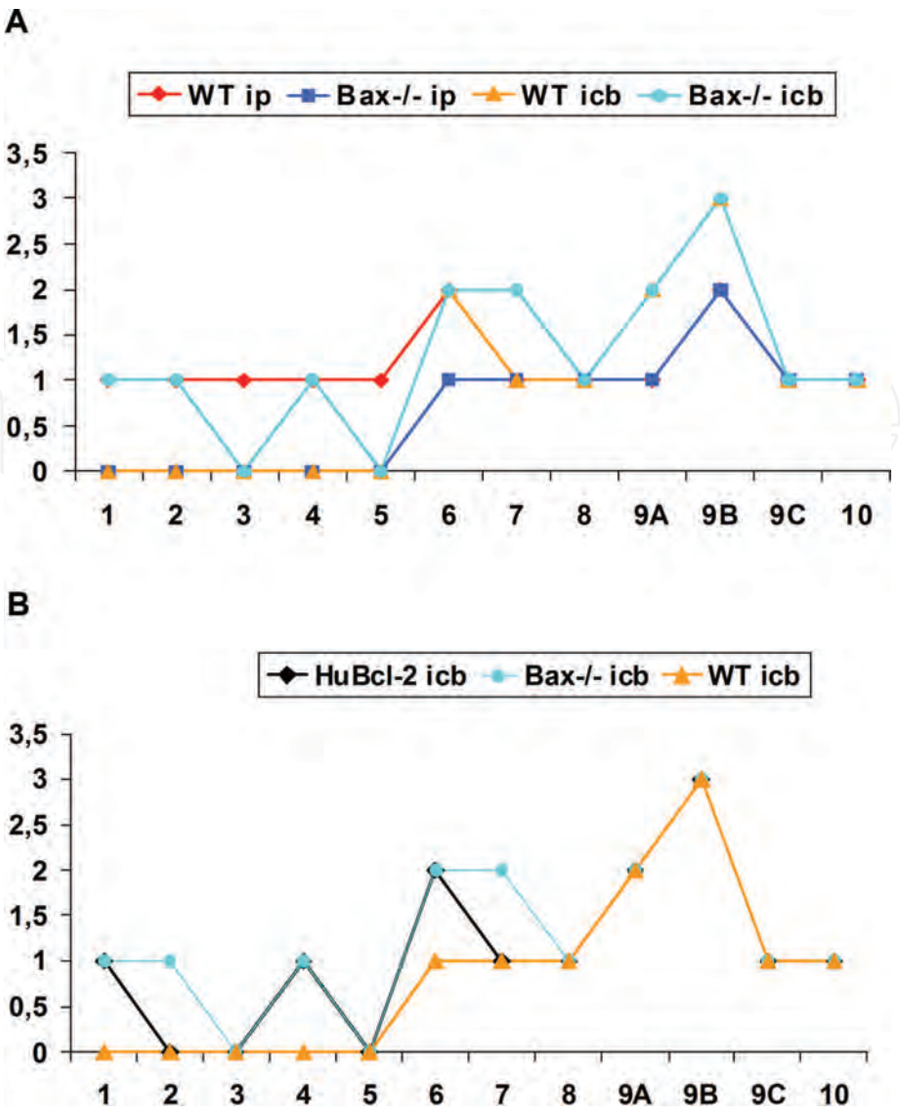

Figure 2.
Spongiosis lesion profiles in the brain of wild-type (WT), Bax$^{-/-}$ and HuBcl-2 mice infected ip. and icb. with the 22L scrapie prion strain. **A.** *Very similar lesion profiles were induced by 22L scrapie ip. in Bax$^{-/-}$ and WT mice. 22L induced more severe cerebellar spongiosis via the icb. route than via the ip. route. 1: cingulate and 2nd motor cortices, 2: lateral and medial septum, 3: caudate putamen, 4: retrosplenial cortex, 5: hippocampus, 6: thalamus, 7: hypothalamus, 8: superior colliculus, 9A: cerebellar molecular layer, 9B: cerebellar granular layer, 9C: cerebellar white matter, 10: medulla.* **B.** *Very similar lesion profiles were induced by 22L scrapie icb. in Bax$^{-/-}$, HuBcl-2 and WT mice.*

and PC death induced by 22L scrapie does not seem to involve BAX and cannot be counteracted by overexpression of the anti-apoptotic factor BCL-2. However, cleaved caspase-3 and -9 were observed in the brains of Bax$^{-/-}$ mice, suggesting that apoptosis may occur through (an) alternative mechanism(s) in TSEs of infectious origin. Indeed, apoptotic features have been reported in the brain of wild-type mice infected with RML, in the absence of Bax upregulation [116], while other proteins involved in cell death including those associated with the mitochondrial inner membrane, the UPS and the endoplasmic-reticulum-associated protein degradation (ERAD) pathway [128] were upregulated.

2.1.3 Prion-induced neuronal death in cerebellar organotypic slice cultures (COCS)

In the recently developed prion cerebellar organotypic slice culture (COCS) assay, progressive spongiform neurodegeneration that closely reproduce features of prion disease can be induced *ex vivo* [117, 129]. Infecting COCS with three different scrapie strains (RML, 22L, 139A) produced three distinct patterns of prion protein

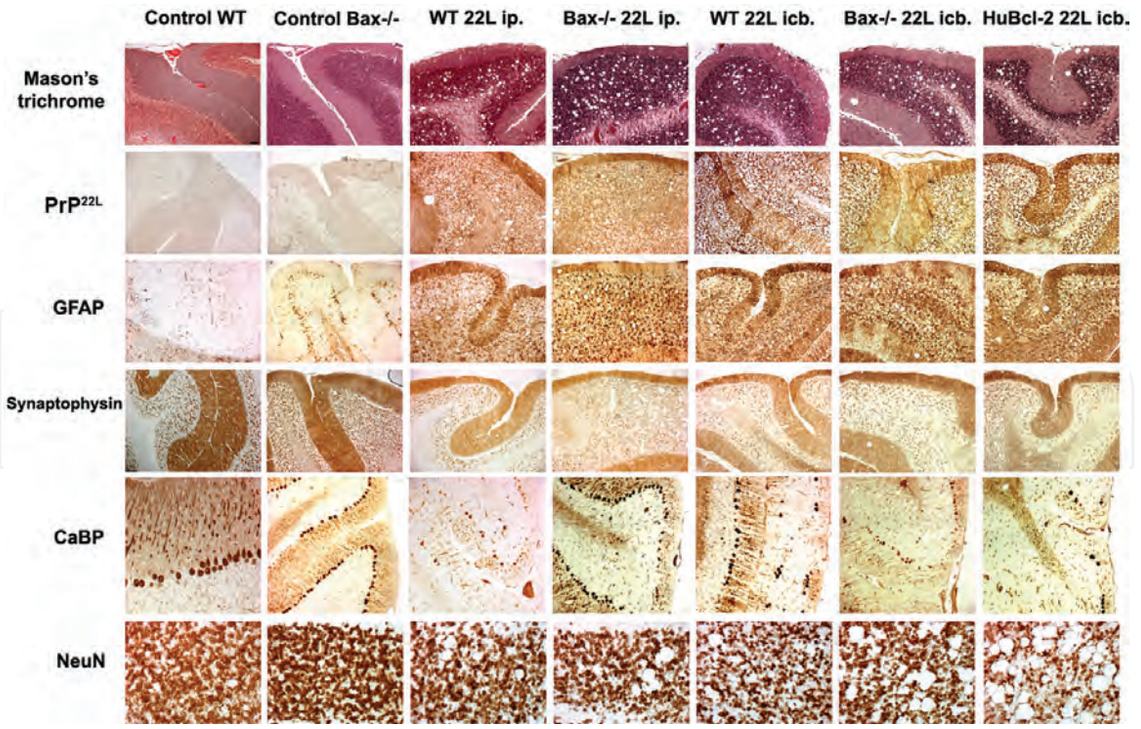

Figure 3.
Anatomopathology of 22L scrapie ip. and icb. in the cerebellum of WT, Bax$^{-/-}$ and HuBcl-2 mice. Neither Bax knockout nor HuBcl-2 overexpression modified vacuolation (Mason's trichrome), astrogliosis (GFAP immunoHRP) and PrP^{22L} accumulation (PrP immunoHRP) patterns in the cerebellar cortex of the 22L ip. and icb. infected Bax$^{-/-}$ and HuBcl-2 mice compared to the WT mice. Synaptophysin and CaBP reveal respectively synapse and PC loss in the cerebellum of all mice. Loss of Neun-immunostained GCs is also prominent in the cerebellum of the WT, Bax$^{-/-}$ and HuBcl-2 infected icb., yet seemed less pronounced in the mice infected ip.

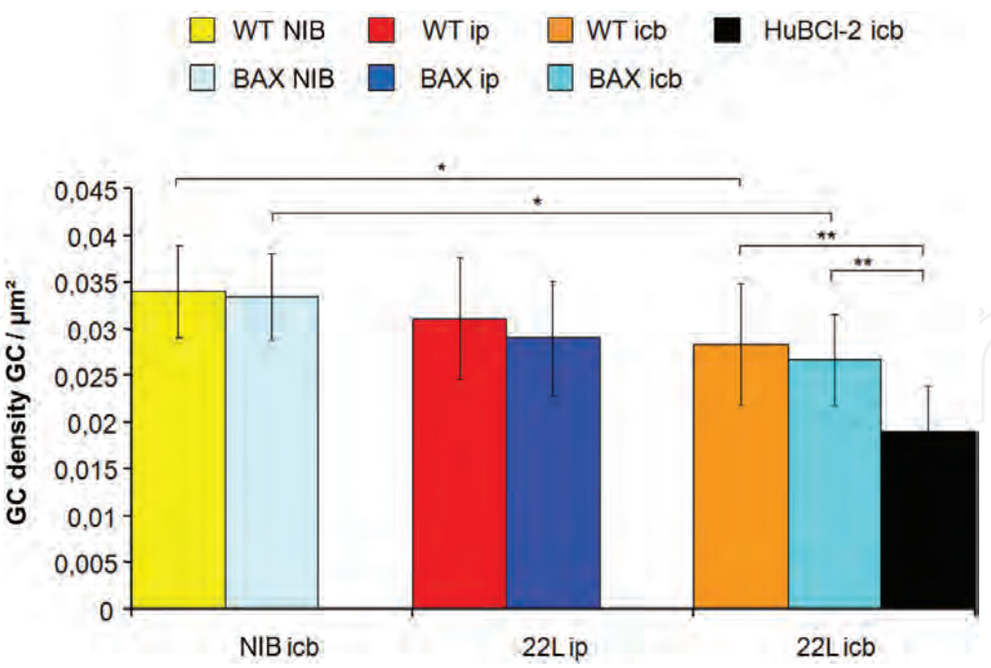

Figure 4.
*Quantitative analysis of cerebellar GCs immunostained for the nuclear marker NeuN revealed a significant loss of neurons in all genotypes infected icb., but not ip. *p < 0.05; **p < 0.01. Whereas Bax$^{-/-}$ and WT mice lost a similar amount of GCs, the HuBcl-2 mice lost more GCs than the WT and Bax$^{-/-}$ mice. NIB, noninfected brain homogenate.*

deposition accompanied by salient features of prion disease pathogenesis such as severe neuronal loss, a pro-inflammatory response, and typical neuropathological changes (spongiform vacuolation, tubulovesicular structures, neuronal dystrophy,

and gliosis). Neurodegeneration did not occur when PrP was genetically removed from neurons and was abrogated by compounds known to antagonize prion replication. Also, calpain inhibitors, but not caspase inhibitors, prevented neurotoxicity and fodrin cleavage; whereas, prion replication was unimpeded indicating that inhibiting calpain uncouples prion replication and neurotoxicity. These data validate the COCS as a powerful model system that faithfully reproduces many morphological hallmarks of prion infections and shows that prion neurotoxicity in cerebellar granule cells is calpain-dependent but caspase-independent.

Furthermore, significant spine loss and altered dendritic morphology, analogous to that seen *in vivo* were induced by RML scrapie in COCS [130], while the deposition pattern and subcellular distribution of PrP^{22L} (i.e., granular deposits associated with neurons, astrocytes, and microglia but not PCs in the neuropil of the PC and molecular layers [131]), closely resembled that observed *in vivo* [59].

Following infection of COCS from C57Bl6/J, ZH-I $Prnp^{0/0}$, and Tga20 PrP-overexpressing mice with brain homogenate from C57Bl6/J infected intracerebrally (ic.) with either 22L or 139A scrapie prions, PrP^{22L} and PrP^{139A} accumulation could be detected on histoblots from wild-type and Tga20 COCS, respectively, 30 and 20 days post infection (dpi), but not on histoblots from ZH-I mice (**Figure 5**). Furthermore, quantitative analysis of PCs in these COCs indicated that a severe loss of neurons was induced by 22L prions in wild-type slices at 30 dpi (22 ± 2 surviving PCs/slice) and in Tga20 slices at 20 dpi (293 ± 68 surviving PCs) as well as by 139A prions in wild-type slices at 30 dpi (145 ± 63 surviving PCs/slice) and in Tga20 slices at 20 dpi (191 ± 31 surviving PCs/slice) compared to noninfected control COCS (220 ± 27 surviving PCs/slice in wild-type slices and 357 ± 71 surviving PCs/slice in Tga20 slices) (**Figure 6**). At 30 dpi, the trilaminar organization of the cerebellar cortex was evident in noninfected COCs, which did not exhibit any clear ultrastructural modifications (**Figure 7**). Nevertheless, numerous vacuoles, autophagosomes, and lysosomes had formed in granule cells infected by 22L and 139A (**Figure 8**). In diseased PCs, autophagosomes with double membranes and rough endoplasmic reticulum (Nissl bodies) formed compartmented organelles of various sizes (1–10 compartments) resembling different stages leading to multivesicular vacuoles (**Figure 9**). Although further investigations are necessary, these ultrastructural

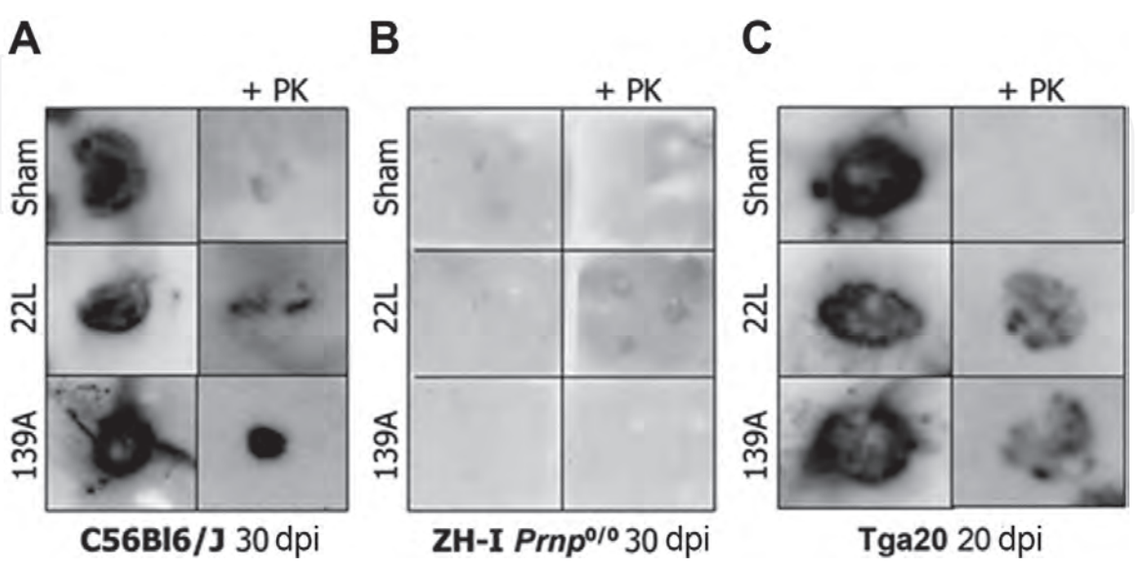

Figure 5.
Histoblots of cultured organotypic cerebellar slices (COCS) infected with the 22L and 139A scrapie strains. PrP^c was detected in histoblots of noninfected (sham) COCS from WT C57Bl6/J (A) and Tga20 PrP-overexpressing (C), but not PrP-deficient ZH-I $PrnP^{0/0}$ (B) mice. PrP^c was completely digested by proteinase K (PK) in these COCS. After 30 and 20 days postinfection (dpi), PK revealed undigested PrP^{22L} and PrP^{139A} respectively in the WT and Tga20, but not ZH-I $Prnp^{0/0}$ infected COCS.

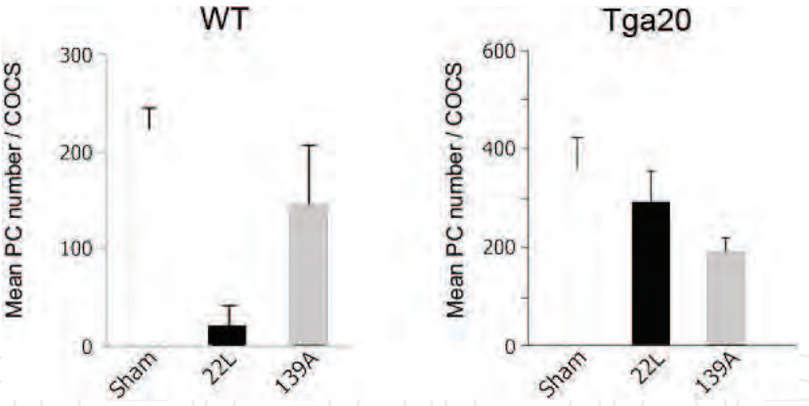

Figure 6.
Mean numbers of CaBP-immunofluorescent PCs in WT and Tga20 COCS noninfected (sham) and infected with 22L and 139A scrapie prions at 30 dpi.

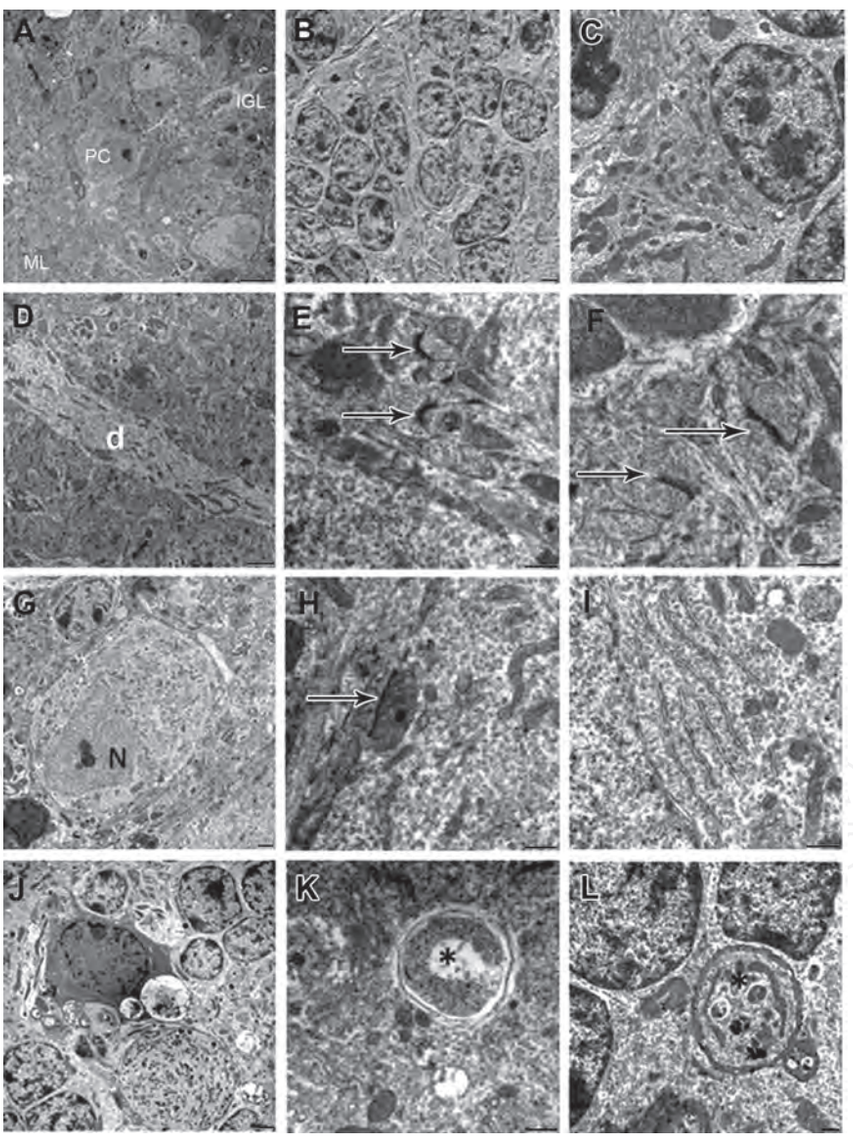

Figure 7.
Ultrastructural features of the C57Bl6/J mouse cerebellar cortex in noninfected COCS after 30 DIV. **A.** *Laminar organization of the cerebellar cortex with PC at the interface between internal granular layer (IGL) and molecular layer (ML).* **B.** *Granule cells in the IGL.* **C.** *IGL neuropil.* **D.** *PC dendrite (d) in the ML neuropil.* **E, F.** *Asymmetrical synapses (arrows) on interneurons dendrites (E) and PC spines (F).* **G.** *PC. N, PC nucleus.* **H.** *A smooth saccule (arrow) typically separates a mitochondrion from the plasma membrane in the PC neuroplasm.* **I.** *Nissl body in the PC neuroplasm.* **J.** *Degenerated cell with electron-dense vacuolated cytoplasm.* **K.** *Autophagic digestion of a mitochondrion (*).* **L.** *Autophagic profiles in a PC axon (*). Scale bars = 10 μm in A, 2 μm in B–D, G, J, 500 nm in E, F, H, I, K, L.*

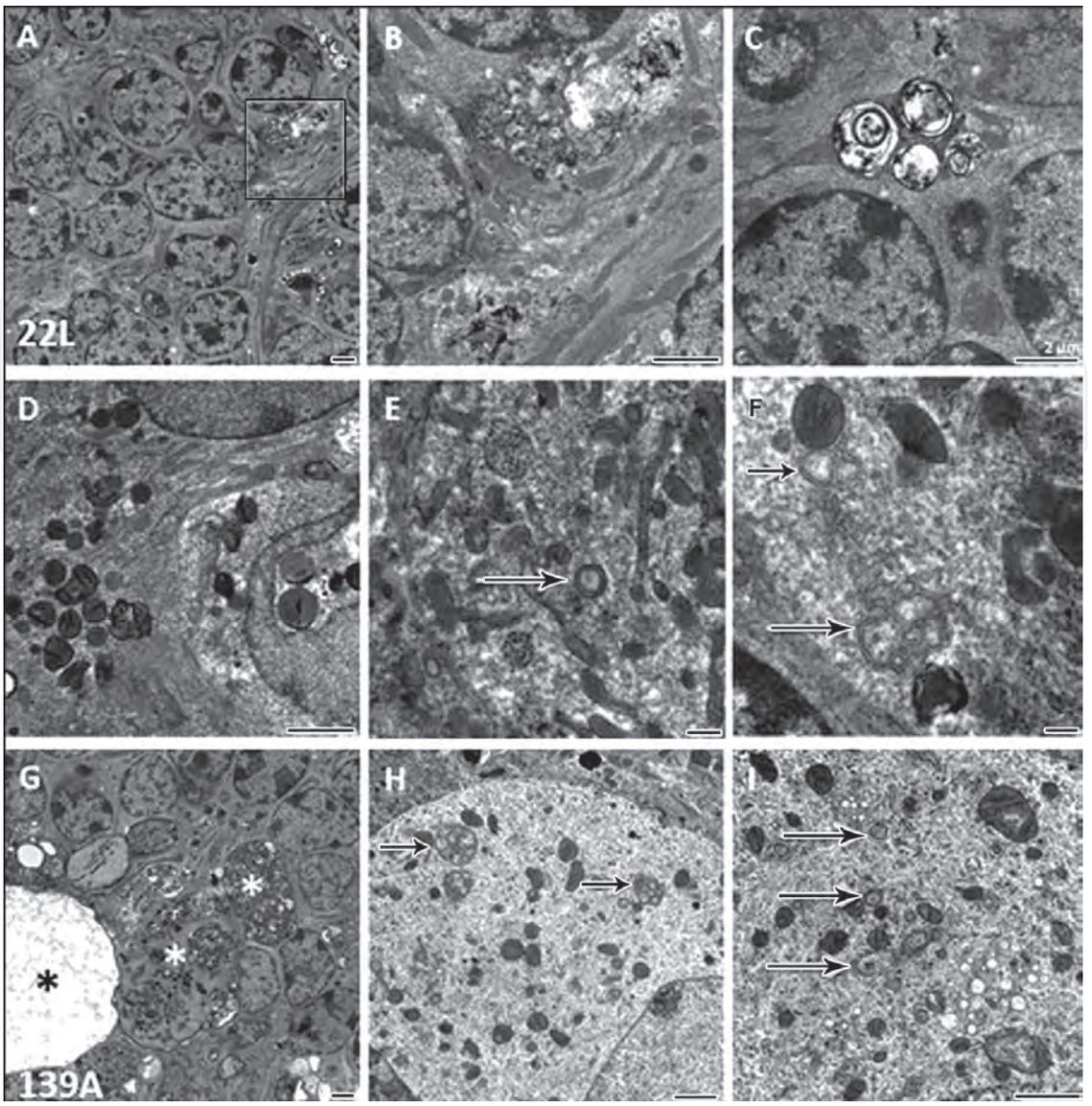

Figure 8.
Cytopathology of the C57Bl6/J mouse cerebellar cortex in COCS infected with 22L (A–F) and 139A (G–L) scrapie prions at 30 dpi. **A.** *IGL.* **B–D.** *Autophagic profiles in the IGL neuropil.* **B.** *Magnification of the inset in A.* **D.** *Electron-dense lysosomes.* **E, F.** *Various stages of ER-derived reticulated organelles (arrows) in the neuroplasm of a PC.* **G.** *Neurodegenerating profiles (*) in the IGL neuropil.* **H, I.** *PC neuroplasm containing different stages of ER-derived reticulated organelles (arrows) and vacuoles. Scale bars = 2 μm in A–D, G–I, 500 nm in E, F.*

alterations were not observed in noninfected slices suggesting that a specific effect of prions links prion-induced ER stress to this morphological ER modification.

2.2 Prion-induced autophagy

Autophagy and apoptosis are activated in many neurodegenerative diseases featured by ubiquitinated misfolded proteins. In neurons, the degradation of abnormal proteins such as α-synuclein in Parkinson's disease, β-amyloid peptide in Alzheimer's disease (AD), or PrP in TSEs occurs by autophagy [14, 132–135]. These cardinal proteins contribute to synaptic dysregulation and altered organelles leading to apoptosis. The neurodegenerating neurons exhibit robust accumulation of cytosolic autophagosomes (see [14] for review, **Figure 10**) suggesting a dysregulation of the autophagic flux resulting from autophagic stress, due to an imbalance between protein synthesis and degradation [136]. Autophagy reduces intraneuronal aggregates and slows down the progression of clinical disease in experimental models of AD [137–139] and prion diseases [140, 141]. Thus, dysregulation of the autophagic

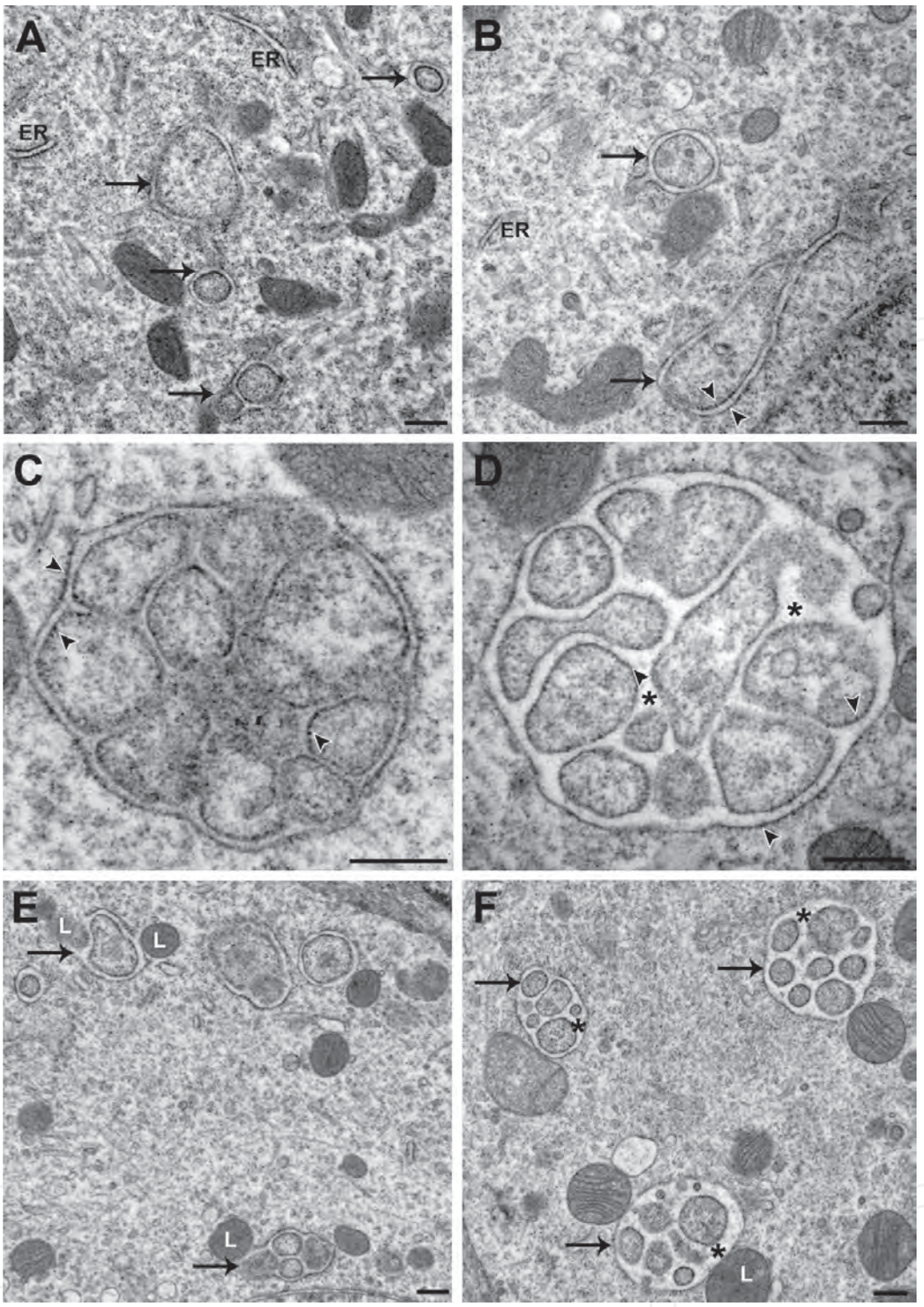

Figure 9.
Cytopathological formation and evolution of ER-derived profiles in PCs of COCS infected with 139A scrapie prions at 30 dpi. **A, B**. *Reticulation and sequestration of neuroplasm by ER saccules forming small double-membrane vesicles (arrows) containing ribosome-like particles (arrowheads in B) on both external and internal faces. ER, endoplasmic reticulum.* **C, D**. *Large compartmented ER-derived organelles which still display membrane-bound ribosomes (arrowheads). C. High magnification of* **Figure 8H**. *D. See the enlargement between membranes (*). **E**. Fusion (arrows) of small ER-derived double-membraned vacuoles with lysosomes (L).* **F**. *Large ER-derived double-membraned vacuoles with enlarged intermembrane space (*) transforming into multivesicular vacuoles (arrows). Scale bars = 500 nm.*

flux impairs the elimination of misfolded proteins and damaged organelles which then accumulate in the cytoplasm and contribute to cell dysfunction and death [142].

Together, spongiform vacuolation of the neuropil, synaptolysis, accompanied by neuronal cell loss and gliosis constitute the classical neuropathological quartet of TSEs. The typical "spongiform vacuoles" are believed to result from autophagy and develop within neuronal elements, myelinated axons, and myelin sheaths

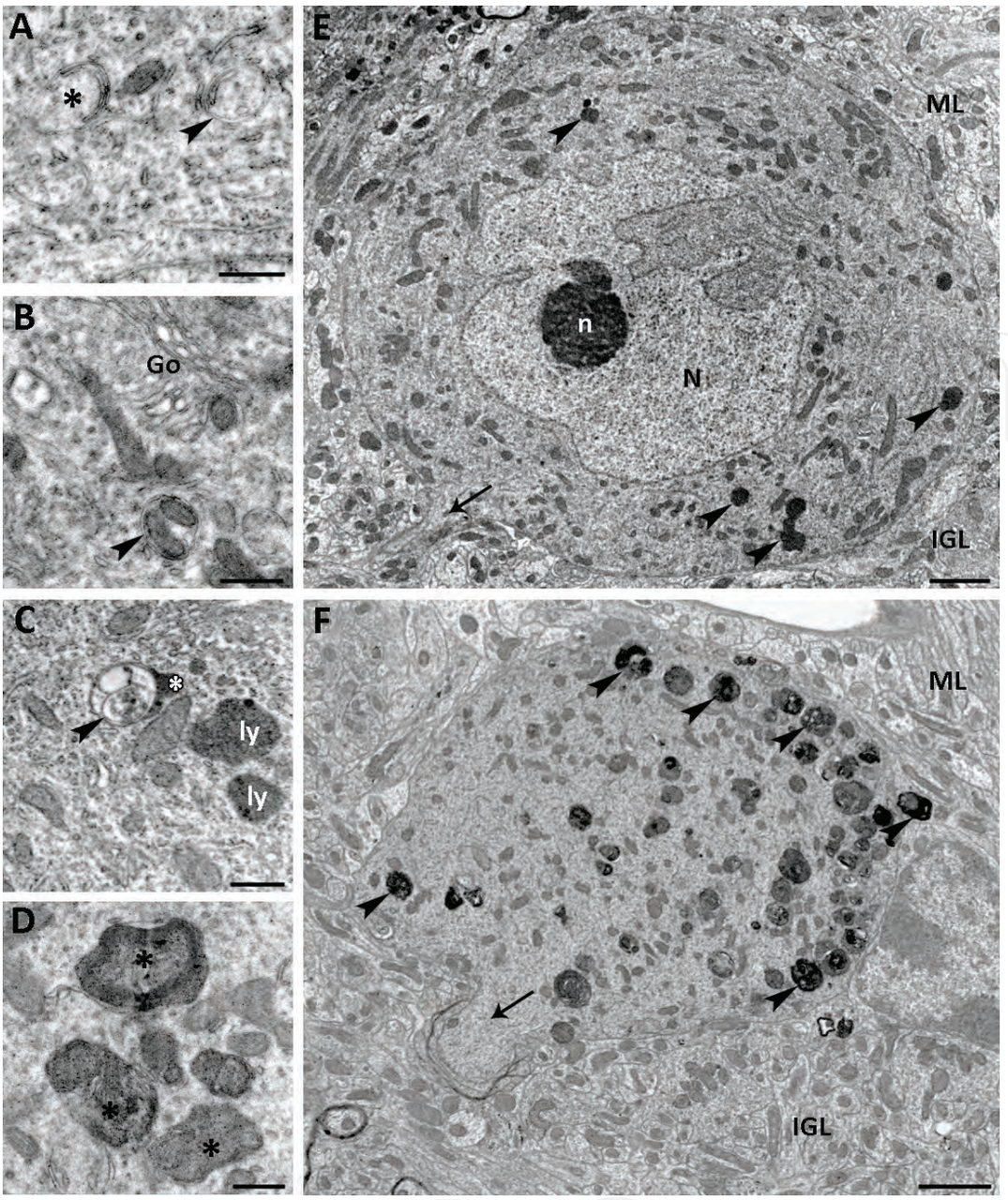

Figure 10.
Autophagy in PCs of 4.5 (A–E) and 12 (F) month-old control $Bax^{+/+}$; $Prnp^{+/+}$ (E) and $Bax^{-/-}$;Ngsk $Prnp^{0/0}$ (A–D, F) mice. Ultrastructural autophagic stages from phagophores to autolysosomes. **A**. *Phagophore (*) and double-membraned autophagosome (arrowhead).* **B**. *Sequestration of two mitochondria in an autophagosome (arrowhead). Go, Golgi dichtyosome.* **C**. *Fusion of an autophagosome (arrowhead) with a lysosome (*). Ly, lysosomes.* **D**. *Autolysosomes (*). A–D. Scale bars = 500 nm.* **E**. *The somato-dendritic cytoplasm of this control $Bax^{+/+}$; $Prnp^{+/+}$ PC contains a few lysosomes and lipofuchsin bodies (arrowheads). N, nucleus; n, nucleolus.* **F**. *Autophagic PC with numerous autophagic organelles (arrowheads) accumulating in the neuroplasm. ML, molecular layer. IGL, internal granular layer. E, F. Arrows show PC axon. Scale bars = 2 μm.*

[143, 144]. Autophagic vacuoles are increased in prion-diseased neurons [64, 65, 145], and the scrapie responsive gene 1 (SRG1) protein is overexpressed and bound to neuronal autophagosomes in the brain of scrapie- and BSE-infected animals and CJD-diseased humans [146, 147]. In addition, LC3-II, a marker of autophagosomes is increased in the cytosol of neurons in scrapie-infected hamsters and CJD- and FFI-diseased patients.

Recent evidence indicated that PrP^c, but not truncated PrP devoid of the N-terminal octapeptide repeat region, exerts a negative control on the induction of autophagy [148]. Thus, the loss or subversion of PrP^c function resulting from prion infection may upregulate autophagy in diseased neurons [16]. While

autophagy-inducing agents increased cellular clearance of PrP^{TSE} [149–151], blocking the fusion of autophagosomes with lysosomes allowed visualization of PrP^{TSE} in the autophagosomes suggesting that degradation of endosomal PrP^{TSE} is by autophagy [134]. However, saturation of the autolysosomal degradation process can release PrP^{TSE} aggregates and degradation enzymes into the neuroplasm contributing to autophagy upregulation and neuronal death [134]. Nevertheless, although autophagy-inducing agents delayed disease onset and PrP^{TSE} accumulation in the CNS of mice [152], survival time was not modified [153]. Along this line, neither autophagy-inducing nor -inhibiting treatments altered the time course or amplitude of prion-induced neuronal death, strongly suggesting that autophagy in protein misfolding diseases is a secondary mechanism in the neurodegenerative process [141, 154].

3. Neuronal death in prion protein-deficient mice

3.1 Impaired autophagy in Zrch-1 prion protein-deficient mice

With the exception of the *Prnp*-knockout models in which ectopic expression of Doppel (Dpl) in the CNS leads to PC death, most other *Prnp*-knockout mouse models do not show gross abnormalities indicating that PrP^c may be dispensable for embryonic development and adulthood. Nevertheless, PrP-deficient mice exhibit an increased predilection for seizures, motor and cognitive disabilities, reduced synaptic inhibition, and long term potentiation in the hippocampus. Also, altered development of the granule cell layer, dysregulation of the cerebellar network and age-dependent spongiform changes with reactive astrogliosis have been observed [155, 156]. In cultures of PrP-deficient hippocampal neurons, autophagy is upregulated in the absence of serum or by hydrogen peroxide-induced oxidative stress [148, 157] suggesting that suppression of the protective effects of PrP^c could impair the autophagic flux in PrP-deficient neurons *in vivo*. Indeed, ultrastructural examination of hippocampus and cerebral cortex of ZH-I $Prnp^{0/0}$ mice revealed an accumulation of autophagosomes containing incompletely digested material increasing from 3 to 12 months of age [158]. In addition, an ultrastructural examination of PCs in the cerebellum of ZH-I $Prnp^{0/0}$ mice revealed significant autophagic accumulation in the somato-dendritic compartment of these neurons from 6 to 14.5 months of age (**Figure 11**). Since autophagic cell death is known to induce neurodegeneration [136, 159, 160], these signs of autophagy blockade could reflect a sustained, progressive autophagic neuronal loss in the CNS of the ZH-I $Prnp^{0/0}$ mice.

3.2 Neuronal loss in Dpl-expressing Ngsk prion protein-deficient mice

Nagasaki (Ngsk) PrP-deficient mice which have a deletion of the entire *Prnp* gene [161–163] develop progressive cerebellar ataxia, which was later discovered to result from the absence of a splice acceptor site in exon 3 of *Prnp* [164]. This leads to the aberrant overexpression of the *Prnd* gene encoding the PrP^c paralogue Dpl [165, 166] that causes selective degeneration of cerebellar PCs. Notably, the reintroduction of *Prnp* in mice overexpressing *Prnd* in the brain rescued the phenotype, suggesting a functional link between the two proteins [167]. Dpl has been shown to have intrinsic neurotoxic properties in cerebellar neurons [168] and has been proposed to interfere with PrP^c and affect cell survival [100]. According to this hypothesis, PrP^c and Dpl bind a common ligand LPrP, where PrP^c binding induces a cell survival signal while Dpl binding activates a death signaling cascade. In PrP^c-deficient *Prnp*-knockout mice that do not express Dpl, the existence of a protein

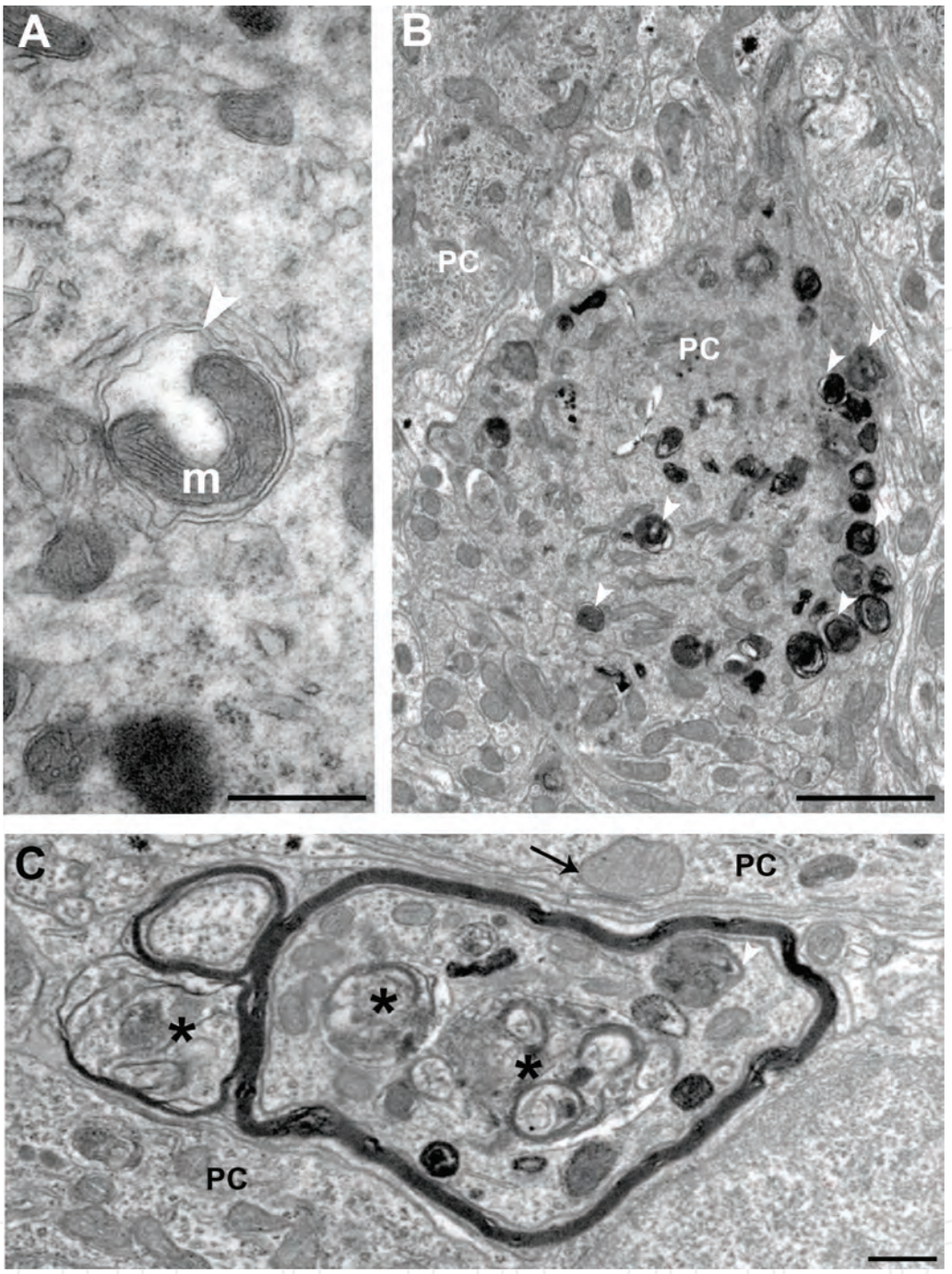

Figure 11.
Autophagy in ZH-I Prnp$^{0/0}$ PCs. **A.** *Mitophagy in the PC neuroplasm of a 4.5 months-old ZH-I Prnp$^{0/0}$ mouse. Arrowhead shows the double membrane of an autophagic vacuole sequestrating a mitochondrion (m). Scale bar = 500 nm.* **B, C.** *12 months-old ZH-I Prnp$^{0/0}$ mice. PC layer. B. Autophagic PC containing numerous autophagosomes and autolysosomes (arrowheads). Scale bar = 2 μm. C. PC layer. Degenerating PC axons containing autophagosomes and lysosomes (*). Scale bar =500 nm.*

π has been proposed to induce a cell survival signal when bound to LPrP [169]. For the moment, LPrP and π remain to be identified, as well as the neuronal death pathways involved in Dpl-induced PC loss.

Because Dpl neurotoxicity depends on PrP^{c}-deficiency in PCs, investigating the underlying neurotoxic mechanism may provide important insight into the neuroprotective function of PrP^{c}. The resistance of the PC population to neurotoxicity increased in the cerebellum of Ngsk mice, which were either deficient for the pro-apoptotic factor Bax [121] or over-express the anti-apoptotic factor Bcl-2 [170]. Although this suggests that an intrinsic apoptotic process is involved in the death of the Ngsk *Prnp*$^{0/0}$ PCs, a significant PC loss still occurred in both

(Bax$^{-/-}$; Ngsk *Prnp*$^{0/0}$) and (HuBcl-2; Ngsk *Prnp*$^{0/0}$) double mutants. Thus, the Ngsk condition, i.e., Dpl neurotoxicity and PrP-deficiency, could activate BAX-independent mechanisms in the Ngsk *Prnp*$^{0/0}$ PCs. These neurons exhibited robust autophagy well before significant neuronal death in the cerebellar cortex of the Ngsk *Prnp*$^{0/0}$ mice [135, 171] suggesting that either "reactive" autophagy is initially induced as a neuroprotective response to Dpl neurotoxicity or impaired autophagy results from PrP-deficiency as in ZH-I *Prnp*$^{0/0}$ mice (see above and [158]). Indeed, the increased expression of the autophagic markers SCRG1, LC3-II, and P62 proteins without any changes in mRNA levels, indicates that the ultimate steps of autophagic degradation are impaired in Ngsk *Prnp*$^{0/0}$ PCs [135]. Probably due to this impairment of autophagic proteolysis, LC3-II-, and Lamp-1-labeled autophagosomes and autolysosomes [172] accumulate in the Ngsk *Prnp*$^{0/0}$ PCs. How apoptosis and autophagy are involved in Ngsk *Prnp*$^{0/0}$ PC death remains to be determined.

To further investigate the role of autophagy in the death of Ngsk *Prnp*$^{0/0}$ PCs, a quantitative analysis of autophagic PCs was performed at the ultrastructural level in the cerebellum of Ngsk *Prnp*$^{0/0}$, *Bax*$^{-/-}$; Ngsk *Prnp*$^{0/0}$, ZCH-I *Prnp*$^{0/0}$ and control *Bax*$^{+/+}$;*Prnp*$^{+/+}$ mice (**Figure 12**). At 4.5 months of age, equivalent amounts of autophagic somato-dendritic compartments and axons of PCs were found in the cerebella of Ngsk *Prnp*$^{0/0}$ and *Bax*$^{-/-}$; Ngsk *Prnp*$^{0/0}$ mutants and were significantly more than those in ZCH-I *Prnp*$^{0/0}$ and control *Bax*$^{+/+}$;Prnp$^{+/+}$ cerebella. Interestingly, the amounts of autophagic axons and somato-dendritic compartments of PCs in the ZCH-I *Prnp*$^{0/0}$ and control *Bax*$^{+/+}$;*Prnp*$^{+/+}$ cerebella were not different. These data suggest that while autophagy induction is already visible in PCs with the Ngsk condition, it is not induced in control *Bax*$^{+/+}$;*Prnp*$^{+/+}$ PCs, nor in the absence of PrP^{c} in the ZCH-I *Prnp*$^{0/0}$ PCs. Thus, autophagy seems to be induced by Dpl neurotoxicity in the Ngsk condition whether BAX is present or not; whereas PrP-deficiency alone has no autophagy-inducing effect at this age (**Figure 13**).

At 6.5–7 months of age, the amount of autophagic somato-dendritic compartments and axons of PC were significantly decreased in *Bax*$^{-/-}$; Ngsk *Prnp*$^{0/0}$ cerebella compared with Ngsk *Prnp*$^{0/0}$ cerebella. Consequently, the amount of autophagic PC profiles in the *Bax*$^{-/-}$; Ngsk *Prnp*$^{0/0}$ and ZH-I *Prnp*$^{0/0}$ cerebella was equivalent, yet more than in the control *Bax*$^{+/+}$;*Prnp*$^{+/+}$ cerebella. Furthermore, autophagic PC somato-dendritic compartments and axons did not change from 4.5 to 6.5–7 months of age in the *Bax*$^{-/-}$; Ngsk *Prnp*$^{0/0}$, whereas many more PCs were autophagic in the 6.5–7 month-old compared to the 4.5 month-old Ngsk *Prnp*$^{0/0}$ cerebella. This increase was also observed in ZH-I *Prnp*$^{0/0}$ cerebella, while no autophagic PCs were found in 6.5–7 month-old control *Bax*$^{+/+}$;*Prnp*$^{+/+}$ cerebella (**Figure 13**).

This suggests that BAX-deficiency modulates autophagy in Ngsk *Prnp*$^{0/0}$ PCs after 4.5 months of age. Autophagy in the ZH-I *Prnp*$^{0/0}$ PCs had increased to the same level as observed in the *Bax*$^{-/-}$;Ngsk *Prnp*$^{0/0}$ cerebella. Thus, the persistent autophagy in the PCs of the *Bax*$^{-/-}$;Ngsk *Prnp*$^{0/0}$ double mutants is likely related to PrP-deficiency. Also, autophagy- and *Bax*-dependent apoptosis are likely to occur in the same PCs that are rescued by *Bax* deletion.

At 12 months of age, the amount of autophagic somato-dendritic compartments and axons of PCs in *Bax*$^{-/-}$;Ngsk *Prnp*$^{0/0}$ cerebella was equivalent to that found in 4.5 month-old cerebella suggesting that autophagy remains stable in this PC population, at a level similar to that maintained in the ZH-I *Prnp*$^{0/0}$, and this likely results from PrP-deficiency. Indeed, many more autophagic PC somato-dendritic compartments and axons were observed in ZH-I *Prnp*$^{0/0}$ cerebella than in the cerebella of 12 month-old control *Bax*$^{+/+}$;*Prnp*$^{+/+}$ mice which did not contain autophagic PCs. However, the autophagic PC somato-dendritic compartments were

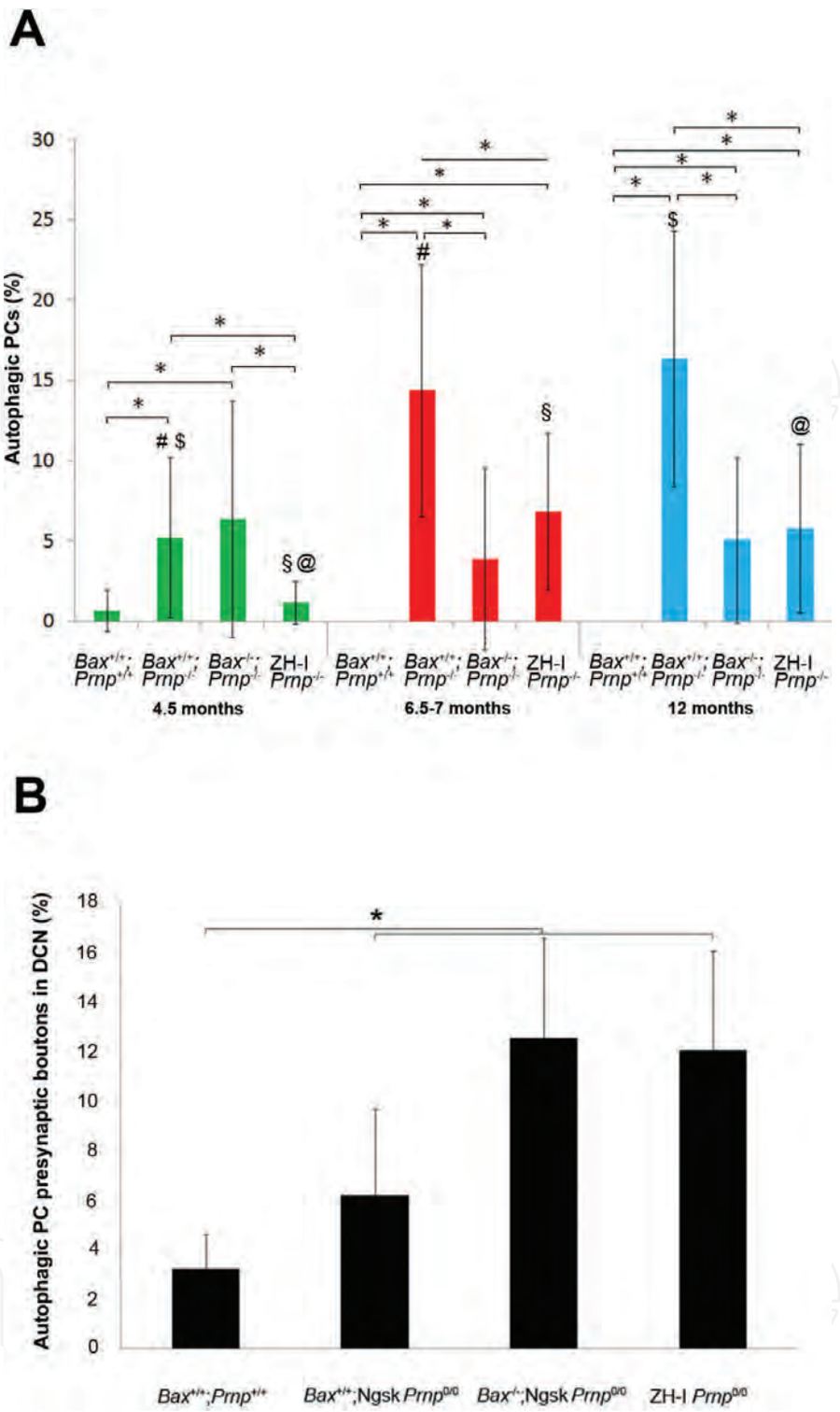

Figure 12.
Quantitative analysis of autophagy in PCs of control Bax$^{+/+}$;Prnp$^{+/+}$ and PrP-deficient Bax$^{+/+}$;Ngsk Prnp$^{0/0}$, Bax$^{-/-}$;Ngsk Prnp$^{0/0}$ and ZH-I Prnp$^{0/0}$ mutant mice. Autophagic somato-dendritic and axonal profiles were counted in 200 PCs in transverse cerebellar sections (50 PCs per hemisphere and hemivermis) from each mouse at 4.5, 6.5–7 and 12 months of age (n = 3 mice/age/genotype). PC soma, primary dendrite and axons were autophagic when containing three or more autophagic profiles (phagophore, autophagosome, autophagolysosome). Data are given as mean values ± standard deviation (SD). Statistical comparisons between ages and genotypes were performed using a two-tailed Student's t test (Statistica). **A.** *Mean percentages of autophagic PC somato-dendritic and axonal compartments. *, #, @, $, §: p < 0.01.* **B.** *Mean percentages of autophagic PC presynaptic boutons making symmetrical synapses on somato-dendritic profiles of deep cerebellar neurons. The PC presynaptic boutons were autophagic when containing at least one autophagic organelle. Autophagic PC presynaptic boutons were counted in 300 presynaptic boutons selected randomly in either left or right fastigial, interposed and dentate nuclei (100 boutons/nucleus) in three 12 month-old mice of each genotype. Statistical comparisons between genotypes were performed using a two-tailed Student's t test (Statistica) and given as mean values ± standard deviation (SD). *, p < 0.01.*

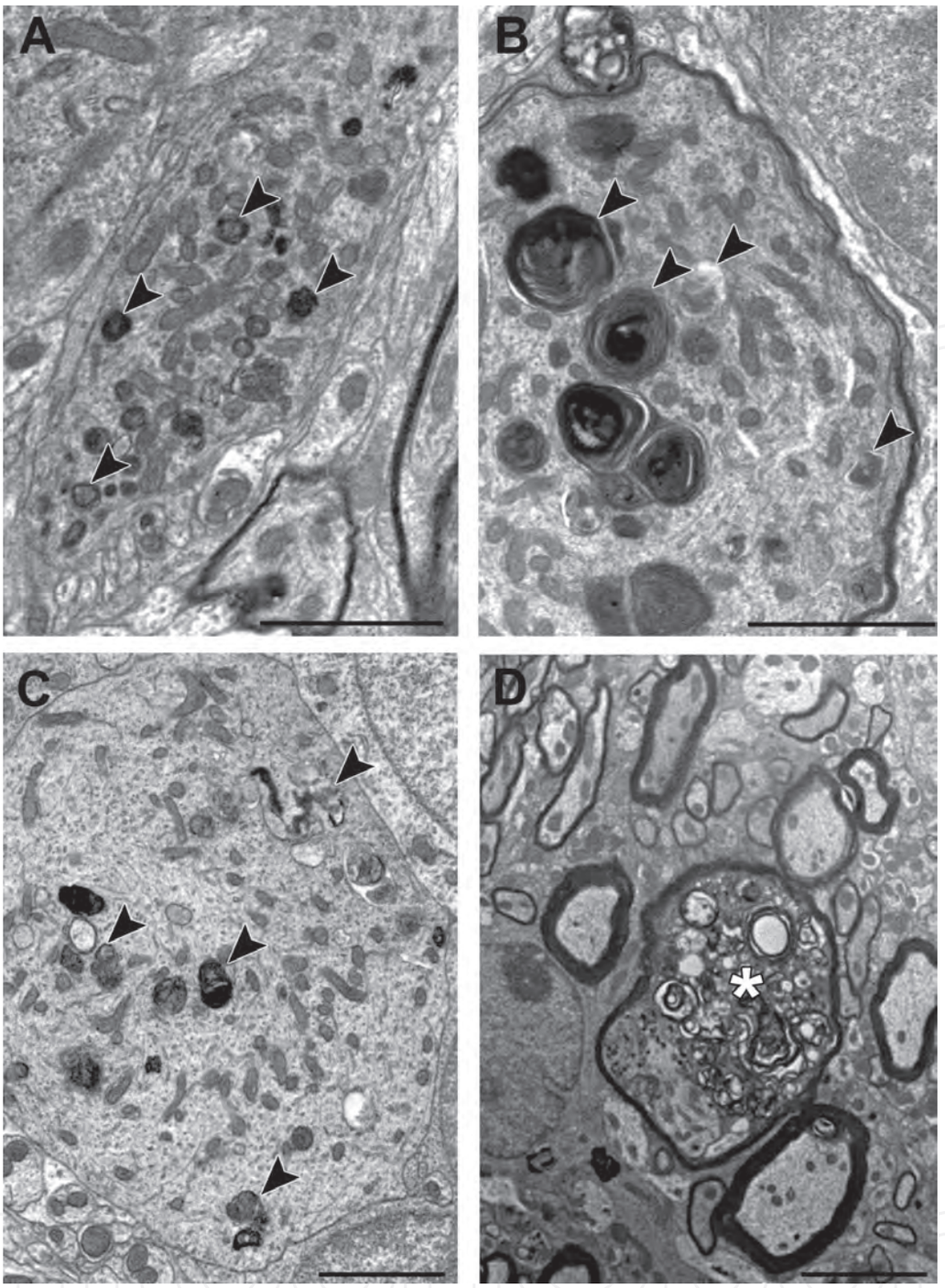

Figure 13.
Autophagy in PCs of 7 (A, B) and 12 (C, D) month-old $Bax^{-/-}$;Ngsk $Prnp^{0/0}$ mice. **A**. *PC-like somato-dendritic profile containing numerous autophagic vacuoles and autolysosomes (arrowheads) in the PC layer.* **B**. *Autolysosomes (arrowheads) in a dystrophic PC-like, myelinated axonal profile in the internal granular layer.* **C**. *Autophagic vacuoles and autolysosomes in a PC-like somato-dendritic profile.* **D**. *Autophagic PC-like myelinated axon (*). Scale bars = 2 μm.*

still more in Ngsk $Prnp^{0/0}$ cerebella (16.36 ± 7.9) compared with $Bax^{-/-}$;Ngsk $Prnp^{0/0}$ (5.08 ± 5) cerebella, and there was a significant increase from 6.5–7 (14.38 ± 7.8) to 12 months of age. The increased amount of autophagic PC axons in $Bax^{-/-}$;Ngsk $Prnp^{0/0}$ cerebella was stable during this same period (3.9 ± 5.6 at 6.5–7 months; 5.08 ± 5.1 at 12 months), suggesting that the initiation of axonal autophagy peaks at 6.5–7 months of age (**Figure 12**) [135, 171, 173–176]. In agreement, an examination of autophagy in the presynaptic terminals of PCs impinging on the somato-dendritic compartments of the deep nuclear neurons in the fastigial, interposed and dentate

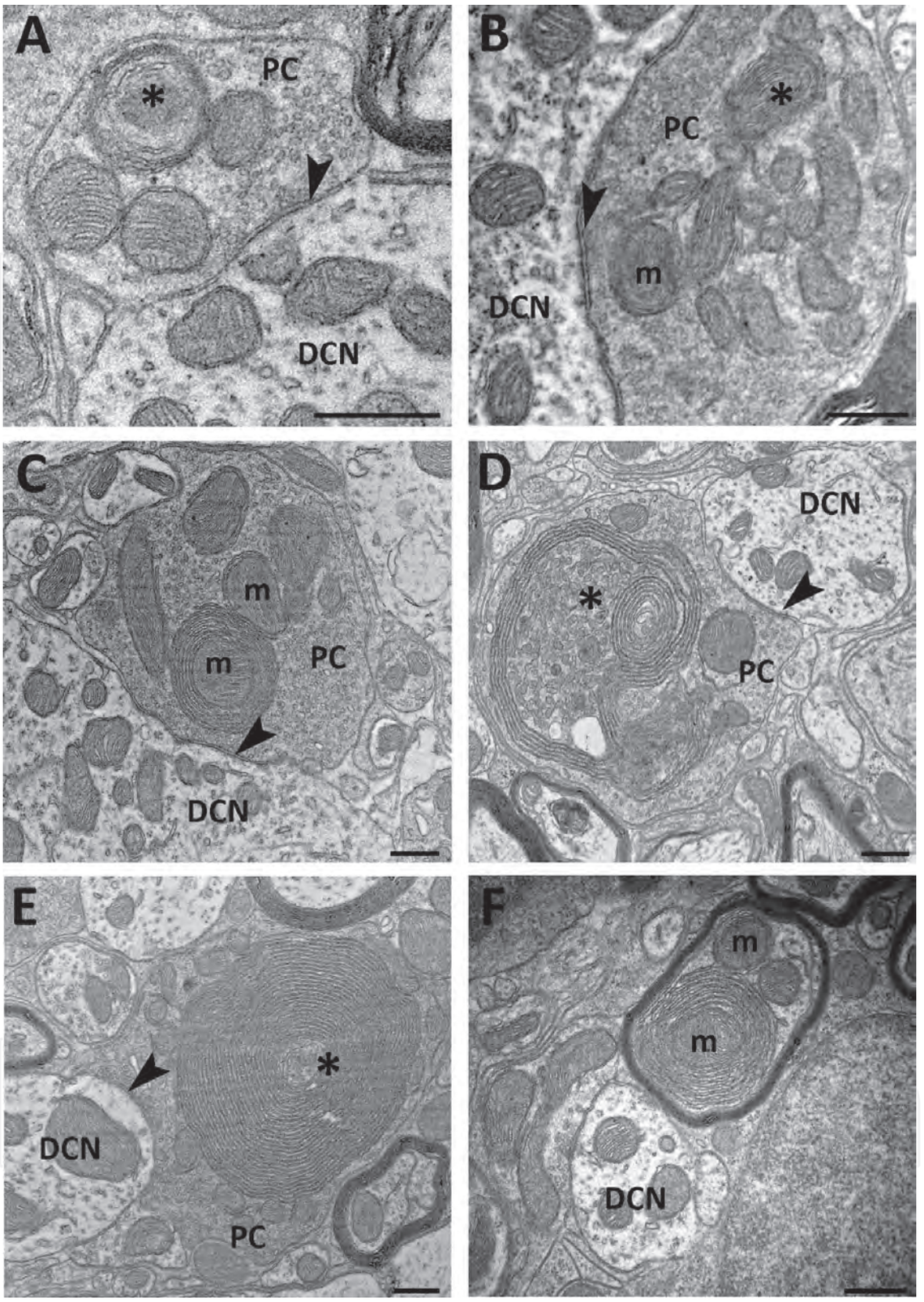

Figure 14.
Autophagy in the deep cerebellar nuclei of 13 month-old Ngsk (A, C–F) and 10 month-old ZH-I (B) Prnp$^{o/o}$ mice. **A–E.** *PC presynaptic boutons establishing symmetrical synapses (arrowheads) with somato-dendritic profiles of deep cerebellar neurons (DCN) and containing different stages of double-membrane wraps sequestrating neuroplasm (* in A, B, D, E) and mitochondria (m in C, F).* **F.** *Myelinated PC-like axon with mitophagic profiles. Scale bars = 500 nm.*

deep cerebellar nuclei, revealed a significantly greater amount of autophagic PC presynaptic boutons in the deep nuclei of all mutants compared to control *Bax*$^{+/+}$;*Prnp*$^{+/+}$ mice (**Figure 14**).

The absence of BAX not only protected some PCs from neurotoxicity in the cerebellum of the Ngsk $Prnp^{0/0}$ mice [121], but also decreased the number of autophagic neurons suggesting that the PCs rescued by *Bax* deficiency do not display activated autophagy, whereas the autophagic PCs in the $Bax^{-/-}$;Ngsk $Prnp^{0/0}$ cerebellum are likely to result from PrP-deficiency as in the ZH-I $Prnp^{0/0}$ cerebellum. Nevertheless, the persistent loss of $Bax^{-/-}$;Ngsk $Prnp^{0/0}$ PCs could result from an increased sensitivity of these PCs to the Ngsk condition compared to ZH-I $Prnp^{0/0}$ PCs.

The complex pattern of neuronal death observed in neurodegenerative diseases is believed to involve an extensive interplay between the major cell death pathways [177, 178]. This is likely the case in prion-infected, as well as PrP-deficient neurons such as PCs. We further investigated PC death in Ngsk $Prnp^{0/0}$ and ZH-I $Prnp^{0/0}$ COCS by measuring PC survival and development using morphometric methods [179] in COCS from these PrP-deficient mice. Similar timing and amplitude of PC growth impairment and death were observed in all PrP-deficient genotypes. Indeed, PC surface, perimeter, and dendritic extension increased between 7 and 21 DIV in the wild-type COCS, while no significant variation of surface and perimeter could be measured in the PrP-deficient mutant COCS during this period (**Figure 15**). Similarly, wild-type and PrP-deficient PCs displayed equivalent maximal dendritic extension after 7 days *ex vivo*, but wild-type PCs continued to increase their maximal dendritic length until 21 DIV, while the dendrites of PrP-deficient PCs did not grow during this period [14, 180]. Thus, PrP-deficient PCs exhibit a similar developmental deficit which seems to be independent of Dpl expression in COCS.

The neurotoxic effects of PrP-deficiency were quantitatively analyzed by counting PCs at 3, 5, 7, 12, and 21 days in COCS from wild-type, Ngsk $Prnp^{+/0}$, Ngsk $Prnp^{0/0}$, and ZH-I $Prnp^{0/0}$. Whereas, wild-type PCs' numbers remained stable during the whole period, severe PC loss (68–69%) had occurred at 7 DIV and slightly increased up to 21 DIV in all PrP-deficient mutant COCS. PC loss displayed similar kinetics and amplitude in Ngsk $Prnp^{+/0}$, Ngsk $Prnp^{0/0}$, and ZH-I $Prnp^{0/0}$ COCS suggesting that despite detectable levels of 15–20 kDa glycosylated form of Dpl in the Ngsk $Prnp^{0/0}$ COCS (**Figure 16**), it may be not implicated in PC death in *ex vivo* cultures.

Furthermore, at the ultrastructural level, whereas autophagic organelles were rare in wild-type PCs after 7 and 12 DIV, Ngsk $Prnp^{0/0}$ PCs contained numerous autophagosomes and autophagolysosomes at different maturation stages (**Figure 17**). During the period of PC death in the $Prnp^{0/0}$ COCS (i.e., 3, 5, and 7 DIV) Western blotting of apoptotic and autophagic markers revealed a 4- to 5-fold increase in markers of autophagosomal formation such as LC3B-II (at 5 DIV), p62, and beclin-1 (at 3 and 5 DIV) in the ZH-I and Ngsk $Prnp^{0/0}$ COCS and the lysosomal receptor LAMP-1 in the Ngsk $Prnp^{0/0}$ COCS at 7 DIV (**Figure 18**). Increased amounts of activated caspase-3 indicated the apoptosis in protein extracts of COCS from both $Prnp^{0/0}$ genotypes as early as 3DIV [14].

This morphometric and quantitative analysis of COCS suggests that PrP-deficiency, rather than Dpl neurotoxicity, is responsible for the neuronal growth deficit and loss *ex vivo*. Indeed, the neurotoxic properties of Dpl did not seem to contribute to Ngsk PC loss in the COCS, whereas Dpl-induced PC loss is detectable in 6-month-old Ngsk $Prnp^{0/0}$ mice. A possible explanation for this difference is that COCS are not mature enough to model 6-month-old cerebellar tissue. Nevertheless, in Ngsk $Prnp^{0/0}$ and ZH-I $Prnp^{0/0}$ COCs, activation of autophagy and apoptosis is contemporaneous with the atrophy and death of PCs during the first week of culture suggesting that PrP-deficiency is solely responsible for neuronal death in this

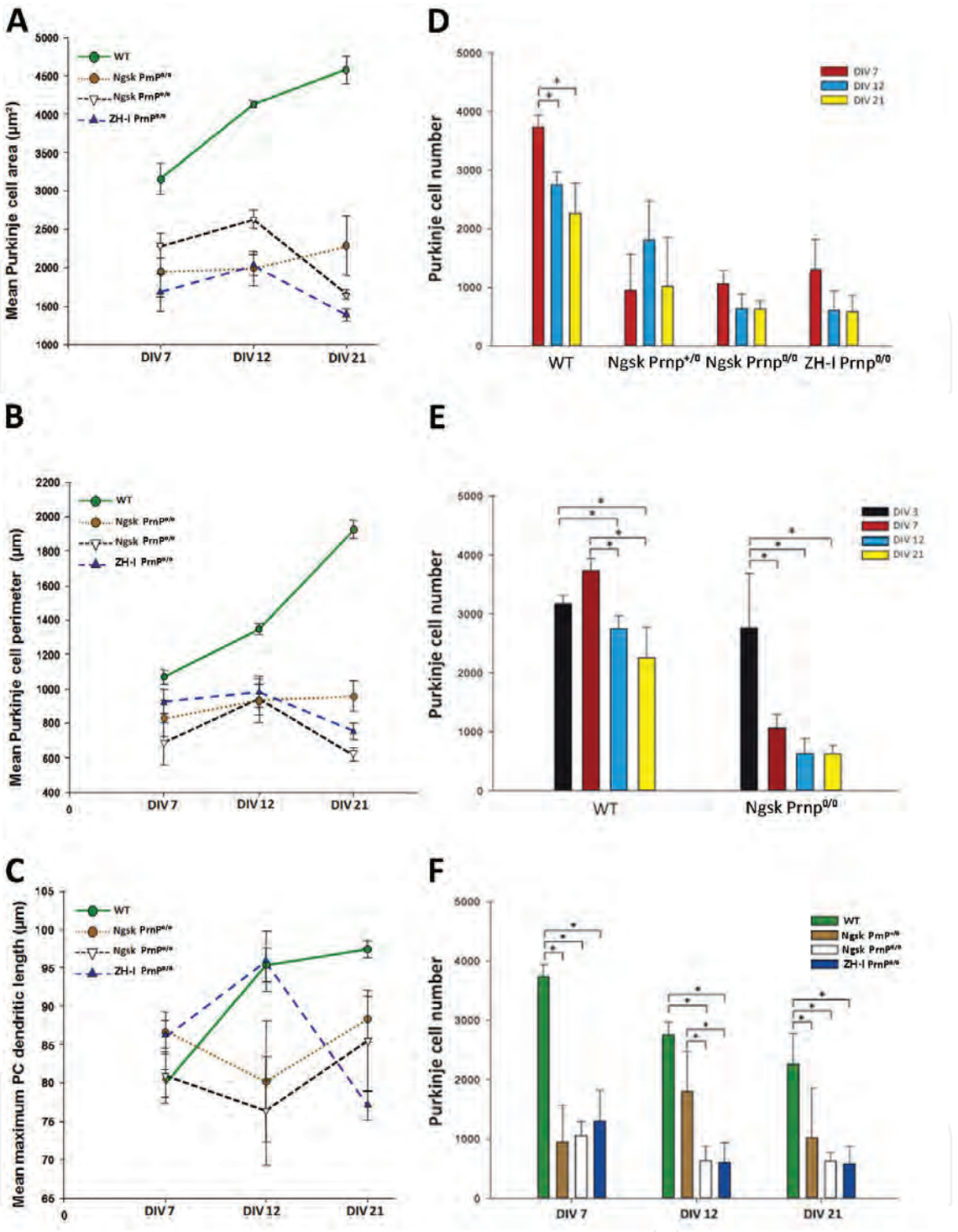

Figure 15.
PC growth deficits and loss in PrP-deficient COCS. **A**, **B**. *PC area (A) and perimeter (B) of WT PCs increased from DIV7 to DIV21, whereas both dimensions in Ngsk Prnp$^{+/0}$, Ngsk Prnp$^{0/0}$ and ZH-I Prnp$^{0/0}$ PCs did not change during the same period. A. At DIV7, WT PC area was larger than area of PrP-deficient PCs.* **C**. *While the longest dendrite of WT PCs had significantly grown from DIV7 to DIV21, the longest dendrite of PrP-deficient PCs displayed similar growth impairment suggesting that in both Ngsk and ZH-I conditions, PrP-deficiency is responsible for PC growth deficits.* **D–F**. *PC loss occurred progressively during the DIV7-DIV21 period in WT COCS (40% at DIV21) while similar loss of PrP-deficient PCs had occurred in the Ngsk Prnp$^{+/0}$, Ngsk Prnp$^{0/0}$ (40%) and ZH-I Prnp$^{0/0}$ (55%) COCS as early as DIV7. E. The Ngsk Prnp$^{0/0}$ COCS had lost many more PCs than the WT COCS over the DIV3-DIV7 period indicating a neurotoxic effect during this period that is attributable to PrP-deficiency since the Ngsk and the ZH-I conditions induced similar neuronal loss at DIV7.*

ex vivo system and that PrP^{c} is neuroprotective for cerebellar PCs. As ZH-I *Prnp*$^{0/0}$ PCs survive *in vivo*, PC death in ZH-I *Prnp*$^{0/0}$ and Ngsk *Prnp*$^{0/0}$ COCS could result from a noxious exacerbation of PrP-deficiency by *ex vivo* conditions.

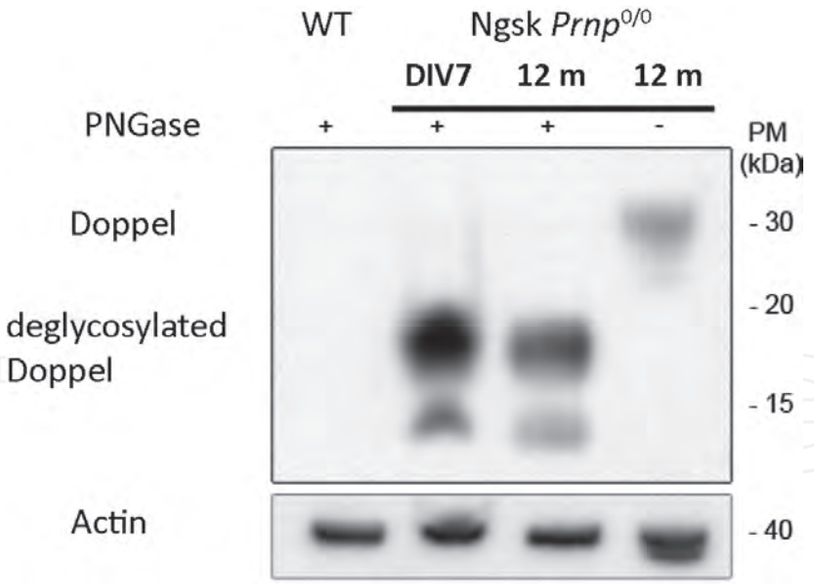

Figure 16.
Western blot of Dpl in Ngsk Prnp$^{0/0}$ DIV7 COCS and 12 month-old mouse cerebellum. Dpl was detected in a Ngsk Prnp$^{0/0}$ COCS at DIV7 and in situ in the cerebellar extract from a 12 month-old Ngsk Prnp$^{0/0}$ mouse but not in the cerebellum of a wild-type (WT) mouse. Dpl migrates at 15–20 kDa after deglycosylation by peptide N-glucosidase (PNGase).

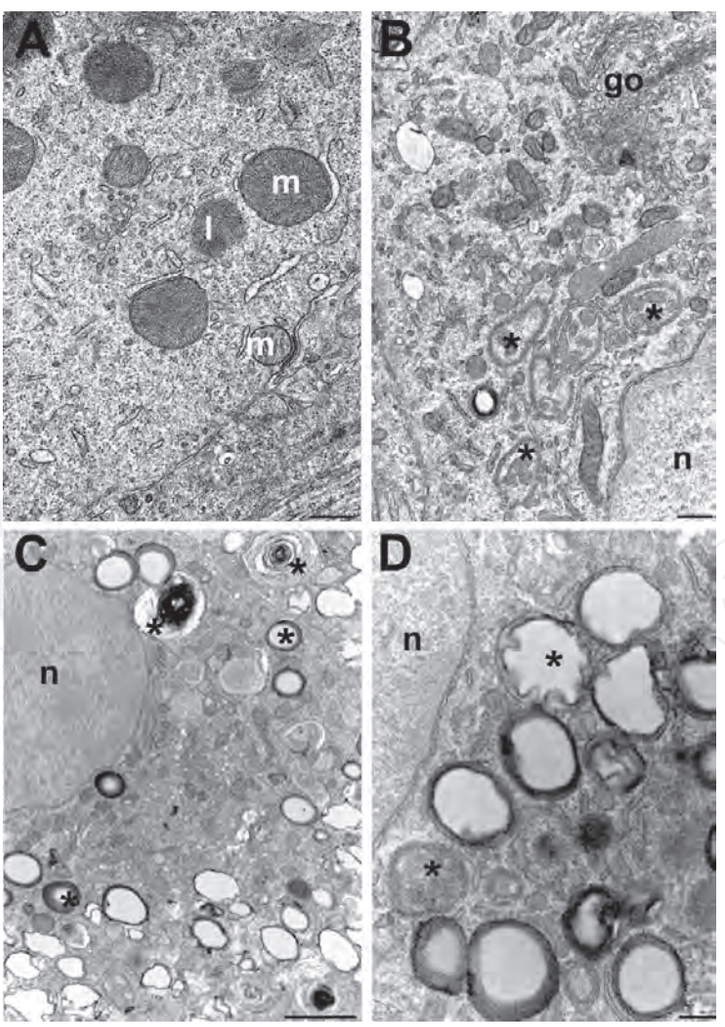

Figure 17.
Autophagy in Ngsk Prnp$^{0/0}$ PCs ex vivo. **A**. *PC cytoplasm in a 12 DIV WT COCS. m, mitochondrion; l, lysosome. Scale bar = 500 nm.* **B–D**. *Autophagic PC cytoplasm in 7 DIV Ngsk Prnp$^{0/0}$ COCSs. Asterisks indicate nascent autophagic vacuoles in B and different maturation stages of autophagolysosomes in C and D. n, nucleus. Scale bar = 2 μm.*

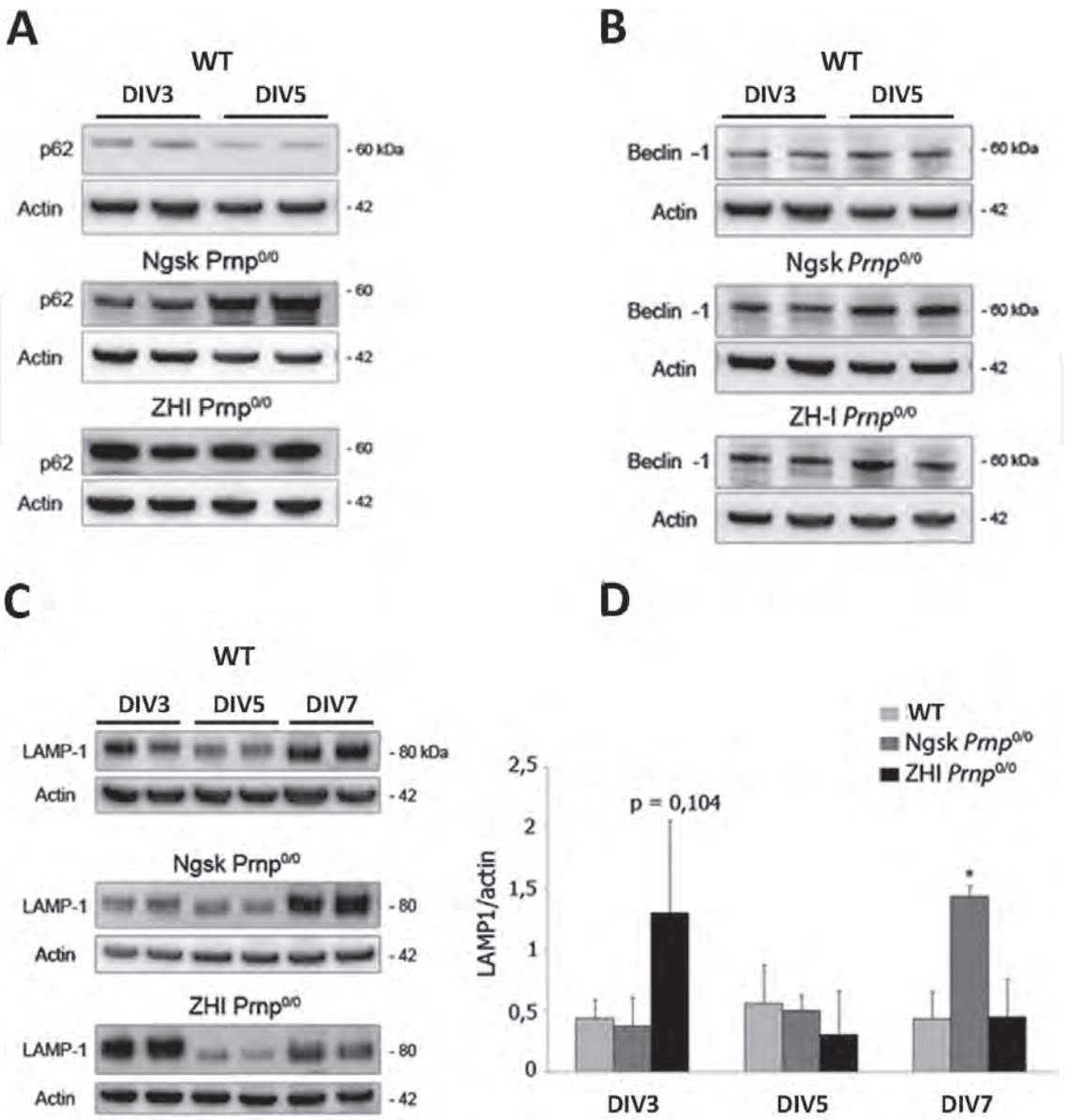

Figure 18.
Western blot of autophagic markers p62, beclin-1 and LAMP-1. **A.** *p62 and* **B.** *Beclin-1. The markers were weakly expressed in WT COCS, but increased in DIV3 and DIV5 COCS from PrP-deficient mice.* **C, D.** *LAMP-1 did not vary in WT and ZH-1 COCS from DIV3 to DIV7, but increased in DIV7 Ngsk Prnp$^{0/0}$ COCS indicating increased lysosomal activity ($p < 0.05$; $n = 3$ mice/genotype and DIV).*

4. Conclusion

Although the contribution of apoptosis to prion-induced death of central neurons including cerebellar ones is strongly supported, our studies of scrapie-infected PCs show that although caspase-3 is activated, the pro-apoptotic BAX/BCL-2-dependent mitochondrial pathway is not involved in the prion-induced death of these neurons. This is also the case for BSE-induced death of hippocampal and thalamic neurons [119], suggesting that prions exert neurotoxicity through BAX-independent activation of caspase-3. Ultrastructural evidence of ER stress and robust autophagy in the scrapie-infected cerebellar neurons both *in vivo* and *ex vivo* implicate them in these BAX-independent neurotoxic mechanisms. Furthermore, the autophagic blockade resulting from prion protein-deficiency in ZH-I and Ngsk *Prnp*$^{0/0}$ mice may contribute to neuronal death in infectious prion-diseased cerebellar neurons. In Ngsk *Prnp*$^{0/0}$ cerebellar neurons, Dpl neurotoxicity and PrP-deficiency contribute to neuronal death probably through an interplay between autophagic blockade and BAX-dependent apoptosis.

DOI: http://dx.doi.org/10.5772/intechopen.80701

Author details

Audrey Ragagnin[1], Qili Wang[1], Aurélie Guillemain[1], Siaka Dole[1], Anne-Sophie Wilding[1], Valérie Demais[1,2], Cathy Royer[1,2], Anne-Marie Haeberlé[1], Nicolas Vitale[1], Stéphane Gasman[1], Nancy Grant[1] and Yannick Bailly[1*]

1 Intracellular Membrane Trafficking in the Nervous and Neuroendocrine System, INCI, CNRS UPR3212, University of Strasbourg, Strasbourg, France

2 In Vitro Imaging Platform, CNRS UPS 3156, University of Strasbourg, Strasbourg, France

*Address all correspondence to: byan@inci-cnrs.unistra.fr

References

[1] Collinge J. Prion diseases of human and animals: Their causes and molecular basis. Annual Review of Neuroscience. 2001;**24**:519-550

[2] Morales R. Prion strains in mammals: Different conformations leading to disease. PLoS Pathogens. 2017;**13**:e1006323. DOI: 10.1371/journal.ppat.1006323

[3] Ironside JW, Ritchie DL. Head MW prion diseases. Handbook of Clinical Neurology. 2018;**145**:393-403. DOI: 10.1016/B978-0-12-802395-2.00028-6

[4] Babelhadj B, Di Bari MA, Pirisinu L, Chiappini B, Gaouar SBS, Riccardi G, et al. Prion disease in dromedary camels, Algeria. Emerging Infectious Diseases. Jun 2018;**24**(6):1029-1036. DOI: 10.3201/eid2406.172007

[5] Prusiner S. Novel proteinaceous infection particles cause scrapie. Science. 1982;**216**:136-144

[6] Brandner S, Raeber A, Sailer A, Blättler T, Fischer M, Weissmann C, et al. Normal host prion protein (PrPC) is required for scrapie spread within the central nervous system. Proceedings of the National Academy of Sciences of the United States of America. 1996;**93**:13148-13151

[7] Aguzzi A, Polymenidou M. Mammalian prion biology: One century of evolving concepts. Cell. 2004;**116**:313-327

[8] Büeler HR, Fischer M, Lang Y, Bluethmann H, Lipp HP, DeArmond SJ, et al. Normal development and behaviour of mice lacking the neuronal cell-surface PrP protein. Nature. 1992;**356**:577-582. DOI.org/10.1038/356577a0

[9] Manson JC, Clarke AR, Hooper ML, Aitchison L, McConnell I, Hope J. 129/Ola mice carrying a null mutation in PrP that abolishes mRNA production are developmentally normal. Molecular Neurobiology. 1994;**8**:121-127

[10] Nuvolone M, Hermann M, Scorce S, Russo G, Tiberi C, Schwarz P, et al. Strictly co-isogenic C57BL/6J-*Prnp*$^{-/-}$ mice: A rigorous resource for prion science. The Journal of Experimental Medicine. 2016;**213**:313-327

[11] Büeler H, Aguzzi A, Sailer A, Greiner RA, Autenried P, Aguet M, et al. Mice devoid of PrP are resistant to scrapie. Cell. 1993;**73**:1339-1347

[12] Mallucci GR, Ratte S, Asante EA, Linehan J, Gowland I, Jefferys JGR, et al. Post-natal knockout of prion protein alters hippocampal CA1 properties but does not result in neurodegeneration. The EMBO Journal. 2002;**21**:202-210

[13] Wulf MA, Senatore A, Aguzzi A. The biological function of the cellular prion protein: An update. BMC Biology. 2017;**15**:34. DOI: 10.1186/s12915-017-0375-5

[14] Ragagnin A, Guillemain A, Grant NJ, Bailly Y. Neuronal autophagy and prion proteins. In: Bailly YJR, editor. Autophagy—A Double-Edged Sword—Cell Survival or Death? Rijeka, Croatia: InTech Publisher; 2013. pp. 377-419

[15] Legname G. Elucidating the function of the prion protein. PLoS Pathogens. Aug 31, 2017;**13**(8):e1006458. DOI: 10.1371/journal.ppat.1006458

[16] Saa P, Harris D, Cervenakova L. Mechanisms of prion-induced neurodegeneration. Expert Reviews in Molecular Medicine. Apr 8, 2016;**18**:e5. DOI: 10.1017/erm2016.8

[17] Stahl N, Borchelt DR, Hsiao K, Prusiner SB. Scrapie prion protein

contain a phosphatidylinositol glycolipid. Cell. 1987;**51**:229-240

[18] Lainé J, Marc M, Sy M, Axelrad H. Cellular and subcellular morphological localization of normal prion protein in rodent cerebellum. The European Journal of Neuroscience. 2001;**14**:47-56

[19] Bailly Y, Haeberlé AM, Blanquet-Grossard F, Chasserot-Golaz S, Grant N, Schulze T, et al. Prion protein (PrP^c) immunocytochemistry and expression of the green fluorescent protein reporter gene under the control of bovine PrP gene promoter in the mouse brain. The Journal of Comparative Neurology. 2004;**473**:244-269

[20] Jacobson K, Dietrich C. Looking at lipid rafts? Trends in Cell Biology. 1999;**9**:87-91

[21] Mouillet-Richard S, Ermonval M, Chebassier C, Laplanche JL, Lehmann S, Launay JM, et al. Signal transduction through prion protein. Science. 2000;**289**:1925-1928. Epub Sep 16, 2000. DOI: 10.1126/science.289.5486.1925

[22] Linden R, Martins VR, Prado MA, Cammarota M, Izquierdo I, Brentani RR. Physiology of the prion protein. Physiological Reviews. 2008;**88**:673-728

[23] Bendheim PE, Brown HR, Rudelli RD, Scala LJ, Goller NL, Wen GY, et al. Nearly ubiquitous tissue distribution of the scrapie agent precursor protein. Neurology. 1992;**42**:149

[24] Haeberlé AM, Ribaut-Barassin C, Bombarde G, Mariani J, Hunsmann G, Grassi J, et al. Synaptic prion protein immuno-reactivity in the rodent cerebellum. Microscopy Research and Technique. 2000;**50**:66-75

[25] Salès N, Rodolfo K, Hässig R, Faucheux B, Di Giamberardino L, Moya KL. Cellular prion protein localization in rodent and primate brain. The European Journal of Neuroscience. 1998;**10**:2464-2471

[26] Salès N, Hässig R, Rodolfo K, Di Giamberardino L, Traiffort E, Ruat M, et al. Developmental expression of the cellular prion protein in elongating axons. The European Journal of Neuroscience. 2002;**15**:1163-1177

[27] Fournier JG, Escaig-Haye F, Billette de Villemeur T, Robain O. Ultrastructural localization of cellular prion protein (PrPc)in synaptic boutons of normal hamster hippocampus. Comptes Rendus de l'Académie des Sciences, Paris. 1995;**318**:339-344

[28] Herms J, Tings T, Gall S, Madlung A, Giese A, Siebert H, et al. Evidence of presynaptic location and function of the prion protein. The Journal of Neuroscience. 1999;**19**:8866-8875

[29] Mironov A, Latawiec D, Wille H, Bouzamondo-Bernstein E, Legname G, Williamson RA, et al. Cytosolic prion protein in neurons. The Journal of Neuroscience. 2003;**23**:183-193

[30] Borchelt DR, Koliatsos VE, Guarnieri M, Pardo CA, Sisodia SS, Price DL. Rapid anterograde axonal transport of the cellular prion glycoprotein in the peripheral and central nervous systems. The Journal of Biological Chemistry. 1994;**269**:14711-14714

[31] Moya K, Hässig R, Créminon C, Laffont I, Di Giamberardino L. Enhanced detection and retrograde axonal transport of PrPc in peripheral nerve. Journal of Neurochemistry. 2003;**88**:155-160

[32] Jeffrey M, Halliday WG, Bell J, Johnston AR, McLeod NK, Ingham C, et al. Synapse loss associated with abnormal PrP precedes neuronal degeneration

in the scrapie-infected murine hippocampus. Neuropathology and Applied Neurobiology. 2000;**26**:41-54

[33] Siskova Z, Reynolds RA, O'Connor V, Perry VH. Brain region specific presynaptic and postsynaptic degeneration are early components of neuropathology in prion diseases. PLoS One. 2013;**8**(1):e55004. DOI: 110.1371/journal.pone.0055004

[34] Senatore A, Colleoni S, Verderio C, Restelli E, Morini R, Condliffe SB, et al. Mutant PrP suppresses glutamatergic neurotransmission in cerebellar granule neurons by impairing membrane delivery of VGCC α2δ-1 subunit. Neuron. 2012;**74**:300-313. DOI: 10.1016/j.neuron.2012.02.027

[35] Khosravani H, Zhang Y, Tsutsui S, Hameed S, Altier C, Hamid J, et al. Prion protein attenuates excitotoxicity by inhibiting NMDA receptors. The Journal of Cell Biology. 2008;**181**:551-565. DOI: 10.1083/jcb.200711002

[36] Mercer RCC, Ma L, Watts JC, Strome R, Wohlgemuth S, Yang J, et al. The prion protein modulates A-typeK+ currents mediated by Kv4.2 complexes through dipeptidyl aminopeptidase-like protein 6. The Journal of Biological Chemistry. 2013;**288**:37241-37255

[37] Stys PK, You H, Zamponi GW. Copper-dependent regulation of NMDA receptors by cellular prion protein: Implications for neurodegenerative disorders. The Journal of Physiology. 2012;**590**:1357-1368. DOI: 10.1113/jphysiol.2011.225276

[38] Gasperini L, Meneghette E, Pastore B, Benetti F, Legname G. Prion protein and copper cooperatively protect neurons by modulating NMDA receptors through S-nitrosylation. Antioxidants & Redox Signaling. 2015;**22**:772-784

[39] Muller WE, Ushijima H, Schroder HC, Forrest JM, Schatton WF, Rytik PG, et al. Cytoprotective effect of NMDA receptor antagonists on prion protein (PrioSc)-induced toxicity in rat cortical cell cultures. European Journal of Pharmacology. 1993;**246**:261-267

[40] Resenberger UK, Harmeier A, Woerner AC, Goodman JL, Muller V, Krishnan R, et al. The cellular prion protein mediates neurotoxic signalling of eIF2α-sheet-rich conformers independent of prion replication. The EMBO Journal. 2011;**30**:2057-2070. DOI: 10.1038/emboj.2011.86

[41] Carulla P, Llorens F, Matamoros-Angles A, Aguilar-Calvo P, Espinosa JC, Gavín R, et al. Involvement of PrP(C) in kainate-induced excitotoxicity in several mouse strains. Scientific Reports. 2015;**5**:11971. DOI: 10.1038/srep11971

[42] Kleene R, Loers G, Langer J, Frobert Y, Buck F, Schachner M. Prion protein regulates glutamate-dependent lactate transport of astrocytes. The Journal of Neuroscience. 2007;**27**:12331-12340

[43] Watt NT, Taylor DR, Kerrigan TL, Griffiths HH, Rushworth JV, Whitehouse IJ, et al. Prion protein facilitates uptake of zinc into neuronal cells. Nature Communications. 2012;**3**:1134

[44] Beraldo FH, Arantes CP, Santos TG, Machado CF, Roffe M, Hajj GN, et al. Metabotropic glutamate receptors transducer signals for neurite outgrowth after binding of the prion protein to laminin γ1 chain. The FASEB Journal. 2011;**25**:265-279

[45] Um JW, Kaufman AC, Kostylev M, Heiss JK, Stagi M, Takahashi H, et al. Metabotropic glutamate receptor 5 is a coreceptor for Alzheimer eIF2α oligomer bound to cellular prion protein. Neuron. 2013;**79**:887-902

[46] Lauren J, Gimbel DA, Nygaard HB, Gilbert JW, Strittmatter SM. Cellular prion protein mediates impairment of synaptic plasticity by amyloid-β oligomers. Nature. 2009;**457**:1128-1132

[47] Um JW, Nygaard HB, Heiss JK, Kostylev MA, Stagi M, Wortmeyer A, et al. Alzheimer amyloid-β oligomer bound to postsynaptic prion protein activates Fyn to impair neurons. Nature Neuroscience. 2012;**15**:1227-1235

[48] Winklhofer KF, Tatzelt J, Haass C. The two faces of protein misfolding: Gain- and loss-of-function in neurodegenerative diseases. The EMBO Journal. 2008;**27**:336-349

[49] Harris DA, True HL. New insights into prion structure and toxicity. Neuron. 2006;**50**:353-357

[50] Moreno JA, Radford H, Peretti D, Steinert JR, Verity N, Martin MG, et al. Sustained translational repression by eIF2α-P mediates prion neurodegeneration Nature. 2012;**485**:507-511. DOI: 10.1038/nature11058. Erratum in: Nature. 2014;**511**:370

[51] McKinnon C, Goold R, Andre R, Devoy A, Ortega Z, Moonga J, et al. Prion-mediated neurodegeneration is associated with early impairment of the ubiquitin-proteasome system. Acta Neuropathologica. 2016;**131**:411-425. DOI: 10.1007/s00401-015-1508-y

[52] Hegde RS, Tremblay P, Groth D, DeArmond SJ, Prusiner SB, Lingappa VR. Transmissible and genetic prion diseases share a common pathway of neurodegeneration. Nature. 1999;**402**:822-826

[53] Moreno JA, Halliday M, Molloy C, Radford H, Verity N, Axten JM, et al. Oral treatment targeting the unfolded protein response prevents neurodegeneration and clinical disease in prion-infected mice. Science Translational Medicine. Oct 9, 2013;**5**(206):206ra138. DOI: 10.1126/scitranslmed.3006767

[54] Telling GC. The importance of prions. PLoS Pathogens. 2013;**9**:e1003090. DOI: 10.1371/journal.ppat.1003090

[55] Piétri M, Dakowski C, Hannaoui S, Alleaume-Buteaux A, Hernandez-Rapp J, Ragagnin A, et al. PDK1 decreases TACE-mediated α-secretase activity and promotes disease progression in prion and Alzheimer's diseases. Nature Medicine. 2013;**19**:1124-1131

[56] Alleaume-Buteaux A, Nicot S, Piétri M, Baudry A, Dakowski C, Tixador P, et al. Double-edge sword of sustained ROCK activation in prion diseases through neuritogenesis defects and prion accumulation. PLoS Pathogens. 2015;**11**:e1005073

[57] Ezpeleta J, Boudet-Devaud F, Piétri M, Baudry A, Baudouin V, Alleaume-Buteaux A, et al. Protective role of cellular prion protein against TNFα-mediated inflammation through TACE α-secretase. Scientific Reports. 2017;**7**:7671. DOI: 10.1038/s41598-017-08110-x

[58] Hilton KJ, Cunningham C, Reynolds RA, Perry VH. Early hippocampal synaptic loss precedes neuronal loss and associates with early behavioural deficits in three distinct strains of prion disease. PLoS One. 2013;**8**:e68062. DOI: 10.1371/journal.pone.0068062

[59] Ragagnin A, Ezpeleta J, Guillemain A, Boudet-Devaud F, Haeberlé A-M, Demais V, et al. Cerebellar compartmentation of prion pathogenesis. Brain Pathology. 2017;**28**:240-263. DOI: 10.1111/bpa.12503

[60] Kristiansen M, Deriziotis P, Dimcheff DE, Jackson GS, Ovaa H, Naumann H, et al. Disease-associated prion protein oligomers inhibit the 26S proteasome. Molecular Cell. 2007;**26**:175-188

[61] Pietri M, Caprini A, Mouillet-Richard S, Pradines E, Ermonval M, Grassi J, et al. Overstimulation of PrPC signaling pathways by prion peptide 106-126 causes oxidative injury of bioaminergic neuronal cells. The Journal of Biological Chemistry. 2006;**281**:28470-28479

[62] Heiseke A, Aguib Y, Schatzl HM. Autophagy, prion infection and their mutual interactions. Current Issues in Molecular Biology. 2010;**12**:87-98

[63] Sikorska B. Mechanisms of neuronal death in transmissible spongiform encephalopathies. Folia Neuropathologica. 2004;**42**(Suppl B): 89-95

[64] Liberski PP, Brown DR, Sikorska B, Caughey B, Brown P. Cell death and autophagy in prion diseases (transmissible spongiform encephalopathies). Folia Neuropathologica. 2008;**46**:1-25

[65] Sikorska B, Liberski PP, Giraud P, Kopp N, Brown P. Autophagy is a part of ultrastructural synaptic pathology in Creutzfeldt-Jakob disease: A brain biopsy study. The International Journal of Biochemistry & Cell Biology. 2004;**36**:2563-2573

[66] Bruce ME, McBride PA, Jeffrey M, Scott JR. PrP in pathology and pathogenesis in scrapie-infected mice. Molecular Neurobiology. 1994;**8**:105-112

[67] Jeffrey M, McGovern G, Sisó S, González L. Cellular and sub-cellular pathology of animal prion diseases: Relationship between morphological changes, accumulation of abnormal prion protein and clinical disease. Acta Neuropathologica. 2011;**121**:113-134

[68] DeArmond SJ, Sánchez H, Yehiely F, Qiu Y, Ninchak-Casey A, Daggett V, et al. Selective neuronal targeting in prion disease. Neuron. 1997;**19**:1337-1348

[69] Lawson VA, Collins SJ, Masters CL, Hill AF. Prion protein glycosylation. Journal of Neurochemistry. 2005;**93**:793-801

[70] Beekes M, McBride PA. The spread of prions through the body in naturally acquired transmissible spongiform encephalopathies. The FEBS Journal. 2007;**274**:588-605

[71] Fraser H, Dickinson AG. The sequential development of the brain lesion of scrapie in three strains of mice. Journal of Comparative Pathology. 1968;**78**:301-311

[72] Guentchev M, Wanschitz J, Voigtländer T, Flicker H, Budka H. Selective neuronal vulnerability in human prion diseases. Fatal familial insomnia differs from other types of prion diseases. American Journal of Pathology. 1999;**155**:1453-1457

[73] Somerville RA. How independent are TSE agents from their hosts? Prion. 2013;**7**:272-275. DOI: 10.4161/pri.25420

[74] Fraser H. Neuropathology of Scrapie: The Precision of Lesion and their Diversity. Slow Transmissible Diseases of the Nervous System. NY: Academic Press; 1979. pp. 387-406

[75] Kim YS, Carp RI, Callahan SM, Natelli M, Wisniewski HM. Vacuolization, incubation period and survival time analyses in three mouse genotypes injected stereotactically in three brain regions

with the 22L scrapie strain. Journal of Neuropathology and Experimental Neurology. 1990;**49**:106-113

[76] Lucassen PJ, Williams A, Chung WCJ, Fraser H. Detection of apoptosis in murine scrapie. Neuroscience Letters. 1995;**198**:185-188

[77] Williams A, Lucassen P, Ritchie D, Bruce M. PrP deposition, microglial activation and neuronal apoptosis in murine scrapie. Experimental Neurology. 1997;**144**:433-438

[78] Fraser J, Halliday W, Brown D, Belichenko P, Jeffrey M. Mechanisms of scrapie-induced neuronal cell death. In: Court L, Dodet B, editors. Transmissible Subacute Spongiform Encephalopathies: Prion Diseases. Paris: Elsevier; 1996. pp. 107-112

[79] Haw JJ, Gray F, Baudrimont M, Escourolle R. Cerebellar changes in 50 cases of Creutzfeldt-Jakob disease with emphasis on granule cell atrophy variant. Acta Neuropathologica. 1981;**7**:196-198

[80] Berciano J, Berciano MT, Polo JM, Figols J, Ciudad J, Lafarga M. Creutzfeldt-Jakob disease with severe involvement of cerebral white matter and cerebellum. Wirschows Archiv. 1990;**417**:533-538

[81] Budka H, Aguzzi A, Brown P, Brucher JM, Bugiani O, Gullotta F, et al. Neuropathological diagnostic criteria for Creutzfeldt-Jakob disease (CJD) and other human spongiform encephalopathies (prion disease). Brain Pathology. 1995;**5**:459-466

[82] Schulz-Schaeffer WJ, Giese A, Windl O, Kretzschmar HA. Polymorphism at codon 129 of the prion protein gene determines cerebellar pathology in Creutzfeldt-Jakob disease. Clinical Neuropathology. 1996;**15**:353-357

[83] Yang Q, Hashizume Y, Yoshida M, Wang Y. Neuropathological study of cerebellar degeneration in prion disease. Neuropathology. 1999;**19**:33-39

[84] Armstrong R, Ironside J, Lantos P, Cairns N. A quantitative study of the pathological changes in the cerebellum in 15 cases of variant Creutzfeldt-Jakob disease (vCJD). Neuropathology and Applied Neurobiology. 2009;**35**:36-45. DOI: 10.1111/j.1365-2990.2008.00979.x

[85] Faucheux B, Morain E, Diouron V, Brandel J, Salomon D, Sazdovitch V, et al. Quantification of surviving cerebellar granule neurons and abnormal prion protein (PrPSc) deposition in sporadic Creutzfeldt-Jakob disease supports a pathogenic role for small PrPSc deposits common to the various molecular subtypes. Neuropathology and Applied Neurobiology. 2011;**37**:500-512. DOI: 10.1111/j.1365-2990.2011.01179.x

[86] Parchi P, Strammiello R, Giese A, Kretzschmar H. Phenotypic variability of sporadic human prion disease and its molecular basis: Past, present and future. Acta Neuropathologica. 2011;**121**:91-112. DOI: 10.1007/s00401-010-0779-6

[87] Cali I, Miller CJ, Parisi J, Geschwind M, Gambetti P, Schonberger L. Distinct pathological phenotypes of Creutzfelds-Jakob disease in recipients of prion-contaminated growth hormone. Acta Neuropathologica. 2015;**3**:37-46

[88] Apps R, Hawkes R. Cerebellar cortical organization: A one-map hypothesis. Nature Reviews. Neuroscience. 2009;**10**:670-681. DOI: 10.1038/nrn2698

[89] Reeber SL, White JJ, Georges-Jones NA, Sillitoe RV. Architecture and development of olivo-cerebellar circuit topography. Frontiers in Neural

Circuits. 2013;**6**:115. DOI: 10.3389/fncir.2012.00115

[90] Brochu G, Maler L, Hawkes R. Zebrin II: A polypeptide antigen expressed selectively by Purkinje cells reveals compartments in rats and fish cerebellum. The Journal of Comparative Neurology. 1990;**291**:538-552

[91] Armstrong R, Cairns N. Spatial patterns of the pathological changes in the cerebellar cortex in sporadic Creutzfeldt-Jakob disease (sCJD). Folia Neuropathologica. 2003;**41**:183-189

[92] Fujita H, Morita N, Furuichi T, Sugihara I. Clustered fine compartmentalization of the mouse embryonic cerebellar cortex and its rearrangement into the postnatal striped configuration. The Journal of Neuroscience. 2012;**32**:15688-15703. DOI: 10.1523/JNEUROSCI.1710-12.2012

[93] Zhou M, Ottenberg G, Sferrazza GF, Lasmézas CI. Highly neurotoxic monomeric alpha-helical prion protein. Proceedings of the National Academy of Sciences of the United States of America. 2012;**109**:3113-3118. DOI: 10.1073/pnas.1118090109

[94] Mallucci G, Ratte S, Asante EA, Linehan J, Gowland I, Jefferys JG, et al. Post-natal knock-out of prion protein alters hippocampal CA1 properties, but does not result in neurodegeneration. The EMBO Journal. 2002;**21**:202-210

[95] Halliday M, Radford H, Mallucci G. Prions: Generation and spread versus neurotoxicity. The Journal of Biological Chemistry. 2014;**289**:19862-19868

[96] Nakagawa T, Zhu H, Morishima N, Li E, Xu J, Bruce A, et al. Caspase-12 mediates endoplasmic reticulum-specific apoptosis and cytotoxicity by amyloid-β. Nature. 2000;**403**:98-103

[97] Hetz C, Russelakis-Carneiro M, Maundrell K, Castilla J, Soto C. Caspase-12 and endoplasmic reticulum stress mediate neurotoxicity of pathological prion protein. The EMBO Journal. 2003;**22**:5435-5445

[98] Soto C, Satani N. The intricate mechanisms of neurodegeneration in priondiseases. Trends in Molecular Medicine. 2011;**17**:14-24

[99] Mukherjee A, Morales-Scheihing D, Gonzalez-Romero D, Green K, Taglialatela G, Soto C. Calcineurin inhibition at the clinical phase of prion disease reduces neurodegeneration, improves behavioral alterations and increases animal survival. PLoS Pathogens. 2010;**6**:e1001138

[100] Sakudo A, Lee DC, Nakamura I, Taniuchi Y, Saeki K, Matsumoto Y, et al. Cell-autonomous PrP-Doppel interaction regulates apoptosis in PrP gene-deficient neuronal cells. Biochemical and Biophysical Research Communications. 2005;**333**:448-454

[101] Kurschner C, Morgan J. The cellular prion protein (PrP) selectively binds to Bcl-2 in the yeast two-hybrid system. Molecular Brain Research. 1995;**30**:165-168

[102] Kurschner C, Morgan J. Analysis of interaction sites in homo- and heteromeric complexes containing Bcl-2 family members and the cellular prion protein. Molecular Brain Research. 1996;**37**:249-258

[103] Laroche-Pierre S, Jodoin J, Leblanc A. Helix 3 is necessary and sufficient for prion protein's anti-Bax function. Journal of Neurochemistry. 2009;**108**:1019-1031

[104] Kuwahara C, Takeuchi AM, Nishimura T, Haraguchi K, Kubosaki A, Matsumoto Y, et al. Prions prevent

neuronal cell-line death. Nature. 1999;**400**:225-226

[105] Kim BH, Lee HG, Choi JK, Kim JI, Choi EK, Carp RI, et al. The cellular prion protein (PrPC) prevents apoptotic neuronal cell death and mitochondrial dysfunction induced by serum deprivation. Brain Research. Molecular Brain Research. 2004;**124**:40-50

[106] Bounhar Y, Zhang Y, Goodyer CG, LeBlanc A. Prion protein protects human neurons against Bax-mediated apoptosis. The Journal of Biological Chemistry. 2001;**276**:39145-39149

[107] Philot T, Drouet B, Pinçon-Raymond M, Vandekerckhove J, Rosseneu M, Chambaz J. A nonfibrillar form of the fusogenic prion protein fragment [118-135] induces apoptotic cell death in rat cortical neurons. Journal of Neurochemistry. 2000;**75**:2298-2308

[108] O'Donovan CN, Tobin D, Cotter TG. Prion protein fragment PrP-(106-126) induces apoptosis via mitochondrial disruption in human neuronal SH-SY5Y cells. The Journal of Biological Chemistry. 2001;**276**:43516-43523

[109] Lin D, Jodoin J, Baril M, Goodyer CG, Leblanc AC. Cytosolic prion protein is the predominant anti-Bax prion protein form: Exclusion of transmembrane and secreted prion protein forms in the anti-Bax function. Biochimica et Biophysica Acta. 2008;**1783**:2001-2012

[110] Giese A, Groschup MH, Hess B, Kretzschmar HA. Neuronal cell death in scrapie-infected mice is due to apoptosis. Brain Pathology. 1995;**5**:213-221

[111] Jesionek-Kupnicka D, Kordek R, Buczyński J, Liberski PP. Apoptosis in relation to neuronal loss in experimental Creutzfeldt-Jakob disease in mice. Acta Neurobiologiae Experimentalis. 2001;**61**:13-19

[112] Gray F, Chrétien F, Adle-Biassette H, Dorandeu A, Ereau T, Delisle MB, et al. Neuronal apoptosis in Creutzfeldt-Jakob disease. Journal of Neuropathology and Experimental Neurology. 1999;**58**:321-328

[113] Ferrer I. Synaptic pathology and cell death in the cerebellum in Creutzfeldt-Jakob disease. Cerebellum. 2002;**1**:213-222

[114] Drew SC, Haigh CL, Klemm HM, Masters CL, Collins SJ, Barnham KJ, et al. Optical imaging detects apoptosis in the brain and peripheral organs of prion-infected mice. Journal of Neuropathology and Experimental Neurology. 2011;**70**:143-150

[115] Cronier S, Carimalo J, Schaeffer B, Jaumain E, Béringue V, Miquel MC, et al. Endogenous prion protein conversion is required for prion-induced neuritic alterations and neuronal death. The FASEB Journal. 2012;**26**:3854-3861

[116] Sisó S, Puig B, Varea R, Vidal E, Acín C, Prinz M, et al. Abnormal synaptic protein expression and cell death in murine scrapie. Acta Neuropathologica. 2002;**103**:615-626

[117] Falsig J, Sonati T, Herrmann US, Saban D, Li B, Arroyo K, et al. Prion pathogenesis is faithfully reproduced in cerebellar organotypic slice cultures. PLoS Pathogens. 2012;**8**:e1002985

[118] Park SK, Choi SI, Jin JK, Choi EK, Kim JI, Carp RI, et al. Differential expression of Bax and Bcl-2 in the brains of hamsters infected with 263K scrapie agent. Neuroreport. 2000;**11**:1677-1682

[119] Coulpier M, Messiaen S, Hamel R, Fernández de Marco M, Lilin T, Eloit M. Bax deletion does not protect neurons from BSE-induced

death. Neurobiology of Disease. 2006;**23**:603-611

[120] Chiesa R, Piccardo P, Dossena S, Nowoslawski L, Roth KA, Ghetti B, et al. Bax deletion prevents neuronal loss but not neurological symptoms in a transgenic model of inherited prion disease. Proceedings of the National Academy of Sciences of the United States of America. 2005;**102**:238-243

[121] Heitz S, Lutz Y, Rodeau J-L, Zanjani H, Gautheron V, Bombarde G, et al. BAX contributes to Doppel-induced apoptosis of prion protein-deficient Purkinje cells. Developmental Neurobiology. 2007;**67**:670-686

[122] Selimi F, Doughty M, Delhaye-Bouchaud N, Mariani J. Target-related and intrinsic neuronal death in Lurcher mutant mice are both mediated by caspase-3 activation. The Journal of Neuroscience. 2000;**20**:992-1000

[123] Zanjani HS, Vogel MW, Martinou JC, Delhaye-Bouchaud N, Mariani J. Postnatal expression of Hu-bcl-2 gene in Lurcher mutant mice fails to rescue Purkinje cells but protects inferior olivary neurons from target-related cell death. The Journal of Neuroscience. 1998;**18**:319-327

[124] Fan H, Favero M, Vogel MW. Elimination of Bax expression in mice increases cerebellar Purkinje cell numbers but not the number of granule cells. The Journal of Comparative Neurology. 2001;**436**:82-91

[125] Zanjani HS, Vogel MW, Delhaye-Bouchaud N, Martinou JC, Mariani J. Increased cerebellar Purkinje cell numbers in mice overexpressing a human bcl-2 transgene. The Journal of Comparative Neurology. 1996;**374**:332-341

[126] Kim YS, Carp RI, Callahan SM, Wisniewski HM. Incubation periods and survival times for mice injected stereotaxically with three scrapie strains in different brain regions. The Journal of General Virology. 1987;**68**:695-702

[127] Zanjani HS, Vogel MW, Delhaye-Bouchaud N, Martinou JC, Mariani J. Increased inferior olivary neuron and cerebellar granule cell numbers in transgenic mice overexpressing the human Bcl-2 gene. Journal of Neurobiology. 1997;**32**:502-516

[128] Moore R. Proteomics analysis of amyloid and nonamylois prion disease phenotype reveals both common and divergent mechanisms of neuropathogenesis. Journal of Proteome Research. 2014;**13**:4620-4634

[129] Falsig J, Julius C, Margalith I, Schwarz P, Heppner FL, Aguzzi A. A versatile prion replication assay in organotypic brain slices. Nature Neuroscience. 2008;**11**:109-117

[130] Campeau JL, Wu G, Bell JR, Rasmussen J, Sim VL. Early increase and late decrease of Purkinje cell dendritic spine density in prion-infected organotypic mouse cerebellar cultures. PLoS One. 2013;**8**:e81776

[131] Wolf H, Hossinger A, Fehlinger A, Büttner S, Sim V, McKenzie D, et al. Deposition pattern and subcellular distribution of disease-associated prion protein in cerebellar organotypic slice cultures infected with scrapie. Frontiers in Neuroscience. Nov 4, 2015;**9**:410. DOI: 10.3389/frins.2015.00410

[132] Webb JL, Ravikumar B, Atkins J, Skepper JN, Rubinsztein DC. Alpha-Synuclein is degraded by both autophagy and the proteasome. The Journal of Biological Chemistry. 2003;**278**:25009-25013

[133] Pickford F, Masliah E, Britschgi M, Lucin K, Narasimhan R, Jaeger PA, et al. The autophagy-related protein

beclin 1 shows reduced expression in early Alzheimer disease and regulates amyloid beta accumulation in mice. The Journal of Clinical Investigation. 2008;**118**:2190-2199

[134] Xu Y, Tian C, Wang SB, Xie WL, Guo Y, Zhang J, et al. Activation of the macroautophagic system in scrapie-infected experimental animals and human genetic prion diseases. Autophagy. 2012;**8**:1604-1620

[135] Heitz S, Grant NJ, Leschiera R, Haeberlé AM, Demais V, Bombarde G, et al. Autophagy and cell death of Purkinje cells overexpressing Doppel in Ngsk Prnp-deficient mice. Brain Pathology. 2010;**20**:119-132

[136] Petersén A, Larsen KE, Behr GG, Romero N, Przedborski S, Brundin P, et al. Expanded CAG repeats in exon 1 of the Huntington's disease gene stimulate dopamine-mediated striatal neuron autophagy and degeneration. Human Molecular Genetics. 2001;**10**:1243-1254

[137] Nixon RA. Autophagy, amyloidogenesis and Alzheimer disease. Journal of Cell Science. 2007;**120**:4081-4091

[138] Spilman P, Podlutskaya N, Hart MJ, Debnath J, Gorostiza O, Bredesen D, et al. Inhibition of mTOR by rapamycin abolishes cognitive deficits and reduces amyloid-beta levels in a mouse model of Alzheimer's disease. PLoS One. 2010;**5**:e9979

[139] Yang DS, Stavrides P, Mohan PS, Kaushik S, Kumar A, Ohno M, et al. Therapeutic effects of remediating autophagy failure in a mouse model of Alzheimer disease by enhancing lysosomal proteolysis. Autophagy. 2011;**7**:788-789

[140] Heiseke A, Aguib Y, Riemer C, Baier M, Schätzl HM. Lithium induces clearance of protease resistant prion protein in prion-infected cells by induction of autophagy. Journal of Neurochemistry. 2009;**109**:25-34

[141] Cortes CJ, Qin K, Cook J, Solanki A, Mastrianni JA. Rapamycin delays disease onset and prevents PrP plaque deposition in a mouse model of Gerstmann-Sträussler-Scheinker disease. The Journal of Neuroscience. 2012;**32**:12396-12405

[142] Cuervo AM, Stefanis L, Fredenburg R, Lansbury PT, Sulzer D. Impaired degradation of mutant alpha-synuclein by chaperone-mediated autophagy. Science. 2004;**305**:1292-1295

[143] Chu C. Autophagic stress in neuronal injury and disease. Journal of Neuropathology and Experimental Neurology. 2006;**65**:423-432

[144] Kovacs G, Budka H. Prion diseases: From protein to cell pathology. The American Journal of Pathology. 2008;**172**:555-565

[145] Boelaard JW, Schlote W, Tateishi J. Neuronal autophagy in experimental Creutzfeldt-Jakob's disease. Acta Neuropathologica. 1989;**78**:410-418

[146] Dron M, Bailly Y, Beringue V, Haeberlé AM, Griffond B, Risold PY, et al. Scrg1 is induced in TSE and brain injuries, and associated with autophagy. The European Journal of Neuroscience. 2005;**22**:133-146

[147] Dron M, Bailly Y, Beringue V, Haeberlé A-M, Griffond B, Risold P-Y, et al. SCRG1, a potential marker of autophagy in transmisible spongiform encephalopathies. Autophagy. 2006;**2**:58-60

[148] Oh JM, Shin HY, Park SJ, Kim BH, Choi JK, Choi EK, et al. The involvement of cellular prion protein in the autophagy pathway in neuronal cells. Molecular and Cellular Neurosciences. 2008;**39**:238-247

[149] Doh-Ura K, Iwaki T, Caughey B. Lysosomotropic agents and cysteine protease inhibitors inhibit scrapie-associated prion protein accumulation. Journal of Virology. 2000;**74**:4894-4897

[150] Beranger F, Crozet C, Goldsborough A, Lehmann S. Trehalose impairs aggregation of PrPSc molecules and protects prion-infected cells against oxidative damage. Biochemical and Biophysical Research Communications. 2008;**374**:44-48. DOI: 10.1016/j.bbrc.2008.06.094

[151] Heiseke A, Aguib Y, Schätzl H. Autophagy, prion infection and their mutual interactions. Current Issues in Molecular Biology. 2010;**12**:11

[152] Yun SW, Ertmer A, Flechsig E, Gilch S, Riederer P, Gerlach M, et al. The tyrosine kinase inhibitor imatinib mesylate delays prion neuroinvasion by inhibiting prion propagation in the periphery. Journal of Neurovirology. 2007;**13**:328-337

[153] Aguib Y, Heiseke A, Gilch S, Riemer C, Baier M, Schätzl HM, et al. Autophagy induction by trehalose counteracts cellular prion infection. Autophagy. 2009;**5**:361-369

[154] Zhou M, Ottenberg G, Sferrazza GF, Hubbs C, Fallahi M, Rumbaugh G, et al. Neuronal death induced by misfolded prion protein is due to NAD+ depletion and can be relieved in vitro and in vivo by NAD+ replenishment. Brain. 2015;**138**:992-1008. DOI: 10.1093/brain/awv002

[155] Weissmann C, Flechsig E. PrP knock-out and PrP transgenic mice in prion research. British Medical Bulletin. 2003;**66**:43-60

[156] Criado JR, Sánchez-Alavez M, Conti B, Giacchino JL, Wills DN, Henriksen SJ, et al. Mice devoid of prion protein have cognitive deficits that are rescued by reconstitution of PrP in neurons. Neurobiology of Disease. 2005;**19**:255-265

[157] Oh JM, Choi EK, Carp RI, Kim YS. Oxidative stress impairs autophagic flux in prion protein-deficient hippocampal cells. Autophagy. 2018:1448-1461

[158] Shin HY, Park JH, Carp RI, Choi EK, Kim YS. Deficiency of prion protein induces impaired autophagic flux in neurons. Frontiers in Aging Neuroscience. 2014;**6**:207. DOI: 10.3389/fnagi.2014.00207

[159] Ko DC, Milenkovic L, Beier SM, Manuel H, Buchanan J, Scott MP. Cell-autonomous death of cerebellar purkinje neurons with autophagy in Niemann-pick type C disease. PLoS Genetics. 2005;**1**:81-95

[160] Sanchez-Varo R, Trujillo-Estrada L, Sanchez-Mejias E, Torres M, Baglietto-Vargas D, Moreno-Gonzalez I, et al. Abnormal accumulation of autophagic vesicles correlates with axonal and synaptic pathology in young Alzheimer's mice hippocampus. Acta Neuropathologica. 2012;**123**:53-70. DOI: 10.1007/s00401-011-0896-x

[161] Sakaguchi S, Katamine S, Nishida N, Moriuchi R, Shigematsu K, Sugimoto T, et al. Loss of cerebellar Purkinje cells in aged mice homozygous for a disrupted PrP gene. Nature. 1996;**380**:528-531

[162] Katamine S, Nishida N, Sugimoto T, Noda T, Sakaguchi S, Shigematsu K, et al. Impaired motor coordination in mice lacking prion protein. Cellular and Molecular Neurobiology. 1998;**18**:731-732

[163] Rossi D, Cozzio A, Flechsig E, Klein MA, Rulicke T, Aguzzi A, et al. Onset of ataxia and Purkinje cell loss in PrP null mice inversely correlated with

Dpl level in brain. The EMBO Journal. 2001;**20**:694-702

[164] Weissmann C, Aguzzi A. PrP's double causes trouble. Science. 1999;**286**:914-915

[165] Moore RC, Lee IY, Silverman GL, Harrison PM, Strome R, Heinrich C, et al. Ataxia in prion protein (PrP)-deficient mice is associated with upregulation of the novel PrP-like protein doppel. Journal of Molecular Biology. 1999;**292**:797-817

[166] Lu K, Wang W, Xie Z, Wong B-S, Li R, Petersen RB, et al. Structural characterization of the recombinant human doppel protein. Biochemistry. 2000;**39**:13575-13583

[167] Moore RC, Mastrangelo P, Bouzamondo E, Heinrich C, Legname G, Prusiner SB, et al. Doppel-induced cerebellar degeneration in transgenic mice. Proceedings of the National Academy of Sciences of the United States of America. 2001;**98**:15288-15293

[168] Lemaire-Vieille C, Bailly Y, Erlich P, Loeuillet C, Brocard J, Haeberlé AM, et al. Ataxia with cerebellar lesions in mice expressing chimeric PrP-Dpl protein. The Journal of Neuroscience. 2013;**33**:1391-1399

[169] Watts JC, Westaway D. The prion protein family: Diversity, rivalry, and dysfunction. Biochimica et Biophysica Acta. 2007;**1772**:654-672

[170] Heitz S, Gautheron V, Lutz Y, Rodeau JL, Zanjani HS, Sugihara I, et al. Bcl-2 conteracts Doppel-induced apoptosis of prion protein-deficient Purkinje cells in the Ngsk *Prnp*$^{0/0}$ mouse. Developmental Neurobiology. 2008;**68**:332-348

[171] Heitz S, Grant NJ, Bailly Y. Doppel induces autophagic stress in prion protein-deficient Purkinje cells. Autophagy. 2009;**5**:422-424

[172] Ding W, Yin X. Sorting, recognition and activation of the misfolded protein degradation pathways through macroautophagy and the proteasome. Autophagy. 2008;**16**:141-150

[173] Wang QJ, Ding Y, Kohtz DS, Mizushima N, Cristea IM, Rout MP, et al. Induction of autophagy in axonal dystrophy and degeneration. The Journal of Neuroscience. 2006;**26**:8057-8068

[174] Yue Z. Regulation of neuronal autophagy in axon: Implication of autophagy in axonal function and dysfunction/degeneration. Autophagy. 2007;**3**:139-141

[175] Yue Z, Friedman L, Komatsu M, Tanaka K. The cellular pathways of neuronal autophagy and their implication in neurodegenerative diseases. Biochimica et Biophysica Acta. 2009;**1793**:1496-1507

[176] Maday S, Wallace KE, Holzbaur EL. Autophagosomes initiate distally and mature during transport toward the cell soma in primary neurons. The Journal of Cell Biology. 2012;**196**:407-417

[177] Nixon RA, Yang DS, Lee JH. Neurodegenerative lysosomal disorders: A continuum from development to late age. Autophagy. 2008;**4**:590-599

[178] Fimia G, Piacentini M. Regulation of autophagy in mammals and its interplay with apoptosis. Cellular and Molecular Life Sciences. 2010;**67**:1581-1588. DOI: 10.1007/s00018-010-0284-z

[179] Metzger F, Kapfhammer JP. Protein kinase C: Its role in activity-dependent Purkinje cell dendritic development and plasticity. Cerebellum. 2003;**2**:206-214

[180] Dole S, Heitz S, Bombarde G, Haeberlé A-M, Demais V, Grant NJ, et al.

New insights into Doppel neurotoxicity using cerebellar organotypic cultures from prion protein-deficient mice. In: Medimond International Proceedings, Monduzzi Editors. Bologna Prion 2010, Salzburg, Austria. Sep 08-11, 2010. pp. 7-14

frontiers in Cellular Neuroscience

REVIEW
published: 23 January 2019
doi: 10.3389/fncel.2019.00002

Phosphatidic Acid: From Pleiotropic Functions to Neuronal Pathology

Emeline Tanguy[1], *Qili Wang*[1], *Hervé Moine*[2] *and Nicolas Vitale*[1]*

[1]Institut des Neurosciences Cellulaires et Intégratives (INCI), UPR-3212 Centre National de la Recherche Scientifique & Université de Strasbourg, Strasbourg, France, [2]Institut de Génétique et de Biologie Moléculaire et Cellulaire (IGBMC), CNRS UMR 7104, INSERM U964, Université de Strasbourg, Illkirch-Graffenstaden, France

Among the cellular lipids, phosphatidic acid (PA) is a peculiar one as it is at the same time a key building block of phospholipid synthesis and a major lipid second messenger conveying signaling information. The latter is thought to largely occur through the ability of PA to recruit and/or activate specific proteins in restricted compartments and within those only at defined submembrane areas. Furthermore, with its cone-shaped geometry PA locally changes membrane topology and may thus be a key player in membrane trafficking events, especially in membrane fusion and fission steps, where lipid remodeling is believed to be crucial. These pleiotropic cellular functions of PA, including phospholipid synthesis and homeostasis together with important signaling activity, imply that perturbations of PA metabolism could lead to serious pathological conditions. In this mini-review article, after outlining the main cellular functions of PA, we highlight the different neurological diseases that could, at least in part, be attributed to an alteration in PA synthesis and/or catabolism.

OPEN ACCESS

Edited by:
Gabriela Alejandra Salvador, Universidad Nacional del Sur, Argentina

Reviewed by:
Richard M. Epand, McMaster University, Canada
Daniel M. Raben, Johns Hopkins University, United States

***Correspondence:**
Nicolas Vitale
vitalen@unistra.fr

Received: 22 October 2018
Accepted: 07 January 2019
Published: 23 January 2019

Citation:
Tanguy E, Wang Q, Moine H and Vitale N (2019) Phosphatidic Acid: From Pleiotropic Functions to Neuronal Pathology. Front. Cell. Neurosci. 13:2. doi: 10.3389/fncel.2019.00002

Keywords: lipid signaling, neuron, neuropathology, phosphatidic acid, phospholipase D

INTRODUCTION

Phosphatidic acid (PA) is a low abundant phospholipid of membranes that, nevertheless, constitutes the original building block from which most glycerophospholipids are synthesized, thus plays an important structural task. Interestingly it was later shown that PA also acts to transmit, amplify, and regulate a great number of intracellular signaling pathways and cellular functions. In cells, PA can be synthesized through different enzymatic pathways (Ammar et al., 2014). Structural PA results from two successive acylation reactions (**Figure 1**). Signaling PA instead, results from three biosynthesis alternative pathways. The first pathway includes the phosphorylation of diacylglycerol (DAG) by any of the 10 DAG-kinases (DGKs) in mammals (**Figure 1**). Hydrolysis of the distal phosphodiester bond in phospholipids by phospholipases D (PLD) constitutes the second pathway (**Figure 1**). Although six different PLDs have been identified in mammals, only PLD1/2 and PLD6 have been shown to synthesize PA from phosphatidylcholine (PC) and cardiolipin (CL), respectively (Jang et al., 2012). The third and final biosynthetic pathway involves acylation of lyso-PA by lyso-PA-acyltransferase (LPAAT) enzymes (**Figure 1**).

Chemically, PA is composed of a glycerol backbone esterified with two fatty acyl chains at positions C-1 and C-2, and with a phosphate at position C-3. The latter confers the specific features of PA compared to the other diacyl–glycerophospholipids. Indeed, the small anionic phosphate headgroup provides to PA a combination of unique cone-shaped geometry and negative charge (Jenkins and Frohman, 2005). At the molecular level, these two characteristics enable PA both to

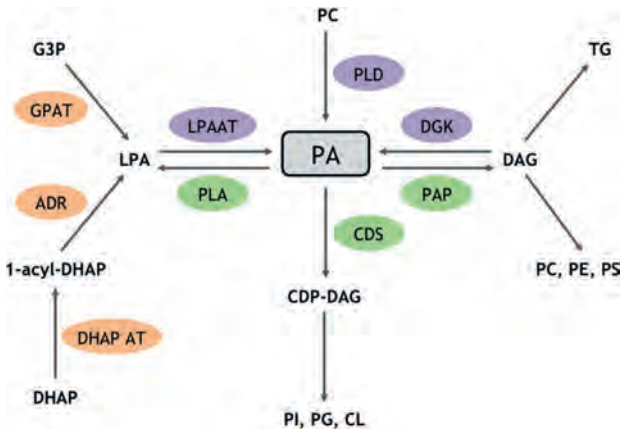

FIGURE 1 | Enzymatic routes for structural and signaling PA metabolism. PA is a major phospholipid for biosynthetic and signaling reactions. Enzymes highlighted in orange are involved in biosynthetic reactions that produce structural PA, whereas enzymes triggering the formation of signaling pools of PA are shown in purple. Enzymes responsible for PA catabolism are shown in green. ADR, Acyldihydroxyacetone-phosphate reductase; CDP, cytidyl phosphatidate; CDS, CDP-diacylglycerol (DAG) synthase; CL, cardiolipin; DHAP, dihydroxyacétone phosphate; DHAP AT, dihydroxyacétone phosphate acyltransferase; G3P, glycerol 3-phosphate; GPAT, glycerol phosphate acyltransferase; PAP, phosphatidic acid phosphatase; PC, phosphatidylcholine; PG, phosphatidylglycerol; PE, phosphatidylethanolamine; PI, phosphatidylinositol; PS, phosphatidylserine; PLA, phospholipase A; TG, triglyceride.

interact with different enzymes to regulate their catalytic activity and/or their association with membrane compartments and also to affect membrane geometry by creating local negative curvatures (Kooijman et al., 2003). As a consequence, PA has been involved in various important cellular functions including membrane trafficking events where membrane rearrangements are necessary (Bader and Vitale, 2009). In this article, we will present some of the most studied PA identified partners, summarize the most well-described cellular processes that require PA and discuss the potential involvement of an alteration in PA synthesis and/or catabolism in different neurological diseases.

PA INTERACTS WITH AND RECRUITS NUMEROUS PROTEINS TO MEMBRANES

Having an overall view of the interaction network of a given molecule is particularly helpful for deciphering the relationships between the constituents of interactomes and characterizing their function in cell signaling. Since the early description of a handful of proteins that bind to PA, at least using the minimal *in vitro* protein-lipid overlay assay, an extensive list of PA interactors has only emerged more recently (Stace and Ktistakis, 2006). For at least some of those, their interaction with PA appears rather specific with little or no interaction with other negatively charged lipids. The position of PA's phosphomonoester headgroup in proximity of the interface of acyl chain headgroup was proposed to be important for binding to specific proteins. Supporting the physiological importance of interactions between PA and proteins, numerous proteins have gained domains that display some level of binding specificity for PA (Jang et al., 2012). Although no clear PA-binding domain can be defined at the three dimensional or secondary structural levels, different factors can influence PA interaction with specific domains in target proteins (Tanguy et al., 2018). For instance, we and others have found that some PA-binding modules possess some levels of specificity for the fatty acyl chains of PA (Kassas et al., 2017). In addition, the local membrane environment surrounding PA also appears to modulate PA binding to these modules (Kassas et al., 2017). Finally, it is most likely that PA-binding domains act first through positively charged residues that initially sample for the negative charge of PA buried within the membrane. This first step is probably followed by a docking state where hydrophobic interaction between hydrophobic residues of the module and the fatty acyl chains of PA stabilize the PA-protein interaction (Potocký et al., 2014; Tanguy et al., 2018). At present, more than 50 different proteins have been shown to directly interact with PA, as extensively reviewed in Jang et al. (2012). Briefly, these PA interactors can be classified in four major families.

Nucleotide-Binding Proteins

Nucleotide (ATP, cAMP, GTP)-binding proteins are important signaling proteins for which the activity is usually regulated by nucleotide binding. Noticeably, the localization and/or activity of many of those proteins are also controlled by PA interaction. This is for instance the case for some of the small GTP-binding proteins of the ADP ribosylation factor (Arf) and Rho (Ras homologous) families that are key players in cytoskeleton remodeling and membrane dynamics. The minimal PA-binding regions of these small GTPases remains however to be defined precisely. Several c-AMP specific phosphodiesterases also interact with PA through their amino-terminal regulatory domains leading to an increase of their enzymatic activity and therefore to a reduction of cAMP levels.

Regulators of GTP-Binding Proteins

The GTPase-activating proteins ArfGAP with GTPase Domain, Ankyrin Repeat and PH domain 1 (AGAP1) and Regulator of G protein Signaling 4 (RGS4) are negative regulators of Arf and Gα GTP-binding proteins, respectively. Intriguingly, while PA stimulates the GTP-hydrolysis activity of AGAP1, it inhibits that of RGS4, highlighting the multiple and sometimes opposite actions of PA on GTP-binding activity. Furthermore, PA has also been shown to recruit and activate different guanine nucleotide-exchange proteins for small GTPases, such as DedicatOr of CytoKinesis 2 (DOCK2) and Son Of Sevenless (SOS), promoting GTP-binding and activation of Rac and Ras, respectively. It is therefore important to have in mind that PA enrichment in particular sub-membrane domains could influence in different and sometimes contradictory manners a given signaling pathway involving GTP-binding proteins by acting at different stages.

Kinases

Protein kinases are among the main signaling regulators with nearly 600 different genes. Among those, protein kinase C (PKC) is one of the largest subgroup and PA modulates the activity of several PKC isoforms. PA also promotes recruitment and activation of the proto-oncogene kinase Raf, acting as a gatekeeper in the ERK1/2 pathway. In addition, PA binding to the FKBP12-rapamycin binding region of mTOR is in competition with FKBP12/rapamycin complex of mTOR and is thus likely to influence nutrient sensing and cell proliferation.

Furthermore, lipid kinases contribute to the great diversity of lipids in cells. Among those, PA is capable to stimulate the action of phosphatidylinositol (PI) 4-phosphate 5-kinase (PI4P5K), to promote the synthesis of PI 4,5-bisphosphate ($PI(4,5)P_2$), a key signaling lipid (Stace and Ktistakis, 2006; Bader and Vitale, 2009). Finally, cytosolic sphingosine kinase that transforms sphingosine into sphingosine-phosphate appears to translocate to the plasma membrane under the control of PA levels, which most likely affects the signaling pathways involving these two lipids. In conclusion, PA binding modules are found in members of the two major kinase families and consequently, the presence of PA in local membrane composition is expected to influence crucial signaling nodes and the various associated key cellular functions.

Phosphatases

In addition to kinases, phosphatases constitute the second important family of signaling proteins that modulate protein activity by removing the phosphate residues added by kinases. The protein-tyrosine phosphatase SHP-1 that negatively modulates signaling pathways involving receptor-tyrosine kinase directly interacts with PA therefore triggering phosphatase activity. Furthermore, PA inhibits the enzymatic activity of protein phosphatase 1 (PP1), involved in many cellular activities such as the metabolism of glycogen, the processing of RNA, and the regulation of cell cycle. In conclusion, although not as well described as for kinases, the regulation of several phosphatases by PA offers the possibility of complex and often paradoxical regulation of signaling pathway by a single lipid family.

THE PLEIOTROPIC CELLULAR FUNCTIONS OF PA

Actin Cytoskeleton Dynamics

Most cellular functions are influenced by precise cell shapes that are under the control of the cytoskeleton proteins network. Among those the dynamics of the cytoskeleton depends on the formation of actin filaments from a pool of cytosolic monomers, and their subsequent association to each other or to cell membranes, pursued by their depolymerization. Most cellular functions actually depend on a permanent remodeling of this actin network and this is orchestrated in large part by actin binding proteins. Interestingly lipids such as phosphoinositides modulate the affinity of these proteins for actin. PA, however, has also been proposed to participate to this regulation (Ammar et al., 2014).

In neurons, the Rho GTPases and related proteins, through the control of the cytoskeleton, modulate various aspects of cell shape including not only neurite outgrowth and differentiation, axonal growth and targeting, but also dendritic spine formation and maintenance (Ammar et al., 2014). As mentioned in the sections "Nucleotide-Binding Proteins" and "Regulators of GTP-Binding Proteins," PA synthesized by either PLD or DGK modulates the activity of some different Rho family of GTPases and their regulators by promoting membrane association and/or through the activation of their regulatory proteins (Chae et al., 2008; Nishikimi et al., 2009; Faugaret et al., 2011; Kurooka et al., 2011; Sanematsu et al., 2013). Alternatively, the p21 activated kinases (PAKs) family that regulates various aspects of neuronal development, through actin cytoskeleton reorganization, is also known for being activated by PA (Daniels et al., 1998; Hayashi et al., 2007). Furthermore, $PI(4,5)P_2$ is a major lipid regulator of the cytoskeleton and PA is an essential building block leading to $PI(4,5)P_2$ synthesis (**Figure 1**). In an alternative pathway, PA stimulates the phospholipid kinase PI4P5K, leading to the phosphorylation of the membrane phospholipid PI(4)P and the formation of $PI(4,5)P_2$ (Honda et al., 1999). In consequence, PA potentially regulates the activity of the three mammalian PI4P5K isozymes that have been described to control actin cytoskeleton reorganization (van den Bout and Divecha, 2009; Roach et al., 2012). Finally, PA levels regulate membrane localization and activity of PKC isoforms α, ε and ζ, all of which are known to affect the morphology of the actin cytoskeleton (Jose Lopez-Andreo et al., 2003).

It is also worth noting that direct interaction of PA with actin-binding proteins has been suggested. Among those potential candidates, the actin-binding protein vinculin known to be involved in neurite outgrowth is a good example (Ito et al., 1982; Johnson and Craig, 1995), but the specificity of these observations remains to be firmly established, since vinculin also binds to other negatively charged lipids, such as $PI(4,5)P_2$.

Membrane Remodeling Events

The secretory pathways have evolved through the establishment of specialized subcellular compartments dedicated to specific biochemical tasks. Membrane trafficking events between these compartments enable particular cells of complex organisms to secrete informative molecules such as hormones, cytokines, and neurotransmitters, for long distance inter-cellular communication. In addition to dedicated and specialized protein machineries, trafficking events of the regulated exocytosis and endocytosis steps also involve remarkable membrane rearrangements that rely on specific lipids (Ammar et al., 2013b). Hence, the first direct molecular data suggesting a role for PLD1-generated PA in hormone release were obtained in chromaffin cells, where overexpression of PLD1, injection of a catalytically-inactive PLD1 mutant (Vitale et al., 2001) or PLD1 silencing (Zeniou-Meyer et al., 2007) affected catecholamine release rates. Using similar approaches, PA synthesized by PLD1 was also shown to govern the regulated secretion of insulin from β-pancreatic cells (Waselle et al., 2005), of von Willebrand factor from endothelial cells (Disse et al., 2009), and acrosomal exocytosis from sperm cells (Lopez et al., 2012; Pelletán et al., 2015). An additional contribution for PA in secretion has been established during the early phase

of azurophilic granules release in neutrophils triggered by anti-neutrophil cytoplasmic antibodies (Williams et al., 2007). Ultimately, different enzymes controlling PA metabolism such as PLDs, LPAATs and DGKs have been proposed to regulate neurotransmission in several neuronal models, suggesting that PA regulates synaptic vesicle release and cycle (Humeau et al., 2001; Schwarz et al., 2011; Tabet et al., 2016a,b; Raben and Barber, 2017).

Intense membrane remodeling also occurs in specialized phagocytic cells, such as in macrophages. Indeed, the ingestion of pathogens, cell debris, or any other solid particle through the formation of phagosomes requires plasma membrane extension and either local lipid synthesis, transfer, or vesicular fusion. PA synthesis by PLD2 has been shown to be important for this early step of phagocytosis, while PA synthesis by PLD1 appears to be also important for the later step of phagosome maturation (Corrotte et al., 2006, 2010). Of note, PA transfer from the ER to plasma membrane during "frustrated phagocytosis," a model where macrophages are plated on IgG-coated plates, has also been suggested to occur from experiments using a combination of lipidomic analysis performed on subcellular fractions and novel PA sensors (Kassas et al., 2017). Furthermore, PA is involved in the invasion and exit of infected cells by apicomplexan parasites (Bullen et al., 2016). It was shown that PA is required for the release of adhesins, perforins and proteases from specialized organelles from these parasites called micronemes (Bullen et al., 2016).

Additional intracellular trafficking events involving intense membrane remodeling have also been shown to require modification in PA levels. To cite only a few, we can also mention that PA critically regulates vesicle budding from the Golgi (Yang et al., 2008), autophagy (Holland et al., 2016), and exosome release (Ghossoub et al., 2014). The mechanisms by which PA promotes membrane rearrangements remain however an unsolved issue (**Figure 2**). The first proposed mode of action of PA in membrane remodeling may depends on its ability to induce membrane curvature and promote fusion, but its ability to specifically regulate the activity of different proteins involved in the vesicle docking and/or recruit crucial fusion proteins has also been proposed (Tanguy et al., 2016, 2018). In a simplified model for membrane fusion a mixture of lipids and proteins appear to be crucial at the fusion site (Tanguy et al., 2016). In principle the intrinsic negative curvatures of accumulating cone-shaped lipids, such as PA in the inner (cis) leaflets of contacting bilayers, should facilitate fusion of merging membranes. But it is worth noting that the promotion of membrane fusion through local modification of membrane curvature also appears to hold true for other cone-shaped lipids such as cholesterol and DAG (Tanguy et al., 2016). Reconstituted membrane fusion assays have been valuable to dissect the role of individual components and on this instance it is important to highlight that PA was observed playing a unique role among cone-shaped lipids in a yeast vacuole fusion assay, suggesting a more complex mode of action of this lipid (Mima and Wickner, 2009). Furthermore, PA could locally accumulate and form microdomains highly negatively charged, which potentially serve as membrane retention sites for several proteins key for exocytosis, such as the SNARE protein syntaxin-1 (Lam et al., 2008), or other membrane remodeling processes (Jenkins and Frohman, 2005). Finally, as a precursor for DAG and PI(4,5)P_2, both known to contribute to numerous membrane remodeling events, PA could also have indirect effects. All these potential contributions of PA in membrane fusion have been reviewed elsewhere (Chasserot-Golaz et al., 2010; Ammar et al., 2013b, 2014; Tanguy et al., 2016), but solving the issue of the mechanistic role of PA in a given membrane remodeling process requires probing these different scenarios (**Figure 2**), which is now in need for novel methods and tools.

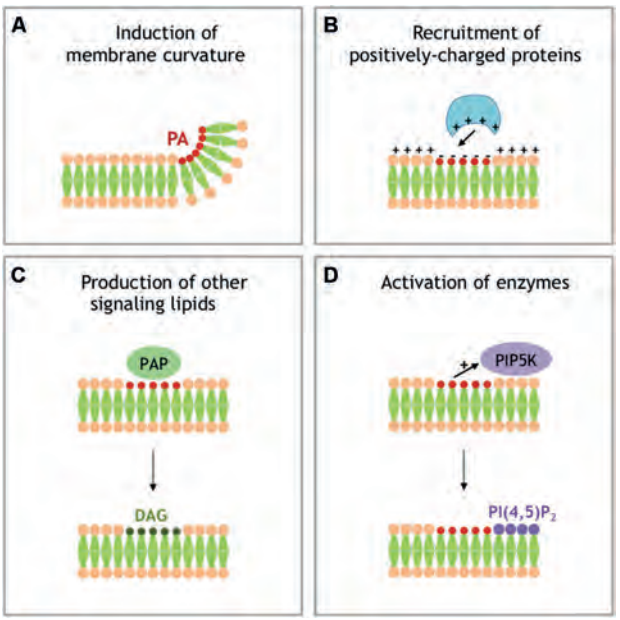

FIGURE 2 | Different models for signaling activity of PA. **(A)** Local accumulation of PA in a single leaflet of membrane generates negative membrane curvature. **(B)** Local accumulation of PA generates local buildup of negative charges that recruit PA effector-containing positively charged domains. **(C)** PAPs transforms PA into DAG, another signaling lipid with specific activity. **(D)** PA stimulates the activity of phosphatidylinositol 4-phosphate 5-kinase (PI4P5K), producing PI 4,5-bisphosphate (PI(4,5)P_2), an additional important signaling lipid.

Apoptosis, Survival, Growth, Proliferation and Migration

Many survival signals including hormones and growth factors activate PA synthesis through the stimulation of PLD activity. Similarly, mitogenic signals trigger cell proliferation, suppression of cell cycle arrest, and prevention of apoptosis. The PLD–PA–Rheb–mTOR and the PLD–PA–MAP kinase pathways are the two main downstream pathways of PLD involved in mitogenic signals and have been described extensively (Foster, 2009). Obviously, future solving of the complex imbrication of these pathways and understanding of the spatiotemporal relationships between PA-generating enzymes, PA-binding partners and PA itself will require development of more specific tools and extensive work.

NEUROLOGICAL DISORDERS POTENTIALLY LINKED TO AN ALTERATION OF PA LEVELS

In all organisms from yeast to mammals, PA was shown to possess signaling activity (Jenkins and Frohman, 2005) and a recent review highlights the apparent mystery of the many roles of PA in plants (Pokotylo et al., 2018). In addition, various PA-generating enzymes were shown to be involved in an increasing number of neuronal pathologies, suggesting a fundamental role of PA in the outcome of these neurodiseases (Tanguy et al., 2018). In the next chapter, we will describe four neuronal pathologies that may be the consequence, at least partially, of an alteration in PA dynamics.

Fetal Alcohol Spectrum Disorders

The damaging effects of alcohol drinking during gestation on the developing fetus are extremely well documented (Ehrhart et al., 2018). Fetal alcohol spectrum disorders (FASDs) is a generic term used to define the birth deficiencies that result from prenatal exposure to alcohol that range from mild to severe. These developmental defects on unborn infants have lifelong physical, behavioral, and cognitive disabilities. As alcohol consumption avoidance during pregnancy is in theory easy to achieve, FASD is in fact considered as one of the largest preventable forms of non-genetic birth disabilities associated with intellectual incapacity.

Although the main effort remains prevention of alcohol consumption during pregnancy, it is also important to understand the underlying pathological mechanisms involved in these effects of ethanol. In addition to the well-recognized ethanol and acetaldehyde toxicity, alcohol intensifies oxidative stress causing consequent effects such as DNA, protein and membrane damages. Additionally, it has been known for over three decades that in the presence of 1%–3% of ethanol, the two best characterized mammalian isoforms PLD1 and PLD2 catalyze a transphosphatidylation reaction. In this case alcohol replaces water during PC hydrolysis, and phosphatidyl alcohols are formed at the expense of PA (Jenkins and Frohman, 2005). Thus, in presence of ethanol, phosphatidylethanol is synthesized while PA is not. Since it is likely that phosphatidylethanol cannot replace PA as a signaling molecule, this was used as a trick to "inhibit" PLD activity (actually prevent PA production), but also in assays to quantify PLD activity (Ammar et al., 2014). It was also shown that ethanol inhibits the mitogenic downstream actions of PA on neuron progenitors (Klein, 2005). Furthermore, it was recently shown that both PLD1 and PLD2 strongly contribute to astroglial proliferation induced by IGF-1 (Burkhardt et al., 2014). Therefore, the perturbation of the IGF1-PLD signaling pathway could, at least in part, explain the teratogenic effects of ethanol observed in FASDs.

Neurological Cancers

Glioblastoma is the most frequent and aggressive brain cancer, with an estimated incidence of near five novel cases per 100,000 persons every year in the USA and Europe. Nearly 200,000 persons die from glioblastoma every year worldwide. It is a relatively difficult cancer to diagnose, as the symptoms are mainly non-specific, including headache and nausea, but leading to alterations of neurological functions such as speech, vision, behavior and memory. Like for many cancer tissues, elevated PLD activity was found in glioblastoma, suggesting that an increase in PA levels is a cause and/or consequence of the pathology (Park et al., 2009). At least part of the survival effect of increased PLD activity on glioblastoma appears to involve the Akt pathway (Bruntz et al., 2014). Interestingly, lipidomic analyses revealed that PA levels are altered in the regions that attract glioblastoma cells, indicating that PA levels control the homing process of glioblastoma (Wildburger et al., 2015). Undoubtedly, a better understanding of the multiple functions of PA in brain tumor development and progression may help to improve treatments and subsequently get a better prognosis for this aggressive cancer.

Intellectual Disability Diseases

Intellectual disability diseases are a common state defined by significant restriction in intellectual capacities and adaptive behavior that happen during childhood, with an overall intelligence quotient bellow 70 together with associated reduction in social, daily living and communication skills. These heterogeneous disease conditions affect 1%–3% of all populations and are thought to result from multiple causes, including environmental, chromosomal and monogenetic alterations. Among the several hundreds of genes involved, some affect brain development, neurogenesis, neuronal migration, or synaptic function (Humeau et al., 2009). Below we will briefly describe the data that support the notion of an alteration of PA levels and/or dynamics in the Fragile-X syndrome (FXS) and the Coffin-Lowry syndrome (CLS).

FXS is a neurodevelopmental pathology accountable for the most common inherited form of intellectual infirmity and autism spectrum disorder. It is generally the consequence of the hypermethylation of CGG expansion repeats (>200) in the 5′ untranslated region of the *FMR1* gene leading to transcription silencing. In a recent study, we pointed DGK kinase-κ (DGKκ) mRNA as the foremost target of Fragile Mental Retardation Protein and found an alteration in PA synthesis in neurons cultured from *Fmr1*-knockout mice after group 1 metabotropic glutamate receptor (mGluRI) stimulation (Tabet et al., 2016a). Silencing DGKκ in CA1 pyramidal neurons modified the immature over mature spine ratio and like in the *Fmr1*-knockout mouse phenotype, reduced LTP and increased LTD (Tabet et al., 2016a). Moreover, the typical *Fmr1*-knockout mouse phenotype on dendritic spine morphology was restored back to normal after overexpression of DGKκ (Tabet et al., 2016a). Finally, DGKκ silencing by shRNA in the mouse reiterated autistic behaviors, such as impaired social interaction, hyperactivity and altered nest-building very much like those seen in the *Fmr1*-knockout mouse model (Tabet et al., 2016a). Based on these observations, it was proposed that a major molecular consequence of the loss of FMRP expression in FXS is to prevent DGKκ translation, leading to an alteration in DAG and PA levels in neurons (Tabet et al., 2016b). A main consequence of this imbalance would be the alteration of the downstream signaling

of DAG and PA required for maturation of dendritic spines and establishment of correct synaptic plasticity (Moine and Vitale, 2018).

Loss of function mutations in the gene encoding Ribosomal S6 Kinase 2 (RSK2) lead to CLS, a rare syndromic form of mental retardation that shows X-linked inheritance. However, the molecular bases of the major neuronal alterations of CLS, such as moderate to severe defect in neurodevelopment, remain indefinable. In agreement with the notion that PLD1-generated PA is key to neurite outgrowth, we observed significant delayed in *Pld1* knockout neuron maturation (Ammar et al., 2013a). These observations were as well found in a mouse model for CLS syndrome since *Rsk2* knockout neurons exhibited developmental delay (Ammar et al., 2013a). Furthermore, RSK2 phosphorylates PLD1 at threonine 147 when exocytosis was triggered (Zeniou-Meyer et al., 2008) or during neurite outgrowth (Ammar et al., 2013a) in PC12 cells. A specific sensor for PA revealed an increase in PA levels at the tips of growing neurites in neurons resulting from PLD1 activation (Ammar et al., 2013a). Interestingly, PLD1 was found to be associated with BDNF positive endosomes (Ammar et al., 2015) and with vesicular structures derived from the trans Golgi, co-labeled by the vesicular SNARE VAMP-7/TiVAMP (Ammar et al., 2013a). The fusion efficiency of these PLD1/VAMP-7 vesicles in the growth cone was severely impaired by RSK2 and PLD1 inhibitors, suggesting that both PLD1 and RSK2 are necessary for membrane provision needed during neurite outgrowth (Ammar et al., 2013a). Accordingly, co-immunoprecipitation and confocal colocalization experiments indicated that RSK2 and PLD1 are found in a complex at the tip end of growing neurites, supporting the observation of an increased PA level at this location (Ammar et al., 2013a). Altogether, these results have highlighted the importance of PA-mediated membrane trafficking in neurite outgrowth and a key role of RSK2 in PA synthesis during this process, by phosphorylation and subsequent activation of PLD1. In consequence, it has been proposed that at least some of the clinical consequences of the CLS might result from an inadequate PA production during neuronal development and function (Zeniou-Meyer et al., 2010).

Neurodegeneration

It is becoming more and more evident that human neurodegenerative diseases such as Alzheimer disease (AD) also have a critical lipidic feature in their outcome. This aspect has been first pointed out by the susceptibility of the ApoE4 allele to AD, but more recently PLDs have also been proposed to contribute to the development of the pathology. It was first shown that PLD1 is involved in the vesicular trafficking of βAPP (Cai et al., 2006) and later that increased expression of APP promoted PLD activity in human astroglioma cells (Jin et al., 2007). Although highly debated, the observation that a rare variant of PLD3 gene confers susceptibility to AD has put PLD and PA on the spotlight (Cruchaga et al., 2014; Heilmann et al., 2015; Lambert et al., 2015; van der Lee et al., 2015). The most compelling evidence that defects in PA production by PLDs are involved in AD comes from an elegant study combining detailed lipidomics with behavioral tests in mouse models. In this study, the authors found that PLD2 knockout fully rescued AD-related synaptic dysfunction and cognitive deficits in a model of AD (Oliveira et al., 2010). The exact nature of the PA imbalance in AD awaits however to be fully defined and the possibility to interfere with AD condition by correcting this imbalance is probably very far from reach.

CONCLUSION

The diversity of mechanisms of PA signaling and physiological functions mostly relies on the fact that PA is synthesized by a complex set of different enzymes involved in diverse array of pathways. PLDs, DGKs, and LPAATs each constitute a big collection of isoenzymes differently localized within cells and displaying cell type specificity. In fact, the specific subcellular distribution, regulation, and/or substrate preferences of these enzymes probably account for the heterogeneity of PA composition in membranes. These aspects, altogether with the capacity of PA-binding modules in proteins to sense the local membrane environment and the type of PA species, offer a hub for the functional diversity of PA from molecular and cellular to physiological functions. There is no doubt that advanced lipidomics in combination with novel imaging tools to follow PA's dynamics will help to gain a better understanding of the apparent paradox of the abundance of function of this simple lipid. Further understanding of the biophysical side of PA's action on membranes is also critically needed to provide novel ideas for the treatment of the growing number of neuronal pathologies linked to the alterations of PA metabolism.

AUTHOR CONTRIBUTIONS

All authors listed have made a substantial, direct and intellectual contribution to the work, and approved it for publication.

FUNDING

This work was supported by Fondation pour la Recherche Médicale and by Fondation Jérôme Lejeune funding to HM.

REFERENCES

Ammar, M. R., Humeau, Y., Hanauer, A., Nieswandt, B., Bader, M. F., and Vitale, N. (2013a). The Coffin-Lowry syndrome-associated protein RSK2 regulates neurite outgrowth through phosphorylation of phospholipase D1 (PLD1) and synthesis of phosphatidic acid. *J. Neurosci.* 33, 19470–19479. doi: 10.1523/JNEUROSCI.2283-13.2013

Ammar, M. R., Kassas, N., Chasserot-Golaz, S., Bader, M. F., and Vitale, N. (2013b). Lipids in regulated exocytosis: what are they doing? *Front. Endocrinol.* 4:125. doi: 10.3389/fendo.2013.00125

Ammar, M. R., Kassas, N., Bader, M. F., and Vitale, N. (2014). Phosphatidic acid in neuronal development: a node for membrane and cytoskeleton rearrangements. *Biochimie* 107, 51–57. doi: 10.1016/j.biochi.2014.07.026

Ammar, M. R., Thahouly, T., Hanauer, A., Stegner, D., Nieswandt, B., and Vitale, N. (2015). PLD1 participates in BDNF-induced signalling in cortical neurons. *Sci. Rep.* 5:14778. doi: 10.1038/srep14778

Bader, M. F., and Vitale, N. (2009). Phospholipase D in calcium-regulated exocytosis: lessons from chromaffin cells. *Biochim. Biophys. Acta* 1791, 936–941. doi: 10.1016/j.bbalip.2009.02.016

Bruntz, R. C., Taylor, H. E., Lindsley, C. W., and Brown, H. A. (2014). Phospholipase D2 mediates survival signaling through direct regulation of Akt in glioblastoma cells. *J. Biol. Chem.* 289, 600–616. doi: 10.1074/jbc.M113.532978

Bullen, H. E., Jia, Y., Yamaryo-Botté, Y., Bisio, H., Zhang, O., Jemelin, N. K., et al. (2016). Phosphatidic acid-mediated signaling regulates microneme secretion in toxoplasma. *Cell Host Microbe* 19, 349–360. doi: 10.1016/j.chom.2016.02.006

Burkhardt, U., Wojcik, B., Zimmermann, M., and Klein, J. (2014). Phospholipase D is a target for inhibition of astroglial proliferation by ethanol. *Neuropharmacology* 79, 1–9. doi: 10.1016/j.neuropharm.2013.11.002

Cai, D., Zhong, M., Wang, R., Netzer, W. J., Shields, D., Zheng, H., et al. (2006). Phospholipase D1 corrects impaired βAPP trafficking and neurite outgrowth in familial Alzheimer's disease-linked presenilin-1 mutant neurons. *Proc. Natl. Acad. Sci. U S A* 103, 1936–1940. doi: 10.1073/pnas.0510710103

Chae, Y. C., Kim, J. H., Kim, K. L., Kim, H. W., Lee, H. Y., Heo, W. D., et al. (2008). Phospholipase D activity regulates integrin-mediated cell spreading and migration by inducing GTP-Rac translocation to the plasma membrane. *Mol. Biol. Cell* 19, 3111–3123. doi: 10.1091/mbc.E07-04-0337

Chasserot-Golaz, S., Coorssen, J. R., Meunier, F. A., and Vitale, N. (2010). Lipid dynamics in exocytosis. *Cell. Mol. Neurobiol.* 30, 1335–1342. doi: 10.1007/s10571-010-9577-x

Corrotte, M., Chasserot-Golaz, S., Huang, P., Du, G., Ktistakis, N. T., Frohman, M. A., et al. (2006). Dynamics and function of phospholipase D and phosphatidic acid during phagocytosis. *Traffic* 7, 365–377. doi: 10.1111/j.1600-0854.2006.00389.x

Corrotte, M., Nyguyen, A. P., Harlay, M. L., Vitale, N., Bader, M. F., and Grant, N. J. (2010). Ral isoforms are implicated in Fcγ R-mediated phagocytosis: activation of phospholipase D by RalA. *J. Immunol.* 185, 2942–2950. doi: 10.4049/jimmunol.0903138

Cruchaga, C., Karch, C. M., Jin, S. C., Benitez, B. A., Cai, Y., Guerreiro, R., et al. (2014). Rare coding variants in the phospholipase D3 gene confer risk for Alzheimer's disease. *Nature* 505, 550–554. doi: 10.1038/nature12825

Daniels, R. H., Hall, P. S., and Bokoch, G. M. (1998). Membrane targeting of p21-activated kinase 1 (PAK1) induces neurite outgrowth from PC12 cells. *EMBO J.* 17, 754–764. doi: 10.1093/emboj/17.3.754

Disse, J., Vitale, N., Bader, M. F., and Gerke, V. (2009). Phospholipase D1 is specifically required for regulated secretion of von Willebrand factor from endothelial cells. *Blood* 113, 973–980. doi: 10.1182/blood-2008-06-165282

Ehrhart, F., Roozen, S., Verbeek, J., Koek, G., Kok, G., van Kranen, H., et al. (2018). Review and gap analysis: molecular pathways leading to fetal alcohol spectrum disorders. *Mol. Psychiatry* 24, 10–17. doi: 10.1038/s41380-018-0095-4

Faugaret, D., Chouinard, F. C., Harbour, D., El azreq, M. A., and Bourgoin, S. G. (2011). An essential role for phospholipase D in the recruitment of vesicle amine transport protein-1 to membranes in human neutrophils. *Biochem. Pharmacol.* 81, 144–156. doi: 10.1016/j.bcp.2010.09.014

Foster, D. A. (2009). Phosphatidic acid signaling to mTOR: signals for the survival of human cancer cells. *Biochim. Biophys. Acta* 1791, 949–949. doi: 10.1016/j.bbalip.2009.02.009

Ghossoub, R., Lembo, F., Rubio, A., Gaillard, C. B., Bouchet, J., Vitale, N., et al. (2014). Syntenin-ALIX exosome biogenesis and budding into multivesicular bodies are controlled by ARF6 and PLD2. *Nat. Commun.* 5:3477. doi: 10.1038/ncomms4477

Hayashi, K., Ohshima, T., Hashimoto, M., and Mikoshiba, K. (2007). Pak1 regulates dendritic branching and spine formation. *Dev. Neurobiol.* 67, 655–669. doi: 10.1002/dneu.20363

Heilmann, S., Drichel, D., Clarimon, J., Fernández, V., Lacour, A., Wagner, H., et al. (2015). PLD3 in non-familial Alzheimer's disease. *Nature* 520, E3–E5. doi: 10.1038/nature14039

Holland, P., Knævelsrud, H., Søreng, K., Mathai, B. J., Lystad, A. H., Pankiv, S., et al. (2016). HS1BP3 negatively regulates autophagy by modulation of phosphatidic acid levels. *Nat. Commun.* 7:13889. doi: 10.1038/ncomms13889

Honda, A., Nogami, M., Yokozeki, T., Yamazaki, M., Nakamura, H., Watanabe, H., et al. (1999). Phosphatidylinositol 4-phosphate 5-kinase α is a downstream effector of the small G protein ARF6 in membrane ruffle formation. *Cell* 99, 521–532. doi: 10.1016/s0092-8674(00)81540-8

Humeau, Y., Gambino, F., Chelly, J., and Vitale, N. (2009). X-linked mental retardation: focus on synaptic function and plasticity. *J. Neurochem.* 109, 1–14. doi: 10.1111/j.1471-4159.2009.05881.x

Humeau, Y., Vitale, N., Chasserot-Golaz, S., Dupont, J. L., Du, G., Frohman, M. A., et al. (2001). A role for phospholipase D1 in neurotransmitter release. *Proc. Natl. Acad. Sci. U S A* 98, 15300–15305. doi: 10.1073/pnas.261358698

Ito, S., Richert, N., and Pastan, I. (1982). Phospholipids stimulate phosphorylation of vinculin by the tyrosine-specific protein kinase of Rous sarcoma virus. *Proc. Natl. Acad. Sci. U S A* 79, 4628–4631. doi: 10.1073/pnas.79.15.4628

Jang, J.-H., Lee, C. S., Hwang, D., and Ryu, S. H. (2012). Understanding of the roles of phospholipase D and phosphatidic acid through their binding partners. *Prog. Lipid Res.* 51, 71–81. doi: 10.1016/j.plipres.2011.12.003

Jenkins, G. M., and Frohman, M. A. (2005). Phospholipase D: a lipid centric review. *Cell. Mol. Life Sci.* 62, 2305–2316. doi: 10.1007/s00018-005-5195-z

Jin, J.-K., Ahn, B.-H., Na, Y.-J., Kim, J.-I., Kim, Y.-S., Choi, E.-K., et al. (2007). Phospholipase D1 is associated with amyloid precursor protein in Alzheimer's disease. *Neurobiol. Aging* 28, 1015–1027. doi: 10.1016/j.neurobiolaging.2006.05.022

Johnson, R. P., and Craig, S. W. (1995). The carboxy-terminal tail domain of vinculin contains a cryptic binding site for acidic phospholipids. *Biochem. Biophys. Res. Commun.* 210, 159–164. doi: 10.1006/bbrc.1995.1641

Jose Lopez-Andreo, M., Gomez-Fernandez, J. C., and Corbalan-Garcia, S. (2003). The simultaneous production of phosphatidic acid and diacylglycerol is essential for the translocation of protein kinase Cε to the plasma membrane in RBL-2H3 cells. *Mol. Biol. Cell* 14, 4885–4895. doi: 10.1091/mbc.e03-05-0295

Kassas, N., Tanguy, E., Thahouly, T., Fouillen, L., Heintz, D., Chasserot-Golaz, S., et al. (2017). Comparative characterization of phosphatidic acid sensors and their localization during frustrated phagocytosis. *J. Biol. Chem.* 292, 4266–4279. doi: 10.1074/jbc.m116.742346

Klein, J. (2005). Functions and pathophysiological roles of phospholipase D in thebrain. *J. Neurochem.* 94, 1473–1487. doi: 10.1111/j.1471-4159.2005.03315.x

Kooijman, E. E., Chupin, V., de Kruijff, B., and Burger, K. N. (2003). Modulation of membrane curvature by phosphatidic acid and lysophosphatidic acid. *Traffic* 4, 162–174. doi: 10.1034/j.1600-0854.2003.00086.x

Kurooka, T., Yamamoto, Y., Takai, Y., and Sakisaka, T. (2011). Dual regulation of RA-RhoGAP activity by phosphatidic acid and Rap1 during neurite outgrowth. *J. Biol. Chem.* 286, 6832–6843. doi: 10.1074/jbc.m110.183772

Lam, A. D., Tryoen-Toth, P., Tsai, B., Vitale, N., and Stuenkel, E. L. (2008). SNARE-catalyzed fusion events are regulated by Syntaxin1A-lipid interactions. *Mol. Biol. Cell* 19, 485–497. doi: 10.1091/mbc.e07-02-0148

Lambert, J. C., Grenier-Boley, B., Bellenguez, C., Pasquier, F., Campion, D., Dartigues, J. F., et al. (2015). PLD3 and sporadic Alzheimer's disease risk. *Nature* 520:E1. doi: 10.1038/nature14036

Lopez, C. I., Pelletán, L. E., Suhaiman, L., De Blas, G. A., Vitale, N., Mayorga, L. S., et al. (2012). Diacylglycerol stimulates acrosomal exocytosis by feeding into a PKC- and PLD1-dependent positive loop that continuously supplies phosphatidylinositol 4,5-bisphosphate. *Biochim. Biophys. Acta* 1821, 1186–1199. doi: 10.1016/j.bbalip.2012.05.001

Mima, J., and Wickner, W. (2009). Complex lipid requirements for SNARE- and SNARE chaperone-dependent membrane fusion. *J. Biol. Chem.* 284, 27114–27122. doi: 10.1074/jbc.m109.010223

Moine, H., and Vitale, N. (2018). Of local translation control and lipid signaling in neurons. *Adv. Biol. Regul.* doi: 10.1016/j.jbior.2018.09.005 [Epub ahead of print].

Nishikimi, A., Fukuhara, H., Su, W., Hongu, T., Takasuga, S., Mihara, H., et al. (2009). Sequential regulation of DOCK2 dynamics by two phospholipids during neutrophil chemotaxis. *Science* 324, 384–387. doi: 10.1126/science.1170179

Oliveira, T. G., Chan, R. B., Tian, H., Laredo, M., Shui, G., Staniszewski, A., et al. (2010). Phospholipase d2 ablation ameliorates Alzheimer's disease-linked synaptic dysfunction and cognitive deficits. *J. Neurosci.* 30, 16419–16428. doi: 10.1523/JNEUROSCI.3317-10.2010

Park, M. H., Ahn, B. H., Hong, Y. K., and Min do, S. (2009). Overexpression of phospholipase D enhances matrix metalloproteinase-2 expression and glioma cell invasion via protein kinase C and protein kinase A/NF-κB/Sp1-mediated signaling pathways. *Carcinogenesis* 30, 356–365. doi: 10.1093/carcin/bgn287

Pelletán, L. E., Suhaiman, L., Vaquer, C. C., Bustos, M. A., De Blas, G. A., Vitale, N., et al. (2015). ADP ribosylation factor 6 (ARF6) promotes acrosomal exocytosis by modulating lipid turnover and Rab3A activation. *J. Biol. Chem.* 290, 9823–9841. doi: 10.1074/jbc.m114.629006

Pokotylo, I., Kravets, V., Martinec, J., and Ruelland, E. (2018). The phosphatidic acid paradox: too many actions for one molecule class? Lessons from plants. *Prog. Lipid Res.* 71, 43–53. doi: 10.1016/j.plipres.2018.05.003

Potocký, M., Pleskot, R., Pejchar, P., Vitale, N., Kost, B., and Zárský, V. (2014). Live-cell imaging of phosphatidic acid dynamics in pollen tubes visualized by Spo20p-derive biosensor. *New Phytol.* 203, 483–494. doi: 10.1111/nph.12814

Raben, D. M., and Barber, C. N. (2017). Phosphatidic acid and neurotransmission. *Adv. Biol. Regul.* 63, 15–21. doi: 10.1016/j.jbior.2016.09.004

Roach, A. N., Wang, Z., Wu, P., Zhang, F., Chan, R. B., Yonekubo, Y., et al. (2012). Phosphatidic acid regulation of PIPKI is critical for actin cytoskeletal reorganization. *J. Lipid Res.* 53, 2598–2609. doi: 10.1194/jlr.m028597

Sanematsu, F., Nishikimi, A., Watanabe, M., Hongu, T., Tanaka, Y., Kanaho, Y., et al. (2013). Phosphatidic acid-dependent recruitment and function of the Rac activator DOCK1 during dorsal ruffle formation. *J. Biol. Chem.* 288, 8092–8100. doi: 10.1074/jbc.m112.410423

Schwarz, K., Natarajan, S., Kassas, N., Vitale, N., and Schmitz, F. (2011). The synaptic ribbon is a site of phosphatidic acid generation in ribbon synapses. *J. Neurosci.* 31, 15996–16011. doi: 10.1523/JNEUROSCI.2965-11.2011

Stace, C. L., and Ktistakis, N. T. (2006). Phosphatidic acid- and phosphatidylserine-binding proteins. *Biochim. Biophys. Acta* 1761, 913–926. doi: 10.1016/j.bbalip.2006.03.006

Tabet, R., Moutin, E., Becker, J. A., Heintz, D., Fouillen, L., Flatter, E., et al. (2016a). Fragile X Mental Retardation Protein (FMRP) controls diacylglycerol kinase activity in neurons. *Proc. Natl. Acad. Sci. U S A* 113, E3619–E3628. doi: 10.1073/pnas.1522631113

Tabet, R., Vitale, N., and Moine, H. (2016b). Fragile X syndrome: are signaling lipids the missing Culprits? *Biochimie* 130, 188–194. doi: 10.1016/j.biochi.2016.09.002

Tanguy, E., Carmon, O., Wang, Q., Jeandel, L., Chasserot-Golaz, S., Montero-Hadjadje, M., et al. (2016). Lipids implicated in the journey of a secretory granule: from biogenesis to fusion. *J. Neurochem.* 137, 904–912. doi: 10.1111/jnc.13577

Tanguy, E., Kassas, N., and Vitale, N. (2018). Protein-phospholipid interaction motifs: a focus on phosphatidic acid. *Biomolecules* 8:E20. doi: 10.3390/biom8020020

van den Bout, I., and Divecha, N. (2009). PIP5K-driven PtdIns(4,5)P2 synthesis: regulation and cellular functions. *J. Cell Sci.* 122, 3837–3850. doi: 10.1242/jcs.056127

van der Lee, S. J., Holstege, H., Wong, T. H., Jakobsdottir, J., Bis, J. C., Chouraki, V., et al. (2015). PLD3 variants in population studies. *Nature* 520, E2–E3. doi: 10.1038/nature14038

Vitale, N., Caumont, A. S., Chasserot-Golaz, S., Du, G., Wu, S., Sciorra, V. A., et al. (2001). Phospholipase D1: a key factor for the exocytotic machinery in neuroendocrine cells. *EMBO J.* 20, 2424–2434. doi: 10.1093/emboj/20.10.2424

Waselle, L., Gerona, R. R., Vitale, N., Martin, T. F., Bader, M. F., and Regazzi, R. (2005). Role of phosphoinositide signaling in the control of insulin exocytosis. *Mol. Endocrinol.* 19, 3097–3106. doi: 10.1210/me.2004-0530

Wildburger, N. C., Wood, P. L., Gumin, J., Lichti, C. F., Emmett, M. R., Lang, F. F., et al. (2015). ESI-MS/MS and MALDI-IMS localization reveal alterations in phosphatidic acid, diacylglycerol, and DHA in glioma stem cell xenografts. *J. Proteome Res.* 14, 2511–2519. doi: 10.1021/acs.jproteome.5b00076

Williams, J. M., Pettitt, T. R., Powell, W., Grove, J., Savage, C. O., and Wakelam, M. J. (2007). Antineutrophil cytoplasm antibody-stimulated neutrophil adhesion depends on diacylglycerol kinase-catalyzed phosphatidic acid formation. *J. Am. Soc. Nephrol.* 18, 1112–1120. doi: 10.1681/asn.2006090973

Yang, J. S., Gad, H., Lee, S. Y., Mironov, A., Zhang, L., Beznoussenko, G. V., et al. (2008). A role for phosphatidic acid in COPI vesicle fission yields insights into Golgi maintenance. *Nat. Cell Biol.* 10, 1146–1153. doi: 10.1038/ncb1774

Zeniou-Meyer, M., Gambino, F., Ammar, M. R., Humeau, Y., and Vitale, N. (2010). The Coffin-Lowry syndrome-associated protein RSK2 and neurosecretion. *Cell. Mol. Neurobiol.* 30, 1401–1406. doi: 10.1007/s10571-010-9578-9

Zeniou-Meyer, M., Liu, Y., Béglé, A., Olanich, M. E., Hanauer, A., Becherer, U., et al. (2008). The Coffin-Lowry syndrome-associated protein RSK2 is implicated in calcium-regulated exocytosis through the regulation of PLD1. *Proc. Natl. Acad. Sci. U S A* 105, 8434–8439. doi: 10.1073/pnas.0710676105

Zeniou-Meyer, M., Zabari, N., Ashery, U., Chasserot-Golaz, S., Haeberlé, A. M., Demais, V., et al. (2007). Phospholipase D1 production of phosphatidic acid at the plasma membrane promotes exocytosis of large dense-core granules at a late stage. *J. Biol. Chem.* 282, 21746–21757. doi: 10.1074/jbc.m702968200

Conflict of Interest Statement: The authors declare that the research was conducted in the absence of any commercial or financial relationships that could be construed as a potential conflict of interest.

Role of Phospholipase D-Derived Phosphatidic Acid in Regulated Exocytosis and Neurological Disease

Emeline Tanguy, Qili Wang, and Nicolas Vitale

Contents

Abstract

Lipids play a vital role in numerous cellular functions starting from a structural role as major constituents of membranes to acting as signaling intracellular or extracellular entities. Accordingly, it has been known for decades that lipids, especially those coming from diet, are important to maintain normal physiological functions and good health. On the other side, the exact molecular nature of these beneficial or deleterious lipids, as well as their precise mode of action, is only starting to be unraveled. This recent improvement in our knowledge is largely resulting from novel pharmacological, molecular, cellular, and genetic tools to study lipids in vitro and in vivo. Among these important lipids, phosphatidic acid plays a unique and central role in a great variety of cellular functions. This review will focus on the proposed functions of phosphatidic acid

E. Tanguy · Q. Wang
Institut des Neurosciences Cellulaires et Intégratives, CNRS UPR 3212 and Université de Strasbourg, Strasbourg, France

N. Vitale (✉)
Institut des Neurosciences Cellulaires et Intégratives, CNRS UPR 3212 and Université de Strasbourg, Strasbourg, France

INSERM, Paris, Cedex 13, France
e-mail: vitalen@inci-cnrs.unistra.fr

Handbook of Experimental Pharmacology, https://doi.org/10.1007/164_2018_180

generated by phospholipase D in the last steps of regulated exocytosis with a specific emphasis on hormonal and neurotransmitter release and its potential impact on different neurological diseases.

Keywords
Exocytosis · Lipid · Neuroendocrine · Neuron · Phosphatidic acid · Phospholipase D

1 Introduction

Complex organisms have evolved through their capacity to maintain global homeostasis. This is usually achieved by numerous cellular processes, of which some require cells to get information from distant cells/organs. Hence, a specific mechanism called regulated exocytosis allows cells to tightly control the release of informative molecules in the extracellular space before they are transported to the target cells/organs. Over the last three decades, considerable insight in this process has been gained through the study of neurotransmitter and hormonal release from neurons and neuroendocrine cells, respectively. As such, the chromaffin cell model, largely described in this review, has been very valuable to delineate the different steps of exocytosis (Bader et al. 2002). The regulated secretory pathway begins in the Golgi apparatus with the formation of specific vesicular structures called synaptic vesicles or dense-core secretory granules that are progressively filled with neurotransmitters, hormones, or neuropeptides to be secreted. After their biogenesis, these secretory vesicles are matured during their transport toward specific regions at the cell periphery, where their journey ends by the fusion with the plasma membrane and vesicular content release into the extracellular space, generally following a rise in cytosolic calcium (Burgess and Kelly 1987). This final stage of the secretory process, known as regulated exocytosis, implies successive docking and the priming of mature granules before merging of vesicular and plasma membranes to enable partial or total release of the secretory vesicle content.

It has been proposed that depending on physiological demand, at least three distinct modes of release co-exist: (1) the so-called “kiss-and-run” mode, when small molecules such as hormones and neurotransmitters are released through a narrow fusion pore, while larger molecules such as neuropeptides are retained in the vesicle; (2) vesicle cavity capture (cavicapture), in which dilation of the fusion pore permits partial release of large molecules but the omega shape of the fusing granule is maintained before closure; and (3) full collapse, wherein the vesicles flatten out in the plane of the plasma membrane, losing their round shape and completely emptying their contents (Taraska et al. 2003; Fulop and Smith 2006; van Kempen et al. 2011). It must be noted that the physiological importance of these different modes of secretion remains to be established and the molecular mechanisms that control the transition between these different modes identified.

Most studies on calcium-regulated exocytosis have focused on the minimal molecular machinery, which involves the formation of a tripartite soluble *N*-ethylmaleimide-sensitive factor attachment protein receptor (SNARE) complex between vesicular and plasma membrane proteins (Jahn and Fasshauer 2012). However, since exocytosis ends by the fusion of two membrane compartments, it is likely that lipids also play a leading role (Tanguy et al. 2016). In the following sections, we review observations detailing the functional roles performed during exocytosis by the simplest glycerophospholipid naturally existing in all-living organisms, phosphatidic acid (PA), and consequently its potential implication in neurological disease. Indeed, although it constitutes only a minor fraction of the total cell lipids, PA has attracted considerable attention for being both a lipid second messenger and a modulator of membrane shape.

2 The Different Sources of Phosphatidic Acid

The pleiotropic functions of PA are the direct consequence of its very simple chemical structure, consisting of two acyl chains linked by ester bonds to glycerol, whose remaining hydroxyl group is esterified with a phosphomonoester group. Hence, the small phosphate headgroup of PA provides a cone-shaped structure generating flexibility and negative curvatures in the context of a lipid bilayer. In addition, the negatively charged phosphomonoester headgroup of PA can carry one or two negative charges, depending on pH and surrounding lipids, and thus can assist in the recruitment of positively charged molecules to membrane surfaces.

There are four major routes of cellular PA production in mammals. Structural PA is synthesized through two acylation reactions: the glycerol 3-phosphate (G-3-P) pathway and the dihydroxyacetone phosphate (DHAP) pathway leading to lysoPA (LPA), a mono-acylated form of PA (Fig. 1a). LPA is subsequently transformed in a second acylation step into PA (Vance and Vance 2004) (Fig. 1a). PA generated from these de novo pathways is a key intermediate in the synthesis of all triacylglycerols and glycerophospholipids, as it is rapidly converted by phosphatidic acid phosphohydrolase (PAP) to diacylglycerol (DAG), which represents a major source for the biosynthesis of these lipids (Vance and Goldfine 2002) (Fig. 1a). Furthermore, PA can be degraded by CDP-DAG synthetase into CDP-diacylglycerol, which is directly used as substrate for the synthesis of phosphatidylinositol (PI), phosphatidylglycerol (PG), and cardiolipin (CL) (Fig. 1a). Finally, the many isoforms of phospholipase A (PLA) can deacylate PA into LPA (Fig. 1a). Three alternative biosynthetic pathways use distinct lipid precursors to produce what is called "signaling" PA. The first pathway involves the phosphorylation of DAG using ATP as a phosphate source by DAG kinase (DGK) to produce PA (Fig. 1a). Ten isoforms of mammalian DGK (α, β, γ, δ, η, k, ε, ζ, ι, and θ) have been cloned, characterized, and classified in five subtypes sharing a conserved catalytic domain and at least two cysteine-rich domains (Topham 2006). The second pathway involves acylation of LPA by specific lysoPA acyltransferases (LPAAT) to generate PA (Jenkins and Frohman 2005) (Fig. 1a). Six human LPAAT isoforms have been cloned and

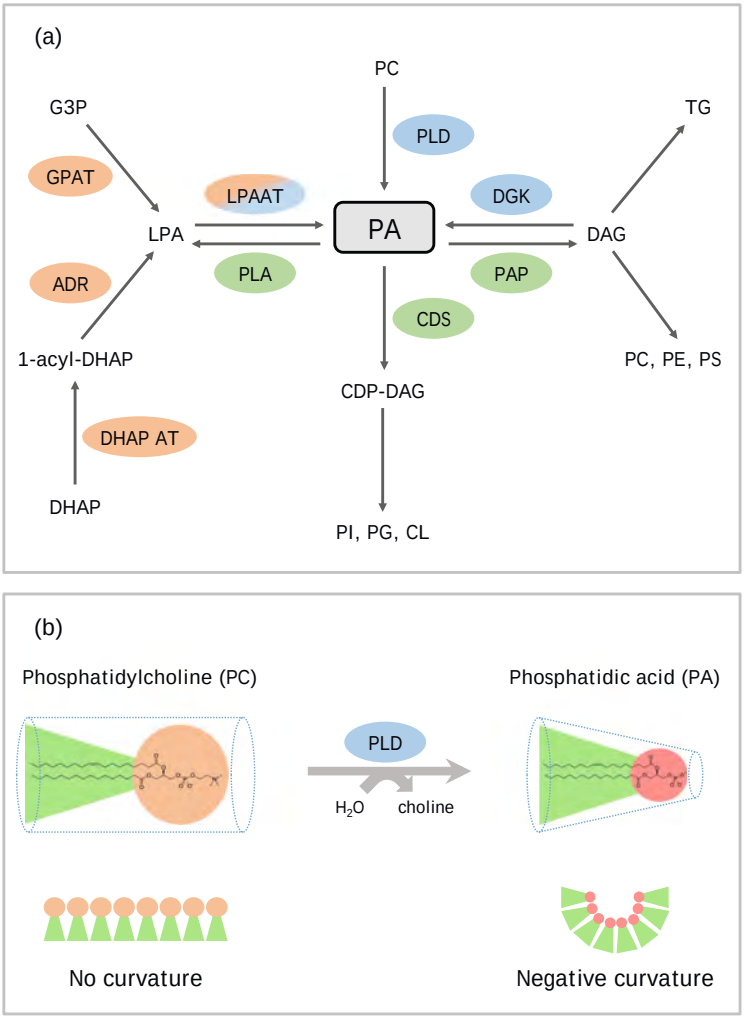

Fig. 1 PA synthesis modifies membrane topology. (**a**) Biosynthetic pathways of structural and signaling PA. PA is a central phospholipid for biosynthetic and signaling reactions. Enzymes in orange denote biosynthetic reactions that lead to structural PA synthesis, whereas enzymes involved in formation of signaling pools of PA are shown in blue. Enzymes involved in PA catabolism are shown in green. (**b**) Phosphatidylcholine hydrolysis by PLD and modification in lipid geometry. The cylindrical PC is transformed into conical PA by enzymatic PLD activity. The accumulation of cone-shaped PA creates regions of negative membrane curvature. Of note, PA exists in a single or a double negative charge mode depending on the local pH environment

characterized (Leung 2001), but more proteins displaying LPAAT activities have been recently identified. For instance, the protein RIBEYE in synaptic ribbon possesses LPAAT activity, providing PA for ultra-fast synaptic release (Schwarz et al. 2011). The third pathway involves phospholipase D (PLD), which catalyzes the

hydrolysis of the distal phosphodiester bond in phosphatidylcholine (PC) to form PA and choline (Fig. 1a). Six isoforms of PLDs have been identified based on sequence homology, but PLD1 and PLD2 are the major isoforms characterized, while thus far no direct PLD activity per se has been demonstrated for PLD3-5 (Frohman 2015). The complexity and diversity of PLD, DGK, and LPAAT families suggest that they are involved in various specific cellular functions and are probably not redundant. In general, signaling PA generated from these enzymes is implicated in multiple cell functions such as cytoskeleton organization, cell survival and proliferation, and membrane and vesicle trafficking (Nelson and Frohman 2015). Intriguingly PC to PA conversion by PLD transforms a cylindrical phospholipid into a conical one (Fig. 1b). Furthermore PA has been shown to produce negative membrane curvature through X-ray diffraction studies (Kooijman et al. 2005). Since biophysical models have proposed that intermediates of the membrane fusion reaction require such cone- or inverted cone-shaped lipid, a direct role of PA as a fusogenic lipid has been proposed (Vitale 2010).

3 A Fusogenic Role of PLD-Generated Phosphatidic Acid in Membrane Fusion

The first elements in favor of a role for PA in regulated exocytosis came from experiments showing a correlation between PLD activation and secretory activity in HL60 cells (Xie et al. 1991; Stutchfield and Cockcroft 1993). Furthermore 1-Butanol, an inhibitor of PA accumulation through the PLD pathway, also strongly affects exocytosis in a number of different cell types (Xie et al. 1991; Stutchfield and Cockcroft 1993; Caumont et al. 1998; Choi et al. 2002). Later, molecular tools established that PLD1 is a key isoform responsible for PA synthesis during catecholamine and insulin secretion (Vitale et al. 2001; Hughes et al. 2004; Huang et al. 2005; Waselle et al. 2005). Accordingly, capacitance recordings from chromaffin cells injected with a dominant-negative form of PLD1 or expressing PLD1 siRNA indicated that PLD1 controls the number of fusion-competent secretory granules docked at the plasma membrane as well as the kinetics of individual fusion events (Vitale et al. 2001; Zeniou-Meyer et al. 2007). Using similar tools, PLD1-generated PA was also reported to contribute actively to the regulated secretion of von Willebrand factor from endothelial cells (Disse et al. 2009). Phagocytosis is another important physiological process that depends on exocytosis of intracellular vesicles. Indeed macrophages engulf and degrade pathogens after generation of extensive plasma membrane protrusions, coming in part from different intracellular membrane compartments. This highly regulated process requires PLD2 activity at the plasma membrane for PA synthesis at the phagocytotic cup, as well as PLD1 activation required for the fusion of intracellular PLD1-positive vesicles with the plasma membrane (Corrotte et al. 2006). Another documented role for PA in secretion relates to the induction of neutrophil exocytosis of azurophilic granules by anti-neutrophil cytoplasmic antibodies (Williams et al. 2007). In apicomplexan parasites, such as *Toxoplasma gondii* and *Plasmodium* spp., specialized organelles termed

micronemes release their contents including adhesins, perforins, and proteases in a PA-dependent manner, critically contributing to invasion and egress from infected cells (Bullen et al. 2016). Sperm acrosome exocytosis also appears to be regulated by PA (Lopez et al. 2012). It must be noted, however, that in the latter case, it is rather DGK-produced PA that is important than PLD-synthesized PA. Nevertheless these results strongly support the notion that PLD-generated PA plays an important role in the last stages of exocytosis but that other sources can also provide PA for efficient secretion.

Many observations support the notion that lipids, in addition to localizing essential components of the exocytotic machinery, also directly contribute to the fusion reaction. The most widely accepted model for membrane fusion involves a combination of protein and lipid elements at the fusion site. It entails the merging of cis-contacting monolayers, leading to the formation of a specific negatively curved lipid structure called the stalk (Chernomordik and Kozlov 2008). The stalk in this case results from the merging of the inner leaflet of the plasma membrane with the outer leaflet of the vesicle prior to fusion pore formation. Cone-shaped lipids, such as PA, have been proposed to facilitate fusion through their intrinsic negative curvatures when accumulated in the inner (cis) leaflets of the contacting bilayers (Fig. 1b). Indeed the property of PA to generate non-bilayer hexagonal II phase membrane domains, particularly in the presence of calcium ions, is well documented (Jouhet 2013). This is important for exocytosis where vesicles have a large positive curvature and the formation of non-bilayer phases may help to lower the energy needed for fusion (Kozlovsky et al. 2002).

In addition to changing membrane topology, PA is unique among anionic lipids because of its small and highly charged headgroup very close to the glycerol backbone. PA tends to form microdomains through intermolecular hydrogen bonding (Boggs 1987; Demel et al. 1992). A partial reduction in charge (e.g., upon divalent cation interaction) reduces electrostatic repulsion between the PA headgroups and increases attractive hydrogen-bonding interactions, possibly resulting in fluid-fluid immiscibility and the formation of PA-enriched microdomains (Garidel et al. 1997). These highly charged microdomains may induce conformational changes in associated proteins (Iversen et al. 2015) and serve as membrane insertion sites for numerous proteins important for exocytosis that tend to accumulate at regions of membrane curvature (Jung et al. 2010; Martens 2010). More directly, PA has been proposed to contribute to many biological processes through its ability to interact with the positively charged domains of numerous proteins (Jenkins and Frohman 2005). PA can also directly serve as source for other lipids, such as DAG, that play positive function in exocytosis. Finally PA stimulates PI kinase to produce PtdIns(4,5)P_2, another key lipid needed for exocytosis (Jones et al. 2000). In fact, it is likely that PA is a critical lipid in any given physiological event through a combination of these functions (Fig. 2).

The biophysical properties of PA also imply that it should rapidly disperse within planar membranes. One possible explanation for the accumulation of PA at the exocytotic site is the occurrence of a PA-binding site that prevents PA diffusion. Such binding of PA to a protein with a highly basic motif has been reported for the

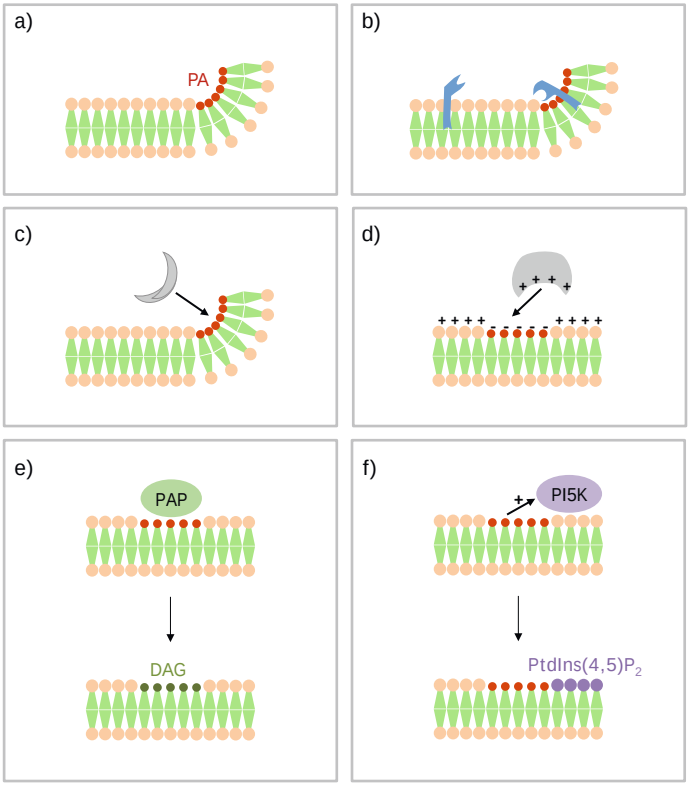

Fig. 2 Model of how PA drives signaling events. (**a**) Local accumulation of PA generates negative membrane curvature or (**b**) membrane-dependent enzymatic activity such as for interfacial activation of lipases. (**c**) Specific curvature-sensing proteins are recruited to PA-induced membrane curved domains. (**d**) Clusters of PA create local negatively charged regions that recruit PA effectors containing positively charged domains. (**e**) PA-phosphatases (PAP) convert PA into DAG, another signaling lipid. (**f**) PA potentiates the activity of PI4P5-kinase, producing PtdIns $(4,5)P_2$, another key signaling lipid

plasma membrane-associated SNARE protein syntaxin-1 (Lam et al. 2008) and for NSF (Jang et al. 2013). A mutation in the polybasic juxtamembrane region of syntaxin-1, which prevents binding to acidic phospholipids such as PA, strongly affects the exocytotic response of chromaffin and PC12 cells, suggesting that PA-binding may be required for the function of syntaxin-1 (Lam et al. 2008). Furthermore, the X-ray structure of this polybasic region of syntaxin-1 confirms that it is important for SNARE complex assembly and that a lipid such as PA may stabilize its orientation (Stein et al. 2009). This idea is further underscored by the observation that cone-shaped lipids that promote negative membrane curvature purify with active zone SNARE proteins (Lewis et al. 2014). Finally the strongest evidence for a direct role of PA in membrane fusion derives from in vitro reconstituted assays that revealed that PA present in a t-SNARE-containing

membrane promoted fusion with a v-SNARE-containing membrane (Vicogne et al. 2006) and studies involving a liposomal flotation assay for fusion with purified yeast vacuolar SNARE chaperones Sec17p/Sec18p and the multifunctional HOPS complex with the Sec1-Munc18 family. In the latter assay, PA was one of the lipids shown to be critical for SNARE complex assembly and fusion (Mima and Wickner 2009).

Intracellular PA levels are tightly controlled, i.e., PA is maintained at very low levels under resting conditions. Visualization of the local formation of PA has necessitated the design of a novel PA-specific sensor derived from the yeast homologue of SNAP25. Ultrastructural analysis revealed PA accumulation near docking sites at the plasma membrane during exocytosis in chromaffin cells (Zeniou-Meyer et al. 2007). Supporting the notion that the intrinsic curvature of PA in the inner leaflet of the plasma membrane contributes to the regulation of fusion pore formation and/or expansion, extracellular application of the inverted cone-shaped lipid lysophosphatidylcholine (LPC) partially rescued secretion from PLD1-depleted cells (Zeniou-Meyer et al. 2007). Interestingly, low levels of PA before exocytosis are probably maintained, since the major source of PA during exocytosis is low-level basal activity PLD1 (Vitale et al. 2001; Hughes et al. 2004). In fact, a complex node of GTPases including Arf6 (Vitale et al. 2002; Béglé et al. 2009), Ral A (Vitale et al. 2005), and Rac1 (Momboisse et al. 2009) and their own regulators (Audebert et al. 2004; Meyer et al. 2006), but also the kinase RSK2, involved in X-linked mental retardation (Zeniou-Meyer et al. 2008), and PtdIns(4,5)P_2 itself (Du et al. 2003), appear altogether to control PLD1 activation for efficient exocytosis in chromaffin cells. Similarly regulators such as Arf6, RalA, and PtdIns(4,5)P_2 have also been identified in the activation of PLD as required for insulin secretion (Grodnitzky et al. 2007; Ljubicic et al. 2009; Waselle et al. 2005).

In conclusion the local buildup of fusogenic lipids such as PA together with other key lipids such as PtdIns(4,5)P_2, DAG, and cholesterol presumably at the neck or near the fusion pore may synergize by changing membrane curvature, together with SNARE-mediated membrane apposition and destabilization, to promote fusion pore formation and/or regulate its stability. The recent development of isoform-specific inhibitors will most likely prove to be useful to define more precisely steps controlled by PLD-generated PA. In addition, the precise localization of these different fusogenic lipids during the short-lived fusion pore formation, expansion, and closure is still unknown and needs important improvement in high-resolution imaging techniques and lipid probes to be adequately addressed. It must be also noted that the contribution of PA in early steps of the secretory pathway have not been as well investigated (Gasman and Vitale 2017). For instance, recent findings suggest that PLD-generated PA mostly affects docking and priming in sea urchin egg fusion (Rogasevskaia and Coorssen 2015) and as well is involved in early steps of sperm acrosomal exocytosis (Lopez et al. 2012).

4 A Role for PLD-Generated PA in Neurological Diseases?

Numerous lipids have been shown to be involved in pre- and post-synaptic functions and neurological diseases (Lauwers et al. 2016). PLD1 largely localizes to neurons in the central nervous system but is also present in oligodendrocytes, while PLD2 is largely found in astrocytes (Kim et al. 2010; Rohrbough and Broadie 2005; Zhang et al. 2004). However, the expression of PLD isoforms in the brain has been relatively controversial in regard to the cell type, isoform expression, and pattern of expression throughout development (Klein 2005). In fact, only a few recent papers have reported the time course of PLD1 expression in maturing neuronal cell cultures, with optimal expression at DIV5-6, then decreasing by more than 50% (Zhu et al. 2012) or 80% (Ammar et al. 2015). It is likely that the relative uncertainty of the PLD isoform expression pattern relies from the limited quality of the anti-PLD antibodies available and from the different types of neuronal culture used in these studies. To date, the strongest evidence that PLD1 may be involved in neurotransmission comes from experiments where injection of catalytically inactive PLD1 protein into presynaptic cholinergic neurons in the buccal ganglion of *Aplysia californica* led to a fast and dose-dependent inhibition of acetylcholine release, suggesting that a rapid exchange of inactive dominant-negative PLD1 for wild-type PLD1 causes a dramatic decrease in the amount of exocytosis (Humeau et al. 2001). These results support the notion that PLD1 generates PA-rich microdomains that recruit or activate proteins required for synaptic vesicle fusion with the plasma membrane (Humeau et al. 2009). These PA-rich domains might also physically bend the membrane to promote mixing of the lipids in the plasma and vesicle membranes during fusion as described previously. Since null mutations in RSK2, a kinase that regulates PLD1 activity, are responsible for the symptoms of the Coffin Lowry Syndrome disease, it has been proposed that alteration of PLD1 activation could explain the intellectual disabilities of patients through at least partially inhibiting neurotransmitter exocytosis (Zeniou-Meyer et al. 2008, 2010). Conversely, PLD2 has been implicated in the modulation of glutamate transporter function (Mateos et al. 2012) and the internalization of mGluR (Bhattacharya et al. 2004), both of which could potentially affect synaptic activity. Alteration of the DAG-PA balance could also be responsible for some of the cellular and behavioral symptoms observed in a mouse model of fragile X disease (Tabet et al. 2016a, b).

In the presence of low amounts of ethanol, PLD produces phosphatidylethanol at the expense of PA. So although ethanol does not inhibit PLD activity per se, it has long been used as disruptor of signaling pathways that involve PLD activation (Frohman 2015). As indicated above, PA is a lipid second messenger in its own right, with several downstream targets that relate to cell proliferation. Ethanol, on the other hand, has long been known to suppress proliferation of brain cells, especially astrocytes in vitro and in vivo. Astrocytes are more sensitive than neurons to ethanol, at least concerning proliferation. Thus, the inhibition of astroglial proliferation by ethanol has been suggested to be responsible for some features of fetal alcohol syndrome. Children born from heavy-drinking pregnant women have characteristic facial features and reduced brain and body weights, with microcephaly indicating a

delay in growth and maturation of the brain (Guerri and Renau-Piqueras 1997; Guizzetti et al. 1997). As numerous studies have validated the activation of PLD in the brain by mitogenic and growth factors, it is likely that PLD1/2-generated PA plays an important role in normal brain development and that alteration of these PLD activities is responsible for some of the brain developmental pathologies.

In addition to its effect on cell proliferation, PLD is also likely to play a role in neuronal development by promoting extension of neurites. PLD activity has been implicated in neurite outgrowth in various neuronal models for over two decades, but most of the original findings relied on the use of ethanol as a non-specific inhibitor of PA synthesis, and in most cases the PLD isoform involved was not identified (Klein 2005). Using a combination of knockout mice, a gene-silencing approach, and the recently described isoform-specific PLD inhibitors, it has more recently been demonstrated that PLD1 contributes to neurite outgrowth, dendrite branching, and spine development (Ammar et al. 2013). It is also worth mentioning that the GTPase RalB promotes neuronal branching through a pathway involving PLD (Lalli and Hall 2005). Conversely, however, using different methods to modulate protein levels and neuronal type, PLD1 has been described to negatively regulate dendritic branching in hippocampal neurons (Zhu et al. 2012). Interestingly, PLD1 was recently shown to participate in the BDNF signaling pathway in cortical neurons, supporting the notion of neuronal development regulation by PLD (Ammar et al. 2015).

The data discussed above implicate the PLD pathway in brain development, but PLD-generated PA has also been shown to be involved in neurodegeneration. Indeed, increased PLD activity has been found in Alzheimer brains postmortem (Kanfer et al. 1996), and other studies have noted that β-amyloid increases PLD expression and activity (Klein 2005). Moreover, synucleins, which are present in amyloid plaques in Alzheimer's disease and in Parkinson's disease, interact with and inhibit PLD (Jenco et al. 1998; Ahn et al. 2002; Payton et al. 2004). However, mass spectrometry analysis of Huntington's disease mouse brains reveals modification of the levels of few PA species (Vodicka et al. 2015). Of note, it was recently suggested that α-synuclein may cross-bridge vesicular SNARE and acidic phospholipids such as PA to facilitate SNARE-dependent vesicle docking, suggesting a possible link between these diseases and alteration of vesicular trafficking regulated by PLD (Lou et al. 2017). Furthermore both oxidative and antioxidative compounds have been reported to modulate PLD activity in neuronal and glial cells (Oh et al. 2000; Servitja et al. 2000; Kim et al. 2004a, b). Interestingly, PLD1 appears to regulate the intracellular trafficking of preselinin 1/γ-secretase (Liu et al. 2009), while the memory deficit in a transgenic model of Alzheimer disease was rescued when the PLD2 gene was ablated (Oliveira et al. 2010). In line with this finding, lipidomic analysis revealed that levels of several PA species were modified in this mouse model and in Alzheimer's disease brain patients (Oliveira et al. 2010). PLD activities were also investigated in acute neurodegeneration induced by brain ischemia. In vitro, acute hypoxia did not change PLD activity in hippocampal slices (Klein et al. 1993), but global ischemia in vivo diminished PLD activity in rat brain (Nishida et al. 1994). A massive increase in PLD1 expression was observed in reactive astrocytes from the hippocampus at 7 to 10 days after forebrain ischemia in vivo (Lee et al. 2000). Increased PLD expression

apparently accompanies astrogliosis, repair, and remodeling of tissue after ischemia, and astrogliosis during inflammation could underlie increased PLD1 expression in scrapie-infected mouse brain (Jin et al. 2005) and in sciatic neurons during experimental autoimmune neuritis (Shin et al. 2002). Prenatal stress induces brain abnormalities of the offspring, with disruption of dendritic profiles, spine distribution, and adult neurogenesis, all of which can lead to pain hypersensitivity that is dependent on PLD1 signaling (Sun et al. 2013). Finally, compression injury of rat spinal cord (Jung et al. 2010), cryoinjury in rat cortex (Kim et al. 2004a), and kainate-induced seizures in rat hippocampus (Kim et al. 2004c) lead to increased PLD activity in astrocytes. Taken together, these pioneer studies contributed to the notion that PLD expression and activity accompany normal brain development and remodeling and that alterations of PLD-generated PA levels correlate and/or are directly responsible for different human neurological diseases. It is evident that understanding the exact role of PA in these pathologies remains the next challenge.

5 Conclusion

The last two decades have seen generation of substantial evidence that PA synthesized by different enzymatic pathways contributes to normal and pathological conditions. Among these strong indications is a direct contribution of PLD-generated PA in the last steps of regulated exocytosis, a key process that allows cells to release informative molecules such as hormones, neurotransmitters, and neuropeptides. Despite our increased understanding, the exact molecular steps affected and targets of PA action are still elusive. In addition, recent lipidomic analyses have revealed that, based on their fatty acid composition, three to four dozen distinct species of PA co-exist in most cells (Andreyev et al. 2010; Kassas et al. 2017; Oliveira et al. 2010). The function of each of these PA species, however, remains completely unknown. Therefore, the development of novel tools to further decipher the role of each PA species in regulated exocytosis, neurological diseases, and many other key cellular functions is now required. This is especially important as membrane-lipid therapies are expected to become new efficient treatments for many human pathologies (Escribá 2017).

References

Ahn BH, Rhim H, Kim SY, Sung YM, Lee MY, Choi JY, Wolozin B, Chang JS, Lee YH, Kwon TK, Chung KC, Yoon SH, Hahn SJ, Kim MS, Jo YH, Min DS (2002) alpha-Synuclein interacts with phospholipase D isozymes and inhibits pervanadate-induced phospholipase D activation in human embryonic kidney-293 cells. J Biol Chem 277(14):12334–12342

Ammar MR, Humeau Y, Hanauer A, Nieswandt B, Bader MF, Vitale N (2013) The Coffin-Lowry syndrome-associated protein RSK2 regulates neurite outgrowth through phosphorylation of phospholipase D1 (PLD1) and synthesis of phosphatidic acid. J Neurosci 33(50):19470–19479

Ammar MR, Thahouly T, Hanauer A, Stegner D, Nieswandt B, Vitale N (2015) PLD1 participates in BDNF-induced signalling in cortical neurons. Sci Rep 5:14778

Andreyev AY, Fahy E, Guan Z, Kelly S, Li X, McDonald JG, Milne S, Myers D, Park H, Ryan A, Thompson BM, Wang E, Zhao Y, Brown HA, Merrill AH, Raetz CR, Russell DW, Subramaniam S, Dennis EA (2010) Subcellular organelle lipidomics in TLR-4-activated macrophages. J Lipid Res 51(9):2785–2797

Audebert S, Navarro C, Nourry C, Chasserot-Golaz S, Lécine P, Bellaiche Y, Dupont JL, Premont RT, Sempéré C, Strub JM, Van Dorsselaer A, Vitale N, Borg JP (2004) Mammalian Scribble forms a tight complex with the betaPIX exchange factor. Curr Biol 14(11):987–995

Bader MF, Holz RW, Kumakura K, Vitale N (2002) Exocytosis: the chromaffin cell as a model system. Ann N Y Acad Sci 971:178–183

Béglé A, Tryoen-Tóth P, de Barry J, Bader MF, Vitale N (2009) ARF6 regulates the synthesis of fusogenic lipids for calcium-regulated exocytosis in neuroendocrine cells. J Biol Chem 284 (8):4836–4845

Bhattacharya M, Babwah AV, Godin C, Anborgh PH, Dale LB, Poulter MO, Ferguson SS (2004) Ral and phospholipase D2-dependent pathway for constitutive metabotropic glutamate receptor endocytosis. J Neurosci 24(40):8752–8761

Boggs JM (1987) Lipid intermolecular hydrogen bonding: influence on structural organization and membrane function. Biochim Biophys Acta 906(3):353–404

Bullen HE, Jia Y, Yamaryo-Botté Y, Bisio H, Zhang O, Jemelin NK, Marq JB, Carruthers V, Botté CY, Soldati-Favre D (2016) Phosphatidic acid-mediated signaling regulates microneme secretion in toxoplasma. Cell Host Microbe 19(3):349–360

Burgess TL, Kelly RB (1987) Constitutive and regulated secretion of proteins. Annu Rev Cell Biol 3:243–293

Caumont AS, Galas MC, Vitale N, Aunis D, Bader MF (1998) Regulated exocytosis in chromaffin cells. Translocation of ARF6 stimulates a plasma membrane-associated phospholipase D. J Biol Chem 273(3):1373–1379

Chernomordik LV, Kozlov MM (2008) Mechanics of membrane fusion. Nat Struct Mol Biol 15(7):675–683

Choi WS, Kim YM, Combs C, Frohman MA, Beaven MA (2002) Phospholipases D1and D2 regulate different phases of exocytosis in mast cells. J Immunol 168(11):5682–5689

Corrotte M, Chasserot-Golaz S, Huang P, Du G, Ktistakis NT, Frohman MA, Vitale N, Bader MF, Grant NJ (2006) Dynamics and function of phospholipase D and phosphatidic acid during phagocytosis. Traffic 7(3):365–377

Demel RA, Yin CC, Lin BZ, Hauser H (1992) Monolayer characteristics and thermal behaviour of phosphatidic acids. Chem Phys Lipids 60:209–223

Disse J, Vitale N, Bader MF, Gerke V (2009) Phospholipase D1 is specifically required for regulated secretion of von Willebrand factor from endothelial cells. Blood 113:973–980

Du G, Altshuller YM, Vitale N, Huang P, Chasserot-Golaz S, Morris AJ, Bader MF, Frohman MA (2003) Regulation of phospholipase D1 subcellular cycling through coordination of multiple membrane association motifs. J Cell Biol 162(2):305–315

Escribá PV (2017) Membrane-lipid therapy: a historical perspective of membrane-targeted therapies – from lipid bilayer structure to the pathophysiological regulation of cells. Biochim Biophys Acta 1859(9 PtB):1493–1506

Frohman MA (2015) The phospholipase D superfamily as therapeutic targets. Trends Pharmacol Sci 36(3):137–144

Fulop T, Smith C (2006) Physiological stimulation regulates the exocytic mode through calcium activation of protein kinase C in mouse chromaffin cells. Biochem J 399(1):111–119

Garidel P, Johann C, Blume A (1997) Nonideal mixing and phase separation in phosphatidylcholine-phosphatidic acid mixtures as a function of acyl chain length and pH. Biophys J 72(5):2196–2210

Gasman S, Vitale N (2017) Lipid remodelling in neuroendocrine secretion. Biol Cell 109 (11):381–390

Grodnitzky JA, Syed N, Kimber MJ, Day TA, Donaldson JG, Hsu WH (2007) Somatostatin receptors signal through EFA6A-ARF6 to activate phospholipase D in clonal beta-cells. J Biol Chem 282(18):13410–13418

Guerri C, Renau-Piqueras J (1997) Alcohol, astroglia, and brain development. Mol Neurobiol 15 (1):65–81

Guizzetti M, Catlin M, Costa LG (1997) The effects of ethanol on glial cell proliferation: relevanceto the fetal alcohol syndrome. Front Biosci 2:e93–e98

Huang P, Altshuller YM, Hou JC, Pessin JE, Frohman MA (2005) Insulin-stimulated plasma membrane fusion of Glut4 glucose transporter-containing vesicles is regulated by phospholipase D1. Mol Biol Cell 16(6):2614–2623

Hughes WE, Elgundi Z, Huang P, Frohman MA, Biden TJ (2004) Phospholipase D1 regulates secretagogue-stimulated insulin release in pancreatic p-cells. J Biol Chem 279:27534–27541

Humeau Y, Vitale N, Chasserot-Golaz S, Dupont JL, Du G, Frohman MA, Bader MF, Poulain B (2001) A role for phospholipase D1 in neurotransmitter release. Proc Natl Acad Sci U S A 98 (26):15300–15305

Humeau Y, Gambino F, Chelly J, Vitale N (2009) X-linked mental retardation: focus on synaptic function and plasticity. J Neurochem 109(1):1–14

Iversen L, Mathiasen S, Larsen JB, Stamou D (2015) Membrane curvature bends the laws of physicsand chemistry. Nat Chem Biol 11(11):822–825

Jahn R, Fasshauer D (2012) Molecular machines governing exocytosis of synaptic vesicles. Nature 490(7419):201–207

Jang HJ, Yang YR, Kim JK, Choi JH, Seo YK, Lee YH, Lee JE, Ryu SH, Suh PG (2013) Phospholipase C-γ1 involved in brain disorders. Adv Biol Regul 53(1):51–62

Jenco JM, Rawlingson A, Daniels B, Morris AJ (1998) Regulation of phospholipase D2: selective inhibition of mammalian phospholipase D isoenzymes by alpha- and beta-synucleins. Biochemistry 37(14):4901–4909

Jenkins GM, Frohman MA (2005) Phospholipase D: a lipid centric review. Cell Mol Life Sci 62 (19–20):2305–2316

Jin JK, Kim NH, Min DS, Kim JI, Choi JK, Jeong BH, Choi SI, Choi EK, Carp RI, Kim YS (2005) Increased expression of phospholipase D1 in the brains of scrapie-infected mice. J Neurochem 92(3):452–461

Jones DH, Morris JB, Morgan CP, Kondo H, Irvine RF, Cockcroft S (2000) Type I phosphatidylinositol 4-phosphate 5-kinase directly interacts with ADP-ribosylation factor 1 and is responsible for phosphatidylinositol 4,5-bisphosphate synthesis in the golgi compartment. J Biol Chem 275(18):13962–13966

Jouhet J (2013) Importance of the hexagonal lipid phase in biological membrane organization. Front Plant Sci 4:494

Jung AG, Labarrera C, Jansen AM, Qvortrup K, Wild K, Kjaerulff O (2010) A mutational analysis of the endophilin-A N-BAR domain performed in living flies. PLoS One 5:e9492

Kanfer JN, Singh IN, Pettegrew JW, McCartney DG, Sorrentino G (1996) Phospholipid metabolism in Alzheimer's disease and in a human cholinergic cell. J Lipid Mediat Cell Signal 14 (1–3):361–363

Kassas N, Tanguy E, Thahouly T, Fouillen L, Heintz D, Chasserot-Golaz S, Bader MF, Grant NJ, Vitale N (2017) Comparative characterization of phosphatidic acid sensors and their localization during frustrated phagocytosis. J Biol Chem 292(10):4266–4279

Kim J, Min G, Bae YS, Min DS (2004a) Phospholipase D is involved in oxidative stress-induced migration of vascular smooth muscle cells via tyrosine phosphorylation and protein kinase C. Exp Mol Med 36(2):103–109

Kim SY, Ahn BH, Min KJ, Lee YH, Joe EH, Min DS (2004b) Phospholipase D isozymes mediate epigallocatechin gallate-induced cyclooxygenase-2 expression in astrocyte cells. J Biol Chem 279(37):38125–38133

Kim SY, Min DS, Choi JS, Choi YS, Park HJ, Sung KW, Kim J, Lee MY (2004c) Differential expression of phospholipase D isozymes in the hippocampus following kainic acid-induced seizures. J Neuropathol Exp Neurol 63:812–820

Kim M, Moon C, Kim H, Shin MK, Min do S, Shin T (2010) Developmental levels of phospholipase D isozymes in the brain of developing rats. Acta Histochem 112(1):81–91

Klein J (2005) Functions and pathophysiological roles of phospholipase D in the brain. J Neurochem 94(6):1473–1487
Klein J, Holler T, Cappel E, Köppen A, Löffelholz K (1993) Release of choline from rat brain under hypoxia: contribution from phospholipase A2 but not from phospholipase D. Brain Res 630 (1–2):337–340
Kooijman EE, Chupin V, Fuller NL, Kozlov MM, de Kruijff B, Burger KN, Rand PR (2005) Spontaneous curvature of phosphatidic acid and lysophosphatidic acid. Biochemistry 44 (6):2097–2102
Kozlovsky Y, Chernomordik LV, Kozlov MM (2002) Lipid intermediates in membrane fusion: formation, structure, and decay of hemifusion diaphragm. Biophys J 83(5):2634–2651
Lalli G, Hall A (2005) Ral GTPases regulate neurite branching through GAP-43 and the exocyst complex. J Cell Biol 171(5):857–869
Lam IP, Siu FK, Chu JY, Chow BK (2008) Multiple actions of secretin in the human body. Int Rev Cytol 265:159–190
Lauwers E, Goodchild R, Verstreken P (2016) Membrane lipids in presynaptic function and disease. Neuron 90(1):11–25
Lee MY, Kim SY, Min DS, Choi YS, Shin SL, Chun MH, Lee SB, Kim MS, Jo YH (2000) Upregulation of phospholipase D in astrocytes in response to transient forebrain ischemia. Glia 30(3):311–317
Leung DW (2001) The structure and functions of human lysophosphatidic acid acyltransferases. Front Biosci 6(1):D944–D953
Lewis KT, Maddipati KR, Taatjes DJ, Jena BP (2014) Neuronal porosome lipidome. J Cell MolMed 18(10):1927–1937
Liu Y, Zhang YW, Wang X, Zhang H, You X, Liao FF, Xu H (2009) Intracellular trafficking of presenilin 1 is regulated by beta-amyloid precursor protein and phospholipase D1. J Biol Chem 284(18):12145–12152
Ljubicic S, Bezzi P, Vitale N, Regazzi R (2009) The GTPase RalA regulates different steps of the secretory process in pancreatic beta-cells. PLoS One 4(11):e7770
Lopez JA, Brennan AJ, Whisstock JC, Voskoboinik I, Trapani JA (2012) Protecting a serial killer: pathways for perforin trafficking and self-defence ensure sequential target cell death. Trends Immunol 33(8):406–412
Lou X, Kim J, Hawk BJ, Shin YK (2017) α-Synuclein may cross-bridge v-SNARE and acidic phospholipids to facilitate SNARE-dependent vesicle docking. Biochem J 474(12):2039–2049
Martens S (2010) Role of C2 domain proteins during synaptic vesicle exocytosis. Biochem Soc Trans 38:213–216
Mateos MV, Giusto NM, Salvador GA (2012) Distinctive roles of PLD signaling elicited by oxidative stress in synaptic endings from adult and aged rats. Biochim Biophys Acta 1823 (12):2136–2148
Meyer MZ, Déliot N, Chasserot-Golaz S, Premont RT, Bader MF, Vitale N (2006) Regulation of neuroendocrine exocytosis by the ARF6 GTPase-activating protein GIT1. J Biol Chem 281 (12):7919–7926
Mima J, Wickner W (2009) Phosphoinositides and SNARE chaperones synergistically assemble and remodel SNARE complexes for membrane fusion. Proc Natl Acad Sci U S A 106 (38):16191–16196
Momboisse F, Lonchamp E, Calco V, Ceridono M, Vitale N, Bader MF, Gasman S (2009) betaPIX-activated Rac1 stimulates the activation of phospholipase D, which is associated with exocytosis in neuroendocrine cells. J Cell Sci 122(Pt 6):798–806
Nelson RK, Frohman MA (2015) Physiological and pathophysiological roles for phospholipase D. J Lipid Res 56(12):2229–2237
Nishida A, Emoto K, Shimizu M, Uozumi T, Yamawaki S (1994) Brain ischemia decreases phosphatidylcholine-phospholipase D but not phosphatidylinositol-phospholipase C in rats. Stroke 25(6):1247–1251

Oh SO, Hong JH, Kim YR, Yoo HS, Lee SH, Lim K, Hwang BD, Exton JH, Park SK (2000) Regulation of phospholipase D2 by H(2)O(2) in PC12 cells. J Neurochem 75(6):2445–2454

Oliveira TG, Chan RB, Tian H, Laredo M, Shui G, Staniszewski A, Zhang H, Wang L, Kim TW, Duff KE, Wenk MR, Arancio O, Di Paolo G (2010) Phospholipase d2 ablation ameliorates Alzheimer's disease-linked synaptic dysfunction and cognitive deficits. J Neurosci 30 (49):16419–16428

Payton JE, Perrin RJ, Woods WS, George JM (2004) Structural determinants of PLD2 inhibition by alpha-synuclein. J Mol Biol 337(4):1001–1009

Rogasevskaia TP, Coorssen JR (2015) The role of phospholipase D in regulated exocytosis. J Biol Chem 290(48):28683–28696

Rohrbough J, Broadie K (2005) Lipid regulation of the synaptic vesicle cycle. Nat Rev Neurosci 6 (2):139–150

Schwarz K, Natarajan S, Kassas N, Vitale N, Schmitz F (2011) The synaptic ribbon is a site of phosphatidic acid generation in ribbon synapses. J Neurosci 31(44):15996–16011

Servitja JM, Masgrau R, Pardo R, Sarri E, Picatoste F (2000) Effects of oxidative stress on phospholipid signaling in rat cultured astrocytes and brain slices. J Neurochem 75(2):788–794

Shin EY, Ma EK, Kim CK, Kwak SJ, Kim EG (2002) Src/ERK but not phospholipase D is involved in keratinocyte growth factor-stimulated secretion of matrix metalloprotease-9 and urokinase-type plasminogen activator in SNU-16 human stomach cancer cell. J Cancer Res Clin Oncol 128 (11):596–602

Stein A, Weber G, Wahl MC, Jahn R (2009) Helical extension of the neuronal SNARE complex into the membrane. Nature 460:525–528

Stutchfield J, Cockcroft S (1993) Correlation between secretion and phospholipase D activation in differentiated HL60 cells. Biochem J 293(Pt3):649–655

Sun H, Xia M, Shahane SA, Jadhav A, Austin CP, Huang R (2013) Are hERG channel blockers also phospholipidosis inducers? Bioorg Med Chem Lett 23(16):4587–4590

Tabet R, Moutin E, Becker JA, Heintz D, Fouillen L, Flatter E, Krężel W, Alunni V, Koebel P, Dembélé D, Tassone F, Bardoni B, Mandel JL, Vitale N, Muller D, Le Merrer J, Moine H (2016a) Fragile X Mental Retardation Protein (FMRP) controls diacylglycerol kinase activity in neurons. Proc Natl Acad Sci U S A 113:E3619–E3628

Tabet R, Vitale N, Moine H (2016b) Fragile X syndrome: are signaling lipids the missing culprits? Biochimie 130:188–194

Tanguy E, Carmon O, Wang Q, Jeandel L, Chasserot-Golaz S, Montero-Hadjadje M, Vitale N (2016) Lipids implicated in the journey of a secretory granule: from biogenesis to fusion. J Neurochem 137(6):904–912

Taraska JW, Perrais D, Ohara-Imaizumi M, Nagamatsu S, Almers W (2003) Secretory granules are recaptured largely intact after stimulated exocytosis in cultured endocrine cells. Proc Natl Acad Sci U S A 100(4):2070–2075. Epub 21 Jan 2003

Topham MK (2006) Signaling roles of diacylglycerol kinases. J Cell Biochem 97(3):474–484 Review

van Kempen GT, vanderLeest HT, van den Berg RJ, Eilers P, Westerink RH (2011) Three distinct modes of exocytosis revealed by amperometry in neuroendocrine cells. Biophys J 100 (4):968–977

Vance DE, Goldfine H (2002) Konrad Bloch – a pioneer in cholesterol and fatty acid biosynthesis. Biochem Biophys Res Commun 292(5):1117–1127

Vance JE, Vance DE (2004) Phospholipid biosynthesis in mammalian cells. Biochem Cell Biol 82 (1):113–128

Vicogne J, VollenweiderD SJR, Huang P, Frohman MA, Pessin JE (2006) Asymmetric phospholipid distribution drives in vitro reconstituted SNARE-dependent membrane fusion. Proc Natl Acad Sci U S A 103:14761–14766

Vitale N (2010) Synthesis of fusogenic lipids through activation of phospholipase D1 by GTPases and the kinase RSK2 is required for calcium-regulated exocytosis in neuroendocrine cells. Biochem Soc Trans 38(Pt 1):167–171

Vitale N, Caumont AS, Chasserot-Golaz S, Du G, Wu S, Sciorra VA, Morris AJ, Frohman MA, Bader MF (2001) Phospholipase D1: a key factor for the exocytotic machinery in neuroendocrine cells. EMBO J 20(10):2424–2434

Vitale N, Chasserot-Golaz S, Bader MF (2002) Regulated secretion in chromaffin cells: an essential role for ARF6-regulated phospholipase D in the late stages of exocytosis. Ann N Y Acad Sci 971:193–200

Vitale N, Mawet J, Camonis J, Regazzi R, Bader MF, Chasserot-Golaz S (2005) The small GTPase RalA controls exocytosis of large dense core secretory granules by interacting with ARF6-dependent phospholipase D1. J Biol Chem 280(33):29921–29928

Vodicka P, Mo S, Tousley A, Green KM, Sapp E, Iuliano M, Sadri-Vakili G, Shaffer SA, Aronin N, DiFiglia M, Kegel-Gleason KB (2015) Mass spectrometry analysis of wild-type and knock-in Q140/Q140 Huntington's disease mouse brains reveals changes in glycerophospholipids including alterations in phosphatidic acid and lyso-phosphatidic acid. J Huntingtons Dis 4(2):187–201

Waselle L, Gerona RR, Vitale N, Martin TF, Bader MF, Regazzi R (2005) Role of phosphoinositide signaling in the control of insulin exocytosis. Mol Endocrinol 19(12):3097–3106. Epub 4 Aug 2005

Williams JM, Pettitt TR, Powell W, Grove J, Savage CO, Wakelam MJ et al (2007) Antineutrophil cytoplasm antibody-stimulated neutrophil adhesion depends on diacylglycerol kinase-catalyzed phosphatidic acid formation. J Am Soc Nephrol 18(4):1112–1120

Xie MS, Jacobs LS, Dubyak GR (1991) Activation of phospholipase D and primary granule secretion by P2-purinergic- and chemotactic peptide-receptor agaonists is induced during granulocyte differenciation of HL-60 cells. J Clin Invest 88:45–54

Zeniou-Meyer M, Zabari N, Ashery U, Chasserot-Golaz S, Haeberlé AM, Demais V, Bailly Y, Gottfried I, Nakanishi H, Neiman AM, Du G, Frohman MA, Bader MF, Vitale N (2007) Phospholipase D1 production of phosphatidic acid at the plasma membrane promotes exocytosis of large dense-core granules at a late stage. J Biol Chem 282(30):21746–21757

Zeniou-Meyer M, Liu Y, Béglé A, Olanich ME, Hanauer A, Becherer U, Rettig J, Bader MF, Vitale N (2008) The Coffin-Lowry syndrome-associated protein RSK2 is implicated in calcium-regulated exocytosis through the regulation of PLD1. Proc Natl Acad Sci U S A 105 (24):8434–8439

Zeniou-Meyer M, Gambino F, Ammar MR, Humeau Y, Vitale N (2010) The Coffin-Lowry syndrome-associated protein RSK2 and neurosecretion. Cell Mol Neurobiol 30(8):1401–1406

Zhang Y, Huang P, Du G, Kanaho Y, Frohman MA, Tsirka SE (2004) Increased expression of two phospholipase D isoforms during experimentally induced hippocampal mossy fiber outgrowth. Glia 46(1):74–83

Zhu YB, Kang K, Zhang Y, Qi C, Li G, Yin DM, Wang Y (2012) PLD1 negatively regulates dendritic branching. J Neurosci 32(23):7960–7969

OCL 2018, 25(4), D408

https://doi.org/10.1051/ocl/2018024

OCL Oilseeds & fats Crops and Lipids

Topical issue on:
LIPIDS & BRAIN IV: LIPIDS IN ALZHEIMER'S DISEASE
LIPIDS & BRAIN IV : LES LIPIDES DANS LA MALADIE D'ALZHEIMER

Available online at:
www.ocl-journal.org

REVIEW OPEN ACCESS

Topical Issue

Different species of phosphatidic acid are produced during neuronal growth and neurosecretion

Emeline Tanguy[1], Qili Wang[1], Pierre Coste de Bagneaux[1], Laetitia Fouillen[2], Tamou Thahouly[1], Mohamed-Raafet Ammar[1] and Nicolas Vitale[1,3,*]

[1] Institut des Neurosciences Cellulaires et Intégratives, CNRS UPR 3212, Université de Strasbourg, 5 rue Blaise Pascal, 67000 Strasbourg, France
[2] Laboratoire de Biogénèse Membranaire, UMR-5200 CNRS, Plateforme Métabolome, Université de Bordeaux, 33883 Villenave D'Ornon, France
[3] INSERM, 75654, Paris cedex 13, France

Received 24 January 2018 – Accepted 15 March 2018

Abstract – Although originally restricted to their structural role as major constituents of membranes, lipids are now well-defined actors to integrate intracellular or extracellular signals. Accordingly, it has been known for decades that lipids, especially those coming from diet, are important to maintain normal physiological functions and good health. This is especially the case to maintain proper cognitive functions and avoid neuronal degeneration. But besides this empiric knowledge, the exact molecular nature of lipids in cellular signaling, as well as their precise mode of action are only starting to emerge. The recent development of novel pharmacological, molecular, cellular and genetic tools to study lipids *in vitro* and *in vivo* has contributed to this improvement in our knowledge. Among these important lipids, phosphatidic acid (PA) plays a unique and central role in a great variety of cellular functions. This article will review the different findings illustrating the involvement of PA generated by phospholipase D (PLD) and diacylglycerol kinases (DGK) in the different steps of neuronal development and neurosecretion. We will also present lipidomic evidences indicating that different species of PA are synthesized during these two key neuronal phenomena.

Keywords: exocytosis / neuroendocrine / neuron / phospholipase D / phosphatidic acid

Résumé – Différentes formes d'acide phosphatidique sont produites au cours de la croissance neuronale et la neurosécrétion. Bien qu'originalement restreints à leur rôle majeur de constituants principaux des membranes, il est maintenant communément admis que certains lipides possèdent également une fonction importante d'intégration des signaux intra- ou extra-cellulaires. En accord avec cette notion, cela fait des décennies qu'il est reconnu que les lipides, principalement *via* l'alimentation, jouent un rôle crucial dans le maintien de l'homéostasie de nombreuses fonctions physiologiques et dans la santé humaine au sens large. Ceci est particulièrement le cas pour la conservation d'un niveau optimal des fonctions cognitives et pour lutter contre la dégénérescence neuronale. Toutefois, malgré ces connaissances empiriques, la nature exacte des lipides impliqués, ainsi que les mécanismes d'action mis en jeu peinent à émerger. Le développement récent de nouveaux outils génétiques, moléculaires, et pharmacologiques pour étudier les lipides *in vitro* et *in vivo* permettent à présent d'améliorer nos connaissances. Parmi ces lipides, l'acide phosphatidique joue un rôle particulier et central dans diverses fonctions cellulaires essentielles. Cet article résume les observations récentes qui illustrent que l'acide phosphatidique, produit par deux voies enzymatiques distinctes impliquant les phospholipases D et les diacylglycérol-kinases, est impliqué dans le développement neuronal et la neurosécrétion. Pour finir, nous présentons des résultats d'analyses lipidomiques qui indiquent que différentes formes de l'acide phosphatidique sont produites au cours de ces deux processus neuronaux majeurs.

Mot clés : acide phosphatidique / exocytose / neuroendocrine / neurone / phospholipase D

*Correspondence: vitalen@inci-cnrs.unistra.fr

1 Introduction

Normal brain function requires the establishment of specific neuronal networks mediated by synapses (*i.e.* structures allowing chemical or electrical communication between neurons). Indeed, during their development, neurons exhibit various morphological and structural changes including axon and dendrite outgrowth, dendritic branching and ramification and spine development that ultimately allow synapse formation and maintenance, which are critical events in the establishment of neuronal networks (Dotti *et al.*, 1988). Further, neuronal development and maturation require plasma membrane expansion and rearrangement provided essentially by two membrane trafficking mechanisms: exocytosis and endocytosis (Gasman and Vitale, 2017). In a first part, exocytosis supports intracellular membrane supply required for the plasma membrane enlargement as well as neurotrophines receptor and neuronal adhesion molecules membrane expression that insure synapse formation and maintenance (Sytnyk *et al.*, 2017). In a second part, endocytosis insures intercellular signal integration required as well for synaptic formation and specificity. Moreover, membrane lipids composition has emerged as an important player during membrane trafficking and cell signaling. Further, it is tempting to speculate that specific lipids and their dynamics are critically important for membrane reorganization and neuronal development.

Among all the lipids, phosphatidic acid (PA) appears to have a particular function in these membrane-related phenomena's. PA is the simplest glycerophospholipid and plays a key structural role as a precursor of most glycerophospholipids, but it is also considered as an important player in the transmission, amplification and regulation of a variety of intracellular signaling and cellular functions (Ammar *et al.*, 2014). At the molecular level, this signaling PA could interact with various proteins to modulate their catalytic activity and/or their membrane association including GTPases, kinases, phosphatases, nucleotide binding proteins and phospholipases (Ammar *et al.*, 2013a, 2014). Furthermore, many PA partners have been involved in the modulation of actin dynamics and membrane trafficking as well as neuronal development. In this article, we will describe and discuss our observations suggesting that PA contributes to the cellular and molecular mechanisms that govern neuronal development and neurosecretion. Moreover, we will present our recent findings suggesting that various PA species are differently synthetized during neurite outgrowth and neurosecretion.

2 PA is involved in neurosecretion

The PA biosynthetic pathway involves mostly three families of enzymes (Fig. 1): phospholipases D (PLD), diacylglycerol kinases (DGK), and lysophosphatidic-acyl-transferases (LPAAT), which has made difficult accurate modulation of cellular PA to evaluate its contribution to neuronal function. Use of ethanol as an inhibitor of PA synthesis by PLD was at first probably the most used approach and has led to the notion that PLD-generated PA plays a role in various membrane trafficking events, especially during endocytosis and regulated exocytosis in different cell types

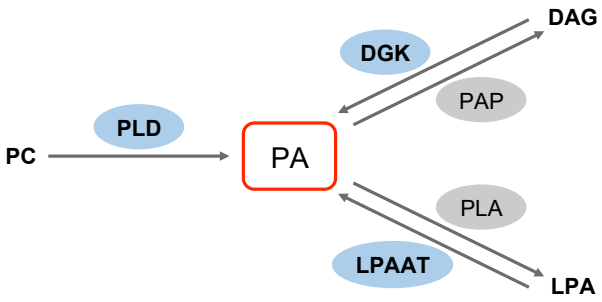

Fig. 1. Biosynthetic pathways of structural and signaling PA. PA is a central phospholipid for biosynthetic and signaling reactions. Enzymes in blue denote biosynthetic reactions that lead to structural and signaling PA synthesis whereas enzymes involved in PA catabolism are shown in grey.

including chromafin cells, neurons, epithelial and mast cells (Caumont *et al.*, 1998; Bader and Vitale, 2009; Ammar *et al.*, 2013a; Kassas *et al.*, 2017; Tanguy *et al.*, 2016,2018). Molecular tools and pharmacological inhibitors of PLDs have indicated that among PLDs, PLD1 is the isoform mostly involved in membrane trafficking. It must be noted however, that DGK-generated PA has been reported to be involved as well in membrane trafficking (Lopez *et al.*, 2012).

Chromaffin cells are neuroendocrine cells originating from the neural crest and have taken a prominent place in the models that have provided important insight into the molecular machinery underlying the successive steps of neurosecretion and exocytosis at large (Bader *et al.*, 2002). Thus, by offering the opportunity to combine the use of recent electrophysiological and biophysical techniques allowing single-vesicle resolution together with specific biochemical modifications in the machinery involved in exocytosis, chromaffin cells allowed the identification of most molecular players that orchestrate the formation, targeting, docking, and fusion of secretory granules. In fact, our early evidence obtained from chromaffin cells injected with a dominant-negative PLD1 mutant supported a function for PLD1-generated PA in the late steps of exocytosis, such as membrane fusion and/or pore expansion (Vitale *et al.*, 2001). Similarly, injection in *Aplysia* neurons blocked ACh release by reducing the number of active presynaptic releasing sites supporting evidence that PLD1 also plays a major role in neurotransmission, most likely by controlling the fusogenic status of presynaptic release sites (Humeau *et al.*, 2001). Later, PLD1 silencing experiments reinforced this model as a decrease in the fusion rate of single secretory granule release was observed (Zeniou-Meyer *et al.*, 2007). Interestingly, RSK2 was shown to be an important regulator of PLD1 activity in neurosecretion (Vitale, 2010). Since loss-of-function mutations of RSK2 are responsible for the Coffin-Lowry syndrome (CLS), an X-linked inherited mental retardation disease, the later observations suggest that the symptoms of CLS could result from alteration of neuronal development but also neuronal activity (Zeniou-Meyer *et al.*, 2008). Using similar tools, PLD1-generated PA was also reported to contribute actively to the regulated secretion of insulin from β-pancreatic cells (Waselle *et al.*, 2005), and of von Willebrand factor from endothelial cells (Disse *et al.*, 2009). Another established role for PA in secretion relates to

the induction of neutrophil exocytosis from azurophilic granules by anti-neutrophil cytoplasmic antibodies (Williams *et al.*, 2007). Moreover, the ability of apicomplexan parasites to invade and later exit infected cells relies on specialized organelles termed micronemes that release their contents including adhesins, perforins and proteases in a PA-dependent manner (Bullen *et al.*, 2016).

Yet, the mechanism(s) by which PA promotes membrane fusion remains debated. It may be linked to its ability to generate membrane curvature and facilitate fusion, modulate specific protein activity involved in the docking of vesicles and/or recruit key proteins required for the fusion process (Tanguy *et al.*, 2018). The most widely accepted model for membrane fusion involves a combination of protein and lipid elements at the fusion site. Cone-shaped lipids, such as PA, have been proposed to facilitate fusion through their intrinsic negative curvatures when accumulating in the inner (cis) leaflets of contacting bilayers. Furthermore, PA forms highly charged microdomains, which serve as membrane insertion sites for numerous proteins important for exocytosis (Lam *et al.*, 2008) and could induce conformational changes in associated proteins (Iversen *et al.*, 2015). More directly, PA has been proposed to contribute to many biological processes through its ability to interact with positively charged domains of numerous proteins (Jenkins and Frohman, 2005). Finally, PA can also directly serve as source for synthesis of DAG, or activate PI-5 kinase producing PtdIns(4,5)P_2, both lipids playing positive function in exocytosis.

3 PA is involved in neuronal outgrowth and development

Ethanol as an inhibitor of PA synthesis by PLDs was also widely used in the field of neuron development and has led to a well-accepted model where PLD-generated PA is crucial to neurite outgrowth in a variety of neuronal cell models (Kanaho *et al.*, 2009). In agreement with this model, we recently observed that neuronal maturation was significantly delayed in cortical *Pld1* knockout neurons culture (Ammar *et al.*, 2013b). However, the mechanisms implicating PA in the underlying membrane trafficking events remained elusive. Using the cell culture models of PC12 cells treated by neuronal growth factor (NGF), which have been widely used as a model to assess neurite outgrowth, we found that the PA sensor Spo20p-GFP accumulated at the plasma membrane following NGF stimulation as well as at the tips of growing neurites. Moreover, we found that PLD1 inhibition abolished PA accumulation induced by NGF, suggesting that PLD1 activation mediates PA synthesis in this process (Ammar *et al.*, 2013b). Interestingly, we found that PLD1 is associated to the trans Golgi-derived vesicular structures containing VAMP-7/TiVAMP, a SNARE protein involved in neurite outgrowth (Martinez-Arca *et al.*, 2000). Moreover, we have shown that PLD1 positive-vesicles move anterogradly and retrogradly in the developing neurites and accumulate at the growth cone (Ammar *et al.*, 2013b). Furthermore, we found that the specific PLD1 inhibitors dramatically reduced membrane supply required for neurite outgrowth by reducing the fusion rate of these VAMP-7 positive vesicles (Ammar *et al.*, 2013b). This appears as the first direct involvement of PA-mediated membrane trafficking in neurite outgrowth (Fig. 2). Of note, expression of the PA sensor Spo20-GFP in PC12 cells strongly reduces the number and length of the NGF-induced neurites most likely as a consequence of PA quenching by the probe (Ammar *et al.*, 2013b). It is thus tempting to speculate that PA acts in part by recruiting key proteins at the vesicle fusion site during neurite outgrowth (Fig. 2).

Pld1 knockout also affects a later step in neuronal development with a specific reduction in the number of secondary branching dendrites in cortical neurons. Additionally, the density of the spines, the tiny protrusions (0.5 μm wide, 2 μm long) on neuronal dendrites that receive the majority of excitatory synaptic inputs, is significantly reduced in *Pld1*$^{-/-}$ cortical neurons and this reduction in spine density specifically affects mushroom and branched spines, which are the forms of mature spines (Ammar *et al.*, 2013b). Accordingly, a previous report showed that the GTPase RalB promotes branching through a pathway involving PLD (Lalli and Hall, 2005). Altogether, these results imply critical functions of PLD1-produced signaling PA in early stages of neuronal growth and development, largely through an effect on cytoskeleton organization (Fig. 2). Intriguingly we found that neurons cultured from mice lacking ribosomal S6 kinase 2 (*Rsk2*), a model for the CLS (Humeau *et al.*, 2009), exhibit a significant delay in growth in a similar way to that shown by neurons cultured from *Pld1* knockout mice (Ammar *et al.*, 2013b). Furthermore, gene silencing of *Rsk2* as well as acute pharmacological inhibition of RSK2 in PC12 cells strongly impaired NGF-induced neurite outgrowth like it was found after *Pld1* silencing or PLD1 inhibition (Ammar *et al.*, 2013b). Expression of phosphomimetic PLD1(T147D) or PLD1 (T147E) mutants rescued the inhibition of neurite outgrowth in PC12 cells silenced for RSK2, revealing that PLD1 is a major target for RSK2 in neurite formation and allowing us to propose that the loss of function mutations in *RSK2* that leads to CLS and neuronal deficits are related to defects in neuronal growth due to impaired RSK2-dependent PLD1 activity resulting in a reduced vesicle fusion rate and membrane supply. On the other hand, we also found that PLD1 regulates BDNF signaling endosomes in cortical neurons *via* ERK1/2 and CREB. This effect could explain in part the reduction of dendritic ramification observed in *Pld1*$^{-/-}$ cortical neurons (Ammar *et al.*, 2015).

PA generated by DGK also seems to modulate dendrite ramification and spines maturation. For instance, overexpression of wild-type DGKβ promotes dendrite outgrowth and spine maturation in transfected hippocampal neurons, whereas a kinase-dead mutant DGK has no effect (Hozumi *et al.*, 2009). Accordingly, reduced number of branches and spines was found in primary cultured hippocampal neurons from DGKβ knockout compared to the wild type (Shirai *et al.*, 2010). DGKζ has also been reported to be important for the maintenance of dendritic spines and the regulation of the PA/DAG balance at excitatory synapses (Kim *et al.*, 2009, 2010) (Fig. 2). Indeed the C-terminal PDZ-binding motif of DGKζ interacts with the PDZ domains of the postsynaptic density protein PSD-95, an abundant postsynaptic scaffolding protein that regulates excitatory synaptic structure and function. This interaction promotes synaptic localization of DGKζ. Functionally, DGKζ overexpression increases spine density in cultured hippocampal neurons in a manner that

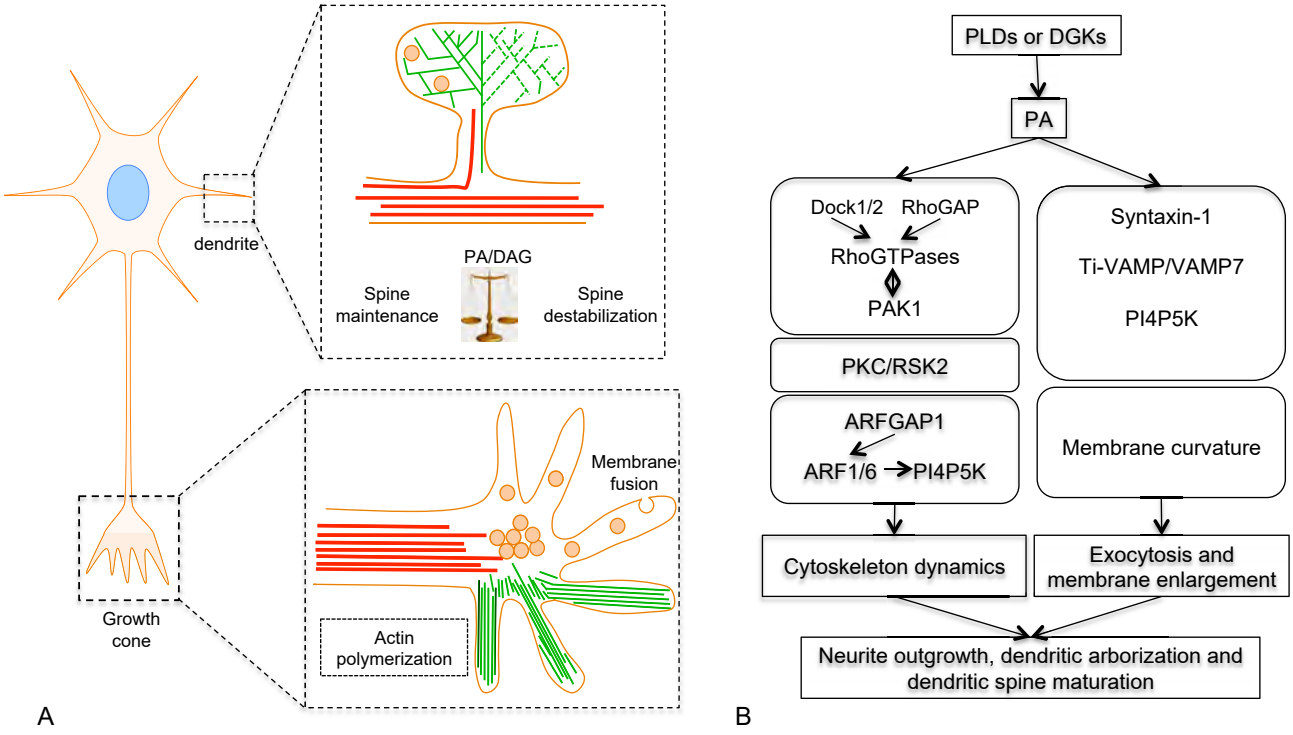

Fig. 2. PA is involved in axon and dendrite outgrowth, dendrite branching and spine formation. A) Schematic representation of growth cone and dendritic spines with actin cytoskeleton (green) and microtubules (red) as well as trafficking vesicles. In dendrites, PA/DAG balance controls the actin cytoskeleton dynamics whereas in growth cones, PA is involved in neurite outgrowth by controlling actin organization and vesicular trafficking for membrane supply. B) Examples of potential molecular targets of PA involved in cytoskeleton dynamics and vesicular exocytosis.

requires DGK catalytic activity but also PSD-95 binding, whereas knockdown of DGKζ decreases spine density. Moreover, mice deficient for *dgkζ* expression show a reduction in spine density in hippocampal CA1 pyramidal neurons and exhibit reduced excitatory synaptic transmission. Time-lapse imaging of *dgkζ*–deficient neurons revealed impaired spine maintenance but not formation (Kim *et al.*, 2009). Finally, it was recently reported that *Dgkκ* silencing in CA1 region of mouse organotypic hippocampal slices causes a strong increase of abnormally long and multi-headed spines and a marked decrease of the proportion of mature spines whereas spine density remains unaffected (Tabet *et al.*, 2016a). In addition, reduced *Dgkκ* expression accelerated spine turnover, as indicated by the increased rate of spine formation and elimination, associated with spine instability (Tabet *et al.*, 2016a). Interestingly these structural defects are very similar to those previously observed in the *Fmr1*$^{-/y}$ mice, a model for fragile X syndrome (He and Portera-Cailliau, 2013), and it was shown that *Dgkκ* overexpression within *Fmr1*$^{-/y}$ neurons could rescue the dendritic spine phenotype (Tabet *et al.*, 2016a,b). Taken together, these data also reveal a key role of DGK-generated PA in dendritic ramification and spine formation and maturation.

4 PA synthesis during neurosecretion and neuronal growth

Like all phospholipids, PA comes in different flavors based on the fatty acid composition. Indeed although in mammalian cells only saturated fatty acids are found in sn1 position, in the sn2 position fatty acids can be saturated, mono-unsaturated, or poly-unsaturated. We performed a lipidomic analysis on cultured PC12 cells stimulated for exocytosis by a 10-minute incubation with a depolarizing K^+ solution to identify the different PA species produced during neurosecretion. The levels of medium and long carbon chains mono- and poly-unsaturated forms of PA were increased after cell stimulation (Fig. 3). These results highlight the potential importance of different PA species in catecholamine secretion. In conclusion, the local build-up of different PA species together with other key lipids such PtdIns(4,5)P_2, DAG, and cholesterol presumably at the neck or near the fusion pore could contribute by changing membrane curvature, together with SNARE mediated membrane apposition and destabilization, to promote fusion pore formation and/or regulate its stability. It must also be noted that the contribution of PA in early steps of the secretory pathway has not been as well investigated (Gasman and Vitale, 2017).

Similarly, we performed a lipidomic analysis on cultured PC12 cells treated with NGF for 3 days. Among the 10 most abundant PA species detected, a specific increase in the long carbon chain forms 38:1, 38:2 and 40:6 was found, whereas levels of other PA especially saturated ones were not modified (Fig. 3). This observation therefore suggests that mono-unsaturated, bis-unsaturated, and/or the omega 3 poly-unsaturated forms of PA contribute to neurite outgrowth and neuronal development. In line with this finding, it has been known for a long time that dietary omega 3 poly-unsaturated lipids such as docosahexanoicacid (DHA) and eicosapentae-

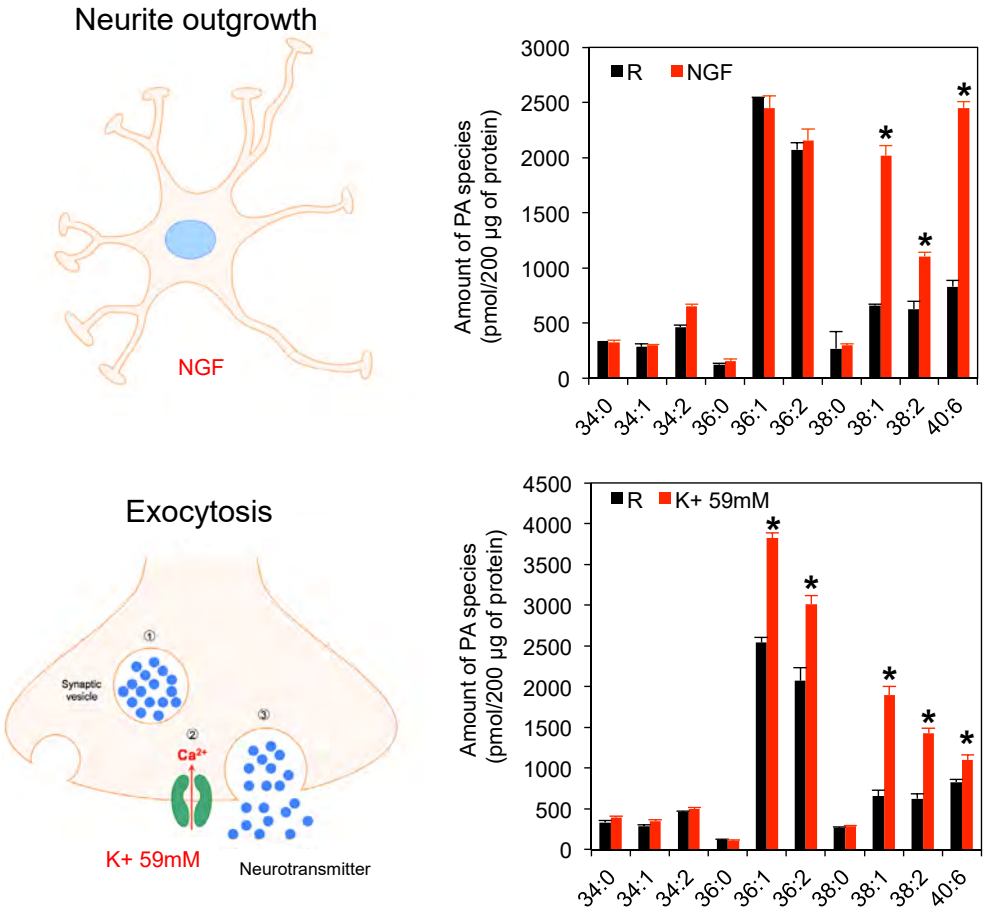

Fig. 3. Synthesis of different PA species during neurosecretion and neurite outgrowth. PC12 cells were either treated with 10 µM of NGF for 3 days to stimulate neurite outgrowth (Ammar *et al.*, 2013a,b) or with a 59 mM potassium solution for 10-minutes to stimulate catecholamine neurosecretion (Béglé *et al.*, 2009). Cells were washed with ice cold PBS, before being lyzed as described previously (Vitale *et al.*, 2002). Proteins levels were quantified and levels of 40 different PA species were estimated in 200 µg fractions by lipidomic analysis (Kassas *et al.*, 2017). The levels of the 10 most abundant PA species are shown and expressed as pmol/200 µg of proteins. The total carbon chain length and saturation is indicated for each PA species. Results were obtained from 3 independent experiments ($^{*}p < 0.001$).

noic acid (EPA) have a beneficial cognitive effects (Cardoso *et al.*, 2016). Although many important functions for the brain have been attributed to DHA for instance, the mechanism of its incorporation into glycerophospholipids is unknown. Of interest, lysophosphatidic acid acyltransferases 4 (LPAAT4) has been recently suggested to play a role for maintaining DHA in neural membranes (Eto *et al.*, 2014). A combination of lipidomic approach and specific inhibitors for the multiple families of enzymes involved in the production and metabolism of PA will be helpful to define more precisely the nature of distinct PA species involved in the different steps of neuronal development and activity.

5 Conclusion

In this paper, we investigated the possibility that the fatty-acyl chain composition affects the functions of PA in neuronal development and exocytosis, an aspect of PA that has not been investigated with care yet. For instance, do the various PAs displaying saturated, mono-, bi- or poly-unsaturated fatty acids have similar effects on membrane topology or recruit the same proteins? These questions are especially relevant in the context of neuronal development and degeneration, since many studies have highlighted key functions of dietary lipids in human cognitive activity (Tolias *et al.*, 1998; Haast and Kiliaan 2015). We indeed found that neurite outgrowth and neurosecretion stimulation increased levels of multiple PA species. Interestingly, however, some of these increased PA species are similar and some others are not, suggesting that convergent and divergent mechanisms involving these different PA forms are present in these two important neuronal processes. The numerous genetic models now available, the recent progress in lipidomics, and some novel tools to study PA's function will be helpful to clarify the intriguing questions raised by these findings.

This work also opens new avenue on the possible contribution of PA and enzymes involved in PA synthesis in various neuronal pathologies such as Alzheimer's disease and autism spectrum disorders. In line with this possibility, the group of Gil di Paolo reported that PLD2 knockdown efficiently prevented cognitive loss in a mice model of

Alzheimer's disease (Oliveira *et al.*, 2010). Finally, the findings that an alteration of DAG/PA balance could be responsible for some of the symptoms of fragile X syndrome (Tabet *et al.*, 2016a,b), also points to perturbation of PA synthesis as a major source of neuronal malfunction.

Acknowledgments. This work was supported by grants from "La Ligue Contre le Cancer" and from "Fondation pour la Recherche Médicale" to NV. The Metabolome facility of Bordeaux was supported by the grant MetaboHUB-ANR-11-INBS-0010.

References

Ammar MR, Humeau Y, Hanauer A, Nieswandt B, Bader MF, Vitale N. 2013a. The Coffin-Lowry syndrome-associated protein RSK2 regulates neuritis outgrowth through phosphorylation of phospholipase D1 (PLD1) and synthesis of phosphatidic acid. *J Neurosci* 33(50): 19470–19479.

Ammar MR, Kassas N, Chasserot-Golaz S, Bader MF, Vitale N. 2013b. Lipids in regulated Eexocytosis: what are they doing? *Front Endocrinol (Lausanne)* 4: 125.

Ammar MR, Kassas N, Bader MF, Vitale N. 2014. Phosphatidic acid in neuronal development: a node for membrane and cytoskeleton rearrangements. *Biochimie* 107: 51–57. DOI: 10.1016/j.biochi.2014.07.026.

Ammar MR, Thahouly T, Hanauer A, Stegner D, Nieswandt B, Vitale N. 2015. PLD1 participates in BDNF-induced signalling in cortical neurons. *Sci Rep* 5: 14778.

Bader MF, Vitale N. 2009. Phospholipase D in calcium-regulated exocytosis: lessons from chromaffin cells. *Biochim Biophys Acta* 1791(9): 936–941.

Bader MF, Holz RW, Kumakura K, Vitale N. 2002. Exocytosis: the chromaffin cell as a model system. *Ann N Y Acad Sci* 971: 178–83.

Béglé A, Tryoen-Tóth P, de Barry J, Bader MF, Vitale N. 2009. ARF6 regulates the synthesis of fusogenic lipids for calcium-regulated exocytosis in neuroendocrine cells. *J Biol Chem* 284(8): 4836–4845.

Bullen HE, Jia Y, Yamaryo-Botté Y, *et al.* 2016. Phosphatidic acid-mediated signaling regulates microneme secretion in toxoplasma. *Cell Host Microbe* 19(3): 349–360.

Cardoso C, Afonso C, Bandarra NM. 2016. Dietary DHA and health: cognitive function ageing. *Nutr Res Rev* 29(2): 281–294.

Caumont AS, Galas MC, Vitale N, Aunis D, Bader MF. 1998. Regulated exocytosis in chromaffin cells. Translocation of ARF6 stimulates a plasma membrane-associated phospholipase D. *J Biol Chem* 273(3): 1373–1379.

Disse J, Vitale N, Bader MF, Gerke V. 2009. Phospholipase D1 is specifically required for regulated secretion of von Willebrand factor from endothelial cells. *Blood* 113(4): 973–980.

Dotti CG, Sullivan CA, Banker GA. 1988. The establishment of polarity by hippocampal neurons in culture. *J Neurosci* 8(4): 1454–1468.

Eto M, Shindou H, Shimizu T. 2014. A novel lysophosphatidic acid acyltransferase enzyme (LPAAT4) with a possible role for incorporating docosahexaenoic acid into brain glycerophospholipids. *Biochem Biophys Res Commun* 443(2): 718–724.

Gasman S, Vitale N. 2017 Lipid remodelling in neuroendocrine secretion. *Biol Cell* 109(11): 381–390.

Haast RA, Kiliaan AJ. 2015. Impact of fatty acids on brain circulation, structure and function. *Prostaglandins Leukot Essent Fatty Acids* 92: 3–14.

He CX, Portera-Cailliau C. 2013. The trouble with spines in fragile X syndrome: density, maturity and plasticity. *Neuroscience* 251: 120–128.

Hozumi Y, Watanabe M, Otani K, Goto K. 2009. Diacylglycerol kinase beta promotes dendritic outgrowth and spine maturation in developing hippocampal neurons. *BMC Neurosci* 10: 99.

Humeau Y, Vitale N, Chasserot-Golaz S, *et al.* 2001. A role for phospholipase D1 in neurotransmitter release. *Proc Natl Acad Sci USA* 98(26): 15300–15305.

Humeau Y, Gambino F, Chelly J, Vitale N. 2009. X-linked mental retardation: focus on synaptic function and plasticity. *J Neurochem* 109(1): 1–14.

Iversen L, Mathiasen S, Larsen JB, Stamou D. 2015. Membrane curvature bends the laws of physics and chemistry. *Nat Chem Biol* 11(11): 822–825.

Jenkins GM, Frohman MA. 2005. Phospholipase D: a lipid centric review. *Cell Mol Life Sci* 62(19-20): 2305–2316.

Kanaho Y, Funakoshi Y, Hasegawa H. 2009. Phospholipase D signalling and its involvement in neurite outgrowth. *Biochim Biophys Acta* 1791(9): 898–904.

Kassas N, Tanguy E, Thahouly T, *et al.* 2017. Comparative characterization of phosphatidic acid sensors and their localization during frustrated phagocytosis. *J Biol Chem* 292(10): 4266–4279.

Kim K, Yang J, Zhong XP, *et al.* 2009. Synaptic removal of diacylglycerol by DGKzeta and PSD-95 regulates dendritic spine maintenance. *EMBO J* 28(8): 1170–1179.

Kim K, Yang J, Kim E. 2010. Diacylglycerol kinases in the regulation of dendritic spines. *J Neurochem* 112(3): 577–587.

Lalli G, Hall A. 2005. Ral GTPases regulate neurite branching through GAP-43 and the exocyst complex. *J Cell Biol* 171(5): 857–869.

Lam IP, Siu FK, Chu JY, Chow BK. 2008. Multiple actions of secretin in the human body. *Int Rev Cytol* 265: 159–190.

Lopez JA, Brennan AJ, Whisstock JC, Voskoboinik I, Trapani JA. 2012. Protecting a serial killer: pathways for perforin trafficking and self-defence ensure sequential target cell death. *Trends Immunol* 33(8): 406–412.

Martinez-Arca S, Alberts P, Zahraoui A, *et al.* 2000. Role of tetanus neurotoxin insensitive vesicle-associated membrane protein (TI-VAMP) in vesicular transport mediating neurite outgrowth. *J Cell Biol* 149(4): 889–900.

Oliveira TG, Chan RB, Tian H, *et al.* 2010. Phospholipase d2 ablation ameliorates Alzheimer's disease-linked synaptic dysfunction and cognitive deficits. *J Neurosci* 30(49): 16419–16428.

Shirai Y, Kouzuki T, Kakefuda K, *et al.* 2010. Essential role of neuron-enriched diacylglycerol kinase (DGK), DGKbeta in neurite spine formation, contributing to cognitive function. *PLoS One* 5(7): e11602.

Sytnyk V, Leshchyns'ka I, Schachner M. 2017. Neural cell adhesion molecules of the immunoglobulin superfamily regulate synapse formation, maintenance, and function. trends. *Neurosci* 40(5): 295–308.

Tabet R, Moutin E, Becker JA, *et al.* 2016a. Fragile X mental retardation protein (FMRP) controls diacylglycerol kinase activity in neurons. *Proc Natl Acad Sci USA* 113(26): E3619–3628.

Tabet R, Vitale N, Moine H. 2016b. Fragile X syndrome: are signaling lipids the missing culprits? *Biochimie* 130: 188–194.

Tanguy E, Carmon O, Wang Q, Jeandel L, Chasserot-Golaz S, Montero-Hadjadje M, Vitale N. 2016. Lipids implicated in the

journey of a secretory granule: from biogenesis to fusion. *J Neurochem* 137(6): 904–912.

Tanguy E, Wang Q, Vitale N. 2018. Role of phospholipase D-derived phosphatidic acid in regulated exocytosis and neurological disease. *Handb Exp Pharmacol*. (in press).

Tolias KF, Couvillon AD, Cantley LC, Carpenter CL. 1998. Characterization of a Rac1-and RhoGDI-associated lipid kinase signaling complex. *Mol Cell Biol* 18(2): 76270.

Vitale N. 2010. Synthesis of fusogenic lipids through activation of phospholipase D1 by GTPases and the kinase RSK2 is required for calcium-regulated exocytosis in neuroendocrine cells. *Biochem Soc Trans* 38(1): 167–171.

Vitale N, Caumont AS, Chasserot-Golaz S, *et al.* 2001. Phospholipase D1: a key factor for the exocytotic machinery in neuroendocrine cells. *EMBO J* 20(10): 2424–2434.

Vitale N, Chasserot-Golaz S, Bader MF. 2002. Regulated secretion in chromaffin cells: an essential role for ARF6-regulated phospholipase D in the late stages of exocytosis. *Ann N Y Acad Sci* 971: 193–200.

Waselle L, Gerona RR, Vitale N, Martin TF, Bader MF, Regazzi R. 2005. Role of phosphoinositide signaling in the control of insulin exocytosis. *Mol Endocrinol* 19(12): 3097–3106.

Williams JM, Pettitt TR, Powell W, *et al.* 2007. Antineutrophil cytoplasm antibody-stimulated neutrophil adhesion depends on diacylglycerol kinase-catalyzed phosphatidic acid formation. *J Am Soc Nephrol* 18(4): 1112–1120

Zeniou-Meyer M, Zabari N, Ashery U, *et al.* 2007. Phospholipase D1 production of phosphatidic acid at the plasma membrane promotes exocytosis of large dense-core granules at a late stage. *J Biol Chem* 282(30): 21746–21757.

Zeniou-Meyer M, Liu Y, Béglé A, *et al.* 2008. The Coffin-Lowry syndrome-associated protein RSK2 is implicated in calcium-regulated exocytosis through the regulation of PLD1. *Proc Natl Acad Sci USA* 105(24): 8434–8439.

Cite this article as: Tanguy E, Wang Q, Bagneaux PCd, Fouillen L, Thahouly T, Ammar M-R, Vitale N. 2018. Different species of phosphatidic acid are produced during neuronal growth and neurosecretion. *OCL* 25(4): D408.

frontiers in Cellular Neuroscience

REVIEW
published: 23 January 2019
doi: 10.3389/fncel.2019.00002

Phosphatidic Acid: From Pleiotropic Functions to Neuronal Pathology

Emeline Tanguy[1], *Qili Wang*[1], *Hervé Moine*[2] *and Nicolas Vitale*[1]*

[1]Institut des Neurosciences Cellulaires et Intégratives (INCI), UPR-3212 Centre National de la Recherche Scientifique & Université de Strasbourg, Strasbourg, France, [2]Institut de Génétique et de Biologie Moléculaire et Cellulaire (IGBMC), CNRS UMR 7104, INSERM U964, Université de Strasbourg, Illkirch-Graffenstaden, France

Among the cellular lipids, phosphatidic acid (PA) is a peculiar one as it is at the same time a key building block of phospholipid synthesis and a major lipid second messenger conveying signaling information. The latter is thought to largely occur through the ability of PA to recruit and/or activate specific proteins in restricted compartments and within those only at defined submembrane areas. Furthermore, with its cone-shaped geometry PA locally changes membrane topology and may thus be a key player in membrane trafficking events, especially in membrane fusion and fission steps, where lipid remodeling is believed to be crucial. These pleiotropic cellular functions of PA, including phospholipid synthesis and homeostasis together with important signaling activity, imply that perturbations of PA metabolism could lead to serious pathological conditions. In this mini-review article, after outlining the main cellular functions of PA, we highlight the different neurological diseases that could, at least in part, be attributed to an alteration in PA synthesis and/or catabolism.

OPEN ACCESS

Edited by:
Gabriela Alejandra Salvador, Universidad Nacional del Sur, Argentina

Reviewed by:
Richard M. Epand, McMaster University, Canada
Daniel M. Raben, Johns Hopkins University, United States

***Correspondence:**
Nicolas Vitale
vitalen@unistra.fr

Received: 22 October 2018
Accepted: 07 January 2019
Published: 23 January 2019

Citation:
Tanguy E, Wang Q, Moine H and Vitale N (2019) Phosphatidic Acid: From Pleiotropic Functions to Neuronal Pathology. Front. Cell. Neurosci. 13:2. doi: 10.3389/fncel.2019.00002

Keywords: lipid signaling, neuron, neuropathology, phosphatidic acid, phospholipase D

INTRODUCTION

Phosphatidic acid (PA) is a low abundant phospholipid of membranes that, nevertheless, constitutes the original building block from which most glycerophospholipids are synthesized, thus plays an important structural task. Interestingly it was later shown that PA also acts to transmit, amplify, and regulate a great number of intracellular signaling pathways and cellular functions. In cells, PA can be synthesized through different enzymatic pathways (Ammar et al., 2014). Structural PA results from two successive acylation reactions (**Figure 1**). Signaling PA instead, results from three biosynthesis alternative pathways. The first pathway includes the phosphorylation of diacylglycerol (DAG) by any of the 10 DAG-kinases (DGKs) in mammals (**Figure 1**). Hydrolysis of the distal phosphodiester bond in phospholipids by phospholipases D (PLD) constitutes the second pathway (**Figure 1**). Although six different PLDs have been identified in mammals, only PLD1/2 and PLD6 have been shown to synthesize PA from phosphatidylcholine (PC) and cardiolipin (CL), respectively (Jang et al., 2012). The third and final biosynthetic pathway involves acylation of lyso-PA by lyso-PA-acyltransferase (LPAAT) enzymes (**Figure 1**).

Chemically, PA is composed of a glycerol backbone esterified with two fatty acyl chains at positions C-1 and C-2, and with a phosphate at position C-3. The latter confers the specific features of PA compared to the other diacyl–glycerophospholipids. Indeed, the small anionic phosphate headgroup provides to PA a combination of unique cone-shaped geometry and negative charge (Jenkins and Frohman, 2005). At the molecular level, these two characteristics enable PA both to

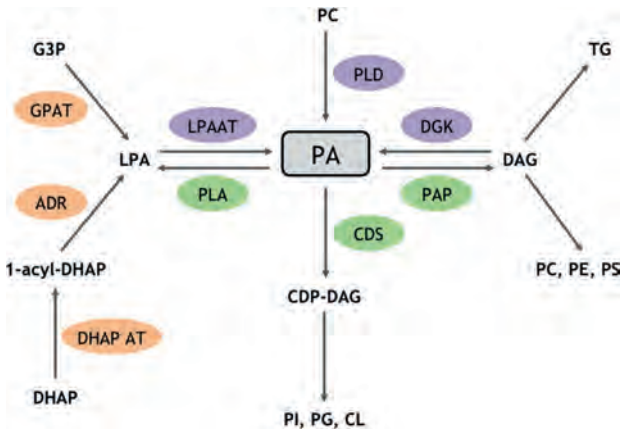

FIGURE 1 | Enzymatic routes for structural and signaling PA metabolism. PA is a major phospholipid for biosynthetic and signaling reactions. Enzymes highlighted in orange are involved in biosynthetic reactions that produce structural PA, whereas enzymes triggering the formation of signaling pools of PA are shown in purple. Enzymes responsible for PA catabolism are shown in green. ADR, Acyldihydroxyacetone-phosphate reductase; CDP, cytidyl phosphatidate; CDS, CDP-diacylglycerol (DAG) synthase; CL, cardiolipin; DHAP, dihydroxyacétone phosphate; DHAP AT, dihydroxyacétone phosphate acyltransferase; G3P, glycerol 3-phosphate; GPAT, glycerol phosphate acyltransferase; PAP, phosphatidic acid phosphatase; PC, phosphatidylcholine; PG, phosphatidylglycerol; PE, phosphatidylethanolamine; PI, phosphatidylinositol; PS, phosphatidylserine; PLA, phospholipase A; TG, triglyceride.

interact with different enzymes to regulate their catalytic activity and/or their association with membrane compartments and also to affect membrane geometry by creating local negative curvatures (Kooijman et al., 2003). As a consequence, PA has been involved in various important cellular functions including membrane trafficking events where membrane rearrangements are necessary (Bader and Vitale, 2009). In this article, we will present some of the most studied PA identified partners, summarize the most well-described cellular processes that require PA and discuss the potential involvement of an alteration in PA synthesis and/or catabolism in different neurological diseases.

PA INTERACTS WITH AND RECRUITS NUMEROUS PROTEINS TO MEMBRANES

Having an overall view of the interaction network of a given molecule is particularly helpful for deciphering the relationships between the constituents of interactomes and characterizing their function in cell signaling. Since the early description of a handful of proteins that bind to PA, at least using the minimal *in vitro* protein-lipid overlay assay, an extensive list of PA interactors has only emerged more recently (Stace and Ktistakis, 2006). For at least some of those, their interaction with PA appears rather specific with little or no interaction with other negatively charged lipids. The position of PA's phosphomonoester headgroup in proximity of the interface of acyl chain headgroup was proposed to be important for binding to specific proteins. Supporting the physiological importance of interactions between PA and proteins, numerous proteins have gained domains that display some level of binding specificity for PA (Jang et al., 2012). Although no clear PA-binding domain can be defined at the three dimensional or secondary structural levels, different factors can influence PA interaction with specific domains in target proteins (Tanguy et al., 2018). For instance, we and others have found that some PA-binding modules possess some levels of specificity for the fatty acyl chains of PA (Kassas et al., 2017). In addition, the local membrane environment surrounding PA also appears to modulate PA binding to these modules (Kassas et al., 2017). Finally, it is most likely that PA-binding domains act first through positively charged residues that initially sample for the negative charge of PA buried within the membrane. This first step is probably followed by a docking state where hydrophobic interaction between hydrophobic residues of the module and the fatty acyl chains of PA stabilize the PA-protein interaction (Potocký et al., 2014; Tanguy et al., 2018). At present, more than 50 different proteins have been shown to directly interact with PA, as extensively reviewed in Jang et al. (2012). Briefly, these PA interactors can be classified in four major families.

Nucleotide-Binding Proteins

Nucleotide (ATP, cAMP, GTP)-binding proteins are important signaling proteins for which the activity is usually regulated by nucleotide binding. Noticeably, the localization and/or activity of many of those proteins are also controlled by PA interaction. This is for instance the case for some of the small GTP-binding proteins of the ADP ribosylation factor (Arf) and Rho (Ras homologous) families that are key players in cytoskeleton remodeling and membrane dynamics. The minimal PA-binding regions of these small GTPases remains however to be defined precisely. Several c-AMP specific phosphodiesterases also interact with PA through their amino-terminal regulatory domains leading to an increase of their enzymatic activity and therefore to a reduction of cAMP levels.

Regulators of GTP-Binding Proteins

The GTPase-activating proteins ArfGAP with GTPase Domain, Ankyrin Repeat and PH domain 1 (AGAP1) and Regulator of G protein Signaling 4 (RGS4) are negative regulators of Arf and Gα GTP-binding proteins, respectively. Intriguingly, while PA stimulates the GTP-hydrolysis activity of AGAP1, it inhibits that of RGS4, highlighting the multiple and sometimes opposite actions of PA on GTP-binding activity. Furthermore, PA has also been shown to recruit and activate different guanine nucleotide-exchange proteins for small GTPases, such as DedicatOr of CytoKinesis 2 (DOCK2) and Son Of Sevenless (SOS), promoting GTP-binding and activation of Rac and Ras, respectively. It is therefore important to have in mind that PA enrichment in particular sub-membrane domains could influence in different and sometimes contradictory manners a given signaling pathway involving GTP-binding proteins by acting at different stages.

Kinases

Protein kinases are among the main signaling regulators with nearly 600 different genes. Among those, protein kinase C (PKC) is one of the largest subgroup and PA modulates the activity of several PKC isoforms. PA also promotes recruitment and activation of the proto-oncogene kinase Raf, acting as a gatekeeper in the ERK1/2 pathway. In addition, PA binding to the FKBP12-rapamycin binding region of mTOR is in competition with FKBP12/rapamycin complex of mTOR and is thus likely to influence nutrient sensing and cell proliferation.

Furthermore, lipid kinases contribute to the great diversity of lipids in cells. Among those, PA is capable to stimulate the action of phosphatidylinositol (PI) 4-phosphate 5-kinase (PI4P5K), to promote the synthesis of PI 4,5-bisphosphate ($PI(4,5)P_2$), a key signaling lipid (Stace and Ktistakis, 2006; Bader and Vitale, 2009). Finally, cytosolic sphingosine kinase that transforms sphingosine into sphingosine-phosphate appears to translocate to the plasma membrane under the control of PA levels, which most likely affects the signaling pathways involving these two lipids. In conclusion, PA binding modules are found in members of the two major kinase families and consequently, the presence of PA in local membrane composition is expected to influence crucial signaling nodes and the various associated key cellular functions.

Phosphatases

In addition to kinases, phosphatases constitute the second important family of signaling proteins that modulate protein activity by removing the phosphate residues added by kinases. The protein-tyrosine phosphatase SHP-1 that negatively modulates signaling pathways involving receptor-tyrosine kinase directly interacts with PA therefore triggering phosphatase activity. Furthermore, PA inhibits the enzymatic activity of protein phosphatase 1 (PP1), involved in many cellular activities such as the metabolism of glycogen, the processing of RNA, and the regulation of cell cycle. In conclusion, although not as well described as for kinases, the regulation of several phosphatases by PA offers the possibility of complex and often paradoxical regulation of signaling pathway by a single lipid family.

THE PLEIOTROPIC CELLULAR FUNCTIONS OF PA

Actin Cytoskeleton Dynamics

Most cellular functions are influenced by precise cell shapes that are under the control of the cytoskeleton proteins network. Among those the dynamics of the cytoskeleton depends on the formation of actin filaments from a pool of cytosolic monomers, and their subsequent association to each other or to cell membranes, pursued by their depolymerization. Most cellular functions actually depend on a permanent remodeling of this actin network and this is orchestrated in large part by actin binding proteins. Interestingly lipids such as phosphoinositides modulate the affinity of these proteins for actin. PA, however, has also been proposed to participate to this regulation (Ammar et al., 2014).

In neurons, the Rho GTPases and related proteins, through the control of the cytoskeleton, modulate various aspects of cell shape including not only neurite outgrowth and differentiation, axonal growth and targeting, but also dendritic spine formation and maintenance (Ammar et al., 2014). As mentioned in the sections "Nucleotide-Binding Proteins" and "Regulators of GTP-Binding Proteins," PA synthesized by either PLD or DGK modulates the activity of some different Rho family of GTPases and their regulators by promoting membrane association and/or through the activation of their regulatory proteins (Chae et al., 2008; Nishikimi et al., 2009; Faugaret et al., 2011; Kurooka et al., 2011; Sanematsu et al., 2013). Alternatively, the p21 activated kinases (PAKs) family that regulates various aspects of neuronal development, through actin cytoskeleton reorganization, is also known for being activated by PA (Daniels et al., 1998; Hayashi et al., 2007). Furthermore, $PI(4,5)P_2$ is a major lipid regulator of the cytoskeleton and PA is an essential building block leading to $PI(4,5)P_2$ synthesis (**Figure 1**). In an alternative pathway, PA stimulates the phospholipid kinase PI4P5K, leading to the phosphorylation of the membrane phospholipid PI(4)P and the formation of $PI(4,5)P_2$ (Honda et al., 1999). In consequence, PA potentially regulates the activity of the three mammalian PI4P5K isozymes that have been described to control actin cytoskeleton reorganization (van den Bout and Divecha, 2009; Roach et al., 2012). Finally, PA levels regulate membrane localization and activity of PKC isoforms α, ε and ζ, all of which are known to affect the morphology of the actin cytoskeleton (Jose Lopez-Andreo et al., 2003).

It is also worth noting that direct interaction of PA with actin-binding proteins has been suggested. Among those potential candidates, the actin-binding protein vinculin known to be involved in neurite outgrowth is a good example (Ito et al., 1982; Johnson and Craig, 1995), but the specificity of these observations remains to be firmly established, since vinculin also binds to other negatively charged lipids, such as $PI(4,5)P_2$.

Membrane Remodeling Events

The secretory pathways have evolved through the establishment of specialized subcellular compartments dedicated to specific biochemical tasks. Membrane trafficking events between these compartments enable particular cells of complex organisms to secrete informative molecules such as hormones, cytokines, and neurotransmitters, for long distance inter-cellular communication. In addition to dedicated and specialized protein machineries, trafficking events of the regulated exocytosis and endocytosis steps also involve remarkable membrane rearrangements that rely on specific lipids (Ammar et al., 2013b). Hence, the first direct molecular data suggesting a role for PLD1-generated PA in hormone release were obtained in chromaffin cells, where overexpression of PLD1, injection of a catalytically-inactive PLD1 mutant (Vitale et al., 2001) or PLD1 silencing (Zeniou-Meyer et al., 2007) affected catecholamine release rates. Using similar approaches, PA synthesized by PLD1 was also shown to govern the regulated secretion of insulin from β-pancreatic cells (Waselle et al., 2005), of von Willebrand factor from endothelial cells (Disse et al., 2009), and acrosomal exocytosis from sperm cells (Lopez et al., 2012; Pelletán et al., 2015). An additional contribution for PA in secretion has been established during the early phase

of azurophilic granules release in neutrophils triggered by anti-neutrophil cytoplasmic antibodies (Williams et al., 2007). Ultimately, different enzymes controlling PA metabolism such as PLDs, LPAATs and DGKs have been proposed to regulate neurotransmission in several neuronal models, suggesting that PA regulates synaptic vesicle release and cycle (Humeau et al., 2001; Schwarz et al., 2011; Tabet et al., 2016a,b; Raben and Barber, 2017).

Intense membrane remodeling also occurs in specialized phagocytic cells, such as in macrophages. Indeed, the ingestion of pathogens, cell debris, or any other solid particle through the formation of phagosomes requires plasma membrane extension and either local lipid synthesis, transfer, or vesicular fusion. PA synthesis by PLD2 has been shown to be important for this early step of phagocytosis, while PA synthesis by PLD1 appears to be also important for the later step of phagosome maturation (Corrotte et al., 2006, 2010). Of note, PA transfer from the ER to plasma membrane during "frustrated phagocytosis," a model where macrophages are plated on IgG-coated plates, has also been suggested to occur from experiments using a combination of lipidomic analysis performed on subcellular fractions and novel PA sensors (Kassas et al., 2017). Furthermore, PA is involved in the invasion and exit of infected cells by apicomplexan parasites (Bullen et al., 2016). It was shown that PA is required for the release of adhesins, perforins and proteases from specialized organelles from these parasites called micronemes (Bullen et al., 2016).

Additional intracellular trafficking events involving intense membrane remodeling have also been shown to require modification in PA levels. To cite only a few, we can also mention that PA critically regulates vesicle budding from the Golgi (Yang et al., 2008), autophagy (Holland et al., 2016), and exosome release (Ghossoub et al., 2014). The mechanisms by which PA promotes membrane rearrangements remain however an unsolved issue (**Figure 2**). The first proposed mode of action of PA in membrane remodeling may depends on its ability to induce membrane curvature and promote fusion, but its ability to specifically regulate the activity of different proteins involved in the vesicle docking and/or recruit crucial fusion proteins has also been proposed (Tanguy et al., 2016, 2018). In a simplified model for membrane fusion a mixture of lipids and proteins appear to be crucial at the fusion site (Tanguy et al., 2016). In principle the intrinsic negative curvatures of accumulating cone-shaped lipids, such as PA in the inner (cis) leaflets of contacting bilayers, should facilitate fusion of merging membranes. But it is worth noting that the promotion of membrane fusion through local modification of membrane curvature also appears to hold true for other cone-shaped lipids such as cholesterol and DAG (Tanguy et al., 2016). Reconstituted membrane fusion assays have been valuable to dissect the role of individual components and on this instance it is important to highlight that PA was observed playing a unique role among cone-shaped lipids in a yeast vacuole fusion assay, suggesting a more complex mode of action of this lipid (Mima and Wickner, 2009). Furthermore, PA could locally accumulate and form microdomains highly negatively charged, which potentially serve as membrane retention sites for several proteins key for exocytosis, such as the SNARE protein syntaxin-1 (Lam et al., 2008), or other membrane remodeling processes (Jenkins and Frohman, 2005). Finally, as a precursor for DAG and PI(4,5)P_2, both known to contribute to numerous membrane remodeling events, PA could also have indirect effects. All these potential contributions of PA in membrane fusion have been reviewed elsewhere (Chasserot-Golaz et al., 2010; Ammar et al., 2013b, 2014; Tanguy et al., 2016), but solving the issue of the mechanistic role of PA in a given membrane remodeling process requires probing these different scenarios (**Figure 2**), which is now in need for novel methods and tools.

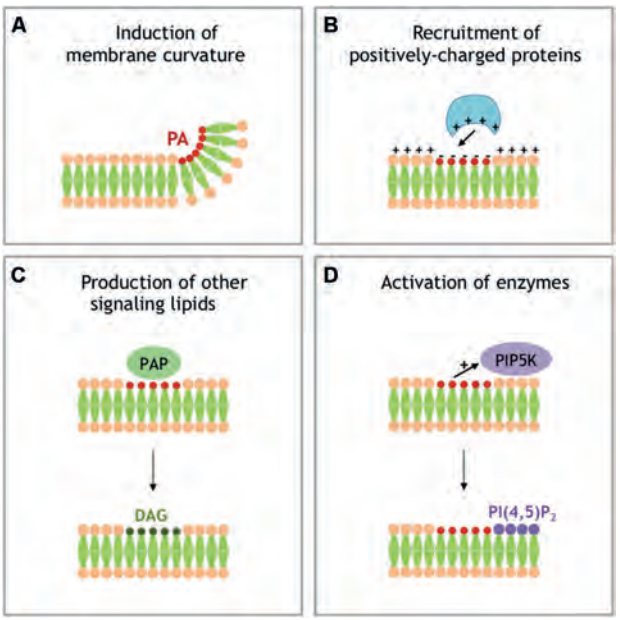

FIGURE 2 | Different models for signaling activity of PA. **(A)** Local accumulation of PA in a single leaflet of membrane generates negative membrane curvature. **(B)** Local accumulation of PA generates local buildup of negative charges that recruit PA effector-containing positively charged domains. **(C)** PAPs transforms PA into DAG, another signaling lipid with specific activity. **(D)** PA stimulates the activity of phosphatidylinositol 4-phosphate 5-kinase (PI4P5K), producing PI 4,5-bisphosphate (PI(4,5)P_2), an additional important signaling lipid.

Apoptosis, Survival, Growth, Proliferation and Migration

Many survival signals including hormones and growth factors activate PA synthesis through the stimulation of PLD activity. Similarly, mitogenic signals trigger cell proliferation, suppression of cell cycle arrest, and prevention of apoptosis. The PLD–PA–Rheb–mTOR and the PLD–PA–MAP kinase pathways are the two main downstream pathways of PLD involved in mitogenic signals and have been described extensively (Foster, 2009). Obviously, future solving of the complex imbrication of these pathways and understanding of the spatiotemporal relationships between PA-generating enzymes, PA-binding partners and PA itself will require development of more specific tools and extensive work.

NEUROLOGICAL DISORDERS POTENTIALLY LINKED TO AN ALTERATION OF PA LEVELS

In all organisms from yeast to mammals, PA was shown to possess signaling activity (Jenkins and Frohman, 2005) and a recent review highlights the apparent mystery of the many roles of PA in plants (Pokotylo et al., 2018). In addition, various PA-generating enzymes were shown to be involved in an increasing number of neuronal pathologies, suggesting a fundamental role of PA in the outcome of these neurodiseases (Tanguy et al., 2018). In the next chapter, we will describe four neuronal pathologies that may be the consequence, at least partially, of an alteration in PA dynamics.

Fetal Alcohol Spectrum Disorders

The damaging effects of alcohol drinking during gestation on the developing fetus are extremely well documented (Ehrhart et al., 2018). Fetal alcohol spectrum disorders (FASDs) is a generic term used to define the birth deficiencies that result from prenatal exposure to alcohol that range from mild to severe. These developmental defects on unborn infants have lifelong physical, behavioral, and cognitive disabilities. As alcohol consumption avoidance during pregnancy is in theory easy to achieve, FASD is in fact considered as one of the largest preventable forms of non-genetic birth disabilities associated with intellectual incapacity.

Although the main effort remains prevention of alcohol consumption during pregnancy, it is also important to understand the underlying pathological mechanisms involved in these effects of ethanol. In addition to the well-recognized ethanol and acetaldehyde toxicity, alcohol intensifies oxidative stress causing consequent effects such as DNA, protein and membrane damages. Additionally, it has been known for over three decades that in the presence of 1%–3% of ethanol, the two best characterized mammalian isoforms PLD1 and PLD2 catalyze a transphosphatidylation reaction. In this case alcohol replaces water during PC hydrolysis, and phosphatidyl alcohols are formed at the expense of PA (Jenkins and Frohman, 2005). Thus, in presence of ethanol, phosphatidylethanol is synthesized while PA is not. Since it is likely that phosphatidylethanol cannot replace PA as a signaling molecule, this was used as a trick to "inhibit" PLD activity (actually prevent PA production), but also in assays to quantify PLD activity (Ammar et al., 2014). It was also shown that ethanol inhibits the mitogenic downstream actions of PA on neuron progenitors (Klein, 2005). Furthermore, it was recently shown that both PLD1 and PLD2 strongly contribute to astroglial proliferation induced by IGF-1 (Burkhardt et al., 2014). Therefore, the perturbation of the IGF1-PLD signaling pathway could, at least in part, explain the teratogenic effects of ethanol observed in FASDs.

Neurological Cancers

Glioblastoma is the most frequent and aggressive brain cancer, with an estimated incidence of near five novel cases per 100,000 persons every year in the USA and Europe. Nearly 200,000 persons die from glioblastoma every year worldwide. It is a relatively difficult cancer to diagnose, as the symptoms are mainly non-specific, including headache and nausea, but leading to alterations of neurological functions such as speech, vision, behavior and memory. Like for many cancer tissues, elevated PLD activity was found in glioblastoma, suggesting that an increase in PA levels is a cause and/or consequence of the pathology (Park et al., 2009). At least part of the survival effect of increased PLD activity on glioblastoma appears to involve the Akt pathway (Bruntz et al., 2014). Interestingly, lipidomic analyses revealed that PA levels are altered in the regions that attract glioblastoma cells, indicating that PA levels control the homing process of glioblastoma (Wildburger et al., 2015). Undoubtedly, a better understanding of the multiple functions of PA in brain tumor development and progression may help to improve treatments and subsequently get a better prognosis for this aggressive cancer.

Intellectual Disability Diseases

Intellectual disability diseases are a common state defined by significant restriction in intellectual capacities and adaptive behavior that happen during childhood, with an overall intelligence quotient bellow 70 together with associated reduction in social, daily living and communication skills. These heterogeneous disease conditions affect 1%–3% of all populations and are thought to result from multiple causes, including environmental, chromosomal and monogenetic alterations. Among the several hundreds of genes involved, some affect brain development, neurogenesis, neuronal migration, or synaptic function (Humeau et al., 2009). Below we will briefly describe the data that support the notion of an alteration of PA levels and/or dynamics in the Fragile-X syndrome (FXS) and the Coffin-Lowry syndrome (CLS).

FXS is a neurodevelopmental pathology accountable for the most common inherited form of intellectual infirmity and autism spectrum disorder. It is generally the consequence of the hypermethylation of CGG expansion repeats (>200) in the 5′ untranslated region of the *FMR1* gene leading to transcription silencing. In a recent study, we pointed DGK kinase-κ (DGKκ) mRNA as the foremost target of Fragile Mental Retardation Protein and found an alteration in PA synthesis in neurons cultured from *Fmr1*-knockout mice after group 1 metabotropic glutamate receptor (mGluRI) stimulation (Tabet et al., 2016a). Silencing DGKκ in CA1 pyramidal neurons modified the immature over mature spine ratio and like in the *Fmr1*-knockout mouse phenotype, reduced LTP and increased LTD (Tabet et al., 2016a). Moreover, the typical *Fmr1*-knockout mouse phenotype on dendritic spine morphology was restored back to normal after overexpression of DGKκ (Tabet et al., 2016a). Finally, DGKκ silencing by shRNA in the mouse reiterated autistic behaviors, such as impaired social interaction, hyperactivity and altered nest-building very much like those seen in the *Fmr1*-knockout mouse model (Tabet et al., 2016a). Based on these observations, it was proposed that a major molecular consequence of the loss of FMRP expression in FXS is to prevent DGKκ translation, leading to an alteration in DAG and PA levels in neurons (Tabet et al., 2016b). A main consequence of this imbalance would be the alteration of the downstream signaling

of DAG and PA required for maturation of dendritic spines and establishment of correct synaptic plasticity (Moine and Vitale, 2018).

Loss of function mutations in the gene encoding Ribosomal S6 Kinase 2 (RSK2) lead to CLS, a rare syndromic form of mental retardation that shows X-linked inheritance. However, the molecular bases of the major neuronal alterations of CLS, such as moderate to severe defect in neurodevelopment, remain indefinable. In agreement with the notion that PLD1-generated PA is key to neurite outgrowth, we observed significant delayed in *Pld1* knockout neuron maturation (Ammar et al., 2013a). These observations were as well found in a mouse model for CLS syndrome since *Rsk2* knockout neurons exhibited developmental delay (Ammar et al., 2013a). Furthermore, RSK2 phosphorylates PLD1 at threonine 147 when exocytosis was triggered (Zeniou-Meyer et al., 2008) or during neurite outgrowth (Ammar et al., 2013a) in PC12 cells. A specific sensor for PA revealed an increase in PA levels at the tips of growing neurites in neurons resulting from PLD1 activation (Ammar et al., 2013a). Interestingly, PLD1 was found to be associated with BDNF positive endosomes (Ammar et al., 2015) and with vesicular structures derived from the trans Golgi, co-labeled by the vesicular SNARE VAMP-7/TiVAMP (Ammar et al., 2013a). The fusion efficiency of these PLD1/VAMP-7 vesicles in the growth cone was severely impaired by RSK2 and PLD1 inhibitors, suggesting that both PLD1 and RSK2 are necessary for membrane provision needed during neurite outgrowth (Ammar et al., 2013a). Accordingly, co-immunoprecipitation and confocal colocalization experiments indicated that RSK2 and PLD1 are found in a complex at the tip end of growing neurites, supporting the observation of an increased PA level at this location (Ammar et al., 2013a). Altogether, these results have highlighted the importance of PA-mediated membrane trafficking in neurite outgrowth and a key role of RSK2 in PA synthesis during this process, by phosphorylation and subsequent activation of PLD1. In consequence, it has been proposed that at least some of the clinical consequences of the CLS might result from an inadequate PA production during neuronal development and function (Zeniou-Meyer et al., 2010).

Neurodegeneration

It is becoming more and more evident that human neurodegenerative diseases such as Alzheimer disease (AD) also have a critical lipidic feature in their outcome. This aspect has been first pointed out by the susceptibility of the ApoE4 allele to AD, but more recently PLDs have also been proposed to contribute to the development of the pathology. It was first shown that PLD1 is involved in the vesicular trafficking of βAPP (Cai et al., 2006) and later that increased expression of APP promoted PLD activity in human astroglioma cells (Jin et al., 2007). Although highly debated, the observation that a rare variant of PLD3 gene confers susceptibility to AD has put PLD and PA on the spotlight (Cruchaga et al., 2014; Heilmann et al., 2015; Lambert et al., 2015; van der Lee et al., 2015). The most compelling evidence that defects in PA production by PLDs are involved in AD comes from an elegant study combining detailed lipidomics with behavioral tests in mouse models. In this study, the authors found that PLD2 knockout fully rescued AD-related synaptic dysfunction and cognitive deficits in a model of AD (Oliveira et al., 2010). The exact nature of the PA imbalance in AD awaits however to be fully defined and the possibility to interfere with AD condition by correcting this imbalance is probably very far from reach.

CONCLUSION

The diversity of mechanisms of PA signaling and physiological functions mostly relies on the fact that PA is synthesized by a complex set of different enzymes involved in diverse array of pathways. PLDs, DGKs, and LPAATs each constitute a big collection of isoenzymes differently localized within cells and displaying cell type specificity. In fact, the specific subcellular distribution, regulation, and/or substrate preferences of these enzymes probably account for the heterogeneity of PA composition in membranes. These aspects, altogether with the capacity of PA-binding modules in proteins to sense the local membrane environment and the type of PA species, offer a hub for the functional diversity of PA from molecular and cellular to physiological functions. There is no doubt that advanced lipidomics in combination with novel imaging tools to follow PA's dynamics will help to gain a better understanding of the apparent paradox of the abundance of function of this simple lipid. Further understanding of the biophysical side of PA's action on membranes is also critically needed to provide novel ideas for the treatment of the growing number of neuronal pathologies linked to the alterations of PA metabolism.

AUTHOR CONTRIBUTIONS

All authors listed have made a substantial, direct and intellectual contribution to the work, and approved it for publication.

FUNDING

This work was supported by Fondation pour la Recherche Médicale and by Fondation Jérôme Lejeune funding to HM.

REFERENCES

Ammar, M. R., Humeau, Y., Hanauer, A., Nieswandt, B., Bader, M. F., and Vitale, N. (2013a). The Coffin-Lowry syndrome-associated protein RSK2 regulates neurite outgrowth through phosphorylation of phospholipase D1 (PLD1) and synthesis of phosphatidic acid. *J. Neurosci.* 33, 19470–19479. doi: 10.1523/JNEUROSCI.2283-13.2013

Ammar, M. R., Kassas, N., Chasserot-Golaz, S., Bader, M. F., and Vitale, N. (2013b). Lipids in regulated exocytosis: what are they doing? *Front. Endocrinol.* 4:125. doi: 10.3389/fendo.2013.00125

Ammar, M. R., Kassas, N., Bader, M. F., and Vitale, N. (2014). Phosphatidic acid in neuronal development: a node for membrane and cytoskeleton rearrangements. *Biochimie* 107, 51–57. doi: 10.1016/j.biochi.2014.07.026

Ammar, M. R., Thahouly, T., Hanauer, A., Stegner, D., Nieswandt, B., and Vitale, N. (2015). PLD1 participates in BDNF-induced signalling in cortical neurons. *Sci. Rep.* 5:14778. doi: 10.1038/srep14778

Bader, M. F., and Vitale, N. (2009). Phospholipase D in calcium-regulated exocytosis: lessons from chromaffin cells. *Biochim. Biophys. Acta* 1791, 936–941. doi: 10.1016/j.bbalip.2009.02.016

Bruntz, R. C., Taylor, H. E., Lindsley, C. W., and Brown, H. A. (2014). Phospholipase D2 mediates survival signaling through direct regulation of Akt in glioblastoma cells. *J. Biol. Chem.* 289, 600–616. doi: 10.1074/jbc.M113.532978

Bullen, H. E., Jia, Y., Yamaryo-Botté, Y., Bisio, H., Zhang, O., Jemelin, N. K., et al. (2016). Phosphatidic acid-mediated signaling regulates microneme secretion in toxoplasma. *Cell Host Microbe* 19, 349–360. doi: 10.1016/j.chom.2016.02.006

Burkhardt, U., Wojcik, B., Zimmermann, M., and Klein, J. (2014). Phospholipase D is a target for inhibition of astroglial proliferation by ethanol. *Neuropharmacology* 79, 1–9. doi: 10.1016/j.neuropharm.2013.11.002

Cai, D., Zhong, M., Wang, R., Netzer, W. J., Shields, D., Zheng, H., et al. (2006). Phospholipase D1 corrects impaired βAPP trafficking and neurite outgrowth in familial Alzheimer's disease-linked presenilin-1 mutant neurons. *Proc. Natl. Acad. Sci. U S A* 103, 1936–1940. doi: 10.1073/pnas.0510710103

Chae, Y. C., Kim, J. H., Kim, K. L., Kim, H. W., Lee, H. Y., Heo, W. D., et al. (2008). Phospholipase D activity regulates integrin-mediated cell spreading and migration by inducing GTP-Rac translocation to the plasma membrane. *Mol. Biol. Cell* 19, 3111–3123. doi: 10.1091/mbc.E07-04-0337

Chasserot-Golaz, S., Coorssen, J. R., Meunier, F. A., and Vitale, N. (2010). Lipid dynamics in exocytosis. *Cell. Mol. Neurobiol.* 30, 1335–1342. doi: 10.1007/s10571-010-9577-x

Corrotte, M., Chasserot-Golaz, S., Huang, P., Du, G., Ktistakis, N. T., Frohman, M. A., et al. (2006). Dynamics and function of phospholipase D and phosphatidic acid during phagocytosis. *Traffic* 7, 365–377. doi: 10.1111/j.1600-0854.2006.00389.x

Corrotte, M., Nyguyen, A. P., Harlay, M. L., Vitale, N., Bader, M. F., and Grant, N. J. (2010). Ral isoforms are implicated in Fcγ R-mediated phagocytosis: activation of phospholipase D by RalA. *J. Immunol.* 185, 2942–2950. doi: 10.4049/jimmunol.0903138

Cruchaga, C., Karch, C. M., Jin, S. C., Benitez, B. A., Cai, Y., Guerreiro, R., et al. (2014). Rare coding variants in the phospholipase D3 gene confer risk for Alzheimer's disease. *Nature* 505, 550–554. doi: 10.1038/nature12825

Daniels, R. H., Hall, P. S., and Bokoch, G. M. (1998). Membrane targeting of p21-activated kinase 1 (PAK1) induces neurite outgrowth from PC12 cells. *EMBO J.* 17, 754–764. doi: 10.1093/emboj/17.3.754

Disse, J., Vitale, N., Bader, M. F., and Gerke, V. (2009). Phospholipase D1 is specifically required for regulated secretion of von Willebrand factor from endothelial cells. *Blood* 113, 973–980. doi: 10.1182/blood-2008-06-165282

Ehrhart, F., Roozen, S., Verbeek, J., Koek, G., Kok, G., van Kranen, H., et al. (2018). Review and gap analysis: molecular pathways leading to fetal alcohol spectrum disorders. *Mol. Psychiatry* 24, 10–17. doi: 10.1038/s41380-018-0095-4

Faugaret, D., Chouinard, F. C., Harbour, D., El azreq, M. A., and Bourgoin, S. G. (2011). An essential role for phospholipase D in the recruitment of vesicle amine transport protein-1 to membranes in human neutrophils. *Biochem. Pharmacol.* 81, 144–156. doi: 10.1016/j.bcp.2010.09.014

Foster, D. A. (2009). Phosphatidic acid signaling to mTOR: signals for the survival of human cancer cells. *Biochim. Biophys. Acta* 1791, 949–949. doi: 10.1016/j.bbalip.2009.02.009

Ghossoub, R., Lembo, F., Rubio, A., Gaillard, C. B., Bouchet, J., Vitale, N., et al. (2014). Syntenin-ALIX exosome biogenesis and budding into multivesicular bodies are controlled by ARF6 and PLD2. *Nat. Commun.* 5:3477. doi: 10.1038/ncomms4477

Hayashi, K., Ohshima, T., Hashimoto, M., and Mikoshiba, K. (2007). Pak1 regulates dendritic branching and spine formation. *Dev. Neurobiol.* 67, 655–669. doi: 10.1002/dneu.20363

Heilmann, S., Drichel, D., Clarimon, J., Fernández, V., Lacour, A., Wagner, H., et al. (2015). PLD3 in non-familial Alzheimer's disease. *Nature* 520, E3–E5. doi: 10.1038/nature14039

Holland, P., Knævelsrud, H., Søreng, K., Mathai, B. J., Lystad, A. H., Pankiv, S., et al. (2016). HS1BP3 negatively regulates autophagy by modulation of phosphatidic acid levels. *Nat. Commun.* 7:13889. doi: 10.1038/ncomms13889

Honda, A., Nogami, M., Yokozeki, T., Yamazaki, M., Nakamura, H., Watanabe, H., et al. (1999). Phosphatidylinositol 4-phosphate 5-kinase α is a downstream effector of the small G protein ARF6 in membrane ruffle formation. *Cell* 99, 521–532. doi: 10.1016/s0092-8674(00)81540-8

Humeau, Y., Gambino, F., Chelly, J., and Vitale, N. (2009). X-linked mental retardation: focus on synaptic function and plasticity. *J. Neurochem.* 109, 1–14. doi: 10.1111/j.1471-4159.2009.05881.x

Humeau, Y., Vitale, N., Chasserot-Golaz, S., Dupont, J. L., Du, G., Frohman, M. A., et al. (2001). A role for phospholipase D1 in neurotransmitter release. *Proc. Natl. Acad. Sci. U S A* 98, 15300–15305. doi: 10.1073/pnas.261358698

Ito, S., Richert, N., and Pastan, I. (1982). Phospholipids stimulate phosphorylation of vinculin by the tyrosine-specific protein kinase of Rous sarcoma virus. *Proc. Natl. Acad. Sci. U S A* 79, 4628–4631. doi: 10.1073/pnas.79.15.4628

Jang, J.-H., Lee, C. S., Hwang, D., and Ryu, S. H. (2012). Understanding of the roles of phospholipase D and phosphatidic acid through their binding partners. *Prog. Lipid Res.* 51, 71–81. doi: 10.1016/j.plipres.2011.12.003

Jenkins, G. M., and Frohman, M. A. (2005). Phospholipase D: a lipid centric review. *Cell. Mol. Life Sci.* 62, 2305–2316. doi: 10.1007/s00018-005-5195-z

Jin, J.-K., Ahn, B.-H., Na, Y.-J., Kim, J.-I., Kim, Y.-S., Choi, E.-K., et al. (2007). Phospholipase D1 is associated with amyloid precursor protein in Alzheimer's disease. *Neurobiol. Aging* 28, 1015–1027. doi: 10.1016/j.neurobiolaging.2006.05.022

Johnson, R. P., and Craig, S. W. (1995). The carboxy-terminal tail domain of vinculin contains a cryptic binding site for acidic phospholipids. *Biochem. Biophys. Res. Commun.* 210, 159–164. doi: 10.1006/bbrc.1995.1641

Jose Lopez-Andreo, M., Gomez-Fernandez, J. C., and Corbalan-Garcia, S. (2003). The simultaneous production of phosphatidic acid and diacylglycerol is essential for the translocation of protein kinase Cε to the plasma membrane in RBL-2H3 cells. *Mol. Biol. Cell* 14, 4885–4895. doi: 10.1091/mbc.e03-05-0295

Kassas, N., Tanguy, E., Thahouly, T., Fouillen, L., Heintz, D., Chasserot-Golaz, S., et al. (2017). Comparative characterization of phosphatidic acid sensors and their localization during frustrated phagocytosis. *J. Biol. Chem.* 292, 4266–4279. doi: 10.1074/jbc.m116.742346

Klein, J. (2005). Functions and pathophysiological roles of phospholipase D in thebrain. *J. Neurochem.* 94, 1473–1487. doi: 10.1111/j.1471-4159.2005.03315.x

Kooijman, E. E., Chupin, V., de Kruijff, B., and Burger, K. N. (2003). Modulation of membrane curvature by phosphatidic acid and lysophosphatidic acid. *Traffic* 4, 162–174. doi: 10.1034/j.1600-0854.2003.00086.x

Kurooka, T., Yamamoto, Y., Takai, Y., and Sakisaka, T. (2011). Dual regulation of RA-RhoGAP activity by phosphatidic acid and Rap1 during neurite outgrowth. *J. Biol. Chem.* 286, 6832–6843. doi: 10.1074/jbc.m110.183772

Lam, A. D., Tryoen-Toth, P., Tsai, B., Vitale, N., and Stuenkel, E. L. (2008). SNARE-catalyzed fusion events are regulated by Syntaxin1A-lipid interactions. *Mol. Biol. Cell* 19, 485–497. doi: 10.1091/mbc.e07-02-0148

Lambert, J. C., Grenier-Boley, B., Bellenguez, C., Pasquier, F., Campion, D., Dartigues, J. F., et al. (2015). PLD3 and sporadic Alzheimer's disease risk. *Nature* 520:E1. doi: 10.1038/nature14036

Lopez, C. I., Pelletán, L. E., Suhaiman, L., De Blas, G. A., Vitale, N., Mayorga, L. S., et al. (2012). Diacylglycerol stimulates acrosomal exocytosis by feeding into a PKC- and PLD1-dependent positive loop that continuously supplies phosphatidylinositol 4,5-bisphosphate. *Biochim. Biophys. Acta* 1821, 1186–1199. doi: 10.1016/j.bbalip.2012.05.001

Mima, J., and Wickner, W. (2009). Complex lipid requirements for SNARE- and SNARE chaperone-dependent membrane fusion. *J. Biol. Chem.* 284, 27114–27122. doi: 10.1074/jbc.m109.010223

Moine, H., and Vitale, N. (2018). Of local translation control and lipid signaling in neurons. *Adv. Biol. Regul.* doi: 10.1016/j.jbior.2018.09.005 [Epub ahead of print].

Nishikimi, A., Fukuhara, H., Su, W., Hongu, T., Takasuga, S., Mihara, H., et al. (2009). Sequential regulation of DOCK2 dynamics by two phospholipids during neutrophil chemotaxis. *Science* 324, 384–387. doi: 10.1126/science.1170179

Oliveira, T. G., Chan, R. B., Tian, H., Laredo, M., Shui, G., Staniszewski, A., et al. (2010). Phospholipase d2 ablation ameliorates Alzheimer's disease-linked synaptic dysfunction and cognitive deficits. *J. Neurosci.* 30, 16419–16428. doi: 10.1523/JNEUROSCI.3317-10.2010

Park, M. H., Ahn, B. H., Hong, Y. K., and Min do, S. (2009). Overexpression of phospholipase D enhances matrix metalloproteinase-2 expression and glioma cell invasion via protein kinase C and protein kinase A/NF-κB/Sp1-mediated signaling pathways. *Carcinogenesis* 30, 356–365. doi: 10.1093/carcin/bgn287

Pelletán, L. E., Suhaiman, L., Vaquer, C. C., Bustos, M. A., De Blas, G. A., Vitale, N., et al. (2015). ADP ribosylation factor 6 (ARF6) promotes acrosomal exocytosis by modulating lipid turnover and Rab3A activation. *J. Biol. Chem.* 290, 9823–9841. doi: 10.1074/jbc.m114.629006

Pokotylo, I., Kravets, V., Martinec, J., and Ruelland, E. (2018). The phosphatidic acid paradox: too many actions for one molecule class? Lessons from plants. *Prog. Lipid Res.* 71, 43–53. doi: 10.1016/j.plipres.2018.05.003

Potocký, M., Pleskot, R., Pejchar, P., Vitale, N., Kost, B., and Zárský, V. (2014). Live-cell imaging of phosphatidic acid dynamics in pollen tubes visualized by Spo20p-derive biosensor. *New Phytol.* 203, 483–494. doi: 10.1111/nph.12814

Raben, D. M., and Barber, C. N. (2017). Phosphatidic acid and neurotransmission. *Adv. Biol. Regul.* 63, 15–21. doi: 10.1016/j.jbior.2016.09.004

Roach, A. N., Wang, Z., Wu, P., Zhang, F., Chan, R. B., Yonekubo, Y., et al. (2012). Phosphatidic acid regulation of PIPKI is critical for actin cytoskeletal reorganization. *J. Lipid Res.* 53, 2598–2609. doi: 10.1194/jlr.m028597

Sanematsu, F., Nishikimi, A., Watanabe, M., Hongu, T., Tanaka, Y., Kanaho, Y., et al. (2013). Phosphatidic acid-dependent recruitment and function of the Rac activator DOCK1 during dorsal ruffle formation. *J. Biol. Chem.* 288, 8092–8100. doi: 10.1074/jbc.m112.410423

Schwarz, K., Natarajan, S., Kassas, N., Vitale, N., and Schmitz, F. (2011). The synaptic ribbon is a site of phosphatidic acid generation in ribbon synapses. *J. Neurosci.* 31, 15996–16011. doi: 10.1523/JNEUROSCI.2965-11.2011

Stace, C. L., and Ktistakis, N. T. (2006). Phosphatidic acid- and phosphatidylserine-binding proteins. *Biochim. Biophys. Acta* 1761, 913–926. doi: 10.1016/j.bbalip.2006.03.006

Tabet, R., Moutin, E., Becker, J. A., Heintz, D., Fouillen, L., Flatter, E., et al. (2016a). Fragile X Mental Retardation Protein (FMRP) controls diacylglycerol kinase activity in neurons. *Proc. Natl. Acad. Sci. U S A* 113, E3619–E3628. doi: 10.1073/pnas.1522631113

Tabet, R., Vitale, N., and Moine, H. (2016b). Fragile X syndrome: are signaling lipids the missing Culprits? *Biochimie* 130, 188–194. doi: 10.1016/j.biochi.2016.09.002

Tanguy, E., Carmon, O., Wang, Q., Jeandel, L., Chasserot-Golaz, S., Montero-Hadjadje, M., et al. (2016). Lipids implicated in the journey of a secretory granule: from biogenesis to fusion. *J. Neurochem.* 137, 904–912. doi: 10.1111/jnc.13577

Tanguy, E., Kassas, N., and Vitale, N. (2018). Protein-phospholipid interaction motifs: a focus on phosphatidic acid. *Biomolecules* 8:E20. doi: 10.3390/biom8020020

van den Bout, I., and Divecha, N. (2009). PIP5K-driven PtdIns(4,5)P2 synthesis: regulation and cellular functions. *J. Cell Sci.* 122, 3837–3850. doi: 10.1242/jcs.056127

van der Lee, S. J., Holstege, H., Wong, T. H., Jakobsdottir, J., Bis, J. C., Chouraki, V., et al. (2015). PLD3 variants in population studies. *Nature* 520, E2–E3. doi: 10.1038/nature14038

Vitale, N., Caumont, A. S., Chasserot-Golaz, S., Du, G., Wu, S., Sciorra, V. A., et al. (2001). Phospholipase D1: a key factor for the exocytotic machinery in neuroendocrine cells. *EMBO J.* 20, 2424–2434. doi: 10.1093/emboj/20.10.2424

Waselle, L., Gerona, R. R., Vitale, N., Martin, T. F., Bader, M. F., and Regazzi, R. (2005). Role of phosphoinositide signaling in the control of insulin exocytosis. *Mol. Endocrinol.* 19, 3097–3106. doi: 10.1210/me.2004-0530

Wildburger, N. C., Wood, P. L., Gumin, J., Lichti, C. F., Emmett, M. R., Lang, F. F., et al. (2015). ESI-MS/MS and MALDI-IMS localization reveal alterations in phosphatidic acid, diacylglycerol, and DHA in glioma stem cell xenografts. *J. Proteome Res.* 14, 2511–2519. doi: 10.1021/acs.jproteome.5b00076

Williams, J. M., Pettitt, T. R., Powell, W., Grove, J., Savage, C. O., and Wakelam, M. J. (2007). Antineutrophil cytoplasm antibody-stimulated neutrophil adhesion depends on diacylglycerol kinase-catalyzed phosphatidic acid formation. *J. Am. Soc. Nephrol.* 18, 1112–1120. doi: 10.1681/asn.2006090973

Yang, J. S., Gad, H., Lee, S. Y., Mironov, A., Zhang, L., Beznoussenko, G. V., et al. (2008). A role for phosphatidic acid in COPI vesicle fission yields insights into Golgi maintenance. *Nat. Cell Biol.* 10, 1146–1153. doi: 10.1038/ncb1774

Zeniou-Meyer, M., Gambino, F., Ammar, M. R., Humeau, Y., and Vitale, N. (2010). The Coffin-Lowry syndrome-associated protein RSK2 and neurosecretion. *Cell. Mol. Neurobiol.* 30, 1401–1406. doi: 10.1007/s10571-010-9578-9

Zeniou-Meyer, M., Liu, Y., Béglé, A., Olanich, M. E., Hanauer, A., Becherer, U., et al. (2008). The Coffin-Lowry syndrome-associated protein RSK2 is implicated in calcium-regulated exocytosis through the regulation of PLD1. *Proc. Natl. Acad. Sci. U S A* 105, 8434–8439. doi: 10.1073/pnas.0710676105

Zeniou-Meyer, M., Zabari, N., Ashery, U., Chasserot-Golaz, S., Haeberlé, A. M., Demais, V., et al. (2007). Phospholipase D1 production of phosphatidic acid at the plasma membrane promotes exocytosis of large dense-core granules at a late stage. *J. Biol. Chem.* 282, 21746–21757. doi: 10.1074/jbc.m702968200

Conflict of Interest Statement: The authors declare that the research was conducted in the absence of any commercial or financial relationships that could be construed as a potential conflict of interest.

Journal of Neurochemistry

JOURNAL OF NEUROCHEMISTRY | 2016

doi: 10.1111/jnc.13577

REVIEW

Lipids implicated in the journey of a secretory granule: from biogenesis to fusion

Emeline Tanguy,*[,1] Ophélie Carmon,†[,1] Qili Wang,* Lydie Jeandel,† Sylvette Chasserot-Golaz,* Maité Montero-Hadjadje† and Nicolas Vitale*

*Institut des Neurosciences Cellulaires et Intégratives (INCI), UPR-3212 Centre National de la Recherche Scientifique & Université de Strasbourg, Strasbourg, France

†INSERM U982, Laboratoire de Différenciation et Communication Neuronale et Neuroendocrine, Institut de Recherche et d'Innovation Biomédicale, Université de Rouen, Mont-Saint-Aignan, France

Abstract

The regulated secretory pathway begins with the formation of secretory granules by budding from the Golgi apparatus and ends by their fusion with the plasma membrane leading to the release of their content into the extracellular space, generally following a rise in cytosolic calcium. Generation of these membrane-bound transport carriers can be classified into three steps: (i) cargo sorting that segregates the cargo from resident proteins of the Golgi apparatus, (ii) membrane budding that encloses the cargo and depends on the creation of appropriate membrane curvature, and (iii) membrane fission events allowing the nascent carrier to separate from the donor membrane. These secretory vesicles then mature as they are actively transported along microtubules toward the cortical actin network at the cell periphery. The final stage known as regulated exocytosis involves the docking and the priming of the mature granules, necessary for merging of vesicular and plasma membranes, and the subsequent partial or total release of the secretory vesicle content. Here, we review the latest evidence detailing the functional roles played by lipids during secretory granule biogenesis, recruitment, and exocytosis steps.

Keywords: exocytosis, lipid, membrane, microdomain, secretion, secretory granule budding.

J. Neurochem. (2016) 10.1111/jnc.13577

This article is part of a mini review series on Chromaffin cells (ISCCB Meeting, 2015).

The secretory pathway is an essential cellular activity that requires synthesis, modification, sorting, and release of secretory proteins/molecules outside cells, as well as transport of cell surface components. These proteins are first created on endoplasmic reticulum (ER)-bound ribosomes and translocated into the ER lumen, where they are folded, assembled, and N-glycosylated (Braakman and Bulleid 2011). Cargo proteins (either membrane associated or soluble) are conveyed from the ER exit sites to the entry side of the Golgi apparatus and then successively pass through the different Golgi stacks, where the proteins undergo maturation and processing (Wilson *et al.* 2011). At the trans-Golgi network (TGN), proteins are sorted into specific vesicular carriers for transport and distribution to their ultimate destinations, including the endolysosomal system and the plasma membrane, by the constitutive or regulated exocytosis pathway (Gerdes 2008). On one side, all cell types recycle membranes, proteins, and extracellular matrix components through constitutive secretory vesicles that are transported directly to the cell surface where they

Received December 24, 2015; revised manuscript received January 20, 2016; accepted February 3, 2016.

Address correspondence and reprint requests to Nicolas Vitale, Institut des Neurosciences Cellulaires et Intégratives (INCI), UPR-3212 Centre National de la Recherche Scientifique & Université de Strasbourg, 5 rue Blaise Pascal, 67084 Strasbourg, France. E-mail: vitalen@unistra.fr

Maité Montero-Hadjadje, INSERM U982, Laboratoire de Différenciation et Communication Neuronale et Neuroendocrine, Institut de Recherche et d'Innovation Biomédicale, Université de Rouen, 76821 Mont-Saint-Aignan, France. E-mail: maite.montero@univ-rouen.fr

[1]These authors contributed equally to this work.

Abbreviations used: AA, arachidonic acid; AP, adaptor protein; AQP, aquaporin; BAR, Bin/amphiphysin/Rvs; CAPS, calcium-activator protein for secretion; CERT, ceramide transport protein; DAG, diacylglycerol; ER, endoplasmic reticulum; ISG, immature secretory granules; LPA, lysophosphatidic acid; LPC, lyso-phosphatidylcholine; MSG, mature secretory granules; PA, phosphatidic acid; PE, phosphatidylethanolamine; PI(3)P, phosphatidylinositol-3-phosphate; PI(3,5)P2, phosphatidylinositol 3,5-bisphosphate; PI(4)P, phophatidylinositol 4-phosphate; PI(4,5)P2, phosphatidylinositol 4,5-bisphosphate; PI3K, phosphatidylinositol 3-kinase; PKD, protein kinase D; PLD, phospholipase D; PS, phosphatidylserine; PUFA, polyunsaturated fatty acid; SNARE, soluble *N*-ethylmaleimide-sensitive factor attachment protein receptor; TGN, trans-Golgi network; VAMP, vesicle-associated membrane protein; V-ATPase, vacuolar H-ATPase.

fuse with the plasma membrane in the absence of any kind of stimuli. On the other side, the regulated pathway is a trademark of specialized secretory cells, such as neurons, endocrine, and exocrine cells, and requires the accumulation of the secretory material into dedicated organelles, the secretory granules (Vázquez-Martínez *et al.* 2012). The latter are transported through the cytoplasm toward the cell periphery, where they are exocytosed after stimulation of the cell (Burgess and Kelly 1987).

In addition to the function of important protein players in the journey of a secretory granules, lipids also contribute to key steps. Cell membranes are indeed composed of a broad spectrum of lipids with specific properties that can directly influence membrane topology, dynamics, and tasks. In addition, the lipid composition and transbilayer arrangement vary strikingly between organelles and there is compelling evidence that the collective properties of bulk lipids profoundly define organelle identity and function (Holthuis and Menon 2014). Of particular interest are changes in the physical properties of the membrane that are directly under the control of lipids, and mark the transition from early to late organelles in the secretory pathway. These include bilayer thickness, lipid packing density, and surface charge. Here, we highlight the latest evidence supporting the notion that in addition to the collective action of bulk lipids, specific minor lipids directly control directionality and functionality of the secretory pathway.

Lipids and biogenesis of secretory granules

Lipids involved in formation of budding sites at the TGN membrane

The biogenesis of secretory granules destined for the regulated secretory pathway begins like other transport vesicles by active budding at the TGN membrane. This process needs several concomitant events: the sorting of cargo and membrane components, the membrane curvature, and the recruitment of cytosolic proteins. A role for lipids in the formation of post-Golgi carriers has long been proposed, including their interactions with enzymes and other membrane-associated proteins. The development of cellular lipidomic approaches (especially mass spectrometry) has revealed (i) that the Golgi membrane of the mammalian cell contains the same lipids as those found in the plasma membrane, but in different proportions and (ii) that the two leaflets of the Golgi membrane bilayers display specific lipid compositions, sphingolipids being enriched in the lumenal leaflet, whereas phosphatidylserine (PS) and phosphatidylethanolamine are concentrated in the cytosolic leaflet (van Meer and de Kroon 2011). Beside these lipids, the recruitment of enzymes at the cytosolic face of the TGN membrane contributes to its remodeling through the generation of lipid metabolites, such as diacylglycerol (DAG), phosphatidic acid (PA), and phosphoinositides (Ha *et al.* 2012). These lipids play a central role in the formation of secretory granules. For instance, the accumulation of PA in the TGN membrane is a key factor for the budding of secretory granules (Siddhanta and Shields 1998). At low pH and high calcium concentrations, PA adopts a conical shape that favors changes in membrane topology (Kooijman *et al.* 2003). DAG also exhibits a conical shape and its accumulation in the TGN membrane has been found to facilitate membrane curvature leading to the budding of secretory granules (Asp *et al.* 2009).

The Golgi membrane also exhibits a dynamic lipid asymmetry, with the ability of cholesterol, DAG, and other glycerophospholipids to translocate spontaneously or in P4-ATPase-stimulated manner (Tang *et al.* 1996). Flippases generally maintain lipid asymmetry, but their lipid transfer activity between the two leaflets can also potentially lead to membrane curvatures that drive the budding of post-Golgi vesicles (Leventis and Grinstein 2010).

Cells are able to maintain differences in lipid composition between their organelles despite the lateral diffusion of lipids in cellular membranes. The physical differences between glycerolipids and sphingolipids make them segregate in the presence of cholesterol (Marsh 2009). In the Golgi membrane, for example, domains with different lipid compositions are targeted with unique transmembrane proteins into separate secretory vesicles. This segregation of lipids and proteins forms the sorting mechanism which cells use to maintain the specific composition of their membranes (van Meer *et al.* 2008). Originally, lipid self-organization was considered to be the major driving force behind lateral membrane organization. The formation of such functional lipid micro- or nano-domains in the bilayer remains difficult to visualize because of the lack of effective lipid probes to study molecule dynamics in living cells. Although this self-organization plays an essential role, it is plausible that membrane proteins influence lipid organization, and conversely that protein function and clustering are under the control of lipids. Notwithstanding the so-called ‘lipid rafts’ in Golgi membrane have been predicted to regulate the function and clustering of proteins involved in the budding of secretory granules (Surma *et al.* 2012).

Lipids involved in protein recruitment at the budding sites

The enrichment of secretory granule membrane in sphingolipids and cholesterol suggests their participation in the formation of functional microdomains involved in the budding of these organelles from the Golgi membrane (Wang and Silvius 2000). Lipid microdomains are implicated in the sorting of proteins destined for the regulated secretory pathway (Tooze *et al.* 2001), as they possess the ability to attract peripheral proteins such as carboxypeptidase E (Dhanvantari and Loh 2000), prohormone convertase PC2 (Blázquez *et al.* 2000), and secretogranin III (Hosaka *et al.*

2004). These proteins act as chaperones by tethering soluble or aggregated proteins to the secretory granule membrane (Dikeakos and Reudelhuber 2007). In secretory cells, lipid microdomains also attract aquaporins (AQP), which are transmembrane proteins that remove water, thereby allowing the condensation of aggregated granule proteins in the TGN (Arnaoutova *et al.* 2008). In the low pH and high calcium conditions found in the Golgi compartment, members of a family of soluble proteins called chromogranins induce aggregation of proteins destined to the regulated secretory pathway (Montero-Hadjadje *et al.* 2008). TGN acidification is achieved by proton pumps of the vacuolar H-ATPase (V-ATPase) family (Schapiro and Grinstein 2000). Interestingly, Li *et al.* (2014) have demonstrated that the signaling lipid phosphatidylinositol 3,5-bisphosphate (PI(3,5)P2) is a significant regulator of V-ATPase assembly and activity. Furthermore, phosphoinositides on the cytosolic surface recruit organelle-specific effector proteins of vesicle trafficking and signal transduction (Di Paolo and De Camilli 2006). For example, the serine/threonine protein kinase D (PKD) is recruited by binding to DAG and the GTPase ARF1, and this promotes the production of phophatidylinositol 4-phosphate (PI(4)P) by activating the lipid kinase PI(4)-kinase IIIß. At the TGN, PI(4)P can recruit lipid transfer proteins, such as oxysterol-binding protein 1 and ceramide transport protein that control sphingolipid and sterol levels, respectively. Ceramide transport protein-mediated transport of ceramide to the TGN has been proposed to increase the local production of DAG, which is converted into PA and lysophosphatidic acid; all these lipids being necessary for fission of secretory vesicles. PKD also regulates the recruitment of Arfaptin-1 (a Bin/amphiphysin/Rvs domain protein) to PI(4)P at the TGN membrane (Cruz-Garcia *et al.* 2013). In this study, Arfaptin-1 also appears important for the sorting of chromogranin A, a member of the chromogranin family, to the regulated secretory pathway in human BON carcinoid tumor cells. These results suggest that DAG-dependent PKD recruitment is crucial for the biogenesis of secretory granules. Indeed, PKD-mediated Arfaptin-1 phosphorylation is necessary to ensure the fission of secretory granules at the TGN of pancreatic β cells (Gehart *et al.* 2012). Such a role is compatible with previous reports showing that other cellular components, such as chromogranin-induced prohormone aggregates are important for driving TGN vesicle budding after their association with membrane rafts (Gondré-Lewis *et al.* 2012).

The journey of secretory granules begins

Hormone precursors, along with other proteins of the regulated secretory pathway in neuroendocrine cells, are sorted and packaged into immature secretory granules that bud off from the TGN. These organelles are rapidly conveyed to the cell periphery through their interaction with microtubules via kinesin motors (Park *et al.* 2009). The maturation process comprises an acidification-dependent processing of cargo, condensation of the secretory granule content, and removal of lipids and proteins not destined for mature secretory granules. The acidification process occurs along the regulated secretory route resulting in a decrease in pH from the TGN (6.5–6.2), to immature secretory granules (6.3–5.7), and finally to mature secretory granules (5.5–5.0). In chromaffin cells, an increase in the proton pump density and a diminution in proton permeability of the granule membrane allow a pH drop (Apps *et al.* 1989). Moreover, the selective V-ATPase inhibitor bafilomycin A1 demonstrated the role of acidification on trafficking of specific granule proteins through the regulated secretory pathway in PC12 cells (Taupenot *et al.* 2005), a process potentially under the control of phosphoinositide levels.

During maturation in endocrine and exocrine cells, granules decrease in size as their content undergoes condensation, along with the concomitant efflux of Na^+, K^+, Cl^-, and water from the granules. Water removal is ensured by the lipid microdomain-associated AQP. AQP1 is found in secretory granules of pituitary and chromaffin cells, as well as in synaptic vesicles and pancreatic zymogen granules, whereas AQP5 is found in parotid gland secretory vesicles (Ishikawa *et al.* 2005; Arnaoutova *et al.* 2008). They facilitate condensation of granular content during maturation. Upon their arrival at the cell periphery, secretory granules are trapped in the dense cortical actin network. Myosin Va together with Rab3D regulate distinct steps of the granule maturation, with an essential role of myosin Va in membrane remodeling (Kögel and Gerdes 2010) and a crucial function of Rab3D in the cargo processing (Kögel *et al.* 2013). Interestingly in yeast, oxysterol-binding protein Osh4p-recruited PI(4)P and Rab proteins are in association with a myosin V type (Myo2p) in the membrane of secretory compartments and are implicated in vesicle maturation (Santiago-Tirado *et al.* 2011).

Membrane remodeling also induces a decrease of the size of secretory granules. The presence of a clathrin coat on patches of secretory granule membrane causes shrinkage of material, mediated by the clathrin adaptator protein (AP)-1 (Dittie *et al.* 1996). As a result, membrane proteins like vesicle-associated membrane protein 4 (VAMP4), furin, and mannose 6-phosphate receptors, which have a canonical AP-1-binding site in their cytosolic domain, are present in immature secretory granules, but not anymore in mature secretory granules (Klumperman *et al.* 1998; Teuchert *et al.* 1999; Hinners *et al.* 2003). AP-1 accumulates at the cytosolic face of TGN membrane likely through PI(4)P interaction (Wang *et al.* 2003). Their transport along microtubules toward the cortical actin, a step that has not been linked to lipid yet, and the concomitant granular modifications result in the maturation and storage of secretory granules, competent for exocytosis.

Lipids and exocytosis of secretory granules

And the journey of secretory granules ends

The final stage of the secretory pathway is regulated exocytosis, a well-defined multistep process triggered by an exocytotic stimulus (Pang and Südhof 2010). The molecular machinery underlying regulated exocytosis involves assembly of a tripartite soluble *N*-ethylmaleimide-sensitive factor attachment protein receptor (SNARE) complex between plasma and granular proteins as well as accessory proteins (Jahn and Fasshauer 2012). Extensive work over the last two decades has also shed light on the importance of lipids in the exocytosis process. In the following sections, the major contributions of membrane lipids for each step of secretory granule exocytosis will be described.

Lipids involved in formation of exocytotic sites and the docking step

Mature granules, once tethered, are recruited to exocytotic sites and this represents the initial contact between secretory granules and plasma membrane. Some lipids, such as cholesterol, phosphatidylinositol 4,5-bisphosphate (PI(4,5)P2), and sphingolipids are clustered in ordered microdomains in plasma membrane, also called membrane rafts. Biochemical and high-resolution imaging observations indicate that these detergent-resistant microdomains serve to concentrate and regulate SNARE proteins, arguing for the constitution of active exocytotic sites (Salaün *et al.* 2005). Spatial definition of exocytotic sites is cholesterol dependent, as depletion of cholesterol from the plasma membrane negatively affects cluster integrity and results in reduced secretory activity by neuroendocrine cells (Lang *et al.* 2001). Furthermore, we have demonstrated that PI(4,5)P2-enriched microdomains co-localize with SNARE clusters and docked secretory granules from analysis of immunogold labeled plasma membrane sheets (Umbrecht-Jenck *et al.* 2010).

PI(4,5)P2 plays a critical role in translocating secretory vesicles to the plasma membrane (Wen *et al.* 2011), but also binds and regulates a large subset of proteins involved in the docking step, and therefore plays an essential role in granule recruitment at exocytotic sites (recently reviewed by Martin 2015). For instance, by modulating actin polymerization, PI(4,5)P2 controls actin-based delivery of secretory vesicles to exocytotic sites (Trifaró *et al.* 2008). Moreover, PI(4,5)P2 clusters organized by syntaxin-1A could act as a platform for granule docking in membrane rafts (Honigmann *et al.* 2013). Studies in chromaffin cells have demonstrated that generation of microdomains is positively regulated by recruitment of annexin A2, a calcium- and PI(4,5)P2-binding protein present at docking sites near SNARE complexes (Chasserot-Golaz *et al.* 2005; Umbrecht-Jenck *et al.* 2010). Using 3D electron tomography, we have recently shown that annexin A2 generates lipid domains sites by connecting cortical actin and docked secretory granules to active fusion sites (Gabel *et al.* 2015). The actin-bundling activity of annexin A2 promotes the formation of ganglioside GM1-enriched microdomains, increases the number of morphologically docked granules at the plasma membrane, and controls the number and the kinetic of individual exocytotic events.

Altogether, these findings raise the possibility that exocytotic sites are defined by specific lipids, such as cholesterol and PI(4,5)P2, that contribute to sequestering or stabilizing components of the exocytotic machinery. There are also indications that other lipids contribute to the establishment of exocytotic sites. For instance, PS resides mostly in the cytosolic leaflet of plasma membrane in unstimulated conditions. However, during exocytosis of secretory granules in numerous secretory cell types, notably neuroendocrine cells, PS translocates to the outer leaflet (Vitale *et al.* 2001). An ultrastructural analysis has recently demonstrated that PS is externalized in the vicinity of the docking sites of secretory granules, although the functional relevance of this PS externalization for fusion is still under debate (Ory *et al.* 2013). Another lipid implicated in regulated exocytosis is PA. Silencing of the PA-producing enzyme phospholipase D1 (PLD1) and the ectopic expression of a catalytically dead PLD1 form in chromaffin cells affected the number of exocytotic events, as revealed by capacitance recordings and carbon fiber amperometry (Zeniou-Meyer *et al.* 2007). In line with these observations, PA has recently been proposed to regulate docking in sea urchin eggs (Rogasevskaia and Coorssen 2015). Finally, analysis of plasma membrane SNARE microdomains in chromaffin cells by total internal reflection fluorescent microscopy suggests that exogenous addition of the polyunsaturated fatty acid arachidonic acid (AA) enhances docking of granules (García-Martínez *et al.* 2013). Thus, investigations using novel high-resolution imaging techniques combined with acute modifications of individual lipid composition in a given membrane will probably further elucidate the contribution of lipids to the organization of the exocytotic platform.

Lipids regulating molecular mechanisms of priming steps

Priming steps depend on molecular events, essentially involving SNARE complex assembly, and are necessary to render vesicles fusion competent (Klenchin and Martin 2000). There is also growing evidence that lipids are implicated in priming, as indicated by lipid reorganization provoked by inositol kinases and lipases during this step. Phosphoinositides such as PI(4,5)P2 seem to be key regulators of secretion, not only by regulating the docking step but also by controlling the size and refilling rate of the readily releasable pool of granules. Electrophysiological studies modulating PI(4,5)P2 levels and using over-expressed PI(4,5)P2 fluorescent probes revealed that a high level of PI(4,5)P2 in chromaffin cells positively modulates secretion by increasing the size of the primed vesicle pool,

whereas the constants of the fusion rate were not affected (Milosevic *et al.* 2005). In agreement with this concept, we recently found that the HIV protein Tat sequesters plasmalemmal PI(4,5)P2 in neuroendocrine cells and subsequently reduces the number of exocytotic events, without significantly affecting the kinetics of fusion (Tryoen-Toth *et al.* 2013). Moreover, *in vitro* experiments using liposomes have previously reported that PI(4,5)P2 can recruit priming factors such as calcium-activator protein for secretion (CAPS), which facilitates SNARE-dependent fusion (James *et al.* 2008). However, it seems that a well-regulated balance between plasmalemmal PI(4,5)P2 synthesis and breakdown is mandatory for exocytosis. Indeed, DAG production through hydrolysis of PI(4,5)P2 by phospholipase C is crucial for exocytosis in mast cells (Hammond *et al.* 2006). As for PI(4,5)P2, DAG formation is essential for priming, leading to activation of protein kinase C and Munc-13, which then modulate the function of syntaxin-1A (Sheu *et al.* 2003; Bauer *et al.* 2007).

On the granule membrane, phosphoinositides have also been implicated in priming. For instance, experiments on permeabilized chromaffin cells have shown that synthesis of phosphatidylinositol-3-phosphate (PI(3)P) on secretory granules positively regulates secretion. Formation of PI3P is mediated by an isoform of phosphatidylinositol 3-kinase (PI3K), PI3K-C2α, particularly enriched on chromaffin granule membranes, suggesting that PI3K-C2α production of PI(3)P has a specific role in the ATP-dependent priming phase of exocytosis (Meunier *et al.* 2005). Genetic and pharmalogical inhibition of PI3K-C2α activity resulted in a complete inhibition of secretion, suggesting that PI(3)P synthesis is necessary for exocytosis to occur (Meunier *et al.* 2005). This notion has been validated by experiments showing that stimulation of exocytosis up-regulated PI(3)P levels on granules, whereas enzymatic conversion of PI3P in PI(3,5)P2 negatively affected exocytosis (Osborne *et al.* 2008; Wen *et al.* 2008). A similar effect on insulin secretion has been reported in pancreatic β cells with impaired PI3K-C2α activity (Dominguez *et al.* 2011). Taken together, PI(3)P production by PI3K-C2α on chromaffin granule membrane can be proposed to act as an essential priming signal for secretory granules, although the effectors directly involved remain to be characterized. Altogether these observations suggest that phosphoinositide metabolism is finely regulated to control the number of fusion-competent granules.

Other lipids have recently emerged as additional modulators of the priming step. AA, a polyunsaturated fatty acid of the omega-6 family has been described to potentiate exocytosis from chromaffin cells (Vitale *et al.* 1994, 2010; Latham *et al.* 2007). *In vitro* assays on protein interactions have revealed that AA can directly interact with SNAREs, like syntaxin-1a or syntaxin-3, and potentiate their assembly with SNAP-25 (Darios and Davletov 2006). Interestingly, this effect of AA on SNARE complex formation *in vitro* can be reproduced by other omega-3 and omega-6 fatty acids, suggesting that polyunsaturated lipids may physiologically regulate SNARE complex assembly by targeting syntaxin isoforms (Darios and Davletov 2006). Along this line, work with snake phospholipase acting as neurotoxin substantiates the notion that free fatty acids and lysophopholipids promote neurosecretion (Rigoni *et al.* 2005). Furthermore, production of sphingosine, *via* hydrolysis of vesicular membrane sphingolipids, also facilitated SNARE complex assembly by activating the vesicular SNARE synaptobrevin (Darios *et al.* 2009). Finally, *in vitro* fusion assays have demonstrated that PA binds syntaxin-1 and promotes SNARE complex assembly (Lam *et al.* 2008; Mima and Wickner 2009).

'Fusogenic lipids' for membrane merging and release of content

Many observations are in agreement that lipids have also a crucial role in the fusion reaction. Thus, the most widely accepted lipidic model for membrane fusion is the stalk pore model, defined by the merging of cis-contacting monolayers, leading to a negatively curved lipid structure called a stalk (Chernomordik and Kozlov 2008). During exocytosis, the outer leaflet of the granule and the inner leaflet of the plasma membrane seemingly form the stalk. As a result of differences in the geometry of lipids, lipid composition of membranes presumably influences the structure of the stalk and subsequently efficacy of exocytosis. Theoretically, cone-shaped lipids such as cholesterol, DAG, or PA, which have intrinsic negative curvatures when found in the inner (cis) leaflets of contacting bilayers could promote fusion. On the contrary, inverted cone-shaped lipids (PS, gangliosides, or lysophospholipids) are supposed to be present in the outer (trans) leaflets. This concept has been partially validated using reconstituted fusion assays and directly by adding lipids to cell cultures. These results indicate that PA, DAG, and cholesterol, may promote fusion by changing the spontaneous curvature of membranes (Ammar *et al.* 2013).

PA is present in the inner leaflet of the plasma membrane, but presumably in very small quantities in resting conditions. Based on the pivotal role of this lipid in exocytosis (Bader and Vitale 2009), the visualization of local formation of PA has been a recurring issue. Use of PA-specific probes coupled to ultrastructural analysis allowed us to visualize PA accumulation at the plasma membrane in stimulated chromaffin cells, near morphological docking sites (Zeniou-Meyer *et al.* 2007). Moreover, silencing of PLD1 has suggested that PA production is necessary to facilitate membrane fusion after early steps of exocytosis, probably by modifying membrane topology in the proximity of docking sites. In favor of this model, extracellular lyso-phosphatidylcholine (LPC) application partially rescued secretion from PLD1-depleted cells (Zeniou-Meyer *et al.* 2007). PLD1 activity at the plasma membrane, and subsequently PA

synthesis during exocytosis, is itself regulated by PI(4,5)P2 (Du *et al.* 2003). As PA is also an essential co-factor of PI5K, which produces PI(4,5)P2, a positive feedback loop for the synthesis of these two lipids may be activated during exocytosis (Cockcroft 2009).

In conclusion, the local accumulation of different fusogenic lipids, such as PA, PI(4,5)P2, DAG, and cholesterol at or near granule docking sites may have a synergistic effect on membrane curvature and thereby promote fusion. However, the precise localization of these lipids during the course of the fusion pore formation, expansion, and closure remains elusive and requires significant advances in imaging techniques and lipid sensors. Finally, a novel mass spectrometry method has recently revealed that saturated free fatty acids are actively generated in stimulated neurosecretory cells and neurons (Narayana *et al.* 2015), but at present it is not known if these fatty acids have a direct role in exocytosis or if they are degradation products of fusogenic lipids.

Ending the journey or a new beginning?

Membrane fusion during exocytosis can occur through three different modes in secretory cells, depending on the physiological demand: kiss and run, cavicapture, or full-collapse fusion. After full-collapse fusion of the granules upon stimulation, the secretory granule membrane components can be entirely recycled by a clathrin-mediated compensatory endocytotic process (Ceridono *et al.* 2011). Molecular mechanisms underlying the preservation of granule mem-

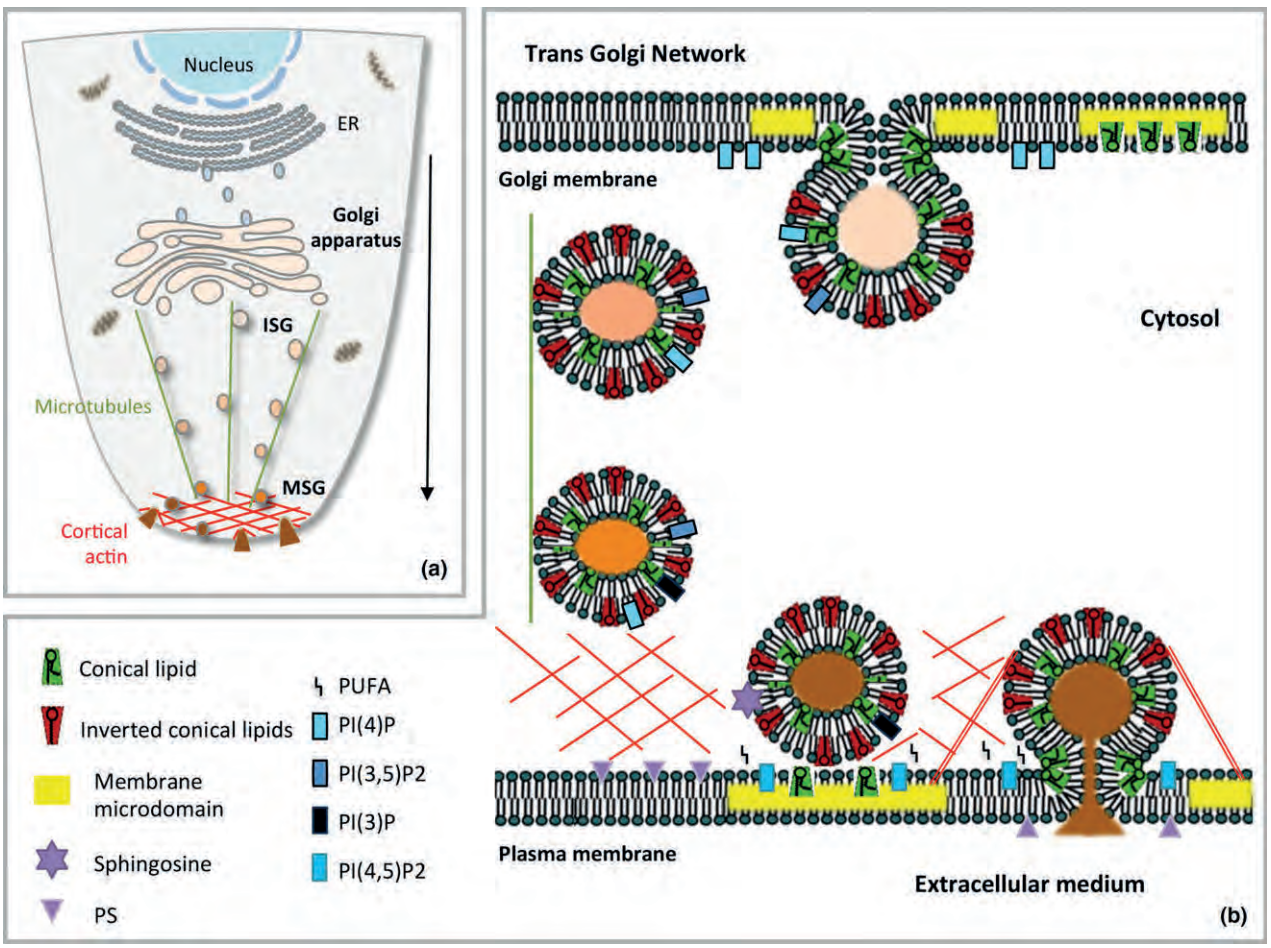

Fig. 1 Model highlighting the importance of lipids from secretory granule biogenesis to fusion. (a) The regulated secretory pathway from the Golgi apparatus to the plasma membrane. Immature secretory granules (ISG) are transported along microtubules from the trans-Golgi network (TGN) up to the cortical actin. During their active transport they are converted into mature secretory granules (MSG). (b) Lipids involved in the journey of secretory granules. Specific minor lipids directly control directionality and functionality of the regulated secretory pathway. Conical lipids include cholesterol, diacylglycerol, phosphatidic acid, and phosphatidylethanolamine. Inverted conical lipids include lysophospholipids and PI(4,5)P2. Omega-6 and omega-3 forms of polyunsaturated fatty acids (PUFA) are released in the cytosol by phospholipases. Membrane microdomains enriched in cholesterol, gangliosides, and sphingolipids are highlighted at the budding membrane of the TGN and at the exocytotic sites of the plasma membrane.

brane identity after fusion with plasma membrane remains unclear, but it has been proposed that specific lipid microdomains might contribute to prevent diffusion of granular components. Hence, exo-endocytosis coupling leads then to recycling of post-exocytotic internalized granule membrane back to the Golgi apparatus, starting a new life for the secretory granule (Houy *et al.* 2013). Recently lipids generated upon exocytosis have been proposed to contribute to the exo-endocytosis coupling (Yuan *et al.* 2015).

Conclusion

Lipids undoubtedly appear to contribute to almost every step along the regulated secretory pathway from the biogenesis of secretory granules to the exocytosis process (Fig. 1). However, despite the important advances in our understanding, many important answers remain far beyond our reach. The contribution of individual molecular lipid species is not known. Addressing this issue will require following the dynamics of individual lipid species at the nanometric scale, an aspect that may be achieved through the development of mass spectrometric imaging. Clearly this remains one of the most challenging issues in modern cell biology, given the large number of lipid molecules to analyze. Probing the physiological relevance of these lipids in different secretory processes is another challenging aspect for the near future. Indeed there is no doubt that an alteration of the fine cellular lipid balance, either as a consequence of an alteration of lipid metabolism or a bad diet, could contribute to dysfunction of the secretory pathway. On the other hand, determining the influence of lipid shape to membrane topology during the different steps of membrane remodeling across the secretory pathway will probably require better *in vitro* modeling of the different steps involved.

Acknowledgements and conflict of interest disclosure

We thank Dr N. Grant for critical reading of the manuscript. This work was supported by the Ministère de l'Enseignement Supérieur et de la Recherche, a grant from La Ligue contre le Cancer to NV, and by a grant from the Région Haute-Normandie to MM-H. The authors declare no conflict of interest.

References

Ammar M. R., Kassas N., Chasserot-Golaz S., Bader M.-F. and Vitale N. (2013) Lipids in regulated exocytosis: what are they doing? *Front. Endocrinol.* **4**, 125.

Apps D. K., Percy J. M. and Perez-Castineira J. R. (1989) Topography of a vacuolar-type H+-translocating ATPase: chromaffin-granule membrane ATPase I. *Biochem. J.* **263**, 81–88.

Arnaoutova I., Cawley N. X., Patel N., Kim T., Rathod T. and Loh Y. P. (2008) Aquaporin 1 is important for maintaining secretory granule biogenesis in endocrine cells. *Mol. Endocrinol.* **22**, 1924–1934.

Asp L., Kartberg F., Fernandez-Rodriguez J. *et al.* (2009) Early stages of Golgi vesicle and tubule formation require diacylglycerol. *Mol. Biol. Cell* **20**, 780–790.

Bader M.-F. and Vitale N. (2009) Phospholipase D in calcium-regulated exocytosis: lessons from chromaffin cells. *Biochim. Biophys. Acta* **1791**, 936–941.

Bauer C. S., Woolley R. J., Teschemacher A. G. and Seward E. P. (2007) Potentiation of exocytosis by phospholipase C-coupled G-Protein-Coupled Receptors requires the priming protein Munc13-1. *J. Neurosci.* **27**, 212–219.

Blázquez M., Thiele C., Huttner W. B., Docherty K. and Shennan K. I. (2000) Involvement of the membrane lipid bilayer in sorting prohormone convertase 2 into the regulated secretory pathway. *Biochem. J.* **349**, 843–852.

Braakman I. and Bulleid N. J. (2011) Protein folding and modification in the mammalian endoplasmic reticulum. *Annu. Rev. Biochem.* **80**, 71–99.

Burgess T. L. and Kelly R. B. (1987) Constitutive and regulated secretion of proteins. *Annu. Rev. Cell Biol.* **3**, 243–293.

Ceridono M., Ory S., Momboisse F. *et al.* (2011) Selective recapture of secretory granule components after full collapse exocytosis in neuroendocrine chromaffin cells. *Traffic* **12**, 72–88.

Chasserot-Golaz S., Vitale N., Umbrecht-Jenck E., Knight D., Gerke V. and Bader M.-F. (2005) Annexin 2 promotes the formation of lipid microdomains required for calcium-regulated exocytosis of dense-core vesicles. *Mol. Biol. Cell* **16**, 1108–1119.

Chernomordik L. V. and Kozlov M. M. (2008) Mechanics of membrane fusion. *Nat. Struct. Mol. Biol.* **15**, 675–683.

Cockcroft S. (2009) Phosphatidic acid regulation of phosphatidylinositol 4-phosphate 5-kinases. *Biochim. Biophys. Acta* **1791**, 905–912.

Cruz-Garcia D., Ortega-Bellido M., Scarpa M., Villeneuve J., Jovic M., Porzner M., Balla T., Seufferlein T. and Malhotra V. (2013) Recruitment of arfaptins to the trans-Golgi network by PI(4)P and their involvement in cargo export. *EMBO J.* **32**, 1717–1729.

Darios F. and Davletov B. (2006) Omega-3 and omega-6 fatty acids stimulate cell membrane expansion by acting on syntaxin 3. *Nature* **440**, 813–817.

Darios F., Wasser C., Shakirzyanova A. *et al.* (2009) Sphingosine facilitates SNARE complex assembly and activates synaptic vesicle exocytosis. *Neuron* **62**, 683–694.

Dhanvantari S. and Loh Y. P. (2000) Lipid raft association of carboxypeptidase E is necessary for its function as a regulated secretory pathway sorting receptor. *J. Biol. Chem.* **275**, 29887–29893.

Di Paolo G. and De Camilli P. (2006) Phosphoinositides in cell regulation and membrane dynamics. *Nature* **443**, 651–657.

Dikeakos J. D. and Reudelhuber T. L. (2007) Sending proteins to dense core secretory granules: still a lot to sort out. *J. Cell Biol.* **177**, 191–196.

Dittie A. S., Hajibagheri N. and Tooze S. A. (1996) The AP-1 adaptor complex binds to immature secretory granules from PC12 cells, and is regulated by ADP-ribosylation factor. *J. Cell Biol.* **132**, 523–536.

Dominguez V., Raimondi C., Somanath S. *et al.* (2011) Class II Phosphoinositide 3-Kinase regulates exocytosis of insulin granules in pancreatic cells. *J. Biol. Chem.* **286**, 4216–4225.

Du G., Altshuller Y. M., Vitale N., Huang P., Chasserot-Golaz S., Morris A. J., Bader M.-F. and Frohman M. A. (2003) Regulation of phospholipase D1 subcellular cycling through coordination of multiple membrane association motifs. *J. Cell Biol.* **162**, 305–315.

Gabel M., Delavoie F., Demais V., Royer C., Bailly Y., Vitale N., Bader M.-F. and Chasserot-Golaz S. (2015) Annexin A2-dependent actin bundling promotes secretory granule docking to the plasma membrane and exocytosis. *J. Cell Biol.* **210**, 785–800.

García-Martínez V., Villanueva J., Torregrosa-Hetland C. J., Bittman R., Higdon A., Darley-Usmar V. M., Davletov B. and Gutiérrez L. M. (2013) Lipid metabolites enhance secretion acting on SNARE microdomains and altering the extent and kinetics of single release events in bovine adrenal chromaffin cells. *PLoS ONE* **8**, e75845.

Gehart H., Goginashvili A., Beck R., Morvan J., Erbs E., Formentini I., De Matteis M. A., Schwab Y., Wieland F. T. and Ricci R. (2012) The BAR domain protein arfaptin-1 controls secretory granule biogenesis at the trans-Golgi network. *Dev. Cell* **23**, 756–768.

Gerdes H.-H. (2008) Membrane traffic in the secretory pathway. *Cell. Mol. Life Sci.* **65**, 2777–2780.

Gondré-Lewis M. C., Park J. J. and Loh Y. P. (2012) Cellular mechanisms for the biogenesis and transport of synaptic and dense-core vesicles. *Int. Rev. Cell Mol. Biol.* **299**, 27–115.

Ha K. D., Clarke B. A. and Brown W. J. (2012) Regulation of the Golgi complex by phospholipid remodeling enzymes. *Biochim. Biophys. Acta* **1821**, 1078–1088.

Hammond G. R. V., Dove S. K., Nicol A., Pinxteren J. A., Zicha D. and Schiavo G. (2006) Elimination of plasma membrane phosphatidylinositol (4,5)-bisphosphate is required for exocytosis from mast cells. *J. Cell Sci.* **119**, 2084–2094.

Hinners I., Wendler F., Fei H., Thomas L., Thomas G. and Tooze S. A. (2003) AP-1 recruitment to VAMP4 is modulated by phosphorylation-dependent binding of PACS-1. *EMBO Rep.* **4**, 1182–1189.

Holthuis J. C. M. and Menon A. K. (2014) Lipid landscapes and pipelines in membrane homeostasis. *Nature* **510**, 48–57.

Honigmann A., van den Bogaart G., Iraheta E. *et al.* (2013) Phosphatidylinositol 4,5-bisphosphate clusters act as molecular beacons for vesicle recruitment. *Nat. Struct. Mol. Biol.* **20**, 679–686.

Hosaka M., Suda M., Sakai Y., Izumi T., Watanabe T. and Takeuchi T. (2004) Secretogranin III binds to cholesterol in the secretory granule membrane as an adapter for chromogranin A. *J. Biol. Chem.* **279**, 3627–3634.

Houy S., Croisé P., Gubar O., Chasserot-Golaz S., Tryoen-Tóth P., Bailly Y., Ory S., Bader M.-F. and Gasman S. (2013) Exocytosis and endocytosis in neuroendocrine cells: inseparable membranes!. *Front. Endocrinol.* **4**, 135.

Ishikawa Y., Yuan Z., Inoue N., Skowronski M. T., Nakae Y., Shono M., Cho G., Yasui M., Agre P. and Nielsen S. (2005) Identification of AQP5 in lipid rafts and its translocation to apical membranes by activation of M3 mAChRs in interlobular ducts of rat parotid gland. *Am. J. Physiol. Cell Physiol.* **289**, 1303–1311.

Jahn R. and Fasshauer D. (2012) Molecular machines governing exocytosis of synaptic vesicles. *Nature* **490**, 201–207.

James D. J., Khodthong C., Kowalchyk J. A. and Martin T. F. J. (2008) Phosphatidylinositol 4,5-bisphosphate regulates SNARE-dependent membrane fusion. *J. Cell Biol.* **182**, 355–366.

Klenchin V. A. and Martin T. F. (2000) Priming in exocytosis: attaining fusion-competence after vesicle docking. *Biochimie* **82**, 399–407.

Klumperman J., Kuliawat R., Griffith J. M., Geuze H. J. and Arvan P. (1998) Mannose 6-phosphate receptors are sorted from immature secretory granules via adaptor protein AP-1, clathrin, and syntaxin 6-positive vesicles. *J. Cell Biol.* **141**, 359–371.

Kögel T. and Gerdes H. H. (2010) Roles of myosin Va and Rab3D in membrane remodeling of immature secretory granules. *Cell. Mol. Neurobiol.* **30**, 1303–1308.

Kögel T., Rudolf R., Hodneland E., Copier J., Regazzi R., Tooze S. A. and Gerdes H. H. (2013) Rab3D is critical for secretory granule maturation in PC12 cells. *PLoS ONE* **8**, e57321.

Kooijman E. E., Chupin V., de Kruijff B. and Burger K. N. J. (2003) Modulation of membrane curvature by phosphatidic acid and lysophosphatidic acid. *Traffic* **4**, 162–174.

Lam A. D., Tryoen-Toth P., Tsai B., Vitale N. and Stuenkel E. L. (2008) SNARE-catalyzed fusion events are regulated by syntaxin1A–lipid interactions. *Mol. Biol. Cell* **19**, 485–497.

Lang T., Bruns D., Wenzel D., Riedel D., Holroyd P., Thiele C. and Jahn R. (2001) SNAREs are concentrated in cholesterol-dependent clusters that define docking and fusion sites for exocytosis. *EMBO J.* **20**, 2202–2213.

Latham C. F., Osborne S. L., Cryle M. J. and Meunier F. A. (2007) Arachidonic acid potentiates exocytosis and allows neuronal SNARE complex to interact with Munc18a. *J. Neurochem.* **100**, 1543–1554.

Leventis P. A. and Grinstein S. (2010) The distribution and function of phosphatidylserine in cellular membranes. *Annu. Rev. Biophys.* **39**, 407–427.

Li S. C., Diakov T. T., Xu T., Tarsio M., Zhu W., Couoh-Cardel S. and Weisman L. S., Kane P. M. (2014) The signaling lipid PI(3,5)P_2 stabilizes V_1-V(o) sector interactions and activates the V-ATPase. *Mol. Biol. Cell* **25**, 1251–1262.

Marsh D. (2009) Cholesterol-induced fluid membrane domains: a compendium of lipid-raft ternary phase diagrams. *Biochim. Biophys. Acta* **1788**, 2114–2123.

Martin T. F. J. (2015) PI(4,5)P2-binding effector proteins for vesicle exocytosis. *Biochim. Biophys. Acta* **1851**, 785–793.

van Meer G. and de Kroon A. I. P. M. (2011) Lipid map of the mammalian cell. *J. Cell Sci.* **124**, 5–8.

van Meer G., Voelker D. and Feigenson G. (2008) Membrane lipids - where they are and how they behave. *Nat. Rev. Mol.* **9**, 112–124.

Meunier F. A., Osborne S. L., Hammond G. R., Cooke F. T., Parker P. J., Domin J. and Schiavo G. (2005) Phosphatidylinositol 3-kinase C2α is essential for ATP-dependent priming of neurosecretory granule exocytosis. *Mol. Biol. Cell* **16**, 4841–4851.

Milosevic I., Sørensen J. B., Lang T., Krauss M., Nagy G., Haucke V., Jahn R. and Neher E. (2005) Plasmalemmal phosphatidylinositol-4,5-bisphosphate level regulates the releasable vesicle pool size in chromaffin cells. *J. Neurosci.* **25**, 2557–2565.

Mima J. and Wickner W. (2009) Complex lipid requirements for SNARE- and SNARE chaperone-dependent membrane fusion. *J. Biol. Chem.* **284**, 27114–27122.

Montero-Hadjadje M., Vaingankar S., Elias S., Tostivint H., Mahata S. K. and Anouar Y. (2008) Chromogranins A and B and secretogranin II: evolutionary and functional aspects. *Acta Physiol.* **192**, 309–324.

Narayana V. K., Tomatis V. M., Wang T., Kvaskoff D. and Meunier F. A. (2015) Profiling of free fatty acids using stable isotope tagging uncovers a role for saturated fatty acids in neuroexocytosis. *Chem. Biol.* **22**, 1552–1561.

Ory S., Ceridono M., Momboisse F. *et al.* (2013) Phospholipid scramblase-1-induced lipid reorganization regulates compensatory endocytosis in neuroendocrine cells. *J. Neurosci.* **33**, 3545–3556.

Osborne S. L., Wen P. J., Boucheron C., Nguyen H. N., Hayakawa M., Kaizawa H., Parker P. J., Vitale N. and Meunier F. A. (2008) PIKfyve negatively regulates exocytosis in neurosecretory cells. *J. Biol. Chem.* **283**, 2804–2813.

Pang Z. P. and Südhof T. C. (2010) Cell biology of Ca^{2+}-triggered exocytosis. *Curr. Opin. Cell Biol.* **22**, 496–505.

Park J. J., Koshimizu H. and Loh Y. P. (2009) Biogenesis and transport of secretory granules to release site in neuroendocrine cells. *J. Mol. Neurosci.* **37**, 151–159.

Rigoni M., Caccin P., Gschmeissner S., Koster G., Postle A. D., Rossetto O., Schiavo G. and Montecucco C. (2005) Equivalent effects of snake PLA2 neurotoxins and lysophospholipid-fatty acid mixtures. *Science* **310**, 1678–1680.

Rogasevskaia T. P. and Coorssen J. R. (2015) The role of phospholipase D in regulated exocytosis. *J. Biol. Chem.* **290**, 28683–28696.

Salaün C., Gould G. W. and Chamberlain L. H. (2005) Lipid raft association of SNARE proteins regulates exocytosis in PC12 cells. *J. Biol. Chem.* **280**, 19449–19453.

Santiago-Tirado F. H., Legesse-Miller A., Schott D. and Bretscher A. (2011) PI4P and Rab inputs collaborate in myosin-V-dependent transport of secretory compartments in yeast. *Dev. Cell* **20**, 47–59.

Schapiro F. B. and Grinstein S. (2000) Determinants of the pH of the Golgi complex. *J. Biol. Chem.* **275**, 21025–21032.

Sheu L., Pasyk E. A., Ji J., Huang X., Gao X., Varoqueaux F., Brose N. and Gaisano H. Y. (2003) Regulation of insulin exocytosis by Munc13-1. *J. Biol. Chem.* **278**, 27556–27563.

Siddhanta A. and Shields D. (1998) Secretory vesicle budding from the trans-Golgi network is mediated by phosphatidic acid levels. *J. Biol. Chem.* **273**, 17995–17998.

Surma M. A., Klose C. and Simons K. (2012) Lipid-dependent protein sorting at the trans Golgi network. *Biochim. Biophys. Acta* **1821**, 1059–1067.

Tang X., Halleck M. S., Schlegel R. A. and Williamson P. (1996) A subfamily of P-type ATPases with aminophospholipid transporting activity. *Science* **272**, 1495–1497.

Taupenot L., Harper K. L. and O'Connor D. T. (2005) Role of H+-ATPase-mediated acidification in sorting and release of the regulated secretory protein chromogranin A: evidence for a vesiculogenic function. *J. Biol. Chem.* **280**, 3885–3897.

Teuchert M., Schäfer W., Berghöfer S., Hoflack B., Klenk H. D. and Garten W. (1999) Sorting of furin at the trans-Golgi network. Interaction of the cytoplasmic tail sorting signals with AP-1 Golgi-specific assembly proteins. *J. Biol. Chem.* **274**, 8199–8207.

Tooze S. A., Martens G. J. M. and Huttner W. B. (2001) Secretory granule biogenesis: rafting to the SNARE. *Trends Cell Biol.* **11**, 116–122.

Trifaró J.-M., Gasman S. and Gutiérrez L. M. (2008) Cytoskeletal control of vesicle transport and exocytosis in chromaffin cells: cytoskeleton and the secretory vesicle cycle. *Acta Physiol.* **192**, 165–172.

Tryoen-Toth P., Chasserot-Golaz S., Tu A., Gherib P., Bader M.-F., Beaumelle B. and Vitale N. (2013) HIV-1 Tat protein inhibits neurosecretion by binding to phosphatidylinositol 4,5-bisphosphate. *J. Cell Sci.* **126**, 454–463.

Umbrecht-Jenck E., Demais V., Calco V., Bailly Y., Bader M.-F. and Chasserot-Golaz S. (2010) S100A10-mediated translocation of annexin-A2 to SNARE proteins in adrenergic chromaffin cells undergoing exocytosis. *Traffic* **11**, 958–971.

Vázquez-Martínez R., Díaz-Ruiz A., Almabouada F., Rabanal-Ruiz Y., Gracia-Navarro F. and Malagón M. M. (2012) Revisiting the regulated secretory pathway: from frogs to human. *Gen. Comp. Endocrinol.* **175**, 1–9.

Vitale N., Thiersé D., Aunis D. and Bader M.-F. (1994) Exocytosis in chromaffin cells: evidence for a MgATP-independent step that requires a pertussis toxin-sensitive GTP-binding protein. *Biochem. J.* **300**, 217–227.

Vitale N., Caumont A.-S., Chasserot-Golaz S., Du G., Wu S., Sciorra V. A., Morris A. J., Frohman M. A. and Bader M.-F. (2001) Phospholipase D1: a key factor for the exocytotic machinery in neuroendocrine cells. *EMBO J.* **20**, 2424–2434.

Vitale N., Thiersé D. and Bader M.-F. (2010) Melittin promotes exocytosis in neuroendocrine cells through the activation of phospholipase A_2. *Regul. Pept.* **165**, 111–116.

Wang T. and Silvius J. R. (2000) Different sphingolipids show differential partitioning into sphingolipid/cholesterol-rich domains in lipid bilayers. *Biophys. J* . **79**, 1478–1489.

Wang Y. J., Wang J., Sun H. Q., Martinez M., Sun Y. X., Macia E., Kirchhausen T., Albanesi J. P., Roth M. G. and Yin H. L. (2003) Phosphatidylinositol 4 phosphate regulates targeting of clathrin adaptor AP-1 complexes to the Golgi. *Cell* **114**, 299–310.

Wen P. J., Osborne S. L., Morrow I. C., Parton R. G., Domin J. and Meunier F. A. (2008) Ca2+-regulated pool of phosphatidylinositol-3-phosphate produced by phosphatidylinositol 3-kinase C2α on neurosecretory vesicles. *Mol. Biol. Cell* **19**, 5593–5603.

Wen P. J., Osborne S. L., Zanin M. *et al.* (2011) Phosphatidylinositol (4,5)bisphosphate coordinates actin-mediated mobilization and translocation of secretory vesicles to the plasma membrane of chromaffin cells. *Nat. Commun.* **2**, 491.

Wilson C., Venditti R., Rega L. R., Colanzi A., D'Angelo G. and De Matteis M. A. (2011) The Golgi apparatus: an organelle with multiple complex functions. *Biochem. J.* **433**, 1–9.

Yuan T., Liu L., Zhang Y. *et al.* (2015) Diacylglycerol guides the hopping of clathrin-coated pits along microtubules for exo-endocytosis coupling. *Dev. Cell* **35**, 120–130.

Zeniou-Meyer M., Zabari N., Ashery U. *et al.* (2007) Phospholipase D1 production of phosphatidic acid at the plasma membrane promotes exocytosis of large dense-core granules at a late stage. *J. Biol. Chem.* **282**, 21746–21757.

Qili WANG

Interaction entre la sous unité V0 de la V-ATPase et le facteur d'échange ARNO et son implication fonctionnelle dans l'exocytose régulée

Résumé

Alors que s'accumulent des donnés épidémiologiques qui suggèrent une importance fondamentale des lipides de l'alimentation dans l'homéostasie cellulaire et le développement de nombreuses pathologies humaines, peu d'informations sur leurs fonctions spécifiques sont disponibles à ce jour. Ceci est particulièrement le cas pour la neurosecretion qui dépend de la fusion d'organites vésiculaires avec la membrane plasmique. Des études récentes ont montré le rôle clé de la compartimentalisation lipidique au niveau des sites d'exocytose et par ailleurs validées la notion de lipides fusogéniques, comme pour l'acide phosphatidique (PA).

La V-ATPase, via ses domaines V0 et V1 est à la fois impliquée dans le remplissage en neurotransmetteurs des vésicules, mais aussi dans leur fusion. Nous montrons ici que V0a1 interagit avec le facteur d'échange pour Arf6 ARNO. En bloquant cette interaction, nous avons observé une réduction de l'activation d'Arf6, de l'activité PLD et de l'exocytose, avec une modification de la cinétique des événements unitaires d'exocytose. Nous proposons que la dissociation de V1 de V0 pourrait représenter un signal permettant l'activation de la voie Arf6-ARNO-PLD1 et ainsi promouvoir la synthèse de PA requise à une exocytose efficace dans les cellules neuroendocrines.

Mots-clés : acide phosphatidique - cellule neuroendocrine - lipides - phospholipase D - exocytose - V-ATPase

Abstract

Lipids play key cellular functions and are involved in many human diseases and little information is available on their exact function. This is especially the case in neurosecretion that relies on the fusion of specific membrane organelle with the plasma membrane for which relatively little attention has been paid to the necessary role of lipids. Recent studies have established the importance of lipid compartmentalization at the exocytotic sites and validated the contribution of fusogenic lipids such as phosphatidic acid (PA) for membrane fusion.

The V-ATPase is involved both in the charging of secretory vesicle and the membrane fusion for secretion of vesicle. Indeed the V1 and V0 subdomains were shown to dissociate during stimulation allowing subunits of the vesicular V0 to interact with different proteins of the secretory machinery. We show here that V0a1 interacts with the exchange factor ARNO and promotes Arf6 activation during exocytosis in neuroendocrine cells. Interfering with the V0a1-ARNO interaction prevented phospholipase D (PLD) activation, phosphatidic acid synthesis during exocytosis, and altered the kinetic parameters of individual fusion events. We suggest that V1 dissociation from V0 could represent the signal that triggers the activation of the ARNO-Arf6-PLD1 pathway and promotes PA synthesis needed for efficient exocytosis in neuroendocrine cells.

Key words: Exocytosis - lipids - neuroendocrine cell - phospholipase D - phosphatidic acid - V-ATPase